ACTA PHYSICA

ACADEMIAE SCIENTIARUM HUNGARICAE

TOMUS XVI FASCICULUS 1

AKADÉMIAI KIADÓ, BUDAPEST
1963

ACTA PHYS. HUNG.

ACTA PHYSICA

A MAGYAR TUDOMÁNYOS AKADÉMIA FIZIKAI KÖZLEMÉNYEI

SZERKESZTŐSÉG ÉS KIADÓHIVATAL: BUDAPEST V., ALKOTMÁNY UTCA 21.

Az *Acta Physica* német, angol, francia és orosz nyelven közöl értekezéseket a fizika tárgyköréből.

Az *Acta Physica* változó terjedelmű füzetekben jelenik meg: több füzet alkot egy kötetet.

A közlésre szánt kéziratok a következő címre küldendők:

Acta Physica, Budapest 502, Postafiók 24.

Ugyanerre a címre küldendő minden szerkesztőségi és kiadóhivatali levelezés.

Az *Acta Physica* előfizetési ára kötetenként belföldre 80 forint, külföldre 110 forint. Megrendelhető a belföld számára az Akadémiai Kiadónál (Budapest V., Alkotmány utca 21. Bankszámla 05-915-111-46), a külföld számára pedig a „Kultúra" Könyv- és Hírlap Külkereskedelmi Vállalatnál (Budapest I., Fő u. 32. Bankszámla 43-790-057-181 sz.), vagy annak külföldi képviseleteinél és bizományosainál.

Die *Acta Physica* veröffentlichen Abhandlungen aus dem Bereiche der Physik in deutscher, englischer, französischer und russischer Sprache.

Die *Acta Physica* erscheinen in Heften wechselnden Umfanges. Mehrere Hefte bilden einen Band.

Die zur Veröffentlichung bestimmten Manuskripte sind an folgende Adresse zu richten:

Acta Physica, Budapest 502, Postafiók 24.

An die gleiche Anschrift ist auch jede für die Redaktion und den Verlag bestimmte Korrespondenz zu senden.

Abonnementspreis pro Band: 110 forint. Bestellbar bei dem Buch- und Zeitungs-Aussenhandels-Unternehmen »Kultúra« (Budapest I., Fő u. 32. Bankkonto Nr. 43-790-057-181) oder bei seinen Auslandsvertretungen und Kommissionären.

ACTA PHYSICA

ACADEMIAE SCIENTIARUM HUNGARICAE

TOMUS XVI

AKADÉMIAI KIADÓ, BUDAPEST
1964

ACTA PHYSICA

Tomus XVI

INDEX

PAIS APPROXIMATE FORMULA FOR THE PHASE SHIFT AND ELECTRON SCATTERING IN THE THOMAS-FERMI THEORY

By

T. TIETZ

UNIVERSITY ŁÓDŹ, DEPARTMENT OF THEORETICAL PHYSICS, ŁÓDŹ, POLAND

(Presented by A. Kónya. — Received 5. XI. 1961)

In this paper we calculate the phase shifts by means of a simplified PAIS method fos the THOMAS-FERMI and analytical HARTREE potentials. The calculation presented in thir paper shows that our method gives more accurate results for the phase shifts than the BORN approximation, having moreover the advantage that it is much more practical than the PAIS method.

For the scattering of electrons by a central field, the scattering amplitude $f(\vartheta)$, as known, is given by the following FAXEN—HOLTZMARK formula [1]:

$$f(\vartheta) = \frac{1}{2ik} \sum_{l=0}^{\infty} (2l+1)\,(e^{2i\delta_l} - 1)\,P_l(\cos\vartheta) = \tag{1}$$

$$= \frac{1}{k} \sum_{l\infty 0}^{\infty} (2l+1) \left[\delta_l - \frac{2}{3}\,\delta_l^3 + \ldots + i\left(\delta_l^2 - \frac{1}{3}\,\delta_l^4 + \ldots\right)\right] P_l(\cos\vartheta)\,.$$

The usual first BORN approximation for the phase shift $\delta_l^{(1)}$ is obtained if δ_l is small; as is known the former has the form [2]

$$\delta_l^{(1)} = -\frac{\pi m}{\hbar^2} \int_0^{\infty} V(r)\, J_{l+\frac{1}{2}}^2(kr)\, r\, dr\,, \tag{2}$$

where $J_{l+\frac{1}{2}}(kr)$ denotes the Bessel function characterizing the free particle solutions. The BORN approximation for the phase shifts for small quantum number l does not give adequate numerical values. Therefore PAIS [3] gave another method for the determination of the phase shifts δ_l. The PAIS method consists in the following. We write the radial wave equation in the form

$$\frac{d^2 w_l}{dr^2} + \left[k^2 - \frac{l(l+1) - c^2}{r^2}\right] w_l = 0\,, \tag{3}$$

where c is a constant. Since the solution w_l must satisfy the following boundary

conditions

$$w_l(0) = 0 \quad \text{and} \quad w_l(\infty) \to \sin\left(kr - \frac{l\pi}{2} + \delta_l\right) \tag{4}$$

the constant c fulfils the relation

$$\left(l + \frac{1}{2}\right) - 2\delta_l/\pi = \sqrt{\left(l + \frac{1}{2}\right)^2 - c^2}\,. \tag{5}$$

The phase shift δ_l must fulfil the following relation, as it has been shown by PAIS with help of the variational method and by the author [4] in another way:

$$\frac{2\,l + 1 - (2\delta_l/\pi)}{2\,l + 1 - (4\,\delta_l/\pi)}\,\delta_l = -\frac{m\pi}{\hbar^2}\int_0^\infty r V(r)\, J^2_{l+\frac{1}{2}(-2\delta_l/\pi)}(kr)\,dr\,. \tag{6}$$

For small quantum number l the PAIS phase shifts δ_l are significantly better than the BORN phases $\delta_l^{(1)}$. The PAIS method has the disadvantage that in many cases δ_l given by equ. (6) can be calculated only numerically, since δ_l fulfils a complicated transcendental equation. Therefore it is advantageous to represent the PAIS method in such an approximation which allows to calculate δ_l by a simple method. If we develop δ_l in a series in powers of the interaction potential $V(r)$, namely

$$\delta_l = \delta_l^{(1)} + \delta_l^{(2)} + \ldots \tag{7}$$

and δ_l is small, then $\delta_l^{(2)}$ is given by

$$\delta_l^{(2)} = \frac{2}{\pi}\left(a_l - \frac{\delta_l^{(1)}}{2l+1}\right)\delta_l^{(1)}, \quad \text{where} \quad a_l = -\left(\frac{\partial\delta_p^{(1)}}{\partial p}\right)_{p=l+\frac{1}{2}}. \tag{8}$$

The BORN phase shifts $\delta_l^{(1)}$ appearing in equ. (8) are given by equ. (2). In this paper, using formulas (2), (7) and (8), we shall calculate the phase shifts for the THOMAS—FERMI [5] and the analytical representation of HARTREE potentials and we shall compare our results with the results obtained numerically. The interaction potential $V(r)$ based on the THOMAS—FERMI or HARTREE scheme [6] may be written

$$V(r) = (-Ze^2/r)\,(Z_p/Z)\,. \tag{9}$$

The Coulomb potential of the nucleus is modified by the factor Z_p/Z representing the screening effect of the orbital electrons on the nucleus. The function Z_p/Z satisfies the conditions $Z_p/Z \to 1$ as $\tau \to 0$ and $Z_p/Z \to 0$ as $r \to \infty$.

Tabulated numerical values of the quantity Z_p/Z exist for a number of atoms and ions. RUARK [7], BYATT [8], ROZENTAL [9] and MOLIÈRE [10] have shown that Z_p/Z can be represented analytically as follows:

$$Z_p/Z = \Sigma_n c_n e^{-b_n x}, \tag{10}$$

where c_n and b_n are constants given in Table I.

Table I

Numerical values of the constants c_n and b_n according to equ. (10) for exponential fits of Z_p/Z and the THOMAS-FERMI function $\Phi(x)$

Element	Z_p/Z (one term)		Z_p/Z (series of terms)					
	c_1	b_1	c_1	c_2	c_3	b_1	b_2	b_3
He	1.00	1.60	1.25	—0.25	—	1.75	3.845	—
Be	—	—	1.00	—0.48	0.48	0.574	1.081	3.06
C	—	—	1.25	—0.44	0.19	0.828	1.41	4.29
N	1.00	0.95	1.20	—0.32	0.12	0.904	1.43	9.65
O	1.00	0.919	1.25	—0.35	0.10	0.991	1.63	18.3
F	1.00	0.907	—	—	—	—	—	—
Ne	1.00	0.978	—	—	—	—	—	—
A*	—	—	0.84	—0.24	0.40	0.566	1.056	3.25
A	—	—	0.659	0.341	—	0.574	2.77	—
K	—	—	0.124	0.68	0.196	0.0514	0.765	2.80
Ca	—	—	0.20	0.56	0.24	0.195	0.770	3.08
Cr	1.00	0.731	1.00	—0.20	0.20	0.731	1.26	3.70
Fe	—	—	0.25	0.56	0.19	0.335	0.828	3.76
Zn	—	—	0.22	0.78	—	0.319	1.081	—
Ge	—	—	0.22	0.78	—	0.263	1.165	—
As	—	—	0.295	0.705	—	0.387	1.295	—
Br	—	—	0.360	0.640	—	0.366	1.485	—
Kr*	—	—	0.335	0.60	0.065	0.290	1.33	7.00
Kr	—	—	0.415	0.51	0.075	0.378	1.48	7.00
W	—	—	0.19	0.72	0.09	0.216	0.970	15.00
Hg	—	—	0.19	0.56	0.25	0.257	0.779	3.16
$\Phi(x)$ ROZENTHAL	—	—	0.255	0.581	0.164	0.246	0.947	4.356
$\Phi(x)$ MOLIÈRE	—	—	0.35	0.55	0.1	0.3	1.2	6.00

* These expressions contain a polarization correction. Some of the exponential fits Z_p/Z contain the exchange correction and some do not. Those of Z_p/Z which contain the exchange correction can be found in A. J. FREEMAN, Phys. Rev., **91**, 1410, 1953 as well as in D. R. HARTREE, Reports on Progress in Physics (The Physical Society, London, 1946), Vol. **11**, p. 113. More details concerning the Z_p/Z are to be found in the paper of W. J. BYATT, Phys. Rev., **104**, 1298, 1956.

The dimensionless quantity x appearing in equ. (10) is related with r as follows [11]:

$$r = x/\mu \quad \text{and} \quad \mu = 0.88534\, a_0/Z^{1/3}. \tag{11}$$

Z is the atomic number and a_0 the first Bohr radius of the hydrogen atom. The potential $V(r)$ appearing in equ. (9) can be written by means of equ. (10) and (11) as

$$V(r) = -\frac{Ze^2}{r} \Sigma_n c_n e^{-\frac{b_n r}{\mu}}. \tag{12}$$

Since [12]

$$J^2_{l+\frac{1}{2}}(kr) = \frac{2}{\pi} \int_0^{\pi/2} J_{2l+\frac{1}{2}}(2kr\cos\vartheta)\, d\vartheta \tag{13}$$

and [12]

$$J_{2l+1}(2\,kr\cos\vartheta) = \frac{2}{\pi} \int_0^{\pi/2} \sin[2\,kr\cos\vartheta\sin\psi]\sin(2\,l+1)\,\psi\, d\psi\,, \tag{14}$$

a_l appearing in formula (8) can be written as

$$a_l = -\frac{8m\,Ze^2}{\pi\hbar^2} \Sigma_n c_n \int_0^{\infty} e^{-\frac{b_n r}{\mu}} dr \int_0^{\pi/2}\int_0^{\pi/2} \times \\ \times \psi \sin[2\,kr\cos\vartheta\sin\psi]\cos(2\,l+1)\,\psi d\,\psi d\vartheta\,. \tag{15}$$

The integrals over r and ϑ can be easily carried out so that

$$a_l = -\frac{4m\,Ze^2}{\pi\hbar^2} \Sigma_n c_n \int_0^{\pi/2} \frac{\psi\cos(2\,l+1)\,\psi}{\sqrt{(b_n/\mu)^2 + 4\,k\sin^2\psi}} \ln \times \\ \times \frac{\sqrt{(b_n/\mu)^2 + 4\,k^2\sin^2\psi} + 2\,k\sin\psi}{\sqrt{(b_n/\mu)^2 + 4k^2\sin^2\psi} - 2\,k\sin\psi}\, d\psi. \tag{16}$$

The integral appearing in the last formula can be calculated only numerically. If we write the last formula for a_l in atomic units we obtain

$$a_l = -\frac{4Z}{\pi} \Sigma_n c_n \int_0^{\pi/2} \frac{\varphi\cos(2\,l+1)\,\varphi}{\sqrt{(b_n/\mu)^2 + 8\,E\sin^2\varphi}} \times \\ \ln \frac{\sqrt{(b_n/\mu)^2 + 8\,E\sin^2\varphi} + 2\sqrt{2\,E}\sin\varphi}{\sqrt{(b_n/\mu)^2 + 8\,E\sin^2\varphi} - 2\sqrt{2\,E}\sin\varphi}\, d\varphi\,, \tag{17}$$

where E is the energy of the incident electrons and its unit equals twice the ionization energy of the normal state of the hydrogen atom and is 27,23 eV, and in atomic units it is $0.88534\, Z^{-1/3}$. The constants b_n and c_n are to be found in Table I. The BORN approximation $\delta_l^{(1)}$ for the potential equ. (12) in atomic units is given by

$$\delta_l^{(1)} = \frac{Z}{\sqrt{2E}} \Sigma_n c_n Q_l \left(1 + \frac{1}{2}\left(\frac{b_n}{\mu\sqrt{2E}}\right)^2\right), \tag{18}$$

where the Q_l are Legendre polynomials of the second kind. Formulas (18), (17) and (8) allow us to calculate the phase shifts δ_l given by equ. (7). In Table II we have collected some numerical results for He for incident electron energies in the voltage range $16 \leqslant V \leqslant 340$.

Table II

A comparison of the phase shifts δ_l equs. (7) and (8) with $\delta_l^{(1)}$ equ. (18) and numerical values

Voltage	l	$\delta_l^{(1)}$ (BORN equ. 18)	Our results for $\delta_l = \delta_l^{(1)} + \delta_l^{(2)}$ equ. (7) and equ. (8)	Numerical values for δ_l (Mc. DOUGALL)
16	1	0.0536	0.0731	0.070
49	1	0.1340	0.1875	0.186
121	1	0.2276	0.2796	0.272
	2	0.0892	0.0924	0.0946
	3	0.0492	0.04917	—
340	1	0.2668	0.3389	0.308
	2	0.1364	0.1415	0.1524

Table II shows that our results for δ_l are significantly better than the BORN phases $\delta_l^{(1)}$ and only a little worse than the corresponding numerical values. Equ. (6) in our case can be presented analytically, but the phases fulfil a transcendental equation of infinite order. Our formula, equ. (17), is much simpler for practical calculations than equ. (6). Table II shows that our results for δ_l agree quite well with the exact MCDOUGALL [13] values. At the high energies our results for δ_l are equivalent with the corresponding results $\delta_l^{(1)}$ for the BORN approximation.

REFERENCES

1. H. Faxen and J. Holtzmark, Zs. f. Phys., **45**, 307, 1928.
2. N. F. Mott and H. S. W. Massey, The Theory of Atomic Collisions, Oxford, Clarendon Press, 1949.
3. A. Pais, Proc. Cambridge Phil. Soc., **42**, 45, 1946.
4. T. Tietz, ЖЭТФ, **37**, 293, 1959.
5. P. Gombás, Die statistische Theorie des Atoms und ihre Anwendungen, Springer-Verlag, Vienna, 1949; see also Encyclopedia of Physics Vol. **36**, Springer-Verlag, Berlin-Göttingen-Heidelberg, 1956.
6. W. J. Byatt, Phys. Rev., **104**, 1298, 1956.
7. A. E. Ruark, Phys. Rev., **57**, 62, 1940.
8. See ref. [6].
9. S. Rozental, Zs. f. Phys., **98**, 742, 1936.
10. G. Molière, Z. Naturforsch., **2***a*, 133, 1947.
11. See ref. [5].
12. A. Kratzer and W. Franz, Transzendente Funktionen, Akademische Verlagsgesellschaft, Geest und Portig K.-G. Leipzig, 1960.
13. McDougall, Proc. Roy. Soc., **136**, 549, 1932.

ПРИБЛИЖЕННАЯ ФОРМУЛА ПАЙСА ДЛЯ СДВИГА ФАЗ И РАССЕЯНИЯ ЭЛЕКТРОНОВ В ТЕОРИИ ТОМАСА—ФЕРМИ

Т. ТИТЦ

Р е з ю м е

В данной работе определяется сдвиг фаз упрощенным методом Пайса для потенциала Томаса—Ферми и аналитического потенциала Хартри. Вычисления, проведённые в работе, показывают, что применённый нами метод даёт более точные результаты для сдвига фаз, чем борновское приближение. Данный метод имеет определённое преимущество перед методом Пайса, заключающееся в его практичности.

THE SCATTERING AND POLARIZATION OF ELECTRONS BY HARTREE AND THOMAS-FERMI ATOMS

By

T. TIETZ

UNIVERSITY ŁÓDŹ, DEPARTMENT OF THEORETICAL PHYSICS, ŁÓDŹ, POLAND

(Presented by A. Kónya. — Received 3. II. 1962)

Using the analytical fits for the effective nuclear charge and the theory of scattering of a beam of particles by a centre of force in the relativistic case, we discuss the asymmetry in double scattering. We have presented the theory in such a simple manner that the asymmetry in double scattering can be calculated without any difficulty in an analytical way. This paper gives a generalization of the paper of MOHR and TASSIE.

Introduction

It is known that the scattering of electrons in gases and thin foils provides information on the interaction of electrons with atomic and nuclear fields. Experiments have been carried out for different energies of incident electrons. The experiments have confirmed that the theory of HARTREE [1] and of THOMAS—FERMI [2] described very well the atomic field in a great range of the energies of the incident electrons. Using BYATT's [3] fits for the HARTREE field as well as approximations for the THOMAS—FERMI functions and the theory of electron scattering we shall discuss the scattering of polarized electrons by atoms in a relativistic case. To discuss the polarization of electrons by double scattering we use the DIRAC theory for elastic scattering of electrons by atoms.

Theory

We start from the DIRAC equation, which we write in the SCHRÖDINGER form, namely [4]

$$\frac{d^2 G_l}{dr^2} + \left[k^2 - \frac{l(l+1)}{r^2} - \frac{2m}{\hbar^2}\right] V(r)\, G_l = 0\,, \tag{1}$$

where m is the electron rest mass and l is the quantum number: $l = 0, 1, 2, 3, \ldots$. The central potential $V(r)$ is the modified DIRAC potential and can be expressed in the following form:

$$V = \gamma\, Z_p\, e^2/r + Z_p^2\, e^4/2\, mc^2 - 3\, \alpha'^2/4\, \alpha^2 + \alpha''/2\, \alpha\,, \tag{2}$$

where

$$\alpha = (E - V + mc^2)/\hbar c. \tag{3}$$

E is the total energy, Z_p is the effective nuclear charge at a distance r and the primes denote derivatives with respect to r. The symbol γ appearing in equ. (2) is given by

$$\gamma = (1 - v^2/c^2)^{-1/2}, \tag{4}$$

where v is the velocity of the incident electron and c is the velocity of light. k appearing in the DIRAC equ. (1) means

$$k = \gamma mv/\hbar. \tag{5}$$

The charge of the electron is denoted by e and $\hbar$ is the Planck constant. In the DIRAC theory the cross section for the scattering of electrons by atoms per unit solid angle in the direction ϑ of the beam of unpolarized electrons is given as follows [5]:

$$I(\vartheta) = |f|^2 + |g|^2, \tag{6}$$

where the scattering amplitudes $f(\vartheta)$ and $g(\vartheta)$ are given in the DIRAC theory by the following formula:

$$2\,ikf(\vartheta) = \sum_l \{(l+1)[\exp(2i\eta_l) - 1] + l[\exp(2i\eta_{-l-1}) - 1]\} P_l(\cos\vartheta). \tag{7}$$

and

$$2\,ikg(\vartheta) = \sum_l [\exp(2i\eta_{-l-1}) - \exp(2i\eta_l)]\, P_l^1(\cos\vartheta). \tag{8}$$

P_l and P_l^1 are the Legendre polynomials, η_l and η_{-l-1} are the phase shifts of the regular and irregular solutions of the DIRAC equation at the origin, which we denote by G_l and G_{-l-1}. These solutions have the following asymptotic form for large r:

$$G_{l,-l-1} \sim \sin(kr - l\pi/2 + \eta_{l,-l-1}). \tag{9}$$

Taking into consideration the detailed theory of double scattering worked out by MOTT we can write the asymmetry in double scattering in the THOMAS—FERMI and HARTREE theory as follows:

$$2\delta = 2\,|fg^* - f^* g|^2/(|f|^2 + |g|^2)^2. \tag{10}$$

To calculate the cross-section $I(\vartheta)$ and the asymmetry in double scattering we must know the scattering amplitudes $f(\vartheta)$ and $g(\vartheta)$. Formulas (7) and (8)

for $f(\vartheta)$ and $g(\vartheta)$ show that if the phase shifts η_l and η_{-l-1} are known the mentioned scattering amplitudes can be calculated. The further part of this paper shows that it is sufficient to know η_l, since η_{-l-1} can be easily calculated directly from η_l. It is known that in case of a pure Coulomb field the phase shifts η^c_{-l-1} of the irregular solution G^c_{-l-1} can be represented analytically by the following formula [6]:

$$\exp(2i\eta^c_{-l-1}) = \frac{l - i\gamma_1'}{\varrho_l - i\gamma_1} \frac{\Gamma(\varrho_l + 1 - i\gamma_1)}{\Gamma(\varrho_l + 1 + i\gamma_1)} \exp\left[-\pi i(\varrho_l - l)\right]. \quad (11)$$

If we note that the phase shift of the regular solution $\exp(2i\eta^c_l)$ is obtained from (11) by replacing l by $-l-1$ everywhere except in the last factor which becomes $\exp[-\pi i(\varrho_{l+1} - l)]$, this means that for η^c_l we obtain the expression

$$\exp(2i\eta_l c) = \frac{(-l-1) - i\gamma_1'}{\varrho_{-l-1} - i\gamma_1} \frac{\Gamma(\varrho_{-l-1} + 1 - i\gamma_1)}{\Gamma(\varrho_{-l-1} + 1 + i\gamma_1)} \exp\left[-\pi i(\varrho_{l+1} - l)\right]. \quad (12)$$

The symbols appearing in formulas (11) and (12) have the following meaning

$$\alpha = Ze^2/\hbar c \quad \text{and} \quad \varrho = (l^2 - \alpha^2)^{1/2}, \quad (13)$$

and further

$$\gamma_1 = Ze^2/\hbar v \quad \text{and} \quad \gamma_1' = \left(1 - \frac{v^2}{c^2}\right)^{1/2} \gamma_1. \quad (14)$$

For a Coulomb field the phases η^c_l and η^c_{-l-1} may be readily calculated from equ. (11) and (12). Equs. (11) and (12) allow us, as we shall see below, to correct the phase shifts in case of THOMAS—FERMI and HARTREE fields. The interaction potential $V_H(r)$ based on the HARTREE or THOMAS—FERMI scheme may be written in the non-relativistic case as

$$V_H(r) = (-Ze^2/r)(Z_p/Z). \quad (15)$$

The Coulomb potential of the nucleus is modified by the factor Z_p/Z representing the screening effect of the orbital electrons on the nucleus. The function Z_p/Z satisfies the conditions $Z_p/Z \to 1$ as $r \to 0$ and $Z_p/Z \to 0$ as $r \to \infty$. Tabulated numerical values of the quantity Z_p/Z exist for a number of atoms and ions. According to RUARK [7] the screening effect of the orbital electron on the nucleus Z_p/Z can be represented as follows:

$$Z_p/Z = \sum_n c_n e^{-b_n X}. \quad (16)$$

The constants c_n appearing in equ. (13) must satisfy the condition $\sum_n c_n = 1$ but otherwise the constants c_n and b_n are adjustable. The best values for the constants c_n and b_n after BYATT for several Z in case of a HARTREE field as well as for the THOMAS—FERMI field are to be found in Table I of [12]. The dimensionless variable x appearing in equ. (16) is related to r as follows:

$$x = \frac{r}{\mu}, \quad \text{where} \quad \mu = \frac{1}{4}\left(\frac{9\pi^2}{2}\right)^{1/3} \frac{a_0}{Z^{1/3}} = \frac{0.88534 a_0}{Z^{1/3}} . \tag{17}$$

In formula (17) Z is the atomic number and a_0 is the first radius of the hydrogen atom. Since it is impossible to solve exactly the DIRAC equ. (1) for the potential (2) and to obtain exact phase shifts η_l and η_{-l-1} we must apply some restrictions concerning the potential V given by equ. (2). If we neglect all the terms in Z_p^2 and a in equ. (2) as small in comparison with the term Z_p we see that

$$V(r) = -\gamma V_H(r) = (\gamma Z e^2/r)(Z_p/Z), \tag{18}$$

where γ is given by equ. (4). Substituting this potential into equ. (1) we obtain the radial SCHRÖDINGER wave equation modified by the factor γ. The simplified potential (18) allows us to calculate approximate values of the phase shifts η_l^0. Using the BORN approximation we obtain the following formula for the phase shifts in case of the potential (18):

$$\eta_l^0 = (\gamma Z/k a_0) \sum_n c_n Q_l \left(1 + \frac{1}{2}\left(\frac{b_n}{\mu k}\right)^2\right). \tag{19}$$

In this formula the Q_l are spherical harmonics of the second kind which may be calculated for the lowest l from explicit expressions and then from the recurrence formula and for the higher l from the asymptotic expansions. If we apply the W. K. B. method for the phase shift we obtain using the potential (18) for the phase shifts η_0^l the following formula:

$$\eta_l^0 = (\gamma Z/k a_0) \sum_n c_n K_0 \left(\frac{b_n}{\mu}\left(l + \frac{1}{2}\right) \middle/ k\right). \tag{20}$$

Formulas (19) and (20) are convenient for calculating η_l^0. The constants b_n and c_n appearing in these formulas can be found in case of HARTREE and THOMAS—FERMI fields in Table I of [12]. If we wish to obtain more accurate values for the phase shifts in case of the potential (18) we can apply the PAIS formula. In this case we must use the following expressions [8]:

$$\frac{2l + 1 - (2\eta_l^P/\pi)}{2l + 1 - (4\eta_l^P/\pi)} \eta_l^P = \frac{\pi m}{\hbar^2} \int_0^\infty V(r) J_{l+\frac{1}{2}}^2(kr)\, r\, dr, \tag{21}$$

where the potential $V(r)$ is given by formula (18). The PAIS formula for the phase shifts η_l^P in case of small phase shifts goes over into formula (19), i.e. into the BORN approximation. Formula (21) gives better values for the phase shifts but it requires more numerical calculations. It has been shown that the PAIS formula can be written in the following form [9]:

$$\eta_l^P = \eta_l^0 + \frac{2}{\pi}\left(a_l - \frac{\eta_l^0}{2l+1}\right)\eta_l^0, \quad \text{where} \quad a_l = -\left(\frac{\partial \eta_p^0}{\partial p}\right)_{p=l+\frac{1}{2}}. \tag{22}$$

In formula (22) η_l^0 is given by equ. (19) or (20). η_l^P as given by the last formula is more convenient for the calculation of the phase shifts than the original formula (21) given by PAIS. Now we can discuss the necessary correction to be added to these phases to allow for the effect of spin, i.e. for the use of the complete expression (2) for V. The phase shifts for the Coulomb field η_l^c and η_{-l-1}^c as it has been said, may be easily calculated from equs. (11) and (12). They differ by a small amount from the phases η_l^0 for a Coulomb field with neglect of spin. The difference is nearly the same as the corresponding difference for HARTREE or THOMAS—FERMI fields, the error being unimportant for small l, while for large l the difference is small in any case. The difference is added to the value of η_l^0 previously calculated, to give the required phases η_l and η_{-l-1} for the HARTREE or THOMAS—FERMI field with spin.

Conclusion

It has been shown that it is possible to calculate from the above theory the cross-section $I(\vartheta)$ for scattering per unit solid angle in the direction η of the beam of unpolarized electrons of rest mass m, velocity v, and charge e given by formula (6), and further it has been shown that the presented procedure gives the method for calculating the asymmetry in double scattering given by formula (10). The author of this paper has shown previously [10] that formulas (19) and (20) give sensible results in comparison with the numerical results. This paper gives a generalization of the scattering and polarization of electrons by atoms calculated by MOHR and TASSIE only for gold, since it allows to calculate the asymmetry in double scattering for any THOMAS—FERMI and some HARTREE atoms [11].

REFERENCES

1. N. F. MOTT and H. S. W. MASSEY, The Theory of Atomic Collisions, Oxford, Clarendon Press, 1949.
2. P. GOMBÁS, Die statistische Theorie des Atoms und ihre Anwendungen, Vienna, Springer-Verlag, 1949; Encyclopedia of Physics Vol. **36**, Springer-Verlag, Berlin—Göttingen—Heidelberg, 1956.

3. W. J. Byatt, Phys. Rev., **104**, 1298, 1956.
4. C. B. O. Mohr and L. J. Tassie, Proc. Phys. Soc., **A67**, 711, 1954.
5. See ref. [1].
6. See ref. [1].
7. A. E. Ruark, Phys. Rev., **57**, 62, 1940.
8. A. Pais, Proc. Camb. Phil. Soc., **42**, 45, 1946.
9. T. Tietz, Ann. d. Phys., **9**, 295, 1962.
10. T. Tietz, Il Nuovo Cim., **10**, 553, 1958.
11. T. Tiez, Acta Phys. Hung., **12**, 151, 1960.
12. T. Tietz, Acta Phys. Hung., **16**, 1, 1963.

РАССЕЯНИЕ И ПОЛЯРИЗАЦИЯ ЭЛЕКТРОНОВ АТОМАМИ ХАРТРИ И ТОМАСА—ФЕРМИ

Т. ТИТЦ

Р е з ю м е

Применяя аналитические формулы для эффективного заряда ядра, а также и для теории рассеяния потока частиц силовыми центрами в релятивистком случае, дискутируется ассиметрия в двойном рассеянии. Излагается теория, дающая возможность для определения ассиметрии в двойном рассеянии аналитическими методами без каких-либо трудностей. В статье обобщается работа Мора и Тасси.

TREATMENT OF THE H_2^+-ION BY MEANS OF ONE-, TWO- AND THREE-CENTER WAVE FUNCTIONS

By

I. TAMÁSSY-LENTEI and Á. BÁBA

INSTITUTE OF THEORETICAL PHYSICS, KOSSUTH LAJOS UNIVERSITY, DEBRECEN

(Presented by A. Kónya. — Received 28. IX. 1962)

The ground state energy of H_2^+ is calculated with one- and multi-center wave functions by means of the variational method. By using hydrogen-like one-center wave functions a bound state is found even with $1s$ function if it is centered near one of the nuclei. Results can be improved by taking the linear combination of two or three of the one-center wave functions of the type $1s$, $2s$, $2p_z$, $3d_z$. By varying the position of the center we get the best results when the center is either located in one of the nuclei or in the middle point between the nuclei. A better approximation can be obtained with the two-center linear combination of $1s$ type wave functions centered on the two nuclei. The results can be essentially improved with the three-center wave function which is a linear combination of $1s$ wave functions centered on the two nuclei and on the middle point. In this case the energy and the internuclear distance are $E = -0.5972\ e^2/a_0$ and $R = 2a_0$, respectively, corresponding to the exact values $-0.60263\ e^2/a_0$ and $2\ a_0$.

Properties of molecules cannot be calculated exactly in quantum chemistry because of mathematical difficulties, but can be determined only approximately.

When deciding between different approximations one should always bear in mind two things: first, the necessary calculations should not be oversized; secondly, the results should possibly give good agreement with the experiment. In actual cases one must find the right middle-way between these two contrary points of view.

In what follows we shall investigate, in the case of the one-electron H_2^+-ion, in what measure the results depend on the fact whether one- or more-center wave functions are used in the calculations.

I. Previously numerous calculations have been done with one-center wave functions in the case of several molecules, among others for H_2^+ [1]. The Hamiltonian* of H_2^+, as is well known, is

$$H = -\frac{1}{2}\Delta - \frac{1}{r_a} - \frac{1}{r_b} + \frac{1}{R}, \tag{1}$$

where a and b denote the positions of the protons. For the notations we refer to the Figure.

* In the following we use atomic units.

In central approximation the actual form of the wave function and the position of the centrum is essential. We consider in the following the widely used hydrogenlike functions defined by

$$\psi_{nlm} = R_{nl}(r)\, Y_{lm}(\vartheta, \varphi)\,, \tag{2}$$

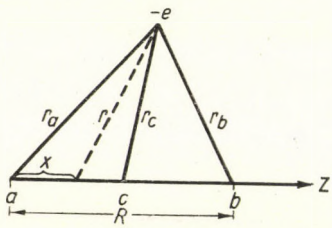

Fig. 1

where R_{nl} is the normalized radial wave function, which can be expressed in terms of the $(2\,l+1)$th derivative of the $(n+l)$th Laguerre polynomial as follows:

$$R_{nl}(r) = -\left\{\frac{(n-l-1)!}{[(n+l)!]^3\, 2n}\right\}^{1/2} \left(\frac{2Z}{na_0}\right)^{3/2} e^{-\frac{\varrho}{2}} \varrho^l L_{n+l}^{2l+1}(\varrho)\,, \tag{3}$$

with $\varrho = \dfrac{2Zr}{na_0}$.

The spherical harmonic $Y_{lm}(\vartheta_1\varphi)$ — the normalized angular wave function — is expressed in terms of the associated Legendre polynomial as follows:

$$Y_{lm}(\vartheta, \varphi) = \sqrt{\frac{2\,l+1}{4\pi}\,\frac{(l-|m|)!}{(l+|m|)!}}\; P_l^{|m|}(\cos\vartheta)\, e^{im\varphi}\,. \tag{4}$$

The ground state of hydrogen-like problems is obtained by putting $n=1$, $l=m=0$. The wave function is in this case spherically symmetrical:

$$\psi_{1s} = \left(\frac{Z_{1s}^3}{\pi}\right)^{1/2} e^{-Z_{1s}r}\,. \tag{5}$$

In the hydrogen-like case Z_{1s} obviously denotes the nuclear charge.

If, for the treatment of H_2^+, we choose (5) as a trial function then it is convenient to regard Z_{1s} as a variational parameter and to determine it from the variational requirement that the energy

$$E = \int \psi^* H \psi\, dv \tag{6}$$

should be a minimum for the system. In the calculation of the energy only simple one- or two-center integrals are involved which can be treated, for example in elliptical coordinates, quite easily.

The question arises where to put the centre of the wave function of the type (5). One possibility is the middle point $\left(x = \frac{R}{2}\right)$ between the two nuclei. In this case there is no binding even if both Z_{1s} and R are varied simultaneously, as it can be seen from Table I. We get a little better result if we take for center one of the nuclei ($x = 0$ or $x = R$). Nevertheless, there is no binding in this case either.

Table I

Energy values calculated with function (5) for the experimental internuclear distance ($R = 2$), after variation of R for wave functions centered on the nucleus ($x = 0$), on the middle point $\left(x = \frac{R}{2}\right)$ and for the position of the center which gives the lowest energy. Results are given in atomic units with the best variational parameter values. The corresponding exact values are: $E = -0.60263$, $R = 2$ [6].

R	2			∞	3.1	1.8
x	0	0.2	$R/2 = 1$	0	0.1	$R/2 = 0.9$
E	—0.475356	—0.491132	—0.466864	—0.5	—0.501408	—0.470369
Z_{1s}	1.1	1	0.9	1	1	0.95

The best result is obtained by varying Z_{1s}, R and x simultaneously. In this way we get stable molecules, with center of the wave function near the nucleus ($x = 0.1$) though the binding is extremely weak. That the center is not in the middle point in the case of the best energy, as it is to be expected from symmetry reasons, is obviously due to the fact that, though the attraction of the proton, which is farther away, exercised on the electron is very small, the interaction with the other proton will be so strong that this results in a larger interaction energy than that resulting from the equal attraction of the two protons in the middle-centered case.

This is also understandable if we take into account the fact that the electron density is large in between and near the two protons. The function ψ_{1s} centered on the middle point between the protons makes the density large in this region, but does not do so in the proximity of the protons. The importance of the value of the density in the neighbourhood of the nuclei can be seen from the fact that if the wave function is such that it is large in the neighbourhood of one of the nuclei but small at the other nucleus (for $x = 0.1$), we can explain binding, while in the case $x = \frac{R}{2}$ we cannot.

A better value for the energy can be obtained if we take the linear combination of hydrogen-like wave functions as it has been done in [1]. Let us, besides (5), consider the further hydrogen-like functions

$$\psi_{2s} = \left[\frac{3Z_{2s}}{\pi(Z_{1s}^2 - Z_{1s}Z_{2s} + Z_{2s}^2)}\right]^{1/2}\left[1 - \frac{Z_{1s}+Z_{2s}}{3}\,r\right]e^{-Z_{2s}r},$$

$$\psi_{2p_z} = \left[\frac{Z_{2p_z}^5}{32\pi}\right]^{1/2} r e^{-\frac{Z_{2pz}r}{2}} \cdot \cos\vartheta\,, \tag{7}$$

$$\psi_{3d_z} = \frac{1}{81}\left[\frac{Z_{3d_z}^7}{6\pi}\right]^{1/2} r^2 e^{-\frac{Z_{3dz}r}{3}}(3\cos^2\vartheta - 1),$$

(in case of ψ_{2s} we used the Fock—Petrashen form orthogonal to ψ_{1s}) and take the wave function in the form

$$\psi = \sum_i c_i \psi_i \qquad (i = 1s, 2s, 2p_z, 3d_z). \tag{8}$$

Here let us take into account in the sum, besides ψ_{1s}, one or two of the functions enumerated.

The integrals appearing in the evaluation of (6) are all well-known one- and two-center integrals. The energy is obtained from the usual secular equation

$$\| H_{ik} - ES_{ik} \| = 0\,, \tag{9}$$

where

$$H_{ik} = \int \psi_i^* H \psi_k \, dv \quad \text{and} \quad S_{ik} = \int \psi_i^* \psi_k \, dv\,.$$

The results obtained from the independent variation of the parameters Z_i, R and x are found in Table II. Now the different wave functions give the best result when centered either on one proton or on the middle point. In between, we would have at the most a small relative minimum. Deviation from this was found only in the case of the function ψ_{1s}.

The best result is obtained from the linear combination of ψ_{1s}, ψ_{2s} and ψ_{3d_z} by putting the center in the middle point. (Here for symmetry reasons the function ψ_{2p_z} does not combine with the other functions.) Although with the correct choice of the center, in a one-center system, we can obtain a stable molecule even with the ground state wave function ψ_{1s}, it is obvious that the wave functions ψ_{2s} and ψ_{3d_z} play an important role in obtaining the correct wave function and contribute essentially to the lowering of the energy of the molecule. This is obviously connected with the fact that although the linear combination of ψ_{1s}, ψ_{2s} and ψ_{3d_z} in the case $x = \frac{R}{2}$ makes the density large between the protons, it increases, at the same time because of its

Table II

Energy values calculated with functions of type (8) for the experimental internuclear distance ($R = 2$), after variation of R for wave functions centered on the nucleus ($x = 0$), on the middle point $\left(x = \frac{R}{2}\right)$. Results are given in atomic units with the best variational parameter values

$\psi = \sum_i c_i \psi_i$	x	0	$R/2 = 1$	0	$R/2$
$i = 1s, 2s$	R	2		∞	1.8
	E	—0.47747	—0.515983	—0.5	—0.520526
	Z_{1s}	1	1.4	1	1.4
	Z_{2s}	0.8	1.6	arbitrary	1.7
$1s, 2p_z$	R	2		2.3	see $1s$
	E	—0.519592	see $1s$	—0.522577	
	Z_{1s}	1		1	
	Z_{2p}	2.3		2.1	
$1s, 3d_z$	R	2		3.6	2
	E	—0.483021	—0.518411	—0.500898	—0.518411
	Z_{1s}	1.1	0.9	1	0.9
	Z_{3d}	1.4	6.4	3.1	6.4
$1s, 2p_z, 3d_z$	R	2		2.1	see $1s, 3d_z$
	E	—0.54223	see $1s, 3d_z$	—0.5424	
	Z_{1s}	1		1	
	Z_{2p}	2.2		2.2	
	Z_{3d}	4.3	see $1s, 3d_z$	4.3	see $1s, 3d_z$
$1s, 2s, 3d_z$	R	2		3.6	1.9
	E	—0.48547	—0.56919	—0.500057	—0.57040
	Z_{1s}	0.9	1.1	0.9	1.1
	Z_{2s}	0.8	2.2	0.8	2.2
	Z_{3d}	4.4	6.6	4.4	6.6

form, the density also in the proximity of the protons in comparison with the value obtained with ψ_{1s}.

By taking the linear combination of more wave functions results can be improved, as it can be seen from (1), but the convergence is very slow.

Thus in the case of one-center functions the nuclei and the middle point have a special significance: the best results are obtained if the functions are centered on these points. It can now be seen that the position of the center is very important.

II. In the case of molecules it is quite natural that one uses wave functions centered on the nuclei, in particular two-center functions for diatomic molecules. For H_2^+ such a function is

$$\psi = c_a \psi_a + c_b \psi_b , \tag{10}$$

where

$$\psi_i = \left(\frac{\lambda_i^3}{\pi}\right)^{1/2} e^{-\lambda_i r_i}, \qquad (i = a, b) .$$

Essentially the same molecular orbital has already been used by FINKELSTEIN and HOROWITZ [2]. Into these calculations also only one- and two-center integrals enter and the energy can be obtained from the corresponding secular equation.

From the simultaneous variation of λ_i and R we get

$$\lambda_a = \lambda_b = 1.24 , \quad E = -0.586505 , \quad R = 2 .$$

As it is expected ψ_a and ψ_b take part in the binding with equal weight. (The case $\lambda_a \neq \lambda_b$, or the variation of R would give a change only in the fourth decimal.)

Hence, even with the simplest hydrogen-like two-center wave function ψ_{1s}, centered on nuclei, one can obtain reasonably good results. Nevertheless, in this case the electron density is not sufficiently large between the nuclei and, moreover, it is too high in the neighbourhood of the protons.

A better result can be obtained if also the wave function centered on the nuclei is considered to be a linear combination of hydrogen-like wave functions. So with a function of type

$$\psi = N [\psi_{1s_a} + k \psi_{2p_{za}} + \psi_{1s_b} + k \psi_{2p_{zb}}]$$

we obtain for the energy as a result of the variational process

$$E = -0.60035$$

for the values $Z_{1s} = 1.25$, $Z_{2p_z} = 3$ and $R = 2$ $(k = 0{,}13643)$.*

* These values are recalculation of the results of B. N. DICKINSON (J. Chem. Phys., 1, 317, 1933)

III. In the cases that have been considered the best results have been obtained with the wave functions centered on the nuclei. Since with these wave functions the interproton densities are not sufficiently large, it is natural to try to improve results by adding to (10) a wave function which is centered on the middle point.

To do this consider

$$\psi = A(\psi_a + \psi_b) + B\psi_c, \tag{11}$$

a three-center function, where

$$\psi_i = \left(\frac{\lambda_i^3}{\pi}\right)^{1/2} e^{-\lambda_i r_i} \qquad (i = a, b, c)$$

and the origin of r_c is in the middle point of the straight line connecting the protons.

The only three-center integral appearing in the energy (6) is of the type

$$\int \frac{\psi_a \psi_c}{r_b} dv. \tag{12}$$

The exact form of this, for $\lambda_a = \lambda_c$, can be found for example in PREUSS [3].** The results of the variation are

$$\lambda_a = \lambda_b = \lambda_c = 1.28, \qquad E = -0.597201, \qquad R = 2.$$

Hence, exactly the experimental value is obtained for the internuclear distance: moreover the energy is also greatly improved.

The three-center integral (12) cannot be evaluated exactly for $\lambda_a \neq \lambda_c$, but can be estimated to a high degree of accuracy (to within 0.5%) with the aid of the ČIŽEK [4] approximation formula. The integrals

$$A_k\left(1, \frac{R}{2}\frac{\lambda_c + \lambda_a}{2}\right) = \int_1^\infty \xi^k e^{-\frac{R}{2}\cdot\frac{\lambda_c+\lambda_a}{2}\xi} d\xi$$

and

$$B_l\left(\frac{R}{2}\frac{\lambda_c - \lambda_a}{2}\right) = \int_{-1}^1 \xi^l e^{-\frac{R}{2}\cdot\frac{\lambda_c-\lambda_a}{2}\xi} d\xi$$

** On page 25 of the quoted work the factor $\bar{a}$, in the first term of formula (3.22), is superfluous, as can be checked on hand of the original paper of G. S. GORDADSE (Zs. f. Phys., **96**, 542, 1935).

entering the formula are tabulated for instance in MILLER—GERHAUSER—MATSEN [5]. For the experimental internuclear distance $R = 2$, A_k and B_l are given for those values of λ_a and λ_c which are simultaneously even or odd multiples of 0.125. In such units the energy minimum is obtained for the values $\lambda_a = \lambda_b = \lambda_c = 1.25$ which, of course, approximates less satisfactorily the exact value than that obtained for $\lambda_a = \lambda_b = \lambda_c = 1.28$. Only a very little improvement can be obtained, if in (11) ψ_a and ψ_b are not centered on the nuclei. The result is $E = -0.598389$, if $x = 0.04$, $\lambda_a = \lambda_b = \lambda_c = 1.27$ and $R = 2$.

It seems from the above considerations that the number of centers of the wave function is important, since this strongly influences the values obtained for the energy. — Similar treatment has been proposed for molecular calculations by PARR [7].

We should like to express our gratitude to J. ČIŽEK for making available his results before publication and for helping us in the evaluation of the integrals.

LITERATURE

1. R. GÁSPÁR, Acta Phys. Hung., **7**, 151, 1957.
2. B. N. FINKELSTEIN and G. E. HOROWITZ, Zs. f. Phys., **48**, 118, 1928.
3. H. PREUSS, Integraltafeln zur Quantenchemie, Vierter Band, Springer Verlag, Berlin, 1960.
4. J. ČIŽEK, Mol. Phys., **6**, 19, 1962.
5. J. MILLER, J. M. GERHAUSER and F. A. MATSEN, Quantum Chemistry Integrals and Tables University of Texas, Austin, 1959.
6. D. R. BATES, K. LEDSHAM and A. L. STEWART, Phil. Trans. Roy. Soc. (London), A **246**, 215, 1953.
7. R. G. PARR, J. Chem. Phys., **26**, 428, 1957.

ИССЛЕДОВАНИЕ ОСНОВНОГО СОСТОЯНИЯ ИОННОЙ МОЛЕКУЛЫ H_2^+ ОДНО-, ДВУХ- И ТРЁХЦЕНТРОВЫМИ ВОЛНОВЫМИ ФУНКЦИЯМИ

И. ТАМАШИ-ЛЕНТЕИ и А. БАБА

Резюме

Для определения энергии основного состояния H_2^+ проводились вычисления одно- и многоцентровыми волновыми функциями с помощью вариационного метода. Применяя водородоподобные одноцентровые волновые функции, для энергии связи довольно хорошее значение получается даже в случае единственной функции типа $1s$, центрированной очень близко к одному из протонов. Результаты значительно улучшаются, если взять линейные комбинации двух или трёх одноцентровых функций типа $1s$, $2s$, $2p_z$ и $3d_z$; при вариации центра наилучшее значение получается в случае центрирования на одно из ядер и на центр. Линейной комбинацией двухцентровых волновых функций типа $1s$, центрированных на два ядра, можно добиться лучшего приближения. Значительное улучшение добивается трёхцентровой волновой функцией, полученной в случае линейной комбинации функций типа $1s$, и центрированной на два ядра и на центр. В данном случае для энергии получено $E = -0{,}5972\ e^2/a_0$, для расстояния между ядрами $R = 2a_0$; точные значения $-0{,}60263\ e^2/a_0$ и $2a_0$ соответственно.

RADIOMETRIC IDENTIFICATION OF FISSION PRODUCT FRACTIONS NOT SORBED BY HUMIC ACIDS

By

MÁRIA SZILÁGYI

INSTITUTE OF NUCLEAR RESEARCH OF THE HUNGARIAN ACADEMY OF SCIENCES (ATOMKI), DEBRECEN

(Presented by A. Szalay. — Received 1. X. 1962)

Although humic acids bind the greater part of U-fission products, it had been found that there exist some fission products that are not fixed on humic preparations (e.g. Nb—95, J—131). In the course of our present investigations we have identified some further fission products that are not sorbed in our testing conditions (Ru—103, Te—127^m, Se—79, Sb—125). Their identification was carried out by means of radiometric methods.

Introduction

In an earlier paper [1] we have explained that nowadays there exists a very great chance that living matter may be polluted by fission products. This may happen partly through fission products spreading at the time of experimental atomic explosions, partly through the fission products contained in the industrial waste of atomic plants.

In the course of their investigations SZALAY and his collaborators [1—3] have proved that humus substances occurring in nature in large quantities are exceptionally suitable for the binding of fission products. This property of humic substances has first been investigated, using inactive substances, by means of chemical analytical procedure, and than using radioactive isotopes by applying the tracer method [2, 3]. In order to extend our knowledge to the sorption properties of the possible largest number of fission products, we have conducted investigations with a composite of fission products [1]. The results obtained in that series of experiments have been summarized in Table I. In this Table only those fission products are shown the fission yield of which reaches at least one per mille and the half-period of which is longer than one month. Our classification shows that of a large group of fission products (first column) it has been possible to establish without any doubt that they get bound by humic preparations. There are references in the literature concerning the adsorption of fission products on humic preparations [4], but as to the question whether there exist fission products that will not be bound by humic substances — and if so which they are — we have found no information. It appeared from our experiments that there do exist such isotopes (Table I, middle column) and that the adsorption properties found

Table I

Grouping according to sorption properties of fission products with a longer half-period than 30 days (on account of its properties, J—131 belongs to the place marked, but because of its short half-period it is put in parentheses (Acta Phys. Hung., XIII/4, 1961)

Firmly fixed by humic acids	Not fixed	Not investigated
Sr—89	J—129	Rb—87
Sr—90	(J—131)	Ru—103
Y—91	Nb—95	Ru—106
Zn—93	Kr—85	Cd—115^m
Cs—135		Sn—123
Cs—137		Te—127^m
Ce—141		Te—129^m
Ce—144		Tc—99
Nd—144		Se—79
Pm—147		Pd—107
Sm—147		Sn—121^m
Sm—151		Sb—125
Eu—155		Te—125

so far cannot be generalized for all fission products. Therefore, the isotopes shown in column 3 of Table I will be investigated in detail in this paper in order to get information on their adsorption properties and to include them in the appropriate column (1 or 2) of Table I.

The fission products needed for the examinations were obtained by irradiating U_3O_8 in a reactor. The bulk of the fission products could be separated from uranium through the ether-nitric acid solvent extraction method [1]. Since the sorption properties of fission products separated from uranium had been dealt with before, we here investigate the sorption properties of fission products that do not separate from uranium during ether-nitric acid solvent extraction, thus further enlarging Table I.

The investigations have been carried through by making a column of the humic preparation — applying the method well-known from the technique of ion exchangers — and by pouring on this column a drop of uranyl nitrate ($1n$) solution that contained the smaller quantity of fission products after the etheric extraction [1]. According to our hypothesis the humic preparation was to bind the uranyl ion, and of the fission products those present in cation form in the given experimental conditions. On the other hand, those of anion form could be eluted of the column by means of a p_H — 5 HCl solution.

In the following we shall report on the method by which it was possible to identify the isotopes in the eluate fractions.

Experiments

1. Ru—103. The eluate fraction was evaporated and its γ-spectrum was investigated. The spectra are shown in Fig. 1. For the sake of comparison, the following three γ-spectra are shown together:

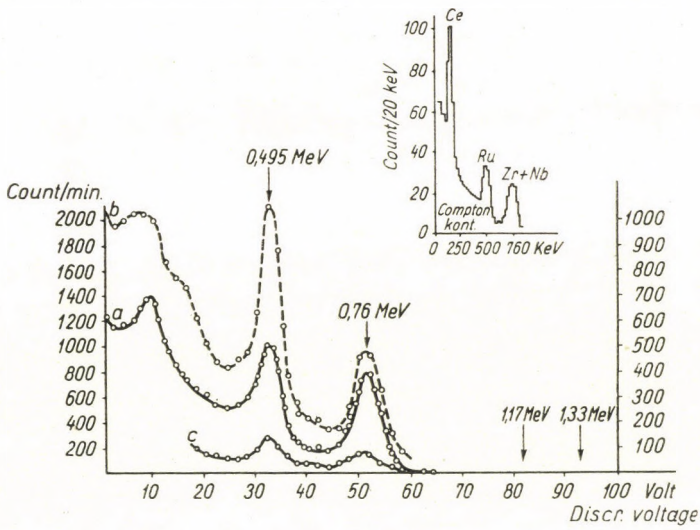

Fig. 1. "a": the γ-spectrum of the uranyl nitrate solution after the etheric extraction of irradiated U_3O_8. It contains some residual fission products. "b": the γ-spectrum ($p_H \sim 5$) of the first eluate fraction gained after this had flown through a humus column of this uranyl nitrate. "c": the γ-spectrum of the same preparation as that used for curve "b", but after a period of 10 months. In the upper right corner of the Figure in a smaller scale the curve of K. LIEBSCHER [5] has been reproduced which was used for comparison when evaluating our measurements

The curve marked "a" was obtained by photographing the γ-spectrum of the uranyl nitrate solution prior to sorbing on humus. Two characteristic lines are very well visible in the spectrum at 0.76 and 0.495 MeV.

The curve marked "b" was obtained by the γ-spectrometric measuring of the eluate fraction prepared with the $p_H \sim$ 5 HCl solution. It is seen from the spectrum that the intensity ratio of the 0.76 and 0.495 MeV lines has changed after sorption because the intensity of the 0.76 MeV-energy radiation decreased.

The curve marked "c" was obtained in the following way: the preparation producing curve "b" was left untouched for 10 months, then its γ-spectrum was taken in measuring conditions identical with the previous ones. It can be seen that both characteristic lines have almost entirely disappeared.

For the evaluation and systematization of these results we have found K. LIEBSCHER's [5] and his collaborators' work very helpful. In 1958 and 1959 they investigated the fission product content of natural waters in and

around Vienna. The measurements were carried out by evaporating the samples of water and by identifying the components of its activity γ-spectrometrically. In the right upper corner of Fig. 1 a curve obtained by them is also shown for the sake of comparison. This γ-spectrum is very similar, almost identical with our measurements mentioned above. We also ascribe the 0.495 MeV-energy spectral line to the presence of isotope Ru—103, as we had already identified the isotopes Zr, Nb and Ce in a previous investigation [1].

Thus the sorption experiment may be evaluated as follows:

The uranyl nitrate stock solution used contains uranium and its short-life decay products (U_{x1}, U_{x2}) which are in balance with it: in addition of the fission products it contains the entire quantity of Ru—103. (Fig. 1, curve "a"). Passing through a humus column, the uranyl ion together with its

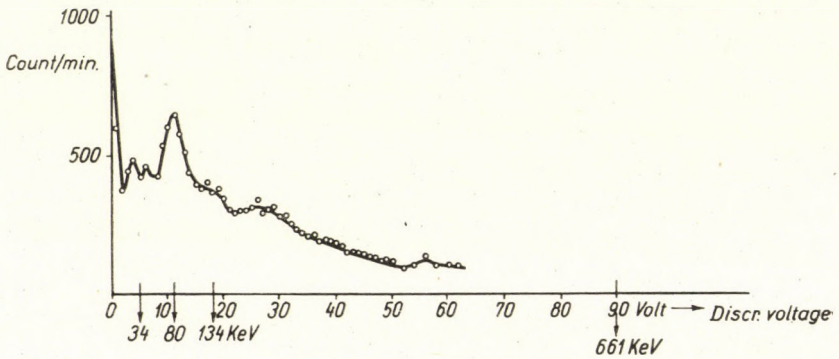

Fig. 2. A more detailed investigation in the low γ-energy ranges of the spectra shown in Fig. 1. The calibrating energies are marked on the abscissa at the appropriate points

radioactive daughter products, as well as the isotope Zr—95 is bound by the humic preparation. Ru—103 and Nb—95, the daughter element of Zr—95, will not be bound, but collect in the receiver (Fig. 1, curve "b"). If the spectrum of the preparation is photographed again after 10 months, in accordance with the half-periods the disappearance of the two characteristic lines (Fig. 1, curve "c") may be observed. Ru—103 will decay into isotope Rh—103 with a half-period of $T = 39.8$ days; Rh—103 will, through isomeric transmutation and emitting 40 KeV-energy γ-radiation, transmute into the stable isotope Rh—103 with a half-period of 57 minutes. We should like to mention that the isotope Rh—103 is always present in preparations that contain Ru—103, but we do not discuss its sorption on humic acids and its γ-spectrum here.

2. Te—127^m. In the following we have carried out a more detailed investigation into those parts of the spectra in Fig. 1 which appear at low γ-energies. The results are shown in Fig. 2.

This spectrum shows a dominating photopeak of small intensity at 88 KeV. Considering that the presence of an isotope with a longer half-period has to be reckoned with, we have taken as the other parameter the energy of the β-radiation rather than the half-period. For this purpose we have first placed the preparation in a solution, then gained through paper electrophoresis [6] the isotope that emits the above-mentioned 88 KeV-energy γ-radiation; then the β-absorption in aluminium of this preparation, containing by now but a single isotope, was determined. The results of the measurements are shown in Fig. 3. According to the Figure, the half layer thickness is 220 mg/cm^2, which

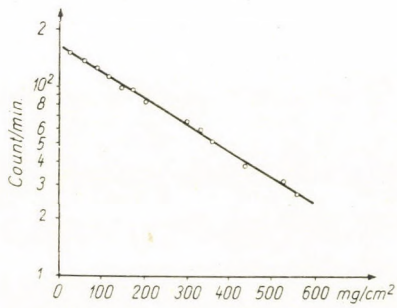

Fig. 3. The β-absorption curve in Al of the preparate identified as isotope Te—127^m

corresponds to a β-radiation of about 0.7 MeV energy. There is no isotope among the fission products that emits 88 KeV γ- and 0.7 MeV β-radiation. Looking, however, at the following decay relation the results of measurements will become understandable.

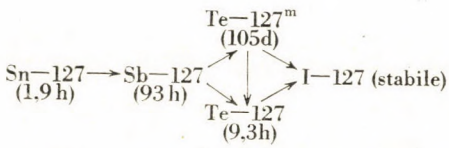

Taking into account the half-periods shown here, it is evident that the γ-line of 88 KeV energy belongs to the isotope Te—127^m, and the β-radiation of 0.7 MeV energy to isotope Te—127, considering the fact that the experiments were begun 6 months after the neutron activation of U_3O_8.

3. Se—79. In the course of the paper-electrophoretic investigation mentioned above, we found at the side of the band extending towards the anode an activity maximum which showed a 0.16 MeV energy β-radiation only and which was not accompanied by γ-radiation. Following this we measured the intensity of the preparation by means of a GM-tube counter

for nearly a year, but were not able to prove any notable decrease in activity. Summing up these findings, it may be stated that here is an isotope behaving as an anion in electrophoretic conditions, as well as showing an anionic character in relation to humic preparations, emitting no γ-radiation, but very soft 0.16 MeV β-particles only, having a very long life and being present in the fission product composite in very small quantities only. Although no Se—79 will directly be produced in fissions, its mother element As—79 will be produced with a maximum yield ($5.6 \cdot 10^{-2}\%$) in the course of the 4 hour activation of the U_3O_8 in the reactor:

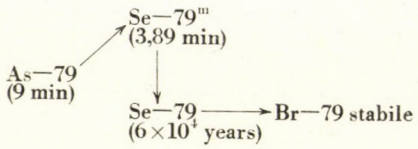

Evaluating the transmutation scheme shown here it appears that after the cessation of the irradiation in the reactor As—79 will transmute into isotope Se—79 in 1 to 2 hours. Thus at the time (chosen by us) of the investigation it was possible to identify isotope Se—79 only.

4. Sb—125 *and* Rb—87. The sorption properties of these isotopes were determined through the application of pure isotope preparations because their quantity was too small to separate these isotopes from the above-mentioned complete fission product composite. For tracer investigations preparations of the isotopes Sb—124 and Rb—86 were used. We have found that in the conditions of our experiments the isotope Sb showed an anionic character and the isotope Rb a cationic one.

Evaluation

These investigations show that there are a number of isotopes among fission products that will not bind on humic preparations (at $p_H \sim 5$), and that belong, as regards their chemical character, to the group of amphoteric elements or to those of a decidedly negative (anionic) character. Table II illustrates the new information gained by the investigations detailed here of the sorption properties of fission products with respect to humic preparations. This Table II shows the isotopes appearing in Table I, but in a different arrangement. Considering the fact that the different isotopes of any chemical element behave in the same way with respect to humic preparations, we have, according to the results of the investigation of the sorption properties of isotope Ru—103, transferred Ru—106 also to the middle column of this Table, etc.

Table II

This Table shows fission products with a half-period longer than 30 days (with a fission yield $> 1‰$) grouped in accordance with our latest investigations

Well fixed	Not fixed	Under investigation
Sr—89	J—129	Cd—115^m
Sr—90	J—131	Sn—123
Y—91	Nb—95	Tc—99
Zr—93	Kr—85	Pd—107
Cs—135	Se—79	Sn—121^m
Cs—137	Ru—103	
Ce—141	Ru—106	
Ce—144	Te—127^m	
Nd—144	Te—129^m	
Pm—147	Sb—125	
Sm—147	Te—125	
Sm—151		
Eu—155		
Rb—87		

Finally I should like to express my gratitude to Prof. A. SZALAY, Director of the Institute of Nuclear Research of the Hungarian Academy of Sciences, for his interest in my work, and to all my colleagues who have extended help in my experimental work.

REFERENCES

1. A. SZALAY and M. SZILÁGYI, Acta Phys. Hung., **13**, 421, 1961.
2. I. SZABÓ, MTA Mat. Fiz. Oszt. Közl., **8**, 393, 1958.
3. S. SZALAY and M. SZILÁGYI, MTA Mat. Fiz. Oszt. Közl., **11**, 47, 1961.
4. R. WINKLER and E. LEIBNITZ, Kernenergie, **3**, 992, 1960.
5. K. LIEBSCHER, F. HABASHI and I. SCHÖNFELD, Atompraxis, **7**, 1, 1961.
6. M. SZILÁGYI, Dissertation for the degree of Dr. Faculty of Sciences, Kossuth Lajos University, Debrecen.

РАДИОМЕТРИЧЕСКАЯ ИДЕНТИФИКАЦИЯ ПРОДУКТОВ ДЕЛЕНИЯ УРАНА НЕ АБСОРБИРОВАННЫХ ГУМИНОВЫМИ КИСЛОТАМИ

М. СИЛАДЬИ

Р е з ю м е

Как раньше было установлено нами, некоторые продукты деления (Nb—95, J—131) не связываются на гумусовом препарате. В ходе настоящих исследований идентифицировались дальнейшие продукты деления, не показывающие сорбционные свойства при наших условиях опыта (Ru—103, Te—127^m, Se—79, Sb—125). Идентификация производилась радиометрическим методом.

TRANSIENT LIFETIME IN CASE OF RECOMBINATION THROUGH EXCITED STATES IN NON-DEGENERATED SEMICONDUCTORS

By

G. PATAKI

RESEARCH INSTITUTE FOR TECHNICAL PHYSICS OF THE HUNGARIAN ACADEMY OF SCIENCES, BUDAPEST

(Presented by G. Szigeti. — Received 10. XII. 1962)

The present paper deals with the model of recombination given by A. V. RZHANOV [3], near equilibrium, in the transient case. From the approximative roots of the characteristic equation, τ_r renders the stationary lifetime given in [3] for an arbitrary concentration of recombination centres, while the second root τ_t gives the generalization of the transient lifetime in the SHOCKLEY-READ model for the recombination through excited states.

As it is well known, in the SHOCKLEY—READ [1] and R. N. HALL [2] theory of the recombination it is an essential assumption that the electrons or holes remain in the recombination centres only for a negligibly short time. A generalization of the model S—R, where the recombination takes place through excited states was given in A. V. RZHANOV's paper [3], thus the trapping time can be essential in the lifetime determination. Generalization in this respect is of special importance as M. LAX [4] was successful in giving the correct orders of magnitude of the capture cross-sections supposing the cascade process to take place through the excited states. Studying the existence of the excited levels, lately BONTCH—BRUEVITCH and GLASKO [5] referred to the fact that it is not impossible to capture the electron through one level, provided the maximum phonon energy is sufficiently great relative to the binding energy of the excited level. The "simple cascade" model, examined in [3] considers two excited states (one for the electrons, one for the holes) and gives a corrected form of the lifetime at a small concentration N_t of the recombination centres, for a steady state. Fig. 1 shows the levels and the possible transitions supposed by this model.

The present paper deals with the examination of this model in the transient case. We write down the approximative expression of the two first lifetimes in case of small excitation and at an arbitrary concentration N_t of centres. From these the first one, τ_r, gives the stationary lifetime, described by RZHANOV for a small N_t; while the second root, τ_t, of the characteristic equation is the generalization of the transient lifetime for the above model, which was determined in the papers of D. J. SANDIFORD [6], G. K. WERTHEIM [7] and G. PATAKI [8].

On the basis of [3] the time dependence of the recombination can be described as follows:

$$\frac{dn}{dt} = -C_n\left[(N_t - N_t^{**} - p + n)\,n - n_0\frac{N_{t0}^*}{n_{t0}^*}n_t^*\right],$$

$$\frac{dp}{dt} = -C_p\left[(p - n - n_t^*)\,p - p_0\frac{n_{t0}}{N_{t0}^{**}}N_t^{**}\right],$$

$$\frac{dn_t^*}{dt} = C_n\left[(N_t - N^{**} - p + n)\,n - n_0\frac{N_{t0}^*}{n_{t0}^*}n_t^*\right] - \tag{1}$$

$$- r_n\left[n_t^* - \frac{n_{t0}^*}{n_{t0}}(p - n - n_t^*)\right],$$

$$\frac{dN_t^{**}}{dt} = C_p\left[(p - n - n_t^*)\,p - p_0\frac{n_{t0}}{N_{t0}^{**}}N_t^{**}\right] -$$

$$- r_p\left[N_t^{**} - \frac{N_{t0}^{**}}{N_{t0}^*}(N_t - N_t^{**} - p + n)\right],$$

where — besides the usual notation — the concentrations correspond to the following states of the recombination centres:

n_t electrons in the ground state,
n_t^* electrons in the excited E_t^* state,
N_t^* the ground state is not filled,
N_t^{**} hole in the excited E_t^{**} state and
C_n, C_p the parameters of transitions from the conduction or valence band to the excited states,
r_n, r_p the parameters of transitions from the excited states to the ground state (see Fig. 1).

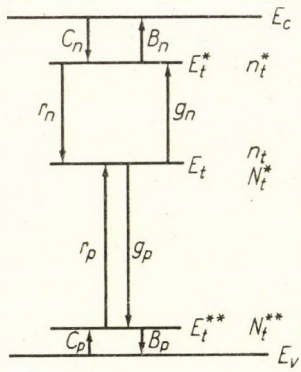

Fig. 1. Model of recombination through excited states (after RZHANOV)

Index zero indicates the equilibrium values. In writing down the above equations the following two conditions were taken into consideration:

$$n_t + n_t^* + N_t^* + N_t^{**} = N_t\,, \tag{2}$$

$$n_t + n_t^* + n = p\,, \tag{3}$$

of which the meaning of the first one is obvious, equ. (3) expresses the condition of electrical neutrality. For the sake of definiteness the charge condition of the recombination centres was taken as neutral.[1]

For the case of equilibrium the electron distribution over the different excited states and charge conditions was given in thepaper of W. SHOCKLEY and J.T. LAST [9], as well as P.T. LANDSBERG [10], while the values concerning the above model are given in paper [3], equ. (3). The equs. (1) represent a system of non-linear differential equations for the concentrations to be determined. After linearization the system of equations can be expressed in matrix form in the following way:

$$\dot{\alpha} + A\alpha = 0\,, \tag{4}$$

where the elements of the column-vector α are: δn, δp, δn_t^*, δN_t^{**} and the matrix A (after some manipulation) is:

$$\begin{vmatrix} \alpha' A_n & -A_n & -A_n \dfrac{n_1^*}{n_0} & -A_n \\ \beta' A_p & A_p(1+\beta') & -A_p & -A_p \dfrac{p_1^{**}}{p_0} \\ -\alpha' A_n & \left[A_n - r_n \dfrac{n_1}{n_1^*}\right] & \left[A_n \dfrac{n_1^*}{n_0} + r_n\left(1+\dfrac{n_1}{n_1^*}\right)\right] & A_n \\ -\beta' A_p & -\left[A_p(1+\beta') - r_p \dfrac{p_1}{p^{**}}\right] & A_p & \left[A_p \dfrac{p_1^{**}}{p_0} + r_p\left(1+\dfrac{p_1}{p_1^{**}}\right)\right] \end{vmatrix}. \tag{5}$$

[1] More generally, in case the number of charges at a lower charge condition is s and at an upper charge condition $s+1$ (e.g. $s>0$ is equivalent to the negative and $s<0$ to the positive charge) the condition of neutrality becomes

$$(s+1)(n_t + n_t^*) + s(N_t^* + N_t^{**}) + n = p\,,$$

which can, on the basis of (2), be brought into the form

$$sN_t + n_t + n_t^* + n = p\,.$$

As sN_t is constant, the cases $s=0$ and $s \neq 0$ lead to the same condition of neutrality for the quantities δn, δp, δn_t, δn_t^*, i.e. even if recombination takes place through different charge states (and accordingly if different mechanisms are possible) the lifetimes are given by similar phenomenological relations.

The following notations were introduced:

$$\begin{aligned} A_n &= C_n n_0 ; \qquad A_p = C_p p_0 , \\ \alpha' &= \frac{N_{t0}^*}{n_0} ; \qquad \beta' = \frac{n_{t0}}{p_0} , \\ n_1^* &= n_0 \frac{N_{t0}^*}{n_{t0}^*} ; \qquad n_1 = n_0 \frac{N_{t0}^*}{n_{t0}} , \\ p_1^{**} &= p_0 \frac{n_{t0}}{N_{t0}^{**}} ; \qquad p_1 = p_0 \frac{n_{t0}}{N_{t0}^*} . \end{aligned} \tag{6}$$

From the notations (6) it can be seen that n_1, p_1, are the electron or hole concentration if the Fermi level is E_t. Similarly n_1^*, p_1^{**} mean the electron or hole concentration if $F_0 = E_t^*$ or $F_0 = E_t^{**}$. The characteristic equation for the lifetime τ is:

$$\left| A - \frac{1}{\tau} I \right| = 0 , \tag{7}$$

where A is matrix (5) and I is the idem matrix.

After doing the simple but long calculation, the coefficients of the equation of the fourth degree can be determined. For simplicity's sake the coefficients are given for the case when the conditions

$$\frac{n_1}{n_1^*} \ll 1 , \quad \frac{p_1}{p_1^{**}} \ll 1 \tag{8}$$

are fulfilled, and as the excited states (E_t^*, E_t^{**}) are far from the E_t level, the inequalities (8) are valid in general. Taking into account what has been said above the coefficients of the equation

$$b_0 \tau^4 + b_1 \tau^3 + b_2 \tau^2 + b_3 \tau + b_4 = 0 \tag{9}$$

are

$$\begin{aligned} b_0 &= + A_n A_p r_n r_p \left[\alpha' \left(1 + \frac{p_1}{p_0} \right) + \beta' \left(1 + \frac{n_1}{n_0} \right) + \alpha' \beta' \right], \\ b_1 &= - r_n r_p \left[A_n \left(1 + \alpha' + \frac{n_1}{n_0} \right) (1 + \delta) + A_p \left(1 + \beta' + \frac{p_1}{p_0} \right) (1 + \varepsilon) \right], \\ b_2 &= + r_n r_p [1 + \varepsilon + \delta + \varepsilon\delta] , \\ b_3 &= - \left[A_n \left(1 + \alpha' + \frac{n_1^*}{n_0} \right) + A_p \left(1 + \beta' + \frac{p_1^{**}}{p_0} \right) + r_n + r_p \right], \\ b_4 &= + 1 , \end{aligned} \tag{10}$$

where the following notations were introduced:

$$\varepsilon \equiv \frac{A_n n_1^*}{r_n n_0} = \frac{C_n n_1^*}{r_n}; \qquad \delta \equiv \frac{A_p p_1^{**}}{r_p p_0} = \frac{C_p p_1^{**}}{r_p} .$$

The roots of equ. (9) of the fourth degree can be determined exactly and numerically as well. In this way, however, the results are not perspicuous. Therefore we shall give the two roots of equ. (9) approximately. It is well known that if the roots of equ. (9) are essentially different ($\tau_1 \gg \tau_2 \gg \tau_3 \gg \tau_4$) the following approximation is valid:

$$\tau_i \approx -\frac{b_i}{b_{i-1}} . \tag{11}$$

As the first two roots are known to be very different from each other and from the others (the mean lifetime and the filling time of the centre) the first two roots, τ_r and τ_t lifetimes can be determined on the basis of (11). At present we neglect the other two lifetimes, as they are essentially shorter. According to equ. (11) making use of the coefficients given in (10) we get

$$\tau_r \approx \frac{A_n\left(1+\alpha'+\frac{n_1}{n_0}\right)(1+\delta)+A_p\left(1+\beta'+\frac{p_1}{p_0}\right)(1+\varepsilon)}{A_n A_p\left[\alpha'\left(1+\frac{p_1}{p_0}\right)+\beta'\left(1+\frac{n_1}{n_0}\right)+\alpha'\beta'\right]} - , \tag{12}$$

$$\tau_t \approx \frac{1+\varepsilon+\delta+\varepsilon\delta}{A_n\left(1+\alpha'+\frac{n_1}{n_0}\right)(1+\delta)+A_p\left(1+\beta'+\frac{p_1}{p_0}\right)(1+\varepsilon)} . \tag{13}$$

If we take into consideration that the relations

$$n_0 \alpha' = N_t\left(1+\frac{p_1}{p_0}\right)^{-1},$$

$$p_0 \beta' = N_t\left(1+\frac{n_1}{n_0}\right)^{-1}$$

valid in case of $\varepsilon = 0$, $\delta = 0$ remain correct in good approximation when

$\varepsilon \neq 0$, $\delta \neq 0$,[2] we obtain after some transformations

$$\tau_r \approx \frac{C_n\left[n_0 + n_1 + N_t\left(1+\frac{p_1}{p_0}\right)^{-1}\right](1+\delta) + C_p\left[p_0 + p_1 + N_t\left(1+\frac{n_1}{n_0}\right)^{-1}\right](1+\varepsilon)}{N_t C_n C_p\left[n_0 + p_0 + N_t\frac{p_1}{p_0}\right)^{-1}\left(1+\frac{n_1}{n_0}\right)^{-1}]}, \tag{14}$$

$$\tau_t \approx \frac{1+\varepsilon+\delta+\varepsilon\delta}{C_n\left[n_0 + n_1 + N_t\left(1+\frac{p_1}{p_0}\right)^{-1}\right](1+\delta) + C_p\left[p_0 + p_1 + N_t\left(1+\frac{n_1}{n_0}\right)^{-1}\right](1+\varepsilon)}. \tag{15}$$

Thus equ. (14) and (15) give the two longer lifetimes of recombination through excited states. Expression (14) renders the stationary lifetime for small values of N_t, given by RZHANOV in paper [3]. It is obvious that if the new parameters (ε and δ) of the theory are zero, we obtain the respective expressions of the S—R model (e.g. [8], equ. (8), (9)).

The lifetimes (14) and (15) are formally identical with the lifetimes of the S—R model, if we replace C_n and C_p by effective capture constants as follows:

$$C_n' \equiv \frac{C_n}{1+\varepsilon}; \quad C_p' \equiv \frac{C_p}{1+\delta},$$

these give account of the inner transitions, too. Accordingly

$$C_n' \leqslant C_n \qquad \text{and} \qquad C_p' \leqslant C_p \quad (\varepsilon \geqslant 0;\ \delta \geqslant 0).$$

While the capture from the conduction band is determined by C_n, the value of r_n limits the rate of transition to the ground state. Examining the process of the whole recombination (on the basis of the model represented in Fig. 1) it is seen that both C_n and r_n (i.e. C_p and r_p) are figuring in the actually measurable lifetime. Thus the last step has also to be considered and the energy loss of the electron must be provided for (by excitation of one or more phonons, perhaps by some other mechanism), as e.g. in the temperature dependence of C_n', C_p', ε and δ must be taken into account as well.

Lifetimes (14) and (15) refer to bulk recombination. We should like to deal with the question of surface recombination centres at another occasion.

[2] It is sufficient to remark that because of condition (8) $\frac{n_{t0}^*}{n_{t0}} \ll 1$ and $\frac{N_{t0}^{**}}{N_{t0}^*} \ll 1$ similarly. That means, that in a thermal equilibrium the excited states can be neglected in comparison with the ground states.

REFERENCES

1. W. Shockley and W. Read, Phys. Rev., **87**, 835, 1952.
2. R. N. Hall, Phys. Rev., **87**, 387, 1952.
3. A. V. Rzhanov, Soviet Physics-Solid State, **3**, 3691, 1961.
4. M. Lax, Phys. Rev., **119**, 1502, 1960.
5. V. L. Bontch-Bruevitch and V. B. Glasko, Soviet Physics-Solid State, **4**, 510, 1962.
6. D. J. Sandiford, Phys. Rev., **105**, 524, 1957.
7. G. K. Wertheim, Phys. Rev., **109**, 1086, 1958.
8. G. Pataki, Acta Phys. Hung., **13**, 119, 1961.
9. W. Schockley and J. T. Last, Phys. Rev., **107**, 392, 1957.
10. P. T. Landsberg, Solid State Physics in Electronics and Telecommunication, Academic Press, 1960, pp. 436—455.

НЕСТАЦИОНАРНОЕ ВРЕМЯ ЖИЗНИ В СЛУЧАЕ РЕКОМБИНАЦИИ, ПРОИСХОДЯЩЕЙСЯ ЧЕРЕЗ ВОЗБУЖДЕННЫЕ СОСТОЯНИЯ В НЕВЫРОЖДЕННЫХ ПОЛУПРОВОДНИКАХ

Г. ПАТАКИ

Р е з ю м е

В статье была исследована модель рекомбинации, данная А. В. Ржановым в работе [3], вблизи равновесия, в нестационарном случае. Из приближенных корней характеристического уравнения τ_r дает стационарное время жизни, полученное в [3], при любой концентрации рекомбинационных центров, в то время как τ_l дает обобщение нестационарного времени жизни модели Шокли—Рида на случай рекомбинации происходящейся через возбужденные состояния.

THE HYDRODYNAMICAL MODEL OF WAVE MECHANICS I

THE MOTION OF A SINGLE PARTICLE IN A POTENTIAL FIELD

By

L. JÁNOSSY and M. ZIEGLER

CENTRAL RESEARCH INSTITUTE OF PHYSICS, BUDAPEST

(Received 11. XII. 1962)

The problem is investigated as to how far the wave equation representing a quantum-mechanical system can be transformed by change of variables into a system of equations which have the form of the classical equation of motion of a deformable medium. In the present paper we carry out this investigation in the case of a single charged particle moving under the influence of an outside potential.

I. Basic conceptions

§ 1. The difficulties connected with the physical interpretation of the wave function ψ have renewed interest in the hydrodynamical model of wave mechanics, i.e. in a model in which the fundamental equations of motion refer to classical quantities by which ψ may be replaced. Summarizing our considerations to be presented in a number of papers, we shall analyse the problem of how far it is possible to replace the wave mechanical description of a system by one mathematically equivalent and of the form of the classical equations of motion of an elastic medium.

Our attempt is not new, similar considerations have been given already e.g. by MADELUNG [1] and later by EHRENFEST [2] and TAKABAYASI [3]. (See also our short communication [4].) Further a number of papers have been published in connection with the classical analogy of quantum mechanics which are to a certain degree similar to ours as regards the mathematical formalism but which are different as regards their aim. (We mention here e.g. L. DE BROGLIE [5] and K. NOVOBÁTZKY [6].) On another occasion we shall summarize the wide literature on the subject.

§ 2. The simplest case, i.e. the motion of a particle of mass m and charge e under the influence of forces which can be derived from a potential V can be described by the SCHRÖDINGER wave equation

$$-\frac{\hbar^2}{2m}\nabla^2\psi + V\psi = i\hbar\frac{\partial\psi}{\partial t}, \tag{1}$$

where the wave function ψ is a function of the coordinates and of the time. We may write for short $\psi(\boldsymbol{r}, t) = \psi$. Similarly V may depend on both $\boldsymbol{r}$ and t, thus we may write $V(\boldsymbol{r}, t) = V$.

According to the generally accepted interpretation of the wave function $|\psi|^2$ is a probability density, i.e. $|\psi|^2 \, d\tau$ is the probability to find the particle (which is supposed to be pointlike) inside the volume element $d\tau$ [7]. SCHRÖDINGER's original idea [8] was that $|\psi|^2$ represents a true density, i.e. the particle is smeared over space with a mass density ϱ_m and electric charge density ϱ_e so that

$$\varrho_m = m\varrho\,, \quad \varrho_e = e\varrho \quad \text{with} \quad \varrho = |\psi|^2\,. \tag{2}$$

Later, reluctantly, SCHRÖDINGER had to give up his original idea and to accept BORN's probability interpretation.

The considerations connected with the hydrodynamical model automatically renew the question as to the interpretation of $|\psi|^2$. The density defined by (2) appears as one of the variables of the hydrodynamical model, thus the classical picture of the system described by the wave function corresponds to a medium with density $\varrho = \varrho(\boldsymbol{r}, t)$ spread out over space and moving under the influence of outer forces, the elastic stresses occurring inside the medium.

§ 3. SCHRÖDINGER already pointed out that the velocity of flow can be expressed in terms of ψ as follows:

$$\varrho \boldsymbol{v} = -\frac{i\hbar}{2m}(\psi^* \operatorname{grad}\psi - \psi \operatorname{grad}\psi^*)\,. \tag{3}$$

The quantities defined by (2) and (3) satisfy together with (1) the following relation

$$\operatorname{div}(\varrho \boldsymbol{v}) + \frac{\partial \varrho}{\partial t} = 0\,. \tag{4}$$

This is the so-called continuity equation, which can be derived from the SCHRÖDINGER equation. Thus $\boldsymbol{v}$ and ϱ can be taken to describe velocity and density distribution of a moving medium.

It should be noted that adding a term rot χ (where χ is some arbitrary vector quantity) to the definition (3) of $\boldsymbol{v}$, the continuity equation (4) would also be satisfied. In the present approximation we may take this term to be zero. We shall return to the exact determination of the form of χ when dealing with the hydrodynamical model describing the electron having spin and magnetic moment, i.e. when χ can be determined by comparison with the experimental results.

Multiplying (4) by m and e, respectively, we obtain the continuity equation for the flow of mass $\operatorname{div} \boldsymbol{p} + \frac{\partial \varrho_m}{\partial t} = 0$ and that for the electric

current div $\boldsymbol{i} + \frac{\partial \varrho_e}{\partial t} = 0$, we merely have to suppose

$$\begin{aligned} \boldsymbol{p} &= m\varrho\boldsymbol{v} = \varrho_m \boldsymbol{v}, \\ \boldsymbol{i} &= e\varrho\boldsymbol{v} \ = \varrho_e \boldsymbol{v}, \end{aligned} \tag{5}$$

where $\boldsymbol{p}$ is the density of momentum and $\boldsymbol{i}$ the density of electric current in suitable units.

Integrating (4) over the whole of space (changing in the second term the order of integration and differentiation and supposing that $\varrho\boldsymbol{v}$ tends sufficiently strongly to zero at infinity), we find

$$\frac{d}{dt} \int \varrho \, d\tau = 0 .$$

Thus the density integrated over the whole space is constant in time and — to be compatible with the wave equation — has to be given the value 1, i.e.

$$\int \varrho \, d\tau = 1 . \tag{6}$$

Using the normalization (6) we obtain for total mass and total charge of the medium the initially given values m and e.

II. Equation of motion

§ 4. So as to obtain a dynamical description of our system it is necessary to consider the acceleration of the elements of the medium. According to hydrodynamics the acceleration of an element of a moving medium is given by the total derivative of the velocity, i.e.

$$\boldsymbol{a} = \frac{d\boldsymbol{v}}{dt} = \frac{\partial \boldsymbol{v}}{\partial t} + (\boldsymbol{v} \operatorname{grad}) \boldsymbol{v} , \tag{7}$$

where the partial derivative $\frac{\partial \boldsymbol{v}}{\partial t}$ expresses the rate of change of velocity in a fixed point. Instead of (7) we can also write, taking into account the continuity equation (4):

$$\varrho \frac{d\boldsymbol{v}}{dt} = \frac{\partial (\varrho \boldsymbol{v})}{\partial t} + \operatorname{Div} (\varrho \boldsymbol{v} \circ \boldsymbol{v}) , \tag{8}$$

where Div is the tensor divergence and $\circ$ designates the direct product.

Differentiating (3) with respect to time and expressing the time derivatives of ψ^* and ψ in terms of their spatial derivatives with help of the wave equ. (1), we get from (8):

$$\varrho_m \frac{d\boldsymbol{v}}{dt} = -\varrho \operatorname{grad}(V + Q) \tag{9}$$

with

$$Q = -\frac{\hbar^2}{2m} \frac{\nabla^2 \varrho^{1/2}}{\varrho^{1/2}} . \tag{10}$$

In place of (9) and (10) one may also write

$$\varrho_m \frac{d\boldsymbol{v}}{dt} = -\varrho \operatorname{grad} V - \operatorname{Div} \mathfrak{Q} , \tag{9a}$$

with the tensor given by the relation

$$\mathfrak{Q} = -\frac{\hbar^2}{4m} \varrho (\nabla \circ \nabla) \ln \varrho \tag{10a}$$

or writing down the i, k-th component of the tensor

$$Q_{ik} = -\frac{\hbar^2}{4m} \varrho \frac{\partial^2 \ln \varrho}{\partial x_i \, \partial x_k} .$$

We find that equs. (9), (10) [or (9a) and (10a)] together with the continuity equation (4) give a complete set of equations of motion. Indeed, if we impose an initial condition upon $\boldsymbol{v}$ and ϱ

$$\boldsymbol{v}(\boldsymbol{r}, 0) = \boldsymbol{v}_0(\boldsymbol{r}) \quad \text{and} \quad \varrho(\boldsymbol{r}, 0) = \varrho_0(\boldsymbol{r})$$

their time distribution can be determined uniquely from the above system of equations.

§ 5. The equs. (4), (9) and (10) are exactly of the form which is to be expected for the classical equations of motion of an elastic medium. Q plays the role of an inner potential and

$$\boldsymbol{F}_i = -\operatorname{grad} Q \tag{11}$$

is the stress appearing as the result of deformation.

That $\boldsymbol{F}_i$ as given by (11) can be regarded as classical stress can be seen from the following remarks:

1. If $\varrho = \text{const.}$, then $Q = \text{const.}$ and $\boldsymbol{F}_i = 0$, thus stress appears only at places where the density of the medium is non-uniform. In a given point, Q depends only upon the density in this point and the spatial derivatives of the density, thus we may say that Q in a given point is determined by the density distribution in the immediate vicinity of that point, just as is to be expected in an elastic medium.

2. It follows from (11) and (10) [or (10a)] that

$$\int \varrho \boldsymbol{F}_i \, d\tau = 0 \,, \tag{12}$$

i.e. the inner forces resulting from the stress have no resultant. Thus the rate of change of momentum of the system is given by the integral over the outer forces only; or denoting by

$$\boldsymbol{R} = \int \varrho \boldsymbol{r} \, d\tau$$

the coordinate vector of the centre of gravity of our system, we find

$$m\ddot{\boldsymbol{R}} = \dot{\boldsymbol{P}} = \int \varrho \boldsymbol{F}_o \, d\tau \,, \tag{13}$$

where

$$\boldsymbol{F}_o = -\operatorname{grad} V \,. \tag{13a}$$

Equation (13) expresses the law of EHRENFEST.

3. The moment of force produced by the inner forces can be written

$$\boldsymbol{K}_i = \int \varrho \, [\boldsymbol{r} \times \boldsymbol{F}_i] \, d\tau = -\int [\boldsymbol{r} \times \operatorname{Div} \mathfrak{Q}] \, d\tau \,.$$

Integrating by parts, we find, remembering that $\mathfrak{Q}$ is a symmetric tensor [see (10a)]:

$$\boldsymbol{K}_i = 0 \,.$$

Thus the inner forces produce no moment of force. We find therefore for the total moment of force of the system in analogy to (13):

$$\boldsymbol{K} = \int \varrho \, [\boldsymbol{r} \times \boldsymbol{F}_o] \, d\tau \,, \tag{14}$$

i.e. the change of angular momentum is caused by the moment of the outer forces only. In particular, we note that the angular momentum of the system will change continuously provided the outer forces produce a non-vanishing moment.

Taking together the three remarks made above, we see that the equs (4), (9) and (10) describing the motion of our medium are indeed of the type of classical equations of motion. The fact that the constant $\hbar$ appears in the expression giving the potential Q does not affect the classical nature of the equation. Indeed, $\hbar$ may be regarded as a constant characteristic of the elastic properties of an atomic system. Obviously no description can be successful which does not make use of $\hbar$.

III. Connection between hydrodynamical equations and the wave equation

§ 6. In the following we discuss how far it is possible to establish a one to one correspondence between the descriptions of a system by a wave function on the one hand and the hydrodynamical variables ϱ and $\boldsymbol{v}$ on the other.

For this purpose it is convenient to express the wave function ψ with help of two real functions $R = R(r, t)$ and $S = S(r, t)$ in the form

$$\psi = Re^{iS}. \tag{15}$$

Introducing (15) into the expressions for the density (2) we find

$$\varrho = R^2 \tag{16a}$$

and further from equ. (3) for the velocity of flow

$$\boldsymbol{v} = \frac{\hbar}{m} \operatorname{grad} S. \tag{16b}$$

(It should be noted that the above expression for $\boldsymbol{v}$ is valid only for points in which $\varrho \neq 0$; at points where $\varrho = 0$, $\boldsymbol{v}$ may have singularities.)

If, however, we want to determine from given distributions of ϱ and $\boldsymbol{v}$ the wave function ψ satisfying the wave equation, we have to express R and S through ϱ and $\boldsymbol{v}$. Reversing (16) we obtain

$$R = \sqrt{\varrho}, \tag{17a}$$

$$S = \frac{m}{\hbar} \int_{r_0}^{r} \boldsymbol{v}\, d\boldsymbol{r} + S_0, \tag{17b}$$

where $\boldsymbol{r}_0$ is a constant vector and S_0 a function of time only. Thus from a given distribution of ϱ and $\boldsymbol{v}$ functions R and S may be determined on the

basis of (17), and further using (15) the corresponding ψ function fulfilling the wave equation may be built up. If we require ψ to be a single-valued function of the coordinates according to (15) $\boldsymbol{v}$ may still be multi-valued having values differing by integer multiples of 2π from each other, i.e.

$$\oint \boldsymbol{v}\, d\boldsymbol{r} = 2\pi\hbar \frac{k}{m}, \quad k = 0, \pm 1, \pm 2, \ldots, \tag{18}$$

where the path of integration must avoid points for which $\varrho = 0$, otherwise it may be an arbitrary closed path. The expression (18) relating to the velocity, together with the normalization (6) of the density may be regarded as initial conditions. Indeed (as can be shown easily), if they are fulfilled at a time $t = 0$ they remain so for all later times.

Equ. (18) is equal to Thomson's law of vortices in a field.

§ 7. So as to check whether ψ constructed from the distributions of ϱ and $\boldsymbol{v}$ obeys indeed the wave equation, we insert the ψ function thus obtained into the wave equation. Doing so we find that the wave equation is indeed fulfilled, provided we take $\boldsymbol{r}_0$ to be an arbitrary vector independent of time and put

$$S_0 = -\frac{1}{\hbar}\int_0^t E(t)\, dt$$

with

$$E = \left(V + Q + \frac{1}{2} m\boldsymbol{v}^2\right)_{\boldsymbol{r}=\boldsymbol{r}_0}.$$

Thus the explicit expression for ψ satisfying (1) can be written

$$\psi = \sqrt{\varrho} \exp\left\{\frac{i}{\hbar}\int_{\boldsymbol{r}_0}^{\boldsymbol{r}} \boldsymbol{v}\, d\boldsymbol{r} - \frac{i}{\hbar}\int_0^t E(t)\, dt\right.$$

We see thus that owing to the arbitrary value of $\boldsymbol{r}_0$, ψ is determined except for a constant phase factor; thus ψ may be replaced by $\psi' = \psi e^{i\gamma}$ (with $\nabla\gamma = \dot{\gamma} = 0$), ψ' corresponding to the same hydrodynamical distribution as ψ. However, in the usual considerations of wave mechanics such a phase factor is regarded as unimportant, thus we can conclude that essentially there exists a one to one correspondence between the solutions of the wave equation and the hydrodynamical equations (4), (9) provided only solutions obeying initial conditions (6), (18) are considered.

IV. Stationary states

§ 8. The Schrödinger wave equation (1) admits so-called stationary solutions of the form

$$\psi(r,t) = \varphi(r)\, e^{-\frac{i}{\hbar}Et} \tag{19}$$

when the potential energy $V(r)$ does not depend on the time.

The amplitude of the n-th stationary solution is determined by the equation

$$-\frac{\hbar^2}{2m}\nabla^2\varphi_n + V\varphi_n = E_n\varphi_n\,, \tag{20}$$

where the constants E_n are the energy eigenvalues and the functions φ_n are the normalized eigenfunctions.

The corresponding hydrodynamical variables are of course independent of time, i.e. introducing (19) into (2) and (3) we get for the density and velocity of flow, respectively:

$$\begin{aligned} \varrho &= \varphi_n^*(r)\,\varphi_n(r)\,, \\ \varrho\boldsymbol{v} &= -\frac{i\hbar}{2m}\left[\varphi_n^*(r)\,\nabla\varphi_n(r) - \nabla\varphi_n^*(r)\,\varphi_n(r)\right]. \end{aligned} \tag{21}$$

a) Let us consider first the case when the amplitude of the stationary solution is real, i.e. $\varphi_n(r) = \varphi_n^*(r)$. (It should be noted that a function ψ of real amplitude multiplied by a constant phase factor can also be regarded as a real solution in accordance with what we have said above.) As can be seen from (21) in this case

$$\frac{\partial\varrho}{\partial t} = 0 \quad \text{and} \quad \boldsymbol{v} = 0\,,$$

which means that the real stationary solutions correspond to states in which the medium representing the particle considered is at rest. The inner potential can be expressed with help of the amplitude function, taking into account (2), (10) and (19) in the form

$$Q = -\frac{\hbar^2}{2m}\,\frac{\nabla^2\varphi_n(r)}{\varphi_n(r)}\,.$$

Using the amplitude equation (20) we have

$$Q = E_n - V$$

or forming the gradient and taking into account (11), (13)

$$\boldsymbol{F}_o + \boldsymbol{F}_i = 0\,,$$

i.e. the stress produced by the inner forces exactly balances the outer forces arising from the potential V.

A well-known example for this case is provided by the ground state of the H-atom. The inner potential corresponding to the wave function $\varphi_1(r) = Ce^{-\frac{r}{r_H}}$ has the form

$$Q = -\frac{me^4}{2\hbar^2} + \frac{e^2}{r} = E_1 - V(r)\,,$$

where E_1 is the energy constant of the ground state and $V(r)$ represents the Coulomb potential. As can be seen Q obtained for this case produces a stress which exactly compensates the Coulomb attraction of the nucleus. The medium is in a state of stress but does not move.

b) Essentially complex solutions of the amplitude equation (20) correspond to states, where

$$\frac{\partial \varrho}{\partial t} = 0\,, \qquad \boldsymbol{v} = -\frac{i\hbar}{2m}\,\mathrm{grad}\,\ln\frac{\varphi_n(r)}{\varphi_n^*(r)}\,.$$

In such a state $\boldsymbol{v} \neq 0$, but $\frac{\partial \boldsymbol{v}}{\partial t} = 0$, these are characteristic expressions for a stationary flow.

As both the charge density ϱ_e and the current density i are constant in time, such a configuration produces stationary electric and magnetic fields, it does, however, not radiate.

For such a distribution grad $(V + Q) \neq 0$, i.e. the inner stress does not compensate exactly the outer force. We find with help of (7) and (9):

$$m\,(\boldsymbol{v}\,\mathrm{grad})\,\boldsymbol{v} = -\,\mathrm{grad}\,(V + Q)\,.$$

As can be seen easily, the uncompensated stress produces forces which are necessary to maintain the state of stationary flow.

A simple example for this case is provided by the $2\,p^1$ state of the H-atom to which belongs the wave function

$$\varphi_2(r) = C\,\frac{x + iy}{2r_H}\,e^{-\frac{r}{2r_H}}\,.$$

We find in this case

$$V + Q = E_2 - \frac{\hbar^2}{2m}\,\frac{1}{x^2 + y^2}$$

(with the energy constant of the $2p^1$ state: $E_2 = -\frac{me^4}{8\hbar^2}$). Thus as can be seen easily from this equation the inner and outer forces do not compensate each other and there remains an uncompensated attractive force, which varies proportional to $(x^2 + y^2)^{-3/2}$.

We find further, introducing $\varphi_2(r)$ into (3), that the medium rotates around the z-axis. The angular velocity in a point $\boldsymbol{r}$ is given by

$$\omega = \frac{\hbar}{m} \frac{1}{x^2 + y^2} .$$

The centripetal force, which is needed to make the elements move along circular paths with such velocities is provided by that part of the stress which is not compensated by the Coulomb attraction of the nucleus and which has the form

$$F_C = m\,\omega^2 (x^2 + y^2)^{1/2} = \frac{\hbar^2}{m} (x^2 + y^2)^{-3/2} .$$

§ 9. Solutions of the wave equation (1) can be represented as linear combinations of stationary solutions. Thus a solution $\psi(\boldsymbol{r}, t)$ can be written in the form:

$$\psi(\boldsymbol{r}, t) = \sum c_\nu \varphi_\nu(\boldsymbol{r})\, e^{-\frac{i}{\hbar} E_\nu t} , \tag{22}$$

where the stationary solutions form a normalized set. The corresponding charge and current densities can be obtained when introducing (22) into (2) and (3); we get thus:

$$\varrho = \sum \varrho_{\nu\mu} \cos(\omega_{\nu\mu} t + \alpha_{\nu\mu}) , \tag{23}$$

where

$$\omega_{\nu\mu} = \frac{E_\nu - E_\mu}{\hbar} \tag{24}$$

and $\varrho_{\nu\mu}$, $\alpha_{\nu\mu}$ are functions of the coordinates only, i.e.

$$\varrho_{\nu\mu} = |c_\nu c_\mu \varphi_\nu(\boldsymbol{r})\, \varphi_\mu(\boldsymbol{r})| ,$$

$$\alpha_{\nu\mu} = \frac{1}{2i} \ln \frac{c_\mu c_\nu^* \varphi_\mu \varphi_\nu^*}{c_\mu^* c_\nu \varphi_\mu^* \varphi_\nu} .$$

Similarly we find

$$\varrho \boldsymbol{v} = \sum \boldsymbol{p}_{\nu\mu} \cos(\omega_{\nu\mu} t + \beta_{\nu\mu}) , \tag{25}$$

where the $\boldsymbol{p}_{\nu\mu}$ and $\beta_{\nu\mu}$ can be also expressed explicitly in terms of the c_ν and φ_ν.

Equs. (23), (24) and (25) show that the medium in the non-stationary state vibrates with frequencies $\omega_{\nu\mu}$, which are exactly the Bohr frequencies. The terms with $\nu = \mu$ represent a constant charge and current density. This stationary motion is superimposed by the oscillation.

We see thus that the fluid representing the particle under investigation has its equilibrium configurations given by the eigenfunctions of the stationary states.

On the effect of some outer disturbance the medium starts to oscillate with frequencies $\omega_{\nu\mu}$ around its equilibrium configuration and as the medium is charged it emits electromagnetic radiation of those frequencies. The total dipole moment which is responsible for the emitted radiation can be written in the form:

$$\boldsymbol{d}_{\nu\mu} = -2\, c_\nu c_\mu e \int \boldsymbol{r}\, \varphi_\nu^* \varphi_\mu \, d\tau \,.$$

Frequencies belonging to a vanishing dipole moment do not occur in first approximation. Indeed, the current distribution inside the atom in a state described by the wave function

$$\psi = c_1 \varphi_1 e^{-\frac{i}{\hbar} E_1 t} + c_2 \varphi_2 e^{-\frac{i}{\hbar} E_2 t}$$

in the case $\boldsymbol{d}_{12} = 0$ is such that part of the medium oscillates with frequency ω_{12}, the phases of the oscillation being distributed in such a way that the radiation emitted by one part of the charged medium is opposite in phase to that emitted by the remaining part and in a first approximation the radiations emitted by the two parts extinguish each other by interference.

Considering the second approximation we obtain the so-called quadrupole radiation. Such a quadrupole radiation with its characteristic distribution of intensity and polarization is indeed observed in case of the forbidden lines when $\boldsymbol{d}_{\nu\mu} = 0$.

We note that the hydrodynamical model accounts also for the "elastically bound electron" which was postulated by HERTZ to explain the optical properties of atoms.

The main difficulty encountered by HERTZ was to explain how it is possible that an electron could be excited so as to vibrate with a series of frequencies.

This difficulty is overcome by the hydrodynamical concept. It is seen that the elastic forces derived from the inner potential Q together with the outside potential V provide a dynamical system, the characteristic frequencies of which are exactly the optical frequencies. Further, the modes of vibration

of this system are in accordance with the polarization and intensity distribution of the observed spectral lines.

In a later article we shall present our considerations for the case when the electromagnetic field is also taken into account. Following on this we shall deal with the hydrodynamical model of the electron with spin.

REFERENCES

1. E. MADELUNG, Z. f. Phys., **40**, 322, 1926.
2. P. EHRENFEST, Z. f. Phys., **45**, 455, 1927.
3. T. TAKABAYASI, Prog. of Theor. Phys., **8**, 143, 1952; **9**, 187, 1953.
4. L. JÁNOSSY, Z. f. Phys., **169**, 79, 1962.
5. L. DE BROGLIE, Compt. Rend., **236**, 1453, 1953.
6. K. NOVOBÁTZKY. Ann. d. Phys., **9**, 406, 1951.
7. M. BORN, Z. f. Phys., **37**, 963, 1926; **38**, 803, 1926.
8. E. SCHRÖDINGER, Ann. d. Phys., **79**, 361, 489, 1926; **80**, 437, 1926; **81**, 109, 1926.

ГИДРОДИНАМИЧЕСКАЯ МОДЕЛЬ ВОЛНОВОЙ МЕХАНИКИ I

Л. ЯНОЩИ и М. ЦИГЛЕР

Р е з ю м е

Рассматривается проблема о возможностях преобразования, путём замены переменных, волнового уравнения квантовомеханической системы в систему уравнений, обладающую формой классического уравнения движения деформирующейся среды. В представленной работе мы изучаем этот вопрос для одной заряженной частицы, движущейся под влиянием внешнего потенциала.

DIE BERECHNUNGEN DER $1sns^1S$-ZUSTÄNDE DES WASSERSTOFFMOLEKÜLS AUF GRUND DER METHODE DER MOLEKÜLBAHNEN

Von

F. BERENCZ

JÓZSEF ATTILA UNIVERSITÄT, INSTITUT FÜR THEORETISCHE PHYSIK, SZEGED

(Vorgelegt von A. Kónya. — Eingegangen: 10. I. 1963)

Es wird die Bindungsenergie des $1s2s^1S$-Zustandes des Wasserstoffmoleküls auf Grund der Methode der Molekülbahnen berechnet, weiterhin werden Molekülintegrale zwischen 1s- und 2s-Elektronen angegeben.

Einleitung

Es ist wohlbekannt, dass die Wellenfunktion der Elektronenkonfiguration eines Moleküls auf Grund von zwei verschiedenen und einander ergänzenden Näherungsmethoden berechnet werden kann. Die erste Methode geht von den separierten Atomen und von den Elektronenbahnen der Atome aus und berücksichtigt nachträglich, dass im Molekülbindungszustand die Elektronenwolken der Atome sich umrichten. Diese Methode ist die sogenannte VB (Valence-Bond)-Methode [1]. Diese Methode liefert offenbar dann gute Resultate, wenn die Entfernung der Atome gross ist, denn in diesem Falle kann die Umrichtung der Atomhülle wirklich als Perturbation angesehen werden. Da in den Molekülen die Entfernung der Atome im allgemeinen klein ist, kann die VB-Methode kein befriedigendes Resultat geben. Die andere Methode geht von der Anordnung der Atomkerne des schon fertigen Moleküls aus und untersucht das Verhalten der einzelnen Elektronen in dem durchschnittlichen, von den positiven Kernen und den anderen Elektronen hervorgerufenen sogenannten Self-Consistent-Potentialfeld. Diese Methode ist die sogenannte MO (Molecular Orbital)-Methode, zu deren Ausarbeitung HUND [2], MULLIKEN [3], HÜCKEL [4] und LENNARD-JONES [5] beigetragen haben. Diese Methode ist zur Bestimmung der Eigenschaften der Moleküle mit starker Bindung geeignet. Die Annahme nämlich, dass die einzelnen Elektronen sich in dem durchschnittlichen, von den positiven Kernen und den anderen Elektronen hervorgerufenen Potentialfeld bewegen, ist umsoweniger erfüllt, je grösser die Atomentfernungen sind. Auf Grund der MO-Methode wurden viele Rechnungen bezüglich des Wasserstoffmoleküls durchgeführt, COULSON [6] konnte sogar feststellen, dass 3,63 eV der beste Wert der Bindungsenergie sei, der sich auf Grund der Molekülbahnrechnungen ergeben könne. Durch diesen Erfolg wurden viel später FROST und BRAUNSTEIN [7] zur Einführung der CMO (Correlated Molecular Orbital)-Methode angeregt. Im folgenden wer-

den die Molekülbahnrechnungen auf die $1sns\,^1S$-Zustände ($n \geq 2$) des Wasserstoffmoleküls ausgedehnt und dann mit Hilfe der CMO-Methode erweitert. Mit diesen Rechnungen vermehrt sich die Zahl der bekannten Molekülintegrale zwischen $1s$- und ns-Elektronen in grossem Masse.

Die Rechenmethode

Bezeichnet man die Molekülbahnen der einzelnen, das Molekül aufbauenden Elektronen mit $\psi_1, \psi_2, \ldots, \psi_n$, so kann man gemäss HUND, MULLIKEN, HÜCKEL und LENNARD-JONES die Eigenfunktion des Moleküls auf Grund des Modells der Eigenfunktionen der freien Systeme in folgender Weise konstruieren:

$$\psi = \psi_1 \cdot \psi_2 \cdots \psi_n . \tag{1}$$

Die Molekülbahnen der einzelnen Elektronen lassen sich aber auf Grund der LCAO (Linear Combination of Atomic Orbitals)-Methode [8] als Linearkombinationen der einzelnen Atombahnen aufschreiben.

Die Wasserstoffeigenfunktionen der ns-Zustände werden durch den folgenden Zusammenhang geliefert:

$$ns(r) = -\frac{1}{n^{3/2}\sqrt{\pi}} \exp\left(-\frac{r}{n}\right) R_n(r), \tag{2}$$

wo

$$R_n(r) = 1 - \frac{n-1}{1!\,2!}\left(\frac{2r}{n}\right) + \frac{(n-1)(n-2)}{2!\,3!}\left(\frac{2r}{n}\right)^2 - \ldots . \tag{3}$$

Die auf Grund der LCAO-Methode aufgeschriebenen Molekülbahnen des ersten Elektrons im Grundzustande und des zweiten Elektrons im angeregten Zustande haben nach (2) und (3) die folgende Gestalt:

$$1s(r_{a1}) + 1s(r_{b1}) = \frac{1}{\sqrt{\pi}}\left[\exp(-r_{a1}) + \exp(-r_{b1})\right], \tag{4}$$

$$2s(r_{a2}) + 2s(r_{b2}) = \frac{1}{2\sqrt{2\pi}}\left\{\left[\exp\left(-\frac{r_{a2}}{2}\right)\right]\left(1 - \frac{1}{2}r_{a2}\right) + \left[\exp\left(-\frac{r_{b2}}{2}\right)\right]\left(1 - \frac{1}{2}r_{b2}\right)\right\}. \tag{5}$$

Unter Berücksichtigung von (4) und (5) kann die Molekülbahn des $1s2s\,^1S$-Zustandes des Wasserstoffmoleküls nach (1) in der folgenden Form angegeben

werden:

$$\psi_2 = \frac{1}{2\sqrt{2\pi}}\left[\exp(-r_{a1}) + \exp(-r_{b1})\right]\left\{\left[\exp\left(-\frac{r_{a2}}{2}\right)\right]\left(1-\frac{1}{2}r_{a2}\right) + \left[\exp\left(-\frac{r_{b2}}{2}\right)\right]\left(1-\frac{1}{2}r_{b2}\right)\right\}. \tag{6}$$

Die Elektronenenergie wird dann auf Grund des folgenden Zusammenhanges berechnet:

$$E_2 = \frac{\int \psi_2 H \psi_2 \, d\tau}{\int \psi_2^2 \, d\tau}, \tag{7}$$

wo

$$H = H_a + H_b - \frac{1}{r_{b1}} - \frac{1}{r_{a2}} + \frac{1}{r_{12}} + \frac{1}{R} \tag{8}$$

und

$$H_a = -\frac{1}{2}\Delta_1 - \frac{1}{r_{a1}}, \qquad H_b = -\frac{1}{3}\Delta_2 - \frac{1}{r_{b2}}. \tag{9}$$

Mit der Molekülbahn (6) ergab sich bei 1,32 Å Kernabstand für die Bindungsenergie der Wert 1,52 eV.

* * *

Ich danke auch an dieser Stelle Fräulein E. GYÖRY für die Hilfe bei den numerischen Rechnungen.

Anhang

Bei der Berechnung der Elektronenenergie mussten mehrere Integrale bestimmt werden, welche bisher in der Literatur noch nicht vorgekommen sind. Es sei bemerkt, dass SUGIURA [9] als erster Zweizentrenintegrale für 1*s*-Elektronen berechnete, weiterhin treten bei ROSEN [10] Integrale für 2*s*- und 2*p*-Elektronen auf. Bei DELBRÜCK [11] befinden sich in den Molekülenintegralen schon $2s^2$-Elektronen, bei BARTLETT und FURRY [12] aber $2s^2$-, 2*s*-, 2*p*-Elektronen. BARTLETT [13] gab auch Integrale zwischen 2*p*-Elektronen an. Austauschintegrale zwischen $2s^2$-, 2*s*-, 2*p*- und $2p^2$-Elektronen findet man bei BLEICH und MAYER [14], bei SKLAR und LYDDANE [16], sowie bei WHEATLEY und LINNETT [17]. PARR und CRAWFORD [18] sowie HIRSCHFELDER und LINNETT [19] beschäftigen sich mit Integralen zwischen 2*p*-

Elektronen. FROST und BRAUNSTEIN [7], BERENCZ [20] und PAUNCZ [21] berechneten zahlreiche Integrale mit 1s-Elektronen und KOPINECK [22] mit 2s- und 2p-Elektronen. Zum Schluss sei die Arbeit von KOTANI, AMEMIYA und SIMOSE [23] erwähnt, die zahlreiche Hilfsintegrale zur Berechnung von Austausch- und anderen Wechselwirkungsintegralen tabelliert haben.

Bei der Berechnung des $1s2s\,^1S$-Zustandes des Wasserstoffmoleküls kommen Integrale zwischen 1s- und 2s-Elektronen vor. Diese seien folgendermassen bezeichnet:

$$I(\alpha,\beta,\gamma,\delta,s,t,n,v) = \frac{1}{\pi^2}\iint \exp(-\alpha r_{a1} - \beta r_{b1}) \exp(-\gamma r_{a2} - \delta r_{b2})\, r_{a1}^{s} r_{b1}^{t} r_{a2}^{u} r_{b2}^{v} \frac{1}{r_{12}}\, d\tau_1\, d\tau_a . \tag{10}$$

Bei der Berechnung der Integrale wird die Methode von KOTANI und seinen Mitarbeitern benutzt. Der Integrand wird in elliptischen Koordinaten dargestellt und die gegenseitige Entfernung der beiden Elektronen wird durch die NEUMANN'sche Reihenentwicklung berücksichtigt. Unsere Integrale wurden mit Hilfe der folgenden Hilfsintegrale ausgedrückt:

$$\begin{aligned}
A_n(\alpha) &= \int_1^\infty e^{-\alpha\mu}\,\mu^n\,d\mu\,,\\
B_n(\beta) &= \int_{-1}^{+1} e^{\beta\nu}\,\nu^n\,d\nu\,,\\
G_\tau^\nu(l,\beta) &= \int_{-1}^{+1} P_\tau^\nu(\nu_i)\, e^{-\beta\nu_i}\,\nu_i^l\,(1-\nu_i^2)^{\frac{\nu}{2}}\,d\nu_i\,,\\
H_\tau^\nu(i,\alpha,k,\beta) &= \int_1^\infty\int_1^\infty e^{-\alpha\mu_1} e^{-\beta\mu_2}\,\mu_1^i\,\mu_2^k\,Q_\tau^\nu(\mu_+)\,P_\tau^\nu(\mu_-)\times\\
&\qquad\times(\mu_1^2-1)^{\frac{\nu}{2}}\,(\mu_2^2-1)^{\frac{\nu}{2}}\,d\mu_1\,d\mu_2\,.
\end{aligned} \tag{11}$$

Die neuen Integrale ergaben sich wie folgt:

$$\begin{aligned}
&I(2,0,1,0,0,0,0,0) =\\
&= \frac{R^5}{8}\,[H_0^0(2,R;2,\tfrac{1}{2}R)\,G_0^0(0,R)\,G_0^0(0,\tfrac{1}{2}R) + C_1 -\\
&\quad - H_0^0(2,R,0,\tfrac{1}{2}R)\,G_0^0(0,R)\,G_0^0(2,\tfrac{1}{2}R) - C_2 -\\
&\quad - H_0^0(0,R,2,\tfrac{1}{2}R)\,G_0^0(2,R)\,G_0^0(0,\tfrac{1}{2}R) - C_3 +\\
&\quad + H_0^0(0,R;0,\tfrac{1}{2}R)\,G_0^0(2,R)\,G_0^0(2,\tfrac{1}{2}R) + C_4].
\end{aligned}$$

$$I\,(2,\,0,\,1,\,0,\,0,\,0,\,\underline{1},\,0) =$$

$$= \frac{R^6}{16}\,[H_0^0\,(2,\,R;\,3,\,\tfrac{1}{2}\,R)\,G_0^0\,(0,\,R)\,G_0^0\,(0,\,\tfrac{1}{2}\,R) + C_5 +$$
$$+ H_0^0\,(2,\,R;\,2,\,\tfrac{1}{2}\,R)\,G_0^0\,(0,\,R)\,G_0^0\,(1,\,\tfrac{1}{2}\,R) + C_6 -$$
$$- H_0^0\,(2,\,R;\,1,\,\tfrac{1}{2}\,R)\,G_0^0\,(0,\,R)\,G_0^0\,(2,\,\tfrac{1}{2}\,R) - C_7 -$$
$$- H_0^0\,(2,\,R;\,0,\,\tfrac{1}{2}\,R)\,G_0^0\,(0,\,R)\,G_0^0\,(3,\,\tfrac{1}{2}\,R) - C_8 -$$
$$- H_0^0\,(0,\,R;\,3,\,\tfrac{1}{2}\,R)\,G_0^0\,(2,\,R)\,G_0^0\,(0,\,\tfrac{1}{2}\,R) - C_9 -$$
$$- H_0^0\,(0,\,R;\,2,\,\tfrac{1}{2}\,R)\,G_0^0\,(2,\,R)\,G_0^0\,(1,\,\tfrac{1}{2}\,R) - C_{10} +$$
$$+ H_0^0\,(0,\,R;\,1,\,\tfrac{1}{2}\,R)\,G_0^0\,(2,\,R)\,G_0^0\,(2,\,\tfrac{1}{2}\,R) + C_{11} +$$
$$+ H_0^0\,(0,\,R;\,0,\,\tfrac{1}{2}\,R)\,G_0^0\,(2,\,R)\,G_0^0\,(3,\,\tfrac{1}{2}\,R) + C_{12}]\,.$$

$$I\,(2,\,0,\,1,\,0,\,0,\,0,\,2,\,0) =$$

$$= \frac{R^7}{32}\,[H_0^0\,(2,\,R;\,4,\,\tfrac{1}{2}\,R)\,G_0^0\,(0,\,R)\,G_0^0\,(0,\,\tfrac{1}{2}\,R) + C_{13} +$$
$$+ 2\,H_0^0\,(2,\,R;\,3,\,\tfrac{1}{2}\,R)\,G_0^0\,(0,\,R)\,G_0^0\,(1,\,\tfrac{1}{2}\,R) + 2\,C_{14} -$$
$$- 2\,H_0^0\,(2,\,R;\,1,\,\tfrac{1}{2}\,R)\,G_0^0\,(0,\,R)\,G_0^0\,(3,\,\tfrac{1}{2}\,R) - 2\,C_{15} -$$
$$- H_0^0\,(2,\,R;\,0,\,\tfrac{1}{2}\,R)\,G_0^0\,(0,\,R)\,G_0^0\,(4,\,\tfrac{1}{2}\,R) - C_{16} -$$
$$- H_0^0\,(0,\,R;\,4,\,\tfrac{1}{2}\,R)\,G_0^0\,(2,\,R)\,G_0^0\,(0,\,\tfrac{1}{2}\,R) - C_{17} -$$
$$- 2\,H_0^0\,(0,\,R;\,3,\,\tfrac{1}{2}\,R)\,G_0^0\,(2,\,R)\,G_0^0\,(1,\,\tfrac{1}{2}\,R) - 2\,C_{18} +$$
$$+ 2\,H_0^0\,(0,\,R;\,1,\,\tfrac{1}{2}\,R)\,G_0^0\,(2,\,R)\,G_0^0\,(3,\,\tfrac{1}{2}\,R) + 2\,C_{19} +$$
$$+ H_0^0\,(0,\,R;\,0,\,\tfrac{1}{2}\,R)\,G_0^0\,(2,\,R)\,G_0^0\,(4,\,\tfrac{1}{2}\,R) + C_{20}]\,.$$

$$I\,(1,\,1,\,1,\,0,\,0,\,0,\,0,\,0) =$$

$$= \frac{R^5}{12}\,\{[3\,H_0^0\,(2,\,R;\,2,\,\tfrac{1}{2}\,R) - H_0^0\,(0,\,R;\,2,\,\tfrac{1}{2}\,R)]\,G_0^0\,(0,\,\tfrac{1}{2}\,R) -$$
$$-[3\,H_0^0\,(2,\,R;\,0,\,\tfrac{1}{2}\,R) - H_0^0\,(0,\,R;\,0,\,\tfrac{1}{2}\,R)]\,G_0^0\,(2,\,\tfrac{1}{2}\,R) -$$
$$- 2\,H_2^0\,(0,\,R;\,2,\,\tfrac{1}{2}\,R)\,G_2^0\,(0,\,\tfrac{1}{2}\,R) -$$
$$- 2\,H_2^0\,(0,\,R;\,0,\,\tfrac{1}{2}\,R)\,G_2^0\,(2,\,\tfrac{1}{2}\,R)\}.$$

$$I\,(1,\,1,\,1,\,0,\,0,\,0,\,1,\,0) =$$

$$= \frac{R^6}{24}\,\{[3\,H_0^0\,(2,\,R;\,3,\,\tfrac{1}{2}\,R) - H_0^0\,(0,\,R;\,3,\,\tfrac{1}{2}\,R)]\,G_0^0\,(0,\,\tfrac{1}{2}\,R) +$$
$$+ [3\,H_0^0\,(2,\,R;\,2,\,\tfrac{1}{2}\,R) - H_0^0\,(0,\,R;\,2,\,\tfrac{1}{2}\,R)]\,G_0^0\,(1,\,\tfrac{1}{2}\,R) -$$

$$- [3\, H_0^0 (2, R; 1, \tfrac{1}{2} R) - H_0^0 (0, R; 1, \tfrac{1}{2} R)]\, G_0^0 (2, \tfrac{1}{2} R) -$$
$$- [3\, H_0^0 (2, R; 0, \tfrac{1}{2} R) - H_0^0 (0, R; 0, \tfrac{1}{2} R)]\, G_0^0 (3, \tfrac{1}{2} R) -$$
$$- 2\, H_2^0 (0, R; 3, \tfrac{1}{2} R)\, G_2^0 (0, \tfrac{1}{2} R) - 2\, H_2^0 (0, R; 2, \tfrac{1}{2} R)\, G_2^0 (1, \tfrac{1}{2} R) +$$
$$+ 2\, H_2^0 (0, R; 1, \tfrac{1}{2} R)\, G_2^0 (2, \tfrac{1}{2} R) + 2\, H_2^0 (0, R; 0, \tfrac{1}{2} R)\, G_2^0 (3, \tfrac{1}{2} R)\} .$$

$$I (1, 1, 1, 0, 0, 0, 2, 0) =$$

$$= \frac{R^7}{48}\{[\, 3\, H_0^0 (2, R; 4, \tfrac{1}{2} R) - H_0^0 (0, R; 4, \tfrac{1}{2} R)]\, G_0^0 (0, \tfrac{1}{2} R) +$$
$$+ 2[3\, H_0^0 (2, R; 3, \tfrac{1}{2} R) - H_0^0 (0, R; 3, \tfrac{1}{2} R)]\, G_0^0 (1, \tfrac{1}{2} R) -$$
$$- 2[3\, H_0^0 (2, R; 1, \tfrac{1}{2} R) - H_0^0 (0, R; 1, \tfrac{1}{2} R)]\, G_0^0 (3, \tfrac{1}{2} R) -$$
$$- [3\, H_0^0 (2, R; 0, \tfrac{1}{2} R) - H_0^0 (0, R; 0, \tfrac{1}{2} R)]\, G_0^0 (4, \tfrac{1}{2} R) -$$
$$- 2\, H_2^0 (0, R; 4, \tfrac{1}{2} R)\, G_2^0 (0, \tfrac{1}{2} R) - 4\, H_2^0 (0, R; 3, \tfrac{1}{2} R)\, G_2^0 (1, \tfrac{1}{2} R) +$$
$$+ 4\, H_2^0 (0, 2; 1, \tfrac{1}{2} R)\, G_2^0 (3, \tfrac{1}{2} R) + 2\, H_2^0 (0, R; 0, \tfrac{1}{2} R)\, G_2^0 (4, \tfrac{1}{2} R)\}.$$

$$I (2, 0, \tfrac{1}{2}, \tfrac{1}{2}, 0, 0, 0, 0) =$$

$$= \frac{R^0}{12}\{[3\, H_0^0 (2, R; 2, \tfrac{1}{2} R) - H_0^0 (2, R; 0, \tfrac{1}{2} R)]\, G_0^0 (0, R) -$$
$$- [3\, H_0^0 (0, R; 2, \tfrac{1}{2} R) - H_0^0 (0, R; 0, \tfrac{1}{2} R)]\, G_0^0 (2, R) -$$
$$- 2\, H_2^0 (2, R; 0, \tfrac{1}{2} R)\, G_2^0 (0, R) + 2\, H_2^0 (0, R; 0, \tfrac{1}{2} R)\, G_2^0 (2, R)\}.$$

$$I (2, 0, \tfrac{1}{2}, \tfrac{1}{2}, 0, 0, \underline{1}, 0) =$$

$$= \frac{R^6}{120}\{5[3\, H_0^0 (2, R; 3, \tfrac{1}{2} R) - H_0^0 (2, R; 1, \tfrac{1}{2} R)]\, G_0^0 (0, R) -$$
$$- 5[3\, H_0^0 (0, R; 3, \tfrac{1}{2} R) - H_0^0 (0, R; 1, \tfrac{1}{2} R)]\, G_0^0 (2, R) +$$
$$+ 3[5\, H_1^0 (2, R; 2, \tfrac{1}{2} R) - 3\, H_1^0 (2, R; 0, \tfrac{1}{2} R)]\, G_1^0 (0, R) -$$
$$- 3[5\, H_1^0 (0, R; 2, \tfrac{1}{2} R) - 3\, H_1^0 (0, R; 0, \tfrac{1}{2} R)]\, G_1^0 (2, R) -$$
$$- 10\, H_2^0 (2, R; 1, \tfrac{1}{2} R)\, G_2^0 (0, R) + 10\, H_2^0 (0, R; 1, \tfrac{1}{2} R)\, G_2^0 (2, R) -$$
$$- 6\, H_3^0 (2, R; 0, \tfrac{1}{2} R)\, G_3^0 (0, R) + 6\, H_3^0 (0, R; 0, \tfrac{1}{2} R)\, G_3^0 (2, R)\}.$$

$$I (2, 0, \tfrac{1}{2}, \tfrac{1}{2}; 0, 0, 0, 1) =$$

$$= \frac{R^6}{120}\{5[3\, H_0^0 (2, R; 3, \tfrac{1}{2} R) - H_0^0 (2, R; 1, \tfrac{1}{2} R)]\, G_0^0 (0, R) -$$
$$- 5[3\, H_0^0 (0, R; 3, \tfrac{1}{2} R) - H_0^0 (0, R; 1, \tfrac{1}{2} R)]\, G_0^0 (2, R) -$$
$$- 3[5\, H_1^0 (2, R; 2, \tfrac{1}{2} R) - 3\, H_1^0 (2, R; 0, \tfrac{1}{2} R)]\, G_1^0 (0, R) +$$

$$+ 3\,[5\,H_1^0(0,R;2,\tfrac{1}{2}R) - 3\,H_1^0(0,R;0,\tfrac{1}{2}R)]\,G_1^0(2,R) -$$
$$- 10\,H_2^0(2,R;1,\tfrac{1}{2}R)\,G_2^0(0,R) + 10\,H_2^0(0,R;1,\tfrac{1}{2}R)\,G_2^0(2,R) +$$
$$+ 6\,H_3^0(2,R;0,\tfrac{1}{2}R)\,G_3^0(0,R) - 6\,H_3^0(0,R;0,\tfrac{1}{2}R)\,G_3^0(2,R)\}\,.$$

$$I(2,0,\tfrac{1}{2},\tfrac{1}{2},0,0,\underline{1},\underline{1}) =$$
$$= \frac{R^7}{168}\{[105\,H_0^0(2,R;4,\tfrac{1}{2}R) - 70\,H_0^0(2,R;2,\tfrac{1}{2}R) +$$
$$+ 21\,H_0^0(2,R;0,\tfrac{1}{2}R)]\,G_0^0(0,R) -$$
$$- [105\,H_0^0(0,R;4,\tfrac{1}{2}R) - 70\,H_0^0(0,R;2,\tfrac{1}{2}R) +$$
$$+ 21\,H_0^0(0,R;0,\tfrac{1}{2}R)]\,G_0^0(2,R) -$$
$$- [140\,H_2^0(2,R;2,\tfrac{1}{2}R) - 60\,H_2^0(2,R;0,\tfrac{1}{2}R)]\,G_2^0(0,R) +$$
$$+ [140\,H_2^0(0,R;2,\tfrac{1}{2}R) - 60\,H_2^0(0,R;0,\tfrac{1}{2}R)]\,G_2^0(2,R) +$$
$$+ 24\,H_4^0(2,R;0,\tfrac{1}{2}R)\,G_4^0(0,R) -$$
$$- 24\,H_4^0(0,R;0,\tfrac{1}{2}R)\,G_4^0(2,R)\}\,.$$

$$I(1,1,\tfrac{1}{2},\tfrac{1}{2},0,0,0,0) =$$
$$= \frac{R^5}{90}[45\,H_0^0(2,R;2,\tfrac{1}{2}R) - 15\,H_0^0(2,R;0,\tfrac{1}{2}R) -$$
$$- 15\,H_0^0(0,R;2,\tfrac{1}{2}R) + 5\,H_0^0(0,R;0,\tfrac{1}{2}R) +$$
$$+ 4\,H_2^0(0,R;0,\tfrac{1}{2}R)]\,.$$

$$I(1,1,\tfrac{1}{2},\tfrac{1}{2},0,0,\underline{1},0) =$$
$$= \frac{R^6}{180}[45\,H_0^0(2,R;3,\tfrac{1}{2}R) - 15\,H_0^0(2,R;1,\tfrac{1}{2}R) -$$
$$- 15\,H_0^0(0,R;3,\tfrac{1}{2}R) + 5\,H_0^0(0,R;1,\tfrac{1}{2}R) +$$
$$+ 4\,H_2^0(0,R;1,\tfrac{1}{2}R)]\,.$$

$$I(1,1,\tfrac{1}{2},\tfrac{1}{2},0,0,\underline{1},\underline{1}) =$$
$$= \frac{R^7}{2520}[315\,H_0^0(2,R;4,\tfrac{1}{2}R) - 210\,H_0^0(2,R;2,\tfrac{1}{2}R) +$$
$$+ 63\,H_0^0(2,R;0,\tfrac{1}{2}R) - 105\,H_0^0(0,R;4,\tfrac{1}{2}R) +$$
$$+ 70\,H_0^0(0,R;2,\tfrac{1}{2}R) - 21\,H_0^0(0,R;0,\tfrac{1}{2}R) +$$
$$+ 56\,H_2^0(0,R;2,\tfrac{1}{2}R) - 24\,H_2^0(0,R;0,\tfrac{1}{2}R)]\,.$$

$C_i = 3\,H_1^0G_1^0G_1^0 + 5\,H_2^0G_2^0G_2^0 + 7\,H_3^0G_3^0G_3^0 + 9\,H_4^0G_4^0G_4^0$ mit den Argumenten in den betreffenden Reihen.

LITERATUR

1. W. Heitler and F. London, Z. Phys., **44**, 455, 1927.
2. F. Hund, Z. Phys., **73**, 1, 1931.
3. R. S. Mulliken, J. Chem. Phys., **1**, 492, 1933; **3**, 375, 1935; Chem. Rev., **9**, 347, 1931.
4. E. Hückel, Z. Phys., **60**, 423, 1930; **72**, 310, 1931.
5. J. Lennard-Jones, Trans. Faraday Soc., **25**, 668, 1929.
6. C. A. Coulson, Proc. Cambridge Phil. Soc., **34**, 204, 1938.
7. A. A. Frost and J. Braunstein, J. Chem. Phys., **19**, 1133, 1951.
8. W. Ritz, J. f. reine und angew. Math., **131**, 1, 1909.
9. Y. Sugiura, Z. Phys., **45**, 484, 1927.
10. N. Rosen, Phys. Rev., **38**, 255, 2099, 1931.
11. M. Delbrück, Ann. Phys., **5**, 36, 1930.
12. J. H. Bartlett und B. H. Furry, Phys. Rev., **38**, 1615, 1931; **39**, 209, 1932.
13. J. H. Bartlett, Phys. Rev., **37**, 507, 1931.
14. W. E. Bleich und J. E. Mayer, J. Chem. Phys., **2**, 252, 1934.
15. A. L. Sklar, J. Chem. Phys., **6**, 645, 1938.
16. A. L. Sklar und R. H. Lyddane, J. Chem. Phys., **7**, 374, 1939.
17. P. J. Wheatley und J. W. Linnett, Trans. Faraday Soc., **45**, 897, 1949.
18. R. G. Parr und B. L. Crawford, J. Chem. Phys., **16**, 1049, 1948.
19. J. O. Hirschfelder und J. W. Linnett, J. Chem. Phys., **18**, 130, 1950.
20. F. Berencz, Acta Phys. Hung., **6**, 423, 1957; **10**, 1, 1959; **9**, 381, 1959.
21. R. Pauncz, Acta Phys. Hung., **4**, 237, 1954.
22. H. J. Kopineck, Z. Naturforschg., **5**, 420, 1950.
23. M. Kotani, A. Amemiya und T. Simose, Proc. Phys. Math. Soc. Japan, **20**, extra No 1, 1938; **22**, extra No 2, 1940.

ОПРЕДЕЛЕНИЕ $1s2s\,^1S$-СОСТОЯНИЯ МОЛЕКУЛЫ ВОДОРОДА МЕТОДОМ МОЛЕКУЛЯРНЫХ ОРБИТ

Ф. БЕРЕНЦ

Резюме

Применением метода молекулярных орбит в работе определяется энергия связи $1s2s\,^1S$-состояния молекулы водорода. Определяются молекулярные интегралы между $1s$- и $2s$-электронами.

RELAXATION OF THE LONG-RANGE ORDER PARAMETER IN THE DOMAINS OF ORDER OF THE ALLOY Cu_3Au*

By

H. ELKHOLY

PHYSICS DEPARTMENT, FACULTY OF SCIENCE, CAIRO UNIVERSITY, EGYPT – U. A. R.

(Presented by Z. Gyulai .— Received 17. I. 1963)

Data are reported, which describe the isothermal time variation of the Hall constant and the electrical resistance of an annealed specimen following a quench from different high temperatures (below T_c) to approximately the same low temperature. It was found that the kinetical equations of NOWICK and WEISBERG failed to interpret the results, and instead it was shown that the kinetics of ordering inside a domain depends on both the lower and the higher temperatures of the heat treatment and can be described by a function of the form $\psi(T_2, T_1)\ \varphi(t)$.

Introduction

At as early a date as 1936, a careful study of ordering kinetics in the alloy Cu_3Au by SYKES and EVANS [1] showed that the process of formation of order from the disordered state was far more complex than had originally been [2] supposed. It was shown that ordering took place by a process of nucleation and growth.

Recently, extensive work on Cu_3Au alloy has been carried out by NAGY and ELKHOLY [3], [4] in an attempt to separate the different phenomena arising during the course of ordering transformation. They analysed the kinetics of that alloy dividing it into several distinct steps, which were ascribed to various physical processes. First an embryo formation process was observed. The second step was due to the establishment of equilibrium order within the domains themselves. The third process, with an exponential time dependence, was found to correspond to domain wall elimination.

The present work is a completion of the above-mentioned work. It describes the change in the kinetics of long-range order in an already long-range ordered specimen. This work differs from that of BURNS and QUIMBY [5] in that it utilizes for the first time the Hall coefficient together with resistivity measurements, second in that the investigation is extended to a range of time much greater than that used by other investigators [5], [6], and third in that the results here could not be interpreted in terms of the kinetic equations predicted from the theory of NOWICK and WEISBERG [7].

* This work has been carried out by the author in Budapest in The Central Research Institute of Physics during his leave of absence in Hungary in 1961.

Experimental method*

An alloy of atomic composition of $25.90 \pm 0.05\%$ gold and $74.10 \pm 0.05\%$ copper served as our sample. This alloy was prepared from pure gold and copper and was melted in a graphite crucible by high frequency technique. In order to make the alloy more homogeneous it was remelted several times. After remelting, the alloy was homogenized by heating in hydrogen for 10 hours at 800 °C. The resulting ingot was rolled to a thickness of 20 microns. After machining, the sample was annealed in hydrogen for 10 hours at 700°C. The sample had the form of a flat plate 10 cm long, 1 cm wide and 0.002 cm thick. Three Hall probes were cut from the sample itself; two probes at one side and 4 mm apart, and one probe at the other side of the sample. The sample and its holder were sealed into a glass bulb and evacuated up to 10^{-5} mm Hg. The sample was heated by a 200 watts electric furnace surrounding the glass bulb and controlled up to $\pm$ 0.1°C by a proportional temperature regulator. Both Hall voltages and electrical resistance were measured on the same sample. The Hall voltages were measured by a d.c. photocell galvanometer of a maximum voltage sensitivity of 2×10^{-8} volts per one division of a scale. A magnetic field of 11.800 oersted and a sample current of approximately 2 A were used. The electrical resistance was determined by measuring the current passing through the sample, and the potential drop between the two Hall probes, lying on one side of the sample, by means of a potentiometer—galvanometer system.

Results and discussion

Figs. 1 and 2 show the isothermal time variation of the Hall coefficient (R_H) and the electrical resistance (r) of an annealed specimen following a quench from different high temperatures, below T_c (indicated at each curve)

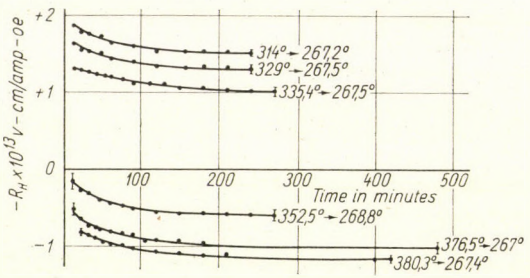

Fig. 1. Isothermal time variation of the Hall constant R_H of an annealed specimen following a quench from different indicated high temperatures to approximately 267.5 °C

* For a detailed description of the experimental arrangements, see reference [8].

to a fixed lower temperature of approximately 267.5°C (the exact values of the lower temperatures are indicated at each curve). The quench to the lower temperature was done after the sample had been annealed at the higher

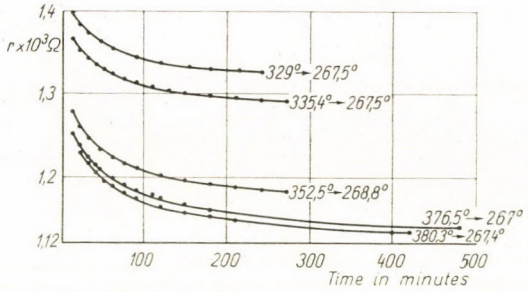

Fig. 2. Isothermal time variation of the resistance r of an annealed specimen following a quench from different indicated high temperatures to approximately 267.5 °C

temperature for several hours (ranging from 8 to 30 hours) till equilibrium was nearly obtained and a domain structure of equilibrium order and average domain size was established. The following features of the graphs are particularly to be noted for future reference:

a) Roughly about 80% of the change in R_H and r dependent on the total order occurs before the first observation is made: hence only about 20% of the complete ordering process is observed. This means that most of the changes occur in the first 10 minutes which we could not measure due to the construction of the sample which prevents temperature equilibrium to be established before 5—10 minutes have elapsed.

b) The shape of these graphs is radically different from that of single-step heat treatment reported in references [3, 4]. It is clear from the quick saturation shown by the graphs that the rate of ordering here is rather large in comparison with the rate of ordering in a single-step measurement. Actually these graphs describe the true kinetics of ordering free from domain growth phenomena, and therefore correspond to the relaxation of the long-range order parameters S in the domains.

c) The rate of ordering in a domain increases with the decrease of the difference between the annealing temperature (the higher temperature) and the temperature to which the sample is quenched (the lower temperature).

d) It is clear from Figs. 1 and 2 that, as the temperature of annealing (the higher temperature) increases, the equilibrium values of $-R_H$ and r successively decrease. Here the sample was quenched to the same lower temperature (approximately 267.5°C) which means that the function of the long-range order parameter S is the same, and this difference in the equilibrium values of $-R_H$ and r is mainly due to the effect of the higher temperature,

resp. to the effect of domain size. This fact is conclusive evidence for the supposition of NAGY and ELKHOLY [3, 4] that the higher the temperature of ordering, the bigger the domain size and the less the domain wall density (decrease of the values of $-R_H$ and r).

It should be mentioned that the kinetic equations of NOWICK and WEISBERG failed to fit the data represented by Figs. 1 and 2. Anyhow, from the following simple mathematical considerations, one finds that the kinetics of ordering inside a domain may be described by a function of the form $\psi(T_2, T_1)\,\varphi(t)$.

Consider the curves of Fig. 2, and suppose that the kinetics here can be expressed in the form:

$$r(T_2, t) = C(T_1) + \psi(T_2, T_1)\,\varphi(t), \qquad T_1 > T_2, \tag{1}$$

where $C(T_1)$ corresponds to the effect of domain size, $\psi(T_2, T_1)$ corresponds to the effect of the equilibrium long-range order parameter S at the lower and the higher temperatures, and $\varphi(t)$ is the universal function of time.

Consider two measurements at different higher temperatures T_1 and T_1', quenched to the same lower temperature T_2 (as is the case in our measurements). In this case we have:

$$r(T_2, t) = C(T_1) + \psi(T_2, T_1)\,\varphi(t). \tag{2}$$

$$r'(T_2, t) = C(T_1') + \psi(T_2, T_1')\,\varphi(t). \tag{3}$$

From eq. (3) we have

$$\varphi(t) = \frac{r'(T_2, t) - C(T_1')}{\psi(T_2, T_1')}. \tag{4}$$

Substituting eq. (4) into eq. (2) we get

$$r(T_2, t) = K_1 + K_2 r'(T_2, t), \tag{5}$$

where

$$K_1 = C(T_1) - C(T')\,\frac{\psi(T_2, T_1)}{\psi(T_2, T_1')}$$

and

$$K_2 = \frac{\psi(T_2, T_1)}{\psi(T_2, T_1')}.$$

Therefore, if the kinetics of ordering inside a domain can be represented by a function of the form $\psi(T_2, T_1)\,\varphi(t)$, then there must be a linear relationship between the resistivity values at the same instant. This was in fact

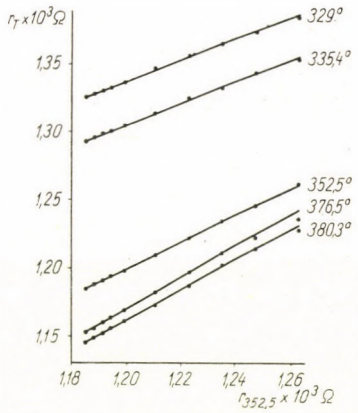

Fig. 3. A plot showing the linear relationship between r at 352.5 °C and r at different indicated temperatures, at the same time

found, and is clear from Fig. 3 which shows the relations between r at 352.5°C and r at different temperatures at the same time.

Acknowledgement

The author is greatly indebted to Prof. E. NAGY and to Mr. I. NAGY for their helpful assistance and discussions.

REFERENCES

1. C. SYKES and H. EVANS, J. Inst. Met., **58**, 255, 1936.
2. W. L. BRAGG and E. J. WILLIAMS, Proc. Roy. Soc., A **145**, 699, 1934; A **151**, 540, 1935.
3. E. NAGY and I. NAGY, J. Phys. Chem. Solids, **23**, 1605, 1962.
4. H. ELKHOLY and E. NAGY, J. Phys. Chem. Solids, **23**, 1613, 1962.
5. F. P. BURNS and S. L. QUIMBY, Phys. Rev., **97**, 1567, 1955.
6. L. R. WEISBERG and S. L. QUIMBY, Phys. Rev., **110**, 338, 1958.
7. A. S. NOWICK and L. R. WEISBERG, Acta Met., **6**, 258, 1958.
8. H. ELKHOLY, Acta Phys. Hung., **13**, 447, 1961.

РЕЛАКСАЦИЯ ДАЛЬНОДЕЙСТВУЮЩИХ ПАРАМЕТРОВ В ДОМЕНАХ, ПОДОБНЫХ СПЛАВУ Cu_3Au

Г. ЭЛЬКОЛИ

Р е з ю м е

Приводятся данные, описывающие изотермическое временное изменение постоянной Холла и электрического сопротивления размягчённого образца, последовательно охлаждённого от различных высоких температур (ниже T_c) приближённо до той же низкой температуры. Найдено, что кинетическое уравнение Новика и Вайсберга не даёт интерпретации результатов. Показывается далее, что кинетика упорядочения внутри домена как при низшей, так и при высшей температурах зависит от термической обработки и имеет форму $\psi(T_2, T_1)\varphi(t)$.

COMMUNICATIONES BREVES

MICRO-INHOMOGENEITIES IN Ge SINGLE CRYSTALS

By

A. Lőrinczy, T. Németh

RESEARCH INSTITUTE FOR TECHNICAL PHYSICS OF THE HUNGARIAN ACADEMY OF SCIENCES,

and

P. Szebeni

INDUSTRIAL RESEARCH INSTITUTE FOR TELECOMMUNICATION TECHNIQUE, BUDAPEST

(Received: 8. II. 1962)

For the manufacture of semiconductor devices the production of Ge single crystals of high purity and homogeneity is required; a demand which seemed to be satisfied by the usual methods. However, in the last ten years a fuller knowledge of the characteristics of Ge showed that in "homogeneous" single crystals there are considerable local fluctuations and micro-inhomogeneities. These fluctuations appear above all in the local variations of the concentration of the dopping material. The phenomenon was first observed by Pfann and Scaff [1], and later others also dealt with this problem [2, 3, 4]. The presence of the inhomogeneities in Ge single crystals is of great importance, since the internal electric field strength arising under the influence of the concentration gradient is comparable to e.g. the drawing field of the diffusion transistor and on the other hand the examination of the fluctuations can give fuller information on the growing mechanism of the single crystals. Our investigations were carried out on Ge single crystals produced by horizontal zone melting. From the single crystals, parallel to the growing direction (111), slices were cut out which were examined after grinding and chemical polishing. The best result concerning the detection of the striations was obtained by the anodic etching of Ge in 10% KOH solution at 70°C. The optimal value of the current density was 0.6—1 A/cm^2. Some minutes are necessary for the striations to appear. The duration of the anodic etching changes depending of the surface treatment. The characteristic lines of the micro-inhomogeneities appear:

on an original Ge surface after one minute,

on a surface ground and etched in CP—4 after two minutes,

on a surface mechanically polished (surface roughness approximately 1 μ) after five minutes.

On a surface ground Al_2O_3 (of a fineness of 305), striations do not appear, even after ten minutes.

During this series of tests an unambiguous relation was found between surface quality and etching time. Striations can be developed on the surface of a Ge sample only if the surface layer damaged in the course of the prepara-

tion of the sample is first removed. The formation of the lines can be explained by the fact that the change of the rate of anodic solution of Ge depends on the concentration of the dopping material.

Such a difference appears, however, only in case of an undamaged lattice structure.

The experimental results are shown in Figs. 1 and 2, where striations developed by the above-mentioned method can be seen on Ge single crystals of *n*- and *p*-type. The striation distance in case of Ge of *n*-type was found

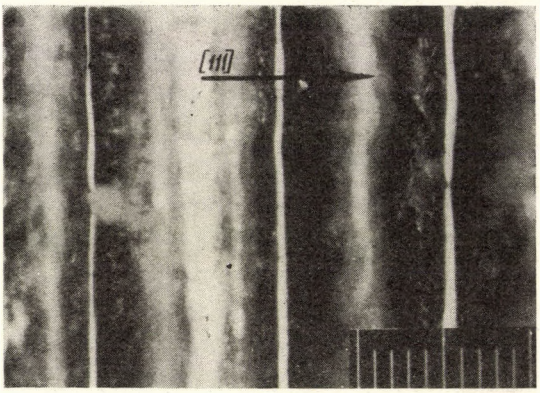

Fig. 1

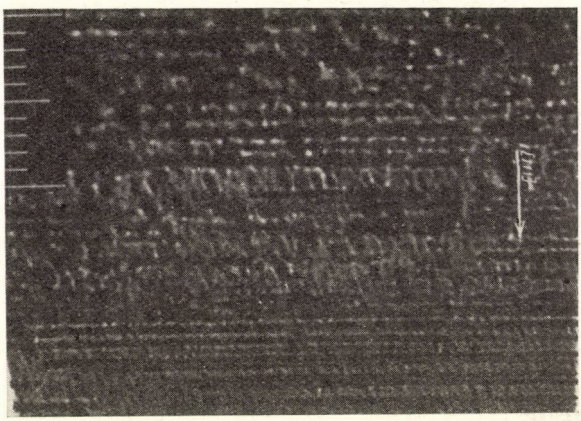

Fig. 2

to be 100 μ, in case of Ge of *p*-type 10 μ. The method by which, at a simultaneous heating of Ge and of the metal plate placed on it, the evaporation of the inhomogeneous Ge gives a picture of a striated structure on the metal, is less suitable. Using nickel on Ge of *n*-type the effect of the striations could be observed.

For the detection of micro-inhomogeneities electrically the most obvious method seems to be micro-scanning of one probe. Onto the ends of a chemically polished sample ohmic contacts were soldered and then the sample was connected to the terminals of a direct current generator. The potential difference between one of the end contacts and the probe placed on the surface was measured. The needle was put on the surface and moved in steps of $20\,\mu$ by means of a micro-manipulator keeping the needle pressure constant. Although in principle the change of the resistivity of the sample can be calculated from the differentiated curve of the potential, it cannot be used for evaluation purposes because of the large errors arising from the uncertainty of the point contact.

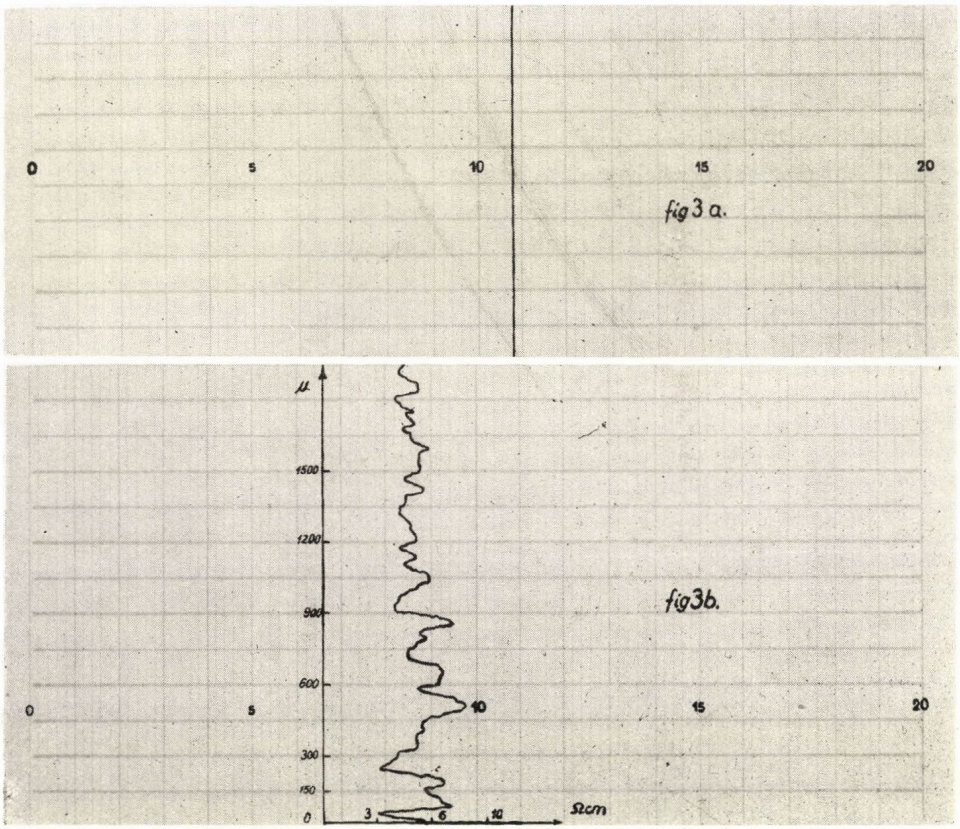

Fig. 3

In order to eliminate the errors of the above-mentioned method, a continuous sliding device of four probes was developed. The sample was fixed on the microscope stage. The micrometer screw of the stage, geared down, was operated continuously by an asynchronous motor. Thus, the

displacement rate of the sample was variable within the speed range of 1—50 μ/sec. The four tungsten needles embedded in resin and arranged in one plane, were put at an angle of 45° onto the surface of the sample. The two exterior needles were connected to the terminals of a current generator and the voltage appearing on the two inner needles was measured by the compensation method.

In Fig. 3 beside the current of constant value (curve 3a) the potential difference appearing on the inner needles (curve 3b) can be seen. These values were registered simultaneously by a compensograph. The measurement can be effectuated also visually, by occasional readings of the null-reading galvanometer of the bridge compensated to the average.

According to our measurements the fluctuation of the resistivity reaches 50%.

The striations detected by us appeared on the whole cross-section of the single crystal, with various periodicities even if the parameters of growing were changed. The distance of the striations was found to depend linearly on the rate of crystal growth and to be inversely proportional to the temperature gradient at the boundary surface of growth. It is remarkable and interesting that single crystals of *n*- and *p*-type containing donor and acceptor impurities show periodicities differing by orders of magnitude from each other. From

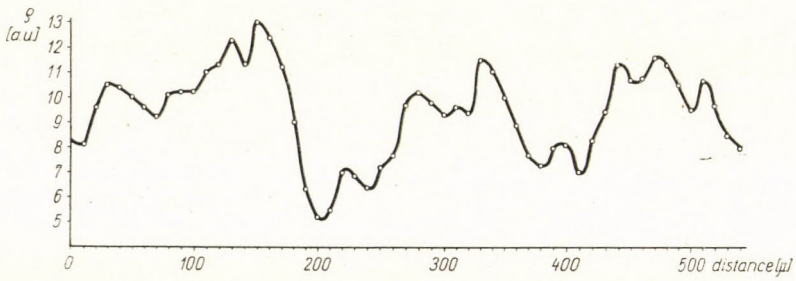

Fig. 4

this we came to the conclusion that the cause of the micro-inhomogeneities found by us must lie in the mechanism of crystal growth. In the course of the examination of the micro-inhomogeneities arising from inner reasons of crystal growth H. UEDA [5] found a relation between the striation period and the parameters of growth. This relation is only partly verified by our experiments. On the other hand, it is definitely refuted by the periodicities of the striations found on Ge of *n*- and *p*-type. Our statement is supported by the results of our experiments in which Ge single crystals were grown under absolutely the same conditions and only the chemical nature of the dopping material was changed in the growth of the single crystals.

Our results contradict the micro-inhomogeneities detected and studied by some authors [2, 3, 4].

These latter micro-inhomogeneities are undoubtedly caused by the mechanical instability of the crystal growing device (this is shown by the fact that the micro-inhomogeneities are to be found only within the surface layer of the single crystal ingots), resp. its heat asymmetry (this is indicated by the micro-inhomogeneities of spiral arrangement).

The aim of our further investigations is to clear up the causes of striation formation, with the help of the methods developed by us and others reported in the literature.

REFERENCES

1. W. Pfann and J. H. Scaff, Metals Trans., **185**, 389, 1949.
2. H. F. Bridges, J. H. Scaff and J. N. Shive, Transistor Technology **1**, 113, 1958.
3. A. C. English, J. Appl. Phys., **31**, 1948, 1960.
4. D. A. Petrov, Dokladi A. N., **139**, 933, 1961.
5. H. Ueda, J. Phys. Soc. Japan, **16**, 61, 1961.

THE EFFECT OF THE NON-ZERO NEUTRINO REST MASS ON THE DECAY RATE OF BOUND μ-MESONS

By

T. NAGY

INSTITUTE OF THEORETICAL PHYSICS, ROLAND EÖTVÖS UNIVERSITY, BUDAPEST

(Received 1. IX. 1962)

The negative μ-mesons in matter are captured atomically and with X-ray emission they reach the 1s state in a very short time. The bound muons disappear either by spontaneous decay or by nuclear capture.

According to the measurements [1] the decay rate of the negative muons (λ_-) is different from that of μ^+-mesons (λ_+): $\lambda_- \ (Z < 10) \approx \lambda_+$, for heavy elements the ratio $R = {}^{\lambda-(z)}/\lambda_+$ considerably decreases, and near $Z = 26$, $R > 1$. The Z-dependence of the decay rate may be expected on a theoretical basis as well: on the one hand the binding reduces the phase space, and on the other hand the muon has a certain momentum distribution which results in time dilatation — these effects tend to decrease $\lambda_-(Z)$ monotonically. At the same time the wave function of the decay electron cannot be considered a plane wave, the effect of the Coulomb field increases its amplitude near the nucleus. This latter effect tends to increase $\lambda_-(Z)$, so we may expect that R will have a maximum at a certain Z.

Recently, some efforts have been made to explain the measured data more exactly. ÜBERALL [2] used an approximation of the form: $R = 1 + a\frac{Z}{137} + b\left(\frac{Z}{137}\right)^2$, but the coefficient of the linear term turned out to be zero, i.e. (b being negative) R decreases monotonically with Z. The more recent calculations [3, 4, 5] have been made with more exact electron and muon wave functions. They have taken into account the finite size of the nucleus, nevertheless the results do not differ essentially from those obtained by ÜBERALL: the theoretical $\lambda_-(Z)$-curve decreases monotonically, and for heavy elements its decrease is less strong than it can be expected from the experiments. PALGI [6] performed a calculation with the assumption of the intermediate boson, but he could not account for the maximum either.

HUFF [5] tried to explain the disagreement between the experimental and theoretical curves by the conditions of the measurement. According to his explanation the discrepancy for heavy elements is caused by the fact that in the case of the bound muons the decay electrons are detected with reduced efficiency in consequence of the considerable modification of

their energy spectrum. To account for the maximum he assumes that the μ-capture γ-rays play a special role near iron. A recent measurement [7], according to which there is no essential difference in the μ-capture γ-spectra of iron and the neighbouring elements, contradicts this assumption.

Now we shall examine whether we can find a better explanation for the experimental data, if we assume that the rest mass of one of the decay neutrinos differs from zero. It is known that to exclude the possibility of the decay $\mu \to e + \gamma$ it has been assumed that two different kinds of neutrinos exist, one of which is connected with the muon, and the other with the electron [8, 9]. Some considerations [10] show that the rest mass of the so-called muon-neutrino (m_ω) can be assumed to be different from zero. The possible upper limit of m_ω is about 8 electron rest masses.

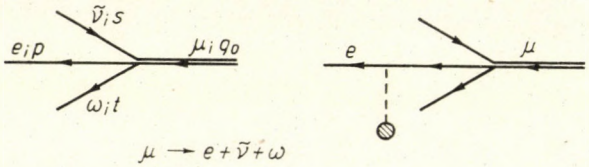

Fig. 1

In the following we shall restrict ourselves to the question whether we get a non-zero linear term in the approximation used by ÜBERALL, if $m_\omega \neq 0$. We take the following form of interaction:

$$H = 2\sqrt{2} f (\bar{\psi}_e O_\alpha \psi_\nu)(\bar{\psi}_\omega O_\alpha \bar{\psi}_\mu) + hc .$$

For the decay rate we get (see Fig. 1):

$$\lambda_- = 4 f^2 \int |\overline{M}|^2 (2\pi)^4 \delta (p + s + t - q) \frac{dq\, dp\, ds\, dt}{(2\pi)^{12}} ,$$

where

$$|\overline{M}|^2 = \frac{1}{8i\, p_0\, t_0\, s_0} \int d\mathfrak{r}\, d\mathfrak{r}'\, A_{\alpha\beta}(\mathfrak{r}, \mathfrak{r}')\, Sp\, B_{\alpha\beta}(\mathfrak{r}, \mathfrak{r}')\, e^{i\mathfrak{k}(\mathfrak{r}' - \mathfrak{r})},$$

$$A_{\alpha\beta}(\mathfrak{r}, \mathfrak{r}') = \sum_\mu (\bar{\varphi}_\mu(\mathfrak{r}')\, \bar{O}_\beta (m_\omega - i\hat{t})\, O_\alpha \varphi_\mu(\mathfrak{r})),$$

$$B_{\alpha\beta}(\mathfrak{r}, \mathfrak{r}') = (m_e - i\hat{p})\, P(\mathfrak{r})\, O_\alpha\, \hat{s}\, \overline{P(\mathfrak{r}')\, O_\beta} ,$$

$$\hat{s} = \gamma_\alpha s_\alpha , \quad \bar{O} = \gamma_4 O^+ \gamma_4 ,$$

$$k = s + t , \quad q = p + k .$$

The corresponding functions are:

$$\varphi_\mu(\mathfrak{r}) = \sqrt{\frac{a^3}{\pi}}\, e^{-ar}\left(1 + \frac{i\gamma}{2}\,\bar{\alpha}\mathfrak{n}\right) u_0\,,$$

$$P(\mathfrak{r}) = e^{-i\mathfrak{p}\mathfrak{r}} - (p_0 + m_\omega \gamma_4 + \nabla)\,\Pi(\mathfrak{r})\,,$$

where

$$\gamma = \frac{Z}{137}, \qquad a = m_\omega \gamma, \qquad \mathfrak{n} = \frac{\mathfrak{r}}{r}\,,$$

$$\Pi(\mathfrak{r}) = \int \frac{d\mathfrak{s}}{(2\pi)^3}\, \frac{e^{i\mathfrak{s}(\mathfrak{r}'-\mathfrak{r})}}{\mathfrak{s}^2 - \mathfrak{p}^2 - i\eta}\, V(\mathfrak{r}')\, e^{-i\mathfrak{p}\mathfrak{r}'}\, d\mathfrak{r}',$$

$$V(\mathfrak{r}) = -\frac{\gamma}{r}\, e^{-\beta r}, \qquad \eta \to 0\,, \qquad \beta \to 0$$

and

$$u_0 = \begin{pmatrix} 1 \\ 0 \\ 0 \\ 0 \end{pmatrix} \quad \text{or} \quad \begin{pmatrix} 0 \\ 1 \\ 0 \\ 0 \end{pmatrix}.$$

In the approximation used here:

$$\lambda_- = \lambda_-^0 + \lambda_-^1\, \gamma\,.$$

Performing the calculations we obtain:

$$\lambda_-^0 = \lambda^+, \quad \lambda_-^1 = 0\,,$$

where λ_+ is the decay rate of the positive muon, calculated with $m_\omega \neq 0$ and $m_e \neq 0$.

Thus we come to the conclusion that the assumption $m_\omega \neq 0$ also fails to explain the maximum of the $R(Z)$ curve near $Z = 26$.

Note. A new measurement has been reported in [11], in which no anomalously high decay rate has been found.

* * *

Acknowledgement. I wish to express my gratitude to Dr. K. NAGY for suggesting this problem, and for his valuable advice.

REFERENCES

1. D. D. YOVANOVITCH, Phys. Rev., **117**, 1580, 1960.
2. H. ÜBERALL, Phys. Rev., **119**, 365, 1960.
3. V. GILINSKY and J. MATTHEWS, Phys. Rev., **120**, 1450, 1960.
4. R. KRÜGER and J. ROTHLEITNER, Z. Physik, **164**, 330, 1961.
5. R. W. HUFF, Ann. Phys., **16**, 288, 1961.
6. L. PALGI, Issl. Teor. Fiz., (Trudy IFA AN ESSR), **16**, 69, 1961.
7. J. V. ALLABY et al., Phys. Rev., **125**, 2077, 1962.
8. T. D. LEE and C. N. YANG, Phys. Rev., **119**, 1410, 1960.
9. S. P. ROSEN, Phys. Rev., Letters, **4**, 613, 1960.
10. J. BAHCALL and R. B. CURTIS, Nuovo Cim., **21**, 423, 1961.
11. L. B. EGOROV et al., International Conference on High Energy Physics, Geneva, 1962.

ON THE POTENTIAL ENERGY FUNCTION OF DIATOMIC MOLECULES

By

M. R. KATTI and D. P. BATRA

DEFENCE SCIENCE LABORATORY, DELHI 6, INDIA

(Received 27. XI. 1962)

Recently, TIETZ [1] has proposed an analytical expression for the dotential energy of diatomic molecules. The function is represented by

$$U(r) = D_e\left[\frac{B}{r(1+Ar)} - \frac{C}{(1+Ar)}\right],$$

where D_e is the dissociation energy and A, B, C are constants. The function fulfils the necessary conditions that any P. E. function must satisfy and as a consequence gives the relations

$$C = 1 + 2Ar_e, \quad B = Ar_e^3 \quad \text{and} \quad K_e = \frac{2D_e A}{r_e(1+Ar_e)},$$

thus connecting A, B, C with the known molecular constants $k_e \cdot r_e$ and D_e. It is claimed by the author that this simple function is one among the few that are convenient to solve the Schrödinger equation when applying the perturbation method. Considering this merit of the expression, it was thought worth while to investigate its applicability and workability in connection with other problems, viz. prediction of molecular constants and construction of P. E. curves. The present note records a few observations in this connection.

Following VARSHNI's [2] analysis of P. E. functions, the above expression yields the following relations for a_e and $\omega_e \varkappa_e$:

$$a_e = \frac{\Delta - 2}{3} \cdot \frac{6B_e^2}{w_e}, \quad w_e \varkappa_e = \frac{4\Delta - \Delta^2 - 1}{3} \cdot \frac{W}{\mu_A},$$

where $Ar_e = \dfrac{\Delta}{1-\Delta}$ and Δ is SUTHERLAND's parameter. The values of a_e and $\omega_e \varkappa_e$ have been evaluated from these relations in the case of 23 diatomic molecules. The relevant molecular constants have been taken from HERZBERG [3]. The nature of the results obtained does not warrant their presentation here, however, it may be remarked that the values of a_e derived are

higher than those due to the relation from MORSE's function, which function has been assessed by VARSHNI [2] as giving highest percentage errors among the various functions considered by him. The relation for $\omega_e x_e$ gives negative values and is thus not applicable to any diatomic molecule.

The constants A, B, C involved in the above expression have been evaluated for all the molecules under consideration here, and in all these cases the three constants turned out to be negative. For N_2 the P. E. function $U(r)$ is represented by the equation

$$U(r) = D_e\left[\frac{1.258\,r - 1.237}{r(1 - 1.033\,r)}\right],$$

which gives negative values for certain values of r, which is meaningless. A similar behaviour is found for a number of molecules. Thus the P. E. function proposed by TIETZ is unsuitable for the type of study indicated above.

Another function

$$U(r) = D_e e^{-ar}\left[\frac{b}{1 - e^{-ar}} - c\right],$$

which is a modification of the one above, has been suggested by TIETZ [4]. Preliminary calculations show that it overcomes the defects of the first expression. In general its performance is similar to that of the function proposed by FROST and MUSULIN [2].

REFERENCES

1. T. TIETZ, Acta Phys. Hung., **13**, 359, 1961.
2. Y. P. VARSHNI, Rev. of Mod. Phys., **29**, 664, 1957.
3. G. HERZBERG, Spectra of Diatomic Molecules, Van Nostrand Company, Inc., Princeton, 1950.
4. T. TIETZ, private communication.

RECENSIONES

R. COURANT, **Methods of Mathematical Physics**

Vol. II., S. XXII + 830, J. Wiley, New York, London, 1962.

Es ist dies nicht eine Neuauflage sondern eine von COURANT verfasste Neuausgabe des zweiten Bandes des berühmten und von den theoretischen Physikern so hoch geschätzten »Courant-Hilbert«. Diese Neuausgabe, die 25 Jahre nach der ersten Ausgabe (in 1937) erschien, trägt naturgemäss der seither erfolgten Entwicklung der Mathematik Rechnung und unterscheidet sich vom deutschen Original, vom II. Band »Methoden der mathematischen Physik«, fast in allen wesentlichen Teilen, wie dies der Verfasser selbst im Vorwort der Neuausgabe feststellt. Das Werk befasst sich mit den partiellen Differentialgleichungen der theoretischen Physik und enthält die folgenden Kapitel. Nach dem I. Kapitel mit dem Titel: Einige einleitende Bemerkungen folgt im II. Kapitel: Die allgemeine Theorie der partiellen Differentialgleichungen erster Ordnung und danach im III. Kapitel: Differentialgleichungen höherer Ordnung. Dem folgen Kapitel IV: Potentialtheorie und Elliptische Differentialgleichungen, Kapitel V: Hyperbolische Differentialgleichungen mit zwei unabhängigen Variablen und Kapitel VI: Hyperbolische Differentialgleichungen für mehr als zwei unabhängige Variablen.

Der Band ist weitgehend unabhängig von dem im selben Verlag erschienenen ersten Band desselben Werkes. Den nun vorliegenden ersten zwei Bänden soll auch ein dritter Band folgen, der sich mit Existenzbeweisen und der Konstruktion der Lösungen befasst.

Die hervorragenden Eigenschaften, insbesondere die Präzisität und Klarheit mit de die schwierigsten Probleme behandelt werden, die der berühmten ersten Ausgabe eigen sind, kennzeichnen auch die Neuausgabe. So wie die erste Ausgabe dieses Meisterwerkes sich in einer der schönsten Epochen der theoretischen Physik als grundlegend erwiesen hat, wird dies auch für die Neuausgabe in der jetzt stattfindenden ausserordentlich raschen Entwicklung unseres Wissensgebietes bestimmt der Fall sein.

P. GOMBÁS

EUGEN MERZBACHER: **Quantum Mechanics**

John Wiley and Sons, Inc., New York—London, 1961, 544 pages

Nowadays, there is hardly any branch of physics which can be approached without a knowledge of quantum mechanics. The purpose of MERZBACHER's book is to give students and working physicists a thorough knowledge of quantum mechanics, enabling them to perform quantum mechanical calculations and to read current theoretical literature. The presentation of the subject is also simple enough to be accessible for self-study and yet sufficiently complete to serve as a handbook for the research worker.

In the first twelve chapters ordinary wave mechanics is developed inductively, enabling the reader to handle energy-level and scattering problems. The discussion of spin as a system with only two basic states is elaborated in Chapter 13. It offers the reader an opportunity to make himself familiar with matrix mechanics and to clarify the physical meaning of a quantum state. In the next two chapters wave and matrix mechanics are united in the general Dirac's bra-ket formulation. This general formulation of quantum dynamics in terms of state vectors and linear operators is subsequently employed throughout the remainder of the book. The bound state and time-dependent perturbation theory is more elaborate than usual; the treatment of the formal theory of scattering is intended as a bridge from elementary quantum mechanics to recent theoretical developments. The final chapter on the theory of angular

momentum should give an idea of the economies in work which group theoretical methods offer.

The 176 exercises are designed to illustrate and supplement the text; the 77 problems, which are given at the chapter endings, are extensions and applications of the subject. The exercises and problems form an integral part of the book.

The book is a fine example of good textbook writing for postgraduate research students and can be strongly recommended.

D. KISDI

E. A. MOELWYN-HUGHES: Physical Chemistry

Second revised edition, Pergamon Press, Oxford—London—New York—Paris, 1961, VII + 1333 pages, 84 s.

Physical chemistry is becoming increasingly important not only in chemical and physical research work, but also in a number of more or less distinct branches of science, such as biology. Consequently, there is an increasing need for textbooks of physical chemistry, which, although not completely elementary, are still easily understandable by university students as well as by researchers and engineers who do not want to become deeply involved in higher mathematics.

One of the most important virtues of MOELWYN-HUGHES' book is the relative simplicity of its mathematics together with an almost unparalleled clarity of the text, which makes the book useful not only for scientists working in physical chemistry, but also for anybody interested in this subject. Although the size of the book (about 1300 pages) indicates that it involves considerably more than a non-specialist may need, the clear-cut arrangement of the chapters and sections makes it easy to select the essential from the superfluous. For the same reason, the book can serve as an excellent textbook for university students who want to pursue the study of up-to-date physical chemistry in greater depth, as well as for a convenient handbook in physio-chemical research work.

The book consists of 24 chapters. The first two chapters present the kinetic-molecular theory, the following two chapters contain a brief discussion of the fundamentals of quantum mechanics involving a discussion of some elementary problems. The fifth chapter deals with the properties of the chemical elements and the periodic table, and it also involves some very elementary nuclear physics. The sixth chapter is devoted to chemical thermodynamics. The seventh deals with intermolecular energy, while the eighth chapter discusses the main connection between micro- and macrophysics: the partition function. The four following chapters are devoted to a discussion of the main properties of isolated molecules. The next seven chapters give a survey of the properties of crystals, gases and liquids, involving a separate discussion of the metallic, the dissolved, the ionic and the "interfacial" state. The twentieth and twenty-first chapters deal with the problem of chemical equilibria in homogeneous and heterogeneous systems, while the last three chapters of the book are devoted to the discussion of reaction kinetics.

In every part of the book equal emphasis is given to the experimental and theoretical side of the problems. In order to facilitate the understanding of the text, some more involved mathematical deductions, which are of less physical importance, are presented in the Appendix. A number of questions are listed at the end of each chapter in order to enable the reader to make certain that the matter has been assimilated.

Except for the parts of the book presenting the fundamentals of quantum mechanics and nuclear physics, which are discussed in a quite elementary way, the book may serve as a starting point in the understanding of more advanced monographs and of the current literature.

In spite of its excellent didactical properties and its conceptual simplicity, the book requires some elementary preliminary knowledge of physical chemistry. This holds particularly for thermodynamics, where without a knowledge of the basic elements there may be some difficulty in understanding some parts of the book. These requirements are, however, considerably less than the subject-matter furnished by the usual university lectures or any elementary textbook.

Pergamon Press has done good work in editing this book, which will certainly become one of the most widely used standard textbooks of physical chemistry.

T. SZONDY

Printed in Hungary

A kiadásért felel az Akadémiai Kiadó igazgatója Műszaki szerkesztő: Farkas Sándor

A kézirat nyomdába érkezett: 1963. III. 30. — Terjedelem: 6,50 (A/5) ív, 16 ábra

63.56922 Akadémiai Nyomda, Budapest — Felelős vezető: Bernát György

The *Acta Physica* publish papers on physics, in English, German, French and Russian.
The *Acta Physica* appear in parts of varying size, making up volumes.
Manuscripts should be addressed to:

Acta Physica, Budapest 502, Postafiók 24.

Correspondence with the editors and publishers should be sent to the same address.
The rate of subscription to the *Acta Physica* is 110 forints a volume. Orders may be placed with "Kultúra" Foreign Trade Company for Books and Newspapers (Budapest I., Fő u. 32. Account No. 43-790-057-181) or with representatives abroad.

Les *Acta Physica* paraissent en français, allemand, anglais et russe et publient des travaux du domaine de la physique.
Les *Acta Physica* sont publiés sous forme de fascicules qui seront réunis en volumes.
On est prié d'envoyer les manuscrits destinés à la rédaction à l'adresse suivante:

Acta Physica, Budapest 502, Postafiók 24.

Toute correspondance doit être envoyée à cette même adresse.
Le prix de l'abonnement est de 110 forints par volume.
On peut s'abonner à l'Entreprise du Commerce Extérieur de Livres et Journaux «Kultúra» (Budapest I., Fő u. 32. — Compte-courant No. 43-790-057-181) ou à l'étranger chez tous les représentants ou dépositaires.

«*Acta Physica*» публикуют трактаты из области физических наук на русском немецком, английском и французском языках.
«*Acta Physica*» выходят отдельными выпусками разного объема. Несколько выпусков составляют один том.
Предназначенные для публикации рукописи следует направлять по адресу:

Acta Physica, Budapest 502, Postafiók 24.

По этому же адресу направлять всякую корреспонденцию для редакции и администрации.
Подписная цена «*Acta Physica*» — 110 форинтов за том. Заказы принимает предприятие по внешней торговле книг и газет «*Kultúra*» (Budapest I., Fő u. 32. Текущий счет: № 43-790-057-181) или его заграничные представительства и уполномоченные.

20,— Ft

INDEX

COMMUNICATIONES BREVES

RECENSIONES

Acta Phys. Hung. Tom. XVI. Fasc. 1. Budapest, 20. VI. 1963.

Index: 26.022

ACTA PHYSICA

ACADEMIAE SCIENTIARUM HUNGARICAE

REDIGIT
P. GOMBÁS

TOMUS XVI FASCICULUS 2

AKADÉMIAI KIADÓ, BUDAPEST
1963

ACTA PHYS. HUNG.

ACTA PHYSICA

A MAGYAR TUDOMÁNYOS AKADÉMIA FIZIKAI KÖZLEMÉNYEI

SZERKESZTŐSÉG ÉS KIADÓHIVATAL: BUDAPEST V., ALKOTMÁNY UTCA 21.

Az *Acta Physica* német, angol, francia és orosz nyelven közöl értekezéseket a fizika tárgyköréből.

Az *Acta Physica* változó terjedelmű füzetekben jelenik meg: több füzet alkot egy kötetet.

A közlésre szánt kéziratok a következő címre küldendők:

Acta Physica, Budapest 502, Postafiók 24.

Ugyanerre a címre küldendő minden szerkesztőségi és kiadóhivatali levelezés.

Az *Acta Physica* előfizetési ára kötetenként belföldre 80 forint, külföldre 110 forint. Megrendelhető a belföld számára az Akadémiai Kiadónál (Budapest V., Alkotmány utca 21. Bankszámla 05-915-111-46), a külföld számára pedig a „Kultúra" Könyv- és Hírlap Külkereskedelmi Vállalatnál (Budapest I., Fő u. 32. Bankszámla 43-790-057-181 sz.), vagy annak külföldi képviseleteinél és bizományosainál.

Die *Acta Physica* veröffentlichen Abhandlungen aus dem Bereiche der Physik in deutscher, englischer, französischer und russischer Sprache.

Die *Acta Physica* erscheinen in Heften wechselnden Umfanges. Mehrere Hefte bilden einen Band.

Die zur Veröffentlichung bestimmten Manuskripte sind an folgende Adresse zu richten:

Acta Physica, Budapest 502, Postafiók 24.

An die gleiche Anschrift ist auch jede für die Redaktion und den Verlag bestimmte Korrespondenz zu senden.

Abonnementspreis pro Band: 110 forint. Bestellbar bei dem Buch- und Zeitungs-Aussenhandels-Unternehmen »Kultúra« (Budapest I., Fő u. 32. Bankkonto Nr. 43-790-057-181) oder bei seinen Auslandsvertretungen und Kommissionären.

SPACE-TIME STRUCTURE AND MASS SPECTRUM OF ELEMENTARY PARTICLES

By

J. I. HORVÁTH

DEPARTMENT OF THEORETICAL PHYSICS, UNIVERSITY OF SZEGED, SZEGED

(Presented by A. Kónya. — Received 12. IX. 1961)

Experiments proving the violation of parity conservation have recently led to the assumption that the structure of the space-time continuum — in agreement with the modern philosophical concept of the space-time world as being determined by real physical interactions — may be anisotropic. In fact, this assumption can be also expressed by saying that the physical fields excited in such an anisotropic space have internal degrees of freedom. In this paper, first of all the derivation of the field equations is discussed for fermions, in particular considering second order equations. Then, it will be proved that a mass spectrum of elementary particles exists and based on a provisional Lagrangian of baryons the mass spectrum of the latter can be calculated in good agreement with the experiments. At the same time an interpretation is suggested of the strangeness and of the multiplicity of the different isodoublets.

§ 1. Introduction

The *a priori* supposition that the structure of the space-time continuum is pseudo-Euclidian, *i.e.* homogeneous and isotropic, is one of the most generally accepted starting points of current theories of elementary particles [1]. In order to see that in fact rather this *a priori* supposition meets the outworn metaphysical concepts of space and time than the modern philosophical cathegory of the space-time world, let us briefly discuss the philosophical concept of the space-time continuum.

Independent of their concrete material content, all events of the material world take place *in space* (side by side) and *in time* (one after another) as well. This means, that the events of the material world can be characterized by four objective parameters: by three data mapping their relative positions (place) and by one determining their succession (time-point). As a matter of fact, the whole of the material events can be regarded as a four-dimensional ensemble of events which in terms of A. D. ALEXANDROV [2] may be denoted as the *space of events*, or in the more usual terms of the theory of relativity — also considering that in fact all material events are continuously dependent on each other — as the *space-time continuum*. From this point of view *the space of events must be the absolute form of existence of the material world.*

The real physical events can only be truly mapped in this way if the geometrical connections among the "points" of the space of events — which are realized in the geometrical structure of the space-time continuum — are

determined by objective connections among the corresponding event, *i.e.* by real material interactions. This means, however, that the space-time continuum, or rather its geometrical structure, depends on the concrete material content, *i.e.* on special physical interactions, of the material world. As matters stand, the space-time continuum and its geometrical structure, respectively, which correspond to the whole of the material events and their objective interactions as well, are unified in the dialectical unity of form and content. From this point of view *the space of events is relative:* indeed, its structure is determined by the concrete features of matter.

To summarize, according to these considerations the space of events and the space-time continuum, respectively, have to be regarded as the objective form of existence of the material world and *by the philosophical cathegory of space-time continuum the absolute and relative features of space and time are represented.* This can also be expressed by saying that the space-time continuum — in spite of the previous metaphysical concept of space and time according to which the Euclidian character of space and the absoluteness of time would be an *a priori* cathegory of the human mind — cannot simply be a geometrical background of physical processes independent of matter, but that its structure is determined by objective interactions. J. BOLYAI was the first scientist who — already a hundred years ago — suggested this idea; it was taken up again by RIEMANN and finally, as a principal idea of EINSTEIN's theory of gravitation scored its revolutional success in macro-physics. So far, this point of view is generally accepted in modern physics.

Nevertheless, the gravitational interactions can be neglected in micro-physics. Therefore, in the case of elementary particles — according to EINSTEIN's theory — it is usually supposed that the structure of the spacet-time world is pseudo-Euclidian. Hence, if we take seriously into account the suggested point of view, one can say that the pseudo-Euclidian character of the space-time world, *i.e.* its homogeneity and isotropy, is rather a consequence of the special symmetry properties of the actual interactions than an *a priori* feature of space-time. In fact, if *e.g.*, the violation of parity conservation can be regarded as a special property of weak interactions, it seems that from the anisotropy of these interactions also the anisotropy of the space may be inferred. The reason for the isotropic structure of the space-time world, in most of the cases, seems to be that the anisotropy of the weak interactions is overlapped by the electromagnetic and strong interactions which have higher or at least another symmetry character. This can also be expressed by saying that the strict insistence on the *a priori* Euclidian (or pseudo-Euclidian) structure of the space-time world can be regarded as a residue of the metaphysical concepts, as it was suggested above.

The important question arises how the space-time anisotropy is to be understood and whether it can be proved at all?

In fact, the spin and the linear polarization of elementary particles, as well as the various internal attributes of elementary particles — such as baryon charge, isospin, hyper charge and isoparity — associated with the abstract concept of isospace (isobaric spin space) and its transformations indicate that there must be some additional intrinsic property of the fields, an additional degree of freedom, which has not been considered in terms of the usual formulation of the theory of elementary particles. *E.g.*, the existence of the spin shows in itself that the point model of elementary particles associated with the familiar local theory of fields does not provide a complete description of the properties of the particles, since the rotational axis connected with the spin angular momentum cannot be explained in a natural manner. Furthermore, the linear polarization — *i.e.* the space-independent correlation of the momentum and the spin angular momentum of fermions — proves that this distinguished direction may be in close connection with the anisotropic internal structure of particles which has not properly been considered previously. The intrinsic anisotropy of particles appears first of all in their handedness by which the asymmetry of right and left is expressed. Of course, on the basis of an extended particle model or based on a rigid-body model this anisotropy could be characterized, but the relativistic formulation of such a theory would be rather difficult and the results of such theories could only be cumberously translated into the language of field theories. Moreover, taking into account the current methods of the theory of elementary particles, it can be noticed that these methods have, from certain points of view, two essentially different features. Some of them are closely connected with geometry and lead to such physical laws as conservation of energy and momentum, etc.; the other are based rather on the abstract concept of the isospace than on current geometrical terms and result in such physical laws as the conservation of charge or the conservation of baryon number, *etc.* In other words, some of the groups of transformations — like translations, rotations and inversions in the four-dimensional space-time continuum — possess an immediate geometrical meaning, but some of the others — such as *e.g.* gauge transformation of first kind, charge conjugation, charge-symmetry and mesoparity transformation — possess none. However, the reality of these latter attributes of elementary particles indicates that the angles of isorotations as well as the planes of isoreflexions are not located in an abstract space, but within space-time itself. This is the reason why several investigations have recently been published to explain the internal degrees of freedom of physical fields as well as to interpret the isospace and its transformations in geometrical terms [6—16]. These proposals are, of course, very different from each other.

My recent investigations in this direction [15, 16] have been based on the supposition that in the anisotropic internal structure of the elementary

particles the anisotropy of the space-time continuum appears. This supposition may be illustrated in simple terms as follows:

In anisotropic spaces the structure of the space is characterized not only by its curvature, but by its torsion too [21]. If the general idea could be accepted that the anisotropy of the space-time world is determined by the anisotropy of the interactions, it should be supposed, of course, that the longitudinal polarization of the particles may be induced by the torsion of the anisotropic space-time world. Consider the following analogy: In the case of the gravitational field the photon with zero rest mass in the most adequate test particle which moves on a geodetical line of the space-time world. As a matter of fact, the deflexion of light in the neighbourhood of the sun, *e.g.*, proves the curvature of the space-time continuum. Analogously, among the fermions the neutrino seems to be a suitable test particle similar to the photon to demonstrate the torsion of the space-time world. Indeed, its rest mass is zero — so that during motion it perfectly adapts itself to the structure of space-time — and its longitudinal polarization is maximal to such an extent that the two-component theory of neutrino admits one kind of neutrinos with helicity (−1). In these terms one may say that the longitudinal polarization of elementary particles demonstrates the space-time asymmetry.

Fort his reason we have recently [15, 16] suggested the unfamiliar idea that the strict adherence to the *a priority* of the pseudo-Euclidian space-time structure may be responsible for the problems connected with the violation of parity conservation predicted by LEE and YANG [3]. In other words, it may be deduced from the anisotropic interactions that the structure of our physical world is richer than it was previously supposed. It seem remarkable that it was possible to suggest a reasonable solution of some problems of the elementary particle theory, such as the geometrical interpretation of isospace and its transformations, *etc.* For the sake of simplicity it was, however, suggested that the dynamics of the local change of the space-time structure due to the anisotropic interactions need provisionally not be investigated; in fact, only the consequences of the actual anisotropy of the space-time world — in the case of different but specialized fields — was discussed. Furthermore, it was supposed that the anisotropy of the space-time continuum can be characterized by the longitudinal polarization of the field quanta which can be regarded as a constant anisotropy parameter a. However, this can be only a provisional supposition. Indeed, in a final theory — considering also the interactions of fields — this constant anisotropy parameter has to be replaced by an anisotropy parameter which depends on space and time: $a = a(x^\mu)$ and which is determined by the interactions of the fields to be considered. This problem will have to be discussed in detail.

In the present paper it will be shown that without any further supposition — having the second order equations of fermions in mind [18—19] — the

mass spectrum of baryons can be calculated in good agreement with the experiments. At the same time the strangeness and multiplicity of isodoublets can be interpreted as well.

§ 2. Geometrical characterization of the space-time anisotropy

The natural geometrical model of an anisotropic space is the line-element geometry [15, 20—22] which is the geometry of an ensemble of line-elements $\{x^\mu, u^\mu\}$ rather than that of points as in current geometries. $\{x^\mu\}$ mean the position co-ordinates of the line-elements and by the contravariant vector density $\{u^\mu\}$ of order (-1), with the transformation law

$$u^{\mu'} = \Delta^{-1} \frac{\partial x^{\mu'}}{\partial x^\mu} u^\mu, \quad \left(\Delta \equiv dt \left| \frac{\partial x^{\mu'}}{\partial x^\mu} \right| \neq 0\right) \tag{2,1}$$

the direction of the line-element $\{x^\mu, u^\mu\}$ is characterized. Since only a direction is defined by the vector density u^μ, the components u^μ are not independent of each other and only their proportions have meaning. Therefore, it is supposed that the metrical fundamental tensor of the space [*i.e.* $g_{\mu\nu} = g_{\mu\nu}(x^\mu, u^\mu)$], the different geometrical and physical quantities, respectively, are homogeneous functions of zero order of these so-called direction co-ordinates u^μ.

The anisotropy of the space in a point $\{x^\mu\}$ can be characterized by the Carathéodorian indicatrix

$$F(x^\mu, l^\mu) = 1, \tag{2,2}$$

where $l^\mu = u^\mu/F$ denote the components of a vector density of unit length in the direction of the line-element $\{x^\mu, u^\mu\}$ and

$$F \equiv \{g_{\mu\nu}(x^\alpha, u^\alpha)\, u^\mu\, u^\nu\}^{2/2} \tag{2,3}$$

means the — so-called — *scalar fundamental function of the space* [15, 16].

If the gravitational interactions are neglected, the space may be considered to be homogeneous and the metrical fundamental tensor does not depend on x^μ. Indeed, for the sake of simplicity let us provisionally suppose that $g_{\mu\nu} = g_{\mu\nu}(u^\alpha)$. Then, the explicit dependence of $g_{\mu\nu}$ on u^α can be calculated easily if it is assumed that the anisotropy of the space-time world is induced by the anisotropy of the interactions. In fact, if the anisotropy of the interaction is determined by the anisotropy parameter α of the interaction considered, it is found [15, 16] that

$$g_{00} = 1, \quad g_{0i} = 0, \quad g_{ik} = -\delta_{ik}\left\{1 + \alpha\, u^3\left[(u^1)^2 + (u^2)^2 + (u^3)^2\right]^{-1/2}\right\}^{-2} \tag{2,4}$$
$$(i, k = 1, 2, 3).$$

Due to this special form of the metrical fundamental tensor the Carathéodorian indicatrix (2,2) obeys the more explicit equation

$$(l^0)^2 + g_{ik}\, l^i\, l^k = 1\,. \tag{2,5}$$

Denoting the co-ordinates of the end-point of l^μ by $\{ y^\mu \}$ we have:

$$(y^0)^2 + g_{ik}\, y^i\, y^k = 1\,. \tag{2,6}$$

By cutting this surface of the four-dimensional space-time continuum by the hyper-plane

$$y_0 = \sqrt{2}\,,$$

in the three-dimensional "spatial" subspace of the space-time continuum the two-dimensional surface

$$\left\{1 + \alpha y^3 \left[(y^1)^2 + (y^2)^2 + (y^3)^2\right]^{-1/2}\right\}^{-2} \left[(y^1)^2 + (y^2)^2 + (y^3)^2\right] = 1 \tag{2,7}$$

can be obtained which has the parametric form:

$$\begin{aligned} y^1 &= (1 + \alpha \cos\vartheta) \sin\vartheta \cos\varphi\,, \\ y^2 &= (1 + \alpha \cos\vartheta) \sin\vartheta \sin\varphi\,, \\ y^3 &= (1 + \alpha \cos\vartheta) \cos\vartheta\,, \end{aligned} \tag{2,8}$$

where (ϑ, φ) are polar angles associated with the three-dimensional Descartesian frame of reference $\{ y^k \}$. Of course, (2,8) is a rotational surface which distinguishes the direction of the y^3-axis of the $\{ y^k \}$ subspace. It is obvious that the distinction of this rotational axis — which can be identified with the spin axis — is covariantly formulated in terms of the Carathéodorian indicatrix. This means, however, that the internal anisotropy of the physical fields and the elementary particles (as their quanta), respectively, associated with the spin angular momentum may be characterized in this way merely in geometrical terms.

In order to take explicitly into account in a covariant way that, in fact, the geometrical and field quantities, respectively, depend only on *three* independent direction co-ordinates, let us introduce three linearly independent vectors λ_i^μ $(i = 1, 2, 3)$ of unit length. Then, the three angles

$$\Theta_i = \arccos \left\{ g_{\mu\nu}\, l^\mu\, \lambda_i^\nu \right\}$$

can be regarded as *inhomogeneous direction co-ordinates.*

The directions of the vectors λ_i^μ can be given — from a geometrical point of view — quite arbitrarily. For the sake of simplicity one can, however, suppose that the λ_i^μ-s are orthogonal by pairs *i.e.*

$$g_{\mu\nu}\lambda_i^\mu\lambda_k^\nu = \delta_{ik}$$

form an orthogonal trieder, the so-called *λ-trieder*. From the definition of the inhomogeneous direction coordinates one can immediately see that they depend on the orientation of the λ-trieder. More recently it was suggested that with help of the λ-trieder and the inhomogeneous direction co-ordinates so far unexpected internal degrees of freedom of physical fields can be characterized [16].

§ 3. Internal degrees of freedom of physical fields

In current field theories the physical fields are characterized by one or several space-time functions $\psi(x_\mu)$, $\psi_a(x^\mu)$ *etc.* — fulfilling certain partial differential equations, the so-called field equations — which have to satisfy definite laws of transformation. In the case of physical fields excited in anisotropic spaces, the fields are analogously characterized by such quantities fulfilling the field equations (s. §4 and [15]) and obeying also definite laws of transformation, however, these functions depend on the line-elements $\{x^\mu, u^\mu\}$, *i.e.* $\psi(x^\mu, u^\mu)$, $\psi_a(x^\mu, u^\mu)$ *etc.* which are, of course, homogeneous functions of zero degree of the direction co-ordinates u^μ.

Instead of the homogeneous direction coordinates let us introduce the inhomogeneous direction co-ordinates Θ_i or — more suitably — rather the quantities $\xi_i \equiv \cos\Theta_i$; then the field quantities depend on the position co-ordinates and on the ξ_i-s as well:

$$\psi_a = \psi_a(x^\mu;\ \xi_1, \xi_2, \xi_3)\,. \tag{3,1}$$

Now, let us take into consideration that the variables x^μ and ξ_i of the field quantity ψ_a satisfy special laws of transformation:

(*i*) The co-ordinates x^μ are transformed in the case of all co-ordinate transformations

$$x^{\mu'} = x^{\mu'}(x^\mu) \qquad \left(\Delta \equiv det\left|\frac{\partial x^{\mu'}}{\partial x^\mu}\right| \neq 0\right) \tag{3,2}$$

in the usual way, however, the inhomogeneous direction co-ordinates are pseudo-scalars of the general group of co-ordinate transformations:

$$\xi_i' = \Delta^{-1}\xi_i\,. \tag{3,3}$$

Let us denote the group of co-ordinate transformations in the following by $\mathcal{G}_x$ and the co-ordinates $\{ x^\mu \}$ as the *external co-ordinates* of the field ψ_a.

(*ii*) On the other hand, the co-ordinates ξ_i change in the case of rotations of the λ-trieder as well as in the case of inversions with respect to the λ-trieder. Nevertheless, this group of transformations — being isomorph with the three-dimensional rotary-reflexion group of transformations — does not involve any change in the case of the external co-ordinates x^μ. The general group of transformations of ξ_i-s

$$\xi_i' = \xi_i'(\xi_i) \qquad \left(\Delta^* \equiv det \left| \frac{\partial \xi_i'}{\partial \xi_i} \right| \neq 0 \right) \tag{3,4}$$

will be denoted in the following by $\mathcal{G}_\xi$ and the inhomogeneous direction co ordinates ξ_i as the internal co-ordinates of the field ψ_a mapping its interna-degrees of freedom.

Indeed, this means last of all that the supposition introduced above — according to which the structure of the space-time world is anisotropic — in other, perhaps more physical, terms corresponds to the fundamental assumption that *the physical fields have also internal degrees of freedom characterized by the internal co-ordinates.*

As a matter of fact, in the case of fields excited in the anisotropic space-time continuum — or in other words in the case of physical fields with internal degrees of freedom — the general group of transformations is a product of those of external and internal co-ordinates, *i.e.* in the following the group

$$\mathcal{G} = \mathcal{G}_x \cdot \mathcal{G}_\xi \tag{3,5}$$

must be considered. Both groups $\mathcal{G}_x$ and $\mathcal{G}_\xi$ have evidently representations with immediate geometrical meaning and just this recognition was the main point of the geometrization of the isospace and its transformations suggested in the recent paper [16]. However, if these considerations are correct at all, one has to conclude that *the integral of action of the field* — being the fundamental quantity of the Lagrangian formalism — *must be an invariant of the general group* $\mathcal{G}$ *introduced above.*

In order to carry out the geometrization of the isospace, let that frame of reference be distinguished in which the metrical fundamental tensor of the space-time continuum does not depend on the external coordinates and which has the explicit form (2,4). In more physical term, this special frame of reference may be taken to be the rest system K^0 of the particle, the time-axis of which can be determined by the momentum four-vector of the particle in a covariant way. Of course, it can be supposed [16], that the vectors λ_i^μ are bare space-like vectors, *i.e.* $\{ \lambda_i^\mu \} = \{ 0, \vec{\lambda}_i \}$, and that they point into the directions of

the principal axes of the Carathéodorian indicatrix (2,2). Furthermore, if the spin of the field does not vanish the direction of the vector $\vec{\lambda}_3$ of the λ-trieder is the same that of the spin vector $\vec{\sigma}$ of the field which makes a precession with the angle $\Theta_3 = \text{const.}$ about the momentum vector of the particle under consideration. In fact, it can be supposed that

$$\vec{\sigma}\,\vec{l} = \mathscr{P}_l, \tag{3,6}$$

where $\mathscr{P}_l$ means the longitudinal polarization of the emitted particle (1). Or, in terms of the theory of relativity

$$\sigma_{\mu\nu} f^{\mu\nu} = P_l\,, \tag{3,7}$$

where $\sigma_{\mu\nu}$ is the spin tensor of the field and $f^{\mu\nu}$ denotes the surface element, the normal vector of which is just the vector density l^α ($\{\alpha, \mu, \nu\}$ cyclical permutation).

The last supposition means, however, that

(*i*) in the case of fields (or elementary particles regarding these as the quanta of the fields) with zero spin the conditions (3,6) and (3,7), respectively, are meaningless and, in fact, the situation is expressed by saying that *no correlation between the external and internal degrees of freedom of the fields exists.*

The isospace is in this case three-dimensional

(*ii*) for fields with non-zero spin the condition (3,6) — or (3,7) — reduces the internal degrees of freedom by one and therefore the isospace is quasi-two-dimensional. In fact, the internal degrees of freedom can be characterized in this case, *e.g.*, by the two internal co-ordinates, ξ_1 and ξ_2.

In the case of fermions with half-integer spin it can be supposed that the ψ_A are the components of a two-component spinor [17—19] and, *e.g.*, for nucleons,

$$\boldsymbol{\psi}(x^\mu;\ \xi_1, \xi_2) = \begin{pmatrix} \psi_\uparrow\ (x^\mu;\ \xi_1, \xi_2) \\ \psi_\downarrow\ (x^\mu;\ \xi_1, \xi_2) \end{pmatrix} = \psi_A\,(x^\mu;\ \xi_1, \xi_2) \qquad (A = \uparrow, \downarrow)\,. \tag{3,8}$$

As a matter of fact, it can be concluded that, *e.g.*, the bosons with zero spin are isotriplets and the fermions with half-integer spin are isodoublets (s. later in § 6).

§ 4. Field equations

Let us suppose that the Lagrangian of the field depends on the metrical fundamental tensor, on the field components and their derivatives. It seems

appropriate to introduce the symbols:

$$\psi_{A,\mu} = \partial_\mu \psi_A \equiv \frac{\partial \psi_A}{\partial x^\mu}; \qquad \psi_{A|i} = \partial_i^* \psi_A \equiv \frac{\partial \psi_A}{\partial \xi_i}. \tag{4,1}$$

Then, the Lagrangian can be implicitly written as follows:

$$\mathscr{L} = |\gamma|^{-1/2} L(\psi_A, \psi_{A,\mu}, \cdots \psi_{A|i}, \cdots), \tag{4,2}$$

where γ denotes the determinant of the metrical fundamental tensor of the internal space

$$\gamma = det\, |\gamma_{ik}| \tag{4,3}$$

with the law of transformation

$$\bar{\gamma}_{ik} = \frac{\partial \bar{\xi}_i}{\partial \xi_r} \frac{\partial \bar{\xi}_k}{\partial \xi_s} \gamma_{rs}. \tag{4,4}$$

From a geometrical point of view we have, of course, no *a priori* restrictions for the structure of the internal space and its structure must be determined by physical factors. It seems, however, that it can provisionally be assumed that the metrical structure of the internal space is Euclidian, *i.e.*

$$\gamma_{ik} = \delta_{ik}, \tag{4,5}$$

where δ_{ik} mean the components of Kronecker's tensor.

According to these considerations the integral of action can be written in the form:

$$\mathscr{J} \equiv \int\int \mathscr{L}\, d^4 x\, d^3 \xi. \tag{4,6}$$

The domain of integration for the external co-ordinates is a four-dimensional domain V_4, and for the internal co-ordinates $-1 \leqq \xi_i \leqq +1$ $(i = 1, 2, 3)$.

On the basis of our fundamental supposition the integral of action is an invariant of the group $\mathscr{G}$ introduced in equ. (3,5). In fact, if we take into account only linear transformations, in the external and internal space as well, the Jacobians Δ and Δ^* respectively, are constants. These transformations are general enough to include such transformations as the Lorentz-transformations and the rotary-reflexion group of the λ-trieder. As a matter of fact — due to (3,2) and (3,4) — we have in this case

$$d^4 x'\, d^4 \xi' = \Delta^{-2} \Delta^*\, d^4 x d^3 \xi \tag{4,7}$$

and consequently one obtains for the Lagrangian the law of transformation

$$\mathscr{L}'(x^{\mu'};\ \xi_i') = \Delta^2 \Delta^{*-1} \mathscr{L}(x^\mu;\ \xi_i). \tag{4,8}$$

But we have

$$|\gamma'|^{1/2} = \Delta^{*-1} |\gamma|^{1/2} \tag{4,9}$$

and, in fact,

$$L'(x^{\mu'};\ \xi_i') = \Delta^2 \Delta^{*-2} L(x^{\mu};\ \xi_i). \tag{4,10}$$

This means, that if the explicit form of the Lagrangian is given, the law of transformation for the field components is determined by (4,10).

The derivation of the field equations and that of the infinitesimal laws of conservation has been discussed in detail in several papers (e.g. [15, 21, 22]); hence, it is not necessary to deal with these problems again.

In respect of the derivation of the field equations we only mention that the variation of $\mathscr{L}$ — which is an invariant of the group $\mathscr{G}$ — has to vanish, *i.e.*

$$\delta \mathscr{J} = \iint |\gamma|^{-1/2} \sum_A \left\{ \frac{\partial L}{\partial \psi_A} \delta\psi_A + \frac{\partial L}{\partial \psi_{A,\mu}} \delta\psi_{A,\mu} + \frac{\partial L}{\partial \psi_{A|i}} \delta\psi_{A|i} \right\} d^4x\, d^3\xi = 0. \tag{4,11}$$

In fact, as usual, $\delta\psi_A$ has to vanish at the limits of the integration domains, therefore, by partial integration one obtains

$$\iint |\gamma|^{-1/2} \sum_A \left\{ \frac{\partial L}{\partial \psi_A} - \partial_\mu \frac{\partial L}{\partial \psi_{A,\mu}} - \partial_i^* \frac{\partial L}{\partial \psi_{A|i}} \right\} \delta\psi_A\, d^4x d^3\xi = 0 \tag{4,12}$$

for all variations of the field components $\delta\psi_A$ and finally, we get the field equations:

$$\frac{\partial L}{\partial \psi_A} - \partial_\mu \frac{\partial L}{\partial \psi_{A,\mu}} - \partial_i^* \frac{\partial L}{\partial \psi_{A|i}} = 0. \tag{4,13}$$

§ 5. The field equations of fermions with half-integer spin

In order to apply the theory to a particular case, let us suppose that the Lagrangian has the following explicit form:

$$L = -\sum_A \left\{ g^{\mu\nu} \partial_\mu \overline{\psi}_A \partial_\nu \psi_A + \gamma^{ik} \partial_i^* \overline{\psi}_A \partial_k^* \psi_A + \varepsilon \overline{\psi}_A \psi \right\}, \tag{5,1}$$

which corresponds to the two-component fermion field without any interactions [17—19]. Substituting this Lagrangian into the integral of action one obtains by variation with respect to $\overline{\psi}_A$ the field equations

$$\partial^\mu \partial_\mu \psi_A + \partial^{*i} \partial_i^* \psi_A - \varepsilon \psi_A = 0, \tag{5,2}$$

where

$$\partial^{\mu} \equiv g^{\mu\nu}\,\partial_{\nu} \quad \text{and} \quad \partial^{*i} \equiv \gamma^{ik}\,\partial^{*}_{k}. \tag{5,3}$$

As a matter of fact, if we suppose that

$$\psi_A(x^{\mu}\,;\ \xi_i) = X_A(x^{\mu})\,\Xi_A(\xi_i) \tag{5,4}$$

equ. (5,2) can be separated:

$$X_A^{-1}\left\{\partial^{\mu}\,\partial_{\mu} X_A\right\} = -\,\Xi_A^{-1}\left\{\partial^{*i}\,\partial^{*}_{i}\,\Xi_A - \varepsilon\Xi_A\right\}, \tag{5,5}$$

and, finally, if the constant of separation is denoted by $\varkappa^2$, we have

$$\begin{aligned} &\left\{\partial^{\mu}\,\partial_{\mu} - \varkappa^2\right\} X_A = 0\,, \\ &\left\{\partial^{*i}\,\partial^{*}_{i} + (\varkappa^2 - \varepsilon)\right\}\Xi_A = 0\,. \end{aligned} \tag{5,6}$$

One can immediately observe that the result obtained is quite analogous to that derived previously in the case of the bilocal theory of fields [15]. However, one has to take into consideration that now the variables have a quite different meaning.

The second equation of (5,6) is the well-known differential equation of an eigenvalue problem for the constant of separation $\varkappa^2$, the spectrum of which — taking into account its meaning in the first equation of (5,6) — becomes the mass-spectrum of the fermions under consideration ($\hbar = c = 1$).

The eigenvalue problem corresponding to the second equation of (5,6) can explicitly be written as follows:

$$\left\{\partial^{*2}_{1} + \partial^{*2}_{2} + (\varkappa^2 - \varepsilon)\right\}\Xi_A = 0\,. \tag{5,7}$$

This equation is, indeed, the differential equation of the eigenvalue problem of the two-dimensional rotator which may be called *isorotator*.

In terms of polar co-ordinates

$$\xi_1 = r\cos\varphi, \quad \xi_2 = r\sin\varphi \qquad (r = \sqrt{2J} = \text{const.}) \tag{5,8}$$

equ. (5,7) can be written in the form

$$\left\{\frac{1}{2J}\,\frac{d^2}{d\varphi^2} + (\varkappa^2 - \varepsilon)\right\}\Xi_A(\varphi) = 0\,, \quad (\hbar = 1) \tag{5,9}$$

where J means the moment of inertia. Considering the usual condition of periodicity $0 \leqq \varphi \leqq 2\pi$ the following eigenvalues and eigenfunctions can be obtained:

$$\varkappa_n^2 = \varepsilon + \frac{1}{2J}\,n^2, \quad (n = 0, \pm 1, \pm 2, \ldots) \tag{5,10}$$

$$\Xi_A^{(n)} = (2\pi)^{-1/2}\exp\left\{in\varphi\right\}. \tag{5,11}$$

The case $n = 0$ has to be excluded, namely, for $n = 0$ the eigenfunction $\Xi_A^{(0)}$ would not depend on the internal co-ordinates; this is in contradiction with the general supposition that all physical quantities have to depend on the internal co-ordinates too. In fact, to express this circumstance explicitly, we introduce the notation

$$n = S + 1, \qquad (S = 0, 1, 2, \ldots). \tag{5,12}$$

Unfortunately, in the expression (5,8) of $\varkappa_S^2$ the constants ε and J are unknown and we have not yet any possibility of obtaining their *a priori* values. This would only be possible in the framework of a non-linear theory where also the interactions of fields are taken into consideration. Nevertheless, one can immediately observe that for $\varkappa_S^2$ in the case $S \geq 2$ the relation

$$\varkappa_S^2 = \varkappa_0^2 + \frac{1}{3}\left[(S+1)^2 - 1\right](\varkappa_1^2 - \varkappa_0^2) \tag{5,13}$$

can be obtained. In fact, for a family of particles if the masses of the first two isodoublets are known, the masses of the heavier isodoublets can be calculated by means of (5,13). This is the case for baryons as it will be shown in the next paragraph.

§ 6. The mass spectrum of baryons

According to our previous result reviewed in § 3 of this paper, the fermions form isodoublets. In fact, this result does not agree with the usual supposition according to which the Σ-mesons form an isotriplet and the Λ^0 particle is an isosinglet. It is, however, in full agreement with the hypothesis of the global baryon-pion interaction suggested by GELL-MANN [23]. In formulating this principle, one has to consider that the pion interaction of hyperons of first order (Λ^0, Σ^+, Σ^0, Σ^-) shows three-dimensional isotropic invariance both if the four particles are divided into two doublets and if they form a singlet and triplet. This remarkable fact has been emphasized also by SCHWINGER [24] who at the same time proposed a possible explanation in the frame of the four-dimensional isospace. In order to overcome the difficulty of SCHWINGER's scheme that in the case of baryons of even order (p, n, Ξ^0, Ξ^-) another subgroup of the six-parametric symmetry group must be identified with the three-dimensional symmetry group of kaons as in the case of baryons of odd order (Λ^0, Σ^+, Σ^0, Σ^-), GELL-MANN's idea has been more recently reinvestigated by KÁROLYHÁZY and MARX [25], whose theory reproduces the important results of GELL-MANN, SCHWINGER and others, but is free from this difficulty.

The theory of KÁROLYHÁZY and MARX has been built up on a four-dimensional mathematical scheme proposed for particles strongly interacting with each other. To describe the pions and the nucleons they need three and two independent components, respectively; therefore, the former are represented by the spinor $\pi_\mu^\nu = \pi_\nu^\mu$ and the latter by a spinor B_α. For the description of the hyperons of first order (Λ^0, Σ^+, Σ^0, Σ^-) a spinor $B_{\alpha,\nu}$ was suggested. In fact, pions, and nucleons have nothing to do with dotted indices, hence, it can be supposed that the number of dotted indices is related to the absolute values of the strangeness of the baryon (which brings KRÓLIKOWSKY's theory [26] to mind):

$$\begin{aligned} &|S| = 0; \quad B_\alpha \; ; \quad p, n, \\ &|S| = 1; \quad B_{\alpha\dot{\sigma}}; \quad \Lambda^\circ, \Sigma^+, \Sigma^\circ, \Sigma^-, \\ &|S| = 2; \quad B_{\beta\dot{\gamma}\dot{\tau}}; \quad \Xi^\circ, \Xi^-, \Omega^+, \Omega^\circ, \Omega^-, \Omega^{--}, \\ &\quad \ldots \qquad \ldots \qquad \ldots \qquad \ldots \qquad \ldots \end{aligned} \tag{6,1}$$

As a matter of fact, the baryons are split into doublets:

$$\begin{pmatrix} B_1 \\ B_2 \end{pmatrix} = \begin{pmatrix} p \\ n \end{pmatrix}; \quad \begin{pmatrix} B_{1\dot{1}} \\ B_{1\dot{2}} \end{pmatrix} = \begin{pmatrix} \Sigma^+ \\ \frac{1}{\sqrt{2}}(\Lambda^\circ - \Sigma^\circ) \end{pmatrix}; \quad \begin{pmatrix} B_{2\dot{1}} \\ B_{2\dot{2}} \end{pmatrix} = \begin{pmatrix} \frac{1}{\sqrt{2}}(\Sigma^\circ + \Lambda^\circ) \\ \Sigma^- \end{pmatrix}; \quad \text{etc.} \tag{6,2}$$

Antibaryons are represented by the complex conjugate of the corresponding spinors, B_α^* *etc.*

Bearing the classification (6,1) of baryons in mind, one observes *that the quantum number S of our isorotator introduced in the last paragraph can be interpreted as the absolute value of the strangeness and the excitation of the isorotator $n = S + 1$ agrees with the number of isodoublets of type (6,2).* Furthermore, one sees that due to the double sign of the quantum number n in equ. (5,10) and (5,11), respectively, $\pm(|n| - 1)$ — with $n \neq 0$ — can immediately be identified with the strangeness of the particles and the double degeneracy of isorotator states may be associated with the well-known property of the scheme of GELL-MANN—NISHIJIMA that the strangeness of baryons and antibaryons have opposite signs.

So far, as only pion-interactions are considered, the masses of the different isodoublets are the same and the mass spectrum of baryons can be described by the relation (5,13). Let us suppose that $\varkappa_0$ and $\varkappa_1$ are equal to the averages of the mass of nucleons and to that of hyperons of first order, then from equ. (5,13) the mass average of the hyperons of second order can be obtained. Our calculations are summarized in Table 1 (the unit of mass is the mass of the electron).

The agreement is satisfactory. The calculated average value of the mass of hyperons of second order differs by 12% from that of xions. As matters stand, this difference may be reasonable, namely, the mass-average of these hyperons must be expected to be somewhat larger than the mass-average of xions.

Table I

Elementary particle	Observed mass	Mass-average	
		observed	calculated
p	$1836{,}03 \pm 0{,}02$	1837	—
n	$1938{,}56 \pm 0{,}02$		
Λ°	$2182{,}39 \pm 0{,}24$		
Σ^+	$2327{,}4 \pm 0{,}69$		
Σ°	$2329 \begin{cases} +1{,}8 \\ -3{,}7 \end{cases}$	2295	—
Σ^-	$2342\,00 \pm 1$		
Ξ°	2585 ± 1	2590	2901,92
Ξ^-	2595 ± 39		

Indeed, in calculating the mass-average of the hyperons of second order — mentioned as the observed mass-average of xions in Table 1 — the masses of the hypothetical Ω particles could not be considered.

The splitting of the degenerate baryon states into isomultiplets is caused first of all by kaon interactions ($\Lambda - \Sigma$ mass-splitting). Electromagnetic interactions will go a step further and distinguish the $\vec{\lambda}_3$ axis of the λ-trieder and thus only the invariance with respect to the rotations about this axis remains. Indeed, the electromagnetic interactions cause further mass splitting: $p - n$, $\Sigma^+ - \Sigma^0$, $\Xi^0 - \Xi^-$, etc.

The Ω particles are hypothetical ones, their mass is about the sum of the xion- and pion-mass. If actually the $\Omega - \Xi$ mass difference is larger than the Ξ mass, then the Ω hyperons decay in a very short time (about 10^{-22} sec) into xions, and this is practically unobservable. Nevertheless, it cannot be omitted from our scheme, as the Σ^0 hyperons the lifetime of which is longer by only a few orders play also a decisive role.

It is, of course, an interesting problem whether the other isodoublets suggested for $S \geq 2$ by the formula (5,13) will be observed in the future.

In order to find also the fine structure of the mass spectrum, one has to consider the interactions of fields too. This will be discussed in a future paper.

REFERENCES

1. P. ROMAN, The Theory of Elementary Particles North-Holland Pc., Amsterdam, 1959.
2. *А. Д. Александров,* Вопросы философии, **13,** 67, 1959.
3. T. D. LEE and G. N. YANG, Phys. Rev., **29,** 295, 1957.
4. S. TANAKA, Progr. Theoret. Phys., **18,** 295, 1957.
5. E. P. WIGNER, Rev. Mod. Phys., **29,** 255, 1957.
6. J. RAYSKI, Acta Phys. Polonica, **17,** 187, 1958.
7. P. HILLTON and J. P. VIGIER, Nuovo Cimento, **18,** 209, 1960.
8. J. A. WHEELER, Neutrinos gravitation and geometry (Rend. d. Int. di Fisica «E. Fermi», Bologna, Corso **11,** 1960.)
9. R. FINKELSTEIN, Ann. of Phys., **12,** 200, 1961.
10. TH. A. MARIS, Nucl. Phys., **24,** 346, 1961.
11. G. R. ALLCOCK, Nucl. Phys., **27,** 204, 1961.
12. H. FRÖHLICH, Proc. Roy. Soc. London, (A) **257,** 147, 283, 1960.
13. H. FRÖHLICH, Helv. Phys. Acta, **33,** 803, 1960.
14. H. FRÖHLICH, Nucl. Phys., **27,** 204, 1961.
15. J. I. HORVÁTH, Suppl. Nuovo Cimento, (X) **9,** 444, 1958.
16. J. I. HORVÁTH, Acta Phys. et Chem. Szeged, **7,** 3, 1961; **9,** 3, 1963.
17. R. P. FEYNMAN, Rochester Conference 1959.
18. R. P. FEYMAN and M. GELL-MANN, Phys. Rev., **101,** 193, 1959.
19. G. MARX, Nucl. Phys., **9,** 337, 1959; **19,** 468, 1959.
20. E. CARTAN, Les Espaces de Finsler, Acta sc. et ind. No. 79, Paris, 1934.
21. J. I. HORVÁTH and A. MOÓR, Indag. Math., **17,** 421, 581, 1955.
22. J. I. HORVÁTH, Acta Phys. et Chem. Szeged, **4,** 3, 1958.
23. M. GELL-MANN, Phys. Rev., **106,** 1297, 1957.
24. J. SCHWINGER, Ann. of Phys., **2,** 407, 1957.
25. F. KÁROLYHÁZY and G. MARX, Acta Phys. Acad. Sci. Hung., **10,** 421, 1958.
26. W. KRÓLIKOWSKY, Bull. Acad. Pol. Sci. Cl., III. **6,** 523, 1958.

ПРОСТРАНСТВЕННО-ВРЕМЕННАЯ СТРУКТУРА И МАСС-СПЕКТР ЭЛЕМЕНТАРНЫХ ЧАСТИЦ

Я. И. ХОРВАТ

Резюме

На основе экспериментальных данных, свидетельствующих о нарушении сохранения паритета, делается предположение, по которому структура пространственно-временных континуумов — в полном согласии с современной философской концепцией о пространственно-временном мире, определённом реальными физическими взаимодействиями — может быть анизотропной. На самом деле, данное предположение эквивалентно тому, что физическое поле, возбуждённое в таком анизотропном пространстве, имеет внутренние степени свободы. В данной работе прежде всего выводится уравнение поля для фермионов, являющееся уравнением второго порядка. Далее доказывается, что масс-спектр элементарных частиц существует и, основываясь на приближенном Лагранжиане барионов, он может быть определён в хорошем согласии с опытными данными. Здесь же предлагается интерпретация редкости и кратности различных изодуплетов.

INVESTIGATION ON THE EXCITATION FUNCTION OF THE NUCLEAR REACTION $Be^9(d, n)B^{10}$ BY ARTIFICIALLY ACCELERATED PARTICLES IN THE 0,5—1,6 MeV ENERGY RANGE

By

E. KOLTAY

INSTITUTE FOR EXPERIMENTAL PHYSICS, KOSSUTH LAJOS UNIVERSITY, DEBRECEN

(Presented by A. Szalay. — Received 19. V. 1962)

The excitation function of the $Be^9(d, n)B^{10}$ nuclear reaction has been taken by an energy-independent neutron detector in the 0,5—1,6 MeV bombarding energy range. The broad peak found near 1 MeV is probably due to concurrent processes of high intensity, taking place above 1 MeV.

Introduction

The nuclear reaction $Be^9(d, n)B^{10}$ is equally significant from the point of view of fundamental nuclear physics and technically. The fact that the last neutron of the target nucleus and the neutron of the deuteron are both very loosely bound (1,667 MeV and 2,226 MeV, respectively) creates special circumstances for the mechanism of the nuclear reaction on the one hand, and on the other it facilitates high neutron yield when bombarding with an artificially accelerated deuteron beam. The investigation of the process from the fundamental point of view, i.e. by interpreting the excitation curves, neutron threshold curves, neutron energy spectra taken with various measuring techniques and the angular distribution curves of the different neutron groups has been in progress for a considerable time, but recent investigations in this field gave rise to new problems as regards the mechanism of the process.

Our investigations are concerned with the following problem: in contrast to conclusions drawn from previous measurements suggesting that the process takes place in such a way that a compound nucleus and deuteron stripping appear simultaneously, BARDES and OWEN [1] conclude from their investigations published in 1960 that the neutrons are partly due to deuteron stripping and partly to a "heavy particle stripping" process. As regards the validity of their conclusion they point out the following problem. On the one hand they consider it possible that when the analysis which they carried out in the Born approximation is replaced by a more accurate distorted-wave calculation, the observed increase of the backward direction neutron intensity can be obtained if only deuteron stripping is assumed, on the other hand they note that the excitation curve shows a dip near 1 MeV. The existence of a resonance would suggest a process taking place through the compound nucleus,

which contradicts the former assumption. In spite of this, their assertion on the mechanism of the reaction can still be admitted, the reason for which is that the results of the measurements carried out by various authors to determine the existence and character of the change observed in the cross-section curve contradict each other [2, 3, 4, 5, 6].

It can be assumed that this effect is due to the increase taking place in the cross section of elastic deuteron scattering in the corresponding energy range, as the increased probability of the new process would decrease the cross-section of the (d, n) reaction and in this case the shape of the excitation function mentioned above would not mean uniquely that the (d, n) reaction takes place with compound nucleus mechanism.

The excitation functions measured at thin targets, published hitherto in the literature, do not provide a sufficient basis for the determination of the existence and origin of the resonance in question. This is due to the fact that the detecting efficiency of the methods used for detecting neutrons is to a large extent energy-dependent and thus owing to the complex structure of the energy spectrum of neutrons emitted in the process the shape of the curves taken by various authors with various experimental techniques greatly deviate from each other and supply no reliable information on the accurate shape of the excitation curve.

To investigate the problem experimentally we have taken the excitation function of the nuclear reaction $Be^9(d, n)B^{10}$ in the 0,5—1,6 MeV bombarding energy range by using an energy-independent gamma background-free neutron intensity measuring technique of 4π geometry. In this way we have succeeded in eliminating the above difficulties underlying the contradiction of measured data.

Experimental method

The bombarding deuteron beam was produced in the 2MV nominal voltage Van de Graaff generator of the Institute for Experimental Physics, Kossuth Lajos University, Debrecen. The description of the generator was published elsewhere [7, 8].

Measurement of bombarding particles

The energy of the bombarding particles was measured by a new reference field generating voltmeter calibrated by nuclear reaction. At the output of the two channels obtained by separating the conventional stator plate system into two independent parts the basic signal proportional to the voltage of the generator and a reference signal proportional to the intensity of the field generated by a reference plate appear separately. The error signal obtained

from the difference of the two signals controls the input of the slow voltage stabilizer acting through the charging current regulator [9]. The regulating circuit used here will serve later on as the slow regulating circuit of the planned precision energy stabilizer. By means of the apparatus used here it was possible to measure the accelerating voltage inside an error limit of 1.5%, i.e. it was stabilized to such a degree. These data satisfy the requirements of our investigations.

To determine the number of bombarding particles we have built a target-current integrator following ELMORE and SANDS [10]. The linearity of this device is better than 1% over a wide range of current.

The measurements have been carried out with a beam not analyzed for e/m.

Measurement of emitted neutrons

For the energy-independent measurement of the absolute number of neutrons emitted in the nuclear process we have used the so-called physical integration measurement of neutron intensity [11, 12, 13]. To determine the intensity of the neutron source this method employs the absolute activity measurement of the artificial radioactive isotope generated in the nuclear reaction by the neutrons to be counted. To prevent the large variation of the cross section of the detecting reaction along the energy spectrum of emitted neutrons from causing an error in the measurement we have employed in each case neutrons thermalized in a moderator for the generation of charged particle activity.

The common basic principle of the measuring methods using thermalized neutrons is that the number of neutrons emitted by the source per unit time — assuming an infinite moderator — equals the total number of neutrons absorbed in the medium per unit time. As the density of the thermal neutrons determining the number of neutrons absorbed in the moderator is a function of the distance from the source, the number of neutrons captured by each volume element of the moderator and the activity of the activation neutron detectors at various points of the moderator vary from point to point. Accordingly, the number Q of neutrons absorbed in the total volume/unit time can be obtained by integrating over the effects represented by the volume elements. If the moderator is a mixture of n components, each of a concentration of N_k atoms/cm^3 and obeying the rule $1/v$, the absolute intensity of the source is given by the equation

$$Q = 4\pi v_t \sum_{k=1}^{n} N\sigma_{k,kt} \int_0^\infty \varrho(r)\, r^2\, dt\,, \tag{1}$$

where $\sigma_{k,t}$ is the neutron capture cross section of the k-th component measured at a thermal neutron velocity v_t, and $\varrho(r)$ is the spatial density of thermal neutrons.

The nuclear process of neutron absorption occurring in the component labelled by index D produces a radioactive final product of intensity $I(r)$, then according to equation

$$I(r) = \varrho(r)_{v_t} \sigma_D n_D \tag{2}$$

the source intensity is given by

$$Q = 4\pi \frac{\sum_{k=1}^{n} N_k \sigma_{k,t}}{\sigma_D n_D} \int_0^\infty I(r) r^2 dr . \tag{3}$$

In physical integration methods the combined task of moderator and detector is performed by the diluted solution of a compound containing nuclei transforming under the effect of thermal neutrons into beta-active isotopes of an appropriate half-life. In such a case by thorough stirring during or after irradiation the activity values originally varying with r are averaged and the average activity of the solution in the total volume directly equals the total number of neutrons absorbed by the detector nuclei per unit time. Instead of measuring the overall activity of the solution we can easily measure the absolute activity of the active nuclei present in a sample of known volume taken from the solution, if Mn^{55} detector nuclei are carried into the solution in the form of $KMnO_4$. In this case the measurements are namely facilitated by the circumstance that owing to the Szilárd—Chalmers process connected with the gamma emission taking place in the detecting reaction $Mn^{55} + n = Mn^{56} + \gamma$ the active Mn^{56} nuclei are obtained in the MnO_2 molecule which can be simply filtered from the solution so that the specific activity of Mn^{56} obtained in this way can be considerably increased.

If the absolute intensity of the preparate obtained on the filter is measured by an end-window Geiger—Müller counter calibrated with a U_3O_8 standard preparate the intensity Q of the source can be given in the following form

$$Q = \frac{I'_{U_3O_8}}{q} \cdot \frac{a}{p(1-w)} \cdot \frac{V}{v} \cdot \frac{\sigma_{Mn} N_{Mn} + \sigma_H N_H}{\sigma_{Mn} N_{Mn}} \frac{S\lambda}{(1-e^{-\lambda T})(1-e^{-\lambda\tau}) e^{-\lambda t}} , \tag{4}$$

where $I'_{U_3O_8}$ is the absolute activity of the unit mass of the standard preparate,

q is the number of pulses given by the unit mass of the standard preparate,

a is a factor correcting for the energy-dependence of window absorption,

p is the efficiency of filtration,
w is the probability of neutron escape due to the finite dimensions of the moderator,
v/V is the relative volume of the sample,
λ is the decay constant of Mn^{56},

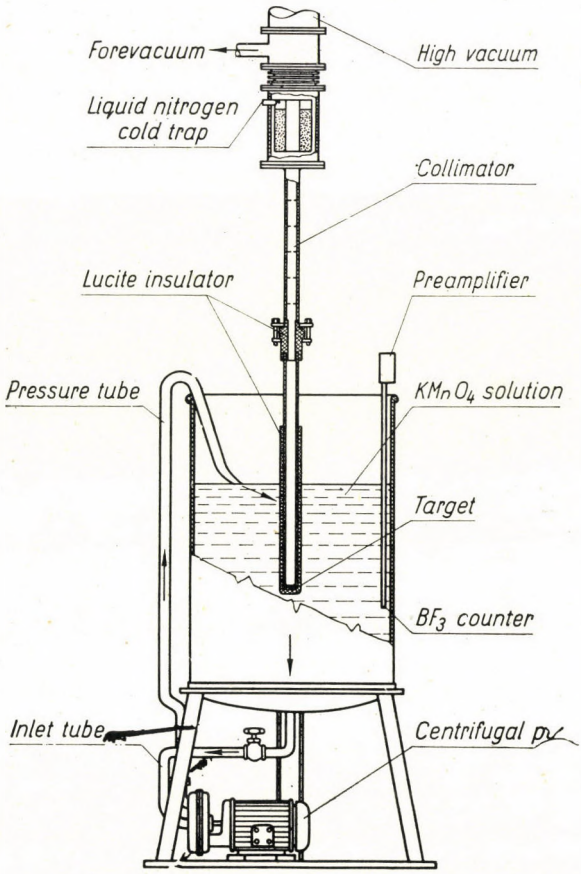

Fig. 1

S is the average number of pulses detected during time T,
τ is the time of activation,
t is the time at which the measurement began, measured from the completion of activation.

In our measurement (Fig. 1) the role of moderator containing a manganese absorbent was played by about 180 litres of $KMnO_4$ solution of 1,8% concentration. The solution was stored in a stainless steel container of cylindri-

cal shape, 62 cm in diameter, filled up to a height of 62 cm. Thorough stirring of the solution was performed by means of a centrifugal pump. The target was at the bottom of a Faraday cage of 70 cm depth in the centre of the moderator. To facilitate the measurement of the target current, the target tube was insulated with plexi from the solution which was at earth potential. Connection to the vacuum system was provided, applying suitable insulation, by a collimator tube 60 cm long, with apertures, through a freeze-out trap filled with liquid nitrogen. Using FIEBIGER's [14] results the parts exposed to deuteron bombardment were made of iron to decrease the "Selbst-target" effect.

The target was a beryllium layer of a thickness of 50 $\mu g/cm^2$.

Results

Having completed the experimental apparatus and elaborated the measuring technique, we measured the excitation function of the process in the energy range 0,5 to 1,6 MeV. Between 1,05 and 1,35 MeV the curve shows a dip, then after a minimum reached at 1,35 MeV it rises again; up to a bombarding energy of 0,9 MeV it runs parallel with the Gamow penetration curve calculated in WKB approximation. In Fig. 2 the measured points have been connected by a continuous line.

Our measurements prove unambiguously the existence of the dip on the excitation curve, considering that the method used for the detection of neutrons is also sensitive to the threshold neutron groups appearing near 1 MeV according to the measurements of BONNER and COOK [15]. Thus the appearance of the dip cannot be interpreted — in contrast to all previous measurements — by the insensitivity of the neutron detecting method in this energy range. As for the origin of the dip on the curve a comparison between the excitation curve and the Gamow penetration curve suggests that the dip is due to the appearance of a concurrent process, or processes, rather than to the existence of a resonance of the assumed compound nucleus.

The data available for the possible concurrent processes are also shown in Fig. 2.

1. At the Manchester conference in September 1961 KNITTER and WÄFFLER [16] reported on the 200 keV broad resonance found at 1,29 MeV in the excitation curve of the reaction $Be^9(d, \gamma)B^{11}$.

2. The investigations of JURIČ and ČIRILOV in 1956 showed that at bombarding energies of 1,162 and 1,358 MeV resonances can be observed in the excitation curve of the elastic scattering process $Be^9(d, d)Be^9$ [17].

3. In 1957 MCCARRY and co-workers found a broad resonance at 1.3 MeV in the excitation curve of the gamma group emitted in the reaction $Be^9(d, p)Be^{10}$ the energy of which was $E\gamma = 3{,}37$ MeV characterized by $Q = 1{,}22$ MeV [18].

It should be noted that the ordinates belonging to each curve are not shown on identical scales but in arbitrary intensity units.

According to what we have said above all four concurrent processes show an increased intensity above the broad dip found by us, and cross the resonance peak close to the abscissa of the minimum. To decide whether the intensity decrease found in the excitation curve can be completely ascribed to the elastic scattering of deuterons — as assumed by BARDES and OWEN —

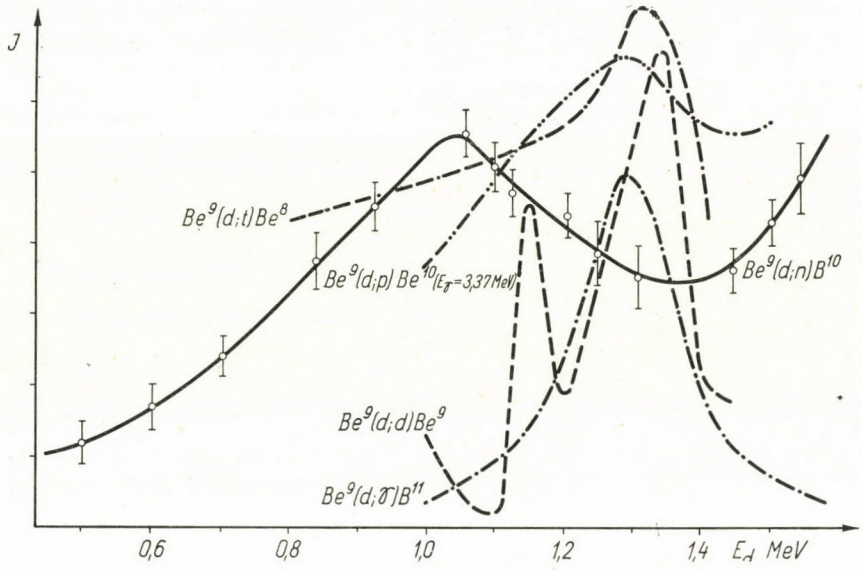

Fig. 2

and whether the energetically possible concurrent processes are responsible for the dip of the curve, we plan to carry out further measurements.

My thanks are due to Prof. A. SZALAY, Doctor of Physical Sciences, for having supported my work and for his continued interest, and to Mr. L. MEDVECZKY for having prepared the beryllium targets used in the investigations.

REFERENCES

1. R. BARDES and G. E. OWEN, Phys. Rev., **120,** 1369, 1960.
2. E. AMALDI et al., Phys. Rev., **51,** 896, 1937.
3. J. E. EVANS et al., Phys. Rev., **75,** 1161, 1949.
4. F. BORELI and B. LALOVIČ, Nature, **176,** 1021, 1955.
5. A. J. SHPETNYI, Soviet Physics JETP, **5,** 357, 1957.
6. G. C. NEILSON et al., Bull. Am. Phys. Soc. **3,** 323, 1958.
7. S. SZALAY et al., Reports of the Institute of Nuclear Physics "ATOMKI", **2,** 3, 1960 (in Hungarian).
8. E. KOLTAY, Nucl. Instr. and Meth., **6,** 45, 1960.
9. E. KOLTAY, Hungarian Physical Journal, **10,** 145, 1962 (in Hungarian).

10. W. Elmore and M. Sands, Electronics Experimental Techniques, New York, 1949.
11. *В. А. Давиденко* и др., Ядерные реакции на легких ядрах (приложение к журналу «Атомная энергия», № 6, 1957, p. 7.
12. *А. С. Ганеев*, и др., ibid. p. 26.
13. E. Koltay, Hungarian Physical Journal, **9**, 89, 1961 (in Hungarian).
14. K. Fiebiger, Z. f. angewandte Physik, **9**, 213, 1957.
15. T. W. Bonner and C. F. Cook, Phys. Rev., **96**, 122, 1954.
16. H. Knitter and H. Wäffler, Paper read at Manchester Conference, 1961.
17. M. K. Jurič and S. D. Čirilov, Bull. of the "Boris Kidrich" **6**, 45, 1956.
18. McCrary et al. Phys. Rev., **108**, 392, 1957.
19. M. K. Jurič, Phys. Rev., **98**, 85, 1955.

ИССЛЕДОВАНИЕ ФУНКЦИИ ВОЗБУЖДЕНИЯ ЯДЕРНОГО ПРОЦЕССА $Be^9/d, n/B^{10}$ ИСКУССТВЕННО УСКОРЕННЫМИ ЧАСТИЦАМИ В ЭНЕРГЕТИЧЕСКОЙ ОБЛАСТИ 0,5 — 1,6 MeV

Е. КОЛТАИ

Резюме

Применением независимого от энергии нейтронного детектора определена кривая возбуждения ядерного процесса $Be^9/d, n/B^{10}$ в энергетической области бомбардировки от 0,5 до 1,6 MeV. За появление широкого пика, обнаруженного в области около 1 MeV, по всей вероятности, вызывает конкурирующий процесс высокой интенсивности, появляющийся выше 1 MeV.

THE SECOND ORDER NON-UNIQUE FORBIDDEN DECAY OF Cl^{36} INTO S^{36}

By

D. BERÉNYI

INSTITUTE FOR NUCLEAR RESEARCH OF THE HUNGARIAN ACADEMY OF SCIENCES, DEBRECEN

(Presented by A. Szalay. — Received 20. XI. 1962)

The internal bremsstrahlung spectrum accompanying the electron-capture decay of Cl^{36} which had not yet been subject to investigation, was studied with scintillation techniques. For the maximum energy the value of 1159 ± 45 keV has been obtained which is, within experimental errors, in good agreement with the value obtained from threshold measurements of the (p, n) reaction. The JAUCH diagram of the internal bremsstrahlung spectrum is linear from 700 keV to the maximum energy.

From the study of the annihilation peak superimposed on the bremsstrahlung spectrum we definitely established the presence of β-decay positrons in the decay of Cl^{36}, in contradiction to current views. The branching ratio of positive β-decay present in the decay of Cl^{36} is $(2{,}3 \pm \pm 0{,}9) \cdot 10^{-3}\%$ and the value of $\log ft$ is 14,3. By accepting a value of 1,7% for the branching ratio of electron capture, the ε_K/β^+ ratio is found to be $(7{,}5 \pm 3{,}0) \cdot 10^2$. This is the first experimental confirmation of the theoretical prediction that for second or higher order forbidden transitions the ratio ε_K/β^+ is increased and is larger than the corresponding value for the allowed transitions (this is ~ 90 in the present case as compared with the experimental value of 750).

1. Introduction

It is known that Cl^{36} decays predominantly (98,9%) with β^--decay into A^{36} and partly (1,7%) with electron capture into S^{36} [1—3]. However, according to the recent tables of KÖNIG, MATTUCH and WAPSTRA [4] and the ground state energy systematics of YAMADA and MATUMOTO [5], the total disintegration energy for the transition $Cl^{36} \rightarrow S^{36}$ is 1138 and 1140 keV, respectively; thus the positive β-decay is also possible energetically.

As to the spins, the value of 2 and 0 can be attributed to the ground state of Cl^{36} and S^{36}, respectively, directly from micro-wave absorption measurements [6]. At the same time the parity of the Cl^{36} ground state is *plus* as can be established from the shape of the β^--spectrum leading to the ground state of A^{36}; the parity of S^{36} is also *plus* since, on the one-hand we are concerned here with the ground state of an even-even nucleus, on the other hand $\log ft = = 13{,}5$ for the electron capture process which corresponds to a second order forbidden transition [6]. Hence for $Cl^{36} \rightarrow S^{36}$ we have $\Delta I = 2$, $\Delta\pi = +1$ i.e. we have to do with a $2^+ \rightarrow 0^+$ non-unique second forbidden transition.

The theory cannot say much about the occurrence of positrons in higher order forbidden transitions. For the case of allowed transitions the calculations

of ZWEIFEL [7—8] give the ratio of electron capture to positron emission as function of the energy and atomic number by taking into account the K-shell only. There have also been some calculations, and in some cases measurements, for different types of first forbidden transitions but no measurement is available at higher order forbidden transitions [9—12]. Numerical calculations for non-unique higher forbidden transitions also do not exist because of the lack of knowledge of nuclear matrix elements. In any case theoretical considerations definitely indicate that for higher order forbidden transitions an increase of the ratio ε/β^+ is to be expected [11—12].

To return to the case of Cl^{36} one can, because of the forbidden nature of the transition, expect fewer positrons than given by ZWEIFEL [7—8] at this energy and atomic number.

There are no reliable data showing the presence of positrons in the decay of Cl^{36}. As far back as 1941 GRAHAME and WALKE [13] observed positron tracks in a cloud chamber originating in a Cl^{36} preparation; however, WU et al. [14] criticized the validity of this conclusion on the grounds that from a thick source there appear positrons even if the sample is purely electron emitting. These authors, from measurements with a magnetic spectrometer, put the upper limit for the ratio of the number of positrons to electrons at 10^{-4}.

Considering these circumstances it seems desirable to search, in the case of Cl^{36}, for positrons by means of the scintillation technique which is more promising as regards the detection of low-intensity positrons. In this case, where γ-radiation is not present, it can be expected that a possible low-intensity annihilation peak will relatively easily be detected.

DREVER and MOLJK performed some measurements on the γ-ray spectrum of Cl^{36}, but the present investigations have been performed under more favourable circumstances.

First we shall examine the internal bremsstrahlung spectrum of Cl^{36} produced by electron capture in order to corroborate the energy differences between the ground states of Cl^{36} and S^{36} as given by KÖNIG et al. [4].

First of all we give a brief summary of the experimental arrangement and conditions.

2. Experimental details

A cylindrical NaI(Tl) crystal of upper diameter of 66 mm and of lower diameter of 42 mm has been used. Its height is 45 mm. This is connected to a RCA 6342A multiplier.*

The pulses pass from the multiplier through a cathode-follower into a wide-band amplifier of amplification $\approx$100 and of band-with 4—5 Mc. The

* The container of the crystal has been made by Mr. GY. MÁTHÉ in our Institute, while the crystal has been produced at the Institute for Medical Physics in Budapest.

amplified signals were analysed by means of a single channel differential discriminator ($\tau \sim 2.10^{-5}$ sec) and counted with a five stage decatron unit. The amplifier, the decatron unit and high-voltage supply are contained in a single box. The arrangement is a somewhat modified version of that described in ref. [15—16].

During the measurement a well-type crystal has also been employed with a similar amplifier and other electronic components as described above. The height, upper diameter and lower diameter of the well-type crystal is 65, 65 and 45 mm, respectively, while the diameter and depth of the hole is 19 and 36 mm, respectively.

The crystal and multiplier have been shielded with a lead (5 cm thick) and an iron (1 cm thick) cylinder.

The measurements have been performed with two Cl^{36} samples. One of them been received from "Совызхимэкспорт" (of 54 μC/g specific activity) and the other from the Amersham "Radiochemical Centre" (of 391 μC/g specific activity). Good specific activity is not essential in these measurements. Both sources used were of $\approx 50\,\mu$C, the Amersham one was, according to the original calibration, of $(50{,}5 \pm 7\%)\,\mu$C. In order to ensure a reproducible geometry in spite of the bad specific activities, the powder sources have been placed in containers shown in Fig. 1. The source of better specific activity has been placed into the container, with longer plexiglass plug. The wall of the plexiglass container and the aluminium cover of the crystal together absorbed all the β^--radiation present.

The source-holder has been placed, except when working with the well-type crystals, in the middle of the upper cover of the crystal's aluminium container. The distance between the upper plane of the crystal and the upper plane of the aluminium cover is 4,5 mm.

3. Investigation of the internal bremsstrahlung

The internal bremsstrahlung originating in the electron capture decay of Cl^{36} has not yet been subject to investigation. Such experiments are difficult to perform because of the intense internal and external bremsstrahlung which has its origin in the negative β-decay of Cl^{36} since, as it has been mentioned, this latter one is the predominant form of the decay of Cl^{36}.

However, the maximum energy of the Cl^{36} β^- spectrum is 715 keV [2] while, on grounds of the energy available for the $Cl^{36} \rightarrow S^{36}$ transition [4] the maximum energy of the electron-capture internal bremsstrahlung should be expected to be about 1140 keV. Thus there seems to be no difficulty to investigate the electron-capture bremsstrahlung in order to confirm the total decay energy value of the Cl^{36}—S^{36} transition known from nuclear reaction investigations.

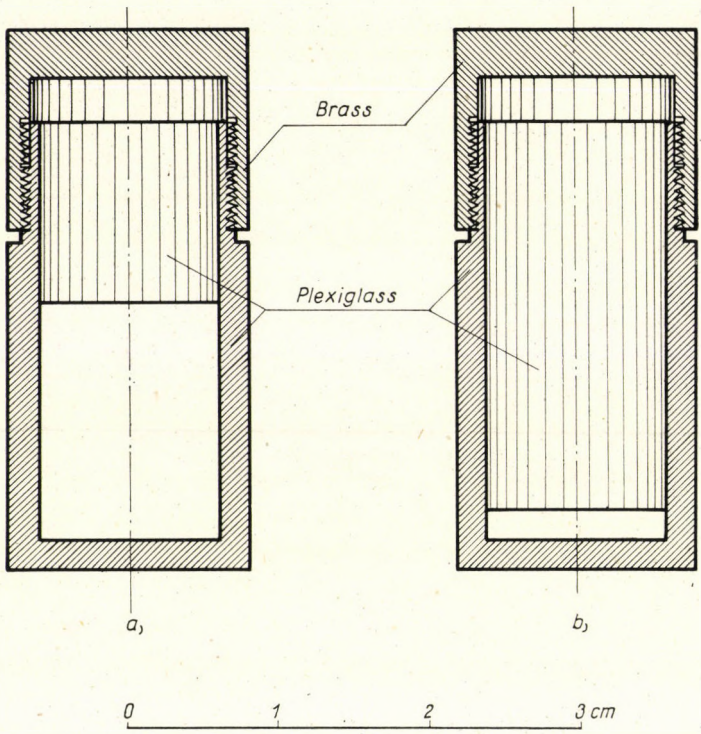

Fig. 1. The containers used for the radioactive samples

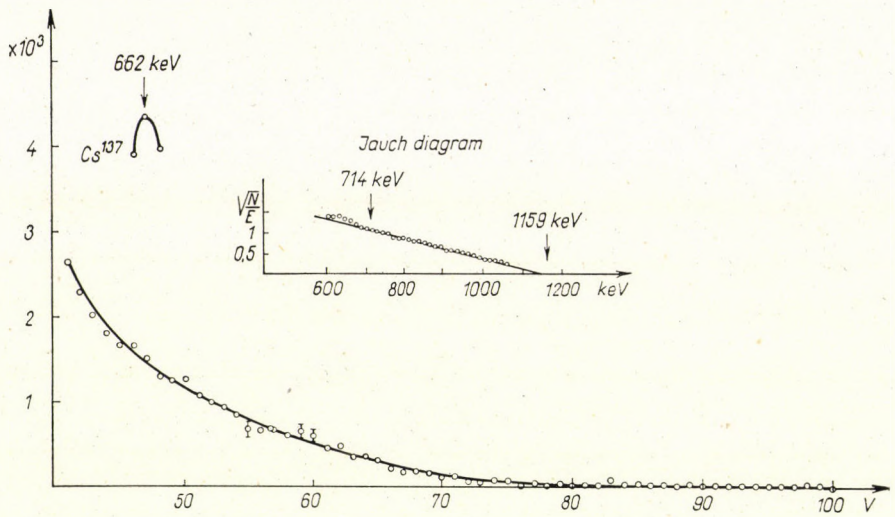

Fig 2. Experimental internal bremsstrahlung of Cl^{36} without any correction, except for the subtraction of background. For the JAUCH diagram every necessary correction has been performed (here the errors due to the corrections might be essentially larger than the diameters of the circles which approximately correspond to the magnitude of the statistical error)

To check the apparatus and the experimental arrangement we took the internal bremsstrahlung of Fe^{55} under the same experimental conditions as with Cl^{36}. (By mixing NaCl to the sample we got the same bad specific activity as that of Cl^{36}.) On the basis of the JAUCH diagram [17—18], the maximum energy of the bremsstrahlung spectrum has been found to be 225 $\pm$ $\pm$10 keV which is in good agreement with experimental data [3]. On the JAUCH diagram under 100 keV the points are not on a straight line which also agrees both with theoretical expectations [19—20] and experimental data [21].

The experimental bremsstrahlung spectrum of Cl^{36}, from about 600 keV to the maximum energy, can be seen in Fig. 2, without any correction, except for the subtraction of background. Individual points correspond to the sum of ten measurements lasting five minutes each, i.e. to measurements lasting 50 minutes.

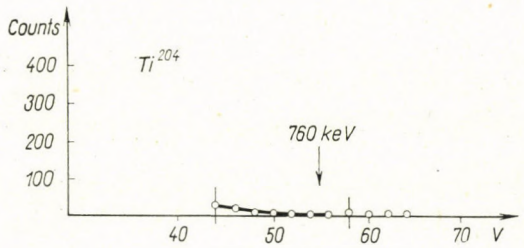

Fig. 3. Check for the presence of superposition in the bremsstrahlung measurement. In the case of Tl^{204}, under conditions identical with those of Cl^{36}, no significant counting rate above the background has been found over the maximum energy of the β-spectrum (background subtracted)

However, the experimental spectrum does not give directly the energy distribution of the continuous γ-ray spectrum since, to the monoenergetic γ-radiation there corresponds, in the scintillation spectrometer, a distribution consisting of a photopeak (total energy peak) and a Compton distribution. Further circumstances, such as the dependence of the sensitivity of the crystal on the energy, also contribute to the distortion of the actual spectrum.

In the given case we first of all investigated whether, in the presence of strong β^- decay, superposition or some other effects will not lead to the distortion of the spectrum also above the maximum of the β^- spectrum. For a check we used Tl^{204}, the maximum of the β^- spectrum of which is at 760 keV. It decays also with electron capture (2,6%) but the available energy for this process is only 376 keV [2, 3]. By putting a 50 μ Csample of this into the container of type *a)*, mixing it with $NaSO_4$, we realized the same experimental conditions as with Cl^{36}. Fig. 3 shows that there is no effect present above the maximum of the β^- spectrum (cf the caption to Fig. 3).

In general in studies of internal bremsstrahlung the following corrections are taken into account: 1. background correction (see for example [23, 24]); 2. correction for the Compton distribution present in the scintillation spectrum

[23, 25, 26]; 3. correction for the energy-dependence of detection efficiency [23—25, 27, 28]; 4. correction for finite resolution [23, 27, 29]; 5. correction for the absorption in the material between crystal and the source [21, 24, 29] and finally, 6. for the escape of the KX-rays of iodine.

The last two of these become significant only at very low energies, thus in our case, where at any rate one cannot measure under 714 keV they can be disregarded. Background has been measured under the same conditions and for the same time intervals as the total effect and has been subtracted in each case from the corresponding value of the latter. The corrections for the Compton distribution and the energy-dependence of the detection efficiency was determined in the following way. From the analysis of standard spectra (Hg^{203}, Cs^{137}, Zn^{65}) we determined the relative positions and height as functions of the energy, of the characteristic points (e.g. the minimum between the photopeak and Compton distribution, height of Compton plateau, etc.) of the scintillation spectrum and compared them with the photopeak (total energy). With the aid of this we decomposed, starting from the high-energy part, into components the internal bremsstrahlung spectrum by means of successive subtraction. The different components, the photopeaks having been increased corresponding to the decrease of relative detection efficiency and the magnitude of the Compton distribution were then again added. For these corrections the graphs from Nuclear Data Tables [22] were used. Finally, the bremsstrahlung spectrum, corrected in this way, was corrected for the finite resolution by using the relation

$$N_{\text{corr}}(E) = N_e(E) - KN'_e(E) - \frac{1}{2} KEN''_e(E),$$

where $N_{\text{corr}}(E)$ is the corrected spectrum, N_e, N'_e and N''_e are the experimental spectrum in our case including all corrections except the correction for finite resolution, and the first and second derivatives at different points of the experimental spectrum, respectively.

$K = W^2(E)/(0{,}693 \cdot 2E)$, in which $W(E)$ is the half-width for a monoenergetic γ-radiation of energy E. The derivatives required were determined according to PALMER and LASLETT, by means of the so-called 7-multiplier method, which is based on the fitting of the best third-order curve [31].

The JAUCH diagram, which represents the linearised spectrum of the internal bremsstrahlung, was constructed with these corrected data. In Fig. 2 it can be seen that the corrected points fit very well a straight line which intersects the x-axis at 1159 keV. From this, by adding the binding energy of the K-shell of Cl, we get 1162 ± 45 for the total decay energy of the transition $Cl^{36} \rightarrow S^{36}$. Estimation of the error given above shows this to be rather large which may be explained by the fact that the error of the individul points

may be significantly greater than the size of the circles representing them in the Figure (the diameter of the circles namely approximately corresponding to the experimental standard deviation). One can say that the value of the total decay energy agrees, within experimental error, with nuclear reaction data [4, 32] and with the value given by the energy systematics of nuclear ground states.

It can be seen from Fig. 2 that the deviation from the straight line on the JAUCH diagram starts at about 700 keV where, however, the presence of the β^- spectrum might have a perturbing effect. The corrected experimental points lie on a straight line though as it has been mentioned, their error might be considerable because of the different corrections. This means, that in spite of the fact, that we have in the case of the electron-capture decay of Cl^{36} a second order forbidden transition, the shape of the internal bremsstrahlung spectrum accompanying the electron capture follows the original MORRISON—SCHIFF theory in the region under study [33].

This fact is irreconciliable neither with present theory concerning the internal bremsstrahlung accompanying electron capture nor with available experimental evidence. Namely those theoretical correction which modify the original MORRISON—SCHIFF theory (electron capture from higher shells, the use of better electron wave functions, etc.), are above all effective in the lower energy domain of the bremsstrahlung spectrum and at higher energies they play a role only in the case of nuclei of larger Z [19, 20, 34]. From this it may be expected that in the case of Cl^{36} (the atomic number of Cl^{36} is lower than that of any other nucleus the internal bremsstrahlung of which has been experimentally investigated) these effects will not be present in the higher energy regions of the spectrum. On the other hand the $Cl^{36} \rightarrow S^{36}$ transition is forbidden in the second order, and thus the internal bremsstrahlung spectrum must also be forbidden in the second order [35].

Further the recent studies of HAYASHI and COMERFORD on the internal bremsstrahlung of Ni^{59} also show that the higher energy part of the JAUCH diagram does not deviate from the straight line. The $Ni^{59} \rightarrow Co^{59}$ $3/2^- \rightarrow 7/2^-$ transition is also forbidden in the second order and the investigation of the bremsstrahlung is not made difficult by electron emission and γ-radiation is not present either. The maximum energy of the internal bremsstrahlung is 1062 keV, so that this is also near to that of Cl^{36}; further its atomic number is not very different from that of Cl^{36}. Under these conditions the JAUCH diagram of the internal bremsstrahlung of Ni^{59} deviates significantly from the straight line only from about 700 keV downwards.

We finally note that in the case of Ni^{59} it is the uncorrected JAUCH diagram which shows the above-mentioned properties. Our JAUCH diagram with uncorrected data (not shown in the figure) shows essentially the same picture as that with the corrected ones, except that it intersects the x-axis at higher energies in the corrected case.

Besides on hand of the JAUCH diagram we checked also with another method whether the MORRISON—SCHIFF theory describes correctly the internal bremsstrahlung of Cl^{36} in the energy range of our investigation.

According to the MORRISON—SCHIFF theory the energy distribution of the bremsstrahlung is described by the relation [28]

$$N(W)\,dW = \frac{n\alpha}{\pi W_0^2}(W_0 - W)^2\,W dW,$$

where n is the total number of K-capture decays, α is the fine structure constant, and W_0 the end point of the spectrum (W_0 and W are given in units of mc^2).

We set the differential discriminator to such a region of the bremsstrahlung spectrum where the spectrum is certainly not disturbed by the bremsstrahlung from the electrons, but where the number of pulses is high enough to get a good statistics. With a 8 V channel width we covered the range between 770 and 880 keV, the middle of which is at 830 keV (see Fig. 2). Integrating the energy distribution, as given by the MORRISON—SCHIFF formula over this interval

$$c\int_{1{,}51}^{1{,}72}(W_0 - W)^2\,W dW\,, \qquad c = \frac{n\alpha}{\pi W_0} = \text{const.},$$

where the constant c can be determined from the known source activity (50,5 μC), the K-capture ratio (1,7%) and the maximum energy of the spectrum (1140 keV), we obtain the number of quanta falling according to theory, into the chosen energy interval. The calculated value was found to be 1,95 quantum/sec.

We were measuring for 30×10 minutes as has been described above at a setting where the channel width is equal to the half width of the monoenergetic line lying in the centre of the channel width i.e. at 830 keV. Background has been measured for the same time interval. After subtracting background the total number of pulses was 25571, i.e. 1,42/sec. After correcting by the aid of the tables of ref. [32, 37] for the photopeak, total spectrum and the absolute efficiency we obtained for the experimental value 26,83 pulses/sec. We note that by choosing the channel width to be equal to the half width of the corresponding monoenergetic photopeak, we approximately counted the pulse number falling in the complete photopeak of corresponding energy.

Comparing the experimental and theoretical values we see that the experimental value is many times larger than the theoretical one calculated width the MORRISON—SCHIFF formula. This remains to also when applying further corrections (e.g. for the Compton distribution of internal bremsstrahlung

of higher energy), though the magnitude of the ratio of experimental and theoretical value will be lower.

SARAF [40] found that also in the case of Ni^{59} the experimental intensity is larger especially in the high-energy part of the spectrum than the MORRISON—SCHIFF values.

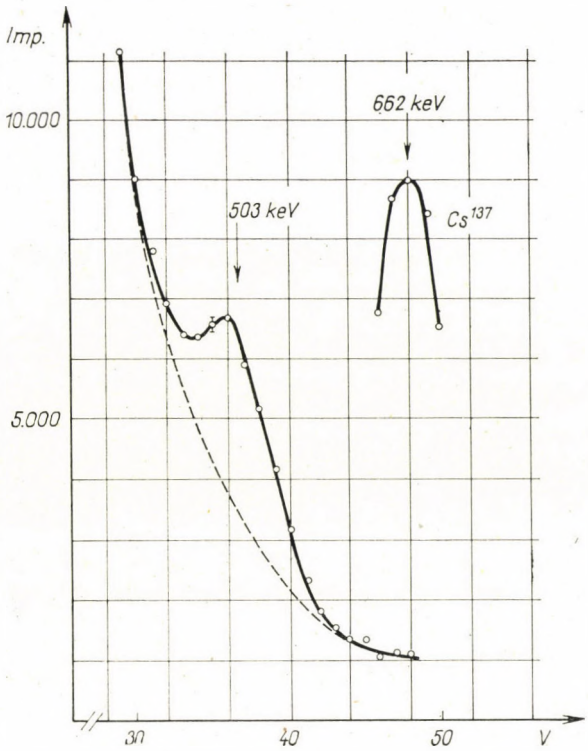

Fig. 4. Scintillation γ-spectrum of Cl^{36} around 500 keV. The different points correspond to the sum of six independent series of measurements (in the series we were measuring for 5 minutes in each point). Background (measured for the same time-interval as the total effect) is subtracted at each point

4. The presence of positrons and the ε_K/β^+ ratio

Above we reported on the investigation of that region of the bremsstrahlung spectrum where more or less only the internal bremsstrahlung spectrum is present. Fig. 4 shows the region of the scintillation γ spectrum around 500 keV under the experimental circumstances explained above, with the Amersham source contained in a *b)* type container shown in Fig. 1. Superimposed on the bremsstrahlung spectrum we have peak at 503 ± 10 keV, which probably originates in the annihilation of positrons. To prove that positrons are present in the $Cl^{36} \rightarrow S^{36}$ transition we have to show that the

peak in question is not caused by impurities and that it is in fact of an annihilation character. However, first of all we must exclude the possibility considered in connection with cloud chamber experiments, according to which positrons may be present in small numbers even in the case of nuclei emitting only electrons. (We note that in our opinion this possibility arises only in the case of spectra of which the maximum energy is above 1,02 MeV). For this purpose the already employed Tl^{204} seems to be most suitable. As it has been explained Tl^{204}, as well as Cl^{36} decays predominantly with negative β decay (into Pb^{204}) and also in a small ratio ($\sim$2,6%) it decays into Hg^{204} by electron capture [2]. The maximum energy of its negative β spectrum is also very near to the 714 keV maximum energy of Cl^{36} (760 keV). However, unlike the case of Cl^{36}, the total decay energy of $Tl^{204} \rightarrow Hg^{204}$ is, according to both nuclearspectroscopic measurements and the most recent mass data, under 400 keV. On this account the possibility of the presence of positive decay positrons is energetically excluded. Fig. 5 shows the scintillation spectrum of Tl^{204} under the experimental conditions described above, in the same energy interval in which the spectrum of Cl^{36} is seen in Fig. 4. The measurement clearly shows that under the given experimental conditions the peak in question cannot come from electrons, since in the case of Tl^{204} nothing similar is found.

That the peak is not due to impurities is proved by the following:

1. The peak is present in the spectrum obtained from different sources (Совызхимэкспорт, Moscow and Radiochemical Centre, Amersham, England) which were of different specific activity.

2. By purifying the source in a cation-exchange column the intensity of the source remains unchanged.

3. Half-life investigations did not lead to a separation of the peak from Cl^{36}. After more than two and half months the height of the peak did not show any decrease.

4. Among nuclei of relatively long half-life none is known which is purely β^+-emitting; further none is known to emit predominantly γ-radiation around 500 keV, relative to which other monoenergetic γ-radiations, if any, are negligible.

There is, however, an experimental and a theoretical argument in favour of the annihilation character of the peak.

Theoretically, it is wholly improbable that there should be a level around 500 keV in an even-even nucleus, as is S^{36}, of magic neutron number. Looking at the light nuclei up to $A = 48$ [6] the first excitation levels of the even-even (i.e. even number of protons and neutrons) nuclei are all above 1 MeV with a jump at magic numbers (Fig. 6). In the Figure we marked also the position of S^{36} (there are no experimental data on the first excited state of S^{36} [6]. Therefore the 503 keV peak of the γ spectrum of Cl^{36} cannot come from the deexcitation of the excited level of S^{36}.

To prove the annihilation character of a 511 keV γ-radiation it is customary to use the fact that the probability is largest for the two annihilation quanta to fly apart at 180°. We also exploited this in a very simple way by the use of the well-type crystal.

It can be seen qualitatively that by putting the source in the hole, we must, when summing the two annihilation radiations, get a peak at 1022 keV,

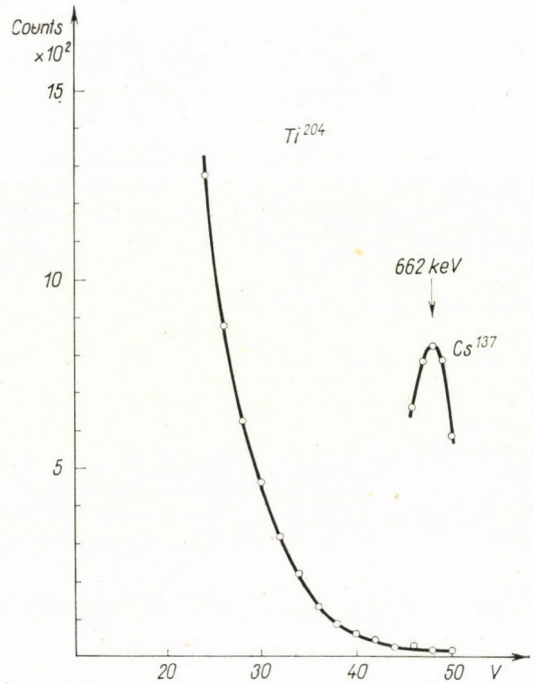

Fig. 5. The bremsstrahlung spectrum of Tl^{204} in the same energy region in which the spectrum of Cl^{36} was taken (background subtracted)

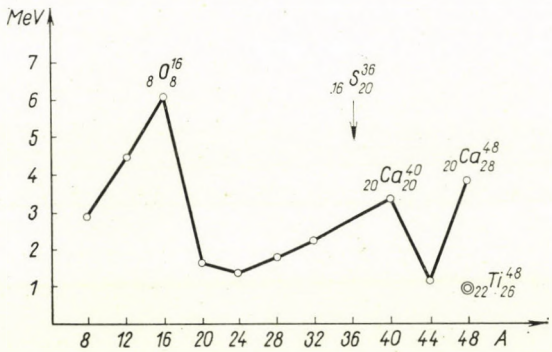

Fig. 6. Positions of the first excited states of even-even nuclei up to $A = 48$ as function of mass number

while if we put the source on a sheet of paper just above the hole we should not get any peak at this energy.

The effect is very definitely present in the case of the positron radiating Na^{22} at the experimental conditions above. By performing the experiment on Cl^{36} we obtained the result shown in Fig. 7.

Against this one might object, that in the case of Cl^{36} the 1020 keV peak in the spectrum taken with the source put in the hole might have its

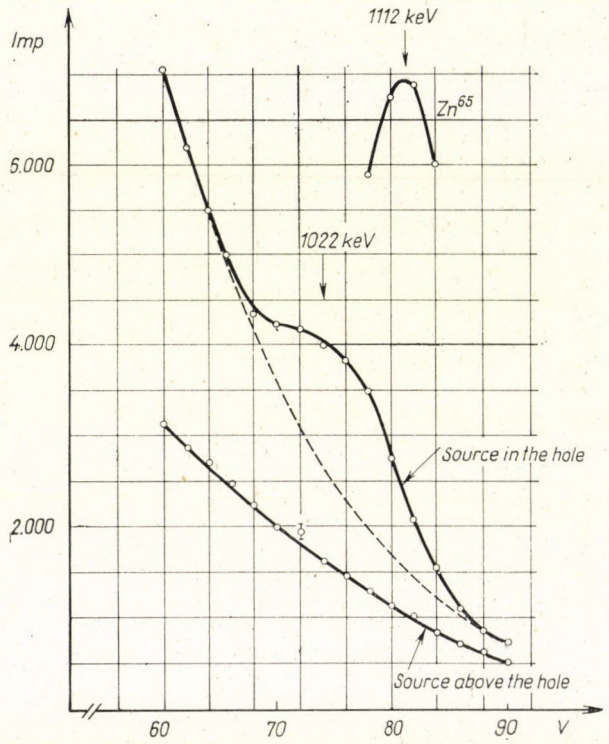

Fig. 7. Scintillation spectrum of Cl^{36} above 1 MeV taken with well-type crystal. The individual points correspond to 20 measurements 5 minutes each, i.e. one point is the result of a measurement of 100 minutes (source activity 50 μC)

origin either in a very small-intensity γ-radiation of about 1020 keV, which is present only because of the solid angle being increased by putting the source in the hole, or in two 500 keV radiations in a cascade originating in the same nucleus.

These objections can be excluded quantitatively. Under exactly the same experimental conditions we measured the intensity ratios for several standard γ-lines above and in the hole (Hg^{203}, Cs^{137}, Mn^{54}, Zn^{65}, Na^{22}). This intensity ratio is shown as function of the energy in Fig. 8. It can be seen from the Figure that the intensity ratio measured above and in the hole around 1000 keV can only be 3 for a direct transition. It can also be easily seen that

in the case of cascade sum-peaks the intensity ratio of the sum-peaks measured in and above the hole is given by the product of the intensity ratios of the component peaks. This, in the case of two radiations of about 500 keV, would be about 10 as can be seen from Fig. 8. If there are both cascade and direct transitions this value must be between 3 and 10. In our case, as it can be seen from Fig. 8, the ratio in question is definitely above 10 even if we take for the height of a possible peak the double standard deviation in the spectrum taken above the hole. We may thus state that *positrons are present without doubt in the decay of* Cl^{36}. The maximum energy of the positron spectrum, according to nuclear reaction data and confirmed by our measurements, is 116 keV.

By preparing from a Cs^{137} solution a source of the same geometry as that of Cl^{36} and using the Nuclear Data Tables (Part 3) [22] and the graphs of the HEATH γ-spectrum cathalogue [37], multiplying by the corresponding detection

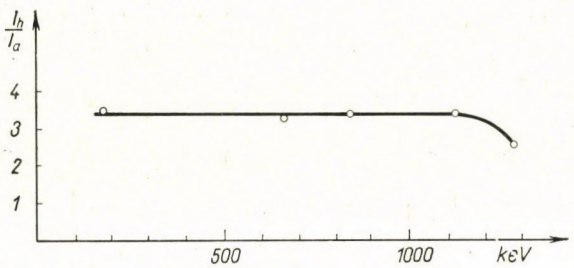

Fig. 8. Intensity ratio of peaks for monoenergetic γ-radiations measured after placing the source into and above the hole

efficiency and the ratio of peak and total spectrum we compared the areas of the Cl^{36} annihilation and the 660 keV total-energy peak of Cs^{137}. From this and from the knowledge of the activities of the standard and the Cl^{36} sources the number of positrons per decay was found to be $(2{,}3 \pm 0{,}9)\ 10^{-3}\,\%$.

From this the value of log *ft* can be calculated with slight extrapolation by means of the MOSZKOVSZKI method [38], if we accept for the maximum energy of the positron spectrum the value of 116 keV and for the half-life of Cl^{36} the value of $2.5 \cdot 10^5$ years [3]. Thus we get $\log ft = 14{,}3$ which means a second order forbidden transition [39].

From the number of positrons per decay and the electron-capture ratio (1,7% according to DREVER and MOLJK [1]) the ratio ε_K/β^+ results in $(7{,}5 \pm \pm 3{,}0) \cdot 10^2$ for the second order forbidden transition $Cl^{36} \rightarrow S^{36}$. At the same time, by extrapolating the graphs prepared with the aid of ZWEIFEL's calculations concerning allowed transitions, we get a value of about 90. Thus our result is in agreement with the theoretical predicitions [11, 12], according to which a definite increase is to be expected for a higher order non-unique forbidden transition in comparison with allowed transitions.

After our measurements were finished a paper was published by DREVER et al. who measured the K/L ratio in the decay $Cl^{36} \rightarrow S^{36}$ and who also did some measurements on the bremsstrahlung spectrum. They obtained for the maximum energy of the internal bremsstrahlung spectrum the value of 1170 $\pm$ $\pm$ 40 keV which is in good agreement with our result. They also found the annihilation peak and the order of magnitude of the ratio ε_K/β^+, calculated from their data, is also in agreement with our value.

Finally I want to express my gratitude to Dr. A. SZALAY, Director of our Institute, Corresponding Member of the Hungarian Academy of Sciences, for his interest in my work and for providing excellent working conditions. Thanks are due to Dr. Cs. UJHELYI and Mr. E. BRÜCHER for the preparation of sources and the radiochemical manipulation and also to Mr. GY. MÁTHÉ for his help with electronic problems.

REFERENCES

1. R. DREVER and A. MOLJK, Phil. Mag., **46,** 1337, 1955.
2. *Б. С. Джелепов* и *Л. К. Пекер,* Схемы распада радиоактивных ядер. Изд. АН СССР. Москва—Ленинград, 1958.
3. Nuclear Data Sheets, National Academy of Sciences — National Research Council, Washington, D. C.
4. L. A. KÖNIG, J. H. E. MATTAUCH and A. H. WAPSTRA, Nucl. Phys., **31,** 18, 1962.
5. M. YAMADA and Z. MATUMOTO, J. Phys. Soc. Japan, **16,** 1947, 1961.
6. LANDOLT—BÖRNSTEIN, Zahlenwerte und Funktionen. Neue Serie. Gruppe I., Bd. I. Springer Vlg., Berlin, G. H., 1961.
7. P. F. ZWEIFEL, Phys. Rev., **96,** 1572, 1954.
8. P. F. ZWEIFEL, Phys. Rev., **107,** 329, 1957.
9. M. L. PERLMAN, J. P. WELKER and M. WOLFSBERG, Phys. Rev., **110,** 381, 1958.
10. P. DEPOMMIER, U. NGUYEN-KHAC et R. BOUCHEZ, Journ. de Phys. Radium, **21,** 456, 1960.
11. R. BOUCHEZ and P. DEPOMMIER, Reports on Prog. in Phys., **23,** 395, 1960.
12. H. BRYSK and M. E. ROSE, Revs. Mod. Phys., **30,** 1169, 1958.
13. D. C. GRAHAME and J. H. WALKE, Phys. Rev., **60,** 909, 1941.
14. C. S. WU, C. H. TOWNES and L. FELDMAN, Phys. Rev., **76,** 692, 1949.
15. GY. MÁTHÉ, Magyar Fizikai Folyóirat, **7,** 129, 1959 (in Hungarian).
16. GY. MÁTHÉ and T. SCHARBERT, Mérés és Automatika, **7,** 1, 1959 (in Hungarian).
17. J. M. JAUCH, AEC Report, ORNL-1102. Oak Ridge National Lab., 1951.
18. T. HAYASHI and J. R. COMERFORD, Jr., Progress Report, TID-6080. Ohio State University, Columbus (Ohio) 1960.
19. R. J. GLAUBER and P. C. MARTIN, Phys. Rev., **95,** 572, 1954.
20. R. J. GLAUBER and P. C. MARTIN, Phys. Rev., 104, 158, 1956.
21. L. MADANSKY and F. RASETTI, Phys. Rev., **94,** 407, 1954.
22. Nuclear Data Tables, Part 3. National Academy of Sciences-National Research Council, Washington, D. C. 1960.
23. R. W. HAYWARD and D. D. HOPPES, Phys. Rev., **104,** 183, 1956.
24. A. BISI, E. GERMAGNOLI, L. ZAPPA and E. ZIMMER, Nuovo Cimento, **2,** 290, 1955.
25. W. S. EMMERICH, S. E. SINGER and J. D. KURBATOV, Phys. Rev., **94,** 113, 1954.
26. J. B. VAN DER KOOI and H. J. VAN DEN BOLD, Physica, **22,** 681, 1956.
27. C. E. ANDERSON, G. W. WHEELER and W. W. WATSON, Phys. Rev., **90,** 606, 1953.
28. S. G. COHEN and S. OFER, Phys. Rev., **100,** 856, 1955.
29. B. SARAF, Phys. Rev., **94,** 642, 1954.
30. T. B. NOVEY, Phys. Rev., **89,** 672, 1953.
31. J. P. PALMER and L. J. LASLETT, AEC Research Report, ISC. 174. Ames Laboratory, 1950.
32. Nuclear Data Tables, 1960. Part 1. National Academy of Sciences-National Research Council, Washington, 1961.

33. P. Morrison and L. J. Schiff, Phys. Rev., **58,** 24, 1940.
34. P. C. Martin and R. J. Glauber, Phys. Rev., **109,** 1307, 1958.
35. R. E. Cutkowsky, Phys. Rev., **95,** 1222, 1954.
36. Gamma Emitters by Half-Life and Energy, Nucleonics, **18,** No. 11. p. 196—197, 1960.
37. R. L. Heath, AEC Res. and Development Rep., IDO-16408. Phillips Petroleum Co., Atomic Energy Division, Idaho Falls, Idaho, 1957.
38. S. A. Moszkowszki, Phys. Rev., **82,** 35, 1951.
39. G. J. Nijgh, A. H. Wapstra and R. Von Lieshout, Nuclear Spectroscopy Tables, North Holland Publ. Co., Amsterdam, 1959.
40. B. Saraf, Phys. Rev., **102,** 466, 1956.
41. P. W. Dougen, K. W. D. Ledingham and R. W. P. Drever, Phil. Mag, **7,** 1222, 1962.

НЕОДНОЗНАЧНО ЗАПРЕЩЕННЫЙ ВО ВТОРОМ ПОРЯДКЕ РАСПАД Cl^{36} В S^{36}

Д. БЕРЕНИ

Резюме

Сцинтилляционной техникой исследуется спектр внутреннего тормозного излучения, сопровождающий распад Cl^{36} с электронным захватом. Данный спектр до настоящего времени не являлся предметом изучения. Для максимальной энергии получено $1159 \pm \pm 45$ keV, которое в пределах погрешности хорошо согласуется с результатом пороговых измерений реакции (p, n). Диаграмма Яуха спектра внутреннего тормозного излучения в области энергии от 700 keV до максимальной представляет собой прямую.

На основании исследования аннигиляционного пика, накладывающегося на спектр тормозного излучения, неоспоримо было установлено присутствие позитронов β-распада в распаде Cl^{36}, что противоречит нынешней точке зрения. Доля участия положительного β-распада в распаде Cl^{36} составляет $(2{,}3 \pm 0{,}9) \cdot 10^{-3}\%$, значение log ft равно 14,3. Взять для доли участия электронного захвата 1,7% (по литературным данным), отношение ε_K/β^+ оказалось равным $(7{,}5 \pm 3{,}0) \cdot 10^2$. Это и есть первое экспериментальное доказательство по отношению теоретического предсказания, согласно которому в случае запрещённых во втором или более высоких приближениях переходов отношение ε_K/β^+ сильно увеличивается и превышает соответствующее значение для разрешенных переходов (последняя величина для данного случая равна ~ 90, против найденного 750).

$\gamma-\gamma$ ANGULAR CORRELATION MEASUREMENT ON THE 0,337 → 1,10 MeV CASCADE IN THE DECAY OF Fe^{59}

By

D. BERÉNYI, GY. MÁTHÉ and T. SCHARBERT

INSTITUTE FOR NUCLEAR RESEARCH OF THE HUNGARIAN ACADEMY OF SCIENCES, DEBRECEN

(Presented by A. Szalay. — Received 18. XII. 1962)

By applying the scintillation method and sum-coincidence circuit the authors carried out $\gamma-\gamma$ angular correlation measurements on the smallest intensity 0,337 → 1,10 MeV cascade in the decay of Fe^{59}, after having reproduced the results known for the 0,145 → 1,29 MeV cascade. For the 0,337→1,10 MeV cascade the angular correlation function is $W(\vartheta) = 1 - (0{,}451 \pm 0{,}156)\, P_2(\cos\vartheta)$, which for the 1,43, 1,29 and 1,10 MeV levels excludes the spin assignments 3/2, 5/2, 7/2; 5/2, 3/2, 7/2; 3/2, 1/2, 7/2 and 5/2, 1/2, 7/2.

In the decay of Fe^{59} three γ-cascades are known at present [1—4]. Of these the most intense (0,192 → 1,10 MeV) has an intensity of only 2,5% as compared to the number of disintegrations of Fe^{59} while the intensities of the 0,145 → 1,29 MeV and 0,337 → 1,10 MeV cascades are only 0,8% and 0,3%, respectively [2]. $\gamma-\gamma$ angular correlation measurements for the γ-cascades occurring in the decay of Fe^{59} have been reported in three cases [6, 7, 2]. Of these cascades only the most intense was known at the time when the first two measurements took place [6, 7] thus, naturally, the measurements were concerned only with this one. Recently, HEATH et al. have carried out measurements not only for the 0,195 → 1,10 MeV but also for the 0,145 → 1,29 MeV cascade. In HEATH et al.'s opinion, such measurements involve considerable difficulties which may be hard to eliminate by present techniques.

By using the scintillation method and sum-coincidence circuit [8] we succeeded in carrying out angular correlation measurements on the lowest intensity 0,337 → 1,10 MeV cascade, after having reproduced the values obtained by HEATH et al. on the 0,145 → 1,29 MeV cascade [2] for the angular correlation coefficient.

We have modified the arrangement used by us previously (for block scheme see [3]) in such a way that after suitable amplification one of the quick signals is given from the trigger crystal directly to the coincidence circuit, the summing circuit being thus avoided [5]. In the sum-coincidence spectrum so taken the sum peak will be missing. The dimensions of the two NaJ(Tl)crystals used were 3,5 ⌀ × 3,5 cm each, the resolving time of the coincidence circuit was $\sim 10^{-7}$ sec. Here random coincidence measurements require special care as the small intensity peaks corresponding to the cascades are superimposed

on a very intense γ-radiation background. Therefore, we have measured the random coincidences in such a manner that the detectors were separated from each other at a distance to prevent true coincidences and in an arrangement completely identical with that of the corresponding angular correlation measurement two independent Fe^{59} sources were used.

The source in the form of ferrichlorid was placed in a glass cylinder of 1,5 mm in outer diameter and 0,5 mm wall thickness. The source — detector separation was 5 cm. The source was adjusted in the centre within 1%, i.e. the counting rate of the movable detector was constant within 1% for all positions. The reliability of the apparatus was checked by an angular correlation measurement on the γ-cascade of Co^{60}.

In the measurements on the 0,337 → 1,1 MeV cascade the standing counter was protected by two lead plates 1 cm thick each, in order that in measurements at 90° and at 120° the two crystals may not "see each other" and thus the Compton scattering from one crystal to the other is prevented.

The measured data were evaluated on the basis of the "maximum likelihood" method by means of an "Ural" type electronic computer [9] at the Department of Computing Techniques of the Central Research Institute of Physics of the Hungarian Academy of Sciences. The angular correlation function best fitting the experimental points for the 0,143 → 1,3 MeV cascade is: $W(\vartheta) = 1 - (0{,}063 \pm 0{,}027)\, P_2(\cos\vartheta)$, whereas for the 0,33 → 1,1 MeV cascade it is: $W(\vartheta) = 1 - (0{,}451 \pm 0{,}156)\, P_2(\cos\vartheta)$. Within the error limit $A_4 = 0$ in both cases. The above values given for A_2 in the angular correlation function are corrected for the finite dimension of the detectors [10].

The value obtained by us for the A_2 angular correlation coefficient in the case of the 0,143 → 1,3 MeV cascade is in sufficiently good agreement with the value obtained by HEATH et al [2].

The results give the following information on the levels of Co^{59} and the transitions between them. The spin of the gorund state of Co^{59} obtained from hyperfine structure and paramagnetic resonance measurements is 7/2 [11]. For the respective spins of the first, second and third excited level, for the transitions of which we have carried out our angular correlation investigations, the shell model predicts that these should be 1/2, 3/2 and 5/2 but it fails to give information on the actual assignment of these values to the individual levels [2]. On the basis of angular correlation measurements and intensity ratio determinations the spin values 5/2, 3/2 and 1/2 have so far been assigned to the 1,10 MeV, 1,29 MeV and 1,43 MeV levels, respectively. This assignment is supported by our measurement on the 0,143 → 1,3 MeV cascade, where, assuming the above spin assignment, the theoretical value of A_2 calculated on the basis of the table given by WAPSTRA et al [12] results in $A_2 = -0.0715$.

At the same time the foregoing spin assignment would give for the angular correlation of the 0,33 → 1,1 MeV cascade the value $A_2 = -0{,}0717$. However,

the difference between this value and $-0{,}451$ measured by us is large, even if the significant error of the experimental value is taken into account. On the other hand, there is no doubt that among the other possible theoretical values (3/2, 5/2, 7/2 — 0,0501; 1/2, 3/2, 7/2 — $-0{,}0715$; 5/2, 3/2, 7/2 — $-0{,}0143$; 3/2, 1/2, 7/2 — 0; 5/2, 1/2, 7/2 — 0) the value $-0{,}0717$ is still comparatively closest to the experimental value, excluding, however, the values 3/2, 5/2, 7/2; 5/2, 3/2, 7/2; 3/2, 1/2, 7/2 and 5/2, 1/2, 7/2 assigned successively.

The discrepancy can probably be explained by the fact that the 1,1 MeV γ-radiation is mixed with a large amount of E2. It did not seem worth-while to carry out a detailed analysis owing to the large error of the experimental values, but if the mixing coefficient is e.g. chosen to be $\delta = 0{,}5$, calculating A_2 we obtain $A_2 = -0{,}486$ and the value A_4 resulting on this assumption is consistent with the fact that in our measurements we obtained $A_4 = 0$ within the error limit.

Our thanks are due to Prof. A. SZALAY, Corresponding Member of the Hungarian Academy of Sciences, for excellent working conditions and for extensive support and to the Department of Computing Techniques of the Central Research Institute of Physics of the Hungarian Academy of Sciences for having carried out the numerical calculations and personally to our colleague Mr. Z. ZÁMORI, for providing all necessary information and assisting in the computations.

REFERENCES

1. J. M. FERGUSON, Nuclear Physics, **12,** 579, 1959.
2. R. L. HEATH, C. W. REICH and D. G. PROCTOR, Phys. Rev., **118,** 1082, 1960.
3. T. SCHARBERT, D. BERÉNYI and GY. MÁTHÉ, Acta Phys. Hung., **12,** 305, 1960.
4. M. KANTOLA and V. SUTELA, Ann. Acad. Sci. Fennicae, Ser. A. **6,** No. 107. p. 1. 1962.
5. GY. MÁTHÉ, Nucl. Phys. to be published.
6. F. R. METZGER, Phys. Rev., **88,** 1360, 1952.
7. D. SCHIFF and F. R. METZGER, Phys. Rev., **90,** 849, 1953.
8. A. M. HOOGENBOOM, Nuclear Instruments, **3,** 57, 1958.
9. RUPP ERZSÉBET, TÓTH IMRE and ZÁMORI ZOLTÁN, Reports of the Central Research Institute of Physics, **10,** 219, 1962. (in Hungarian).
10. M. E. ROSE, Phys. Rev., **91,** 610, 1953.
11. LANDOLT—BÖRNSTEIN, Zahlenwerte und Funktionen. Neue Serie. Gruppe I. Bd. I. Springer Vlg. Berlin, G. H., 1961.
12. A. H. WAPSTRA, G. J. NIJGH and R. VAN LIESHOUT, Nuclear Spectroscopy Tables. North-Holland Publ. Co., Amsterdam, 1959.

ИЗМЕРЕНИЕ $\gamma-\gamma$ УГЛОВОЙ КОРРЕЛЯЦИИ В КАСКАДЕ 0,337 → 1,10 MeV В РАСПАДЕ Fe^{59}

Д. БЕРЕНИ, ДЬ. МАТЕЙ и Т. ШАРБЕРТ

Р е з ю м е

Применением сцинтилляционного метода и схемы сум-совпадений после воспроизведения результатов, известных в случае каскада 0,145 — 1,29 MeV удалось проводить измерения угловой корреляции $\gamma - \gamma$ на каскаде 0,337 ← 1,10 MeV наименьшей интенсивности, наблюдаемой в распаде Fe^{59}.

Для каскада 0,337 → 1,10 MeV функция угловой корреляции $W(\vartheta) = 1 - (0{,}451 \pm \pm 0{,}156)\ P_2\ (\cos\vartheta)$, что по отношению уровней 1,43; 1,29 и 1,10 MeV исключает прикрепление к ним спинов 3/2, 5/2, 7/2; 5/2, 3/2, 7/2; 3/2, 1/2, 7/2 и 5/2, 1/2, 7/2.

EINE ERWEITERUNG DER THEORIE DER ÜBERGANGSSCHICHT

Von

Z. GYULAI und F. BUKOVSZKY*

INSTITUT FÜR EXPERIMENTALPHYSIK DER TECHNISCHEN HOCHSCHULE FÜR BAUTECHNIK UND VERKEHRSWESEN, BUDAPEST

(Eingegangen: 17. I. 1963)

Mit Hilfe der Theorie der Übergangsschicht [1] lässt sich die KOSSELsche Molekularbetrachtungsweise des Kristallwachstums auf die Ausbildung von dickeren (mehrere tausend Ionen enthaltende) Schichten und Spitzen erweitern. Sowohl für die Ausbildung der Schichten wie auch der Spitzen skizzieren wir die Möglichkeit der Ausbildung eines sogenannten KOSSELschen wiederholbaren Schrittes. Bei der Ausbildung eines solchen Schrittes beim Spitzenwachstum spielen auch Ionenpaare ein Rolle, deren grosse Konzentration in der Übergangsschicht dazu reichlich Gelegenheit bietet. Im Falle des Wachsens aus Dämpfen besteht der Dampf schon von vornherein aus Ionenpaaren.

1. Das Ziel der Theorie der Übergangsschicht ist es, die von KOSSEL [2] entwickelte Molekularbetrachtungsweise den praktischen Beobachtungen näher zu bringen. KOSSEL hat nämlich für das Wachstum der Kristalle eine sehr nützliche, sog. molekulare Betrachtung ausgebildet. Zwischen den KOSSELschen molekularen und den beobachteten Vorgängen besteht aber ein grössenordnungsmässiger Unterschied. Die im Mikroskop beobachtbare Wachstumsschicht ist mindestens 0,001 mm dick und enthält ungefähr 10000 Ionenschichten. Es muss also gefragt werden, auf welche Art das von KOSSEL für eine Ionenschicht bestimmte Wachstumsgesetz auf die Anregung eines 10000 Ionenschichten umfassenden Vorganges entscheidend einwirken kann. Es ist die Aufgabe der Theorie der Übergangsschicht diesen Unterschied in der Grössenordnung zu überbrücken.

2. Das Bild der Übergangsschicht ist das folgende: Der Kristall ist mit der gesättigten Lösung in Berührung. Die Ionenkräfte reichen in die Lösung hinein und binden dort einige Ionen und Ionenpaare an die Oberfläche des Kristalls. Auf der Kristalloberfläche befinden sich auch adsorbierte Wassermoleküle, aber die Kraftwirkungen der einzelnen Ionen oder Ionenpaare reichen weiter in die Lösung hinein, und auch sie können einige weitere Ionen auf die Kristallfläche binden. In der unmittelbaren Nähe des Kristalls setzen also kleine Kristallsplitter den Kristall fort, während in einer Entfernung von einigen Mikronen allmählich nur noch die gesättigte Lösung vorhanden ist. Solange jedoch der Kristall wächst, wird entsprechend der ausgeschiedenen Stoffmenge Wasser frei und dieses verdünnt die Lösung in der Nähe der Kristall-

* Gegenwärtige Adresse: The Federal Advanced Teachers' College, Lagos, Nigeria

oberfläche. So findet eine ständige Diffusion von den ferneren konzentrierten Stellen in diese verdünnte Schicht statt. Einfache Diffusionsprozesse können jedoch nicht erklären, auf welche Art der gelöste Stoff aus der verdünnten Schicht auf die Kristalloberfläche diffundieren kann, damit dort infolge Überstättigung das Weiterwachsen des Kristalls möglich wird. Dieses Diffusionsproblem wird durch die oben skizzierte Vorstellung gelöst, nach welcher die Ionenkräfte die Ionen aus der Lösung auf die Oberfläche des Kristalls ziehen und dort binden.

MALICSKÓ und DOMOKOS haben mit Hilfe optischer Messungen [3] das Vorhandensein der Übergangsschicht bewiesen und gezeigt, dass die Kon-

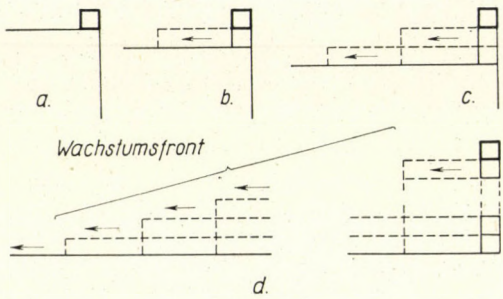

Abb. 1. Das Wachstum der Kristallecken durch die allmähliche Anlagerung der einzelnen Ionen

zentration in der unmittelbaren Nähe der Kristalloberfläche die Sättigungskonzentration auch um ein Vielfaches übersteigen kann. Das ist als Nebenergebnis für sich allein auch sehr interessant.

3. Das weitere Problem besteht darin zu verstehen, wie das von KOSSEL theoretisch vorausgesagte erste sich auf der Kristallspitze anlagernde Ion das Wachstum anregt, sodass sich die Dicke der beobachteten Schicht auf mehrere Mikronen ausdehnen kann.

Setzen wir unseren Gedankengang im KOSSELschen Sinne fort. Wenn sich das erste Ion auf der Spitze festgesetzt hat (siehe Abb. 1*a*), so beginnt daneben sofort die Anlagerung einer Ionenreihe, da das erste Ion schon eine günstigere Lage zur Anlagerung eines neuen Ions geschaffen hat, wie das der Pfeil zeigt. Wenn eine Ionenreihe sich neben diesem Ion schon ausgebildet hat, dann entstehen daneben parallele Reihen, und nach einer gewissen Zeit bildet sich eine quadratische Ionenschicht auf dem Kristall. Ist die erste Ionenebene bis zu einer gewissen Entfernung gewachsen, so ergibt sich über dem ersten Ion wiederum die Möglichkeit zur Anlagerung eines neuen Ions (Abb. 1*b*), womit auf ähnliche Weise eine neue Ionenreihe sich auszubilden beginnt. Diese zweite Ionenreihe bleibt im Verhältnis zur ersten zurück, folgt ihr aber in gewissem Abstand. Auf ähnliche Weise setzt sich ein drittes Ion

auf die Spitze an (Abb. 1*c*), und der Vorgang beginnt von neuem. Der durch das erste Spitzenion angeregte Vorgang vergrössert also die Dicke der sich auflagernden Ionenschicht in vollkommen gleichen, sich immer wiederholenden Schritten.

Das Ergebnis der Berechnungen nach der KOSSELschen Theorie ist in Abb. 2 zu sehen. Für die Ionen der darauffolgenden Ionenreihen sind ähnliche Werte gültig. Bei NaCl ist die Energieeinheit (die innere Bindungsenergie eines Ionenpaares) 5,1 eV. In dieser Energieeinheit drücken wir alle Energiewerte aus.

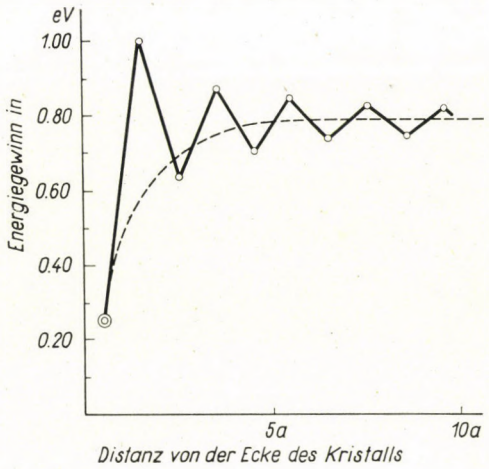

Abb. 2. Der Energiegewinn bei der Anlagerung von Ionen in Reihen auf der Kristallecke (a = zwei Ionenabstände im Gitter)

Der in Abb. 1 dargestellte Vorgang dauert solange an, bis die Anlagerung eines neuen Ions an die Spitze infolge physikalischer Umstände aufhört. Im Abbrechen der Anlagerung spielt das freiwerdende Wasser nach unserer Meinung eine wichtige Rolle, aber auch die Verunreinigungen der Lösung können eine solche Wirkung ausüben.

Es ist uns also gelungen, das im Mikroskop beobachtete Schichtenwachstum zu erklären. Auf Grund des vorher Gesagten besteht also eine Schicht aus den in Abb. 1*d* dargestellten stufenförmigen Reihen. Eine solche Reihe ist als ein zusammengesetzter KOSSELscher wiederholbarer Schritt aufzufassen, wobei sich die schiefe Front in Pfeilrichtung bewegt, was im Mikroskop leicht zu beobachten ist.

4. Daneben gibt es aber auch noch eine andere Form des Kristallwachstums, die man sowohl im Mikroskop wie auch auf Filmaufnahmen beobachten kann, und auf die einer von uns schon in einer früheren Arbeit hingewiesen hat [4]. Diese Erscheinung ist das sog. Spitzenwachstum, das darin besteht,

dass eine Kristallspitze häufig in der diagonalen Richtung zu beiden Seiten symmetrisch vorwärtsschreitet, wie das die Abb. 3 zeigt. Dieses Wachstum der Spitze ist bei der Kristallisation aus einer Lösung oder aus Dampf zu beobachten. Man findet es aber auch bei der Rekristallisation in der festen Phase [5].

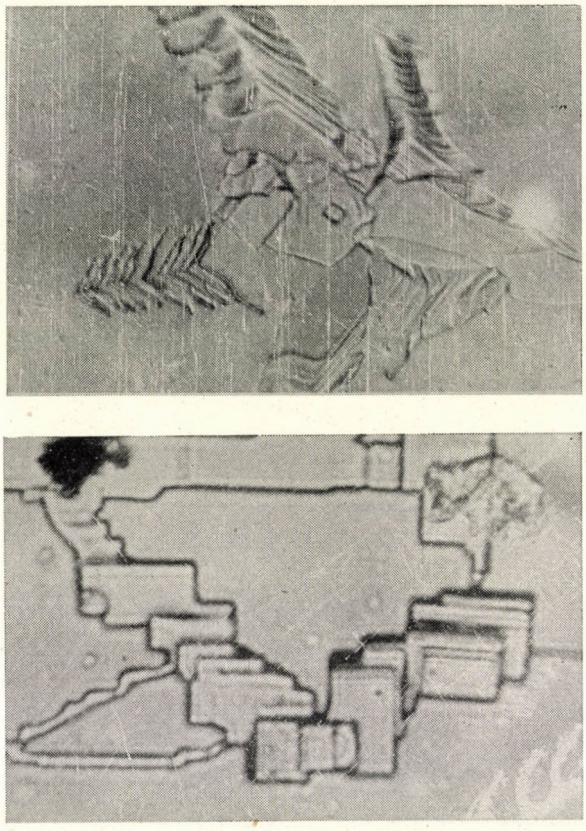

Abb. 3. Zwei mikroskopische Aufnahmen als Beispiele des Spitzenwachstums. Kristallisation aus Dampf auf Glas

Dieses Wachstum der Spitze ist oft eine sehr vehemente Erscheinung, wie man das auf Filmaufnahmen sehen kann, und wie wir das an den Kristallen aus KBr und Fixiersalz ($Na_2S_2O_3$) schon öfter gezeigt haben. Die Filme veranlassen uns zu der Ansicht, dass wir in dem Spitzenwachstum eine sehr wichtige Erscheinung vor uns haben. Wir versuchen daher, uns über das Spitzenwachstum im Sinne von KOSSEL Rechenschaft zu geben. KOSSEL erwähnt am Ende seiner grossen Arbeit, dass am Kristallwachstum Ionenpaare, sogar auch mehrfache Ionenpaare teilnehmen können. Die Anlagerung der Ionenpaare an den Kristall in einem Schritt muss man auch deshalb in Erwägung ziehen, weil bei der

Kristallisation aus Dampf nur die Ionenpaare eine Rolle spielen, da der NaCl-Dampf, wie allgemein bekannt ist, aus Molekülen besteht. Da die mikroskopischen Aufnahmen der Kristallisation aus Lösung und aus Dampf dieselben Formen zeigen, ist anzunehmen, dass der Mechanismus des Kristallwachstums in beiden Fällen ähnlich ist. Aber auch im Falle der Kristallisation aus Lösung ist das Vorhandensein von NaCl-Molekülen wahrscheinlich. Weiterhin wächst die Wahrscheinlichkeit der Anwesenheit von Ionenpaaren noch stark an, da die Ionenkonzentration in der Übergangsschicht das Mehrfache der Sättigungskonzentration erreichen kann.

5. Den Aufbau der Spitze aus Ionenpaaren stellen wir uns folgendermassen vor. An der Spitze A (siehe Abb. 4), lagert sich oben das Ionenpaar

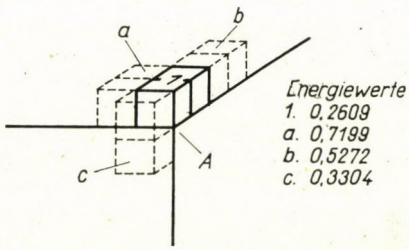

Abb. 4. Der Energiegewinn bei der Anlagerung von Ionenpaaren in der Reihenfolge 1*a*, *b*, *c*

Nr. 1 an. Daneben sind die drei günstigsten Stellen (a, b, c) für die Anlagerung neuer Ionenpaare dargestellt.

Die entsprechenden Energiewerte sind die folgenden:

für das Ionenpaar Nr. 1 0,2609,
für das Ionenpaar a 0,7199,
für das Ionenpaar b 0,5272,
für das Ionenpaar c 0,3304.

Aus den Werten folgt, dass die Anlagerung des folgenden Paares an der Stelle a erfolgt. Der Prozess wiederholt sich, und die weitere Anlagerung erfolgt entsprechend immer an der günstigsten Stelle. Auf diese Weise füllt sich die Reihe auf, und bringt die Ausbildung paralleler Reihen mit sich, woraus schliesslich ein Kern mit quadratischer Oberfläche entsteht. Zur Fortsetzung der Spitze des so entstandenen Oberflächenkerns gibt es drei Möglichkeiten, nämlich entlang der einen der drei aufeinander senkrechten Kanten, wie das Abb. 5 veranschaulicht. Falls die linearen Ausmasse des quadratischen Kerns 10 Ionenabstände betragen, so sind die Energiewerte der möglichen Plätze die folgenden:

für den Platz $\alpha \rightarrow$ 0,2616,
$\beta \rightarrow$ 0,2629,
$\gamma \rightarrow$ 0,2607.

Beim Weiterwachsen kann das Ionenpaar zwischen den drei Lagen frei wählen, da die Energiewerte im wesentlichen gleich sind. Hat sich ein Ionenpaar an einer Stelle angelagert, so beginnt der in Abb. 4 geschilderte Vorgang, und nach der Ausbildung des Oberflächenkerns stellt sich wieder die Ausgangslage ein. Da sich das Ionenpaar an allen drei Seiten mit gleicher Wahrscheinlichkeit anlagern kann, erfolgt die Anlagerung nach allen Richtungen mit der gleichen

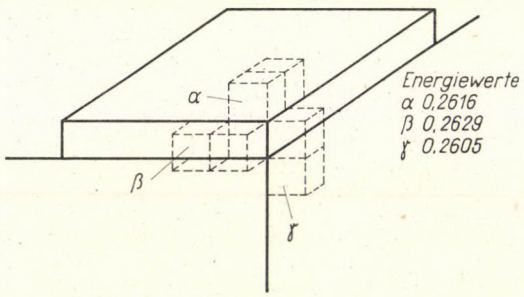

Abb. 5. Die Fälle des alternativen Energiegewinns um die Würfelspitze nach der Ausbildung des Oberflächenkeims

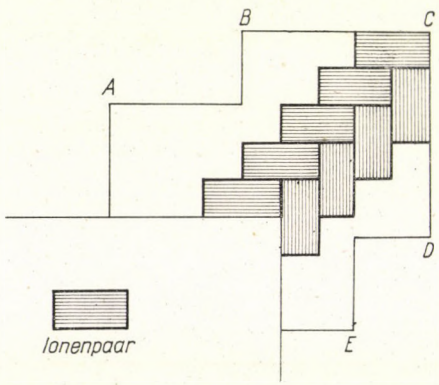

Abb. 6. Zweidimensionales schematisches Bild des Wachstums einer Würfelspitze im Falle der wechselnden Anlagerung der Ionenpaare. Sogenannte zweidimensionale wiederholbare Schritte nach KOSSEL

Häufigkeit, und so wächst die Spitze nach allen Seiten gleichförmig, wie das die Filmaufnahmen zeigen. Wenn der Oberflächenkeim weiterwächst, verschwinden die Energieunterschiede immer mehr, und die in Abb. 5 gezeigten drei Möglichkeiten bleiben demzufolge gleich wahrscheinlich. Die Folge davon ist, dass die Spitze in der Richtung der Körperdiagonale vorwärtsschreitet.

Mit diesen Betrachtungen stellten wir also für das Wachstum der Kristallspitze einen sich wiederholbaren Schritt im Sinne KOSSELS fest. Hier muss man bemerken, dass beim Weiterwachsen der Reihen sich einzelne Ionen genauso

wie Ionenpaare anlagern können, es ist nur nötig, dass jeder Schritt durch die Anlagerung eines Ionenpaares an die Spitze eingeleitet wird.

Zur besseren Anschaulichkeit haben wir in Abb. 6 die Spitzenschritte in zwei Dimensionen dargestellt. Die Anfangsschritte wiederholen sich, infolge der äusseren Umstände bleiben sie jedoch zeitweise stehen, und so entsteht die makroskopische Treppenspitzenform ABCDE.

Zum Aufbaumechanismus der beobachteten Wachstumsgebilde muss man bemerken, dass das hier gegebene Schema sehr viele Variationen erlaubt, sodass es wahrscheinlich ist, dass sich die Vorgänge in der Wirklichkeit auch so abspielen. Dabei können auch Spezialfälle, zu denen z.B. die Dislocationsformen gehören, auftreten. Wir möchten hier die Beobachtung von JESZENSZKY erwähnen, in der dieser neben dem KOSSELschen Schichtenwachstum auch die Spuren eines Spiralwachstums nachwies [5].

Die Beobachtungen zeigen, dass das Spitzenwachstum mit ganz verschiedener Intensität vor sich gehen kann. Man beobachtet sehr schnelle Vorgänge, aber auch sehr langsame. Das Grundschema verwirklicht sich bei jeder Geschwindigkeit, und darin besteht eben seine theoretische Bedeutung. Über die grosse Intensität der Erscheinungen erhalten wir einen anschaulichen Eindruck, wenn wir sie im Mikroskop beobachten oder im Film sehen.

Wir haben im vorstehenden gezeigt, dass die Ausbildung der Spitze eines der wichtigsten Momente des Kristallwachstums darstellt, und wir haben versucht, das ihm zugrundeliegende Schema zu skizzieren.

LITERATUR

1. Z. GYULAI und S. BIELEK, Acta Phys. Hung., **1**, 199, 1952.
2. W. KOSSEL, Leipziger Vorträge, 1928.
3. G. DOMOKOS und L. MALICSKÓ, Acta Phys. Hung., **10**, 185, 1959.
4. Z. GYULAI, Zs. f. Kristallographie (A), **91**, 142, 1935.
5. Z. GYULAI, Zs. f. Phys. Chem., **217**, 428, 1961.

РАЗВИТИЕ ТЕОРИИ ПЕРЕХОДНОГО ГРАНИЧНОГО СЛОЯ

З. ДЮЛАИ и Ф. БУКОВСКИ

Резюме

Молекулярное воззрение Косселя роста кристаллов с использованием переходного слоя распространяется на более толстые слои (содержащие несколько тысяч ионов), а также и на формирование острия. Описывается возможность появления так называемого повторяющегося шага Косселя при формировании как слоя, так и острия. При формировании повторяющегося шага роста острия играют роль и ионные пары, однако большая концентрация, имеющаяся в переходном слое, доставляет изобильную возможность. При росте из паров пар заранее состоит из пар ионов.

ON THE APPLICATION OF X-RAY INTENSITY STATISTICS IN THE CASE OF INORGANIC SUBSTANCES

METHOD FOR DETERMINATION OF CRYSTAL SYMMETRIES AND SPACE GROUPS

By

A. KÁLMÁN

CENTRAL RESEARCH INSTITUTE FOR CHEMISTRY OF THE HUNGARIAN ACADEMY OF SCIENCES, BUDAPEST

(Presented by G. Schay — Received 10. I. 1963)

The present paper deals with the application of the method of intensity statistics to the determination of the crystal symmetries in the cases of the non-ideal, mostly inorganic substances. It was found that in the case of the investigated non-ideal substances the curves of centric, respectively, acentric projections have their own characteristic shapes which strongly differ from each other, as well as from the theoretical $N(z)$-distribution functions. On the basis of these findings it is possible to apply these kinds of centric and acentric $N(z)$-curves to decide whether a centre of symmetry is present or absent in the investigated structures.

Introduction

The crystal structure of α-$K_2Pb_2Si_2O_7$ was recently determined in our laboratory [1]. The oscillation photographs and the powder diffractograms showed no systematical absence of reflections of the hexagonal crystal; thus a large number of space groups was possible.

On the basis of geometrical and crystal chemical considerations and in agreement with the results of McMURDIE's previous investigations [2] we found $P\bar{3}$ to be the most probable space group. To this we had to suppose the presence of a centre of symmetry in the structure without having exactly verified it, as LIEBAU was right in pointing out [3].

Despite of the fact, that our supposition was confirmed by the results of the structure determination ($R = 0{,}07$), we wanted to confirm the presence of a centre of symmetry and so the reliability of the proposed space group, independently of the results of the structure determination.

For this re-investigation we tried to compute the probability distribution of the reflection intensities of α-$K_2Pb_2Si_2O_7$.

The theoretical distribution functions of intensities, introduced by HOWELLS, PHILLIPS and ROGERS [4], i.e.

$$_1N(z) = 1 - \exp(-z)$$

for non-centrosymmetrical, and

$$_{\bar{1}}N(z) = \operatorname{erf}\left(\frac{1}{2}z\right)^{1/2}$$

for centrosymmetrical structures, are valid only if the substance in question is ideally statistical, i.e. if there is a sufficiently large number of atoms with not too different atomic scattering factors randomly distributed in the unit cell.

These conditions are not satisfactorily fulfilled in the case of α-$K_2Pb_2Si_2O_7$ because the unit cell contains the heavy ion Pb^{2+} and the total number of its ions amounts only to 13. Therefore we could not find full agreement between the theoretical curves and the experimental one, calculated from the supervised structure factors* of 82 *h0l* reflections (Fig. 2/A).

Calculations

We tried also to apply SIM's method [6] which took into consideration the presence of a heavy atom in general position to correct the expected deviation of the experimental $N(z)$-curve. SIM's functions $_{\max 1}N(z, r)$ and $_{\max \bar{1}}N(z, r)$ for acentric and centric cases are given in tables as the functions of z and r [7], where:

$$r = \frac{f_H}{\left(\sum_{i=1}^{m} f_i^2\right)^{\frac{1}{2}}} .$$

Here f_H is the scattering factor of the heavy atom and f_i is that of the other atoms numbering m. Computing SIM's functions for the centric and acentric cases ($r = 3{,}7$) and comparing them with our experimental curve, a disagreement could be found again.

Four years ago KEGLEVICH [8] suggested an experimental "analogous" method for the determination of symmetry elements in cases, when the examined compounds contain different kinds of heavy and light atoms and when moreover their number is not too high. To decide whether $SrS_2O_3 \cdot 5H_2O$ belongs to the space group Aa or A2/a KEGLEVICH compared the experimental $N(z)$-curve calculated from *0kl* reflections not with the theoretical functions, but with the experimental ones, obtained from the same *0kl* reflections of $Na_2S_2O_3 \cdot 5H_2O$ (space group: $P2_1/c$ [9]) and of $BaS_2O_3 \cdot H_2O$ (space group: Pbcn [10]). As the curve of $SrS_2O_3 \cdot 5H_2O$ shows a similar shape to that of the two experimental ones and lies between them, in accordance with the fact that the electron number of the Sr^{2+} ion lies between those of Na^+ and Ba^{2+}, it seemed proved that the *0kl* zone of $SrS_2O_3 \cdot 5H_2O$ was also centro-

* For the calculation of the $N(z)$-curve, as SIM previously suggested [5], values of F_{calc} were used. This was necessary because in the space group $P\bar{3}$ $(F_{hkl}) \neq (F_{hk\bar{l}})$ and therefore the values for themselves cannot be determined from the powder diagram, only their arithmetic mean values.

symmetrical, i.e. that its space group was A2/a. This was in agreement with the results of morphological examinations.

In the meantime the author had the opportunity (by the courtesy of K. SASVÁRI) to examine the intensity statistics of the monoclinic $AlNbO_4$. According to the observed extinctions and to the LAUE symmetry, the possible space groups were Cm and C2/m. The $N(z)$-curve, calculated from 98 $h0l$ intensities showed a remarkable departure from the ideal distribution functions, but its shape was similar to that of α-$K_2Pb_2Si_2O_7$ and of the three thiosulphates irrespective of the fact that the chemical composition of these substances was quite different. This fact offers the possibility to determine whether crystals of non-ideal compounds are centric or acentric irrespective of their composition, if we can show that the deviation of their curves from the ideal ones is characteristic and quite different for the centric and acentric cases, respectively.

This thought called our attention to the investigation of the probability distribution of the intensities in a number of cases, where the unit cell contains heavy atoms among light ones and the number of the atoms in the unit cell is small. We have examined more than fifteen such centric and acentric crystal structures. Data belonging to these investigated and mostly inorganic compounds are given in Tables 1, 2 and 3.

We have computed distribution curves only for such projections which are apt to determine the presence or the absence of centres of symmetry in the space group. It can be seen from Figs. 2 and 3 that in the case of the investigated substances the curves of centric, respectively acentric projections have their own characteristic shapes which firmly differ from each other, as well as from the ideal distribution functions.

The points of the acentric distribution curve are always below the theoretical ${}_1N(z)$-function for $z < 0{,}5 \pm 0{,}1$. Then the experimental curve crosses the ${}_1N(z)$-function and rises above it. In some cases it crosses the theoretical ${}_{\bar{1}}N(z)$-function, too.

In the centric case the experimental $N(z)$-curve has always a steep slope up to about $z = 0{,}1$. Near $z = 0{,}1$ it shows an abrupt break, and then forms an almost straight line. With the exception of only a few cases the height of the breaking point B is inversely proportional to the electron number (scattering factor) of the heavy atom, as it is evident from Fig. 1.

On the basis of these results we may regard the examined projections of α-$K_2Pb_2Si_2O_7$ and of $AlNbO_4$ (Fig. 2/B) to be centrosymmetrical. This means that:

1. the space group of lead-potassium-pyrosilicate is centric and this fact confirms the space group to be $P\bar{3}$;

2. the centricity of the $h0l$ zone of $AlNbO_4$ excludes the space group Cm. So only the space group C2/m is possible. This result was confirmed in the meantime by PEDERSEN [11].

This statement makes it possible to confirm also the reliability of the space group in such cases in which difficulties arose in the determination of the presence or the absence of a centre of symmetry.

Table 1

Data of projections which show centric distribution curves

Compounds	Data of the unit cell						Investigated zones			Fig.	Ref.
	space group	a(Å)	b(Å)	c(Å)	angle°	Z	$hk0$	$0kl$	$h0l$		
α-$K_2Pb_2Si_2O_7$	$C_{3i}^1 - P\bar{3}$	5,64	—	7,62	—	1	—	—	82*	2/A	[1]
$Cu_2Cl(OH)_3$ (atacamite)	$C_{2h}^{16} - Pnam$	6,01	9,13	6,84	—	4	65	—	—	2/A	[24]
$(Mn,Fe)Be(PO_4)(OH)$ (väyrynenite)	$C_{2h}^5 - P2_1/a$	5,41	14,49	4,73	102,8	4	210	—	—	2/B	[25]
$CaAl_2Si_2O_8$ (anorthite)	$C_i^1 - P\bar{1}$	8,18	12,87	14,17	93,1 115,8 91,2	8	—	?	—	2/B	[15]
$ScSi_2O_7$ (thortveitite)	$C_{2h}^3 - C2/m$	6,54	8,52	4,67	102,5	2	35	—	—	2/C	[12] [13]
$AlNbO_4$	$C_{2h}^3 - C2/m$	12,13	3,73	6,46	107,2	4	—	—	98	2/B	[11]
$AlICl_6$	$C_2^2 - P2_1$	6,92	11,02	6,11	99,1	2	—	—	74	2/C	[26]
$(CH_3)_3 \cdot SI$	$C_{2h}^2 - P2_1/m$	5,94	8,00	8,92	126,5	2	—	77	75	2/D	[14]

* The number of the used reflections for the calculation of the $N(z)$-cuves.

Table 2

Data of projections which show acentric distribution curves

Compounds	Data of the unit cell						Investigated zones			Fig.	Ref.
	space group	a(Å)	b(Å)	c(Å)	angle°	Z	$hk0$	$0kl$	$h0l$		
$Ba(ClO_4)_2 \cdot 3\,H_2O$	$C_6^6 - P6_3$	7,28	—	9,64	—	2	Calculated from hkl reflections by the authors			3/A	[17]
$Al_2Si_2O_5(OH)_4$ (dickite)	$C_s^4 - Cc$	5,15	8,95	14,42	96,8	4	—	—	46	3/B	[21]
P_4S_5	$C_2^2 - P2_1$	6,41	10,94	6,69	111,7	2	70	86	—	3/C	[27]
$AlICl_6$	$C_2^2 - P2_1$	6,92	11,02	6,11	99,1	2	77	84	—	3/D	[26]

Table 3

Data of projections which show hypercentric distribution curves

Compounds	Data of the unit cell						Investigated zones			Fig.	Ref.
	space group	a(Å)	b(Å)	c(Å)	angle°	Z	$hk0$	$0kl$	$h0l$		
$(NH_4)_2 \cdot WS_4$	D_{2h}^{16} — Pnam	9,52	12,33	7,01	—	4	141	—	—	4/A	[28]
$Cu(ClO_4)_2 \cdot 6\ H_2O$	C_{2h}^5 — $P2_1/c$	5,14	23,17	14,15	90	6	—	124	—	4/A	[30]
$Al_2Si_2O_5(OH)_4$ (dickite)	C_s^4 — Cc	5,15	8,95	14,42	96,8	4	—	63	—	4/B	[21]
P_4S_5	C_2^2 — $P2_1$	16,41	10,94	6,69	111,7	2	—	—	84	4/C	[27]
$Na_2Al_2Si_3O_{10} \cdot 2\ H_2O$ (natrolite)	C_{2v}^{19} — Fdd2	18,30	18,63	6,60	—	8	63	—	—	4/D	[29]

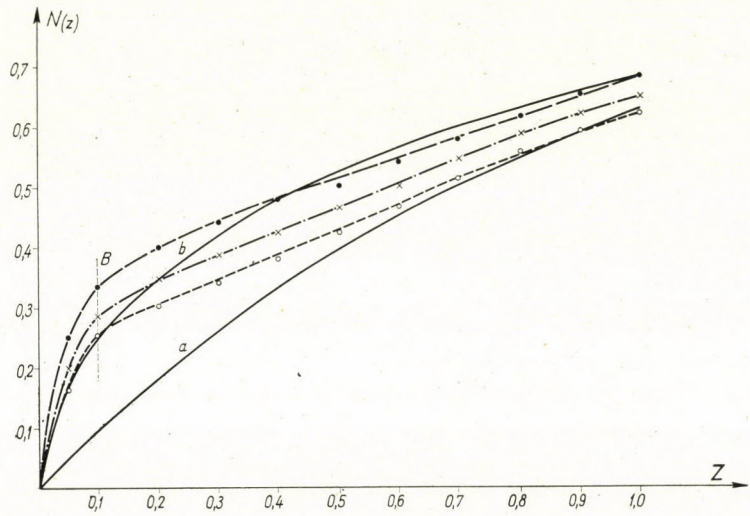

Fig. 1. The experimental $N(z)$-curves for the $0kl$ zones of the following thiosulphates: $Na_2S_2O_3 \cdot 5\ H_2O$ (black circle), $SrS_2O_3 \cdot 5\ H_2O$ (cross), $BaS_2O_3 \cdot H_2O$ (open circle). Curves a and b are the theoretical acentric ${}_1N(z)$ respectively centric ${}_{\bar{1}}N(z)$ functions [8]

3. Reinvestigating the structure of thortveitite BARCLAY, COX and LYNTON [12] examined the intensity statistics for $h0l$ and $0kl$ reflections. The results, which were not reported suggested that both projections were acentric. From that, the probable space group was Cm. On the basis of the result of our $N(z)$-test (Fig. 2/C) for $hk0$ reflections the only space group C2/m is possible. The final result of the above structure re-investigation [13] also confirmed the space group to be C2/m.

4. The $N(z)$-curves for $0kl$ and $h0l$ projections of trimethylsulfonium iodide (Fig. 2/D) seem to justify the reliability of space group $P2_1/m$ [14].

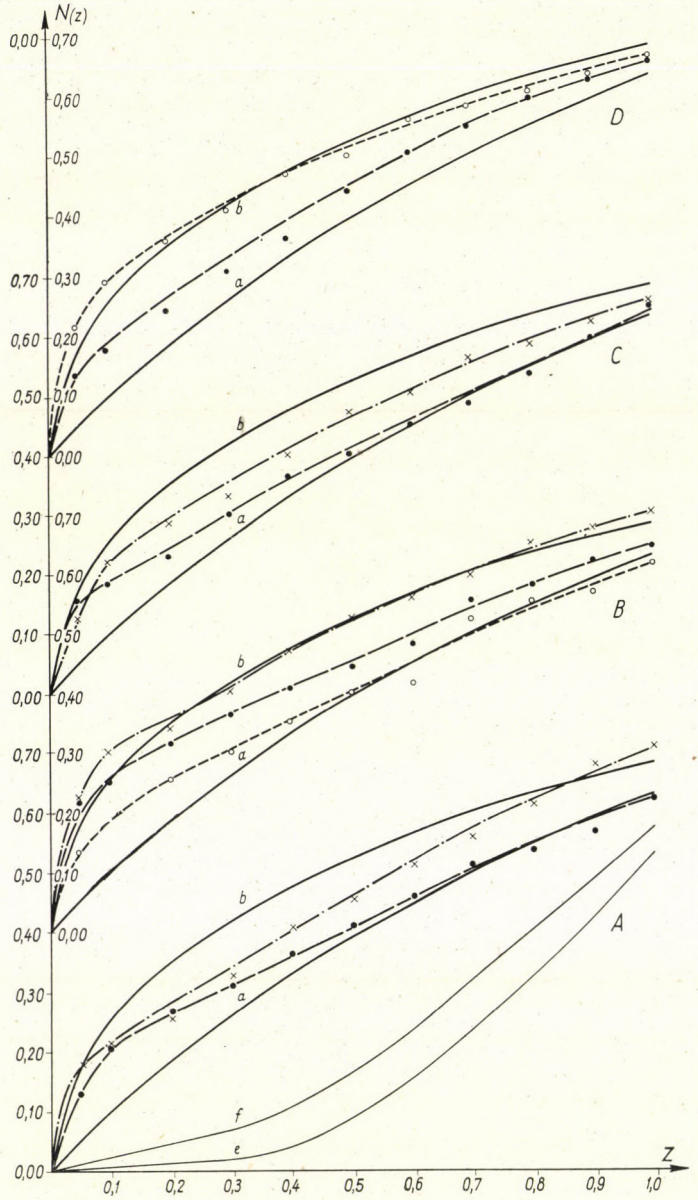

Fig. 2. The experimental $N(z)$-curves of the centric projections

A: $h0l$ zone of α-$K_2Pb_2Si_2O_7$ (black circle) and $hk0$ zone of atacamite (cross); curves a and b are as Fig. 1, e and f are the calculated acentric and centric SIM's functions, respectively, for α-$K_2Pb_2Si_2O_7$.

B: $hk0$ zone of väyrynenite (cross) and $0kl$ zone of anorthite (open circle) [15] and $h0l$ zone of $AlNbO_4$ (black circle)

C: $hk0$ zone of thortveitite (cross) and $h0l$ zone of $AlICl_6$ (black circle)

D: $0kl$ (open circle) and $h0l$ (black circle) zones of $(CH_3)_3 \cdot$ SI

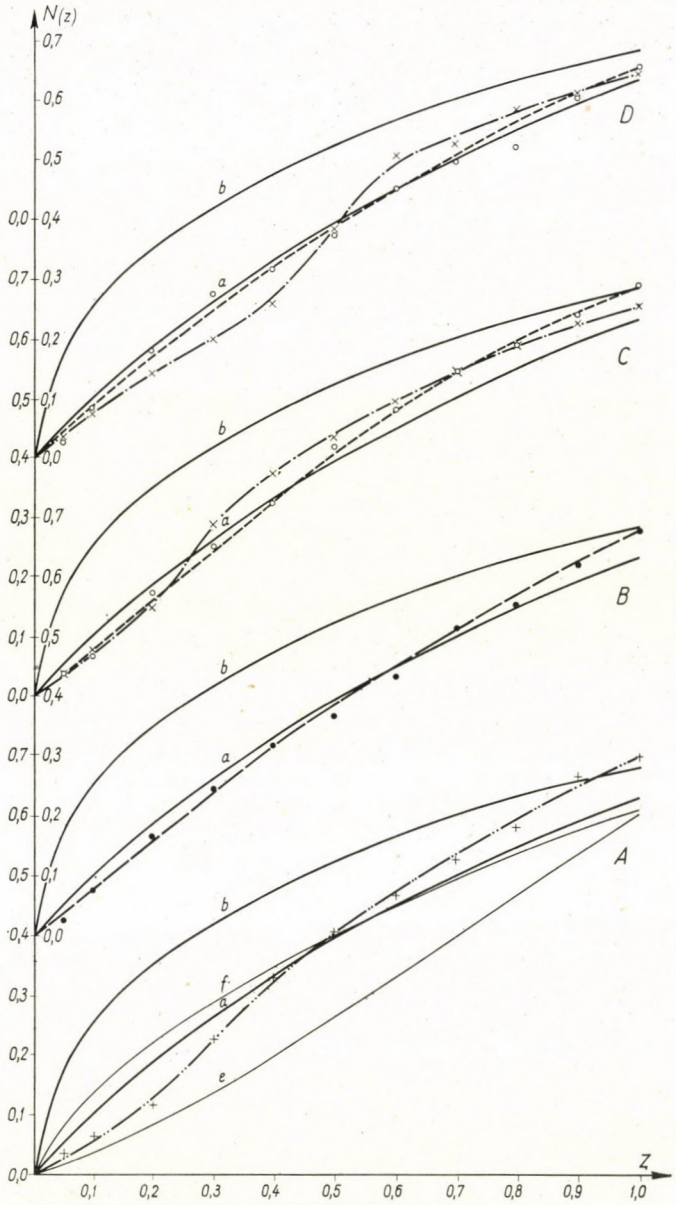

Fig. 3. The experimental $N(z)$-curves for the acentric projections

A: $N(z)$ curve for *hkl* intensities of $Ba(ClO_4)_2 \cdot 3\,H_2O$ [17], curves *e* and *f* are the calculated acentric and centric SIM's ones
B: *h*0*l* zone of dickite
C: *hk*0 (cross) and 0*kl* (open circle) zones pf P_4S_5
D: *hk*0 (cross) and 0*kl* (open circle) zones of $AlICl_6$

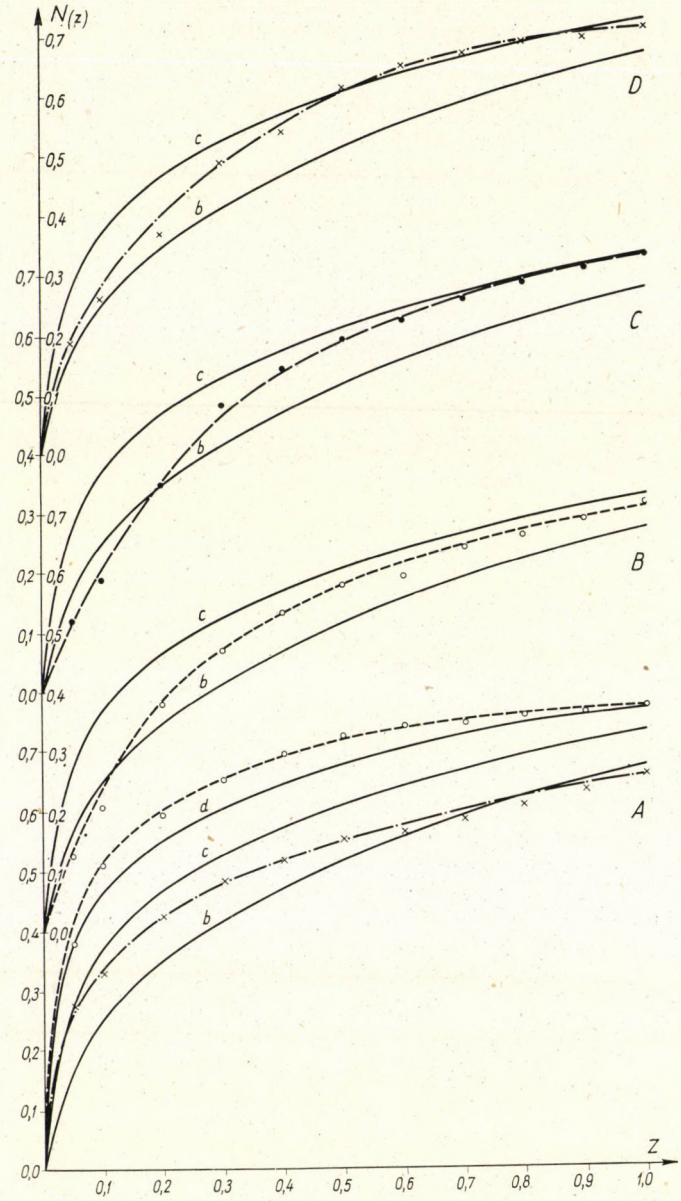

Fig. 4. The experimental $N(z)$ curves for the hypercentric projections
A: $hk0$ zone of $(NH_4)_2WS_4$ (cross) and $0kl$ zone of $Cu(ClO_4)_2 \cdot 6\,H_2O$ (open circle)
B: $0kl$ zone of dickite, C: $h0l$ zone of P_4S_5. D: $hk0$ zone of natrolite; curves *b*, *c* and *d* are the theoretical centric, bicentric and tricentric distribution functions

5. KEMPSTER, MEGAW and RADOSLOVICH [15] recently published the results of the $N(z)$-test for $0kl$ intensities of the triclinic anorthite, which suggested the space group P1. This was not in agreement with the result of the structure determination, while the $P(y)$ statistical test (RAMACHANDRAN, SRINIVASAN [16]) established the space group to be centric. In our opinion the curve obtained from the $N(z)$-test for the $0kl$ projection may also be regarded as revealing a centric distribution (Fig. 2/B).

6. Comparing the $N(z)$-curve for hkl intensities of the hexagonal $Ba(ClO_4)_2 \cdot 3H_2O$ calculated by MANI and RAMASESHAN [17] with the ones for the $0kl$ zone of $AlICl_6$, for the $h0l$ zone of dickite and for the $0kl$ and $hk0$ projections of P_4S_5, we can detect a likeness between the characters of the $N(z)$-curves for the hkl reflections of $Ba(ClO_4)_2 \cdot 3H_2O$ and for the other four acentric projections. Consequently, the $N(z)$-curve for hkl intensities may be considered as being acentric and thus the real space group is $P6_3$.

During the examination of the experimental distribution curves of different chemical compounds we frequently found hypercentric projections among the centric and acentric ones (Fig. 4). The reason for the different degrees of hypercentricity in the inorganic structures (Table 3) is as in the case of organic ones [18, 19, 20] probably the presence of certain kinds of pseudo-centres of symmetry in the unit cell. The $hk0$ projection of $(NH_4)_2WS_4$ (Fig. 4/A) shows a transition from the hypercentric to the examined non-ideal centric distribution. The shapes of the hypercentric $N(z)$-curves for the $hk0$ intensities of natrolite, the $0kl$ zone of dickite and for the $h0l$ projection of P_4S_5 are similar to each other. The $0kl$ zone of $Cu(ClO_4)_2 \cdot 6H_2O$ shows a very strong hypercentricity, the reason for which is unknown.

In the case of dickite an odd phenomenon was found. Its space group was stated [21] to be Cc. This means that its $hk0$, $0kl$ and $h0l$ projections ought to show acentric distributions. The $N(z)$-curve for the $h0l$ projection satisfied this condition, but the $0kl$ zone showed a hypercentric distribution. These two results are inconsistent with each other. HARGREAVES and WATSON [22] describe a similar phenomenon shown by β-naphtol, the space group of which is Ia. According to these authors the $0kl$ reflections gave an acentric, the $h0l$ reflections a hypercentric distribution. This can be explained if we suppose the presence of a pseudo-centre of symmetry between the β-naphtol molecules. Keeping in mind the probable reason for this hypercentricity we can explain the odd behaviour of the $0kl$ projection of dickite, too.

Besides the hypercentric cases we have found, of course, such ones in which the $N(z)$-curves were not similar to the centric and acentric ones discussed above, of which only the harmotome ($Ba_2Al_4Si_{12}O_{33} \cdot 12H_2O$) should be mentioned here. On the basis of the structure determination its monoclinic space group is $P2_1$. The authors SADANAGA, MARUMO and TAKEUCHI [23] made

a statistical test for the $0kl$ intensities, but this having suggested rather the space group $P2_1/m$, than $P2_1$, we supervised their computation and found it to be correct. We have moreover computed the $N(z)$-curve for the centric $h0l$ zone. As it is to be seen from Table 4 the difference between these two curves is not significant enough to make it possible to state which of them is centric and which acentric.

Table 4

Values of the $N(z)$ curves for $0kl$ and for $h0l$ zones of harmotome

z / Zone	0,05	0,1	0,2	0,3	0,4	0,5	0,6	0,7	0,8	0,9	1,0
$0kl$	0,099	0,161	0,253	0,347	0,410	0,482	0,542	0,577	0,631	0,655	0,693
$h0l$	0,155	0,199	0,287	0,369	0,413	0,476	0,522	0,581	0,601	0,627	0,667

Discussion

The results given above concerning the probable intensity distributions of non-ideal substances confirmed the intensity statistical test proposed by KEGLEVICH to be a useful one and made possible a wider application of this empirical method.

According to our investigations:

1. A part of the chemical, mostly inorganic substances shows such $N(z)$-curves which differ from the theoretical functions, but have their own characteristic shapes, on the basis of which centric and acentric structures or their projections in almost every case can be distinguished from each other.

2. The different compounds show similar centric and acentric distribution curves, respectively, and thus the application of the analogous method is superfluous.

3. For a reliable computation of the $N(z)$-curves of an unknown structure or projection at least 60 to 70 independent reflections have to be used.

Acknowledgements

The author would like to express his sincere thanks to Dr. I. NÁRAY-SZABÓ for his kind interest and valuable advice during the course of this work. Thanks are due to Dr. K. SASVÁRI for many helpful discussions and for experimental data.

REFERENCES

1. I. Náray-Szabó and A. Kálmán, Silikattechn., **12,** 316, 1961.
2. H. F. McMurdie, J. Res. Nat. Bur. Stand., **26,** 489, 1941.
3. F. Liebau, Glastechn. Ber., **35,** 362, 1962.
4. E. R. Howells, D. C. Phillips and D. Rogers, Acta Cryst., **3,** 210, 1950.
5. G. A. Sim, Acta Cryst., **13,** 850, 1960.
6. G. A. Sim, ibid., **11,** 420, 1958.
7. G. A. Sim, ibid., **11,** 123, 1958.
8. L. Keglevich, Acta Chim. Hung., **19,** 469, 1959.
9. P. G. Taylor and C. A. Beevers, Acta Cryst., **5,** 341, 1952.
10. M. Nardelli and G. Fava, Acta Cryst., **15,** 477, 1962.
11. B. F. Pedersen, Acta Chem. Scand., **16,** 421, 1962.
12. G. A. Barclay, E. G. Cox and H. Lynton, Chem. and Ind., 178, 1956.
13. D. W. J. Cruickshank, H. Lynton and G. A. Barclay, Acta Cryst. **15,** 491, 1962.
14. D. E. Zuccaro and J. D. McCullough, Z. Krist., **112,** 401, 1959.
15. C. J. E. Kempster et al., Acta Cryst., **15,** 1005, 1962.
16. G. N. Ramachandran and R. Srinivasan, ibid., **12,** 410, 1959.
17. N. V. Mani and S. Ramaseshan, Z. Krist., **114,** 200, 1960.
18. H. Lipson and M. M. Woolfson, Acta Cryst., **5,** 680, 1952.
19. D. Rogers and A. J. C. Wilson, ibid., **6,** 439, 1953.
20. F. H. Herbstein and F. R. Schoening, ibid., **10,** 657, 1957.
21. R. E. Newnham and G. W. Brindley, ibid., **9,** 759, 1956.
22. A. Hargreaves and H. C. Watson, ibid., **10,** 368, 1957.
23. R. Sadanaga et al., ibid., **14,** 1153, 1961.
24. A. F. Wells, ibid., **2,** 175, 1949.
25. M. E. Mrose and D. E. Appleman, Z. Krist., **117,** 16, 1962.
26. C. G. Vonk and E. H. Wiebenga, Acta Cryst., **12,** 859, 1959.
27. S. v. Houten and E. H. Wiebenga, ibid., **10,** 156, 1957.
28. K. Sasvári, ibid., **16,** 719, 1963.
29. W. M. Meier, Z. Krist., **113,** 430, 1960.
30. N. V. Mani and S. Ramaseshan, ibid., **115,** 7, 1961.

О ПРИМЕНЕНИИ МЕТОДА СТАТИСТИЧЕСКОЙ ИНТЕНСИВНОСТИ РЕНТГЕНОВСКИХ ЛУЧЕЙ В СЛУЧАЕ НЕОРГАНИЧЕСКИХ ВЕЩЕСТВ

МЕТОД ОПРЕДЕЛЕНИЯ КРИСТАЛЛИЧЕСКОЙ СИММЕТРИИ И ПРОСТРАНСТВЕННЫХ ГРУПП

А. КАЛЬМАН

Резюме

Данная работа занимается вопросом применения метода статистической интенсивности для определения кристаллической симметрии в случае неидеальных, главным образом неорганических веществ. Найдено, что в случае рассмотренных неорганических веществ крывые центральной или нецентральной проекций обладают характеристическими для них формами, которые резко отличаются друг от друга, а также и от теоретической функции распределения $N(z)$. На основании данного обнаружения имеется возможность для применения этих центральных и нецентральных кривых $N(z)$ для определения наличия или отсутствия центров симметрии в исследованной структуре.

NEUTRINO RADIATION FROM DEGENERATED GASES

By

G. MARX and T. NAGY

INSTITUTE FOR THEORETICAL PHYSICS, ROLAND EÖTVÖS UNIVERSITY, BUDAPEST

(Presented by K. F. Novobátzky — Received 28. I. 1963)

The production cross-section of neutrino-pairs in the nuclear Coulomb field is calculated. The Coulomb screening is also taken into account. A separate discussion is devoted to the presence of a degenerated electron gas. Its importance is shown for low energies. The results may have some astrophysical consequences, esp. for the interior of degenerated stars, during the late period of their evolution, in the temperature-interval 10^8 — 10^9 °K.

§ 1. Thermal neutrino radiation of a hot plasma

During the longest period of the stellar evolution neutrinos are produced in β-decays, accompanying fusion reactions:

$$ {}_ZN^A \rightarrow {}_{Z-1}N^A + e^+ + \nu , \tag{1} $$

thus the total number of ν's, radiated by the star, is nearly equal to the number of neutrons in the star; the $\bar{\nu}$-radiation can be neglected. In such a case the neutrinos take away no more than a few per cent of the total radiation energy [1]. However, as the star temperature approaches 10^9 °K, processes begin which produce $\nu - \bar{\nu}$ pairs at the expense of the inner thermal energy of the stellar matter. The most important reactions are:

$$ \left.\begin{aligned} e^- + {}_ZN^A &\rightarrow {}_{Z-1}N^A + \nu \\ {}_{Z-1}N^A &\rightarrow {}_ZN^A + e^- + \bar{\nu} \end{aligned}\right\} \quad \text{URCA process [2]} \tag{2} $$

$$ e^- + {}_ZN^A \rightarrow {}_ZN^A + e^- + \nu + \bar{\nu} \quad \text{(Bremsstrahlung-neutrinos[5])} \tag{3} $$

$$ \gamma + e^- \rightarrow e^- + \nu + \bar{\nu} \quad \text{(Compton-neutrinos)} \tag{4} $$

$$ \left.\begin{aligned} \gamma + {}_ZN^A &\rightarrow {}_ZN^A + e^- + e^+ \\ e^- + e^+ &\rightarrow \nu + \bar{\nu} \end{aligned}\right\} \quad \text{(Annihilation-neutrinos[6,7,8])} \tag{5} $$

The analysis of these processes has shown, that the neutrino radiation may become significant and, by chance, for a short time even predominant in the late period of the stellar evolution [3, 7]. However, the situation changes

considerably in a degenerated electron gas. Here the electron states are filled up to a high Fermi level and therefore final states, in which low energy electrons occur, are forbidden. Hence the intensity of the neutrino radiation is diminished by many orders of magnitude. We may assume that in such cases it is the photoneutrino production which plays an important role. In this process the photons of the thermal radiation transform into $\nu - \tilde{\nu}$ pairs and no electrons appear in the final state. The most important reactions are:

$$\gamma + \gamma \quad \rightarrow \quad \nu + \bar{\nu}\,, \tag{6}$$

$$\gamma + {}_Z N^A \rightarrow {}_Z N^A + \nu + \bar{\nu}\,, \tag{7}$$

$$\gamma + \gamma \quad \rightarrow \quad \gamma + \nu + \bar{\nu}\,. \tag{8}$$

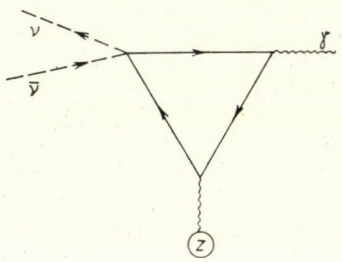

Fig. 1

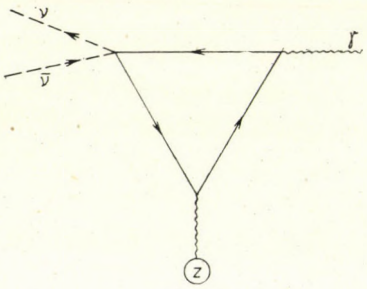

Fig. 2

(The cross sections of these processes contain a factor 1/137 as compared with the reactions (3), (4), (5) and therefore their role can be neglected in a normal gas.)

GELL-MANN has shown that the reaction (6) is forbidden for a local weak interaction. The cross section of the process (7) is larger by a factor Z^2 than that of (8). For this reason it was our purpose to treat the cross section of reaction (7) in more detail. (Preliminary report under [9].) The astronomical aspects of the results have been discussed elsewhere [10].

§ 2. The cross section of the photoneutrino production

The reaction (7), i.e. the transformation $\gamma \rightarrow \nu + \tilde{\nu}$ in the nuclear Coulomb field, can take place according to the graphs of Fig. 1 and 2. The Hamiltonian, corresponding to the weak corner, will be assumed to have the following form:

$$H = \frac{f}{\sqrt{2}} \bar{\psi}_e \gamma_\mu (1 + \gamma_5) \psi_\nu . \bar{\psi}_\nu \gamma_\mu (1 + \gamma_5) \psi_e\,,$$

which, according to the Fiertz identity, can be rearranged as follows:

$$H = \frac{f}{\sqrt{2}} \bar{\psi}_e \gamma_\mu (1 + \gamma_5) \psi_e . \bar{\psi}_\nu \gamma_\mu (1 + \gamma_5) \psi_\nu . \tag{9}$$

On the other hand, the electromagnetic Hamiltonian is

$$H = ie \bar{\psi}_e \gamma_\mu \psi_e (A_\mu + A_\mu^{\text{Coul}}) . \tag{10}$$

On writing down the corresponding S-matrix element one can see that for the vector part of the weak interaction (proportional to $\bar{\psi}_e \gamma_\mu \psi_e$) the sum of the contributions from the two graphs cancel out on account of the Furry theotem, while the contributions coming from the axial vector part (proportional ro $\bar{\psi}_e \gamma_\mu \gamma_5 \psi_e$) are the same; thus the S-matrix element of the process (7) is given by

$$\begin{aligned} S = & - \frac{iZe^3 f}{(2\pi)^3 k_0^{1/2}} (\bar{u}_\nu \gamma_\alpha (1 + \gamma_5) v_{\bar{\nu}}) e_\beta n_\gamma \cdot \\ & \cdot \int M_{\alpha\beta\gamma}(k, q) \frac{\delta(q_0)}{\mathfrak{q}^2 + r_0^{-2}} \cdot \delta(k_r + k_{\bar{\nu}} + q - k) \, d^4 q . \end{aligned} \tag{11}$$

Here k denotes the momentum of the incident photon, q is the momentum of the virtual photon describing the Coulomb interaction, e_β and n_γ stand for the photon polarization and time direction unit vectors, respectively. The screened Coulomb potential of the nucleus is of the form

$$A^{\text{Coul}} = n_\mu \frac{Ze}{4\pi} \frac{e^{-r/r_0}}{r} = n_\mu \frac{Ze}{(2\pi)^3} \int \frac{\delta(q_0)}{\mathfrak{q}^2 + r_0^{-2}} e^{iqx} \, d^4 q . \tag{12}$$

Finally, we have for the contribution $M_{\alpha\beta\delta}(k, q)$ of the electron triangle:

$$M_{\alpha\beta\gamma}(k, q) = \text{Tr} \int \gamma_5 \gamma_\alpha S_C(p + k) \gamma_\beta S_C(p) \gamma_\gamma S_C(p - q) \cdot d^4 p . \tag{13}$$

On evaluating the latter integral one obtains logarithmically divergent expressions. Nevertheless, by an explicit calculation one can verify that these divergent constants vanish and $M_{\alpha\beta\gamma}$ is convergent. In order to avoid the troublesome calculations involved in the evaluation of the remaining complicated integral expressions, we can make use the of equations

$$M_{\alpha\beta\gamma} k_\beta = 0 , \qquad M_{\alpha\beta\gamma} q_\gamma = 0 , \tag{14}$$

expressing gauge invariance. Thus we get

$$\begin{aligned} M_{\alpha\beta\gamma} = & 4i\pi^2 m^2 \{ \varepsilon_{\alpha\beta\gamma\mu} [A (q_\mu k_\varrho q_\varrho + k_\mu q_\varrho q_\varrho) - \\ & - C (q_\mu k_\varrho q_\varrho - k_\mu q_\varrho q_\varrho) + \\ & + k_\sigma q_\tau \varepsilon_{\alpha\beta\sigma\tau} (A q_\gamma - C k_\gamma) + \\ & + \varepsilon_{\alpha\gamma\sigma\tau} (A q_\beta - C k_\beta) - \varepsilon_{\beta\gamma\sigma\tau} (D q_\alpha + G k_\alpha)] \} , \end{aligned} \tag{15}$$

where m is the electron rest mass, and A, C, D, G can be constructed from the following integral expressions:

$$A = \int_0^1 \int_0^{1-\xi} \frac{\xi - \xi^2 - \xi\eta}{1 + m^{-2}\left[q_\varrho q_\varrho (\xi - \xi^2) + 2k_\varrho q_\varrho \xi\eta\right]} d\eta\, d\xi\,, \tag{16}$$

$$B = \int_0^1 \int_0^{1-\xi} \frac{\xi\eta}{1 + m^{-2}\left[q_\varrho q_\varrho (\xi - \xi^2) + 2k_\varrho q_\varrho \xi\eta\right]} d\eta\, d\xi\,, \tag{17}$$

$$C = \int_0^1 \int_0^{1-\xi} \frac{\eta - \eta^2 - \xi\eta}{1 + m^{-2}\left[q_\sigma q_\varrho (\xi - \xi^2) + 2k_\varrho q_\varrho \xi\eta\right]} d\eta\, d\xi$$

as follows:

$$D = A + 2B\,, \qquad G = C + 2B\,.$$

By using (13) we can write down the total cross section summed over the spin directions of the neutrinos:

$$\sigma_{\mathrm{pol}} = \frac{Z^2\,\sigma_0}{2^7\,\pi^6} \iiint \frac{M_{\alpha\sigma\varrho} M_{\beta\tau\omega}}{(\mathfrak{q}^2 + r_0^{-2})^2} \frac{e_\sigma e_\tau n_\varrho n_\omega}{k_0\, k_{\nu 0}\, k_{\bar\nu 0}} \cdot$$
$$\cdot \delta(k_\nu + k_{\bar\nu} + q - k) \cdot (2k_{\nu\alpha} k_{\bar\nu\beta} - \delta_{\alpha\beta} k_{\nu\varrho} k_{\bar\nu\varrho}) \cdot$$
$$\cdot \delta(q_0)\, d^4 h\, d^3 k_\nu\, d^3 k_{\bar\nu}\,.$$

Two integrations can be carried out by making use of the following formula:

$$\iint \delta(k_\nu + k_{\bar\nu} - p) \cdot (2k_{\nu\alpha} k_{\bar\nu\beta} - \delta_{\alpha\beta} k_{\nu\varrho} k_{\bar\nu\varrho}) \frac{d^3 k_\nu\, d^3 k_{\bar\nu}}{k_{\nu 0}\, k_{\bar\nu 0}} =$$
$$= \frac{2\pi}{3} (p_\alpha p_\beta - p_\varrho p_\varrho \delta_{\alpha\beta}) \cdot \tag{18}$$

We can average over the polarization of the incident photon as well. Finally, in order to facilitate the evaluation of the remaining integrals we introduce the following new integration variables:

$$y = \frac{\mathfrak{q}^2}{m^2 E^2}\,, \qquad x = \frac{\mathfrak{q}\mathfrak{k}}{m^2 E^2}\,, \tag{19}$$

where $E = k_0/m$ denotes the energy of the incident photon in electron rest mass units. With these new variables we get

$$\sigma_D(E) = \sigma_0\, Z^2\, D^4\, E^{10} \int_0^4 \int_{y/2}^{\sqrt{y}} \left[A^2(-x^2 y^2 + 4xy^2 - y^3) + \right.$$
$$\left. + 4B^2(-x^4 + x^2 y) + 4AB(-x^3 y + xy^2)\right] \cdot \tag{20}$$
$$\cdot \frac{1}{6(1 + D^2 E^2 y)^2}\, dx\, dy\,,$$

where

$$\sigma_0 = \frac{f^2 m^2}{137^3 \pi^4} = 1{,}33 \cdot 10^{-52} \text{ cm}^2 \tag{21}$$

and

$$D = mr_0 \tag{22}$$

is the parameter characterizing the degree of the screening.

The formula (20) describes the cross section of the processes, illustrated by Figs. 1 and 2 without any approximation. The integration, however, cannot be carried out in full generality. Nevertheless, the cross section, valid for low energies ($E \ll 1$), can easily be obtained, because in this approximation the expressions

$$A(0, x, y) = B(0, x, y) = \frac{1}{24}$$

are constant and by substituting them into (20) we have for the case without screening ($D \to \infty$):

$$\sigma_\infty(E) = \frac{17}{4860} \sigma_0 Z^2 E^6 (1 + 0(E^2)), \tag{23}$$

or for finite screening ($E \ll 1$, $E \ll D^{-1}$)

$$\sigma_D(E) = \frac{2591}{17010} \sigma_0 Z^2 D^4 E^{10} (1 + 0(E^2)). \tag{24}$$

The determination of the high energy behaviour encounters many more difficulties. In any case, it can be seen from the expression (20) that σ_D behaves like $\sim E^2$ for $E \gg 1$, $E \gg D$.

§ 3. Photoneutrinos from a degenerated gas

The electrons of the plasma do not influence the matrix element (11) of the process (7) shown in Figs. 1 and 2, because there are no real electrons in the final state. Nevertheless, in the case of a dense electron gas one has to take into account that on calculating the cross section one obtains a coherent contribution from the process in which (7) is cathalized by the positive energy electrons of the degenerated Fermi gas and not by the negative energy electrons of the Dirac vacuum:

$$\gamma + e_{(i)} + {}_Z N^A \to {}_Z N^A + e_{(f)} + \nu + \bar{\nu}, \tag{25}$$

where the electron states $e_{(i)}$ and $e_{(f)}$ must be the same owing to the Pauli principle. Thus, in the presence of an electron gas background we have to consider the following processes simultaneously:

$$S^{(3)} = S_\alpha + \sum_{p_e} S_\beta(p_e) + \sum_{p_e} \sum_{p_{e'}} S_\gamma(p_e, p'_e). \tag{26}$$

For simplicity, let us consider a completely degenerated electron gas. The simplest way to get the summarized S-matrix element is to re-define the

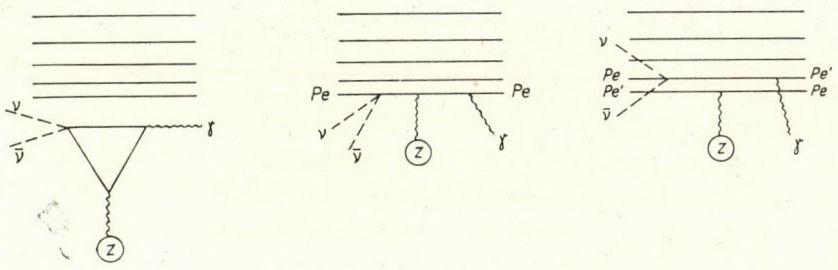

Fig. 3

vacuum state by raising the occupation level from the Dirac level to a positive Fermi level. This procedure can be expressed by the expansion operators $a_\mathfrak{p}$ of ψ_e as follows:

$$< F \,|a_\mathfrak{p}^+ a_\mathfrak{p}|\, F > = \begin{cases} 1, \text{ if } E_\mathfrak{p} < 0 \text{ or } E_\mathfrak{p} > 0 \text{ and } |\mathfrak{p}| < p_F, \\ 0, \text{ if } E_\mathfrak{p} > 0 \text{ and } |\mathfrak{p}| > p_F. \end{cases}$$

By using the new Fermi vacuum we define the electron propagator

$$S'_C(x-y) = < F \,|T\psi(x)\,\overline{\psi}(y)|\, F > = S_C(x-y) + S_{C1}(x-y), \tag{27}$$

where $S_C(x)$ is the usual causal propagator and

$$S_{C1}(x) = \frac{1}{(2\pi)^3} \int\limits_{|\mathfrak{p}|<p_F} (ip_\mu \gamma_\mu - m)\, \varepsilon(p_0)\, \delta(p^2 + m^2)\, e^{ipx}\, d^4 p. \tag{28}$$

The Wick theorem applies also in this case, provided the normal products are referred to the Fermi vacuum. (I. e. we norm to zero the ground state energy containing also the self energy of the electron gas.) So we can immediately write down the common matrix element of the processes shown by Fig. 3 by considering only the graphs of Figs. 1 and 2, i.e. by starting

from a matrix element of the type (11) and using the new $S'_C(x)$ in it instead of $S_C(x)$.

Indeed, by substituting (27) into the matrix element of the type

$$S^{(3)} = \ldots S'_C(p+k)\, S'_C(p)\, S'_C(p+q)\, \delta(q_0)\, \delta(k_\nu + k_{\bar\nu}) \tag{29}$$

we get $S^{(3)} = \ldots S_C(p+k)\, S_C(p)\, S_C(p+q) + S_C(p+k)\, S_C(p)\, S_{C1}(p+q) +$
$+ S_C(p+k)\, S_{C1}(p)\, S_C(p+q) + S_{C1}(p+k)\, S_C(p)\, S_C(p+q) +$
$+ S_C(p+k)\, S_{C1}(p)\, S_{C1}(p+q) + S_{C1}(p+k)\, S_C(p)\, S_{C1}(p+q) +$
$+ S_{C1}(p+k)\, S_{C1}(p)\, S_C(p+q) + S_{C1}(p+k)\, S_{C1}(p)\, S_{C1}(p+q) \cdot$
$\cdot\, \delta(q_0)\, \delta(k_\nu + k_{\bar\nu} + q - k).$

$S_{C1}(p)$ includes a $\delta(p_0 - \sqrt{\mathfrak{p}^2 + m^2})$-function, thus one can integrate over p_0 in the terms containing S_{C1}. All terms but one, containing more than just one S_{C1}, vanish owing to the conditions imposed by the δ-functions on p and the external momenta. One can readily verify that the result obtained in this way is the same one would get by calculating the contributions of the graphs of Fig. 3 in a Dirac vacuum.

Now the exact form of the matrix element is given by

$$S^{(3)} = 2\sqrt{2} f e^2 \left(\bar u_\nu \gamma_\alpha \frac{1+\gamma_5}{2} v_{\bar\nu}\right) \frac{1}{\sqrt{2k_0}} 2\pi\delta(k_0 - k_{\nu 0} - k_{\bar\nu}) \cdot$$
$$\cdot A(\mathfrak{q})\, e_\mu (K_{\alpha\mu} + L_{\alpha\mu}),$$

where

$$K_{\alpha\mu} = i \int \frac{d^4 p}{(2\pi)^4} \operatorname{Tr} \gamma_\alpha \gamma_5 \frac{i\hat p_1 - m}{p_1^2 + m^2} \gamma_4 \frac{i\hat p - m}{p^2 + m^2} \gamma_\mu \frac{i\hat p_2 - m}{p_2^2 + m^2}, \tag{30}$$

$$L_{\alpha\mu} = \int\limits_{|\mathfrak{p}|<p_F} \frac{d^3 p}{(2\pi)^3} \operatorname{Tr} \left[\gamma_\alpha \frac{1+\gamma_5}{2} \frac{i\hat p_1 - m}{p_1^2 + m^2} \gamma_4 \frac{i\hat p - m}{2\varepsilon} \frac{i\hat p_2 - m}{p_2^2 + m^2} - \right.$$
$$+ \frac{1+\gamma_5}{2} \frac{i\hat p - m}{2\varepsilon} \gamma_4 \frac{i\hat p_3 - m}{p_3^2 + m^2} \gamma_\mu \frac{i\hat p_4 - m}{p_4^2 + m^2} +$$
$$\left. + \frac{1+\gamma_5}{2} \frac{i\hat p_5 - m}{p_5^2 + m^2} \gamma_4 \frac{i\hat p_6 - m}{p_6^2 + m^2} \gamma_\mu \frac{i\hat p - m}{2\varepsilon} \right] + F - \tag{31}$$
$$- i \int\limits_{|\mathfrak{p}|<p_F} \frac{d^3 p}{(2\pi)^2} \delta(\varepsilon - \sqrt{(\mathfrak{p} - \mathfrak{q})^2 + m^2}) \cdot$$
$$\cdot \operatorname{Tr} \left[\gamma_\alpha \frac{1+\gamma_5}{2} \frac{i\hat p_1 - m}{2\varepsilon} \gamma_4 \frac{i\hat p - m}{2\varepsilon} \gamma_\mu \frac{i\hat p_2 - m}{p_2^2 + m^2} + \right.$$
$$\left. + \gamma_\alpha \frac{1+\gamma_5}{2} \frac{i\hat p_5 - m}{p_5^2 + m^2} \gamma_\mu \frac{i\hat p_1 - m}{2\varepsilon} \gamma_4 \frac{i\hat p - m}{2\varepsilon} \right].$$

furthermore

$$A(q) = -\frac{Ze}{q^2 + r_0^{-2}},$$

$$\varepsilon = \sqrt{p^2 + m^2},$$

$$p_1 = p - q, \qquad p_3 = p + q, \qquad p_5 = p + k - q,$$

$$p_2 = p - k, \qquad p_4 = p - k + q, \qquad p_6 = p + k.$$

e_μ is the polarization vector of the incoming photon. F in L designates the contributions of the graphs directed in opposite sense. These contributions can be obtained from the given terms by the substitution $p \to -p$ and $1 + \gamma_5 \to \gamma_5 - 1$.

It can be seen that $S^{(3)}$ is the sum of two terms:

$$S^{(3)} = S_D + S_F,$$

the first one describing the process (7) cathalized by the electrons of the Dirac sea and the second one that cathalized by the electrons of the Fermi sea. Accordingly, the cross section, proportional to $|S^{(3)}|^2$, can be written as the sum of three terms:

$$\sigma \sim |S^{(3)}|^2 = |S_D|^2 + |S_F|^2 + (S_D S_F^* + S_D^* S_F),$$

that is

$$\sigma = \sigma_D + \sigma_F + \sigma_{\text{int}}.$$

At a given energy S_D and S_F generally differ by orders of magnitude, therefore in a wide energy range $S^{(3)}$ coincides with S_D, σ with σ_D, calculated in § 2. In another wide energy range $|S_F| \gg |S_D|$, then σ practically coincides with σ_F, thus it can be calculated from S_F, i.e. from $L_{a\mu}$. Finally, there is a third, probably narrow, energy range, where $|S_F|$ and $|S_D|$ are of the same order of magnitude and where both σ_D, σ_F and the interference term σ_{int} are to be taken into account.

In what follows we shall calculate σ_F. There where $\sigma_F \gg \sigma_D$ we have $\sigma \cong \sigma_F$ and where $\sigma_F \ll \sigma_D$, $\sigma \cong \sigma_D$. In the case $\sigma_F \cong \sigma_D$ the calculation of σ_{int} would be needed as well. However, in this range we use interpolation.

From (29) we get

$$\sigma_F = \frac{8f^2 e^6}{2k_0} \frac{Z^2}{(2\pi)^5} \int \delta(k_\nu + k_{\bar{\nu}} + q - k) \frac{1}{(q^2 + r_0^{-2})^2} \cdot \frac{1}{2} \sum_{\nu\bar{\nu}} |M_F|^2 \, d^3 k_\nu \, d^3 k_{\bar{\nu}} \, d^3 q, \tag{32}$$

where

$$M_F = -\left(\bar{u}_\nu \gamma_\alpha \frac{1+\gamma_5}{2} v_{\bar{\nu}}\right) L_{\alpha\mu}.$$

Integration over k_ν and $k_{\bar{\nu}}$ yields

$$\sigma_F = -\frac{1}{3\,(2\pi)^4} f^2 e^6 Z^2 \frac{1}{k_0} \int (s^2 N_{\alpha\alpha} - s_\alpha s_\beta N_{\alpha\beta} - 2s^2 N_{44} + \\ + 2 s_4 s_\alpha N_{\alpha 4}) \frac{d^3 q}{(\mathfrak{q}^2 + r_0^{-2})^2}, \tag{33}$$

where

$$N_{\alpha\beta} = L_{\alpha\mu} L^*_{\beta\mu} \quad \text{and} \quad s = k - q.$$

The general evaluation of the integral would be a hopeless task. Let us consider merely the case when $p_F \ll m$. First we put $k_0 \ll p_F$ and

$$a = \frac{1}{2k_0 r_0} \gg 1. \tag{34}$$

Taking the lowest approximation in k and q we have from (31)

$$L_{\alpha\mu} = \frac{i}{(2\pi)^3} \frac{2}{k_0^2} (W - iY)(k_0 k_\alpha \delta_{\mu 4} + k_0 k_\mu \delta_{\alpha 4} - \\ - ik_0^2 \delta_{\alpha\mu} - k_0 q_\mu \delta_{\alpha 4} - iqk \delta_{\alpha 4} \delta_{\mu 4}), \tag{35}$$

where

$$W = \frac{\pi}{4|\mathfrak{q}|} (4p_F^2 - \mathfrak{q}^2) \ln \left| \frac{2p_F + |\mathfrak{q}|}{2p_F - |\mathfrak{q}|} \right| + \pi p_F,$$

$$Y = \frac{\pi^2}{4|\mathfrak{q}|} (4p_F^2 - \mathfrak{q}) \Theta\left(p_F - \frac{|\mathfrak{q}|}{2}\right),$$

$$\Theta(x) = \begin{cases} 1, & \text{if } x > 0, \\ 0, & \text{if } x < 0. \end{cases}$$

It can easily be seen that

$$s_\alpha L_{\alpha\mu} = 0,$$

$$N_{\alpha\alpha} = \frac{4}{k_0^4 (2\pi)^6} (W^2 + Y^2)(6k_0^4 - 4k_0^2 \mathfrak{q}\mathfrak{k} + k_0^2 \mathfrak{q}^2 + (\mathfrak{q}\mathfrak{k})^2),$$

$$N_{44} = \frac{4}{k_0^4 (2\pi)^6} (W^2 + Y^2)(2k_0^4 - 4k_0^2 \mathfrak{q}\mathfrak{k} + k_0^2 \mathfrak{q}^2 + (\mathfrak{q}\mathfrak{k})^2).$$

Introducing the notations

$$x = \frac{p_F}{k_0}, \quad E = \frac{k_0}{m}, \quad u = \frac{|q|}{2k_0} \tag{36}$$

and

$$w = \frac{1}{2u}(x^2 - u^2) \ln \frac{x+u}{x-u} + x,$$

$$y = \frac{1}{2u}(x^2 - u^2)\, \Theta(x-u),$$

we obtain

$$\sigma_F = \frac{1}{9} Z^2 \sigma_0 E^2 \int_0^1 \frac{w^2 + y^2}{(u^2 + a^2)^2} (3 + 2u - 18u^2 + 12u^3 + 2u^4 - u^6) u^3 \, du,$$

where σ_0 is the quantity introduced in (21). Since $x \gg u$,

$$w \approx 2x,$$

$$y \approx \frac{\pi}{2} \frac{x^2}{u},$$

similarly, in the denominator of the integrand we may put simply a^4 because of $a \gg 1$. Thus σ_F is given by

$$\sigma_F (x \gg 1, a \gg 1) \approx \frac{4}{9} \sigma_0 Z^2 E^6 D^4 \cdot$$

$$\cdot \int_0^1 (w^2 + y^2)(3 + 2u - 18u^2 + 12u^3 + 2u^4 - u^6) u^3 \, du =$$

$$= \frac{11}{90} \pi^2 Z^2 \sigma_0 \frac{p_F^4}{m^4} E^2 D^4 \left[1 + 0\left(\frac{1}{x^2}\right) + 0\left(\frac{1}{a^2}\right)\right]. \tag{37}$$

D is defined by (22). One can see that the cross section goes to zero as $E \to 0$.

Now let k_0 be $\gg p_F$ and $p_F/k_0 \gg a$. Since the integral over q contains a denominator of the form $\left(\frac{q^2}{4k_0^2} + a^2\right)^2$, and $a \ll 1$, the integrand's most

significant contribution comes from the range where $|\mathfrak{q}|/2k_0 \leq a$. Thus in $L_{a\mu}$ we may restrict ourselves to the lowest approximation in $\mathfrak{q}$, because each higher power of $\mathfrak{q}$ gives a higher approximation in a. The approximation we apply depends on whether $|\mathfrak{q}|$ is smaller or bigger than $2p_F$.

If $|\mathfrak{q}|/2 < p_F$, one obtains

$$L_{a\mu} \approx -\frac{2i}{(2\pi)^3 k_0}(W_1 - iY_1)(k_a \delta_{\mu 4} + k_\mu \delta_{a4} - k_4 \delta_{a\mu}). \tag{38}$$

Hence

$$s_a L_{a\mu} = 0\,,$$

$$N_{aa} = \frac{4}{(2\pi)^6 k_0^2}(W_1^2 + Y_1^2)\, 6\, k_0^2\,,$$

$$N_{44} = \frac{4}{(2\pi)^6 k_0^2}(W_1^2 + Y_1^2)\, 2\, k_0^2\,,$$

where

$$W_1 \approx 2\pi p_F \left(1 - \frac{1}{12}\,\frac{\mathfrak{q}^2}{p_F^2}\right),$$

$$Y_1 \approx \frac{\pi^2}{\mathfrak{q}^2}\left(p_F^2 - \frac{\mathfrak{q}^2}{4}\right).$$

If $\frac{|\mathfrak{q}|}{2} > p_F$, we have

$$L_{a\mu} \approx -\frac{2i}{(2\pi)^3 k_0} W_2 (k_a \delta_{\mu 4} + k_\mu \delta_{a4} - k_4 \delta_{a\mu})\,, \tag{39}$$

and

$$s_a L_{a\mu} = 0\,,$$

$$N_{aa} = \frac{4}{(2\pi)^6 k_0^2} W_2^2\, 6\, k_0^2\,,$$

$$N_{44} = \frac{4}{(2\pi)^6 k_0^2} W_2^2\, 2\, k_0^2\,,$$

where

$$W_2 \approx \frac{8\pi p_F^3}{3\mathfrak{q}^2}\left(1 + \frac{4}{5}\,\frac{p_F^2}{\mathfrak{q}^2}\right).$$

Introducing the notations used in (34) and (36) we get

$$\sigma_F\,(1 \gg x \gg a) \approx \frac{1}{3}\,\sigma_0\,Z^2\,E^2\left\{\int_0^x\left[\frac{\pi^2}{4}\,u\,(x^4 - 2u^2\,x^2 + u^4) + \right.\right.$$

$$+ 4x^2\,u^3\left(1 - \frac{2}{3}\,\frac{u^2}{x^2}\right)\Bigg]\frac{du}{(a^2 + u^2)^2} +$$

$$+ \int_x^1 \frac{4}{9}\,x^6\,\frac{1}{u^5}\left(1 + \frac{2}{5}\,\frac{x^2}{u^2}\right)du\Bigg\} \approx \tag{40}$$

$$\approx \frac{\pi^2}{6}\,Z^2\,\sigma_0\,\frac{P_F^4}{m^4}\,D^2\left(1 + 0\left(\frac{a^2}{x^2}\right)\right),$$

i.e. at high energies the cross section becomes constant.

§ 4. Conclusion

Owing to the mathematical complications we failed to determine in full generality the cross section of the reaction $\gamma \to \nu + \bar{\nu}$ taking place in a degenerated electron gas. Nevertheless, it can be concluded also from the calculations performed for special cases that the transformation cathalized by the Fermi sea predominates at low energies ($E \ll 1$). In such a case the screening ($D^{-1} \neq 0$) plays an essential role. (We may use (37).) On the other hand, at very high energies ($E \gg 1$) the transformation cathalized by the Dirac sea will be dominating (this latter continues to increase while σ_F becomes constant), and therefore we may use the formula (20). The screening becomes less important.

It should be noted that for low energies the cross section of the process (7) has been determined also by MATINYAN [11] without his taking into account the screening and the presence of real electrons, and a result different from (23) has been obtained. This difference, however, refers to a practically uninteresting case because at low energies the screening (and as a rule also the degeneration) plays an important role.

The astronomical consequences of our results have been discussed elsewhere [10]. Here we mention only that below 10^9 °K and in the case of strong degeneration the role of the photoneutrino emission can be competing with that of the Compton neutrinos. At higher temperatures the annihilation neutrinos become more significant.

Acknowledgements

The authors wish to thank Dr. G. Pócsik for helpful discussions on gauge invariance, and Dr. F. Károlyházy for his valuable remarks on the modified propagator.

REFERENCES

1. G. Marx and N. Menyhárd, Science, **131,** 299, 1960; Mitteilungen der Sternwarte, Budapest, No. 48, 1960.
2. G. Gamow and M. Schönberg, Phys. Rev., **59,** 539, 1941.
3. H. Y. Chiu, Annals of Physics, **15,** 1, 1961.
4. B. M. Pontecorvo, JETP. USSP, **36,** 1615, 1959; Soviet Physics JETP, **9,** 1148, 1959.
5. G. M. Gandelman and V. S. Pinaev, JETP USSR, **37,** 1072, 1959; Soviet Physics JETP **37,** 764, 1960.
6. R. C. Stabler, thesis, Cornell University.
7. H. Y. Chiu and R. C. Stabler, Phys. Rev., **122,** 1317, 1961.
8. M. Gell-Mann, Phys. Rev. Lett., **6,** 70, 1961.
9. G. Marx and J. Németh, Proceedings of the XIth International Conference on High Energy Physics, CERN, Geneva, 1962.
10. G. Marx and J. Németh, Mitteilungen der Sternwarte Budapest, No. 52, 1963.
11. S. Matinyan and N. Tsilosani, JETP, **41,** 1681, 1961.

ИЗЛУЧЕНИЕ НЕЙТРИНО ПРИ ВЫРОЖДЕННОМ ГАЗЕ

Г. МАРКС и Т. НАДЬ

Резюме

Определяется эффективное сечение образования пар нейтрино фотонами в кулоновском поле ядра. При вычислениях принималась во внимание и экранировка кулоновского поля, отдельно исследовалось влияние возможно присутствующего электронного газа. Данное влияние оказалось значительным при низких энергиях. Результаты могут иметь астрофизическое значение, в первую очередь для внутренней части поздних вырожденных звёзд в области температур $10^8 — 10^9$ К°.

THE ENERGY OF NEUTRONS FROM THE REACTION $Be^9(\alpha, n)C^{12}$

By

L. MEDVECZKY

NUCLEAR RESEARCH INSTITUTE OF THE HUNGARIAN ACADEMY OF SCIENCES, DEBRECEN

(Presented by A. Szalay. — Received 21. II. 1963)

The nuclear reaction was produced by Po^{210} alpha-source. The energy of the neutrons was measured by the photoemulsion method in direction of 30°, 90°, 120°, 150° and 180° (in the laboratory system). The differential cross section for formation of the 4,433 MeV state was found to be 56; 24; 25; 29; and 30 mb/sr $\pm$ 20,4% respectively, in the above-mentioned five directions.

There are a great many reports [1] on the nuclear reaction $Be^9(\alpha, n)C^{12}$. Several workers investigated the dependence of the intensity of radiations from the nuclear reaction on the energy of α-particles producing the reaction. The shape of the excitation curves is very similar for photons and neutrons, both showing marked resonances characteristic of the formation of the compound nucleus.

There have been extensive studies on the angular distribution of neutrons as well as on the $n-\gamma$ angular correlation. The experimental results generally indicate anisotrope angular distribution, the interpretation of which given by the authors, however, is divergent. In the view of JAMES, JONES and WILKINSON [2] as well as that of RISSER, PRICE and CLASS [3] the angular distribution of ground state neutrons of nucleus C^{12} when $E_\alpha \leq 5$ MeV can be explained by the formation of a compound nucleus. TANNER's [4] angular correlation studies essentially also support this view. Among recent examinations [5, 6, 7] GARG, CALVERT and GALE interpret the angular distribution of neutrons arising from the reaction $Be^9(\alpha, n)C^{12}$ and pertaining to the 4,433 MeV level of the nucleus C^{12} by means of a direct reaction mechanism, although the possibility for the formation of a compound nucleus is not excluded either.

Interestingly, when α-particles of higher energy are concerned ($9 < E_\alpha < 14$ MeV), the angular distribution of these neutrons greatly varies at different E_α-energies [8]. This may be caused by the formation of a compound nucleus. The angular distribution belonging to the ground state and second energy level of C^{12} hardly changes in a wide energy region, which is due to a direct nuclear reaction mechanism in addition to identical values of spin and parity (O^+).

Investigations with α-particles of $E_\alpha = 5{,}3$ MeV energy, which we also applied in the study reported here, were made only by GUIER, BERTINI and

ROBERTS [9]. They measured the energy distribution of neutrons only in forward and backward directions. Our measurements, however, were made under more favourable conditions, insofar as the geometrical arrangement of investigations and naturally the technique of measurements are concerned. Moreover, the measurements of neutron energy were made also in directions 30°, 90°, 120° and 150° besides 180°.

Experimental method and results

Exposure of the plates

For producing reaction Po^{210}, an alpha-source was used which had been prepared according to the method generally applied at this Institute [10]. The intensity of the preparation volatilized onto a Pt-Ir disk was 53,34 mC at the beginning of the experiments. The high grade of purity of the alpha-source was checked by measuring the energy distribution of the emitted particles with an electromagnetic alpha spectrometer [11].

The target consisted of a Be-layer evaporated upon a copper disk carefully burnished and electrolytically polished. Both the alpha-source and the target were 3 mm in diameter, and the distance between them was $5 \pm 0{,}01$ mm. During an exposition of about 3 weeks, the alpha-source and the target were enclosed in a glass vacuum container coated with a copper foil on the inside. The pressure in the container was about 10^{-2} Hgmm during irradiation.

The emitted neutrons were detected by the observation of the tracks made by recoil protons arising in the nuclear emulsions. The small surface of the Po-source made it possible for the 200μ thick Agfa K2 nuclear plate to be placed at a distance of 30 mm from the Be-target. While exposed, all the plates were enclosed in a light-proof case cylindric in shape and made of iron. The case was such that ensured the neutrons to be observed from different angles around the source. Measurements were made on plates irradiated in directions of 30°, 90°, 120°, 150° and 180° in the laboratory system. During irradiation, the source together with the case of plates was suspended by a wire. The minimum of other scattering materials in the room was 110 cm.

The nuclear emulsions were processed by temperature-development with amidol [12]. To reduce the shrinkage factor, an aqueous solution of 10% glycerin was applied. The proton tracks were scanned in the usual way. For accuracy in measuring the neutrons, the range-energy relation of Agfa K2 nuclear emulsions was calibrated [13].

Results of measurement

The energy distribution of neutrons arising from the reaction $Be^9(\alpha, n)C^{12}$ was determined in the above-mentioned five directions. Owing to the low

density of tracks, the energy distribution obtained from all directions was summarized from results in measuring several plates.

The scanned volume of emulsions and number of tracks are shown in Table I.

Table I

Direction Laboratory system	Scanned volumes of emulsion (in cc mm)	Number of recoil proton tracks	Background	Corrected number of proton tracks (neutrons)
30°	195	428	29	586
90°	292	385	46	491
120°	292	354	41	437
150°	292	389	46	472
180°	390	532	59	648

About 10 per cent of all the tracks, as determined by the comparative mesurement made on the non-irradiated plates, had to be ascribed to the background.

The number of protons corrected in the usual way — after background reduction — is plotted according to each direction of observation in Figs. 1—5. The neutron energy values calculated on the basis of the levels of C^{12} are indicated by arrows. The Q-value of the ground state of C^{12} for reaction $Be^9(\alpha, n)C^{12}$ was taken as 5,704 MeV [14].

In the energy distribution measured in each direction three different groups of neutrons can be distinguished. Out of these, the one with the highest intensity is that which corresponds to the level of 4,433 MeV, and the energy peaks as well as the calculated values designated by arrows are in good agreement. For the energy of neutrons pertaining to the ground state and the 7,656 MeV level, there is no longer such good agreement. Here, not only the number of events but also the resolving power of measuring methods is less. The uncertainty in the determination of the number of neutrons pertaining to the level of 7,656 MeV is significant only because of the background observable at energies lower than 2,2 MeV. Therefore conclusions are drawn only for neutrons pertaining to the first excited level of C^{12}.

Using the most recent mass values [15] the Q-value for this level is $1{,}302 \pm 0{,}058$ MeV, if it is calculated by the neutron energy values obtained for reaction $Be^9(\alpha, n)C^{12}$. This weighted mean value, within the given standard deviation, is in good agreement with earlier data in the literature.

The neutron intensities obtained in various directions are presented in Fig. 6 in arbitrary units. The error of relative intensities is determined by the uncertainty of determining the volume of the emulsion. In determining the

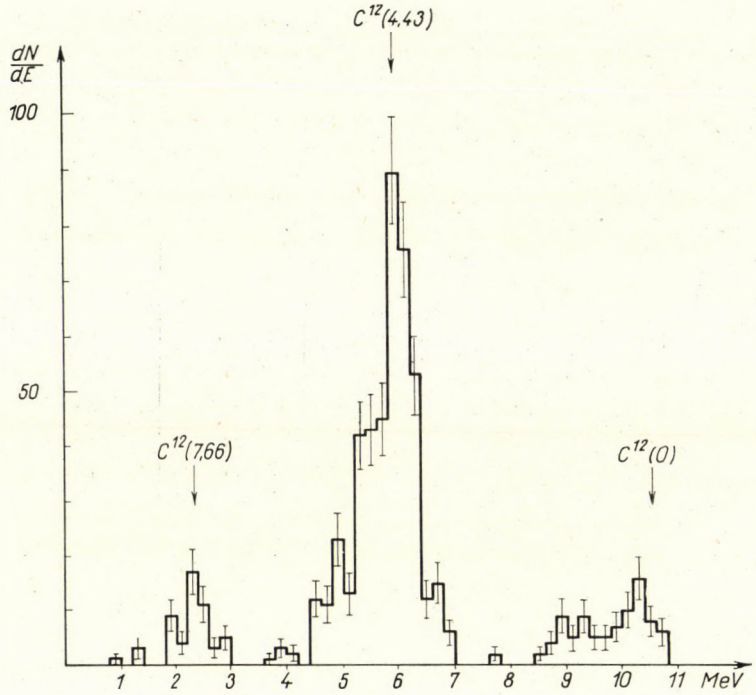

Fig. 1. Neutron energy distribution obtained at 30° (in laboratory system). dN is the corrected number of neutrons in a 0,2 MeV interval (dE). The arrows indicate the energy-level of C^{12} to which the neutron group corresponds

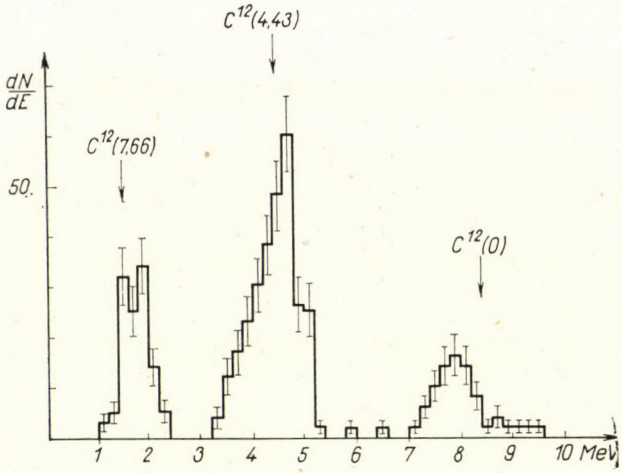

Fig. 2. Neutron energy-distribution observed at 90° in laboratory system. (For signs see the caption of Fig. 1)

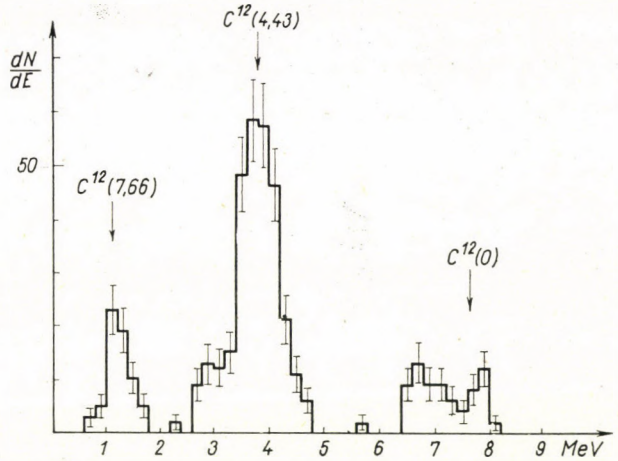

Fig. 3. Neutron energy-distribution observed at 120° in laboratory system. (For signs see the caption of Fig. 1)

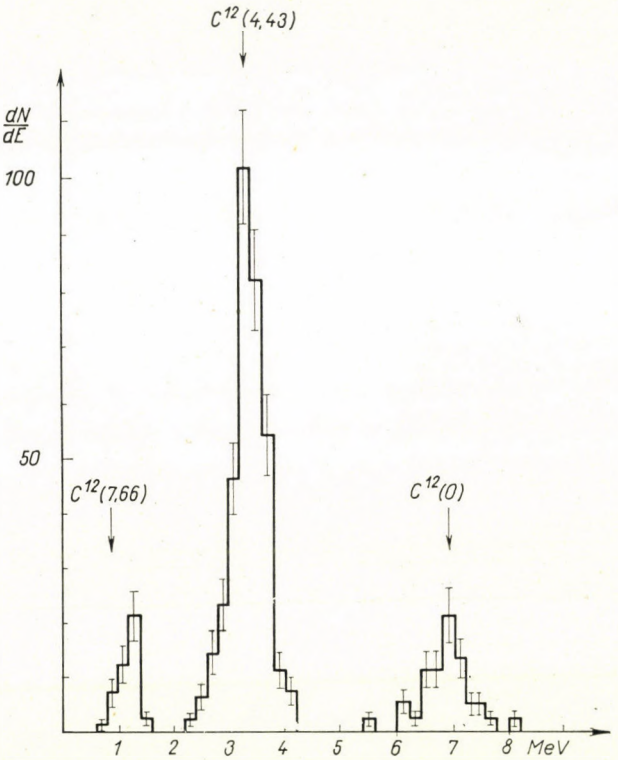

Fig. 4. Neutron energy-distribution observed at 150° in laboratory system. (For signs see the caption of Fig. 1)

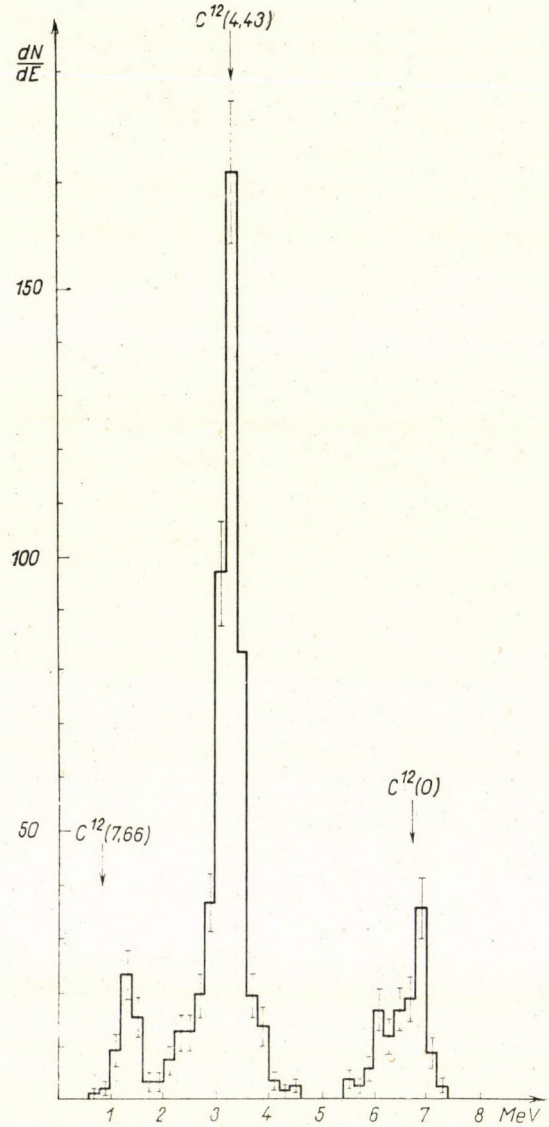

Fig. 5. Neutron energy-distribution observed at 180° in laboratory system. (For signs see the caption of Fig. 1)

error of angles the following factors were considered: *a)* the straggling of α-particles, *b)* the size of the target and *c)* the point of observation. The curve of distribution was obtained by the method of least squares fit, and it can be expressed by the equation:

$$W(\omega) = P_0 + a_1 P_1 + a_2 P_2 + a_3 P_3 ,$$

where P_0, P_1, P_2 and P_3 are Legendre polynominals; the coefficients a_1, a_2, a_3 are equal to 221,8245; 591,4016; 1,7224, respectively.

From the results of our measurement, the differential cross-section of the formation of the 4,433 MeV level of C^{12} is 56 mb in 37° 30′ direction of the centre-of-mass system. This differential cross-section in other directions is less; that is 24 mb/sterrad at 105° 30′; 25 at 133°, 29 at 158° and 30 at 180°. The root mean square error of the differential cross-section values is 20,4%

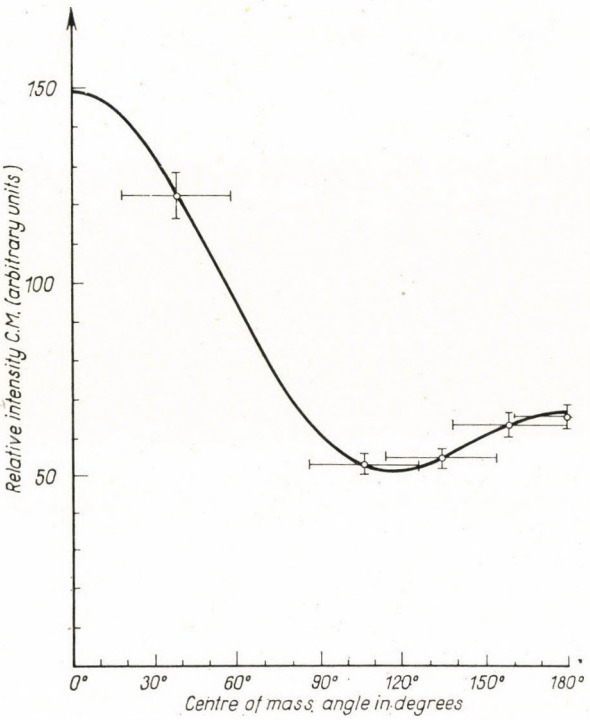

Fig. 6. Angular distribution of the neutrons pertaining to the 4,433 MeV state of the nucleus C^{12}, in the centre-of-mass system

which is given by the following uncertainty factors: *a)* 5,6% in the number of α-particles; *b)* 10% in the thickness of the target; *c)* 6% as the statistical error; *d)* 10% attenuation of neutrons in the emulsion and *e)* 5% as the error in determining the volume of the emulsion.

According to results reported in the literature (Fig. 7) a forward peak is observable in the angular distribution. From the angular distribution of neutrons, conclusions as to the mechanism of the nuclear reaction have only been drawn by GARG at al [7]. In their view, direct reaction mechanism is predominant, although the compound nucleus formation also is possible.

The clarification of the problem is even more complex. Namely the widths of the level on which C^{13} may be formed as a compound nucleus can be com-

pared to the distance of these energy levels. This reaction may be produced even through overlapping levels and so there is not necessarily a symmetry in case of compound nucleus formation to the 90° centre-of-mass angle in the angular distribution of neutrons. Otherwise a detailed evaluation is hindered also by the fact that the spin and parity of these levels of C^{13} are not yet known.

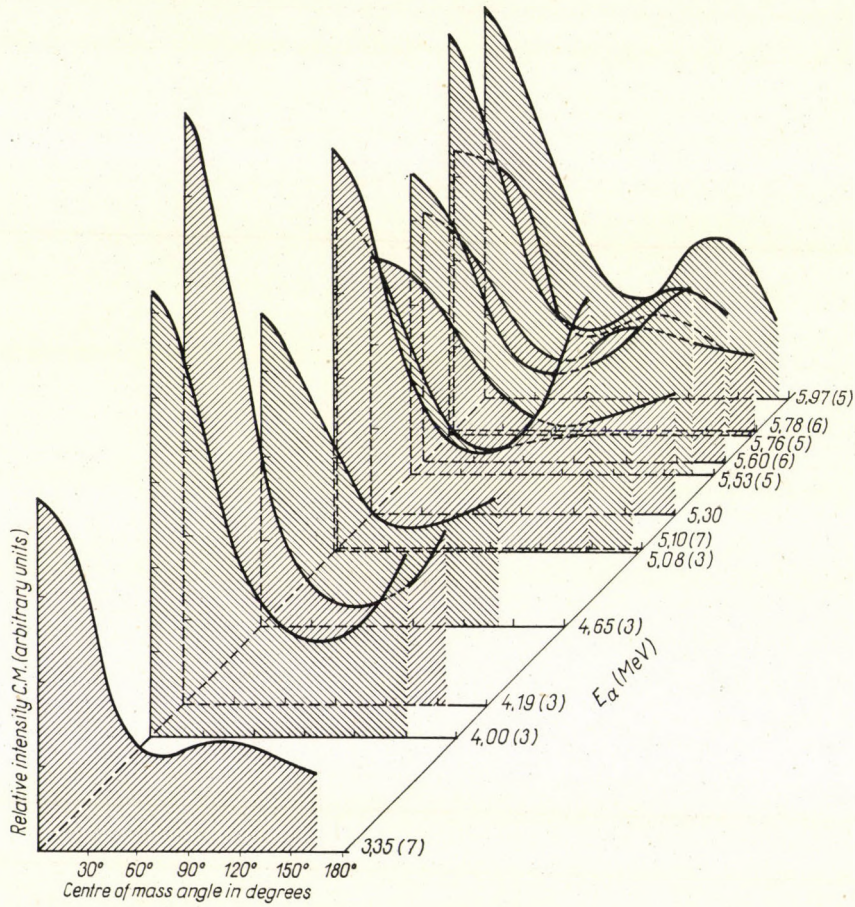

Fig. 7. The relative intensity of neutrons pertaining to the 4,433 MeV level of C^{12} according to the centre-of-mass angles at different E_α-energies. (The numbers in brackets after the E_α-values indicate the corresponding ordinal number of references.) The relative intensities are normalized for 90° centre-of-mass angle

I wish to thank Prof. A. SZALAY for his interest in the subject and his help and for having prepared the Po-source. The valuable discussions with my colleagues, Mrs. B. GYARMATI and Mr. T. BALOGH, Lecturer at the University, Debrecen are also greatly appreciated. Acknowledgement is due to all taking part in processing the emulsions and measuring the tracks for their conscientious and thorough work.

REFERENCES

1. F. AJZENBERG-SELOVE and T. LAURITSEN, Nucl. Phys., **11,** 1, 1959.
2. D. B. JAMES, G. A. JONES and D. H. WILKINSON, Phil. Mag., (8)**1,** 949, 1957.
3. J. R. RISSER, J. E. PRICE and C. M. CLASS, Phys. Rev., **105,** 1288, 1957.
4. N. W. TANNER, Proc. Phys. Soc., **72,** 457, 1958.
5. N. H. GALE and J. B. GARG, Nuovo Cimento Ser. I, **19,** 742, 1961.
6. F. AJZENBERG-SELOVE and P. H. STELSON, Phys. Rev., **120,** 500, 1960.
7. J. B. GARG, J. N. CALVERT and N. H. GALE, Nucl. Phys., **19,** 264, 1960.
8. J. KJELLMAN and A. NILSSON, Ark. Fys., **22,** 277, 1962.
9. W. H. GUIER, H. W. BERTINI and J. H. ROBERTS, Phys. Rev., **85,** 426, 1952.
10. A. SZALAY, Z. Phys., **112,** 29, 1938.
11. T. FÉNYES, private communication.
12. E. BUJDOSÓ and L. MEDVECZKY, Nucl. Instruments, **2,** 270, 1958.
13. L. MEDVECZKY and G. SOMOGYI, Acta Phys. Hung., **13,** 163, 1961.
14. F. AJZENBERG-SELOVE and T. LAURITSEN, Energy Levels of Light Nuclei A = 5 to A = 20.
LANDOLT—BÖRNSTEIN, Neue Serie, Band I/1, Springer, Berlin 1961, p. 34.
15. L. A. KÖNIG, J. H. E. MATTAUCH and A. H. WAPSTRA, Nucl. Phys., **31,** 18, 1962.

ЭНЕРГИЯ НЕЙТРОНОВ, ПОЛУЧЕННЫХ ОТ ЯДЕРНОГО ПРОЦЕССА $Be^9(\alpha, n)C^{12}$

Л. МЕДВЕЦКИ

Резюме

Исследованный ядерный процесс был создан α-источником Po^{210} и тонкой мишенью Be. Энергия нейтронов была измерена фотоэмульсионным методом в направлениях 30°, 90°, 120°, 150° и 180° (в лабораторной системе). Относительно вышеупомянутых пяти направлений для дифференциального состояния 4,433 MeV найдены 56; 24; 25; 29 и 30 миллибарн/стерадиан $\pm$ 20,4%.

COMMUNICATIONES BREVES

THE HELLMANN—FEYNMAN THEOREM IN THE VARIATIONAL METHOD

By

R. GÁSPÁR

INSTITUTE FOR THEORETICAL PHYSICS, KOSSUTH LAJOS UNIVERSITY, DEBRECEN

and

RESEARCH GROUP FOR THEORETICAL PHYSICS, HUNGARIAN ACADEMY OF SCIENCES, BUDAPEST

(Received 25. I. 1963)

Be the Hamiltonian operator of the problem given by H and the variational trial function by $\Phi(\xi_i)$, where the ξ_i are variational parameters. If Φ is normalized then the approximate energy is

$$\varepsilon = < \Phi \,|H|\, \Phi > . \tag{1}$$

The best energy value will be given by the function Φ_0, the parameters ξ_{i0} of which are determined from the equations

$$\begin{aligned} \frac{\partial \varepsilon}{\partial \xi_i} = \frac{\partial}{\partial \xi_i} < \Phi \,|H|\, \Phi > \; = \; < \frac{\partial \Phi}{\partial \xi_i} \,|H|\, \Phi > + \\ + < \Phi \,|H|\, \frac{\partial \Phi}{\partial \xi_i} > = 0 \qquad (i = 1, 2, \ldots, n). \end{aligned} \tag{2}$$

Of course, the Hamiltonian H does not contain variational parameters. If a parameter η is contained in H then Φ_0 will also depend on this parameter.

Φ_0 may depend on η in two ways; *a)* Φ_0 may depend explicitly on η. The most usual case, however, is that when *b)* Φ_0 depends on η only through the minimum value, ξ_{i0}, of the variational parameter ξ_i. But for these values ξ_{i0} (2) is satisfied since ε depends in the same way on ξ_{i0} as on ξ_i if η is constant. By taking this into account we have

$$\frac{d\varepsilon}{d\eta} = \frac{\partial \varepsilon}{\partial \eta} + \sum_{i=1}^{n} \frac{\partial \varepsilon}{\partial \xi_{i0}} \cdot \frac{\partial \xi_{i0}}{\partial \eta} = \frac{\partial \varepsilon}{\partial \eta} . \tag{3}$$

Thus, when differentiating ε, we have to take into account only the explicit dependence of Φ on η. Because of this we have

$$\frac{d\varepsilon}{d\eta} = \frac{\partial \varepsilon}{\partial \eta} = < \Phi \left| \frac{\partial H}{\partial \eta} \right| \Phi > + < \frac{\partial \Phi}{\partial \eta} \,|H|\, \Phi > + < \Phi \,|H|\, \frac{\partial \Phi}{\partial \eta} > \tag{4}$$

and if Φ does not depend explicitly on η

$$\frac{d\varepsilon}{d\eta} = \frac{\partial \varepsilon}{\partial \eta} = <\Phi \left| \frac{\partial H}{\partial \eta} \right| \Phi > . \tag{5}$$

Equs. (4) and (5) give the form of the HELLMANN—FEYNMAN theorem in the variational method.

As it is well known, according to the HELLMANN—FEYNMAN theorem [1], relation (5) holds for the eigenvalue E and the eigenfunction ψ of the eigenvalue problem $H\psi = E\psi$.

Let the Hamiltonian of the atomic system under consideration be given by

$$H = \sum_{i=1}^{N} H_i + \sum_{i>j=1}^{N} \frac{e^2}{r_{ij}} + \sum_{k>l=1}^{\nu} \frac{Z_k Z_l e^2}{R_{kl}}, \tag{6}$$

$$H_i = \frac{\hbar^2}{2m} \Delta_i - \sum_{k=1}^{\nu} \frac{Z_k e^2}{r_{ki}} . \tag{7}$$

The nuclei can, in the adiabatic approximation, be considered to be at rest. r_{ij}, r_{ki}, R_{ki} denote in order the distances between the electrons, those between the kth nucleus and the ith electron, and lastly beetwen the nuclei.

Z_k is the atomic number of the kth nucleus, m the mass of the electron and e the elementary charge.

If $\eta = Z_k$ then

$$\frac{\partial H}{\partial Z_k} = -\frac{e^2}{r_{ki}} + \sum_{l=1}^{\nu}{}' Z_l \, e^2/R_{kl} = -\frac{e^2}{r_{ki}} + \text{constant}, \tag{8}$$

where the prime means that there is no summation for $l = k$. From this, by the aid of (5), we get for the isoelectronic series of helium

$$\left(\frac{\bar{1}}{r}\right)_{\text{variational}} = \left(2Z - \frac{5}{8}\right) \frac{1}{a_0}, \tag{9}$$

if the trial function is $\Phi = A \exp(-\xi r/a_0)$ and $A = (\xi^3/\pi a_0^3)^{1/2}$ is the normalization factor. Further

$$E = \left[\xi^2 - \left(2Z - \frac{5}{8}\right)\xi\right] \frac{e^2}{a_0} \tag{10}$$

and the minimum is at the value $\xi_0 = Z - \frac{5}{16}$.

By using the HYLLERAAS expression [2] for the energy of the isoelectronic series of helium

$$E = \left(Z^2 - \frac{5}{8} Z + 0{,}15744 - 0{,}00876 \frac{1}{Z} + 0{,}00274 \frac{1}{Z^2}\right) \frac{e^2}{a_0}, \qquad (11)$$

we get

$$\left(\frac{\bar{1}}{r}\right)_{\text{exact}} = \left(2Z - \frac{5}{8} + 0{,}00876 \frac{1}{Z^3} - 0{,}00548 \frac{1}{Z^3}\right) \frac{1}{a_0}. \qquad (12)$$

Subtracting (9) from (12) we see from the relation

$$\left(\frac{\bar{1}}{r}\right)_{\text{exact}} - \left(\frac{\bar{1}}{r}\right)_{\text{variational}} = \left(0{,}00876 \frac{1}{Z^2} - 0{,}00548 \frac{1}{Z^3}\right) \frac{1}{a_0} \qquad (13)$$

that the difference between the exact average value and the one calculated with the variational method is very small and tends to zero rapidly with increasing atomic number. Even in the case of the H^- ion the order of magnitude of the difference is 0,00328 a_0^{-1}, and in the case of the He atom 0,00082, while the value of $\left(\frac{\bar{1}}{r}\right)_{\text{variational}}$ in the two cases is 1,375 a_0^{-1} and 3,375 a_0^{-1}, respectively.

REFERENCES

1. H. HELLMANN, Einführung in die Quantenchemie, F. Deuticke, Leipzig, 1937; R. O. FEYNMAN, Phys. Rev., **56**, 340, 1939.
2. E. A. HYLLERAAS, Zs. f. Phys., **48**, 469, 1928; ibid., **54**, 347, 1929; E. A. HYLLERAAS and B. UNDHEIM, ibid., **65**, 759, 1930.

THE HELLMANN—FEYNMAN THEOREM AND THE CORRELATION ENERGY

By

R. GÁSPÁR

INSTITUTE FOR THEORETICAL PHYSICS, KOSSUTH LAJOS UNIVERSITY, DEBRECEN

and

RESEARCH GROUP FOR THEORETICAL PHYSICS, HUNGARIAN ACADEMY OF SCIENCES, BUDAPEST

(Received 28. I. 1963)

The HELLMANN—FEYNMAN theorem [1] states that the exact wave function and energy of an atom or a molceule satisfies the following relation

$$\partial E/\partial\lambda = <\overline{\Psi} \mid \partial H/\partial\lambda \mid \overline{\Psi}>. \tag{1}$$

The proof of the above theorem is rather simple, since the relation

$$\begin{aligned}\partial E/\partial\lambda = \partial <\overline{\Psi} \mid H \mid \overline{\Psi}>/\partial\lambda = <\overline{\Psi} \mid \partial H/\partial\lambda \mid \Psi> + \\ + <\partial\overline{\Psi}/\partial\lambda \mid H \mid \overline{\Psi}> + <\overline{\Psi} \mid H \mid \partial\overline{\Psi}/\partial\lambda>\end{aligned} \tag{2}$$

holds. By making use of the hermiticity of H and of the relation

$$H\overline{\Psi} = E\overline{\Psi} \tag{3}$$

we get

$$\partial E/\partial\lambda = <\overline{\Psi} \mid \partial H/\partial\lambda \mid \overline{\Psi}> + E\{<\partial\overline{\Psi}/\partial\lambda \mid \overline{\Psi}> + <\Psi \mid \partial\overline{\Psi}/\partial\lambda>. \tag{4}$$

Because of the normalisation condition

$$<\overline{\Psi} \mid \overline{\Psi}> = 1 \tag{5}$$

we have by differentiation

$$<\overline{\Psi} \mid \partial\Psi \mid \partial\lambda> + <\partial\overline{\Psi} \mid \partial\lambda \mid \Psi> 0\,. \tag{6}$$

Hence the sum of the last two terms in (4) gives zero and relation (1) holds.

In (1) λ is any parameter contained in the Hamiltonian of the system; it may, for example, be the intensity of the electric or magnetic field, the internuclear distance or the angular coordinate determining the position of the nuclei, which are all real continuously variable parameters. But these parameters may describe also interactions switched on adiabatically or other atomic constants, the values of which change stepwise, such as for example the charge or mass of a particle.

The HELLMANN—FEYNMAN theorem can be applied to HARTREE—FOCK wave functions and total energies calculated with these functions [2]. Be

$$\Psi_{HF} = \| a_1(1)\, a_2(2) \ldots a_n(n) \| \tag{7}$$

the normalized HARTREE—FOCK wave function and

$$E_{HF} = < \Psi_{HF} | H | \Psi_{HF} > \tag{8}$$

the HARTREE—FOCK total energy, where the a_i-s are the one-electron wave functions. By differentiating (8) with respect to λ we get the expression

$$\begin{aligned} \partial E_{HF} / \partial \lambda = < \Psi_{HF} | \partial H / \partial \lambda | \Psi_{HF} > + < \partial \Psi_{HF} / \partial \lambda | H | \Psi_{HF} > + \\ + < \Psi_{HF} | H | \partial \Psi_{HF} / \partial \lambda > . \end{aligned} \tag{9}$$

Differentiating Ψ_{HF} with respect to λ, we have

$$\begin{aligned} \partial \Psi_{HF} / \partial \lambda = \partial a_1 / \partial \lambda\, a_2 \ldots a_n \| + \| a_1\, \partial a_2 / \partial \lambda \ldots a_n \| + \ldots + \\ + \| a_1\, a_2 \ldots \partial a_n / \partial \lambda \| . \end{aligned} \tag{10}$$

Because of the normalisation condition

$$< a_i | a_i > = 1 \tag{11}$$

which holds for any λ, we have

$$Re < \partial a_i / \partial \lambda | a_i > = \frac{1}{2} \partial / \partial \lambda < a_i | a_i > = 0 . \tag{12}$$

If a_i is complex, then the imaginary part can be made zero by multiplying it by a phase-factor of modulus unity [3]. Hence $\partial a_i / \partial \lambda$ is orthogonal to a_i. Even more, it can be considered orthogonal also to the wave function of every other occupied state since, because of a well-known property of determinants, those components of $\partial a_i / \partial \lambda$ which contain the other orbitals do not influence the value of the determinant. Thus the matrix elements $< \partial \Psi_{HF} / \partial \lambda | H | \Psi_{HF} >$ and $< \Psi_{HF} | H | \partial \Psi_{HF} / \partial \lambda >$ are, according to a theorem of BRILLOUIN [4], equal to zero. Hence we have from (9)

$$\partial E_{HF} / \partial \lambda = < \Psi_{HF} | \partial H / \partial \lambda | \Psi_{HF} > , \tag{13}$$

which is the desired result.

If the correlation energy is defined as the difference of the exact (the relativistic corrections subtracted) energy and the HARTREE—FOCK one, from the comparison of (1) and (13) we get the dependence on λ of the correlation energy as follows

$$\begin{aligned} \partial E_{\text{corr}}/\partial\lambda = \partial \Delta E/\partial\lambda = \partial E/\partial\lambda - \partial E_{HF}/\partial\lambda = \\ = <\Psi\,|\,\partial H/\partial\lambda\,|\,\Psi> - <\Psi_{HF}\,|\,\partial H/\partial\lambda\,|\,\Psi_{HF}>. \end{aligned} \tag{14}$$

The Hamiltonian of the system under consideration is

$$H = \sum_{i=1}^{N} H_i + \sum_{i>j=1}^{N} \frac{e^2}{r_{ij}} + \sum_{k>l=1}^{\nu} \frac{Z_k Z_l e^2}{R_{kl}} \tag{15}$$

and

$$H_i = \frac{\hbar^2}{2m} \Delta_i - \sum_{k=1}^{\nu} \frac{Z_k e^2}{r_{ki}}, \tag{16}$$

where the nuclei are, according to the adiabatic approximation, considered to be at rest. r_{ij}, r_{ki} and R_{kl} denote the mutual distances between the electrons, the k-th nucleus and i-th electron, and the nuclei, respectively. Z_k is the atomic number of the k-th nucleus, m the electron mass and e the elementary charge.

If $\lambda = Z_k$, then

$$\partial H/\partial Z_k = -\sum_{i=1}^{N} e^2/r_{ki} + \sum_{l=1}^{\nu}{}' Z_l e^2/R_{kl} = -e^2 \sum_{i=1}^{N} 1/r_{ki} + \text{constant}, \tag{17}$$

where the prime means that there is no summation for $l = k$. In taking into account (17) we have from (14)

$$\begin{aligned} \partial E_{\text{corr}}/\partial Z_k = -e^2 \sum_{i=1}^{N} \{<\Psi\,|\,1/r_{ki}\,|\,\Psi> - <\Psi_{HF}\,|\,1/r_{ki}\,|\,\Psi_{HF}>\} = \\ = -e^2 \sum_{i=1}^{N} \{(\overline{r_{ki}^{-1}})_{\text{exact}} - (\overline{r_{ki}^{-1}})_{HF}\} \approx 0. \end{aligned} \tag{18}$$

This last expression is approximately equal to zero since, according to experience, the nucleus-electron distance calculated in the HARTREE—FOCK approximation, differs very little from the exact value. Hence with the aid of the HELLMANN—FEYNMAN theorem we have proved that the derivative of the correlation energy vanishes within an isoelectronic series, i.e. that the correlation energy is approximately constant. In Table I we collected the correlation energies as given by LÖWDIN [5] and FRÖMAN [6], for the isoelectronic series of helium. In the Table are collected the differences of the experimental and HARTREE—FOCK energies, the relativistic corrections calculated by FRÖMAN with

HARTREE—FOCK functions and the difference of these, i.e. the correlation energy. For the H^- ion it gives the difference between the very accurate calculations of HYLLERAAS and the HARTREE—FOCK value. The Table shows very clearly the constancy of the correlation energy within this isoelectronic series.

Table I

Correlation energies of the isoelectronic series of He. Energies are given in eV

	$E_{exp} - E_{HF}$	E_{rel}	E_{corr}
H^-			—1,08
He	$-1{,}145_2$	$-0{,}003_6$	—1,142
Li^+	—1,197	—0,015	—1,182
Be^{2+}	—1,250	—0,056	—1,194
Be^{3+} ...	—1,345	—0,149	—1,196
C^{4+}	—1.521	—0.324	—1.197

I would like to call attention to the great significance of this empirical theorem known for a long time past; relation (18) greatly simplifies molecular calculations in that the constancy, in a good approximation, of the correlation energy within an isoelectronic series can be taken as well founded also theoretically.

REFERENCES

1. H. HELLMANN, Einführung die Quantenchemie, F. Deuticke, Leipzig, 1937, p. 285; R. P. FEYNMAN, Phys. Rev., **56,** 340, 1939; T. BERLIN, J. Chem. Phys., **19,** 208, 1951.
2. R. E. STANTON, J. Chem. Phys., **36,** 1298, 1962.
3. E. U. CONDON and G. H. SHORTLEY, The Theory of Atomic Spectra, 1953, Cambridge University Press, Cambridge, pp. 30—34.
4. L. BRILLOUIN, Actualités sci. et ind. No. 71, 1933.
5. P. O. LÖWDIN, Advances in Chemical Physics, Interscience Publishers, Inc., New York, 1959. II. pp. 240.
6. A. FRÖMAN, Phys. Rev., **112,** 870, 1958.

CALCULATION OF SOME ATOMIC LOCALIZATION ENERGIES OF VARIOUS POLYCYCLIC HYDROCARBONS

By

G. Biczó, J. Ladik, F. Tüdős and T. A. Berezsnich

CENTRAL RESEARCH INSTITUTE FOR CHEMISTRY OF THE HUNGARIAN ACADEMY OF SCIENCES, BUDAPEST

(Received 12. III. 1963)

For the purpose of planned investigations of the kinetics of polymerization, we have calculated the atomic localization energies for some positions of the polycondensed aromatic hydrocarbons shown in Fig. 1.

Experimental investigations performed in our Laboratory have shown that not only that position of the hydrocarbon takes part in the reaction, to which the least atomic localization energy belongs. Therefore we have calculated this quantity also for some other positions of the molecule still reactive enough which were chosen partly on the basis of their free valences and partly on the strengths of chemical considerations. Only part of these data we could find in the literature.

The atomic localization energies (E_L) have been determined as the difference of the total π electron energy of the parent molecule (E_{π_P}) and the total electron energy of that radical (E_{π_R}) which we get if we omit the $2p_z$ orbital of a C atom from the interaction:

$$E_L = E_{\pi_P} - E_{\pi_R}. \tag{1}$$

The total π electron energies we have obtained in the usual way with the aid of the expression:

$$E_\pi = 2 \sum_i \varepsilon_i , \tag{2}$$

where ε_i denotes the energy of the i-th MO, and the summation is to be extended over all the bonding MO-s.

The individual ε_i-values we have calculated in the simple Hückel approximation neglecting overlap. The solution of the eigenvalue problem of the appropriate matrices has been obtained with the aid of the M3 electronic computer.

Since the results may be useful also in other investigations, in Table I we give all the MO energies, the total π electron energies and the localization energies for the calculated cases.

Table I

MO energies and total π electron energies of some polycyclic aromatic hydrocarbon radicals and the atomic localization energies of their parent hydrocarbons in β units

Radical	I/1* 1. $E\pi_p = 25{,}190$	I/3* $E\pi_p = 25{,}190$	I/6* $E\pi_p = 25{,}190$
	$\varepsilon_i = 0{,}000$	$\varepsilon_i = 0{,}000$	$\varepsilon_i = 0{,}000$
	0,596	0,651	0,606
	0,834	0,798	0,812
	1,166	1,126	1,133
	1,257	1,246	1,217
	1,335	1,515	1,475
	1,670	1,590	1,667
	2,162	2,054	2,060
	2,401	2,466	2,452
	$E\pi_R = 22{,}841$	$E\pi_R = 22{,}890$	$E\pi_R = 22{,}843$
	$E_L = 2{,}349$	$E_L = 2{,}300$	$E_L = 2{,}347$

II/5* 1. $E\pi_p = 25{,}275$	II/6* $E\pi_p = 25{,}275$	III/12* 1. $E\pi_p = 25{,}101$	IV/1* 1. $E\pi_p = 22{,}506$
$\varepsilon_i = 0{,}000$	$\varepsilon_i = 0{,}000$	$\varepsilon_i = 0{,}000$	$\varepsilon_i = 0{,}000$
0,684	0,684	0,653	0,636
0,775	0,816	1,000	0,893
1,130	1,000	1,000	1,213
1,286	1,286	1,246	1,329
1,341	1,317	1,361	1,590
1,787	1,819	1,749	1,991
1,970	1,970	2,131	2,463
2,476	2,509		
$E\pi_R = 22{,}897$	$E\pi_R = 22{,}798$	$E\pi_R = 23{,}000$	$E\pi_R = 20{,}231$
$E_L = 2{,}378$	$E_L = 2{,}477$	$E_L = 2{,}101$	$E_L = 2{,}275$

* The values of the atomic localization energies for these cases are given by KOUTECKÝ et al [4], but they do not give the individual MO energies of the radicals.

1. See ref. [1].

V/8* 2. $E\pi_p = 28{,}222$	V/10* $E\pi_p = 28{,}222$	VI/5 3. $E\pi_p = 34{,}030$	VI/8 $E\pi_p = 34{,}030$
$\varepsilon_i = 0{,}000$	$\varepsilon_i = 0{,}000$	$\varepsilon_i = 0{,}000$	$\varepsilon_i = 0{,}000$
0,605	0,682	0,664	0,500
1,000	0,811	1,000	1,000
1,000	1,000	1,000	1,000
1,000	1,177	1,000	1,000
1,353	1,260	1,000	1,000
1,572	1,652	1,310	1,364
1,831	1,775	1,522	1,526
2,126	2,136	1,750	1,695
2,542	2,541	2,045	2,030
		2,155	2,191
		2,576	2,601
$E\pi_R = 26{,}057$	$E\pi_R = 26{,}072$	$E\pi_R = 32{,}045$	$E\pi_R = 31{,}814$
$E_L = 2{,}165$	$E_L = 2{,}150$	$E_L = 1{,}985$	$E_L = 2{,}216$

VI/10 $E\pi_p = 34{,}030$	VII/1* 2. $E\pi_p = 31{,}253$	VII/3* $E\pi_p = 31{,}253$	VII/6* $E\pi_p = 31{,}253$
$\varepsilon_i = 0{,}000$	$\varepsilon_i = 0{,}000$	$\varepsilon_i = 0{,}000$	$\varepsilon_i = 0{,}000$
0,556	0,610	0,575	0,621
0,772	0,814	0,782	0,845
1,000	0,898	1,000	1,000
1,000	1,191	1,118	1,130
1,177	1,226	1,210	1,228
1,352	1,414	1,500	1,464
1,532	1,705	1,643	1,741
1,660	1,933	1,966	1,824
2,101	2,199	2,179	2,248
2,157	2,600	2,604	2,562
2,591			
$E\pi_R = 31{,}796$	$E\pi_R = 29{,}178$	$E\pi_R = 29{,}155$	$E\pi_R = 29{,}325$
$E_L = 2{,}234$	$E_L = 2{,}075$	$E_L = 2{,}098$	$E_L = 1{,}928$

* See footnote on page 174.
2. See ref. [2].
3. See ref. [3].

VIII/1* 1. $E\pi_p = 28{,}245$	VIII/3* $E\pi_p = 28{,}245$	IX/2 1. $E\pi_p = 31{,}452$	IX/3 $E\pi_p = 31{,}452$
$\varepsilon_i = 0{,}000$	$\varepsilon_i = 0{,}000$	$\varepsilon_i = 0{,}000$	$\varepsilon_i = 0{,}000$
0,584	0,651	0,502	0,633
1,000	1,000	0,824	0,719
1,000	1,000	1,000	1,000
1,000	1,000	1,100	1,079
1,384	1,343	1,334	1,345
1,592	1,554	1,414	1,414
1,770	1,861	1,603	1,611
2,153	2,086	2,017	2,072
2,538	2,558	2,157	2,104
		2,604	2,607
$E\pi_R = 26{,}042$	$E\pi_R = 26{,}106$	$E\pi_R = 29{,}115$	$E\pi_R = 29{,}166$
$E_L = 2{,}203$	$E_L = 21{,}39$	$E_L = 2{,}337$	$E_L = 2{,}286$

IX/4 $E\pi_p = 31{,}452$	IX/6 $E\pi_p = 31{,}452$	X $E\pi_p = 30{,}839$	X/7 $E\pi_p = 30{,}839$
$\varepsilon_i = 0{,}000$	$\varepsilon_i = 0{,}000$	$\varepsilon_i = 0{,}405$	$\varepsilon_i = 0{,}000$
0,662	0,592	0,705	0,657
0,737	0,842	0,823	0,805
1,000	1,000	1,095	1,000
1,102	1,000	1,163	1,114
1,307	1,265	1,358	1,220
1,414	1,527	1,496	1,481
1,608	1,602	1,592	1,518
2,028	1,979	1,969	1,968
2,136	2,181	2,290	2,172
2,614	2,602	2,525	2,471
$E\pi_R = 29{,}218$	$E\pi_R = 29{,}179$	$E\pi_R = -$	$E\pi_R = 28{,}819$
$E_L = 2{,}234$	$E_L = 2{,}273$	$E_L = -$	$E_L = 2{,}020$

* See footnote on page 174.
1. See ref. [1].

X/12	XI/3	XI/5	XI/6
$E\pi_p = 30{,}839$	$E\pi_p = 28{,}336$	$E\pi_p = 28{,}336$	$E\pi_p = 28{,}336$
$\varepsilon_i = 0{,}000$	$\varepsilon_i = 0{,}000$	$\varepsilon_i = 0{,}000$	$\varepsilon_i = 0{,}000$
0,598	0,715	0,651	0,684
0,618	0,760	1,000	0,748
0,912	1,000	1,000	1,000
1,149	1,183	1,000	1,286
1,276	1,346	1,343	1,336
1,470	1,499	1,554	1,414
1,618	1,887	1,861	1,970
1,842	2,104	2,086	2,039
2,073	2,544	2,558	2,549
2,542			
$E\pi_R = 28{,}015$	$E\pi_R = 26{,}072$	$E\pi_R = 26{,}106$	$E\pi_R = 26{,}052$
$E_L = 2{,}824$	$E_L = 2{,}264$	$E_L = 2{,}230$	$E_L = 2{,}284$

XII	XII/3	XII/6	XII/7
$E\pi_p = 34{,}065$	$E\pi_p = 34{,}065$	$E\pi_p = 34{,}065$	$E\pi_p = 34{,}065$
$\varepsilon_i = 0{,}422$	$\varepsilon_i = 0{,}000$	$\varepsilon_i = 0{,}000$	$\varepsilon_i = 0{,}000$
0,742	0,716	0,502	0,666
0,821	0,788	0,748	0,749
1,000	1,000	0,905	0,823
1,128	1,000	1,125	1,102
1,232	1,173	1,227	1,217
1,398	1,293	1,379	1,317
1,575	1,499	1,414	1,490
1,756	1,748	1,723	1,748
2,090	2,034	2,034	1,977
2,245	2,201	2,230	2,245
2,623	2,556	2,573	2,582
$E\pi_R = -$	$E\pi_R = 32{,}017$	$E\pi_R = 31{,}719$	$E\pi_R = 31{,}831$
$E_L = -$	$E_L = 2{,}048$	$E_L = 2{,}346$	$E_L = 2{,}234$

XII/8 $E\pi_p = 34{,}065$	XII/10 $E\pi_p = 34{,}065$	XIII/1 [3] $E\pi_p = 33{,}954$	XIII/4'' $E\pi_p = 33{,}954$
$\varepsilon_i = 0{,}000$	$\varepsilon_i = 0{,}000$	$\varepsilon_i = 0{,}000$	$\varepsilon_i = 0{,}000$
0,616	0,598	0,454	0,469
0,783	0,742	0,740	0,803
1,000	1,000	1,000	1 000
1,000	1,000	1,000	1,000
1,183	1,166	1,236	1,221
1,271	1,378	1,351	1,290
1,575	1,512	1,579	1,569
1,702	1,662	1,626	1,755
1,975	2,064	2,000	1,922
2,233	2,200	2,301	2,247
2,595	2,585	2,542	2,588
$E\pi_R = 31{,}863$	$E\pi_R = 31{,}816$	$E\pi_R = 31{,}658$	$E\pi_R = 31{,}726$
$E_L = 2{,}202$	$E_L = 2{,}249$	$E_L = 2{,}296$	$E_L = 2{,}228$

XIII/5 $E\pi_p = 33{,}954$	XIII/6 $E\pi_p = 33{,}954$
$\varepsilon_i = 0{,}000$	$\varepsilon_i = 0{,}000$
0,627	0,562
1,000	0,682
1,000	1,000
1,000	1,000
1,000	1,209
1,319	1,384
1,528	1,544
1,751	1,680
2,000	1,947
2,223	2,306
2,554	2,555
$E\pi_R = 32{,}005$	$E\pi_R = 31{,}739$
$E_L = 1{,}949$	$E_L = 2{,}215$

3. See ref. [3].

In the Table in the row headed "radical" the Roman numbers denote the parent molecules according to Fig. 1 and the Arabic numbers show, — using again the same numbering as in Fig. 1 — the position of the C atom which is omitted from the interaction.

I. Chrysene

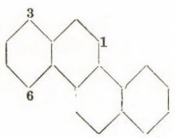

V. 3,4-benzpyrene

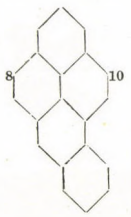

II. Triphenylene

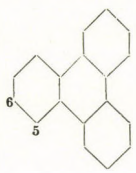

VI. 1,2,3,4-dibenzpyrene

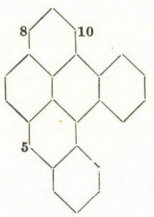

III. 1,2-benzanthracene

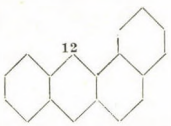

VII. Anthanthrene

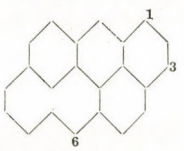

IV. Pyrene

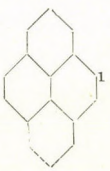

VIII. Perylene

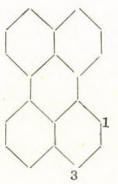

Fig. 1

IX. 1,12-benzperylene

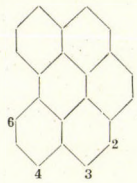

XII. 1,2,4,5-dibenzpyrene

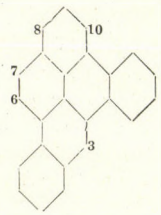

X. 3,4-benztetraphene

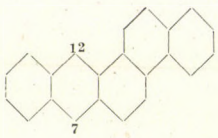

XIII. 3,4;9,10-dibenzpyrene

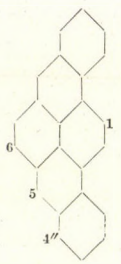

XI. 1,2-benzpyrene

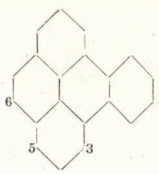

Fig. 1 (continued)

Acknowledgement. We should like to express our gratitude to Mr. J. Szelezsán, and Mr. J. Balatoni for programming the matrix eigenvalue problem for the M3 computer of the Computing Centre of the Hungarian Academy of Sciences.

REFERENCES

1. C. A. Coulson and R. H. Daudel, Dictionary of Molecular Constants, II, 1955.
2. B. Pullman and J. Baudet, Compt. Rend., **237,** 986, 1953.
3. O. Chalvet and J. Peltier, Compt. Rend., **240,** 1709, 1955.
4. J. Kouteczký, R. Zahradnik and J. Cižek, Trans. Faraday Soc., **57,** 169, 1961.

DIE GRÜNEISENSCHE KONSTANTE DES METALLISCHEN Cu-S

Von

I. BIRÓ

PHYSIKALISCHES INSTITUT DER UNIVERSITÄT FÜR TECHNISCHE WISSENSCHAFTEN, BUDAPEST*

(Eingegangen: 20. III. 1963)

In der vorliegenden Arbeit wird die GRÜNEISENsche Konstante für das metallische Kupfer sowie deren Druckabhängigkeit am absoluten Nullpunkt der Temperatur berechnet und zwar auf Grund des von GOMBÁS ausgearbeiteten Metallmodells [1] auf ganz ähnliche Weise, wie die vom Verfasser durchgeführte ähnliche Berechnung für das metallische Ag [2]. Da die Berechnungen denen der zitierten Arbeit weitgehend parallel laufen, können wir uns auf diese beziehen.

Der Ausdruck für die Gitterenergie [3] des metallischen Cu kann in der Umgebung der Gleichgewichtslage als Funktion des Radius R der Elementarkugel folgendermassen dargestellt werden:

$$U = -\frac{A}{R} + \frac{B}{R^n} + C\,, \tag{1}$$

wo die Konstanten A, B und C die folgenden Werte haben:

$$\begin{aligned} A &= \quad 1{,}3456\, e^2\,, \\ B &= \quad 28{,}5498\, e^2\, a_0^5\,, \\ C &= -0{,}04460\, \frac{e^2}{a_0}\,. \end{aligned} \tag{2}$$

e ist der Betrag der Elektronenladung und a_0 der kleinste Bohrsche Wasserstoffradius. Der Exponent der Abstossung n, hat hier den Wert

$$n = 6\,. \tag{3}$$

n ist also verglichen mit Ag ($n = 11$) hier wesentlich kleiner.

Für γ als Funktion des Druckes P am absoluten Nullpunkt der Tempera-

* Hochschulartiges Technikum für Fernmeldetechnik und Meßlere.

tur wurde in [1] folgender Ausdruck abgeleitet:

$$\gamma = \frac{1}{6(n-1)} \left\{ (n+3)(n+2) - 12 - \frac{4}{3} \left[(n+3)(n+2) - 3(n-1) - 12 \right] \varkappa_0 P \right\} \tag{4}$$

$$(\text{wenn } \varkappa_0 P \ll 1),$$

wo $\varkappa_0$ die Kompressibilität am absoluten Nullpunkt der Temperatur beim Druck $P = 0$ bedeutet; es ist also

$$\frac{1}{\varkappa_0} = \frac{1}{12\pi R_0} \left(\frac{d^2 U}{dR^2} \right)_{R=R_0}. \tag{5}$$

R_0 bedeutet den Radius der Elementarkugel in der Gleichgewichtslage. Mit (1) ergibt sich aus (5)

$$\varkappa_0 = 19{,}90 \frac{a_0^4}{e^2} = 0{,}0675 \cdot 10^{-12} \text{ cm}^2/\text{dyn} \tag{6}$$

und mit $n = 6$ aus (4)

$$\gamma = 2 - 2\varkappa_0 P,$$

wo für $\varkappa_0$ der Wert (6) einzusetzen ist.

Für $P = 0$ erhält man den Wert

$$\gamma = 2,$$

der mit dem SLATERschen halbempirischen Wert [4] $\gamma = 1{,}9$ gut übereinstimmt.

LITERATUR

1. P. GOMBÁS, Die statistische Theorie des Atoms und ihre Anwendungen, Springer Verl. Wien, 1949; Handbuch d. Physik, 36/II, S. 108. Springer, Berlin—Göttingen—Heidelberg, 1956; Ann. d. Phys., (6), **17**, 70, 1951; Zs. f. Naturforsch., **15***a*, 531, 1960.
2. I. BIRÓ, Acta Phys. Hung., **13**, 99, 1961.
3. P. GOMBÁS, Acta Phys. Hung., **1**, 301, 1952.
4. J. C. SLATER, Introduction to Chemical Physics, S. 451; Mc. Graw-Hill Book Co., Inc., New-York, London, 1939.

RECENSIONES

MORTON HAMMERMEASH,

Group Theory and its Applications to Physical Problems,

XV + 509, Pergamon Press, London—Paris, 1962.

Obwohl in neuerer Zeit dieses Gebiet von mehreren Autoren in Monographien dargestellt wurde, ist das Erscheinen dieses Werkes besonders zu begrüssen, erstens wegen seiner klaren Darstellungsweise und zweitens aus dem Grunde, dass der Verfasser nur sehr wenige Kenntnisse vom Leser voraussetzt und sich die Mühe nahm den Stoff in einer Weise darzustellen der den Leser in dieses Gebiet einführt und ihn nach Durcharbeitung der wichtigsten Methoden mit den aktuellen physikalischen Anwendungen bekannt macht.

Die ersten fünf Kapitel behandeln allgemeine Prinzipien der Gruppentheorie und die Representation von Gruppen. Die weiteren sieben Kapitel bringen hauptsächlich Anwendungen von gruppentheoretischen Methoden auf physikalische Probleme. Unter anderen ist die Methode von YOUNG sowie die HUNDsche Methode ausführlich diskutiert, dem folgen die kontinuierlichen Gruppen von LIE. Nach einigen Anwendungen auf Kristallprobleme werden im Kapitel 10 die linearen Gruppen im n-dimensionalen Raum und die irreduciblen Tensoren behandelt. Dem folgen Anwendungen auf Atom- und Kernprobleme und schliesslich einige Representationen von endlichen Gruppen.

Das Buch ist sowohl dem Studierenden als auch dem auf diesem Gebiet tätigen Forscher wärmstens zu empfehlen.

P. GOMBÁS

Festkörperphysik

Redakteure Prof. Dr. P. GÖRLICH und Dr. G. SZIGETI, 532 Seiten, Akademie Verlag, Berlin, 1961. Gebunden DM 92.

Der Band vermittelt den Stoff der Vorträge, die auf der gemeinsamen Konferenz der Eötvös Loránd Fizikai Társulat und der Physikalischen Gesellschaft in der Deutschen Demokratischen Republik vom 14.—20. September in Balatonfüred gehalten wurden.

Die Vortragenden der Konferenz waren Mitglieder der beiden Physikalischen Gesellschaften sowie einige Gäste aus der Sowjetunion, der Tschechoslowakei, Bulgarien, Polen, Frankreich und der Deutschen Bundesrepublik.

Die Redakteure des Bandes teilten den Stoff nach Themenkreisen in sechs Teile. In dieser Einteilung enthält der Band 55 Mitteilungen.

Die Themen der 22 Mitteilungen der ersten Gruppe sind: Kristallwachstum, Rekristallisation, Kristallstruktur, Ordnungsvorgänge, Oberflächenzustände. Mit den Fragen des Kristallwachstums und der Kristallisation beschäftigten sich die folgenden Vortragenden: Z. GYULAI bespricht das Wachstum der Alkalihaloide, T. A. HOFFMANN eine Theorie der Kristallkeimbildung; A. SCHNEIDER misst das orientierte Kristallwachstum von n-Alkylaminhydrochloriden, H. POSER die Kondensation des Germaniums aus der Dampfphase, J. PROHÁSZKA, A. HORVÁTH und TH. MILLNER die Wachstumsgeschwindigkeit der Kristallite während der sekundären Rekristallisation von Wolframdrähten. L. BARTHA, J. PROHÁSZKA und T. MILLNER untersuchen den Einfluss von Fremdsubstanzen auf die Rekristallisation der Metalle.

Die Wirkung der Neutronenbestrahlung untersuchen H. RZEWUSKI und B. BURAS an Halbleitern, O. HAUSER und V. KÖHLER an CdS-Kristallen. L. I. PÁL und G. NÉMETH besprechen eine Theorie der durch energiereiche Teilchen verursachten Gitterfehler.

E. NAGY gibt ein Referat über den Einfluss der Gitterfehler auf die Transporteigenschaften der Metalle und Legierungen. E. RÓZSA untersucht die Wanderung der

Leerstellen in Ge und J. AULEYTNER bestimmt die Winkelverteilung der Mosaikblöcke und die Versetzungsdichte in Ge-Einkristallen.

Mit der Frage der Ordnungsvorgänge beschäftigen sich E. NAGY, I. NAGY und J. TÓTH an Cu_3Au, weiterhin L. PÁL und T. TARNÓCZI an Eisen-Aluminiumlegierungen.

I. SZÉP und M. NÉMETH referieren über die Oberflächeneigenschaften des Germaniums, H. H. PLAGEMANN und H. J. SCHNABEL über den Einfluss der umgebenden Gasphase auf die Kenndaten von p—n—p Legierungstransistoren aus Germanium. L. ERNST weist die Adsorption von Sauerstoff an Wolfram mit Hilfe eines Feldemissionsmikroskops nach.

G. E. R. SCHULZE berichtet über die Stapelfehler in LAVES-Phasen. P. SZABÓ behandelt die röntgenographische Nachweisbarkeit der Unordnung feinkristalliner Kohlenstoffe. G. SCHULTZ gibt eine Methode zur Messung der Absorption von Kristallpulvern. GY. TURCSÁNYI untersucht die Spaltbarkeit und Deformation der NaCl-Kristalle, K. ÁRKOSI und Z. MORLIN befassen sich mit der Bildung von Gleitquellen an Alkalihaloiden.

Die sieben Artikel der zweiten Gruppe beschäftigen sich mit den Wirkungen der Störstellen und mit der Reinigung. Der zusammenfassende Artikel von A. MURIN behandelt die Natur der chemischen Fehlstellen in Ionenkristallen. J. NEUGEBAUER, L. IMRE und TH. MILLNER untersuchen die verschiedenen Entstehungsarten des β-Wolframs und seine von Fremdatomen verursachten Eigenschaften. TH. MILLNER, J. PROHÁSZKA und J. NEUGEBAUER diskutieren die Rolle der Verunreinigungen in der sekundären Rekristallisation des Wolframs. Ü. RAYNER behandelt eine Möglichkeit zur Bestimmung der Dotierungs-Randkonzentration in der Basis eines Drifttransistors aus einfachen Strom-Spannungsmessungen. P. SCHMIDT ermittelt den Störstellenzustand von Ge-Einkristallen aus der Temperaturabhängigkeit der Leitfähigkeit. I. SZÉP, G. PÁSZTOR und J. PFEIFER messen die Verteilung der Störstellen in Ge mit Hilfe von Kapazitätsmessungen.

H. E. LONGO und K. SCHLAUBITZ beschreiben eine Zonenschmelzapparatur für Wolfram, wobei das Schmelzen durch Elektronenbeschuss geschieht.

Die acht Mitteilungen der dritten Gruppe befassen sich mit optischen und lichtelektrischen Untersuchungen und mit Rauscheffekten. GY. T. BAUER, GY. GERGELY und J. ÁDÁM messen die Absorptionskante von einigen mikrokristallinen Leuchtstoffen. J. BOROS schreibt über das Termschema von NaCl. E. GRILLOT befasst sich mit den durch Excitonen bedingten optischen Eigenschaften in Halbleitern. R. ANDREJTSCHIN berichtet über eine Abart der photovoltaischen Effekte die er zusammen mit G. NADJAKOW gefunden hat. P. GÖRLICH und H. HORA untersuchen die Polarisationsabhängigkeit an zusammengesetzten Photokathoden. I. TARJÁN, R. VOSZKA und A. SOMLÓ teilen einige neue Ergebnisse über die innere Photoleitfähigkeit röntgenbestrahlter NaCl Kristalle mit. Das Thema von F. FISCHER und I. P. VALKÓ ist der Zusammenhang zwischen der Porosität der Kathodenoberfläche und dem Flickerrauschen. O. LITZMAN behandelt das Frequenzspektrum und die thermodynamischen Funktionen der Kristallgitter mit Fehlstellen.

Mit den Lumineszenzerscheinungen beschäftigen sich zehn Abhandlungen. Die Hälfte der Mitteilungen berichtet über Messergebnisse an ZnS. L. BALÁZS, L. PUSKÁS, J. WEISZBURG und J. SCHANDA referieren über den Einfluss der chemischen Behandlung auf die physikalischen Eigenschaften des elektrolumineszenten ZnS. Z. BODÓ, J. WEISZBURG und J. SCHANDA berichten über neuere Messergebnisse an elektrolumineszentem ZnS. H. ORTMANN referiert über die Grün—Blau-Emission von Zns—Cu-Luminophoren. G. WENDEL berichtet über die Elektrolumineszenz des Cu-aktivierten ZnS. GY. GERGELY und I. HANGOS bringen Beiträge zur Photolyse von ZnS-Phosphoren. I. SOUDEK macht Anmerkungen zum Modell des Lumineszenzvorganges in anorganischen Kristallen.

Mit Lumineszenzerscheinungen an anorganischen Stoffen befassten sich W. THIELEMANN, der einige durch Influenz bedingte Effekte untersuchte, und H. WITZMANN, G. HERZOG und E. GEGNER, die das Emissionsverhalten ceraktivierter Strontiumcarbonatmischphosphore und des Strontiumcerates gemessen haben. Mit der Lumineszenz der organischen Stoffe beschäftigten sich L. HERFORTH und H. HILBIG. Sie haben die Einwirkung von UV-Licht und β-Strahlung auf das Lumineszenzvermögen organischer Substanzen in Lösung und in fester Form untersucht.

Vier Vorträge befassten sich mit den thermischen Eigenschaften der Festkörper. B. FOGARASSY und G. NÉMETH teilen eine Methode zur Berechnung der spezifischen Wärme und Wärmeausdehnung fester Körper mit. W. HEINZE zeigte, dass das Bändermodell der Oxydkathode in der Lage ist, die bei derartigen Kathoden auftretenden Elektronemissionserscheinungen befriedigend zu erklären. E. KRANZ misst thermoelektrische Erscheinungen im Überlappungsgrenzgebiet aufgedampfter dünner Schichten. O. LUCKE behandelt die metallische Modifikation der Materie unter sehr hohem Druck. Er weist darauf hin, dass man solchen Untersuchungen Erkenntnisse über den Aufbau der Himmels-

körper erwarten kann, da die Materie in ihrem Innern in Metallmodifikation ist.

In der letzten Gruppe sind die vierzehn Artikel zusammengefasst, die sich mit elektrischer Leitfähigkeit, mit der Katalyse und mit magnetischen und ferroelektrischen Eigenschaften befassen. H. BERGER bringt Beiträge zum Ausheilen beim Aufdampfen entstandener Gitterstörungen in CdS-Schichten mit Hilfe der Dunkelleitfähigkeit. Die zusammenfassende Abhandlung von K. W. BÖER behandelt die plasmaähnlichen Raumladungserscheinungen, die bei hohen elektrischen Feldstärken in Halbleitern auftreten. H. EIGLER untersucht die Umverteilung der Elektronendichte in CdS- und Ge-Einkristallen infolge der Einwirkung äusserer elektrischer Felder. Das Thema von CH. KLEINT sind die elektrischen und optischen Eigenschaften von Indiumsulfid-Einkristallen. F. THOM misst den Restwiderstand an plastisch verformtem Kupfer. A. ZAREBA untersucht die Einwirkung der Elektronenbestrahlung auf die elektrische Leitfähigkeit des *n*—Ge. H. ROTHER schreibt über die Erscheinungen, die bei hohen Feldstärken in Halbleitern auftreten. W. LUDWIG führt Impedanzmessungen an Selen durch. M. MÁTYÁS befasst sich mit der magnetischen Suszeptibilität von Halbleitern. H. E. MÜSER untersucht die Umpolarisierung von ferroelektrischen Seignettesalzkristallen. H. WITZMANN, H. ANDERSON und K. KINZNER berichten über die katalytischen Eigenschaften des Magnesiumoxyds und seiner Mischphasen. In den letzten drei Artikeln befassen sich J. S. ZHELUDJEW mit Schwingungen der dielektrischen Pendel, V. MEYER mit Festigkeitsmessungen an Cu-Whiskern und L. M. BELJAJEW mit Kristallzüchtung.

Die Mitteilungen sind, abgesehen von zwei englischen, zwei russischen und einer französischen Mitteilung, deutschsprachig.

Die sorgfältige Ausstattung des Bandes entspricht dem guten Ruf der deutschen Verlage.

J. BOROS

J. FAGOT and PH. MAGUE:

Frequency Modulation Theory

Pergamon Press, Oxford, London, New York, Paris, 1961

The authors aim at the presentation, in one book, of problems related to frequency modulated radio transmission. Accordingly the topics treated range from the theory of frequency modulation to the techniques of radio transmission.

The book is divided into five chapters. The first deals with the propagation properties of metre-, decimetre-, centimetre-waves both in optical and over-horizon transmission. The second chapter presents the basic concepts of frequency modulated systems and special emphasis is laid on the problem of signal-to-noise ratio. The third chapter treats different kinds of distortions of frequency modulated signals (e.g. those generated by mismatched waveguides).

After the theoretical foundations, given by the first three chapters, the fourth one treats the transmission properties of multichannel telephone and television signals from the points of view of signal and noise levels and distortion. The last chapter gives a general survey of radio relay techniques.

It is apparent that the authors have tried to give not only a theoretical foundation of the subject but also practically useful formulae and numerical data for the use of design engineers. The book is completed by numerous figures and diagrams.

P. RÓNA

W. B. THOMPSON:

An Introduction to Plasma Physics

Pergamon Press, Oxford, London, New York, Paris, 1962

Interest in plasma physics and its application to the problems of thermonuclear energy production has grown rapidly during the last few years, with the result that many books on this subject have been published recently. As plasma physics embraces an extremely wide field the subject matter of books dealing with it is extremely varied and depends largely on the predilections of the author.

THOMPSON's book is one of the best books on plasma physics; in spite of its being rather short, it contains a concise introduction into the modern theory of the dynamics of completely ionized gases. This book is based on a series of lectures given by the author

at the Atomic Energy Research Establishment at Harwell, the Clarendon Laboratory at Oxford and the Theoretical Physics Department of Imperial College in London.

This book is designed primarily for physics students in their final years and to physicists and engineers working on plasma physics and fusion problems. Experimental results are dealt with only briefly, the emphasis being on a thorough description of the basic theoretical features of the plasma. A knowledge of such a book as "Lehrbuch der theoretischen Physik" by Joos would be quite sufficient to enable the reader to understand this book. The selection of the literature at the end of each chapter is excellent.

The book contains eight chapters and an appendix containing some important formulae and physical constants. The first chapter outlines the subject of plasma physics, the range of its problems and its applications. The second and third deal with the description of the most important properties of plasma, their interrelations and the experimental realization of the plasma state. The three following chapters contain the phenomenological, magnetohydrodynamical theory of plasma. After a short but thorough discussion of the basic equations of magnetohydrodynamics, some of their applications to simple problems are presented followed by an elegant treatment of magnetohydrodynamical waves. The important problem of the stability of the plasma is dealt with in appropriate detail. The subject of Chapter 7 is the motion of charged particles in electromagnetic fields and an elementary treatment of the dielectric properties of the plasma. The last and most extensive chapter is a very thorough introduction into the kinetic theory of the plasma. The author briefly, but very clearly, summarizes the different methods of statistical description of the plasma and their most important applications. It is, however, a pity that the Green-function method is not included.

The treatment by the author is always clear and the presentation of the book is exemplary.

J. Szabó

Kiadásért felel az Akadémiai Kiadó igazgatója Műszaki szerkesztő: Farkas Sándor

A kézirat nyomdába érkezett: 1963. VI. 20. — Terjedelem: 9,75 (A/5) ív, 32 ábra

63.57340 Akadémiai Nyomda, Budapest — Felelős vezető: Bernát György

The *Acta Physica* publish papers on physics, in English, German, French and Russian.
The *Acta Physica* appear in parts of varying size, making up volumes.
Manuscripts should be addressed to:

Acta Physica, Budapest 502, Postafiók 24.

Correspondence with the editors and publishers should be sent to the same address.
The rate of subscription to the *Acta Physica* is 110 forints a volume. Orders may be placed with "Kultúra" Foreign Trade Company for Books and Newspapers (Budapest I., Fő u. 32. Account No. 43-790-057-181) or with representatives abroad.

Les *Acta Physica* paraissent en français, allemand, anglais et russe et publient des travaux du domaine de la physique.
Les *Acta Physica* sont publiés sous forme de fascicules qui seront réunis en volumes.
On est prié d'envoyer les manuscrits destinés à la rédaction à l'adresse suivante:

Acta Physica, Budapest 502, Postafiók 24.

Toute correspondance doit être envoyée à cette même adresse.
Le prix de l'abonnement est de 110 forints par volume.
On peut s'abonner à l'Entreprise du Commerce Extérieur de Livres et Journaux «Kultúra» (Budapest I., Fő u. 32. — Compte-courant No. 43-790-057-181) ou à l'étranger chez tous les représentants ou dépositaires.

«*Acta Physica*» публикуют трактаты из област физических наук на русском немецком, английском и французском языках.
«*Acta Physica*» выходят отдельными выпусками разного объема. Несколько выпусков составляют один том.
Предназначенные для публикации рукописи следует направлять по адресу:

Acta Physica, Budapest 502, Postafiók 24.

По этому же адресу направлять всякую корреспонденцию для реадекции и администрации.
Подписная цена «*Acta Physica*» — 110 форинтов за том. Заказы принимает предприятие по внешней торговле книг и газет «*Kultúra*» (Budapest I., Fő u. 32. Текущий счет: № 43-790-057-181) или его заграничные представительства и уполномоченные.

28,— Ft

INDEX

COMMUNICATIONES BREVES

RECENSIONES

Acta Phys. Hung. Tom. XVI. Fasc. 2. Budapest, 30. IX. 1963.

Index: 26.022

ACTA PHYSICA

ACADEMIAE SCIENTIARUM HUNGARICAE

TOMUS XVI FASCICULUS 3

AKADÉMIAI KIADÓ, BUDAPEST
1963

ACTA PHYS. HUNG.

ACTA PHYSICA

A MAGYAR TUDOMÁNYOS AKADÉMIA FIZIKAI KÖZLEMÉNYEI

SZERKESZTŐSÉG ÉS KIADÓHIVATAL: BUDAPEST V., ALKOTMÁNY UTCA 21.

Az *Acta Physica* német, angol, francia és orosz nyelven közöl értekezéseket a fizika tárgyköréből.

Az *Acta Physica* változó terjedelmű füzetekben jelenik meg: több füzet alkot egy kötetet.

A közlésre szánt kéziratok a következő címre küldendők:

Acta Physica, Budapest 502, Postafiók 24.

Ugyanerre a címre küldendő minden szerkesztőségi és kiadóhivatali levelezés.

Az *Acta Physica* előfizetési ára kötetenként belföldre 80 forint, külföldre 110 forint. Megrendelhető a belföld számára az Akadémiai Kiadónál (Budapest V., Alkotmány utca 21. Bankszámla 05-915-111-46), a külföld számára pedig a „Kultúra" Könyv- és Hírlap Külkereskedelmi Vállalatnál (Budapest I., Fő u. 32. Bankszámla 43-790-057-181 sz.) vagy annak külföldi képviseleteinél és bizományosainál.

Die *Acta Physica* veröffentlichen Abhandlungen aus dem Bereiche der Physik in deutscher, englischer, französischer und russischer Sprache.

Die *Acta Physica* erscheinen in Heften wechselnden Umfanges. Mehrere Hefte bilden einen Band.

Die zur Veröffentlichung bestimmten Manuskripte sind an folgende Adresse zu richten:

Acta Physica, Budapest 502, Postafiók 24.

An die gleiche Anschrift ist auch jede für die Redaktion und den Verlag bestimmte Korrespondenz zu senden.

Abonnementspreis pro Band: 110 Forint. Bestellbar bei dem Buch- und Zeitungs-Aussenhandels-Unternehmen »Kultúra« (Budapest I., Fő u. 32. Bankkonto Nr. 43-790-057-181) oder bei seinen Auslandsvertretungen und Kommissionären.

THEORETICAL DETERMINATION OF THE INTERACTION ENERGY OF NOBLE GAS ATOMS II.

INTERACTION OF NOBLE GAS ATOMS OF DIFFERENT ATOMIC NUMBERS. INTERPOLATION PROBLEMS

By

R. GÁSPÁR

INSTITUTE FOR THEORETICAL PHYSICS, KOSSUTH LAJOS UNIVERSITY, DEBRECEN

and

RESEARCH GROUP FOR THEORETICAL PHYSICS, HUNGARIAN ACADEMY OF SCIENCES, BUDAPEST

(Presented by A. Kónya — Received 28. I. 1963)

A method described in a previous paper is generalized to determine the interaction energy of unlike noble gas atoms. The method facilitates the development of an interpolation procedure, by means of which the interaction energy of unlike noble gas atoms can be determined from the experimental interaction energy of like noble gas atoms. The treatment of the He—A system is followed by a detailed analysis of the He—He interaction potential energy.

§ 1. Introduction

The collision of neutral atoms and molecules has been the subject of remarkable experimental investigations for a considerable time [1]. From experiments on high energy atomic and molecular beams the interaction potential energy of atoms and molecules can be determined. Our previous paper was concerned with the theoretical determination of the collision potential energy of noble gas atoms [2].

In the calculations we used the statistical method, most suitable for use with many-electron systems. First, it was shown that in a very interesting way the collision energy of identical noble gas atoms is obtained in the Thomas—Fermi approximation of the statistical theory of the atom in a special coordinate system as a universal function (independent of atomic number). Plotting the experimental curves in this coordinate system it was found that in the regions belonging to small and intermediate internuclear distance values the shape of the curves was to a good approximation universal within an accuracy permitted by the mean error of the measurements. Thus, in the region where electrostatic forces predominate the theoretical conclusions are intrinsically confirmed by experiment. Second, it was shown that the formulae of the statistical method evaluated with the density determined to an appropriate accuracy, correctly reflect the experimental curves also for larger internuclear distances.

In the present paper we wish to investigate on the one hand whether our theory renders correctly the interaction energy curves of noble gas atoms of different atomic number. On the other hand we wish to deal with interpolation problems.

§ 2. Calculation of interaction energy

To determine the interaction energy we have used the expression

$$U_{12}(\delta) = (-\alpha_1 + \beta_1)\,\varrho_2(\delta) + \beta_2\,\varrho_1(\delta)\,, \tag{1}$$

where ϱ_1 and ϱ_2 are the densities of the neutral noble gas atoms interacting with each other and

$$\alpha_i = 4\pi e \int_0^\infty \gamma_i(r)\, r^2\, dr \tag{2}$$

and

$$\beta_i = \frac{20\pi}{3}\,\varkappa_k \int_0^\infty [\varrho_i(r)]^{2/3}\, r^2\, dr\,. \tag{3}$$

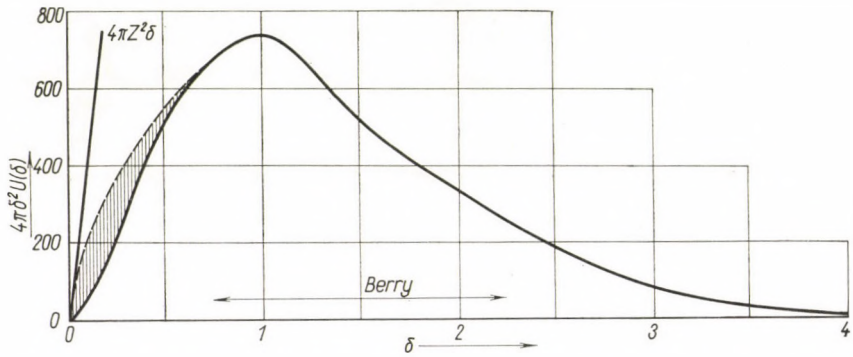

Fig. 1. Potential energy of the argon—argon interaction. The abscissa is given in a_0, and the ordinate in e^2a_0 atomic units

e is the elementary charge and $\varkappa_k = (3/10)\,(3\pi^2)^{2/3}\,e^2a_0$; a_0 is the first Bohr hydrogen radius. The energy expression (1) is asymmetric with respect to the density distributions of the two atoms, which would seem to be rather peculiar, had thorough investigations of the problem not shown that the effect of this on the interaction energy is negligible [3]. However, to determine the interaction energy, (1) can be easily replaced by a symmetric expression. Let us commute in (1) the indices 1 and 2 and add the expression so obtained, also giving $U_{12}(\delta)$ to (1). The new expression of the interaction energy becomes

$$U_{12}(\delta) = 1/2\,\{(-\alpha_1 + 2\beta_1)\,\varrho_2(\delta) + (-\alpha_2 + 2\beta_2)\,\varrho_1(\delta)\}\,. \tag{4}$$

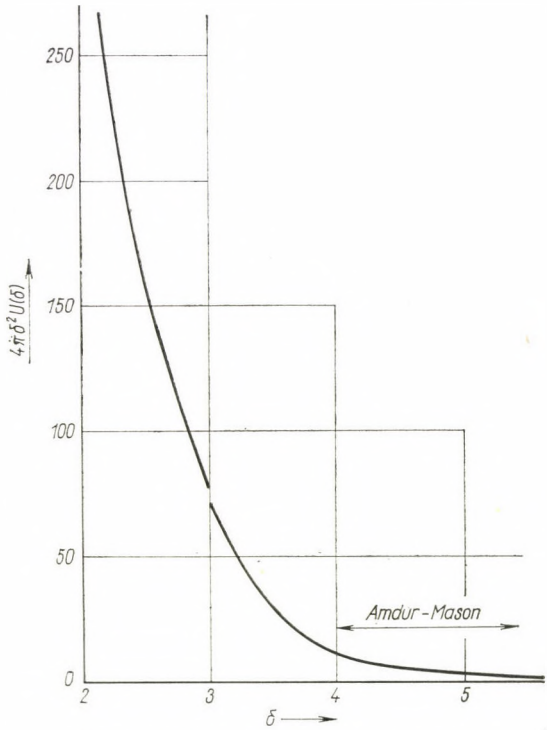

Fig. 2. The enlarged curve of Fig. 1

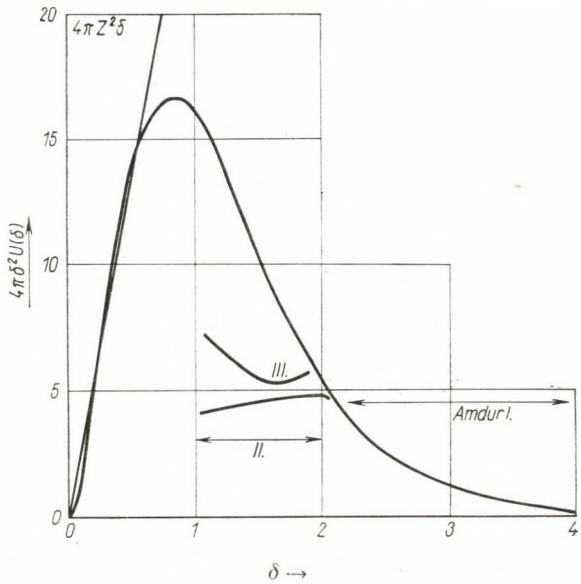

Fig. 3. Potential energy of the helium—helium interaction. The abscissa is given in a_0, and the ordinate in e^2a_0 atomic units

Let us assume that we know the interaction energy of atoms 1 and1′ with the atomic number Z_1 and of atoms 2 and 2′ with the atomic number Z_2

$$U_1(\delta) = (-\alpha_1 + 2\beta_1)\,\varrho_1(\delta)\,, \tag{5}$$

$$U_2(\delta) = (-\alpha_2 + 2\beta_2)\,\varrho_2(\delta)\,. \tag{6}$$

Using (5) and (6), (4) can be transformed in the following manner

$$U_{12}(\delta) = \frac{1}{2}\,\frac{-\alpha_1 + 2\beta_1}{-\alpha_2 + 2\beta_2}\,U_2(\delta) + \frac{1}{2}\,\frac{-\alpha_2 + 2\beta_2}{-\alpha_1 + 2\beta_1}\,U_1(\delta)\,. \tag{7}$$

For simplicity (7) can be written in the form

$$U_{12}(\delta) = \frac{1}{2}\left\{\gamma U_2(\delta) + \frac{1}{\gamma}\,U_1(\delta)\right\}, \tag{8}$$

where

$$\gamma = \frac{-\alpha_1 + 2\beta_1}{-\alpha_2 + 2\beta_2} \tag{9}$$

is constant and can be determined from the theory on the basis of (2) and (3).

The question may arise whether the constant γ might be determined by using the experimental data only. This is possible in the following way. Multiplying the expression (5) by $4\pi\delta^2$ and integrating over δ, we obtain

$$\int_0^\infty 4\pi\delta^2\,U_1(\delta)\,d\delta = (-\alpha_1 + 2\beta_1)\int_0^\infty \varrho_1(\delta)\,4\pi\delta^2\,d\delta = (-\alpha_1 + 2\beta_1)\,N_1\,, \tag{10}$$

where N_1 is the number of electrons in the atom 1. Formula (10) shows that the value of the quantity $U_1(\delta)$ is required throughout the full range of the value of δ. Experimentally $U_1(\delta)$ is known in many cases up to values of δ at which $U_1(\delta)$ assumes very small values. So a problem of some significance is encountered only in the neighbourhood of $\delta = 0$, where $U_1(\delta)$ behaves singularly. As at very small values of δ the screening effect of the electrons is negligible

$$U_1(\delta) \cong \frac{Z_1 Z_1 e^2}{\delta} \tag{11}$$

i.e. only the repulsion of the two nuclei remains and so

$$4\pi\delta^2\,U_1(\delta) \cong 4\pi\,Z_1^2\,e^2\,\delta\,. \tag{12}$$

On the basis of (2) the integrand can be estimated with sufficient accuracy in the neighbourhood of $\delta = 0$.

By graphical interpolation the overall shape of the integrand can be determined in any region required.

In Figs. 1 and 2 the quantity $4\pi\delta^2 U(\delta)$ is plotted for the noble gas atom A. The double arrows mark the range of internuclear distance over which the curves obtained from the experimental data correspond to the experimental results. For illustration we have listed these data in Table 1. In the region not investigated experimentally the curve has been completed by extrapolating the nearest

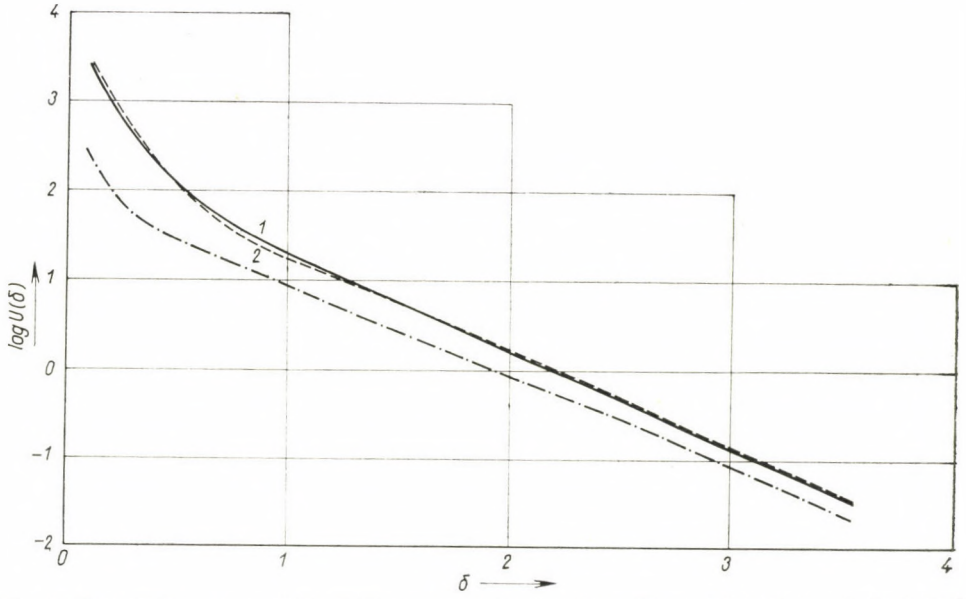

Fig. 4. Potential energy of the helium—argon interaction. The solid and the dashed line represent the theoretical curves, the dashes and dots the curve obtained by interpolating the experimental helium—helium and argon—argon potential energy curves. The ordinate is $\log U(\delta)a_0e^{-2}$, where $U(\delta)$ and δ are plotted in e^2a_0 and a_0 atomic units, respectively

Table 1

The experimental interaction potentials and their ranges of validity

	$U(r)$ in erg.	the range in Å
He — He	$\frac{4{,}62 \cdot 10^{-12}}{r\ 1{,}79}$	$0{,}52 < r < 1{,}02$
	$6{,}18 \cdot \exp(-4{,}65 \cdot r) \cdot 10^{-10}$	$1{,}27 \leq r \leq 2{,}30$
	see Table 1a	$0{,}55 < r < 1$
A — A	$21{,}9 \cdot \exp(-4{,}14\, r) \cdot 10^{-9}$	$0{,}04 \leq r \leq 1{,}02$
	$1{,}36 \cdot 10^{-9}/r^{8{,}33}$	$2{,}18 \leq r \leq 2{,}69$
	$9{,}03 \cdot 10^{-16}/r^{7{,}87}$	$2{,}69 \leq r \leq 2{,}98$

experimental curve. The greatly enlarged curve in Fig. 2 shows that this extrapolation does not involve too great an error. In Fig. 1 the slope of the A—A interaction potential is shown in a smaller range of internuclear distance

The straight line starting from the origo is the one described by equ. (12). The solid curve has been obtained by extrapolating the experimental curve. The dashed line is the one obtained by graphical interpolation, which connects with a continuous tangent the straight line in the origo and the curve determined experimentally. The shaded area shows the maximum deviation of the sector giving an uncertain contribution when integrating over the above curve instead of over the curve extrapolated experimentally.

In Fig. 3 the quantity $4\pi\delta^2 U(\delta)$ has been plotted as a function of δ against the He—He internuclear distance.

Table 1a

The experimental interaction potentials and their range of validity. See Table 1

Å	U in eV
0,55	14,6
0,60	11,5
0,65	9,2
0,70	7,5
0,80	5,1
0,90	4,0
1,0	3,5

Of the experimental results those published in the paper of AMDUR [4] can be very well fitted to the behaviour in the neighbourhood of the origo described by equ. (12). However, the results published in an earlier paper of AMDUR [5] deviate from the foregoing results, which is clearly shown in the Figure. In our opinion further experimental work is required to facilitate a comparison between the theoretical and the experimental results. In Table 2 the values of the constants determined by graphical integration are shown. The Table also includes the constants determined by means of the Hartree and Hartree—Fock density distributions.

The constants so obtained can be used in the relation (7) to determine the interaction energy of unlike noble gas atoms. In Fig. 4 the logarithm of the He—A interaction potential has been plotted as a function of the internuclear distance.

The solid and dashed lines represent the theoretical curves. Curve 1 has been obtained on the basis of the asymmetric formula (1) and the curve 2 on the basis of the symmetric formula (4) with the aid of the Hartree density distribution of He and the Hartree—Fock density distribution of A, respectively. The difference between the two theoretical curves is very slight. The dashed and dotted curve represents the curve interpolated from the He—He and A—

Table 2

Theoretical and experimental values of the interpolation constants

		$N(-\alpha+2\beta)=\int_0^\infty 4\pi\delta^2 U(\delta)d\delta$	Author
He — He	theoretical	87,19	HARTREE [6]
	experimental	25,5	AMDUR—HARKNESS [1]
Ne — Ne	theoretical	646,2	BROWN [7]
	experimental	504	AMDUR—MASON—RICE [1]
A — A	theoretical	3148,6	HARTREE—HARTREE [8]
	experimental	1140	AMDUR—MASON—RICE [1]

A interaction curves with the aid of (7). The relative position of the theoretical and interpolated curves is the same as that of the theoretical and experimental interaction curves of identical atoms.

My thanks are due to Mr. J. GÁTHY for carrying out the numerical calculations and for drawing the figures.

REFERENCES

1. I. AMDUR and A. L. HARKNESS, J. Chem. Phys., **22,** 664, 1954; I. AMDUR and E. A. MASON, J. Chem. Phys., **23,** 415, 1955; ibid., **22,** 670, 1954; ibid. **23,** 2268, 1955; H. W. BERRY, Phys. Rev., **99,** 553, 1955; ibid. **75,** 913, 1949; E. A. MASON and W. E. RICE, J. Chem. Phys., **22,** 843, 1954.
2. R. GÁSPÁR, Acta Phys. Hung., **11,** 71, 1960.
3. P. GOMBÁS, Zs. f. Phys., **93,** 378, 1935.
4. I. AMDUR and R. R. BERTRAND, J. Chem. Phys., **36,** 1078, 1962.
5. I. AMDUR, J. Chem. Phys., **17,** 844, 1949.
6. D. R. HARTREE, Proc. Cambridge Phil. Soc., **34,** 111, 1928.
7. F. W. BROWN, Phys. Rev., **44,** 214, 1933.
8. D. R. HARTREE and W. HARTREE, Proc. Roy. Soc., **166,** 450, 1938.

ТЕОРЕТИЧЕСКОЕ ОПРЕДЕЛЕНИЕ ЭНЕРГИИ ВЗАИМОДЕЙСТВИЯ АТОМОВ БЛАГОРОДНЫХ ГАЗОВ II.

ВЗАИМОДЕЙСТВИЕ АТОМОВ БЛАГОРОДНЫХ ГАЗОВ С РАЗЛИЧНЫМИ ПОРЯДКОВЫМИ НОМЕРАМИ. ИНТЕРПОЛЯЦИОННЫЕ ПРОБЛЕМЫ

Р. ГАШПАР

Р е з ю м е

Производится обобщение метода, изложенного в одной из предыдущих работ, на определение энергии взаимодействия атомов благородных газов с различными порядковыми номерами. Метод даёт возможность для разработки интерполяционного приёма, с помощью которого из энергии взаимодействия атомов одинаковых благородных газов, определённой экспериментально, можно определить интерполяцией энергию взаимодействия атомов различных благородных газов. После подробной дискуссии системы He – A дается детальный анализ потенциальной энергии взаимодействия He — He.

ON THE CALCULATION OF THE ANGULAR RESOLUTION CORRECTION IN ANGULAR CORRELATION MEASUREMENTS

By

D. BERÉNYI and T. BALOGH

INSTITUTE FOR NUCLEAR RESEARCH OF THE HUNGARIAN ACADEMY OF SCIENCES, DEBRECEN

(Presented by A. Szalay — Received 26. II. 1963)

Based in principle on ROSE's [1] calculations closed formulae and tables are given, from which, knowing certain data of the experimental angular resolution curve, the factors for the correction of the angular correlation coefficient for the finite dimensions of detectors are obtained.

In $\gamma - \gamma$ angular correlation measurements and in angular correlation and angular distribution measurements in general, a correction has to be applied owing to the finite dimensions of detectors. The theoretical foundations of the problem were established by ROSE [1] in 1953. However, the actual correction procedure carried out on this basis is rather lengthy.

ROSE's calculations have been followed by other calculations and measurements on the angular resolution correction [2, 3]. The procedure can be carried out with the aid of diagrams, also available for special crystal dimensions and arrangements [4]. Inspite of this the method of CHURCH and KRAUSHAAR [5] is still being applied by many authors, which may be due to the fact that knowing the half width of the experimental angular resolution curve it is simple to calculate the values of the correction factor by means of closed formulae.

The method used by CHURCH and KRAUSHAAR, however, is a rather rough approximation, to be applied directly only if 1. the two radiations are of approximately equal energy and the two detectors are approximately identical, i.e. if the shape of the angular resolution curve is approximately identical for the two detectors; further if 2. the shape of the angular resolution curve can be approximated by a triangle or a Gaussian curve. Obviously, these restrictions are too stringent and do not satisfy the requirements of present experimental practice.

In view of this we have developed a procedure which, based in principle on the method of ROSE, provides closed formulae for the performance of the angular resolution correction as in CHURCH and KRAUSHAAR's method, but this is done in a much more general form, without applying their restrictive assumptions.

According to ROSE [1] if A'_{2k} is an uncorrected angular correlation coefficient, the corrected coefficient A_{2k} is obtained on the basis of the formula

$$A_{2k} = \frac{Q_0}{Q_{2k}} A'_{2k}, \tag{1}$$

where

$$Q_{2k} = J'_{2k}(\gamma_1) J''_{2k}(\gamma_2), \tag{2}$$

i.e.

$$A_{2k} = \frac{J'_0}{J'_{2k}} \frac{J''_0}{J''_{2k}}.$$

Here the single mark relates to one of the crystals and the double mark to the other. The J-s are obtained from the experimental angular resolution curve marked by $\varepsilon(\alpha)$ by integration in the following manner

$$J_{2k} = 2 \int_0^{\frac{\alpha_0}{2}} P_{2k}(\cos\alpha).\ \varepsilon(\alpha) |\sin\alpha|\, d\alpha. \tag{3}$$

$P_{2k}(x)$ is the appropriate $2k$-th order Legendre polynomial, α_0 is the "basic width" of the angular resolution curve (see Figs. 1 and 2).

The problem actually is how to evaluate the integral (3). Applying a suitable approximation for the experimental angular resolution function $\varepsilon(\alpha)$ no integration by means of the clumsy planimeter is required to calculate the correction, but closed formulae can be used.

The function $\varepsilon(\alpha)$ has been approximated in three ways corresponding to the experimental curves occurring in practice: by triangle, trapezoid and Gaussian curve. In the two former cases the integration is straightforward and so J_{2k}, i.e. J_0, J_2 and J_4 actually occurring in practice can be given by means of closed formulae. In the case of the Gaussian curve expansion in a series and approximation was necessary. In the following, formulae obtained for J_0/J_2 and J_0/J_4 and in the approximation by the Gaussian curve for J_0, J_2 and J_4 are given for the various approximations relating to the shape of the $\varepsilon(\alpha)$ curve.

Triangular approximation:

$$\left.\begin{aligned} \frac{J_0}{J_2} &= \frac{6(\delta - \sin\delta)}{\sin^3\delta} \\ \frac{J_0}{J_4} &= \frac{120(\delta - \sin\delta)}{20\sin^3\delta - 21\sin^5\delta} \end{aligned}\right\}. \tag{4}$$

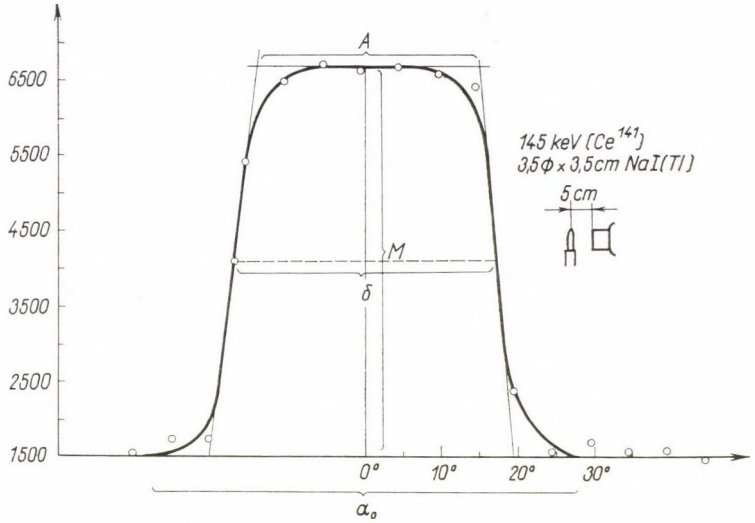

Fig. 1. Angular resolution curve for 145 keV monoenergetic radiation. The radiation passed through a collimating lead channel 10 cm in length. The distance from the end of the collimator oriented towards the crystal to the crystal face was equal to the source-to-crystal distance in angular correlation measurements

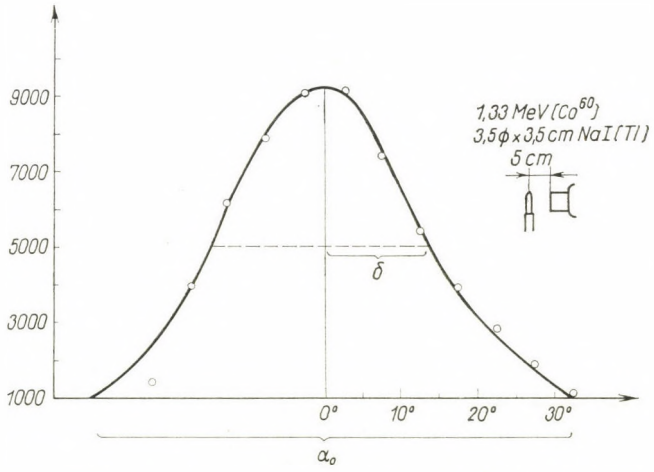

Fig. 2. Angular resolution curve for 1,33 MeV monoenergetic γ-radiation. The experimental conditions are in every respect identical with those prevailing during taking the curve shown in Fig. 1

Trapezoid approximation:

$$\left.\begin{aligned}\frac{J_0}{J_2} &= \frac{2(\delta - A) - 4\sin\frac{\delta - A}{2}\cos\frac{\delta}{2}}{\frac{1}{2}\sin\frac{\delta - A}{2}\cos\frac{\delta}{2} - \frac{1}{6}\sin^3\frac{\delta - A}{2}\cos^3\frac{\delta}{2}} \\ \frac{J_0}{J_4} &= \frac{2(\delta - A) - 4\sin\frac{\delta - A}{2}\cos\frac{\delta}{2}}{\frac{1}{32}\left[2\sin\frac{\delta - A}{2}\cos\frac{\delta}{2} + \frac{5}{3}\sin 3\frac{\delta - A}{2}\cos 3\frac{\delta}{2} - \frac{7}{5}\sin 5\frac{\delta - A}{2}\cos 5\frac{\delta}{2}\right]}\end{aligned}\right\} \quad (5)$$

Gaussian curve approximation

$$J_0 = 0,67764\,\delta - 0,16295\,\delta^3 + e^{-\frac{0,4275}{\delta^2}}(-0,60797\,\delta + 0,16295\,\delta^3) + R_0\,,$$

$$\begin{aligned}J_2 = {} & 0,67764\,\delta - 1,62953\,\delta^3 + 2,13948\,\delta^5 - 1,98670\,\delta^7 + \\ & + e^{-\frac{0,4275}{\delta^2}}(-0,15063\,\delta + 0,89641\,\delta^3 - 1,29003\,\delta^5 + \\ & + 1,98670\,\delta^7) + R_2\,,\end{aligned}$$

$$\begin{aligned}J_4 = {} & 0,67764\,\delta - 5,05179\,\delta^3 + 19,42126\,\delta^5 - 51,14149\,\delta^7 + \\ & + 103,27982\,\delta^9 - 169,79299\,\delta^{11} + \\ & + e^{-\frac{0,4275}{\delta^2}}(0,24977\,\delta + 0,28591\,\delta^3 - 4,78346\,\delta^5 + \\ & + 22,50470\,\delta^7 - 30,68340\,\delta^9 + 169,79299\,\delta^{11}) + R_4\,,\end{aligned} \quad (6)$$

where $|R_0| \leq 0,003$, $|R_2| \leq 0,003$ and $|R_4| \leq 0,003$.

In formulae (4) and (5) δ denotes the total halfwidth (Fig. 1) while in formula (6) this means one half of the half-width (Fig. 2). A is the length of the upper straight line bounding the trapezoid (see Fig. 1). δ and A are expressed in radians or degrees. Thus the triangular and the Gaussian curve approximation require one experimental parameter each, while the trapezoid approximation requires two experimental parameters.

The method of carrying out the correction is shown on the example of the $0,145 \rightarrow 1,29$ MeV cascade occurring in the disintegration of Fe^{59}. First of all it is necessary to take the experimental angular resolution curve for the γ-radiations, the energies of which are from 0,145 and 1,29 MeV. For the method see [6, 7]. In our case these have been taken by using the 145 keV γ-radiation of Ce^{141} and the 1,33 MeV γ-radiation of Co^{60} (Figs. 1 and 2). Reading the corresponding data in Figs. 1 and 2 we obtain J_0/J_2 and J_0/J_4

by means of formulae (5) and (6). (In the actual case referred to above e.g. J_0/J_4 is not necessary, as for nuclear physical reasons $A_4 = 0$.)

To facilitate the calculation of the correction we have compiled the values of J_0/J_2 and J_0/J_4 in Tables for the cases most frequently occurring in practice (trapezoid and Gaussian curve). By taking the angular resolution curve experimentally the actual values of the parameters are determined and by using the corresponding values shown in the Tables the correction factors are obtained simply by taking the product of the two quantities.

Table 1

Trapezoid form

A_0	δ_0	J_0/J_2	J_0/J_4
	30	1,0574	1,2005
26	32	1,0649	1,10512
	34	1,0754	1,2820
	32	1,0626	1,0970
28	34	1,0732	1,2710
	36	1,0820	7,3178
	34	1,0751	1,2449
30	36	1,0795	1,3063
	38	1,0921	1,3613

Table 2

Gaussian curve

δ_0	J_0/J_2	J_0/J_2
8	1,0430	1,1506
9	1,0546	1,1932
10	1,0679	1,2456
11	1,0827	1,3044
12	1,0989	1,3733
13	1,1169	1,4447
14	1,1361	1,5303
15	1,1567	1,6247
16	1,1793	1,7326
17	1,2006	1,8473
18	1,2245	1,9809
19	1,2447	2,1085
20	1,2663	2,2514
21	1,2874	2,4268
22	1,3075	2,5812

The angular correlation correction for the above cascade has also been carried out by integrating (3) graphically by means of a planimeter. For Q_0/Q_2 the result was 1,23, the Tables gave 1,22.

Our thanks are due to Prof. A. SZALAY, Director of this Institute, for his support and excellent working conditions.

REFERENCES

1. M. E. ROSE, Phys. Rev., **91,** 610, 1953.
2. A. L. STANFORD and W. K. RIVERS, Rev. Sci. Instr., **30,** 719, 1959.
3. D. W. GLASGOW, L. W. COLEMAN and L. SCHECTER, Rev. Sci. Instr., **32,** 683, 1961.
4. Nuclear Data Tables, Part 3. National Academy of Sciences-National Research Council, Washington 25, D. C., 1960.

5. E. L. Church and J. J. Kraushaar, Phys. Rev., **88,** 419, 1952.
6. J. S. Lawson, Jr. and H. Frauenfelder, Phys. Rev., **91,** 649, 1953.
7. T. Lindgvist, Ark. f. Fys., **12,** 500, 1957.

О ВВЕДЕНИИ КОРРЕКЦИИ УГЛОВОГО РАЗРЕШЕНИЯ ПРИ ИЗМЕРЕНИИ УГЛОВОЙ КОРРЕЛЯЦИИ

Д. БЕРЕНИ и Т. БАЛОГ

Р е з ю м е

На принципиальной основе вычислений Розе [1] даются закрытые формулы и таблицы. При их помощи, зная соответствующие данные определённой экспериментально кривой углового разрешения, вычисляются факторы, дающие возможность для поправки коэффициента угловой корреляции в случае детекторов конечных размеров.

INVESTIGATIONS ON γ-RADIATION ACCOMPANYING THE BOMBARDMENT OF NUCLEUS Na-23 BY α-PARTICLES OF Po

By

I. ANGELI

INSTITUTE OF NUCLEAR RESEARCH OF THE HUNGARIAN ACADEMY OF SCIENCES, DEBRECEN

(Presented by A. Szalay — Received 28. II. 1963)

The excitation function and energy distribution of γ-radiation emitted by a metal Na-target through the effect of Po α-particles were investigated. The obtained excitation function made it possible to determine a new highly excited level (or group of levels) of the nucleus Al^{27} with certainty and another with probability. From an investigation of the γ-spectrum it has been deduced that the excitation function is related to the nuclear reaction $Na^{23}(\alpha, p)Mg^{26}$. The experimental result for the reaction cross section $\sigma(\alpha, p)$ is consistent with the calculated value.

Introduction

The first suggestion of the appearence of γ-radiation due to the α-bombarding of Na^{23} was made by BOTHE and BECKER [1]. Furthermore WEBSTER [2] and SAVEL [3] proved the definite existence of such γ-radiation. SAVEL [3] determined the energy ($E_\gamma \approx 1{,}7 - 1{,}9$ MeV) by absorption method and measured the intensity at five different energies. M. KOVÁCS [4] obtained a more detailed excitation function, however, the curve gained by her does not show any step relating to the levels of the compound nucleus Al^{27}. SLÄTIS's measurements [5] showed similar results. It was HEYDENBURG and TEMMER [6], [7] who first found resonances in the bombarding energy region $E_\alpha = 1{,}5 - 3{,}6$ MeV.

Our aim was to search for further resonances in the energy interval $E_\alpha = 3{,}6 - 5{,}3$ MeV. The resonances appearing in the excitation function give the highly excited states of the compound nucleus Al^{27}. The disintegration of this nucleus yields a residual nucleus existing generally in an excited state too and the transition into the ground state takes place by emitting γ-radiation.

We measured the intensity of the γ-radiation as a function of the energy of the impinging α-particles *(excitation function)*. The *γ-spectrum* was investigated too; this was necessary for the identification of the residual nucleus.

Experimental arrangements

The measuring apparatus was essentially the same as that used by E. CSONGOR [8], [14], [15] in her investigations of a similar kind on separated Mg isotopes. Therefore we describe here only its main features.

The α-source prepared by Prof. A. SZALAY was a 40—50 mC Po-preparatum deposited into a Pt—Ir disc 3 mm in diameter using the method developed by him [9].

The target we applied to determine the excitation function consisted of a 0,4 mg/cm^2 metal Na layer prepared by means of vacuum evaporation The Po source was placed in the centre of curvature of the spherical-calotte shaped target and so the α-particles arrived at every point of the surface to be radiated with the same energy. It was easy to control the bombarding α-energy by altering the pressure of the argon gas present in the chamber. The energy resolving power was determined by the "straggling" in the gas and the final target thickness. The resolving power curves plotted above the excitation function show what shape the excitation function would have been, if the reaction had taken place only at a single resonance energy E_r.

The γ-radiation was detected by a cylindrical NaJ(T1) crystal of 40 mm $\varnothing \times 30$ mm dimension, and the pulses coming from the photomultiplier reached the decatron tube scaler after passing through the amplifier and a discriminator. In order to eliminate the 0,8 MeV γ-radiation of Po^{210} (which has an intensity a hundred times greater than the effect to be measured) we counted only the pulses originating from γ-rays having an energy higher than 1 MeV.

The γ-spectrum was measured using a thick Na metal layer; the calibration of the single-channel differential discriminator for measuring of γ-energies was carried out by γ-rays of Cs^{137}, Po^{210}, Co^{60} and ThC".

Experimental results

The excitation function (γ-s of higher energy than 1 MeV vs. bombarding energy) is presented in Fig. 1. In the upper part of the figure the resolving power curves are drawn.

Analysing statistically the measured data [10] it can be shown that:

a) It is *certain* that there exists a resonance (or group of resonances) at $E_a = 5{,}00 \pm 0{,}05$ MeV;

b) it is *probable* that there exists a resonance (or group of resonances) at $E_a = 4{,}75 \pm 0{,}05$ MeV;

c) it is *probable* that the sharp rise above $E_a = 5{,}1$ MeV originates from resonance(s).

The *γ-spectrum* was measured at three different voltages of the photomultiplier; Fig. 2 shows the γ-lines appearing in the excitation function with appreciable intensity. The dotted line is the background spectrum.

It can be seen that the 1,84 MeV and 1,13 MeV lines are those which mainly contribute to the γ-spectrum above 1 MeV. The intensity of the 2,55

MeV line is about one order of magnitude lower. These three lines are responsible for the well-defined photo-peaks. Further low-intensity and rather uncertain "peaks" can be found at 2,93 MeV and 3,30 MeV.

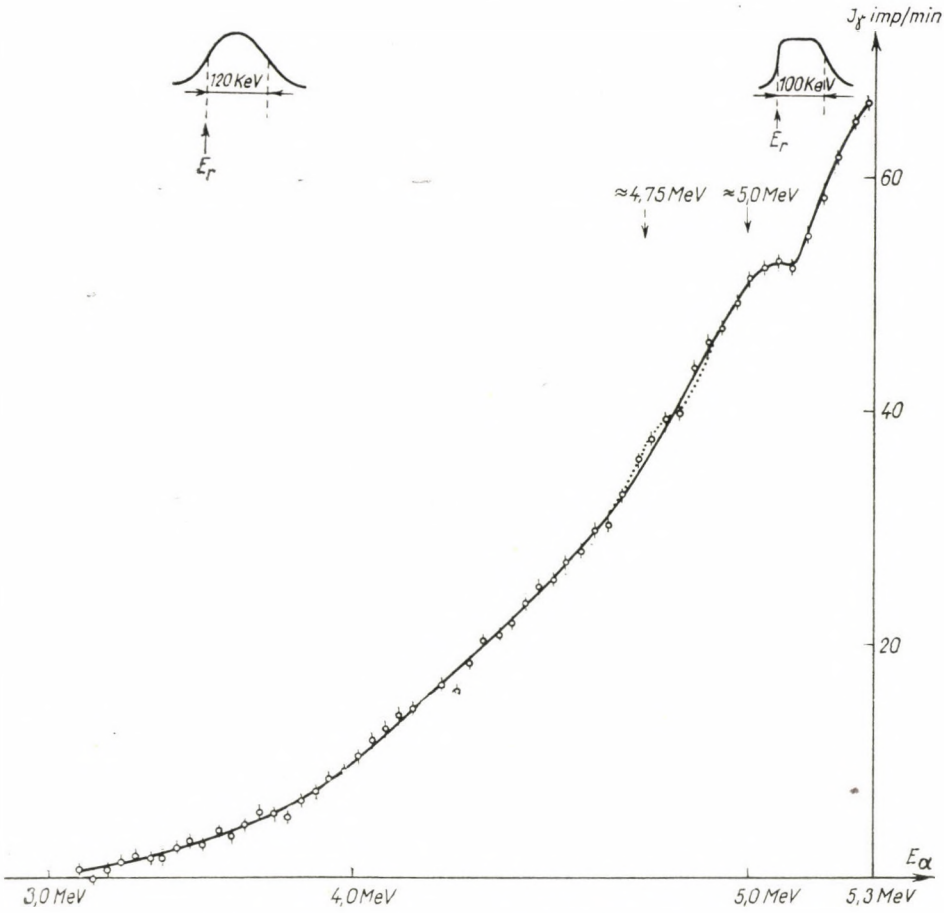

Fig. 1. Excitation function of reaction $Na^{23}/\alpha, p/Mg^{26}$.
Abscissa: Bombarding α-energy (E_α). Ordinate: γ-intensity above the γ-energy 1 MeV (I_γ)

Evaluation of the experimental results

Natural Na consists of a single isotope Na^{23}. This fact renders the evaluation of the measurements easier. It can be concluded from the resonances occurring in the *excitation function* that at the corresponding points the compound nucleus Al^{27} has one or more energy levels lying close to one another,

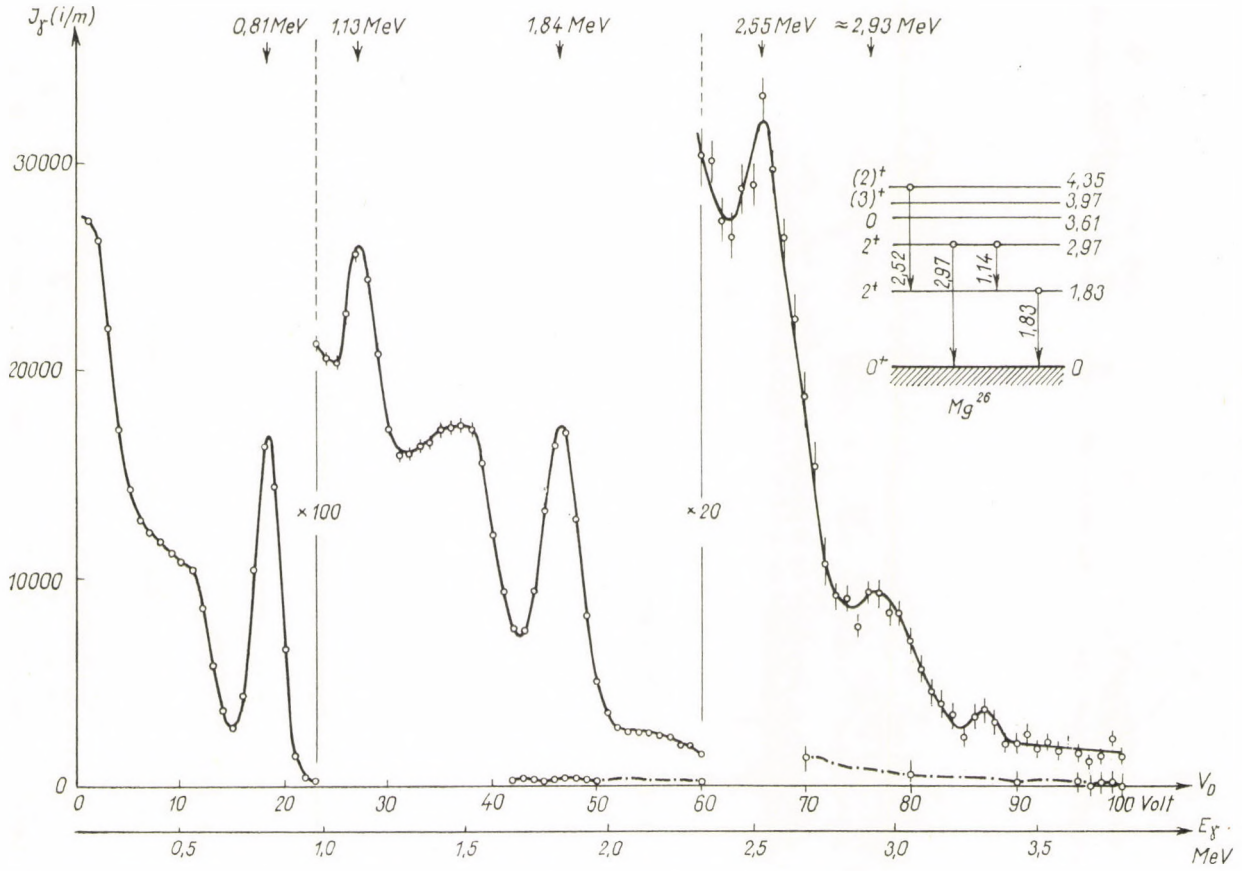

Fig. 2. The energy spectrum of the γ-radiation.
Abscissa: γ-energy (E_γ). Ordinate: γ-intensity (I_γ)

but it must be emphasized that the resolving power of our apparatus was not sufficient to resolve them.

a) certain: $E_{exc.}(Al^{27}) = 14{,}35$ MeV;
b) probable: $E_{exc.}(Al^{27}) = 14{,}14$ MeV;
c) probable: $E_{exc.}(Al^{27}) = 14{,}4$ MeV

(we have accepted 10,094 MeV as the binding energy of the α-particle according to [11]).

Origin of the γ-spectrum lines: Bombarding the nucleus Na^{23} by Po α-particles the following reactions can be taken into account:

$$Na^{23}(\alpha, p)\, Mg^{26}, \qquad Q = +1{,}84 \text{ MeV},$$
$$Na^{23}(\alpha, n)\, Al^{26}, \qquad Q = -2{,}97 \text{ MeV}.$$

Without doubt the 1,84 MeV and 1,13 MeV lines correspond to the transitions

$$1{,}83 \rightarrow 0{,}00$$

and

$$2{,}97 \rightarrow 1{,}83$$

of the residual nucleus Mg^{26}. As to the origin of the 2,55 MeV and 2,97 MeV γ-radiations the most probable possibilities are

$$4{,}35 \rightarrow 1{,}83$$

and

$$2{,}97 \rightarrow 0{,}00\,,$$

respectively. So it can be seen that the γ-radiation of energies above 1 MeV corresponds almost entirely to the transitions between the levels of the residual nucleus Mg^{26}, that is, they come from the reaction (α, p).

The value of the *cross section* obtained from the experimental data is

$$\sigma^*(\alpha, p) = 5{,}5 \pm 2{,}2 \text{ mb}.$$

An approximate calculation carried out on the basis of ref. [12] (not including spin and parity) gives

$$7{,}4 \text{ mb} < \sigma^*(\alpha, p) < 8{,}8 \text{ mb}.$$

$\sigma^*(\alpha, p)$ means that the residual nucleus Mg^{26} was produced in an excited state. However, according to the measurements of MAY and FOSTER [13] the percentage of the reaction $Na^{23}(\alpha, p)\, Mg^{26}$ leading directly to the ground state is very small (about 3—5%), therefore we can say

$$\sigma^*(\alpha, p) = \sigma(\alpha, p).$$

I am greatly indebted to Prof. A. SZALAY, the Director of the Institute for suggesting this problem and for preparing the Po-source. Thanks are also due to Mrs. VERESS for her assistance throughout the measurements.

REFERENCES

1. W. BOTHE and H. BECKER, Naturwiss., **18,** 705, 1930.
2. H. C. WEBSTER, Proc. Roy. Soc., (L) **1360,** 428, 1932.
3. P. SAVEL, Ann. de physique, **4,** 88, 1935.
4. M. KOVÁCS, Phys. Rev., **70,** 895, 1946.
5. H. SLÄTIS, Arkiv f. Mat. Astr. Fys., **350,** No. 31, 1, 1948.
6. N. P. HEYDENBURG and G. M. TEMMER, Phys. Rev., **95,** 629, 1954.
7. G. M. TEMMER and N. P. HEYDENBURG, Phys. Rev., **96,** 426, 1954.
8. E. CSONGOR, Nucl. Phys., **23,** 107, 1961.
9. A. SZALAY, Zs. f. Phys., **112,** 29, 1939.
10. L. JÁNOSSY, private communication.
11. P. M. ENDT and M. DEMEUR, Nuclear Reactions I., 264, North Holland Publ. Comp., Amsterdam, 1959.
12. H. FESCHBACH, M. M. SHAPIRO and V. F. WEISSKOPF, Tables of Penetrabilities for Charged Particle Reaction, NYO-3077, NDA Report, 15B-5, June 15, 1953.
13. J. E. MAY and B. P. FOSTER, Phys. Rev., **90,** 243, 1953.
14. É. CSONGOR, ATOMKI Közlemények III, 1. sz. mell. 1961. (dissertation for degree of candidate).
15. É. CSONGOR, Magyar Fizikai Folyóirat, VIII, 357, 1960.

ИССЛЕДОВАНИЕ γ-ИЗЛУЧЕНИЯ, СОПРОВОЖДАЮЩЕГО БОМБАРДИРОВКУ ЯДРА Na-23 α-ЧАСТИЦАМИ Po

И. АНГЕЛИ

Р е з ю м е

Исследуется функция возбуждения и распределение энергии γ-излучения, эмиттируемого металлической Na-мишенью под действием бомбардировки α-частицами. Полученная функция возбуждения дает возможность для определения нового сильно возбужденного уровня (или группы уровней) ядра Al^{27} с уверенностью, а иного с некоторой вероятностью. На основании исследования γ-спектра можно сделать вывод о том, что функция распределения связана с ядерной реакцией $Na^{23}(\alpha, p)Mg^{26}$. Экспериментальные результаты для поперечного сечения реакции $\sigma(\alpha, p)$ согласуются с вычисленными данными.

ON THE TRANSMISSION FUNCTION OF NEUTRON CHOPPERS WITH STRAIGHT SLITS

By

T. NAGY, I. PAVLICSEK and L. NAGY

CENTRAL RESEARCH INSTITUTE OF PHYSICS OF THE HUNGARIAN ACADEMY OF SCIENCES, BUDAPEST

(Presented by L. Pál — Received 21. III. 1963)

The transmission function is derived for neutron choppers having straight slits using geometrical considerations. Misalignment manifests itself in the shape of the transmission curve and the measured shape permits to locate and estimate any error in alignment. The results of the calculations are verified experimentally.

I. Introduction

The neutron spectrum of a reactor measured by means of a velocity selector has to be corrected for the deformation due to the chopper. The transmission function taking account of this deformation has been calculated for the case of choppers with straight slits by P. A. EGELSTAFF [1], V. I. MOSTOVOI et al. [2] and P. HRASKÓ [3].

The transmission function determined theoretically can be employed only in those cases when an ideal alignment of the collimators, rotor and detector is achieved. Considering now that the heights of the collimator and rotor slits are in general 0,2—2 mm, while their length as a whole may reach even 60—80 cm it is rather hard, for low slit heights even impossible, to obtain by conventional optical and mechanical means an alignment of ideal precision.

Apart from its importance in neutron spectrum measurements, it is of interest to know the extent of misalignment, since such errors may cause substantial reduction in the neutron intensity and this affects disadvantageously the neutron experiments involved.

In the following calculations of the transmission function geometrical considerations will be employed which enable us to determine how the shape of the transmission curve is deformed by any error in alignment. Then by considering the shape of the measured transmission function it is possible to locate the area and extent of misalignment. Bringing about artificial error in the alignment, the calculations are verified by measurements.

II. The transmission function

For simplicity, the rotor and the collimators are each assumed to have one slit only (Fig. 1). h be the height of the slits, z_0 their width. We assume

further the neutrons to fly parallel to one another within the beam and the flux of the neutrons of various velocities to be uniform and constant. The time is reckoned from the instant at which the neutrons can start to stream into the slit of the rotor crossing the plane P_1, that is when the point b of the rotor reaches the point A of the collimator (position $\overline{bA}$). If $t = t_0$ is the time at which the rotor gets into the position $\overline{cD}$, t_0 is the time past which the neutrons cannot leave the rotor. The velocity of the slowest neutrons passing through the rotor is given by $v_0 = \dfrac{2R}{t_0}$; neutrons of lower velocity cannot reach the plane P_2.

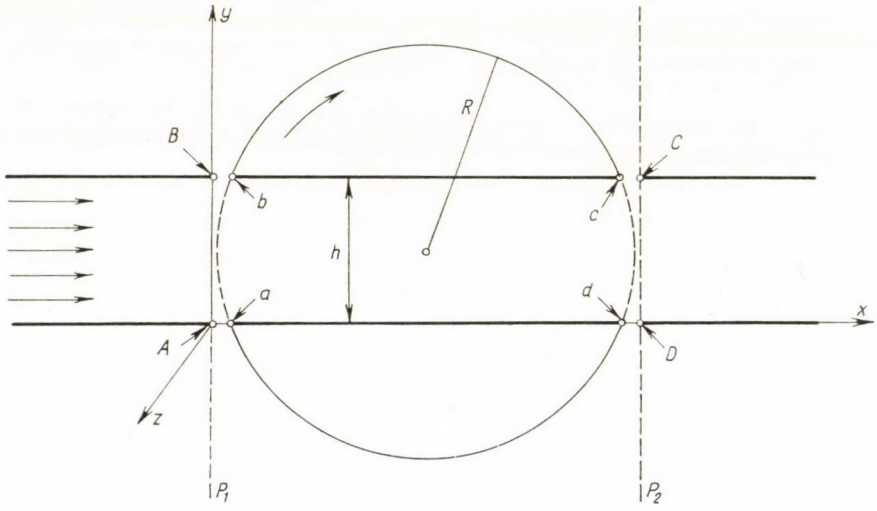

Fig. 1. Cross-sectional view of rotor and collimators normal to the axis of rotation

In Fig. 2 the position of a neutron beam with velocity v satisfying the condition $v_0 \leqslant v \leqslant 2v_0$ is illustrated in the course of its passage through the rotor. In time $\dfrac{t_0}{2}$ the rotor slit gets into a position parallel to the axis x and at this instant the neutrons flying as high as $y = h$ may just get into the rotor, while the neutrons which entered at time $t = 0$ at the position $y = 0$ have already covered the distance $x_0 = v\dfrac{t_0}{2}$ in the direction x. Under the above condition $R \leqslant x_0 \leqslant 2R$. The plane 1 represents the front of neutrons with velocity v getting into the rotor during the time $\dfrac{t_0}{2}$. The volume of the rotor containing the neutrons is now given by $\dfrac{x_0 h}{2} z_0$.

At the time $t_1 = \dfrac{2R - x_0}{v}$ past $\dfrac{t_0}{2}$, the front of neutrons gets into the position 2. During this time the point a of the rotor covers the distance y_1. The neutrons being inside the rotor are now in the volume confined by the planes 2 and $2/a$.

At time $\dfrac{t_0}{2} + t_1$ the neutrons start flying out of the rotor and are leaving the slit in ever increasing numbers across the plane P_2. The number of outgoing neutrons continues to increase until their front gets into a position

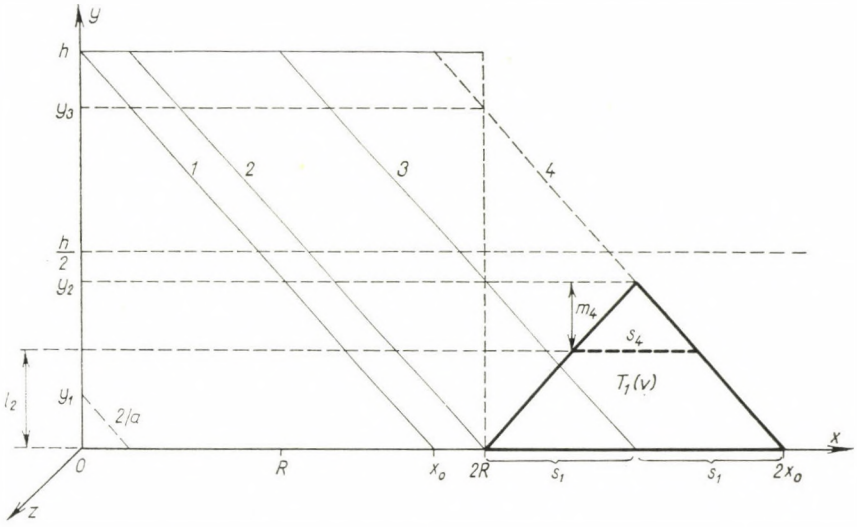

Fig. 2. The position of the neutrons with velocities from v_0 to $2v_0$ transmitted by the rotor in the plane (x, y) at the time $t = t_0$

— denoted by plane 3 — when it meets the point c of the rotor. Let s_1 be the distance in the direction x from the plane 2 to the plane 3, t_2 the time required to fly this distance, and y_2 the ordinate belonging to the abscissa $2R$ of the plane 3.

From the time $\dfrac{t_0}{2} + t_1 + t_2$ there is a linear decrease in the number of neutrons leaving the rotor across plane P_2 until the complete closing of the shutter. Let us denote this period of decrease by t_3. During this period, since $t_3 = t_2$, the front of the neutrons has progressed in the direction x to a further distance s_1. The front is now in the position 4. Denoting the density of neutrons having velocity v by u, the number of neutrons passing the rotor is

$$N_1(v) = T_1(v)\, z_0\, u.$$

Calculating now the area $T_1(v)$ of the triangle of base width $2s_1$, we find

$$N_1(v) = Rhz_0 (1 - 2u + u^2) \qquad (0{,}5 \leqslant u \leqslant 1),$$

where the density of neutrons with velocity v_0 was taken to be equal to unity, thus $u = \dfrac{v_0}{r}$.

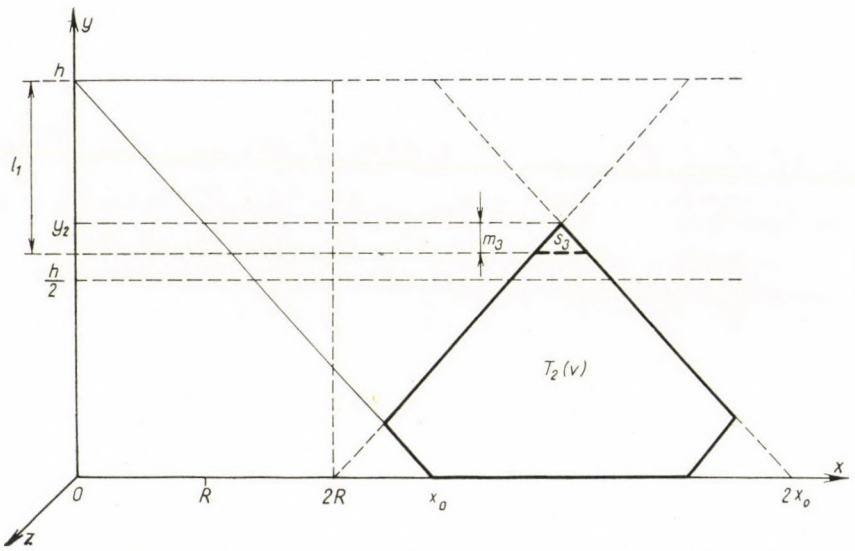

Fig. 3. The position of the neutrons with velocities $v \geqslant 2v_0$ transmitted by the rotor in the plane (x, y) at the time $t = t_0$

From similar geometrical considerations [4] the number of neutrons with velocity $v \geqslant 2v_0$ which have passed through the rotor (Fig. 3) is obtained as

$$N_2(v) = T_2(v)\, z_0\, u = Rhz_0 \left(\frac{1}{2} - u^2\right) \qquad (0 \leqslant u \leqslant 0{,}5)\,.$$

The number of the neutrons of infinite velocity transmitted by the rotor becomes

$$N(\infty) = \frac{1}{2} Rhz_0\,.$$

It follows from the above that the transmission function of the rotor has the form

$$f(u) = \frac{N(v)}{N(\infty)} = \begin{cases} 1 - 2u^2 & (0 \leqslant u \leqslant 0{,}5)\,, \\ 2 - 4u + 2u^2 & (0{,}5 \leqslant u \leqslant 1)\,, \end{cases}$$

illustrated in Fig. 4. The transmission function calculated by MOSTOVOI is also shown in the figure. The difference between the two curves is due to our neglecting the effect of "overtaking" [3] causing a further reduction in the number of neutrons. Since this fact does not affect appreciably the following calculations we shall consider the approximate value of $f(u)$ determined above.

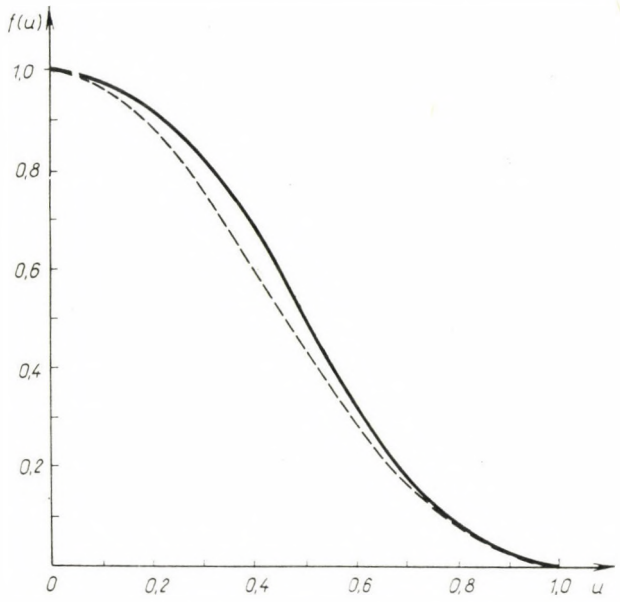

Fig. 4. The transmission function taking into account the "overtaking" effect (dotted line) and neglecting this effect (solid line)

III. The deformation of the transmission function

Let us now consider the cases in which the collimators placed in front and after the rotor are not precisely aligned or the placing of the detector is inadequate.

A misalignment of collimators or detector is equivalent to a good alignment in which a material opaque to neutrons is put into the corresponding place of the slit of the collimator. If this place is in the upper half of the slit it will be called upper screening, and lower screening if the lower half is covered (Fig. 5). Let us consider the transmission function in the above two cases. The effect of the intermediate and combined screenings can be calculated in a similar way.

Since the numbers of neutrons passing through the rotor are proportional to the areas $T_1(v)$ and $T_2(v)$ illustrated in Figs. 2 and 3, respectively, we have to determine the change in these areas due to screenings.

1. *Upper screening*

a) In the case of $v_0 \leqslant v \leqslant 2v_0$ even the screening of the whole upper half of the slit does not affect the number of neutrons passing through the rotor, since the height of the triangle of area $T_1(v)$ will not protrude into the upper half of the slit even if $v = 2v_0$ (Fig. 2).

b) If $v \geqslant 2v_0$, the screening l_1 cuts out of the area $T_2(v)$ a triangle of area $T_3(v)$ of base width s_3 and height m_3 (Fig. 3). For $l_1 \leqslant h - y_2$ the triangle $T_3(v) = 0$ and the neutrons with velocity v or less pass through the rotor without being reduced in number. On the other hand, if $l_1 > h - y_2$ we have $T_3(v) > 0$ and the number of neutrons with velocity v will be proportional to the area $T_2(v) - T_3(v)$.

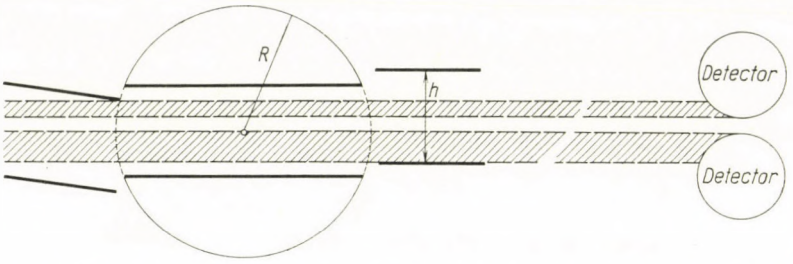

Fig. 5. Cross-sectional view of rotor, collimators and detector normal to the axis of rotation in the case of misalignment. Only the neutrons flying in the dashed strip can reach the counters

Introducing now $\alpha = \dfrac{2l_1}{h}$ to denote relative screening, the transmission function as altered by the upper screening l_1, has the form

$$f(U;u) = 1 - \frac{1}{2}\alpha^2 + 2\alpha u - 4u^2 \qquad \left(0 \leqslant u \leqslant \frac{\alpha}{2}\right).$$

2. *Lower screening*

a) In the case of $v_0 \leqslant v \leqslant 2v_0$ (Fig. 2) the area $T_1(v)$ is reduced by the screening l_2 to a triangle having an area $T_4(v)$ of base width s_4 and height m_4. The transmission function altered by the effect of the lower screening l_2 has the form

$$f(L;u) = \begin{cases} 2 - 4u + 2u^2 + \dfrac{1}{2}\alpha^2 - 2\alpha + 2\alpha u & \left(0{,}5 \leqslant u \leqslant 1 - \dfrac{\alpha}{2}\right), \\ 0 & \left(1 - \dfrac{\alpha}{2} \leqslant u \leqslant 1\right), \end{cases}$$

where $\alpha = \dfrac{2l_2}{h}$.

b) For $v \geqslant 2v_0$ (Figs. 6 and 7), we find

$$f(L;u) = \begin{cases} 1 - 2u^2 - \frac{1}{2}\alpha^2 - 2\alpha u & \left(0 \leqslant u \leqslant \frac{1-\alpha}{2}\right), \\ 2 - 4u + 2u^2 + \frac{1}{2}\alpha^2 - 2\alpha + 2\alpha u & \left(\frac{1-\alpha}{2} \leqslant u \leqslant 0{,}5\right). \end{cases}$$

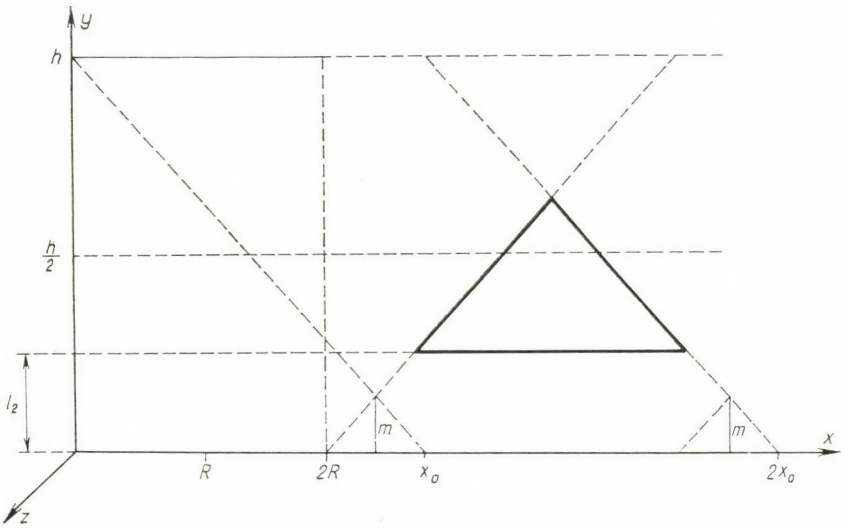

Fig. 6. The position of the neutrons with velocities $v \geqslant 2v_0$ transmitted by the rotor in the plane (x, y) at the time $t = t_0$ when a screening of size $l_2 \geqslant m$ was used (triangle shown by heavy line)

For $\alpha = 0{,}5$ and $\alpha = 1$ the functions $f(L; u)$, $f(U; u)$ as well as $f(u)$ are plotted in Fig. 8. It is apparent from the expressions as well as from the figure that while an upper screening affects the shape of the function $f(u)$ only in the range $0 \leqslant u \leqslant 0{,}5$, a lower screening changes the shape of the function $f(u)$ over its whole extent.

This phenomenon can be used for checking the alignment of the selector. If we compare the measured transmission curve with the theoretical one, the coincidence or difference of the two curves indicates the precision or inaccuracy of the alignment. It is advisable to measure the transmission function in either sense of rotation, since it may happen that for one sense of rotation a small upper screening exists, thus leaving the shape of the transmission function almost unaffected, although in the other sense of rotation it manifests itself as a lower screening to which the shape of the curve is much more sensitive. For satisfactory alignment the transmission functions measured in either sense

of rotation show the same shape. If the alignment is poor, usually two different transmission functions are obtained which permit to determine the character and extent of the misalignment.

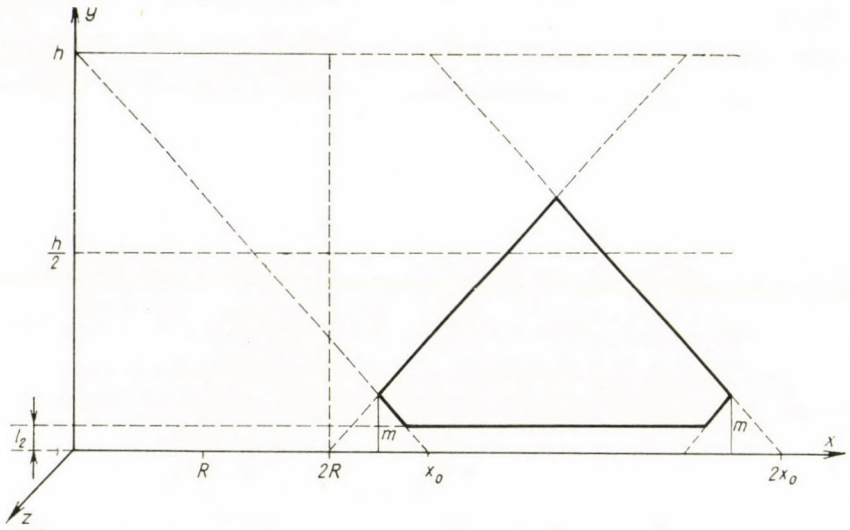

Fig. 7. The position of the neutrons with velocities $v \geqslant 2v_0$ transmitted by the rotor in the plane (x, y) at the time $t = t_0$ when a screening of size $l_2 < m$ was used (pentagon shown by heavy line)

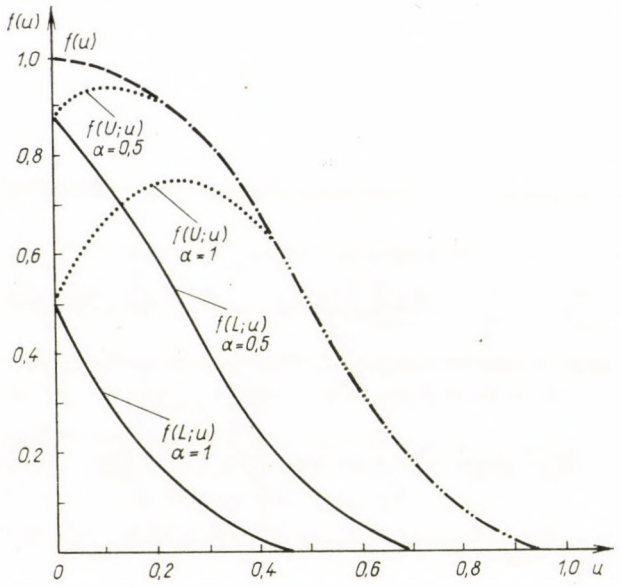

Fig. 8. Transmission curves in the case of lower and upper screenings corresponding to values of $\alpha = 0{,}5$ and $\alpha = 1$, respectively

IV. Experimental investigations

A slow chopper with straight slits [5] was used for the experimental check of the above results. The main features of the chopper are the following. The rotor is a 16 cm diameter bakelite disc. The rotor and the 30 cm long collimators placed before and after the rotor and fixed to the rotor housing, have each three slits of 2×20 mm^2 cross section for the passage of neutrons.

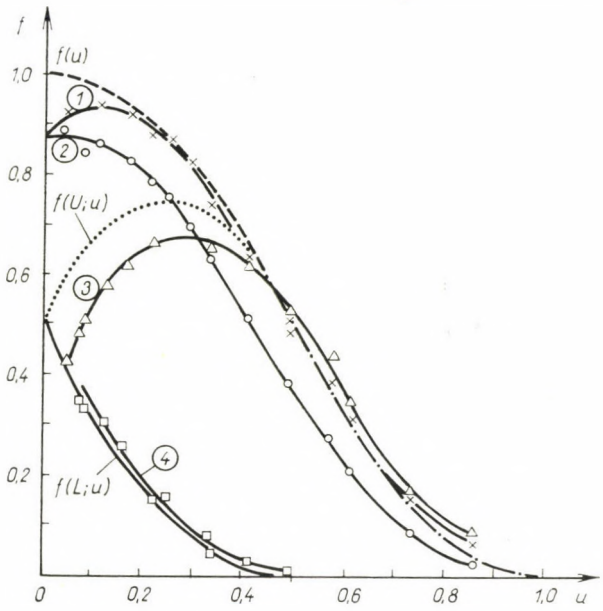

Fig. 9. Calculated and measured transmission functions

The detector consists of three counter tubes filled with BF_3 gas enriched in B^{10} and is placed vertically in the path of the neutron beam at 8 m distance from the rotor. The length of the counters covers the entire beam of neutrons transmitted by the slit of width $h = 2$ mm. In this way any deformation due to the detector was avoided in the transmission curve. The detector signals are passed to a 100-channel time analyser.

First the transmission functions of the chopper were measured rotating the rotor in either sense. Subsequently the transmission functions were measured with artificial screenings corresponding to $a = 1$.

The transmission function No. 1 (Fig. 9) was measured for the clockwise and the curve No. 2 for the anti-clockwise rotation of the rotor. The difference between the two curves indicates — considering the set of curves in Fig. 8 — that the slits of one of the collimators lie lower than the slits of the rotor in the fully opened position. Even the extent of the screening can be

calculated. We have to compute the ratio $f(U; u)$ to $f(L; u)$ for a given value of u and make it equal to the ratio obtained at the corresponding point of the measured curves. The value of a and from this the size of the screening, can be calculated from this equation. In the present case the size of the screening was found to be 0,12 mm.

The curves No. 3 and No. 4 to be seen in Fig. 9 have been measured by insertion of bakelite plates with $h = 1$ mm into the upper parts of the collimator slits and running the rotor first in one, then in the other sense, thus bringing about upper and lower screening, respectively. The shape of each curve is in good agreement with the calculated one. The deviation of the curve No. 3 from $f(U; u)$ is due to the 0,12 mm misalignment in the original setting.

REFERENCES

1. P. A. Egelstaff, J. Nucl. Energy, **1**, 57, 1954.
2. *В. И. Мостовой, М. И. Певзнер* и *А. П. Цитович*, Доклад на Женевской Конференции, **4**, 19, 1955.
3. P. Hraskó, KFKI Közl., **8**, 225, 1960.
4. I. Pavlicsek, T. Nagy and L. Nagy, KFKI Közl., **10**, 189, 1962.
5. L. Nagy, T. Nagy, L. Muzsnay and I. Pavlicsek, KFKI Közl., **8**, 203, 1960.

ФУНКЦИЯ ТРАНСМИССИИ НЕЙТРОННОГО ПРЕРЫВАТЕЛЯ С ПРЯМОЙ ЩЕЛЬЮ

Т. НАДЬ, И. ПАВЛИЧЕК и Л. НАДЬ

Резюме

На основе геометрических соображений выводится функция трансмиссии для нейтронного прерывателя, имеющего прямую щель. О разрегулированности можно судить по форме кривой трансмиссии, и измеренная форма дает возможность для локализации и определения любой ошибки в настройке. Правильность результатов вычисления доказывается экспериментально.

BERECHNUNG DER LICHTZERSTREUUNG MIT DOPPELTER FREQUENZ AUS DER SCHRÖDINGER-GLEICHUNG

Von

TH. NEUGEBAUER

INSTITUT FÜR THEORETISCHE PHYSIK DER ROLAND EÖTVÖS UNIVERSITÄT, BUDAPEST

(Vorgelegt von K. F. Novobátzky — Eingegangen: 14. IV. 1963)

Als Einleitung wird die Frage der Konvergenz der zeitabhängigen quantenmechanischen Störungsrechnung und das Problem der Brauchbarkeit der zweiten Näherung, auch im Fall in dem dieses Verfahren nicht mehr konvergent ist, kurz besprochen. Danach wird das Problem der Vereinigung von zwei Photonen gleicher Frequenz an Molekülen nach der skalaren Schrödingerschen Theorie berechnet. Unsere Formel (32) gibt das erhaltene Resultat an. Da bei diesem Verfahren der magnetische Vektor der Lichtwelle und relativistische Effekte unberücksichtigt bleiben, und es sich ausserdem um einen Effekt zweiter Ordnung handelt, so sind zwar die erhaltenen Resultate denen von dem Verfasser aus der Klein-Gordonschen Gleichung berechneten und denen in der folgenden Arbeit aus der auf das n-Teilchenproblem verallgemeinerten Diracgleichung hergeleiteten weitgehend analog, stimmen jedoch mit diesen nicht vollständig überein. Auf die bei diesem neuen Effekt auftretenden Auswahlregeln, Intensitätsfragen, Beobachtungsmöglichkeiten usw. wird in der vorliegenden Arbeit nicht eingegangen, weil diese am Ende des in diesem Heft folgenden Artikel ausführlich besprochen werden.

Einleitung

Ziel der vorliegenden Untersuchung ist die Berechnung der Intensität des mit doppelter Frequenz gestreuten Lichtes, um theoretische Richtlinien für den experimentellen Nachweis eines solchen Effektes angeben zu können. Die ersten theoretischen Untersuchungen bezüglich der Berechnung der Streuung von Licht an Licht, also der Wechselwirkung von zwei Lichtquanten im Vakuum, rühren von EULER und GOCKEL [1] her. In unserem Falle handelt es sich dagegen um die Wechselwirkung (die Vereinigung) von zwei Lichtquanten an Materie, also um einen Effekt, der um viele Grössenordnungen wahrscheinlicher ist.

Die erste Frage, die hier beantwortet werden muss, ist die, ob es überhaupt noch einen Sinn hat, die quantenmechanische Störungstheorie in diesem Falle (zeitabhängiges Problem) bis zur zweiten Näherung zu erweitern, bzw. ob dieses Verfahren noch konvergent ist. Diesbezüglich liegen erstens Untersuchungen von WILSON [2] vor, der gezeigt hat, dass in den meisten der von ihm untersuchten Fälle die zeitabhängige quantenmechanische Störungsrechnung, wenn auch nicht konvergent, so doch wenigstens asymptotisch ist, ganz ebenso wie das nach POINCARÉ bei der astronomischen Störungstheorie der Fall ist. Es ist übrigens eine bekannte Tatsache, dass einfache Näherungsmethoden oft auch dann noch brauchbare Resultate liefern, wenn die Anwend-

barkeitskriterien dieser Methoden nicht mehr erfüllt sind. Ein klassisches diesbezügliches Beispiel ist die Herleitung der Rutherfordschen Streuformel aus der Bornschen Näherung. Bezüglich dieser Frage seien die Untersuchungen von WIGNER [3], TREES [4], GOLDHAMMER und FEENBERG u. a. [5] erwähnt. Das bekannteste Beispiel für die Brauchbarkeit von semikonvergenten Reihen in der Physik sind jedenfalls die in der Theorie der Diffraktionserscheinungen benutzten halbkonvergenten Entwicklungen der Fresnelschen Integrale. Übrigens zeigt auch die Erfahrung, dass die zweite Näherung der quantenmechanischen Störungsrechnung mit der Erfahrung übereinstimmende Resultate liefert, wenigstens in dem Falle, in dem es sich um die Wechselwirkung von zwei Störungen handelt, und dabei die eine zeitunabhängig die andere dagegen zeitabhängig ist. Diesbezüglich seien die Theorien des diamagnetischen Faraday-effektes [6], des elektrooptischen Kerr-effektes [7] und die der Refraktionsverminderung von Elektrolytlösungen [8] erwähnt. Beim Kerreffekt handelt es sich eigentlich um eine Störung noch höherer Ordnung, weil dieser ja schon in der konstanten Feldintensität quadratisch ist. Besonders das Voigtsche Glied dieses Effektes (dessen Vorhandensein experimentell sichergestellt ist) ist ein typischer Effekt dritter Ordnung, kann also nur mit Hilfe der zweiten Näherung der Eigenfunktion berechnet werden. Ein Effekt zweiter Ordnung wäre ja schon der gewöhnliche (quadratische) Starkeffekt, doch handelt es sich dort um einen zeitunabhängigen Effekt, und ausserdem benützt man zu seiner Berechnung bei Atomspektren ein ganz spezielles mathematisches Verfahren.

Den erwähnten Effekt hat der Verfasser zuerst aus der Klein—Gordonschen Gleichung berechnet. Der theoretische Gedankengang, der zu dem Resultat führte, wurde bereits veröffentlicht [9]. Ausserdem wurde vom Verfasser die Lösung dieses Problems aus der gewöhnlichen skalaren Schrödingergleichung und aus der auf das n-Teilchenproblem verallgemeinerten Diracgleichung berechnet, die erhaltenen Resultate sind (ohne Herleitungen) ebenfalls erschienen [10].

Seit der Veröffentlichung der erwähnten Arbeiten des Verfassers haben sich viele Autoren mit dem Problem der Berechnung der Lichtzerstreuung mit doppelter Frequenz beschäftigt. Wir wollen hier in erster Linie die Arbeiten von KLEINMANN [11], BRAUNSTEIN [12], HENNEBERGER [13] und ARMSTRONG, BLOEMBERGEN, DUCUING und PERSHAN [14] erwähnen.

Im folgenden wollen wir die Herleitung des erwähnten Effektes aus der Schrödingergleichung angeben. In dem der vorliegenden Arbeit in diesem Heft folgenden Artikel werden wir die von der auf das n-Teilchenproblem verallgemeinerten Diracgleichung ausgehenden Berechnungen wiedergeben. Bekanntermeise erhält man in der gewöhnlichen Dispersionstheorie und in der Theorie der Lichtzerstreuung formal genau dieselben Resultate, von welcher der erwähnten Wellengleichungen man auch ausgeht. In unserem Problem

wird das dagegen, wie wir sehen werden, nicht mehr der Fall sein, weil in dieser Näherung das magnetische Feld der Lichtwelle und relativistische Effekte nicht mehr ganz unberücksichtigt bleiben können. Bezüglich der Berechnung aus der Diracschen Theorie wird hier der interessante Fall vorliegen, dass man ein Problem mit Hilfe der auf das n-Teilchenproblem verallgemeinerten Diracgleichung tatsächlich ganz durchrechnen kann.

§ 1

Um unser Problem nach der Schrödingerschen Theorie behandeln zu können, führen wir die folgenden Bezeichnungen ein: u' sei die (zeitabhängige) antisymmetrische Eigenfunktion unseres n-Körperproblems (des Atoms oder Moleküls), V die potentielle Energie des ganzen Systems, mit Δ bezeichnen wir die Summe der sich auf alle n Teilchen beziehenden Laplaceschen Operatoren und endlich mit $\mathfrak{E}_z = \mathfrak{E}_0 \cos 2\pi\nu t$ den elektrischen Vektor der einfallenden Lichtwelle. (Der magnetische Vektor bleibt nach diesem Verfahren unberücksichtigt.) Dann erhalten wir das folgende Störungsproblem:

$$\Delta u' - \frac{8\pi^2 m}{h^2}\left(V + e\sum_{a=1}^{n} z_a \mathfrak{E}_0 \cos 2\pi\nu t\right) u' - \frac{4\pi i m}{h}\frac{\partial u'}{\partial t} = 0\,. \tag{1}$$

Ganz allgemein können wir

$$u'_n = \psi'_n e^{\frac{2\pi i}{h} E_n t} \tag{2}$$

schreiben. Zur Lösung von (1) machen wir den bekannten Ansatz

$$u_n = u_0 + w, \tag{3}$$

wo u_0 die Eigenfunktion des ungestörten n-Körperproblems im Grundzustande bedeutet. Aus (1) und (3) folgt

$$\Delta w - \frac{8\pi^2 m}{h^2} V w - \frac{4\pi i m}{h}\frac{\partial w}{\partial t} = \frac{8\pi^2 m}{h^2} e(\Sigma z)\,\mathfrak{E}_0 \cos 2\pi\nu t\,.\; u_0$$

$$= \frac{4\pi^2 m}{h^2}\,\mathfrak{E}_0\, e\,(\Sigma z)\left\{e^{2\pi i\nu t} + e^{-2\pi i\nu t}\right\} u_0\,. \tag{4}$$

Nach der bekannten Methode sei

$$w = w_+ e^{2\pi i t\frac{E_0+h\nu}{h}} + w_- e^{2\pi i t\frac{E_0-h\nu}{h}}, \tag{5}$$

dann folgt aus (4) und (5), wenn wir noch zur Vereinfachung

$$w_\pm e^{2\pi i\frac{E_0}{h}t} = v_\pm \tag{6}$$

setzen

$$\Delta v_{\pm} - \frac{8\pi^2 m}{h^2} V v_{\pm} + \frac{8\pi^2 m}{h^2} \{E_0 \pm h\nu\} v_{\pm} = \frac{4\pi^2 m}{h^2} \mathfrak{E}_0 e(\Sigma z) \cdot u_0 . \tag{7}$$

Mit Hilfe der Reihenentwicklungen

$$v_{\pm} = \sum_k a_{k\pm} \psi_k \tag{8}$$

folgt weiter

$$v_+ = \frac{1}{2} e \mathfrak{E}_0 \sum_k{}' \frac{\int u_0 \Sigma z \bar{u}_k d\tau}{h\{-\nu(k0) + \nu\}} \cdot u_k \tag{9}$$

und

$$v_- = \frac{1}{2} e \mathfrak{E}_0 \sum_k{}' \frac{\int u_0 \Sigma z \bar{u}_k d\tau}{h(-\nu(k0) - \nu\}} \cdot u_k , \tag{10}$$

wo wir die Bezeichnung $E_k - E_0 = h\nu(k0)$ eingeführt haben. Die bei dem Übergange von einem angeregten in den Grundzustand emittierten Frequenzen werden also positiv.

Für die ganze gestörte Eigenfunktion erhalten wir daher das bekannte Resultat

$$u' = u_0 + \frac{1}{2} \mathfrak{E}_0 e \sum_k{}' \int u_0 \Sigma z \bar{u}_k d\tau \left[\frac{e^{2\pi i \nu t}}{h\{-\nu(k0) + \nu\}} + \frac{e^{-2\pi i \nu t}}{h\{-\nu(k0) - \nu\}} \right] u_k . \tag{11}$$

Der Eigenwertet ändert sich in erster Näherung nicht, weil es — abgesehen von Ausnahmsfällen — keinen linearen Starkeffekt gibt.

Jetzt wollen wir die zweite Näherung berechnen. Es sei

$$u' = u_0 + \frac{1}{2} \mathfrak{E}_0 e \sum_k{}' \int u_0 \Sigma z \bar{u}_k d\tau \left[\frac{e^{2\pi i \nu t}}{h\{-\nu(k0) + \nu\}} + \frac{e^{-2\pi i \nu t}}{h\{-\nu(k0) - \nu\}} \right] u_k + f. \tag{12}$$

Setzen wir (12) in (1) ein, so folgt, wenn wir Glieder bis zur zweiten Ordnung behalten

$$\Delta f - \frac{8\pi^2 m}{h^2} V f - \frac{4\pi i m}{h} \frac{\partial f}{\partial t}$$

$$= \frac{8\pi^2 m}{h^2} \mathfrak{E}_0 e (\Sigma z) \cos 2\pi \nu t \cdot \frac{1}{2} \mathfrak{E}_0 e \sum_k{}' \int u_0 \Sigma z \bar{u}_k d\tau \left[\frac{e^{2\pi i \nu t}}{h\{-\nu(k0) + \nu\}} + \right.$$

$$\left. + \frac{e^{-2\pi i \nu t}}{h\{-\nu(k0) - \nu\}} \right] u_k . \tag{13}$$

Berücksichtigen wir noch in (13), dass $\cos 2\pi\nu t = \frac{1}{2}\left\{e^{2\pi i\nu t} + e^{-2\pi i\nu t}\right\}$ ist, so folgt weiter

$$\Delta f - \frac{8\pi^2 m}{h^2} Vf - \frac{4\pi i m}{h}\frac{\partial f}{\partial t}$$

$$= \frac{8\pi^2 m}{h^2}\mathfrak{E}_0^2 e^2 \frac{1}{4}(\Sigma z)\sum_k{}' \int u_0 \Sigma z\, \bar{u}_k\, d\tau \left[\frac{e^{4\pi i\nu t}}{h\{-\nu(k0)+\nu\}} + \frac{1}{h\{-\nu(k0)+\nu\}} + \right.$$

$$\left. + \frac{e^{-4\pi i\nu t}}{h\{-\nu(k0)-\nu\}} + \frac{1}{h\{-\nu(k0)-\nu\}}\right] u_k$$

$$= \frac{8\pi^2 m}{h^2}\mathfrak{E}_0^2 e^2 \sum_k{}' \left[\frac{e^{4\pi i\nu t}}{h\{-\nu(k0)+\nu\}} + \frac{e^{-4\pi i\nu t}}{h\{-\nu(k0)-\nu\}} - \right.$$

$$\left. - \frac{2\nu(k0)}{h\{\nu^2(k0)-\nu^2\}}\right]\frac{1}{4}(\Sigma z)\int u_0 \Sigma z\, \bar{u}_k\, d\tau \cdot u_k . \tag{14}$$

Zur Lösung dieser Differentialgleichung zerlegen wir f in drei Glieder

$$f = f_1 e^{4\pi i\nu t} + f_2 e^{-4\pi i\nu t} + f_3 \tag{15}$$

Da die linke Seite von (14) in f linear ist, so zerfällt unsere Gleichung mit diesem Ansatz in drei Differentialgleichungen. Es sei weiter

$$f = f_{10} e^{2\pi i t\frac{E_0+2h\nu}{h}} + f_{20} e^{2\pi i t\frac{E_0-2h\nu}{h}} + f_{30} e^{2\pi i t\frac{E_0}{h}} . \tag{16}$$

f_{10}, f_{20} und f_{30} entwickeln wir jetzt nach den ungestörten Eigenfunktionen:

$$f_{10} = \sum_l b_l \psi_l , \quad f_{20} = \sum_l c_l \psi_l \quad \text{und} \quad f_{30} = \sum_l d_l \psi_l . \tag{17}$$

Dann haben wir z. B.

$$\sum b_l h\{-\nu(l0)+2\nu\}\psi_l = \frac{1}{4}\mathfrak{E}_0^2 e^2 \sum_k{}' \int u_0 \Sigma z\, \bar{u}_k\, d\tau .$$

$$\cdot e^{-2\pi i t\frac{E_0}{h}} \cdot \frac{1}{h\{-\nu(k0)+\nu\}}(\Sigma z)\, u_k \tag{18}$$

und daraus folgt mit Hilfe der bekannten Fourierartigen Methode für die b_l

$$b_l = \frac{1}{4}\mathfrak{E}_0^2 e^2 \sum_k{}' \frac{\int u_0 \Sigma z\, \bar{u}_k\, d\tau \cdot \int u_k \Sigma z\, \bar{\psi}_l\, d\tau}{h^2\{-\nu(k0)+\nu\}\cdot\{-\nu(l0)+2\nu\}} e^{-2\pi i t\frac{E_0}{h}} \tag{19}$$

und weiter endlich für f_{10}

$$f_{10} = \frac{1}{4}\mathfrak{E}_0^2 e^2 \sum_{\substack{k,\,l \\ k\neq l}}' \frac{\int u_0 \Sigma z\, \bar{u}_k\, d\tau \cdot \int u_k \Sigma z\, \bar{u}_l\, d\tau}{h^2\{-\nu(k0)+\nu\}\cdot\{-\nu(l0)+2\nu\}}\, e^{-2\pi i t \frac{E_0}{h}} \cdot u_l . \tag{20}$$

Analog erhalten wir

$$f_{20} = \frac{1}{4}\mathfrak{E}_0^2 e^2 \sum_{\substack{k,\,l \\ k\neq l}}' \frac{\int u_0 \Sigma z\, \bar{u}_k\, d\tau \cdot \int u_k \Sigma z\, \bar{u}_l\, d\tau}{h^2\{-\nu(k0)-\nu\}\cdot\{-\nu(l0)-2\nu\}}\, e^{-2\pi i t \frac{E_0}{h}} \cdot u_l \tag{21}$$

und

$$f_{30} = \frac{1}{4}\mathfrak{E}_0^2 e^2 \sum_{\substack{k,\,l \\ k\neq l}}' 2\, \frac{\nu(k0)\int u_0 \Sigma z\, \bar{u}_k\, d\tau \cdot \int u_k \Sigma z\, \bar{u}_l\, d\tau}{h^2\{\nu^2(k0)-\nu^2\}\,\nu(l0)}\, e^{-2\pi i t \frac{E_0}{h}} \cdot u_l . \tag{22}$$

In zweiter Näherung erhalten wir also für die ganze Eigenfunktion aus (3), (5), (11), (16), (20), (21) und (22)

$$u' = u_0 + \frac{1}{2}\mathfrak{E}_0\, e \sum_k' \int u_0 \Sigma z\, \bar{u}_k\, d\tau \left[\frac{e^{2\pi i\nu t}}{h\{-\nu(k0)+\nu\}} + \frac{e^{-2\pi i\nu t}}{h\{-\nu(k0)-\nu\}}\right] u_k$$

$$+ \frac{1}{4}\mathfrak{E}_0^2 e^2 \sum_{\substack{k,\,l \\ k\neq l}}' \int u_0 \Sigma z\, \bar{u}_k\, d\tau \cdot \int u_k \Sigma z\, \bar{u}_l\, d\tau \left[\frac{e^{4\pi i\nu t}}{h^2\{-\nu(k0)+\nu\}\cdot\{-\nu(l0)+2\nu\}} + \right.$$

$$\left. + \frac{e^{-4\pi i\nu t}}{h^2\{-\nu(k0)-\nu\}\cdot\{-\nu(l0)-2\nu\}} + \frac{2\nu(k0)}{h^2\{\nu^2(k0)-\nu^2\}\,\nu(l0)}\right] u_l . \tag{23}$$

Diese gestörte Eigenfunktion ist noch nicht normiert. Die ungestörten Eigenfunktionen haben wir zwar in unseren Berechnungen als normiert angenommen, daraus folgt jedoch noch nicht, dass auch die gestörten normiert sind. Für die Eigenfunktion in erster Näherung ist das zwar tatsächlich der Fall, wie man das ausgehend von der Normiertheit der Eigenfunktionen des ungestörten Problems leicht zeigen kann. Für die zweite Näherung verlangt die Normierungsbedingung erstens, dass im dritten Gliede von (23) $k \neq l$ sein soll. In unserem Problem ist jedoch diese Bedingung automatisch erfüllt, weil im Falle von $k = l$ das eine Matrizenelement in diesem Gliede verschwindet. Diesen Tatbestand kann man auch so ausdrücken, dass er eine Folge davon ist, dass es abgesehen von Ausnahmsfällen (die jedoch bezüglich unseres Problems ganz uninteressant sind) keinen linearen Starkeffekt gibt. Zweitens würde eben wegen der Normierung zu (23) noch das Glied

$$-\frac{1}{2}\sum_k' \left|\mathfrak{E}_0\, e \int u_0 \Sigma z\, \bar{u}_k\, d\tau \left[\frac{e^{2\pi i\nu t}}{h\{-\nu(k0)+\nu\}} + \frac{e^{-2\pi i\nu t}}{h\{-\nu(k0)-\nu\}}\right]\right|^2 u_0 \tag{23a}$$

hinzutreten. Da jedoch in der betrachteten Näherung (23a) nicht das Auftreten von weiteren Gliedern in p_q verursachen würde, so wollen wir hier nicht weiter auf diese Frage eingehen.

Endlich folgt aus (23) für das ganze induzierte Moment (ebenfalls in zweiter Näherung)

$$
\begin{aligned}
-p_q = e\int u'\,\Sigma\, q\,\bar{u}'\,d\tau &= \int u_0\,\Sigma\, q\,\bar{u}_0\,d\tau \\
&+ \mathfrak{E}_0\,e^2 \sum_k{}' \int u_0\,\Sigma\, z\,\bar{u}_k\,d\tau \cdot \int u_k\,\Sigma\, q\,\bar{u}_0\,d\tau \left[\frac{1}{h\{-\nu(k0)+\nu\}} + \right. \\
&\left. + \frac{1}{h\{-\nu(k0)-\nu\}}\right] \cos 2\pi\nu t \\
+\frac{1}{4}\mathfrak{E}_0^2\,e^3 \sum_{\substack{k,\,l\\ k\neq l}}{}' \int u_0\,\Sigma\, z\,\bar{u}_k\,d\tau \cdot \int u_k\,\Sigma\, z\,q\,\bar{u}_l\,d\tau \cdot \int u_l\,\Sigma\, z\,\bar{u}_0\,d\tau &\left[\frac{1}{h^2\{-\nu(k0)+\nu\}\cdot\{-\nu(l0)+\nu\}}\right. \\
+ \frac{1}{h^2\{-\nu(k0)-\nu\}\cdot\{-\nu(l0)-\nu\}} &+ \frac{e^{4\pi i\nu t}}{h^2\{-\nu(k0)+\nu\}\cdot\{-\nu(l0)-\nu\}} + \\
&\left. + \frac{e^{-4\pi i\nu t}}{h^2\{-\nu(k0)-\nu\}\cdot\{-\nu(l0)+\nu\}}\right] \\
+\frac{1}{4}\mathfrak{E}_0^2\,e^3 \sum_{\substack{k,\,l\\ k\neq l}}{}' \int u_0\,\Sigma\, z\,\bar{u}_k\,d\tau \cdot \int u_k\,\Sigma\, z\,\bar{u}_l\,d\tau \cdot \int u_l\,\Sigma\, q\,\bar{u}_0\,d\tau &\left\{\left[\frac{1}{h^2\{-\nu(k0)+\nu\}\cdot\{-\nu(l0)+2\nu\}}\right.\right. \\
&\left. + \frac{1}{h^2\{-\nu(k0)-\nu\}\cdot\{-\nu(l0)-2\nu\}}\right] 2\cos 4\pi\nu t + \\
&\left. + \frac{4\nu(k0)}{h^2\{\nu^2(k0)-\nu^2\}\,\nu(l0)}\right\}. \qquad (24)
\end{aligned}
$$

Das ganze vierte Glied von (24) kann man auch noch folgendermassen schreiben:

$$
\begin{aligned}
&\frac{1}{4}\mathfrak{E}_0^2\,e^3 \sum_{k,\,l}{}' \int u_0\,\Sigma\, z\,\bar{u}_k\,d\tau \cdot \int u_k\,\Sigma\, z\,\bar{u}_l\,d\tau \cdot \int u_l\,\Sigma\, q\,\bar{u}_0\,d\tau \qquad (25)\\
&\cdot\left[\frac{\{2\nu(k0)\,\nu(l0)+4\nu^2\}\,2\cos 4\pi\nu t}{h^2\{\nu^2(k0)-\nu^2\}\cdot\{\nu^2(l0)-4\nu^2\}} + \frac{4\nu(k0)}{h^2\{\nu^2(k0)-\nu^2\}\,\nu(l0)}\right].
\end{aligned}
$$

Im dritten Gliede von (24) stehen in der eckigen Klammer die zeitabhängigen Glieder

$$
\frac{e^{4\pi i\nu t}}{h^2\{-\nu(k0)+\nu\}\cdot\{-\nu(l0)-\nu\}} \text{ und } \frac{e^{-4\pi i\nu t}}{h^2\{-\nu(k0)-\nu\}\cdot\{-\nu(l0)+\nu\}}, \qquad (26)
$$

die mit dem Faktor

$$
\int u_0\,\Sigma\, z\,\bar{u}_k\,d\tau \cdot \int u_k\,\Sigma\, q\,\bar{u}_l\,d\tau \cdot \int u_l\,\Sigma\, z\,\bar{u}_0\,d\tau \qquad (27)
$$

multipliziert sind.

Dieses Produkt ist gegen eine Vertauschung von k und l unempfindlich.

Betrachten wir jetzt die in (26) stehenden Glieder and addieren wir zu dem ersten Gliede, das zu einem beliebigen Paare von k und l gehört, ein zweites, in dem k und l miteinander vertauscht sind, so erhalten wir

$$\frac{1}{h^2\{-\nu(k0)+\nu\}\cdot\{-\nu(l0)-\nu\}}\,2\cos 4\pi\nu t, \tag{28}$$

In einer analogen Weise folgt, wenn wir das zweite Glied in (26) mit einem solchen ersten zusammenziehen, in dem ebenfalls k und l vertauscht sind

$$\frac{1}{h^2\{-\nu(k0)-\nu\}\cdot\{-\nu(l0)+\nu\}}\,2\cos 4\pi\nu t. \tag{29}$$

Addieren wir jetzt (28) und (29), so folgt

$$\frac{2\nu(k0)\,\nu(l0)-2\nu^2}{h^2\{\nu^2(k0)-\nu^2\}\cdot\{\nu^2(l0)-\nu^2\}}\,2\cos 4\pi\nu t. \tag{30}$$

Dieser Ausdruck ist wieder gegenüber einer Vertauschung von k und l invariant, und deshalb können wir endlich das dritte Glied von (24) folgendermassen schreiben:

$$\frac{1}{4}\mathfrak{E}_0^2 e^3 \sum_{\substack{k,l\\k\neq l}}{}' \int u_0 \Sigma z\,\bar{u}_k\,d\tau\cdot\int u_k\,\Sigma q\,\bar{u}_l\,d\tau\cdot\int u_l\,\Sigma z\,\bar{u}_0\,d\tau\cdot$$
$$\cdot\frac{2\nu(k0)\,\nu(l0)+2\nu^2+[2\nu(k0)\,\nu(l0)-2\nu^2]\cos 4\pi\nu t}{h^2\{\nu^2(k0)-\nu^2\}\cdot\{\nu^2(l0)-\nu^2\}} \tag{31}$$

Aus (24), (25) und (31) erhalten wir also für das induzierte Moment die endgültige Formel

$$-p_q = e\int u'\,\Sigma q\,\bar{u}'\,d\tau = e\int u_0\,\Sigma q\,\bar{u}_0\,d\tau$$
$$-\mathfrak{E}_0 e^2 \sum_k{}'\int u_0\,\Sigma z\,\bar{u}_k\,d\tau\cdot\int u_k\,\Sigma q\,\bar{u}_0\,d\tau\,\frac{2\nu(k0)}{h\{\nu^2(k0)-\nu^2\}}\cos 2\pi\nu t$$
$$+\frac{1}{4}\mathfrak{E}_0^2 e^3 \sum_{\substack{k,l\\k\neq l}}{}'\int u_0\,\Sigma z\,\bar{u}_k\,d\tau\cdot\int u_k\,\Sigma q\,\bar{u}_l\,d\tau\cdot\int u_l\,\Sigma z\,\bar{u}_0\,d\tau$$
$$\cdot\frac{2\nu(k0)\,\nu(l0)+2\nu^2+[2\nu(k0)\,\nu(l0)-2\nu^2]\cos 4\pi\nu t}{h^2\{\nu^2(k0)-\nu^2\}\cdot\{\nu^2(l0)-\nu^2\}}$$
$$+\frac{1}{4}\mathfrak{E}_0^2 e^3 \sum_{\substack{k,l\\k\neq l}}{}'\int u_0\,\Sigma z\,\bar{u}_k\,d\tau\cdot\int u_k\,\Sigma z\,\bar{u}_l\,d\tau\cdot\int u_l\,\Sigma q\,\bar{u}_0\,d\tau$$
$$\cdot\left\{\frac{[2\nu(k0)\,\nu(l0)+4\nu^2]2\cos 4\pi\nu t}{h^2\{\nu^2(k0)-\nu^2\}\cdot\{\nu^2(l0)-(2\nu)^2\}}+\frac{4\nu(k0)}{h^2\{\nu^2(k0)-\nu^2\}\,\nu(l0)}\right\}. \tag{32}$$

§ 2

Um die Lichtzerstreuung mit doppelter Frequenz aus der Klein—Gordonschen Gleichung, oder richtiger ausgedrückt aus der Schrödingergleichung ergänzt durch die aus der Klein—Gordonschen Gleichung folgenden und das Vektorpotential enthaltenden Gieder, berechnen zu können, muss zuerst das Vektorpotential

$$\mathfrak{A} = \mathfrak{A}_z = -\frac{c\,\mathfrak{E}_0}{2\pi\nu}\sin 2\pi\nu\left(t-\frac{x}{c}\right) \tag{33}$$

eingeführt werden. Tatsächlich erhält man aus (33)

$$\mathfrak{E}_z = \mathfrak{E}_0 \cos 2\pi\nu\left(t-\frac{x}{c}\right) \tag{34}$$

und

$$\mathfrak{H}_y = -\mathfrak{E}_0 \cos 2\pi\nu\left(t-\frac{x}{c}\right). \tag{35}$$

Setzen wir (33) als Störglied in die erwähnte Gleichung ein, so erhalten wir die gestörte Differentialgleichung

$$\Delta u - \frac{4\pi i m}{h}\frac{\partial u}{\partial t} - \frac{8\pi^2 m}{h^2}(E_0+U)\,u = \frac{2ie}{h\nu}\mathfrak{E}_0 \sin 2\pi\nu\left(t-\frac{x}{c}\right)\cdot\frac{\partial u}{\partial z}. \tag{36}$$

$E_0 = mc^2$ ist hier die Ruheenergie des Elektrons und U bedeutet die potentielle Energie. Die weiteren Rechnungen sind denen, die im § 1 von (1) zu (32) geführt haben, weitgehend analog [9], und man erhält ein zu (32) ähnliches, jedoch damit nicht ganz übereinstimmendes Resultat; da diese letztere Formel jedoch formal vollständig mit der in der folgenden Arbeit aus der Diracschen Theorie hergeleiteten übereinstimmt, so wollen wir hier nicht näher darauf eingehen. Vollständigkeitshalber sei nur noch erwähnt, dass wir bei der zitierten Berechnung aus der Klein—Gordonschen Gleichung das entgegengesetzte Vorzeichen für die Eigenfrequenzen benützt haben, woraus sich das ebenfalls entgegensetzte Vorzeichen im zweiten Gliede unserer Formel (32) und der Formel (58) in der erwähnten Arbeit erklärt.

Auf die bei dem neuen Effekt auftretenden Auswahlregeln, Intensitätsfragen, Beobachtungsmöglichkeiten (besonders mit Hilfe der modernen Lasertechnik) usw. wollen wir hier nicht eingehen, weil diese am Ende der in diesem Heft folgenden Arbeit ausführlich besprochen werden und weil sie ohne jede Änderung auch auf die aus unserer Formel (32) hergeleiteten Resultate anwendbar sind.

LITERATUR

1. H. Euler und B. Gockel, Die Naturwiss., **23,** 246, 1935, H. Euler, Ann. d. Phys. (5) **26,** 398, 1936 und J. Mc. Kenna und P. M. Platzman, Phys. Rev. **129,** 2354, 1963. Vgl. auch R. Karplus und M. Neuman, Phys. Rev., **83,** 776, 1951.
2. H. A. Wilson, Proc. Roy. Soc. London, A **122,** 589, 1929; Vgl. auch P. A. M. Dirac, ebenda **112,** 661, 1926; **114,** 243, 1927; **114,** 710, 1927; und W. Heisenberg, Ann. d. Phys., **9,** 338, 1931.
3. E. P. Wigner, Phys. Rev., **94,** 77, 1954.
4. R. E. Trees, Phys. Rev., **102,** 1553, 1956.
5. P. Goldhammer und E. Feenberg, Phys. Rev., **101** 1233, 1956;
   A. Dalgarno, Proc. Phys. Soc. A. **69,** 784,1956.
   E. Feenberg und P. Goldhammer, Phys. Rev., 105, 750, 1957;
   R. C. Young, L. C. Biedenharn und E. Feenberg, ebenda **106,** 1151, 1957;
   G. Speisman, ebenda, **107,** 1180, 1957.
6. R. de L. Kronig, Z. Physik, **45,** 458, 1927; **47,** 702, 1928;
   L. Rosenfeld, Z. Physik, **57,** 835, 1929;
   R. Serber, Phys. Rev., **41,** 489, 1932.
7. Th. Neugebauer, Z. Physik **73,** 386, 1931, **82,** 660, 1933, **86,** 392, 1933 und **119,** 114, 1942; Acta Phys. Hung. **1,** 167, 1951.
8. Th. Neugebauer, Z. Physik, **99,** 677, 1936; Math u. Naturwiss. Anzeiger d. ung. A. d. Wiss., **56,** 443, 1937.
9. Th. Neugebauer, Acta Phys. Hung., **10,** 221, 1959.
10. Th. Neugebauer, Z. Physik, **155,** 380, 1959.
11. D. A. Kleinman, Phys. Rev., **125,** 87, 19 62, vgl. auch **126,** 1977, 1962 und **128,** 1761, 1962. (Klassische Berechnung des in nichtlinearen dielektrischen Medien auftretenden Effektes).
12. R. Braunstein, Phys. Rev., **125,** 475, 1962.
13. W. C. Henneberger, Bull. Am. Phys. Soc., **7,** 14, 1962. (Berechnung des Effektes aus der Quantenelektrodynamik.)
14. J. A. Armstrong, N. Bloembergen, J. Ducuing und P. S. Pershan, Phys. Rev., **127,** 1918, 1962; N. Bloembergen und P. S. Pershan, ebenda **128,** 606, 1962 und P. S. Pershan, ebenda **130,** 919, 1963.

ВЫЧИСЛЕНИЕ РАССЕЯНИЯ СВЕТА С ДВОЙНОЙ ЧАСТОТОЙ НА ОСНОВЕ УРАВНЕНИЯ ШРЕДИНГЕРА

Т. НАЙГЕБАЕР

Резюме

В введении в первую очередь рассматривается вопрос сходимости зависящегося от времени квантовомеханического пертурбационного исчисления. Далее уделяется внимание проблеме о применимости второго приближения в случае, когда приём не даёт сходящихся результатов. После этого на основании скалярного и нерелятивистского уравнения Шредингера дискутируется вопрос вероятности соединения двух фотонов на молекулах. Полученный результат содержится в уравнении (32). Так как в данном методе, с одной стороны, вектор магнитного поля света и релятивистские эффекты не принимаются во внимание, и речь идёт о второстепенных эффектах, с другой, полученные результаты хотя и аналогичны вычисленным автором на основе теории Клейна—Гордона и вычисленным здесь данным, которые в следующей за данной работой статье обобщены в теории Дирака для проблемы n-частиц, но полностью с ними они не совпадают. Появляющиеся при этом новом эффекте правила отбора, условия интенсивностей и возможности экспериментального наблюдения не дискутируются в данной работе, так как они являются предметом подробного анализа, даваемого автором в конце следующей его работы. Выведённые в упомянутой работе результаты могут быть перенесены без каких-либо изменений и на полученные здесь данные.

BERECHNUNG DER LICHTZERSTREUUNG MIT DOPPELTER FREQUENZ AUS DER AUF DAS n-TEILCHENPROBLEM VERALLGEMEINERTEN DIRACGLEICHUNG

Von

TH. NEUGEBAUER

INSTITUT FÜR THEORETISCHE PHYSIK DER ROLAND EÖTVÖS UNIVERSITÄT, BUDAPEST

(Vorgelegt von K. F. Novobátzky — Eingegangen: 14. IV. 1963)

Die Vereinigung von zwei Photonen gleicher Frequenz an Materie wird aus der auf ein n-Körperproblem verallgemeinerten Diracschen Theorie berechnet, wobei der seltene Fall vorliegt, dass man ein Problem nach dieser Theorie tatsächlich ganz durchrechnen kann. Die Resultate enthalten die Formeln (54) und (57). Danach wird gezeigt, dass auch die in $\mathfrak{E}_0$ quadratischen und dabei zeitunabhängigen Glieder eine physikalische Realität besitzen. Im § 2 werden die Grössenordnungen der Intensitäten der Rayleighstreuung und die der Streuung mit doppelter Frequenz miteinander verglichen, und es wird die Frage besprochen, wie die streuenden Moleküle und die Versuchsbedingungen zu wählen sind, damit der neu berechnete Effekt möglichst gross wird. Am wichtigsten ist dabei das in (57) unterstrichene Glied, welches eine Resonanzverstärkung des neuen Effektes ohne gleichzeitige Verstärkung der Rayleighstreuung ermöglicht. Zuletzt (§ 3) werden noch die Auswahlregeln für die Doppelfrequenzstreuung hergeleitet. Bei Atomen, zweiatomigen homonuklearen Molekülen und symmetrisch gebauten mehratomigen Molekülen verschwindet der Effekt exakt. Am stärksten »doppelfrequenzaktiv« sind dagegen ganz unsymmetrische, mehratomige Moleküle. Mit Hilfe des optischen Masers ist es tatsächlich schon gelungen, das Auftreten des neuen Effektes an zusammenhängender Materie nachzuweisen, theoretisch am interessantesten wäre selbstverständlich der an Molekülen auftretende Effekt, wozu in erster Linie ebenfalls die Lasertechnik die experimentelle Möglichkeit gibt.

Einleitung

In der vorangehenden Arbeit wurde die Lichtzerstreuung mit doppelter Frequenz ausgehend von der skalaren und nichtrelativistischen Schrödingergleichung berechnet. Ziel des vorliegenden Artikels ist es dasselbe Problem nach der auf das n-Teilchenproblem verallgemeinerten Diracgleichung zu behandeln. Es sei gleich bemerkt, dass hier der ganz einzigartige Fall vorliegt, dass es tatsächlich möglich ist, ein Problem nach der auf das n-Teilchenproblem verallgemeinerten Diracschen Theorie ganz durchzurechnen. Die erhaltenen Resultate wurden vom Verfasser ohne deren Herleitung bereits veröffentlicht [1]. In der vorliegenden Arbeit soll die Rechnung, welche zu der erwähnten Formel geführt hat, ausführlich besprochen und ausserdem am Ende der Arbeit die experimentellen Methoden, die zum Nachweis des neuen Effektes dienen können, kritisch betrachtet werden. Die moderne Lasertechnik liefert eine ganz ideale Möglichkeit dazu.

§ 1

Für ein Teilchen lautet die Diracsche Gleichung in den gewohnten Bezeichnungen

$$\left[p_0 + \sum_{k=xyz} \alpha_k p_k + cm\,\alpha_4\right] u = 0\,, \tag{1}$$

wo

$$p_0 = -\frac{h}{2\pi ic}\frac{\partial}{\partial t} + \frac{e}{c}A \tag{2}$$

und

$$p_k = \frac{h}{2\pi i}\frac{\partial}{\partial k} + \frac{e}{c}A_k \tag{3}$$

ist. A bedeutet das skalare Potential und die A_k die Komponenten des Vektorpotentials.

Für ein allgemeines n-Teilchenproblem kann man bekannterweise die Diracsche Gleichung folgendermassen verallgemeinern:

$$\left[p_0 + \sum_{a=1}^{n}\sum_{k=x,y,z}\alpha_k^{(a)}p_k^{(a)} + c\sum_{a=1}^{n}m_a\alpha_4^{(a)} + B\right]u = 0\,. \tag{4}$$

Hier bedeuten

$$p_0 = -\frac{h}{2\pi ic}\frac{\partial}{\partial t} + \frac{e}{c}\sum_{a=1}^{n}A^{(a} \tag{5}$$

und

$$p_k^{(a)} = \frac{h}{2\pi i}\frac{\partial}{\partial k_{(a)}} + \frac{e}{c}A_k^{(a)}, \tag{6}$$

wo $A^{(a)}$ und die $A_k^{(a)}$ das skalare und die Komponenten des Vektorpotentials am Orte des a-ten Teilchens bedeuten. Die Wechselwirkungen der zu dem System gehörenden Teilchen haben wir alle im Operator B zusammengefasst; dieser enthält also erstens sämtliche Glieder, die von den skalaren Potentialen, die von den Ladungen der einzelnen Teilchen verursacht sind, herrühren, also den Ausdruck

$$\frac{e}{2c}\sum_{a=1}^{n}A_0^{(a)} = -\frac{e^2}{2c}\sum_{a,b}^{n}\frac{1}{r_{ab}}, \tag{7}$$

den wir auch noch zu (5) hätten schreiben können und ausserdem die übrigen Wechselwirkungen dieser Teilchen. Auf das Problem der expliziten Form dieser Glieder, das wie bekannt, ein recht verwickeltes Problem ist, kommen wir noch zurück.

Die Eigenfunktion u hat hier 4^n Komponenten. Die Matrizendifferentialgleichung entspricht also einem aus 4^n Gleichungen bestehenden Differentialgleichungssystem. Wir haben z. B.

$$(\alpha_k^{al}\psi)_{b_1 b_2 \ldots b_n} = \sum_{\lambda=1}^{4}(\alpha_k^{al})_{b_l\lambda}\psi_{b_1 b_2 \ldots b_{l-1}\lambda b_{l+1}\ldots b_n}\,. \tag{8}$$

Die elektrische Dichte ist hier folgendermassen definiert

$$\varrho = n\,\varrho' = -\,ne\,\overline{\psi}\psi = -\,ne \sum_{b_1 b_2 \ldots b_n = 1}^{4} \overline{\psi}_{b_1 b_2 \ldots b_n} \psi_{b_1 b_2 \ldots b_n} . \tag{9}$$

Diese Summe besteht aus 4^n Gliedern.

Für die Stromkomponenten haben wir

$$j_k^{(a_l)} = ce\,\overline{\psi}\alpha_k^{(a_l)}\psi\,, \quad u = \psi\, e^{-2\pi i \frac{W}{n} t} . \tag{10}$$

Hier bedeutet k eine der drei Raumkoordinaten und a_l das betreffende Teilchen, zu dem die Stromkomponente gehört. Explizit hat j die Form

$$j_k^{(a_l)} = ce \sum_{b_1 b_2 \ldots b_n \lambda = 1}^{4} \overline{\psi}_{b_1 b_2 \ldots b_n} (\alpha_k^{(a_l)})_{b_l \lambda} \psi_{b_1 b_2 \ldots b_{l-1} \lambda\, b_{l+1} \ldots b_n} . \tag{11}$$

Jetzt wollen wir noch das berühmte Problem der expliziten Form des in (4) eingeführten Wechselwirkungsoperators B kurz besprechen. Das erste Glied dieses Operators, die »naive Coulombsche Wechselwirkung« der Ladungen ohne Retardierung, haben wir bereits in (7) angegeben. Die ersten Ansätze zur Berücksichtigung der weiteren Glieder nach dem Gedankengange der Diracschen Theorie rühren von GAUNT [2] her. Auf ein n-Körperproblem verallgemeinert lautet seine Formel

$$B = -\frac{e^2}{2c} \sum_{a,b}^{n} \frac{1}{r_{ab}} \left[1 - \varrho_a' \varrho_b' (\sigma_a \sigma_b)\right] , \tag{12}$$

wo die ϱ' und die σ Diracsche Matrizen sind. In der runden Klammer steht ein aus Matrizenvektoren gebildetes skalares Produkt. Die Retardierung ist jedoch in der Formel von GAUNT noch nicht berücksichtigt.

BREIT [3] erhielt, ausgehend von einer älteren Untersuchung von C. G. DARWIN [4] bezüglich der richtigen relativistischen Formulierung der klassischen Bewegungsgleichungen eines Zweielektronensystems, eine genauere Formel. Wir geben hier sein Ergebnis ebenfalls auf ein n-Teilchenproblem verallgemeinert an:

$$B = -\frac{e^2}{2c} \sum_{a,b}^{n} \frac{1}{r_{ab}} + \frac{e^2}{4c} \sum_{a,b}^{n} \left[\sum_{k=x,y,z} \frac{\alpha_k^{(a)} \alpha_k^{(b)}}{r_{ab}} + \frac{(\alpha^{(a)} \mathbf{r})(\alpha^{(b)} \mathbf{r})}{r_{ab}^3} \right] . \tag{13}$$

In den runden Klammern stehen wieder skalare Produkte. Die Formel von BREIT ist jedoch nur angenähert relativistisch invariant. (Bis zu Gliedern von der Grössenordnung v^2/c^2.)

Eine streng Lorentzinvariante Form des Wechselwirkungsgliedes von zwei Partikeln rührt von MØLLER [5] her. Sein Resultat ist jedoch seinem physikalischen Inhalte nach bloss annähernd und ist deshalb in erster Linie zur Behandlung von stark relativistischen Problemen (z. B. der Streuung von Elektronen sehr grosser Energie usw.) geeignet, wo die Entwicklung nach v^2/c^2 versagen würde.

Eine vierdimensionale komplett relativistische Gleichung für zwei in Wechselwirkung stehende Fermi—Diracsche Partikel, die sich in gebundenen Zuständen befinden, haben ausgehend von dem von FEYNMAN [6] angegebenen Formalismus SALPETER und BETHE [7] angegeben. Es sei nur noch bemerkt, dass GELL—MANN und LOW [8] die Gleichungen von FEYNMAN aus der Quantenelektrodynamik streng hergeleitet haben.

Die BETHE—SALPETERsche Gleichung lautet für ein Zweikörperproblem, im Falle dass kein äusseres Feld vorhanden ist, in den Bezeichnungen dieser Verfasser:

$$\left[\sum_{\mu}\left(\frac{m_1}{m_1+m_2}P_\mu + p_\mu\right)\gamma_\mu^{(1)} - im_1 c\right]\cdot\left[\sum_{\mu}\left(\frac{m_2}{m_1+m_2}P_\mu - p_\mu\right)\gamma_\mu^{(2)} - im_2 c\right]\psi(x_\nu) = i\,\bar{G}(x_\nu)\,\psi(x_\nu)\,. \tag{14}$$

Hier ist $x_\nu = (\vec{r}, ict)$, $r = \vec{r}_1 - \vec{r}_2$ und $t = t_1 - t_2$ ist »die relative Zeit«. Weiter ist $p_\mu = -i\hbar\dfrac{\partial}{\partial x_\mu}$ und P_μ bedeutet den Moment-Energie-Vierervektor der Bewegung des Massenmittelpunktes.

$\bar{G}(x_\nu)$ ist der eigentliche Wechselwirkungsoperator, der jedoch nur als eine unendliche Reihe darstellbar ist. Jedes Glied dieser Reihe ist ein Lorentzinvarianter Operator und kann aus der erwähnten FEYNMANschen Formulierung der Quantenelektrodynamik hergeleitet werden. Es sei jedoch bemerkt, dass die Konvergenz dieser Reihe problematisch ist.

Eine weitere Methode zur Berücksichtigung dieser Wechselwirkung rührt von TAMM [9] und DANCOFF [10] her, die wie ZIMMERMANN [11] gezeigt hat, mit der BETHE—SALPETERschen Gleichung in Zusammenhang gebracht werden kann.

Bei unserem Problem liegt jedoch der glückliche Fall vor, dass der Wechselwirkungsoperator B während unserer weiteren Rechnungen weider herausfallen wird, sodass unsere Resultate so lange streng richtig bleiben, bis diese Wechselwirkung überhaupt noch als ein auf die Eigenfunktion u' des Systems einwirkender Operator dargestellt werden kann.

Es sei nur noch bemerkt, dass wir hier der Einfachheit halber angenommen haben, dass alle n Teilchen Elektronen sind. Jetzt wissen wir zwar aus den Untersuchungen von R. HOFSTADTER, dass die Nukleonen keine Diracschen Teilchen sind, doch wird man diese trotzdem in guter Näherung durch

die Diracsche Theorie beschreiben können (selbstverständlich unter Berücksichtigung des anomalen magnetischen Momentes) und ausserdem spielt ja in unseren Betrachtungen sowieso nur das Coulombfeld des Kernes eine Rolle, so dass dadurch die Allgemeinheit unserer Betrachtungen nicht beeinträchtigt wird. Selbstverständlich würden bei der Wechselwirkung eines Elektrons und eines Protons unsere Wechselwirkungsglieder ihr Vorzeichen ändern.

Nach diesen Vorbereitungen wollen wir jetzt unser Störungsproblem tatsächlich berechnen. In Formel (1) der vorangehenden Arbeit haben wir in die skalare Schrödingersche Wellengleichung einfach den elektrischen Vektor $\mathfrak{E}_z = \mathfrak{E}_0 \cos 2\pi\nu\left(t - \frac{x}{c}\right)$ eingesetzt, jetzt benötigen wir das dazu gehörende Vektorpotential

$$\mathfrak{A} = \mathfrak{A}_z = -\frac{c\,\mathfrak{E}_0}{2\pi\nu} \sin 2\pi\nu\left(t - \frac{x}{c}\right), \quad \varphi = 0\,. \tag{15}$$

Tatsächlich folgt aus (15) mit Hilfe der Formeln $\mathfrak{H} = \text{rot}\,\mathfrak{A}$ und $\mathfrak{E} = -\,\text{grad}\,\varphi - \frac{1}{c}\dot{\mathfrak{A}}$

$$\mathfrak{E}_z = \mathfrak{E}_0 \cos 2\pi\nu\left(t - \frac{x}{c}\right), \quad \mathfrak{E}_x = \mathfrak{E}_y = 0 \tag{16}$$

und

$$\mathfrak{H}_y = -\,\mathfrak{E}_0 \cos 2\pi\nu\left(t - \frac{x}{c}\right), \quad \mathfrak{H}_x = \mathfrak{H}_z = 0\,. \tag{17}$$

Setzen wir jetzt (15) in (4) ein, so folgt

$$\left[-\frac{h}{2\pi i c}\frac{\partial}{\partial t} + \sum_{a=1}^{n}\sum_{k=x,y,z}\frac{h}{2\pi i}\frac{\partial}{\partial k_{(a)}}\alpha_k^{(a)} + c\sum_{a=1}^{n} m_{(a)}\alpha_4^{(a)} + B\right]u' = \frac{e}{c}A\sum_{a=1}^{n}\alpha_z^{(a)} \sin 2\pi\nu\left(t - \frac{x}{c}\right).u'\,, \tag{18}$$

wo wir zur Abkürzung

$$\mathrm{A} = \frac{c\,\mathfrak{E}_0}{2\pi\nu} \tag{19}$$

gesetzt haben.

Die Eigenwerte und die Eigenfunktionen der ungestörten Gleichung bezeichnen wir mit

$$W_s \quad \text{und} \quad u_s = \psi_s e^{-\frac{2\pi i}{h}W_s t} = \psi_s e^{\frac{2\pi i}{h}E_s t}\,, \tag{20}$$

letztere besitzt 4^n Komponenten. s bezeichnet die Gesamtheit aller einen Zustand charakterisierender Quantenzahlen. Die Bezeichnung $-W_s = E_s$ haben wir nur aus Bequemlichkeitsgründen eingeführt, um nicht überall das negative Vorzeichen explizit hinschreiben zu müssen. E_s bedeutet also nicht den Eigenwert in der Diracschen Theorie, sondern dessen negativen Wert.

Die vollständige Gleichung kann man mit Hilfe des folgenden Ansatzes integrieren:

$$u'_s = \psi_s e^{\frac{2\pi i}{h} E_s t} + w_s = u_s + w_s \,. \tag{21}$$

Setzen wir jetzt (21) in (18) ein und berücksichtigen wir, dass u_s die ungestörte Gleichung befriedigt, so folgt

$$\left[-\frac{h}{2\pi i c}\frac{\partial}{\partial t} + \sum_{a=1}^{n} \sum_{k=x,y,z} \frac{h}{2\pi i}\frac{\partial}{\partial k_{(a)}} \alpha_k^{(a)} + c \sum_{a=1}^{n} m_{(a)} \alpha_4^{(a)} + B \right] w_s$$
$$= \frac{e}{c} A \sum_{a=1}^{n} \alpha_z^{(a)} \sin 2\pi\nu \left(t - \frac{x}{c} \right) \cdot u_s \,. \tag{22}$$

Wir nehmen weiter an (da es sich um sichtbares oder infrarotes Licht handelt), dass das fragliche Molekül klein im Verhältnis zu λ ist, dann können wir das Glied auf der rechten Seite von (22) wie folgt schreiben:

$$\frac{e}{c} A \sum_{a=1}^{n} \alpha_z^{(a)} \frac{1}{2i} \left\{ e^{\frac{2\pi i t}{h}(E_s + h\nu)} - e^{\frac{2\pi i t}{h}(E_s - h\nu)} \right\} \psi_s \,. \tag{23}$$

Für w_s machen wir den bekannten Ansatz

$$w_s = w_s^+ e^{\frac{2\pi i t}{h}(E_s + h\nu)} - w_s^- e^{\frac{2\pi i t}{h}(E_s - h\nu)} \,. \tag{24}$$

Setzen wir jetzt (23) und (24) in (22) ein, so folgt

$$\left[-\frac{1}{c}(E_s \pm h\nu) + \frac{h}{2\pi i} \sum_{a=1}^{n} \sum_{k=x,y,z} \frac{\partial}{\partial k_{(a)}} \alpha_k^{(a)} + c \sum_{a=1}^{n} m_{(a)} \alpha_4^{(a)} + B \right] w_s^{\pm}$$
$$= \frac{eA}{2ic} \sum_{a=1}^{n} \alpha_z^{(a)} \psi_s \,. \tag{25}$$

Die $w_s^{\pm}$ (die aus einer 4^n Komponenten besitzenden Kolonnenmatrix bestehen) entwickeln wir jetzt in Reihen nach den ungestörten Eigenfunktionen (die ebenfalls Kolonnenmatrizen sind und die selbe Zahl von Elementen besitzen:

$$w_s^{\pm} = \sum_{s'} w_{ss'}^{\pm} \psi_{s'} \,. \tag{26}$$

Setzen wir dies in (25) ein, so folgt

$$-\sum_{s'}\frac{1}{c}(E_s \pm h\nu - E_{s'})\, w^{\pm}_{ss'}\psi_{s'} = \frac{eA}{2ic}\sum_{a=1}^{n}\alpha_z^{(a)}\psi_s\,. \tag{27}$$

B ist hier herausgefallen, das problematische Wechselwirkungsglied tritt also im Resultat explizit nicht auf. Die Gleichung (27) multiplizieren wir jetzt mit $\bar{\psi}_{s'}$ und integrieren dann über den ganzen Konfigurationsraum. Wir erhalten

$$-\frac{1}{c}(E_s \pm h\nu - E_{s'})\, w^{\pm}_{ss'} = \frac{eA}{2ic}\int\sum_{a=1}^{n}\bar{\psi}_{s'}\,\alpha_z^{(a)}\psi_s\,d\tau\,, \tag{28}$$

oder wegen (10)

$$-\frac{1}{c}(E_s \pm h\nu - E_{s'})\, w^{\pm}_{ss'} = \frac{A}{2ic^2}\int\sum_{a=1}^{n} j_z^{(a)}(ss')\,d\tau\,. \tag{29}$$

$\sum_{a=1}^{n} j_z^{(a)}(ss') = j_z(ss')$ bedeutet die zu dem Quantensprung $s' \to s$ gehörende

und von allen Partikeln herrührende Stromkomponente; also haben wir

$$-\frac{1}{c}(E_s - E_{s'} \pm h\nu)\, w^{\pm}_{ss'} = \frac{A}{2ic^2}\int j_z(ss')\,d\tau\,. \tag{30}$$

Da weiter

$$div\, j + \frac{\partial\varrho}{\partial t} = 0 \tag{31}$$

und demzufolge (selbstverständlich unter Benützung der zeitabhängigen Eigenfunktionen und Einführung der Bezeichnung $W_{s'} - W_s = E_s - E_{s'} = h\nu(s's)$, mit Hilfe deren die bei dem Übergang von einem angeregten Zustand in den Grundzustand ausgestrahlte Frequenz positiv wird)

$$\mathrm{div}\, j(ss') + 2\pi i\nu(s's)\,\varrho(s\,s') = 0 \tag{32}$$

ist und

$$\int\Big(\sum_{a=1}^{n} q^{(a)}\, div\, j^{(a)}(s\,s')\Big)\,d\tau = -\int j_q(ss')d\tau \tag{33}$$

sein muss, wo q eine Koordinate bedeutet, so kann (30) auch noch folgendermassen geschrieben werden:

$$-(E_s - E_{s'} \pm h\nu)\, w^{\pm}_{ss'} = \frac{A}{2ci}\,2\pi i\nu(s's)\int\sum_{a=1}^{n} z^{(a)}\varrho'(s's)\,d\tau\,. \tag{34}$$

Setzen wir hier noch den Wert von A aus (19) ein, so folgt

$$-(E_s - E_{s'} \pm h\nu)\, w^{\pm}_{ss'} = \frac{1}{2}\frac{\nu(s's)}{\nu}\,\mathfrak{E}_0 \int \sum_{a=1}^{n} z^{(a)}\, \varrho'(ss')\, d\tau\,. \tag{35}$$

Mit Hilfe der Bezeichnung

$$\int \sum_{a=1}^{n} z^{(a)}\, \varrho'(ss')\, d\tau = -P_z(ss') \tag{36}$$

erhalten wir aus (35)

$$w^{\pm}_{ss'} = \frac{1}{2}\frac{\nu(s's)}{\nu}\,\frac{(P(ss'), \mathfrak{E}_0)}{E_s - E_{s'} \pm h\nu}\,. \tag{37}$$

Setzen wir dieses Resultat in (26), das erhaltene in (24) und dieses wieder in (21) ein, so folgt

$$u'_s = \psi_s\, e^{\frac{2\pi i t}{h} E_s t} + \frac{1}{2}\sum_{s'}\frac{\nu(s's)}{\nu}\,(P(ss'), \mathfrak{E}_0)\,\psi_{s'}\left\{\frac{e^{\frac{2\pi i t}{h}(E_s + h\nu)}}{E_s - E_{s'} + h\nu} - \right.$$
$$\left. - \frac{e^{\frac{2\pi i t}{h}(E_s - h\nu)}}{E_s - E_{s'} - h\nu}\right\}. \tag{38}$$

Damit haben wir die gestörte Eigenfunktion in erster Näherung hergeleitet. Zur Berechnung der zweiten Näherung setzen wir weiter

$$u'_s = u_s + \frac{1}{2}\,\mathfrak{E}_0\, e \sum_{s'}\frac{\nu(s's)}{\nu}\, u_{s'} \int \sum_{a=1}^{n} z^{(a)}\, u_s\, \bar{u}_{s'}\, d\tau \left\{\frac{e^{2\pi i \nu t}}{E_s - E_{s'} + h\nu} - \right.$$
$$\left. - \frac{e^{-2\pi i \nu t}}{E_s - E_{s'} - h\nu}\right\} + f, \tag{39}$$

wo f wieder eine aus 4^n Elementen bestehende Kolonnenmatrizenfunktion ist.

Setzen wir diesen Ansatz jetzt in unsere Gleichung (18) ein, die wir in der Form

$$\left[-\frac{h}{2\pi i c}\frac{\partial}{\partial t} + \sum_{a=1}^{n}\sum_{k=x,y,z}\frac{h}{2\pi i}\frac{\partial}{\partial k^{(a)}}\alpha_k^{(a)} + c\sum_{a=1}^{n} m_{(a)}\,\alpha_4^{(a)} + B\right] u'$$
$$= \frac{e}{c} A \sum_{a=1}^{n} \alpha_z^{(a)}\,\frac{e^{2\pi i \nu t} - e^{-2\pi i \nu t}}{2i}\, u' \tag{40}$$

schreiben (Die Abhängigkeit des Argumentes der Sinusfunktion von x haben wir dabei ebenso wie in der von (22) zu (23) führenden Rechnung vernach-

lässigt.) und behalten wir nur Glieder bis zur zweiten Ordnung, so folgt

$$\left[-\frac{h}{2\pi ic}\frac{\partial}{\partial t}+\sum_{a=1}^{n}\sum_{k=x,y,z}\frac{h}{2\pi i}\frac{\partial}{\partial k_{(a)}}\alpha_k^{(a)}+c\sum_{a=1}^{n}m_{(a)}\alpha_4^{(a)}+B\right]f$$

$$=-\frac{1}{2}\frac{e^2}{c}A\,\mathfrak{E}_0\sum_{s'}\frac{\nu(ss')}{\nu}\int\sum_{a=1}^{n}z^{(a)}u_s\,\bar{u}_{s'}\,d\tau\left\{\frac{e^{2\pi i\nu t}}{h\{\nu(s's)+\nu\}}-\frac{e^{-2\pi i\nu t}}{h\{\nu(s's)-\nu\}}\right\}$$

$$\cdot\sum_{a=1}^{n}\alpha_z^{(a)}\,\frac{e^{2\pi i\nu t}-e^{-2\pi i\nu t}}{2i}\,u_{s'}, \tag{41}$$

oder nach weiteren Umformungen

$$\left[-\frac{h}{2\pi ic}\frac{\partial}{\partial t}+\sum_{a=1}^{n}\sum_{k=x,y,z}\frac{h}{2\pi i}\frac{\partial}{\partial k^{(a)}}\alpha_k^{(a)}+c\sum_{a=1}^{n}m_{(a)}\alpha_4^{(a)}+B\right]f$$

$$=-\frac{1}{4i}\frac{e^2}{c}A\,\mathfrak{E}_0\sum_{s'}{}'\frac{\nu(ss')}{\nu}\int\sum_{a=1}^{n}z^{(a)}u_s\,\bar{u}_{s'}\,d\tau\left\{\frac{e^{4\pi i\nu t}}{h\{\nu(s's)+\nu\}}+\frac{e^{-4\pi i\nu t}}{h\{\nu(s's)-\nu\}}\right.$$

$$\left.-\left[\frac{1}{h\{\nu(s's)+\nu\}}+\frac{1}{h\{\nu(s's)-\nu\}}\right]\right\}\sum_{a=1}^{n}\alpha_z^{(a)}u_{s'}. \tag{42}$$

Zur Lösung von (42) zerlegen wir f wieder in drei Glieder (bzw. in drei Kolonnenmatrizen)

$$f=f_1e^{4\pi i\nu t}+f_2e^{-4\pi i\nu t}+f_3. \tag{43}$$

Da die linke Seite von (42) in f linear ist, so zerfällt (42) mit diesem Ansatz in drei Matrizendifferentialgleichungen. Es sei weiter

$$f=f_{10}e^{i2\pi t\frac{E_s+2h\nu}{h}}+f_{20}e^{i2\pi t\frac{E_s-2h\nu}{h}}+f_{30}e^{i2\pi\frac{E_s}{h}t}. \tag{44}$$

Die (aus 4^n Komponenten bestehenden) f_{10}, f_{20} und f_{30} entwickeln wir jetzt nach den ungestörten Eigenfunktionen:

$$f_{10}=\sum_{s''}b_{s''}\psi_{s''},\quad f_{20}=\sum_{s''}c_{s''}\psi_{s''}\text{ und }f_{30}=\sum_{s''}d_{s''}\psi_{s''}. \tag{45}$$

Dann haben wir z. B.

$$-\frac{1}{c}\sum_{s''}b_{s''}(E_s+2h\nu-E_{s''})\psi_{s''}=$$

$$=-\frac{1}{4i}\frac{e^2}{c}A\,\mathfrak{E}_0\sum_{s''}{}'\frac{\nu(ss')}{\nu}\int\sum_{a=1}^{n}z_{(a)}u_s\,\bar{u}_{s'}\,d\tau\,\frac{e^{-2\pi it\frac{E_s}{h}}}{h\{\nu(s's)+\nu\}}\cdot\sum_{a=1}^{n}\alpha_z^{(a)}u_{s'} \tag{46}$$

und zwei analoge Gleichungen.

Aus (46) folgt mit Hilfe der bekannten Fourierartigen Methode für die Entwicklungskoeffizienten $b_{s''}$ [wenn wir ausserdem auch wieder A aus (19) einsetzen]

$$b_{s''} = \frac{1}{4i}\frac{c\mathfrak{E}_0^2}{2\pi}e^2 \sum_{s'}{}' \frac{\nu(ss')}{\nu^2}\int \sum_{a=1}^{n} z^{(a)}\, u_s\, \bar{u}_{s'}\, d\tau \times$$

$$\times \frac{\int \bar{\psi}_{s''} \sum_{a}^{n} \alpha_z^{(a)}\, u_{s'}\, d\tau}{h^2\{\nu(s's)+\nu\}\cdot\{\nu(s''s)+2\nu\}}\, e^{-2\pi i t\frac{E_s}{h}} \tag{47}$$

und analog

$$c_{s''} = \frac{1}{4i}\frac{c\mathfrak{E}_0^2}{2\pi}e^2 \sum_{s'}{}' \frac{\nu(ss')}{\nu^2}\int \sum_{a=1}^{n} z^{(a)}\, u_s\, \bar{u}_{s'}\, d\tau \times$$

$$\times \frac{\int \bar{\psi}_{s''} \sum_{a}^{n} \alpha_z^{(a)}\, u_{s'}\, d\tau}{h^2\{\nu(s's)-\nu\}\cdot\{\nu(s''s)-2\nu\}}\, e^{-2\pi i t\frac{E_s}{h}} \tag{48}$$

und

$$d_{s''} = -\frac{1}{4i}\frac{c\mathfrak{E}_0^2}{2\pi}e^2 \sum_{s'}{}' \frac{\nu(ss')}{\nu^2}\int \sum_{a=1}^{n} z^{(a)}\, u_s\, \bar{u}_{s'}\, d\tau \times$$

$$\times \frac{\int \bar{\psi}_{s''} \sum_{a}^{n} \alpha_z^{(a)}\, u_{s'}\, d\tau}{h^2\{\nu^2(s's)-\nu^2\}\,\nu(s''s)}\, 2\nu(s's)\, e^{-2\pi i t\frac{E_s}{h}}. \tag{49}$$

Setzen wir diese Resultate in (45) ein, so folgt

$$f_{10} = \frac{1}{4i}\frac{c\mathfrak{E}_0^2}{2\pi}e^2 \sum_{s's''}{}' \frac{\nu(ss')}{\nu^2}\,\frac{\int \sum_{a}^{n} z^{(a)}\, u_s\, \bar{u}_{s'}\, d\tau \cdot \int \bar{u}_{s''} \sum_{a}^{n} \alpha_z^{(a)}\, u_{s'}\, d\tau}{h^2\{\nu(s's)+\nu\}\cdot\{\nu(s''s)+2\nu\}}\, u_{s''}\, e^{-2\pi i\frac{E_s}{h}t} \tag{50}$$

$$f_{20} = \frac{1}{4i}\frac{c\mathfrak{E}_0^2}{2\pi}e^2 \sum_{s's''}{}' \frac{\nu(ss')}{\nu^2}\,\frac{\int \sum_{a}^{n} z^{(a)}\, u_s\, \bar{u}_{s'}\, d\tau \cdot \int \bar{u}_{s''} \sum_{a}^{n} \alpha_z^{(a)}\, u_{s'}\, d\tau}{h^2\{\nu(s's)-\nu\}\cdot\{\nu(s''s)-2\nu\}}\, u_{s''}\, e^{-2\pi i\frac{E_s}{h}t} \tag{51}$$

und

$$f_{30} = -$$

$$-\frac{1}{4i}\frac{c\mathfrak{E}_0^2}{2\pi}e^2 \sum_{s's''}{}' \frac{2\nu(ss')\,\nu(s's)}{\nu^2}\,\frac{\int \sum_{a}^{n} z^{(a)}\, u_s\, \bar{u}_{s'}\, d\tau \cdot \int \bar{u}_{s''} \sum_{a}^{n} \alpha_z^{(a)}\, u_{s'}\, d\tau}{h^2\{\nu^2(s's)-\nu^2\}\,\nu(s''s)}\, u_{s''}\, e^{-2\pi i\frac{E_s}{h}t}. \tag{52}$$

Zur Auswertung des Integrals $\int \bar{u}_{s''} \sum_a^n \alpha_z^{(a)} u_{s'} \, d\tau$ kann man ganz analog verfahren wie in den von (28) zu (34) führenden Rechnungen und als Resultat folgt

$$\int \bar{u}_{s''} \sum_a^n \alpha_z^{(a)} u_{s'} \, d\tau = \frac{1}{ce} \int j_z (s' s'') \, d\tau =$$

$$= \frac{1}{ce} 2\pi i \nu (s'' s') \int \sum_a^n z^{(a)} \varrho'(s's'') \, d\tau \, . \tag{53}$$

Endlich erhalten wir also aus (39), (44), (50), (51), (52) und (53) für die ganze Eigenfunktion in zweiter Näherung

$$\begin{aligned} u' = u_s &+ \frac{1}{2} \mathfrak{E}_0 e \sum_{s'} \frac{\nu (s's)}{\nu} \int u_s \sum^n z^{(a)} \bar{u}_{s'} \, d\tau \cdot \\ &\cdot \left\{ \frac{e^{2\pi i \nu t}}{h \{\nu(s's) + \nu\}} - \frac{e^{-2\pi i \nu t}}{h \{\nu (s's) - \nu\}} \right\} u_{s'} + \\ &+ \frac{1}{4} \mathfrak{E}_0^2 e^2 \sum_{s' s''}{}' \frac{\nu (s's) \nu (s''s')}{\nu^2} \cdot \\ &\cdot \frac{\int \sum_a^n z^{(a)} u_s \bar{u}_{s'} \, d\tau \cdot \int \sum_a^n z^{(a)} u_{s'} \bar{u}_{s''} \, d\tau}{h^2 \{\nu (s's) + \nu\} \cdot \{\nu (s''s) + 2\nu\}} e^{4\pi i \nu t} \cdot u_{s''} + \\ &+ \frac{1}{4} \mathfrak{E}_0^2 e^2 \sum_{s' s''}{}' \frac{\nu (s's) \nu (s''s')}{\nu^2} \cdot \\ &\cdot \frac{\int \sum_a^n z^{(a)} u_s \bar{u}_{s'} \, d\tau \cdot \int \sum_a^n z^{(a)} u_{s'} \bar{u}_{s''} \, d\tau}{h^2 \{\nu (s's) - \nu\} \cdot \{\nu (s''s) - 2\nu\}} e^{-4\pi i \nu t} \cdot u_{s''} - \\ &- \frac{1}{4} \mathfrak{E}_0^2 e^2 \sum_{s' s''}{}' \frac{2\nu^2 (s's)}{\nu^2} \nu (s''s') \frac{\int \sum_a^n z^{(a)} u_s \bar{u}_{s'} \, d\tau \cdot \int \sum_a^n z^{(a)} u_{s'} \bar{u}_{s''} \, d\tau}{h^2 \{\nu^2 (s's) - \nu^2\} \nu (s''s)} \cdot u_{s''} \, . \end{aligned} \tag{54}$$

Bezüglich der Normiertheit dieser Eigenfunktion verweisen wir auf das in der vorangehenden Arbeit nach der Formel (23) Gesagte und bemerken nur, dass hier die Bedingung $s' \neq s''$ einfach schon deshalb automatisch erfüllt ist, weil die letzten drei Glieder in (54) mit $\nu(s''s')$ multipliziert sind.

Aus (54) folgt das induzierte Moment ebenfalls in zweiter Näherung:

$$
\begin{aligned}
-p_q = e\int \sum_a^n q^{(a)}\, u'\, \bar{u}'\, d\tau = e\int \sum_a^n q^{(a)}\, u_s\, \bar{u}_s\, d\tau + \\
+ \mathfrak{E}_0\, e^2 \sum_{s'}{}' \int \sum_a^n z^{(a)}\, u_s\, \bar{u}_{s'}\, d\tau \cdot \int \sum_a^n q^{(a)}\, u_{s'}\, \bar{u}_s\, d\tau \cdot \\
\cdot \left\{ \frac{1}{h\{\nu\, s's) + \nu\}} - \frac{1}{h\{\nu\,(s's) - \nu\}} \right\} \frac{\nu\,(s's)}{\nu} \cos 2\pi\,\nu t + \\
+ \frac{1}{4}\, \mathfrak{E}_0^2\, e^3 \sum_{\substack{s'\,s'' \\ s'\neq s''}}{}' \int \sum_a^n z^{(a)}\, u_s\, \bar{u}_{s'}\, d\tau \cdot \int \sum_a^n q^{(a)}\, u_{s'}\, \bar{u}_{s''}\, d\tau \cdot \\
\cdot \int \sum_a^n z^{(a)}\, u_{s''}\, \bar{u}_s\, d\tau \left\{ \frac{1}{h^2\{\nu\,(s's) + \nu\} \cdot \{\nu\,(s''s) + \nu\}} + \right. \qquad (55) \\
+ \frac{1}{h^2\{\nu\,(s's) - \nu\} \cdot \{\nu\,(s''s) - \nu\}} - \frac{e^{i4\pi\nu t}}{h^2\{\nu\,(s's) + \nu\} \cdot \{\nu\,(s''s) - \nu\}} - \\
\left. - \frac{e^{-i4\pi\nu t}}{h^2\{\nu\,(s's) - \nu\} \cdot \{\nu\,(s''s) + \nu\}} \right\} \frac{\nu(s's)\,\nu(s''s)}{\nu^2} + \\
+ \frac{1}{4}\, \mathfrak{E}_0^2\, e^3 \sum_{s'\,s''}{}' \int \sum_a^n z^{(a)}\, u_s\, \bar{u}_{s'}\, d\tau \cdot \int \sum_a^n z^{(a)}\, u_{s'}\, \bar{u}_{s''}\, d\tau \cdot \int \sum_a^n q^{(a)}\, u_{s''}\, \bar{u}_s\, d\tau \cdot \\
\cdot \left\{ \left[\frac{1}{h^2\{\nu\,(s's) + \nu\} \cdot \{\nu\,(s''s) + 2\nu\}} + \right. \right. \\
\left. + \frac{1}{h^2\{\nu\,(s's) - \nu\} \cdot \{\nu\,(s''s) - 2\nu\}} \right] \frac{\nu(s's)\,\nu\,(s''s')}{\nu^2}\, 2\cos 4\pi\,\nu t - \\
\left. - \frac{4\nu^2\,(s's)\,\nu\,(s''s')}{h^2\{\nu^2\,(s's) - \nu^2\}\,\nu\,(s''s) \cdot \nu^2} \right\}.
\end{aligned}
$$

Für die mit den exponentiellen Faktoren multiplizierten Glieder in der geschweiften Klammer im dritten Gliede auf der rechten Seite von (55) kann man den in der vorangehenden Arbeit von (26) zu (31) führenden Gedankengang wiederholen. Daraus folgt für dieses dritte Glied

$$
\begin{aligned}
\frac{1}{4}\, \mathfrak{E}_0^2\, e^3 \sum_{\substack{s'\,s'' \\ s'\neq s''}}{}' \int \sum_a^n z^{(a)}\, u_s\, \bar{u}_{s'}\, d\tau \cdot \int \sum_a^n q^{(a)}\, u_{s'}\, \bar{u}_{s''}\, d\tau \cdot \int \sum_a^n z^{(a)}\, u_{s''}\, \bar{u}_s\, d\tau \cdot \\
\cdot \left\{ - \frac{2\nu\,(s's)\,\nu\,(s''s) - 2\nu^2}{h^2\{\nu^2\,(s's) - \nu^2\} \cdot \{\nu^2\,(s''s) - \nu^2\}} \cdot \frac{\nu\,(s's)\,\nu\,(s''s)}{\nu^2} \cos 4\,\pi\nu t + \right. \qquad (56) \\
\left. + \frac{2\nu\,(s's)\,\nu\,(s''s) + 2\nu^2}{h^2\{\nu^2\,(s's) - \nu^2\} \cdot \{\nu^2\,(s''s) - \nu^2\}} \cdot \frac{\nu(s's)\,\nu\,(s''s)}{\nu^2} \right\}.
\end{aligned}
$$

Endlich haben wir also für das ganze induzierte Moment

$$-p_q = e\int \sum_a^n q^{(a)}\, u'_s\, \bar{u}'_s\, d\tau = e\int \sum_a^n q^{(a)}\, u_s\, \bar{u}_s\, d\tau -$$

$$-\mathfrak{E}_0\, e^2 \sum_{s'}{}' \int \sum_a^n z^{(a)}\, u_s\, \bar{u}_{s'}\, d\tau \cdot \int \sum_a^n q^{(a)}\, u_{s'}\, \bar{u}_s\, d\tau\, \frac{2\nu\,(s's)}{h\{\nu^2\,(s's) - \nu^2\}} \cos 2\pi\nu t +$$

$$+\frac{1}{4}\,\mathfrak{E}_0^2\, e^3 \sum_{\substack{s'\,s'' \\ s'\neq s''}}{}' \int \sum_a^n z^{(a)}\, u_s\, \bar{u}_{s'}\, d\tau \cdot \int \sum_a^n q^{(a)}\, u_{s'}\, \bar{u}_{s''}\, d\tau \cdot$$

$$\cdot \int \sum_a^n z^{(a)}\, u_{s''}\, \bar{u}_s\, d\tau\, \frac{\nu\,(s's)\,\nu\,(s''s)}{\nu^2}\, \cdot$$

$$\cdot\, \frac{2\nu\,(s's)\,\nu\,(s''s) + 2\nu^2 - \{2\nu\,(s's)\,\nu\,(s''s) - 2\nu^2\}\cos 4\pi\nu t}{h^2\{\nu^2\,(s's) - \nu^2\}\cdot\{\nu^2\,(s''s) - \nu^2\}} +$$

$$+\frac{1}{4}\,\mathfrak{E}_0^2\, e^3 \sum_{s'\,s''}{}' \int \sum_a^n z^{(a)}\, u_s\, \bar{u}_{s'}\, d\tau \cdot \int \sum_a^n z^{(a)}\, u_{s'}\, \bar{u}_{s''}\, d\tau \cdot \int \sum_a^n q^{(a)}\, u_{s''}\, \bar{u}_s\, d\tau \cdot$$

$$\cdot\, \frac{\nu\,(s's)\,\nu\,(s''s')}{\nu^2} \cdot \left[-\frac{2\nu\,(s's)\,\nu\,(s''s) + 4\nu^2}{h^2\{\nu^2\,(s's) - \nu^2\}\cdot\{\nu^2\,(s''s) - (2\nu)^2\}}\, 2\cos 4\pi\,\nu t - \right.$$

$$\left. -\frac{4\nu\,(s's)}{h^2\{\nu^2\,(s's) - \nu^2\}\,\nu\,(s''s)} \right]. \qquad (57)$$

Wir müssen noch die Frage beantworten, ob es erlaubt ist, die erste Näherung der Energie in unserer Rechnung zu vernachlässigen. Dieses Glied multipliziert mit der ersten Näherung der gestörten Eigenfunktion müsste nämlich ebenfalls ein Glied von zweiter Ordnung ergeben. Bei der Schrödingerschen Methode kann jedoch solch ein Glied nicht auftreten, weil es ja abgesehen von Ausnahmsfällen keinen linearen Starkeffekt gibt. Bei der Diracschen Methode ist jedoch zu beachten, dass es zwar ebenfalls keinen linearen Starkeffekt, jedoch einen linearen Zeemaneffekt gibt. (Allerdings verschwindet meistens im Grundzustande die Zeemanaufspaltung.) Wir müssen deshalb hier doch noch diese Frage untersuchen.

Aus (19) und (22) erhalten wir für die erste Näherung der Störung des Eigenwertes (die wir mit W_{s1} bezeichnen) in unserem Problem

$$W_{s1} = -E_{s1} = -\frac{\mathfrak{E}_0\, e}{2\pi\,\nu}\int \sum_a^n u_s\, \alpha_z^{(a)}\, \bar{u}_s \sin 2\pi\,\nu\left(t - \frac{x}{c}\right) d\tau. \qquad (58)$$

Berücksichtigen wir wieder — ganz ebenso, wie in den von (22) zu (23) und zu (40) führenden Rechnungen — dass es sich um sichtbares oder infrarotes Licht handelt, und wir deshalb in der in (58) stehenden trigonometrischen Funktion die Abhängigkeit von x vernachlässigen können, so kann

sin $2\pi\nu t$ vor das Integralzeichen geschrieben werden, und das ist der springende Punkt unserer Überlegung.

Nehmen wir jetzt noch (10) in Betracht, so folgt endlich für (58)

$$E_{s1} = \frac{\mathfrak{E}_0}{2\pi\nu c} \sin 2\pi\nu t \cdot \int \sum_a^n j_z^{(a)}(ss)\, d\tau = \frac{\mathfrak{E}_0}{2\pi\nu c} \sin 2\pi\nu t \cdot \int j_z(ss)\, d\tau. \qquad (59)$$

Die Stromkomponente in irgendeiner Koordinatenrichtung muss jedoch in jedem gebundenen Quantenzustande, integriert über den ganzen Raum, verschwinden, und damit haben wir die Vernachlässigung dieses Gliedes in unseren Rechnungen gerechtfertigt.

Würden wir in der Sinusfunktion in (58) die Abhängigkeit von der Koordinate nicht vernachlässigen, so würde tatsächlich ein ganz kleines lineares Glied auftreten. Selbstverständlich müssten wir dann diese Abhängigkeit auch in (23) und (40) einführen. Man rechnet jedoch leicht nach, dass diese Vernachlässigung sehr unbedeutend ist. Man könnte höchstens noch daran denken, dass man bis jetzt nur Lichtzerstreuungseffekte bis zur ersten Ordnung berechnet hat und dass dort diese Vernachlässigung tatsächlich gerechtfertigt ist, bei Effekten zweiter Ordnung jedoch schon viel kleinere Abweichungen wesentlich sein könnten. Eine Abschätzung der Grössenordnung macht das jedoch wenig wahrscheinlich. Übrigens könnte man diese Abhängigkeit der Sinusfunktion in unseren Rechnungen ganz analog dazu berücksichtigen, wie man in der Theorie der Streuung der Röntgenstrahlen den Atomformfaktor einführt. Doch würden damit unsere Formeln noch bedeutend verwickelter werden.

Jetzt wollen wir unsere Resultate, d. h. Formel (32), in der vorangehenden Arbeit und (57) in der vorliegenden miteinander vergleichen. Berücksichtigen wir, dass den in der vorangehenden Arbeit benützten Bezeichnungen für die Quantenzahlen 0, k und l in (57) s, s' und s'' entsprechen, und dass ausserdem den Übergangsmomenten vom Typ $\int u_0 \Sigma e z \bar{u}_k d\tau$ in der Schrödingerschen Theorie nach Dirac $\int \sum_a^n e z^{(a)} u_s \bar{u}_{s'}\, d\tau$ entspricht, so sehen wir, dass unsere erwähnten zwei Resultate zwar weitgehend analog, jedoch nicht ganz übereinstimmend sind, was ja auch zu erwarten war, weil in einer Näherung von so hoher Ordnung relativistische Effekte und das magnetische Feld der Lichtwelle nicht mehr ganz unbedeutend sein können. Selbstverständlich differieren die beiden Formeln nur in den Gliedern zweiter Ordnung. Vollführt man den Grenzübergang $v \to 0$, so gehen (23) und (32) der vorangehenden Arbeit in die bekannten Formeln für das statische Feld über, für (57) ist das jedoch nicht der Fall, was davon herrührt, dass man ein konstantes elektrisches Feld nicht durch ein Vektorpotential beschreiben kann.

Vergleichen wir jedoch unsere Formel (57) mit dem vom Verfasser aus der Klein—Gordonschen Gleichung hergeleiteten Resultate [12] also mit der

Formel (58) der zitierten Arbeit, so sehen wir, dass diese formal vollständig miteinander übereinstimmen. (Beim Vergleich ist zu beachten, dass nach unseren Definitionen $v(s's) = -v(k0)$ ist.) Das spricht dafür, dass die in den Vektorpotentialen quadratischen Glieder der Klein—Gordonschen Gleichung, welche in der zitierten Arbeit vernachlässigt wurden, wenigstens in dem betrachteten Problem keine physikalische Realität besitzen.

Ein weiteres Problem, das noch besprochen werden muss, ist, ob es nicht paradox ist, dass in der Formel (32) der vorangehenden Arbeit und in (57) auch zeitunabhängige Glieder auftreten, bzw. ob es möglich ist, dass eine periodische Störung auch zeitunabhängige Störglieder verursachen soll. Zeitunabhängige Glieder erster Ordnung würden in diesem Fall tatsächlich eine Absurdität bedeuten, solche zweiter Ordnung jedoch nicht, wie man das leicht einsieht, wenn man z. B. an einen unsymmetrischen Oszillator denkt. Tatsächlich verschwinden diese Glieder (und übrigens die ganze zweite Näherung) für kugelsymmetrische Atome und Moleküle, was einfach daraus folgt, dass die drei Übergangsmomente, deren Produkte vor diesen Gliedern stehen, in diesem Falle nicht alle drei gleichzeitig von Null verschieden sein können. Bei unsymmetrischen Molekülen ist dagegen das Auftreten dieser zeitunabhängigen Glieder nicht mehr sinnlos.

In der Formel (32) der vorangehenden Arbeit und in der Formel (57) der vorliegenden haben wir die Grösse des von der Lichtwelle induzierten Dipols in einer ganz willkürlichen mit q bezeichneten Richtung angegeben. Selbstverständlich ist der grösste Effekt dann zu erwarten, wenn wir diese Richtung parallel zu der Richtung des elektrischen Vektors der Lichtwelle wählen. Im folgenden wollen wir also in diesen Formeln z statt q schreiben.

Ein oszillierender Dipol verursacht bekanntermeise in seiner weiteren Umgebung (Wellengebiet) die elektrischen und magnetischen Feldstärken

$$|E| = |H| = \left| \frac{1}{c^2} \frac{\ddot{p}}{r} \sin \vartheta \right| . \tag{60}$$

Daraus folgt für den Poyntingschen Vektor $\mathfrak{S} = \frac{c}{4\pi} [\mathfrak{E}, \mathfrak{H}]$, wenn wir in diese Formel (60) einsetzen

$$S(\vartheta) = \frac{1}{4\pi c^3} \left(\frac{\ddot{p}}{r} \sin \vartheta \right)^2 , \tag{61}$$

und endlich für die gestreute Intensität in der mit der Dipolachse den Winkel ϑ einschliessenden Richtung

$$\Im(\vartheta) = \overline{S(\vartheta)} = \frac{1}{4\pi c^3} \frac{\overline{\ddot{p}^2}}{r^2} \sin^2 \vartheta, \tag{62}$$

wobei das Überstreichen den zeitlichen Mittelwert bedeutet.

Aus (32) der vorangehenden Arbeit und aus (57) in diesem Artikel folgt, dass unser p vom Typ

$$p = A \cos 2\pi \nu t + B + C \cos 4\pi \nu t \tag{63}$$

ist. Differenzieren wir zweimal nach der Zeit, quadrieren das erhaltene Resultat und bilden dann die zeitlichen Mittelwerte, so verschwindet das entstehende bilineare Glied, so dass nur die reinen Quadrate der zeitabhängigen Glieder (also nur reine Rayleigh- und ebenfalls reine Doppelfrequenzstreuung) übrigbleiben.

§ 2

In diesem Paragraphen wollen wir noch die Grössenordnung der zu erwartenden Intensität des Streulichtes abschätzen, bzw. die Intensitäten, die bei der Rayleighstreuung und bei der Streuung mit doppelter Frequenz auftreten, miteinander vergleichen. Aus (32) der vorangehenden Arbeit oder aus (57) folgt, dass die mit $\cos 2\pi\nu t$ und $\cos 4\pi\nu t$ multiplizierten Glieder von den Grössenordnungen

$$\mathfrak{E}_0 P^2 \frac{2}{h\nu} \quad \text{und} \quad \mathfrak{E}_0^2 P^3 \frac{1}{h^2 \nu^2} \tag{64}$$

sind, wo wir mit P die Grössenordnung eines Übergangsmomentes von Typ $\int \sum_a^n z^{(a)} u_s \bar{u}_{s'} \, d\tau$ bezeichnet haben. Die Quadrate dieser Glieder sind

$$\mathfrak{E}_0^2 P^4 \frac{4}{h^2 \nu^2} \quad \text{und} \quad \mathfrak{E}_0^4 P^6 \frac{1}{h^4 \nu^4}, \tag{65}$$

dazu treten noch wegen der zweimaligen Differentiation die Faktoren $(2\pi\nu)^4$ und $(4\pi\nu)^4$ hinzu. Also folgt

$$\frac{\mathfrak{J}_{2\nu}}{\mathfrak{J}_\nu} \approx \frac{16\, \mathfrak{E}_0^4 P^6 \dfrac{1}{h^4 \nu^4}}{\mathfrak{E}_0^2 P^4 \dfrac{4}{h^2 \nu^2}} = \frac{4\, \mathfrak{E}_0^2 P^2}{h^2 \nu^2}, \tag{66}$$

wo wir mit $\mathfrak{J}_\nu$ die bei der Rayleighstreuung und mit $\mathfrak{J}_{2\nu}$ die bei der Streuung mit doppelter Frequenz auftretende Intensität bezeichnet haben. Für die Grössenordnung von P setzen wir 10^{-18} cgs. ein, für h haben wir $6{,}625 \cdot 10^{-27}$ erg sec und für ν benützen wir den Wert $0{,}5 \cdot 10^{15}$ sec^{-1} (NaD-Linie). Dann folgt für (66)

$$\frac{\mathfrak{J}_{2\nu}}{\mathfrak{J}_\nu} \approx 0{,}4\, \mathfrak{E}_0^2 \cdot 10^{-12}. \tag{67}$$

Das Verhältnis der Intensitäten hängt also von der Intensität des Primärlichtes ab, wie das ja auch sein muss. Um einen Begriff von der Grösse des Verhältnisses (67) erhalten zu können, wollen wir zuerst annehmen, dass das einfallende (monochromatische) Licht die Intensität der Sonnenstrahlung auf der Erdoberfläche besitzt; daraus können wir $\mathfrak{E}_0^2$ berechnen. Die Solarkonstante beträgt rund 2 cal/cm^2 in der Minute, also $8{,}372 \cdot 10^7$ erg. Da wir mit $\mathfrak{E}_z = \mathfrak{E}_0 \cos 2\pi\nu t$ den elektrischen Vektor der einfallenden Lichtwelle bezeichnet haben, so folgt für die Intensität des Primärstrahles

$$I = \frac{c}{4\pi} \overline{[\mathfrak{E}, \mathfrak{H}]} = \frac{c}{8\pi} \mathfrak{E}_0^2 \tag{68}$$

und daraus berechnen wir $\mathfrak{E}_0^2 \approx 1{,}2 \cdot 10^{-3}$ cgs-Einheiten. Setzen wir dieses Resultat in (67) ein, so folgt

$$\frac{\mathfrak{J}_{2\nu}}{\mathfrak{J}_\nu} \approx \frac{1}{2} \cdot 10^{-15} . \tag{69}$$

Das ist eine recht kleine Zahl, jedoch sind hier folgende Umstände zu beachten, welche die Grössenordnung von (69) wesentlich erhöhen können:

Erstens hängt die Grösse des Verhältnisses (69) von der Intensität des benützten Lichtes ab, und damit hat man die Möglichkeit, die relative Intensität der Doppelfrequenzstreuung wesentlich zu erhöhen. Die Experimentalphysik besitzt heutzutage die Möglichkeit viel grössere Lichtintensitäten als die erwähnte herzustellen. Die Oberfläche einer Quecksilberhochdruckentladung sendet z. B. mehr Licht aus als die Sonnenoberfläche, deshalb könnte man z. B. $\mathfrak{J}_{2\nu}/\mathfrak{J}_\nu$ etwa um den Faktor

$$\frac{I_{\text{Sonnenoberfläche}}}{I_{\text{Erde}}} = \left(\frac{150 \cdot 10^6 \,\text{Km}}{7 \cdot 10^5 \,\text{Km}} \right)^2 = 4{,}5 \cdot 10^4 \tag{70}$$

erhöhen.

Zweitens — und das ist noch wichtiger — müssen wir beachten, dass in (32) der vorangehenden Arbeit und in (57) der vorliegenden im unterstrichenen Gliede ein doppelter Resonanznenner von Typ

$$\frac{1}{\{\nu^2 (s's) - \nu^2\} \cdot \{\nu^2 (s''s) - (2\nu)^2\}} \tag{71}$$

steht und dieses Resonanzglied geht ausserdem in $\mathfrak{J}_{2\nu}$ noch quadratisch ein. Durch entsprechende Wahl der eingestrahlten Frequenz (ganz nahe zur halben Eigenfrequenz $\nu(s''s)$ der benützten Streusubstanz) können wir also die Intensität des mit doppelter Frequenz gestreuten Lichtes noch um viele Grössenordnungen erhöhen, ohne dass wir damit gleichzeitig auch die Intensi-

tät der Rayleighstreuung erhöhen würden. Dem wird nur durch die in dieser Arbeit nicht berücksichtigten Absorption eine Grenze gesetzt.

Drittens ist ausserdem auch noch zu beachten, dass diese Doppelfrequenzlinie sehr weit entfernt von der Rayleighlinie liegt und die Beobachtungsverhältnisse deshalb viel günstiger als beim Ramaneffekt sind. Man könnte sogar die einfallende Frequenz im Ultraroten wählen, was auch noch mit dem Vorteil verbunden wäre, dass unsere irdischen Lichtquellen eben in diesem Gebiet am stärksten strahlen.

Alles das spricht dafür, dass es auch schon mit unseren gewöhnlichen Lichtquellen möglich sein müsste, das tatsächliche Auftreten des neuen Effektes zu zeigen. Die moderne Masertechnik liefert jedoch eine direkt ideale Möglichkeit zum Nachweis des neuen Effektes, und tatsächlich ist es schon mit Hilfe des optischen Masers gelungen, das Vorhandensein des besprochenen Effektes, wenn auch nicht an Molekülen, so doch an zusammenhängender Materie (an Kristallen, welche nichtlineare Dielektrika sind, wie das den im nächsten Paragraphen hergeleiteten Auswahlregeln entspricht, wenn man diese auf Kristalle überträgt), zu verifizieren. Zuerst ist das mit Hilfe des Rubinmasers an monokristallinen Quarzplatten Franken, Hill, Peters und Weinreich [13] geglückt. Giordmaine [14] ist es gelungen, mit einer ähnlichen Versuchsanordnung die Vereinigung von zwei Photonen verschiedener Frequenz (optical mixing) nachzuweisen. Selbstverständlich können diese an nichtlinearen Dielektrika beobachteten Erscheinungen auch nach der elementaren klassischen Theorie gedeutet werden. Eine weitere Ausarbeitung dieser klassischen Theorie rührt von Kleinmann [15] her. In neuester Zeit ist es sogar gelungen, die Vereinigung von drei Photonen gleicher Frequenz nachzuweisen. Terhune, Maker und Savage [16] benutzten zu diesem Zweck Kalkspatplatten, also ein lineares Dielektrikum und konnten dabei das sehr schwache Auftreten der zweiten Harmonischen (um vier Grössenordnungen kleiner als an Quarzplatten), jedoch auch das auftreten der dritten optischen Harmonischen nachweisen. Eine der hier besprochenen analoge Erscheinung, die Zweiphotonenanregung von Elektronenniveaus, ist es ebenfalls schon geglückt zu zeigen [17]. In neuester Zeit hat sogar dieser Doppelfrequenzeffekt schon eine technische Anwendung gefunden. Aus bekannten physikalischen Gründen besitzt nämlich im Seewasser nicht das rote sondern das grüne Licht das grösste Durchdringungsvermögen. Es ist zwar noch nicht gelungen unmittelbar für dieses Licht einen brauchbaren Laser zu konstruieren, man konnte jedoch den infraroten Strahl eines mit Neodymium versehenen Glaslasers an den nichtlinearen Dielektrika KH_2PO_4 oder $(NH_4)H_2PO_4$ durch Frequenzverdoppelung in einen grünen ($\lambda = 0{,}53\ \mu$) verwandeln [18]. Der Effekt dieser Umwandlung beträgt zwar nur 1—3%, doch hat diese Methode bereits wichtige technische und militärische Anwendungen gefunden. (Z. B. Lokalisation von Unterseebooten und andere Unterseeobjekte, usw.). Es ist

leicht möglich, dass diese neue Methode die zu ähnlichen Zwecken bis jetzt benutzte Sonartechnik vollständig ersetzen wird.

Am interessantesten wäre selbstverständlich die Untersuchung von Molekülen bezüglich des Auftretens des neuen Effektes, weil bei diesen die theoretischen Verhältnisse erstens einfacher sind und ausserdem bei ihnen auch die Resonanzverstärkung des Effektes möglich sein muss. Alle diese Fragen wurden vom Verfasser bereits in einer kleineren Arbeit [19] untersucht.

§ 3

Zuletzt wollen wir noch die Auswahlregeln für den berechneten neuen Effekt herleiten und ausserdem die Frage besprechen, welche Materialen zum Nachweis des neuen Effektes am geeignetesten sein werden. Wie wir schon erwähnt haben, ist erstens selbstverständlich dann der grösste Effekt zu erwarten, wenn wir in (32) der vorangehenden Arbeit oder in (57) $q = z$ setzen. Vor den quadratischen Gliedern steht dann in (57) das Produkt

$$\int \sum_a^n z^{(a)} u_s \bar{u}_{s'} d\tau \cdot \int \sum_a^n z^{(a)} u_{s'} \bar{u}_{s''} d\tau \cdot \int \sum_a^n z^{(a)} u_{s''} \bar{u}_s d\tau, \tag{72}$$

das bekannterweise für Atome und symmetrisch gebaute Moleküle verschwinden muss. Das folgt einfach aus der Auswahlregel für die Nebenquantenzahl, nach der sich diese nur um ± 1 ändern kann, also könnten in (72) nicht alle drei Integrale gleichzeitig von Null verschieden sein. Bei zweiatomigen heteropolaren Molekülen wird jedoch der Effekt im allgemeinen nicht verschwinden, weil sich ja bei diesen die Quantenzahl Λ um ± 1 oder 0 ändern kann (dabei werden wenn sich Λ nicht ändert, Momente entlang der Molekülachse, und wenn sie sich um ± 1 ändert, Momente darauf senkrecht induziert) und deshalb (72) nicht notwendigerweise verschwindet. Allerdings wird bei zweiatomigen Molekülen, die ja meistens recht symmetrisch gebaut sind (ihre Dipolmomente sind meistens klein), der Effekt nur schwach auftreten. Bei homonuklearen zweiatomigen Molekülen verschwindet dagegen der neue Effekt wieder exakt. Es folgt aus der Auswahlregel, dass bei diesen gerade Terme nur mit ungeraden und umgekehrt kombinieren. Also können für solche Moleküle in (72) wieder nicht alle drei Faktoren gleichzeitig von Null verschieden sein. Analog könnte man beweisen, dass auch bei mehratomigen Molekülen, die eine wenigstens zweizählige Symmetrieachse und eine darauf senkrecht stehende Spiegelebene besitzen (z. B. Acetylen, Äthylen, usw.); der neue Effekt verschwindet. Nur die Berücksichtigung von reinen Oszillationsübergängen könnte ganz unwesentliche Abweichungen von diesen Auswahlregeln verursachen.

Wir können unsere Resultate also folgenderweise zusammenfassen: Atome, kugelsymmetrische Moleküle, zweiatomige homonukleare Moleküle und mehratomige Moleküle, welche eine zweizählige Symmetrieachse und eine

darauf senkrecht stehende Symmetrieebene besitzen, sind »doppelfrequenzinaktiv«. Mehratomige unsymmetrisch gebaute Moleküle sind dagegen »doppelfrequenzaktiv« und zwar um so mehr, je unsymmetrischer sie gebaut sind, also ein grosses Dipolmoment besitzen.

Gewisse qualitative Richtlinien bezüglich dieser Frage können wir noch erhalten, wenn wir in (57) in den quadratischen Gliedern statt $\nu(s's)$, $\nu(s''s')$ und $\nu(s''s)$ gewisse Mittelwerte dieser Eigenfrequenzen einführen. Das Summenzeichen bezieht sich dann nur auf das dreifache Produkt (72), das wir dann mit Hilfe eines matrizentheoretischen Satzes (wenn wir beachten, dass die zu den identischen Übergängen gehörenden Matrizenelemente verschwinden), noch umformen können. Wir erhalten

$$\sum_{s's''}{}' \int \sum_a^n z^{(a)}\, u_s\, \bar{u}_{s'}\, d\tau \cdot \int \sum_a^n z^{(a)}\, u_{s'}\, \bar{u}_{s''}\, d\tau \cdot \int \sum_a^n z^{(a)}\, u_{s''}\, \bar{u}_s\, d\tau =$$

$$= \sum_{s''} \int \left(\sum_a^n z^{(a)} \right)^2 u_s\, \bar{u}_{s''}\, d\tau \cdot \int \sum_a^n z^{(a)}\, u_{s''}\, \bar{u}_s\, d\tau = \int \left(\sum_a^n z^{(a)} \right)^3 u_s\, \bar{u}_s\, d\tau. \qquad (73)$$

Es werden also solche Moleküle für die Doppelfrequenzstreuung recht »aktiv« sein, bei denen z^3 über die ganze Ladungsverteilung gemittelt, recht gross sein wird. Eigentlich ist diese Behauptung nicht mit der ganz identisch, dass das Dipolmoment gross sein soll, weil man dasselbe durch eine Mittelung über z erhält.

Weiter ist zur Erzielung eines möglichst grossen Effektes zu verlangen, dass das fragliche unsymmetrische Molekül eine möglichst starke Resonanzfrequenz besitzt, und die eingestrahlte Frequenz ist nach (71) so zu wählen, dass das zweifache dieser Frequenz mit der erwähnten Resonanzfrequenz nahezu übereinstimmt.

Wahrscheinlich werden zum Nachweis des besprochenen Effektes, ebenso wie beim Ramaneffekt, Flüssigkeiten am geeignetesten sein. Es ist zwar wahr, dass bei ihnen infolge der unvermeidlichen Verunreinigungen (Mie-Effekt an suspendierten kleinen Teilchen) die Rayleighstrahlung gegenüber Gasen stark erhöht wird, die viel grössere Dichte wird jedoch diesen Nachteil überkompensieren. Selbstverständlich tritt der Effekt auch an sehr unsymmetrisch gebauten festen Körpern auf, wie wir das schon besprochen haben, doch könnte man bei diesen (71) nicht gut ausnützen, da ja feste Stoffe, abgesehen von Ausnahmsfällen, keine scharfen Resonanzfrequenzen besitzen.

Es sei nur noch erwähnt, dass auch der neue Effekt, ebenso wie die Rayleighstreuung, zu λ^{-4} proportional ist und dass wir bei unseren Rechnungen die Molekülrotation ganz ausser acht gelassen haben. Das haben wir tun können, weil ja die Rotationsfrequenzen im Verhältnis zur Frequenz des eingestrahlten Lichtes klein sind.

Weiter sei noch bemerkt, dass man, ganz analog dem Gedankengange dieser Arbeit, auch das Problem der gleichzeitigen Streuung von zwei Lichtwellen verschiedener Frequenz, bei der auch ein Streustrahl auftritt, dessen Frequenz die Summe der Frequenzen der erwähnten zwei Lichtstrahlen ist, berechnen könnte.

LITERATUR

1. Th. Neugebauer, Z. Physik, **155,** 380, 1959.
2. J. A. Gaunt, Proc. Roy. Soc. London A **122,** 513, 1929; **124,** 163, 1929;
   A. S. Eddington, ebenda, **122,** 358, 1929;
   L. Goldstein, Journ. d. Phys. **1,** 271, 1930.
3. G. Breit, Phys. Rev., **34,** 553, 1929; I. S. Lowen, ebenda, **51,** 190, 1937;
   G. Breit und G. E. Brown, ebenda **74,** 1278, 1948;
   G. Breit und R. E. Meyerott, ebenda, **72,** 1023, 1947 und **75,** 1447, 1949;
   G. Breit, G. E. Brown und J. Arfken, ebenda, **76,** 1299, 1949;
   H. Joos, J. Ferreira und R. H. Zimmermann, Nuovo Cim., **5,** 57, 1957.
4. C. G. Darwin, Phil. Mag., **39,** 537, 1920.
5. C. Møller, Z. Physik, **7**., 786, 1931; Ann. d. Phys., **14,** 531, 1932; Kgl. Danske Videnskab. Selskab. Mat-fys. Medd., **23,** 1, 1945.
6. R. P. Feynman, Phys. Rev., **76,** 749, 1949.
7. E. E. Salpeter und H. A. Bethe, Phys. Rev., **84,** 1232, 1951;
   K. Karplus und A. Klein, ebenda, **87,** 848, 1952;
   J. S. Goldstein, ebenda, **91,** 1516, 1953; Vgl. auch S. S. Schweber, Ann. of Phys., **20,** 61, 1962 und Iwao Sato, J. of Math. Phys., **4,** 24, 1963.
8. M. Gell-Mann und F. Low, Phys. Rev., **84,** 350, 1951.
9. I. Tamm, Journ. Phys. USSR., **9,** 449, 1950.
10. S. M. Dancoff, Phys. Rev., **78,** 382, 1950.
11. W. Zimmermann, Nuovo Cim. Suppl., **1,** 43, 1954.
12. T. H. Neugebauer, Acta Phys. Hung., **10,** 221, 1959.
13. P. A. Franken, A. E. Hill, C. W. Peters und G. Weinreich, Phys. Rev. Letters, **7,** 118, 1961;
    M. Bass, P. A. Franken, A. E. Hill, C. W. Peters, und G. Weinreich, Phys. Rev. Letters, **8,** 18, 1962;
    D. Maker, R. W. Terhune, M. Nisenoff und C. W. Savage, Phys. Rev. Letters, **8,** 21, 1962;
    B. Lax, J. G. Mavroides und D. F. Edwards, Phys. Rev. Letters, **8,** 166, 1962; (theoretische Arbeit) und A. Savage und R. C. Miller, Appl. Opt., **1,** 661, 1962; Vgl. auch P. A. Franken und J. F. Ward, Rev. Mod. Phys., **35,** 23, 1963 (zusammenfassender Bericht) und R. C. Miller, D. A. Kleinman und A. Savage, Phys. Rev. Letters, **11,** 146, 1963.
14. J. A. Giordmaine, Phys. Rev. Letters, **8,** 19, 1962;
    R. C. Miller und A. Savage, Phys. Rev., **128,** 2175, 1962.
15. D. A. Kleinman, Phys. Rev., **125,** 87, 1962 und **128,** 1761, 1962.
16. R. W. Terhune, P. D. Maker und C. W. Savage, Phys. Rev. Letters, **8,** 404, 1962.
17. W. Kaiser und C. G. B. Garrett, Phys. Rev. Letters, **7** ,229, 1961; I. D. Abella, Phys. Rev. Letters, **9,** 453, 1962.
18. Electronics S. 30, Febr. 22, 1963 und S. 7, Febr. 15, 1963; Vgl. auch Elektronics S. 24, June 9, 1961.
19. Th. Neugebauer, Acta Phys. Hung., **14,** 77, 1962.

ВЫЧИСЛЕНИЕ РАССЕЯНИЯ СВЕТА С ДВОЙНОЙ ЧАСТОТОЙ НА ОСНОВЕ УРАВНЕНИЯ ДИРАКА, ОБОБЩЕННОГО ДЛЯ ПРОБЛЕМЫ *n*-ЧАСТИЦ

Т. НАЙГЕБАЕР

Р е з ю м е

В рамках теории Дирака, обобщённой для проблемы *n*-частиц, автором определяется вероятность соединения двух фотонов одинаковой частоты на веществе. Показывается, что здесь имеем дело с тем редким случаем, когда вычисления, направленные на решение проблемы, по этой теории можно довести до конца. Результаты содержатся в формулах (54) и (57). После этого показывается, что и члены второго порядка по $\mathfrak{E}_0$, которые притом не зависят от времени, действительно имеют физический смысл. Во втором параграфе сравниваются интенсивности релеевского рассеяния и рассеяния с двойной частотой, далее освещается вопрос, каким образом нужно выбирать рассеивающие молекулы и условия эксперимента, чтобы определённый вновь эффект был по возможности велик. Самым важным в этом вопросе является член, подчеркнутый в уравнении (57). Он даёт возможность для резонансного усиления нового эффекта без одновременного усиления релеевского рассеяния. В конце (3-й параграф) для нового эффекта выводятся правила отбора. Новый эффект точно исчезает у атомов, молекул с одинаковыми ядрами и многоатомных молекул симметричной структуры. Напротив, усиленно активны в отношении двойной частоты именно многоатомные молекулы полностью асимметричной структуры. При помощи оптического мазера действительно удалось обнаружить появление нового эффекта в случае связанного вещества. Конечно, с теоретической точки зрения наиболее интересным является эффект, появляющийся на молекулах, экспериментальные озможности для которого обеспечиваются в первую очередь техникой лазеров.

THE DEVELOPMENT OF THE CONFIGURATION-INTERACTION METHOD BY THE AID OF THE SPIN-OPERATOR METHOD

By

F. BERENCZ

DEPARTMENT OF THEORETICAL PHYSICS, JÓZSEF ATTILA UNIVERSITY, SZEGED

(Presented by A. Kónya — Received 22. IV. 1963)

When taking all the possible configurations into consideration, the equivalence of the configuration-interaction method developed by the aid of the spin-operator method and the Slater-Pauling method was established on the basis of calculations for the benzene molecule.

Introduction

Only for a certain rather special form of the potential function is the wave equation completely solvable in closed terms; in general, and especially in the field of quantum chemistry, different approximate methods must be applied. In the beginning of the fifties in the theoretical investigation of atoms and molecules the method gained in importance in which the wave function is approximated by the linear combination of given configurations. This method was first applied with success by JUCIS [1] and BOYS [2] to the case of atoms, improving the HARTREE—FOCK method [3], [4]. In the investigation of molecules the molecular orbital method was developed by configuration interaction by CRAIG [5], by COULSON and JACOBS [6], as well as by COULSON, CRAIG and JACOBS [7]. A molecular configuration is a given assignment of electrons to the available one-electron energy levels. It is well known that antisymmetry is required in the coordinates of all electrons in the eigenfunction to ensure the validity of the wave-mechanical PAULI principle. The condition can automatically be fulfilled by giving the function of the molecule in form of a SLATER determinant [8]. The SLATER determinant, however, corresponds to a configuration distributing the electrons in orbitals with given spin eigenfunctions. Generally, one determinant corresponding to a single configuration is not sufficient for a good approximation of the wave function and thus the linear combination of all possible different configurations has to be investigated. This method, which forms the wave function of the molecule from the linear combination of all the possible different configurations is called configuration-interaction method. The drawback of the method lies in the fact that the number of configurations increases extremely rapidly with increasing numbers of electrons.

In the configuration-interaction method the zero-order eigenfunction of a molecule with n electrons has to be constructed as the linear combination $\sum_i c_i \varphi_i$ of the SLATER determinants:

$$\varphi_i = \frac{1}{\sqrt{n!}} \begin{vmatrix} (a\alpha)_1 & (b\alpha)_1 & (c\beta)_1 \dots & (n\alpha)_1 \\ (a\alpha)_2 & (b\alpha)_2 & (c\beta)_2 \dots & (n\alpha)_2 \\ \cdot & & & \\ \cdot & & & \\ \cdot & & & \\ (a\alpha)_n & (b\alpha)_n & (c\beta)_n \dots & (n\alpha)_n \end{vmatrix}, \tag{1}$$

where $a, b, c, \dots, n$ mean orbital eigenfunctions, yet α and β one-particle spin functions and $(a\alpha)_1 = a(1)\,\alpha(1)$, etc. Since each column may contain either $\alpha(i)$ or $\beta(i)$ the degree of the degeneracy of the corresponding energy level is 2^n. On the basis of the RITZ method [9] the energy, to the first order, of the system given by the linear combination of all the possible different configurations can be obtained from the roots of the usual secular equation:

$$|H_{ij} - ES_{ij}| = 0, \tag{2}$$

where

$$H_{ij} = \int \varphi_i^* H \varphi_j \, d\tau \quad \text{and} \quad S_{ij} = \int \varphi_i^* \varphi_j \, d\tau. \tag{3}$$

Since the eigenfunction given by the linear combination of all the possible different configurations has 2^n members, the order of the secular equation is 2^n too. When n is a large number, the problem will be tractable only if the secular determinant can be broken down into a product of determinants of lower order. We have no criterion as to which configurations are important and which can be neglected, therefore we must work out methods for reducing the secular equation. In order to reduce the secular equation we have developed the configuration-interaction method by the aid of the spin-operator method.

The development of the configuration-interaction method by means of the spin-operator method

The development of the configuration-interaction method by the aid of the spin-operator method was discussed in the case of the benzene molecule. It was shown by roentgenographical and electrondiffractional measurements that benzene is a planar molecule with the carbon atoms at the corners of a regular hexagon, and with all C. C. C and C. C. H angles equal to 120°. It is well known that the electron configuration of the C atom is not $(1s)^2\,(2s)^2\,(2p)^2$ in the valence level, but $(1s)^2\,(2s)\,(2p)^3$. Therefore, if we take the plane of the molecule to be the xy plane, we can form three carbon valence bonds with bond angles equal to 120° from the proper linear combination of the s, p_x and p_y carbon orbitals. Now each carbon atom still has one p_z orbitals. The

proper pairing of these create the π-bonds. According to PAULING and WHELAND [10] we assume that the s, p_x and p_y carbon electrons and the hydrogen electrons are localized in σ bonds and we shall calculate the binding energy arising from the interaction of the p_z electrons in the ground state with the configuration-interaction method developed by the aid of the spin-operator-method. Therefore we have to do with a six-electron problem.

In the case of a six-electron system the number of the possible different configurations is $2^6 = 64$; this means, that the zero-order eigenfunction in the configuration-interaction method is built up from the linear combination of 64 SLATER determinants and so the order of the secular equation is 64 too. The first step for reducing the secular equation is to classify the eigenfunctions according to their eigenvalues for S_z. The SLATER determinants contained in the linear combination are eigenfunctions of the operator S_z corresponding to the following eigenvalues in $\hbar$ units:

$$3, \quad 2, \quad 1, \quad 0, \quad -1, \quad -2, \quad -3.$$

The number of eigenfunctions belonging to the eigenvalue $i = 3, 2, 1, 0, -1, -2, -3$ is equal to the possibility of choosing 6 from i, that is $\binom{6}{i}$. That means that the number of eigenfunctions corresponding to the eigenvalues 3, 2, 1, 0, -1, -2, -3 is 1, 6, 15, 20, 15, 6, 1. When we classify the 64 eigenfunctions according to the eigenvalue for S_z, the secular determinant is reduced to 2 one-row, 2 six-row, 2 fifteen-row and 1 twenty-row determinants, since SLATER [14] and CONDON [15] have proved, that

$$H_{ij} = S_{ij} = 0, \tag{4}$$

if φ_i and φ_j have different eigenvalues for S_z.

$$\begin{vmatrix}
\text{one-row} & 0 & 0 & 0 & 0 & 0 & 0 \\
0 & \text{six-row} & 0 & 0 & 0 & 0 & 0 \\
0 & 0 & \text{fifteen-row} & 0 & 0 & 0 & 0 \\
0 & 0 & 0 & \text{twenty-row} & 0 & 0 & 0 \\
0 & 0 & 0 & 0 & \text{fifteen-row} & 0 & 0 \\
0 & 0 & 0 & 0 & 0 & \text{six-row} & 0 \\
0 & 0 & 0 & 0 & 0 & 0 & \text{one-row}
\end{vmatrix} = 0. \tag{5}$$

We are interested only in the ground state, in which the resulting spin is zero, therefore we need only discuss the case with the twenty-row determinant. In the twenty-row determinant there are SLATER determinants which are eigenfunctions for S_z corresponding to the eigenvalue 0. These are as follows:

$$\begin{aligned}
\varphi_1 &= (\alpha\alpha\alpha\,\beta\beta\beta)\,,\\
\varphi_2 &= (\alpha\alpha\,\beta\beta\,\alpha\beta)\,,\\
\varphi_3 &= (\alpha\beta\,\alpha\alpha\,\beta\beta)\,,\\
\varphi_4 &= (\alpha\beta\,\alpha\beta\,\alpha\beta)\,,\\
\varphi_5 &= (\alpha\alpha\,\beta\alpha\,\beta\beta)\,,\\
\varphi_6 &= (\alpha\alpha\,\beta\beta\,\beta\alpha)\,,\\
\varphi_7 &= (\alpha\beta\,\beta\beta\,\alpha\alpha)\,,\\
\varphi_8 &= (\alpha\beta\,\beta\alpha\,\alpha\beta)\,,\\
\varphi_9 &= (\alpha\beta\,\beta\alpha\,\beta\alpha)\,,\\
\varphi_{10} &= (\alpha\beta\,\alpha\beta\,\beta\alpha)\,,\\
\varphi_{11} &= (\beta\alpha\,\beta\alpha\,\alpha\beta)\,,\\
\varphi_{12} &= (\beta\alpha\,\alpha\beta\,\alpha\beta)\,,\\
\varphi_{13} &= (\beta\alpha\,\alpha\beta\,\beta\alpha)\,,\\
\varphi_{14} &= (\beta\alpha\,\alpha\alpha\,\beta\beta)\,,\\
\varphi_{15} &= (\beta\beta\,\alpha\alpha\,\alpha\beta)\,,\\
\varphi_{16} &= (\beta\beta\,\alpha\beta\,\alpha\alpha)\,,\\
\varphi_{17} &= (\beta\alpha\,\beta\alpha\,\beta\alpha)\,,\\
\varphi_{18} &= (\beta\alpha\,\beta\beta\,\alpha\alpha)\,,\\
\varphi_{19} &= (\beta\beta\,\alpha\alpha\,\beta\alpha)\,,\\
\varphi_{20} &= (\beta\beta\beta\,\alpha\alpha\alpha)\,.
\end{aligned} \tag{6}$$

The basis of the further reduction of the twenty-row determinant is the spin-operator method introduced in a previous paper [13], which forms such a linear combination of the φ_i $(i = 1, 2, \ldots, 20)$ eigenfunctions which are eigenfunctions for S^2 corresponding to the eigenvalues $\hbar^2 s(s+1)$. In the case of six electrons the absolute value of the resulting spin can be 0, 1, 2, 3. According to the branching diagram there exist 5 linear independent singlet states, 9 linear independent triplet states, 5 linear independent quintet states and 1 linear independent septet state:

When our spin operator given in a previous paper [13] is operating on the eigenfunctions of the above-mentioned states, according to the theorem given also in that paper [13], the eigenfunctions for S^2 are obtained corresponding to the eigenvalues $\hbar^2 0(0+1)$, $\hbar^2 1(1+1)$, $\hbar^2 2(2+1)$, $\hbar^2 3(3+1)$. It is well known, that if the resulting spin has for example the value 2, then the spin-projections can be 2, 1, 0, -1, -2, that is, the state with the resulting spin 2 is fivefold degenerate and therefore the number of eigenfunctions of S^2 is

also 5. With the application of our spin-operator such eigenfunctions of S^2 can be obtained which correspond to the maximal value for S^2. However, considering the equ. (19) the eigenfunctions related to other eigenvalues for S_z can also be derived. In the case of the singlet state the 5 eigenfunctions for S^2 are also eigenfunctions for S_z related to the eigenvalue 0. In the case of triplet state the eigenvalues for S_z are $+1, 0, -1$ and therefore there are 9 such eigenfunctions among the 27 eigenfunctions of the triplet state which correspond to the eigenvalue 0 for S_z. In the case of quintet state the eigenvalues

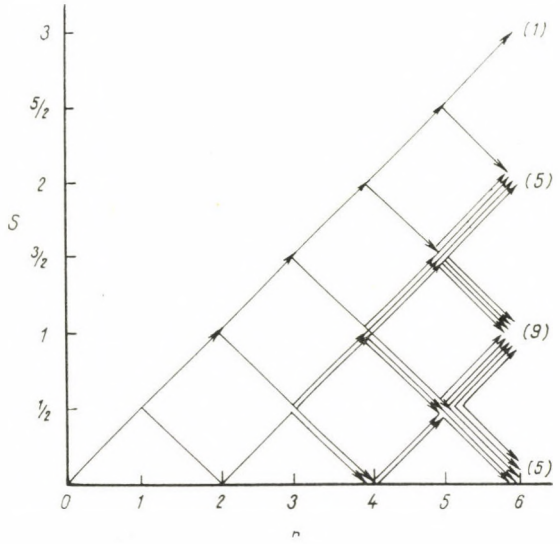

Fig. 1

for S_z are $+2, +1, 0, -1, -2$ and therefore there are 5 eigenfunctions among the 25 eigenfunctions of the quintet states which correspond to the eigenvalue 0 for S_z. Finally, in the case of the septet state the eigenvalues for S_z are $+3, +2, +1, 0, -1, -2, -3$ and therefore there is 1 eigenfunction among the 7 eigenfunctions of the septet state which corresponds to the eigenvalue 0 for S_z. We have also 20 such combinations of eigenfunctions which relate to various eigenvalues for S^2 and to zero eigenvalue for S_z. These eigenfunctions can be constructed with our general spin operator introduced in the paper mentioned [13].

Using the spin-operator method the eigenfunctions which are simultaneous eigenfunctions for S^2 and for S_z corresponding to the eigenvalue 0, can be constructed by the application of our general spin operator to the eigenfunctions of the 5 linear independent singlet states shown in the branching

diagram

$$\psi_1^{0,0} = \frac{1}{6}(3\varphi_1 - \varphi_2 - \varphi_3 - \varphi_4 - \varphi_5 - \varphi_6 + \varphi_7 + \varphi_8 + \varphi_9 - \varphi_{10} + \\ + \varphi_{11} - \varphi_{12} - \varphi_{13} - \varphi_{14} + \varphi_{15} + \varphi_{16} + \varphi_{17} + \varphi_{18} + \varphi_{19} - 3\varphi_{20}),$$

$$\psi_2^{0,0} = \frac{1}{2\sqrt{6}}(2\varphi_2 - \varphi_4 - 2\varphi_6 - \varphi_8 + \varphi_9 + \varphi_{10} - \\ - \varphi_{11} - \varphi_{12} + \varphi_{13} + 2\varphi_{15} + \varphi_{17} - 2\varphi_{19}),$$

$$\psi_3^{0,0} = \frac{1}{2\sqrt{6}}(2\varphi_3 - \varphi_4 + 2\varphi_7 - \varphi_8 - \varphi_9 - \varphi_{10} + \\ + \varphi_{11} + \varphi_{12} + \varphi_{13} - 2\varphi_{14} + \varphi_{17} - 2\varphi_{18}), \tag{7}$$

$$\psi_4^{0,0} = \frac{1}{2\sqrt{2}}(\varphi_4 - \varphi_8 + \varphi_9 - \varphi_{10} + \varphi_{11} - \varphi_{12} + \varphi_{13} - \varphi_{17}),$$

$$\psi_5^{0,0} = \frac{1}{6\sqrt{2}}(-2\varphi_2 - 2\varphi_3 + \varphi_4 + 4\varphi_5 - 2\varphi_6 + 2\varphi_7 - \varphi_8 - \varphi_9 + \varphi_{10} - \\ - \varphi_{11} + \varphi_{12} + \varphi_{13} - 2\varphi_{14} + 2\varphi_{15} - 4\varphi_{16} - \varphi_{17} + 2\varphi_{18} + 2\varphi_{19}).$$

In the triplet state when the general spin operator is operating on the eigenfunctions representing the 9 linear independent triplet states constructed in the branching diagram and equ. (19) is considered, such eigenfunctions for S^2 are obtained, which correspond to the eigenvalue $\hbar^2\, 1(1+1)$ according to the theorem introduced in a previous paper [13] and which are also eigenfunctions for S_2 corresponding to the eigenvalue 0:

$$\psi_1^{1,0} = \frac{1}{6\sqrt{10}}(3\varphi_1 - 2\varphi_2 + 3\varphi_3 - 2\varphi_4 + 3\varphi_5 - 2\varphi_6 + 3\varphi_7 - 2\varphi_8 - \\ - 2\varphi_9 - 2\varphi_{10} - 2\varphi_{11} - 2\varphi_{12} - 2\varphi_{13} + 3\varphi_{14} - 2\varphi_{15} + 3\varphi_{16} - \\ - 2\varphi_{17} + 3\varphi_{18} - 2\varphi_{19} + 3\varphi_{20}),$$

$$\psi_2^{1,0} = \frac{1}{6\sqrt{3}}(3\varphi_1 - \varphi_2 - \varphi_3 - \varphi_4 - \varphi_5 + \varphi_6 - \varphi_7 + \varphi_8 - \varphi_9 + \varphi_{10} + \\ + \varphi_{11} - \varphi_{12} + \varphi_{13} - \varphi_{14} + \varphi_{15} - \varphi_{16} - \varphi_{17} - \varphi_{18} - \varphi_{19} + 3\varphi_{20}),$$

$$\psi_3^{1,0} = \frac{1}{6\sqrt{2}}(2\varphi_2 - \varphi_4 + 2\varphi_6 - \varphi_8 - \varphi_9 - \varphi_{10} - \\ - \varphi_{11} - \varphi_{12} - \varphi_{13} + 2\varphi_{15} - \varphi_{17} + 2\varphi_{19}),$$

$$\psi_4^{1,0} = \frac{1}{6}(\varphi_3 + \varphi_4 - \varphi_7 + \varphi_8 - \varphi_9 - \varphi_{10} - \\ - \varphi_{11} - \varphi_{12} + \varphi_{13} - \varphi_{14} + \varphi_{17} + \varphi_{18}),$$

$$\psi_5^{1,0} = \frac{1}{6\sqrt{3}}(2\varphi_2 - \varphi_3 - \varphi_4 + 2\varphi_5 - 2\varphi_6 - \varphi_7 + \varphi_8 - \varphi_9 + \varphi_{10} + \\ + \varphi_{11} - \varphi_{12} + \varphi_{13} - \varphi_{14} - 2\varphi_{15} + 2\varphi_{16} - \varphi_{17} - \varphi_{18} + 2\varphi_{19}),$$

$$\psi_6^{1,0} = \frac{1}{6\sqrt{6}}(3\varphi_1 + 2\varphi_2 - \varphi_3 + 2\varphi_4 - \varphi_5 - 2\varphi_6 - \varphi_7 - 2\varphi_8 + 2\varphi_9 - \\ - 2\varphi_{10} - 2\varphi_{11} + 2\varphi_{12} - 2\varphi_{13} - \varphi_{14} - 2\varphi_{15} - \varphi_{16} + 2\varphi_{17} - \\ - \varphi_{18} + 2\varphi_{19} + 3\varphi_{20}),$$

$$\psi_7^{1,0} = \frac{1}{6\sqrt{6}}(-2\varphi_2 - 2\varphi_3 + \varphi_4 + 4\varphi_5 + 2\varphi_6 - 2\varphi_7 - \varphi_8 + \varphi_9 - \varphi_{10} - \\ - \varphi_{11} + \varphi_{12} - \varphi_{13} - 2\varphi_{14} + 2\varphi_{15} + 4\varphi_{16} + \varphi_{17} - 2\varphi_{18} - 2\varphi_{19}),$$

$$\psi_8^{1,0} = \frac{1}{6\sqrt{2}}(2\varphi_3 - \varphi_4 - 2\varphi_7 - \varphi_8 + \varphi_9 + \varphi_{10} + \\ + \varphi_{11} + \varphi_{12} - \varphi_{13} - 2\varphi_{14} - \varphi_{17} + 2\varphi_{18}),$$

$$\psi_9^{1,0} = \frac{1}{2\sqrt{6}}(\varphi_4 - \varphi_8 - \varphi_9 + \varphi_{10} + \varphi_{11} - \varphi_{12} - \varphi_{13} + \varphi_{17}). \qquad (8)$$

Also in the quintet state, when the general spin operator is operating on the eigenfunctions representing the 5 linear independent triplet states constructed in the branching diagram and considering equ. (19) such eigenfunctions for S^2 are obtained, which correspond to the eigenvalue $\hbar^2 2(2+1)$ and which are also eigenfunctions for S_z corresponding to the eigenvalue 0:

$$\psi_1^{2,0} = \frac{1}{5\sqrt{2}}(\varphi_1 + \varphi_2 + \varphi_3 + \varphi_4 + \varphi_5 - \varphi_6 - \varphi_7 + \varphi_8 - \varphi_9 - \varphi_{10} + \\ + \varphi_{11} + \varphi_{12} - \varphi_{13} + \varphi_{14} + \varphi_{15} - \varphi_{16} - \varphi_{17} - \varphi_{18} - \varphi_{19} - \varphi_{20}),$$

$$\psi_2^{2,0} = \frac{1}{10\sqrt{3}}(3\varphi_1 - 2\varphi_2 + 3\varphi_3 - 2\varphi_4 + 3\varphi_5 + 2\varphi_6 - 3\varphi_7 - 2\varphi_8 + \\ + 2\varphi_9 + 2\varphi_{10} - 2\varphi_{11} - 2\varphi_{12} + 2\varphi_{13} + 3\varphi_{14} - 2\varphi_{15} - 3\varphi_{16} + \\ + 2\varphi_{17} - 3\varphi_{18} + 2\varphi_{19} - 3\varphi_{20}),$$

$$\psi_3^{2,0} = \frac{1}{6\sqrt{5}}(3\varphi_1 + 2\varphi_2 - \varphi_3 + 2\varphi_4 - \varphi_5 + 2\varphi_6 + \varphi_7 - 2\varphi_8 - 2\varphi_9 + 2\varphi_{10} - 2\varphi_{11} + 2\varphi_{12} + 2\varphi_{13} - \varphi_{14} - 2\varphi_{15} + \varphi_{16} - 2\varphi_{17} + \varphi_{18} - 2\varphi_{19} - 3\varphi_{20})/$$

$$\psi_4^{2,0} = \frac{1}{3\sqrt{10}}(2\varphi_2 - \varphi_3 - \varphi_4 + 2\varphi_5 + 2\varphi_6 + \varphi_7 + \varphi_8 + \varphi_9 - \varphi_{10} + \varphi_{11} - \varphi_{12} - \psi_{13} - \varphi_{14} - 2\varphi_{15} - 2\varphi_{16} + \varphi_{17} + \varphi_{18} - 2\varphi_{19}),$$

$$\psi_5^{2,0} = \frac{1}{\sqrt{30}}(\varphi_3 + \varphi_4 + \varphi_7 + \varphi_8 + \varphi_9 + \varphi_{10} - \varphi_{11} - \varphi_{12} - \varphi_{13} - \varphi_{14} - \varphi_{17} - \varphi_{18}). \tag{9}$$

In the case of the septet state only one eigenfunction for S^2 corresponds to the eigenvalue $\hbar^2\, 3(3+1)$ and this eigenfunction is also that eigenfunction for S_z which corresponds to the eigenvalue 0. It can be obtained considering equ. (13):

$$\psi^{3,0} = \frac{1}{20}(\varphi_1 + \varphi_2 + \varphi_3 + \varphi_4 + \varphi_5 + \varphi_6 + \varphi_7 + \varphi_8 + \varphi_9 + \varphi_{10} + \varphi_{11} + \varphi_{12} + \varphi_{13} + \varphi_{14} + \varphi_{15} + \varphi_{16} + \varphi_{17} + \varphi_{18} + \varphi_{19} + \varphi_{20}). \tag{10}$$

Among the 20 eigenfunctions for S^2 constructed above there are 5 corresponding to the eigenvalue $\hbar^2\, 1(1+1)$, 5 corresponding to the eigenvalue $\hbar^2\, 2(2+1)$ and 1 corresponding to the eigenvalue $\hbar^2\, 3(3+1)$. If the eigenfunctions for S^2 are to be classified according to their eigenvalues, the secular determinant, since the equ. (4) is valid in the case of the eigenfunctions for S^2 too, will be further reduced to 2 five-row, 1 nine-row and 1 one-row determinants:

$$\begin{vmatrix} \text{five-row} & 0 & 0 & 0 \\ 0 & \text{nine-row} & 0 & 0 \\ 0 & 0 & \text{five-row} & 0 \\ 0 & 0 & 0 & \text{one-row} \end{vmatrix} = 0. \tag{11}$$

We are interested only in the ground state, therefore we have only to do with that five-row determinant, in which those eigenfunctions play a role which correspond to the resulting spin zero. Denoting the Coulomb integrals

by Q and taking only the interaction of the neighbouring atoms into consideration according to the HÜCKEL method [14] and further denoting the exchange integrals by α, the above-mentioned five-row secular determinant has the following form:

$$\begin{vmatrix} x-20 & -\sqrt{6} & -\sqrt{6} & -3\sqrt{2} & -5\sqrt{2} \\ -\sqrt{6} & x-9 & 3 & -3\sqrt{3} & -5\sqrt{3} \\ -6 & 3 & x-9 & -3\sqrt{3} & -5\sqrt{3} \\ -3\sqrt{2} & -3\sqrt{3} & -3\sqrt{3} & x+9 & 3 \\ -5\sqrt{2} & -5\sqrt{3} & -5\sqrt{3} & 3 & x-7 \end{vmatrix} = 0, \tag{12}$$

where

$$x = \frac{6(Q-E)}{\alpha}. \tag{13}$$

After some manipulation the previous determinant reduces to

$$\begin{vmatrix} x-12 & 0 & 0 & 0 & 0 \\ 0 & x-20 & -\sqrt{6} & -\sqrt{2} & 0 \\ 0 & -2\sqrt{6} & x-6 & -2\sqrt{3} & 0 \\ 0 & -2\sqrt{2} & -2\sqrt{3} & x-2 & 4x \\ 0 & 0 & 0 & 4x & 17x+36 \end{vmatrix} = 0. \tag{14}$$

Expanding the determinant the following equation is obtained

$$x(x-12)^2(x^2-12x-342) = 0. \tag{15}$$

The roots of this equation are as follows:

$$\begin{aligned} x &= 0, \\ x &= 12, \\ x &= 12, \\ x &= 6(1+\sqrt{13}), \\ x &= 6(1-\sqrt{13}). \end{aligned} \tag{16}$$

The energy expressions according to the equ. (13) have the following forms:

$$\begin{aligned} E &= Q, \\ E &= Q-2\alpha, \\ E &= Q-2\alpha, \\ E &= Q-(1+\sqrt{13})\alpha, \\ E &= Q-(1-\sqrt{13})\alpha. \end{aligned} \tag{17}$$

It is well known that a is a negative quantity, so that the energy of the ground state is

$$E = Q - (1 - \sqrt{13})\, a = Q + 2{,}61\, a. \tag{18}$$

If the configuration-interaction method is developed by the aid of the spin-operator method the ground state energy fo the benzene molecule can be obtained by solving a secular equation of only order 5.

The equivalence of the configuration-interaction method developed by the aid of the spin-operator method and the Slater—Pauling method

On the basis of the calculations for the benzene molecule, when taking all possible configurations into consideration the equivalence of the configuration-interaction method extended by the aid of the spin-operator method and the SLATER [15]—PAULING [16] method can be established. The proof can be summarized in the following points:

1. In the case of the SLATER—PAULING method, similar to our method, the eigenfunction is given in the form of a linear combination of SLATER determinants.

2. It was proved by SLATER that only such eigenfunctions must be used in a linear combination, in which the projection on the axis z of the resulting spin has the same value. In our case this fact is shown by the classification of the eigenfunctions according to the eigenvalues for S_z and then on account of equ. (4) the matrix elements constructed from the eigenfunctions having different eigenvalues will be zero.

3. The next step in the SLATER—PAULING method was the idea of PAULING, according to which linear combinations of only those eigenfunctions has to be looked for, in which the absolute value of the resulting spin has a fixed value. These eigenfunctions are the bond eigenfunctions representing the various numbers of the linear independent bonds; these eigenfunctions can be derived from the RUMER diagram [17]. This step is made in our case when the linear combination of SLATER determinants is constructed on the basis of our general spin operator (in this fact lies the origin of the name spin-operator method) derived from the so called step-up and step-down operators, the eigenfunction being an eigenfunction for S^2. In our case the eigenfunctions related to the spin states of various multiplicity correspond to the bond eigenfunctions representing the various numbers of the linear independent bonds. These eigenfunctions can be constructed from the branching diagram.

4. On the basis of the SLATER—PAULING method numerical calculations were performed by PAULING and WHELAND for the benzene molecule according

to the HÜCKEL method. Although the bond eigenfunctions of PAULING and WHELAND differ from the eigenfunctions constructed with help of the spin-operator method and therefore the secular equation of PAULING and WHELAND naturally has a form other than the secular equation obtained by the spin-operator-method, nevertheless the roots of the secular equation, that is the energies of the various states, are in full agreement.

Appendix

When constructing the eigenfunctions for S^2 the following equation was used on several occasions

$$\varphi(s, s-i) \equiv \frac{1}{2!}\binom{n}{i}^{-\frac{1}{2}} (s^-)^i (\overset{1}{\alpha}\ \overset{2}{\alpha} \ldots \overset{n}{\alpha}), \tag{19}$$

where s means the resulting spin and $s - i$ means the spin projection. This theorem was proved in the appendix of a previous paper [13].

REFERENCES

1. Y. JUCIS, J. Exp. Theor. Phys. USSR, **19,** 565, 1949.
2. S. F. BOYS, Proc. Roy. Soc. **A 200,** 542, 1950.
3. D. R. HARTREE, Proc. Camb. Phil. Soc., **24,** 111, 1927—28.
4. V. FOCK, Z. Phys., **61,** 126, 1930.
5. D. P. CRAIG, Proc. Roy. Soc. **A 202,** 498, 1950.
6. C. A. COULSON and J. JACOBS, Proc. Roy. Soc. **A 206,** 287, 1951.
7. C. A. COULSON, D. P. CRAIG and J. JACOBS, Proc. Roy. Soc. **A 206,** 297, 1951.
8. J. C. SLATER, Phys. Rev., **34,** 1293, 1929.
9. W. RITZ, J. f. reine und angew. Math., **131,** 1, 1909.
10. L. PAULING and G. W. WHELAND, J. Chem. Phys., **1,** 362, 1933.
11. J. C. SLATER, Phys. Rev., **34,** 1293, 1929.
12. E. U. CONDON, Phys. Rev., **36,** 1121, 1930.
13. F. BERENCZ, Proc. Phys. Soc. **A 71,** 152, 1958.
14. E. HÜCKEL, Z. Phys., **70,** 204, 1931; **76,** 628, 1932.
15. J. C. SLATER, Phys. Rev., **38,** 1109, 1931.
16. L. PAULING, J. Chem. Phys., **1,** 280, 1933.
17. G. RUMER, Göttingen Nachr., **377,** 1932.

РАЗРАБОТКА МЕТОДА КОНФИГУРАЦИОННОГО ВЗАИМОДЕЙСТВИЯ СПИН-ОПЕРАТОРНЫМ МЕТОДОМ

Ф. БЕРЕНЦ

Резюме

Принимая во внимание все возможные конфигурации, устанавливается эквивалентность метода конфигурационного взаимодействия, разработанного спин-операторным методом, и методом Слейтера-Полинга. Вся работа базируется на вычислениях, проведенных для молекулы бензола.

ОБНАРУЖЕНИЕ ЯДЕРНЫХ ИЗОМЕРОВ МЕТОДОМ ФОТОАКТИВАЦИИ С ПОМОЩЬЮ ИСТОЧНИКА Co—60

А. ВЕРЕШ

ГОСУДАРСТВЕННЫЙ КОМИТЕТ ПО АТОМНОЙ ЭНЕРГИИ
ИНСТИТУТ ИЗОТОПОВ, БУДАПЕШТ

(Представлено Л. Пал. — Поступило 27. IV. 1963)

В работе определены ядерные изомеры в случае 10 различных стабильных нуклидов. Ядерные изомеры получены путем реакции A (γ, γ') A*, применением источника Co-60 с активностью 1310 Кюри. Эти изомеры были получены таким путём впервые. Из величины фотоактивации было оценено сечение активации и ширина уровня активации. Указаны возможные пути применения данного метода.

Введение

В 1921-ом году появилось первое сообщение [1] по поводу явления ядерных изомеров, но выяснение свойства этого физического явления осуществилось только намного позже, после 1935-го года, когда ядерная изомерия наблюдалась также у исскуственных радиоизотопов [2—4].

С тех пор у многих ядер удалось вызвать и обнаружить метастабильные состояния [5—6] с помощью (γ, n), $(n, 2n)$, (n, γ), (n, α), (n, p), (p, n) и т. д. ядерных реакций. В настоящее время для стабильных изотопов насчитывается около сорока ядерных изомеров, время жизни которых больше одной секунды.

Одним из возможных методов для возбуждения в метастабильное состояние является резонансное возбуждение типа $A(\gamma, \gamma')A^*$. Голдхабер, Хилл и Сциллард [14] с помощью γ-лучей 0,5 грамма Ra не могли обнаружить возбуждение на метастабильный уровень индия, путем In-115 (γ, γ') In-115m ядерной реакции. Отрицательные результаты этого опыта Э. Гус [13] объяснял тем, что энергии γ-лучей радия не равняются энергиям возможных состояний возбуждения индия.

В 1962-ом году автор настоящего сообщения производил исследования [18] с помощью γ-источника Co-60 с активностью 424 кюри на ядрах In-115 и Cd-111. На примере этих ядер удалось впервые обнаружить возбуждение в метастабильное состояние с помощью γ-лучей. Полученные данные активности, времена жизни и энергии несомненно доказали образования ядерных изомеров In-115m и Cd-111m.

Известно кроме того из многих сообщений, что с помощью обладающего непрерывным спектром тормозного излучения, тоже осуществляются ядерные изомеры методом резонансного возбуждения (γ, γ').

Метастабильные состояния разных стабильных ядер исследовали: Валдман и Коллинс [7] — In-115 и Pb, Виденбек [8—10] — Ag, Cd, Hg, Sr, Nb, Au, Kr, Rh, Миллер и Валдман [11] — In-115. Лукенс, Отвош и Вагнер [12] исследовали почти все стабильные элементы с порядковым номером $Z > 4$ за исключением инертных газов. Они обнаружили активность в случае 23 ядер и определили энергии и время жизни у 19 ядерных изомеров.

Исследования, произведенные с помощью рентгеновского излучения, обладающего непрерывным спектром, доказали, что возбуждение ядра происходит не на метастабильный уровень E_m, а на уровень активации $E_a > E_m$. с этого уровня за очень короткое время $\tau < 10^{-10}$ сек ядро может достичь

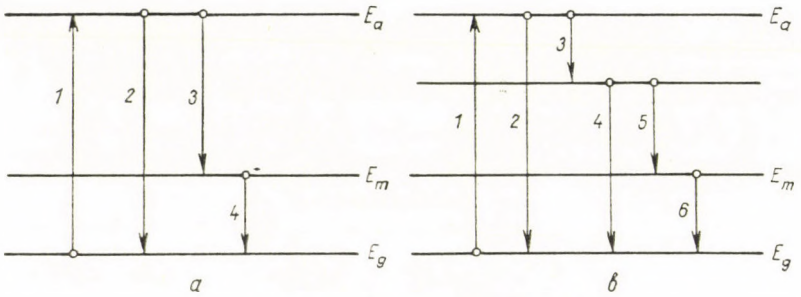

Рис. 1. Возможные схемы возбуждения

а) Простой случай, в котором ядро с активационного уровня проходит частично в основное состояние и частично в метастабильное состояние.

б) Возможный каскадный переход, в котором ядро проходит на метастабильный уровень со прикосновением некоторых промежуточных возбужденных уровней.

метастабильного уровня непосредственным переходом или соприкосновением многих уровней путем каскадного процесса. С метастабильного уровня ядро проходит в стабильное состояние за то время, которое характерно для времени жизни E_m уровня. (см. I.а, I.б рис.)

В настоящей работе сообщается исследование 10 таких стабильных ядер, которые имеют метастабильный уровень со временем жизни больше одной секунды. Опыты производились с помощью источника Co-60, с активностью 1310 кюри.

Условия облучения

а) *Источник*

Источник состоит из кобальтовой трубки с активными размерами ф24/16 × 24 мм. Источник находился в алюминиевом цилиндрическом кожухе, размеры которого 27 × ф 26 мм. Облучаемые мишени были помещены на одном торце цилиндрообразного источника. Для того, чтобы избегать загрязнения от поверхности источника, мишени были положены в алюминиевые

кожухи с толщиной стены 1 мм. Источник находился в свинцовом контейнере, изготовленном в Советском Союзе, который обеспечил защиту от излучения в течение опыта. Введение мишени в контейнер было произведено с помощью дистанционного манипулятора наклоном 90 градусов (см. рис. 2.). Трубчатая часть манипулятора над мишенью с диаметром 30 мм был налит свинцом, с целью избежания выхода интенсивного пучка γ-лучей даже и на время облучения мишени. Это применялось только при исследовании

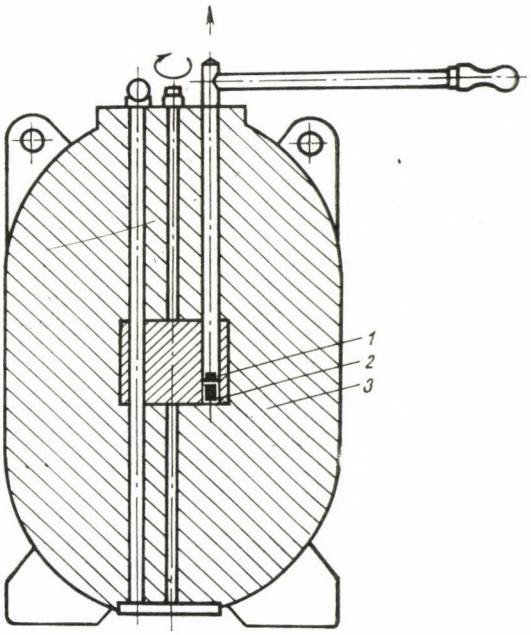

Рис. 2. Схема облучающей установки
1. Мишень,
2. Источник,
3. Свинцовая защита

изомеров, имеющих не очень короткое время полураспада, поскольку вслучае исследования изомеров, имеющих очень короткое время полураспада, после облучения на наше распоряжение оставалось чрезвычайно мало времени для измерения. Эти измерения производились на воздухе и поэтому увеличение фона из-за рассеяния пучка было минимально.

б) *Мишени*

Диаметры облучаемых мишеней 25 мм, их вес и химический состав приведены в табл. I. Время облучения для материалов, имеющих метастабильный уровень с коротким полураспадом, подбиралось в основном так, чтобы

оно превосходило 8—10-и кратный полураспад, который необходим для достижения активности насыщения.

Таблица I

Данные ядер, облученных источником Co—60.

Хим. знак элемента	Вес мишени (г)	Хим. сост. мишени	Время облучения
Se	14	металл	3 мин.
Sr	8,7	окись	25 час.
Y	10	окись	3 мин.
Rh	10	металл. порошок	16 час.
Ag	8	металл	6 мин.
Hf	0,4	окись	3 мин.
Ir	1	металл. порошок	1 мин.
Pt	3,2	металл	3 дня
Au	9,1	металл	1 мин.
Hg	58	металл	5 час.

Метрология

После облучения, измерения полученных активностей производились с помощью датчика, состоящего из кристалла NaJ (Tl) с размерами $1\frac{1''}{2} \times$ $\times 1\frac{3''}{4}$, из фотоумножителя типа EMI 9536B и пересчётной схемы типа GOM. Датчик был присоединен с одной стороны к одноканальному анализатору типа Siemens с интегральным дискриминатором с целью измерения суммы импульсов. Установка содержала в себе автоматический электронный блок для измерения времени, блок, печатающий число импульсов и времени и автоматический пусковой блок, время периода которого можно регулировать от 6- сек. до 400 мин. и так оказался весьма пригодным для определения времени полураспада изомеров в порядке несколько сек. Те же импульсы были зарегистрированы с 128 канальным анализатором типа KFKI с целью определения энергетического спектра выпущенного излучения. Для определения величины активности определили эффективность детектора для разных энергий γ-квантов частично по расчёту и частично с известными γ-линиями Cs-137, Cd-109 и Co-60 изотопов, таким образом, что приготовили источник с известной активностью, имеющий форму облученной мишени. Градуировка энергетической шкалы и исследование линейности производились тоже с источниками Cs-137, Cd-109 и Co-60 изотопов. Энергетическая разрешающая

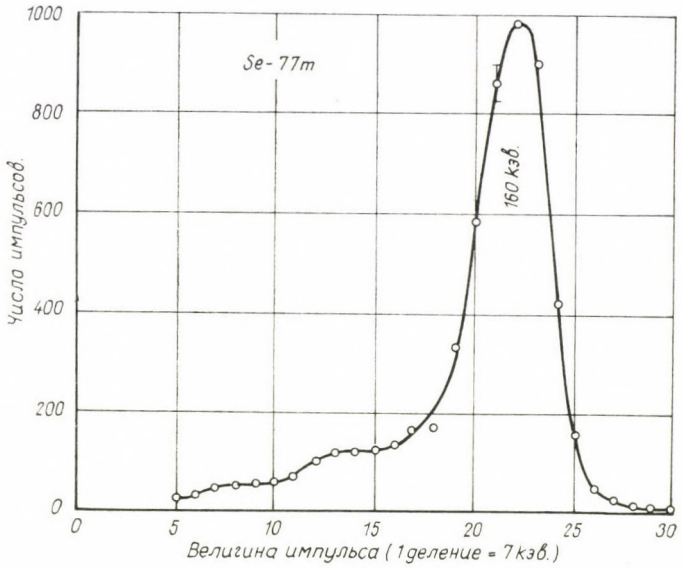

Рис. 3. Энергетический спектр Se-77m

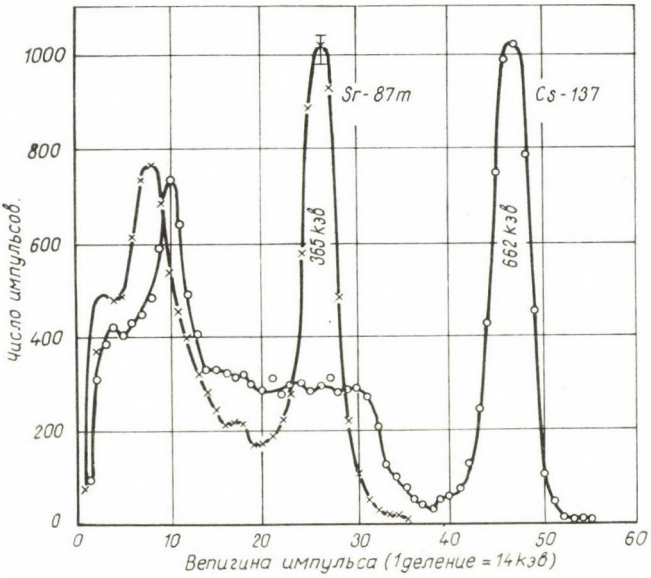

Рис. 4. Энергетический спектр Sr-87m и градуирующий спектр Cs-137

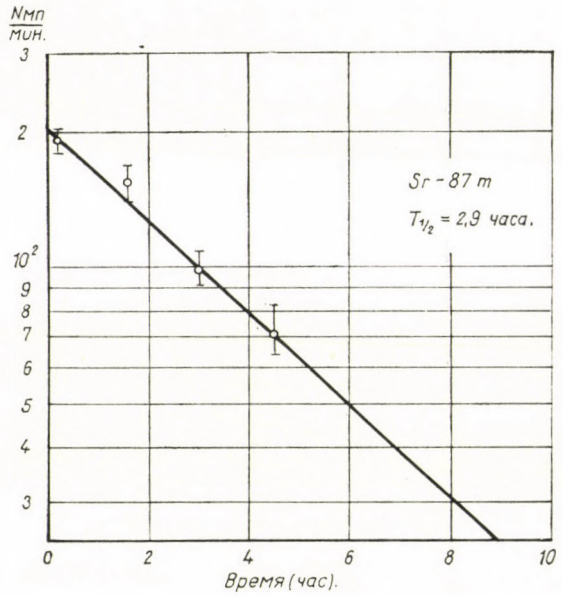

Рис. 5. Кривая распада Sr-87m

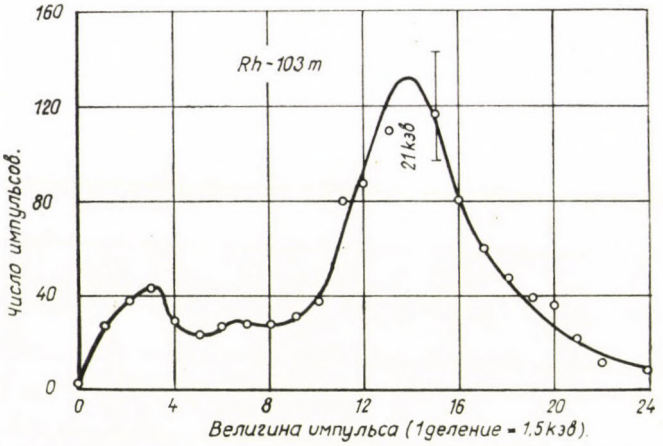

Рис. 6. Энергетический спектр Rh-103m

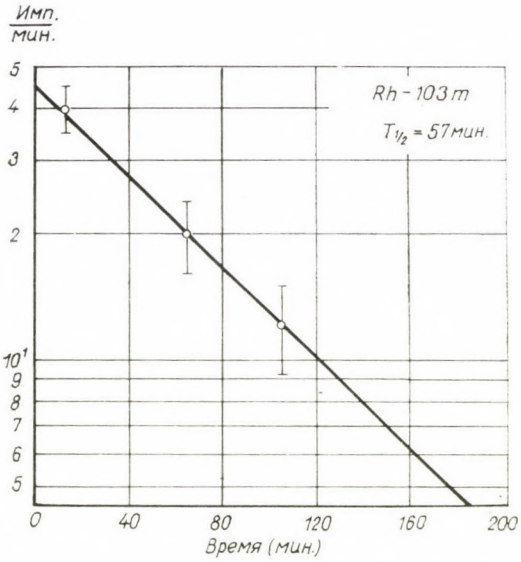

Рис. 7. Кривая распада Rh-103m

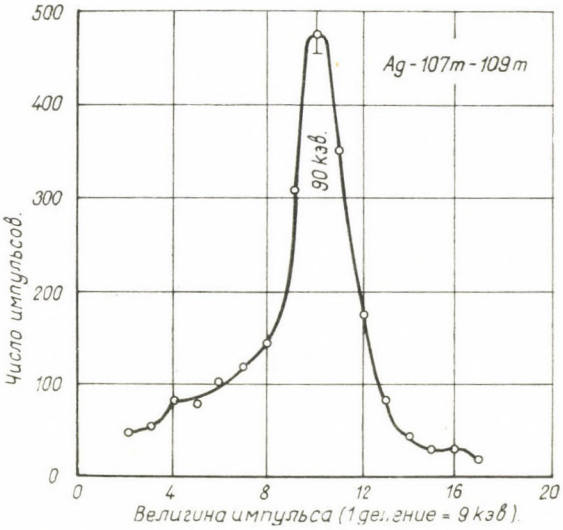

Рис. 8. Энергетический спектр Ag-107m — 109m

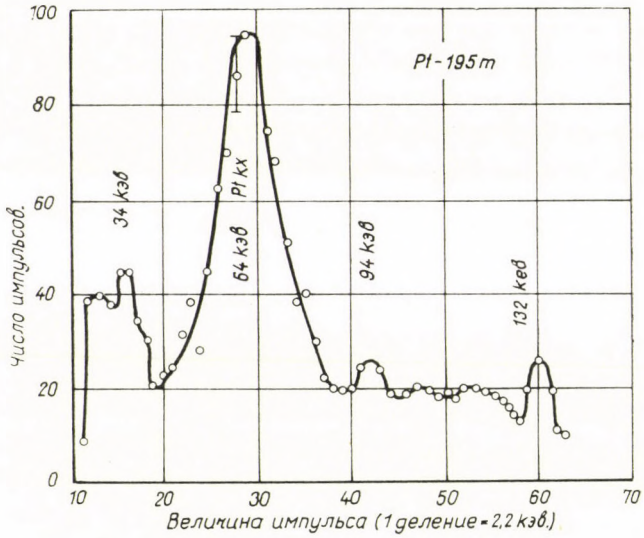

Рис. 9. Энергетический спектр Pt-195m

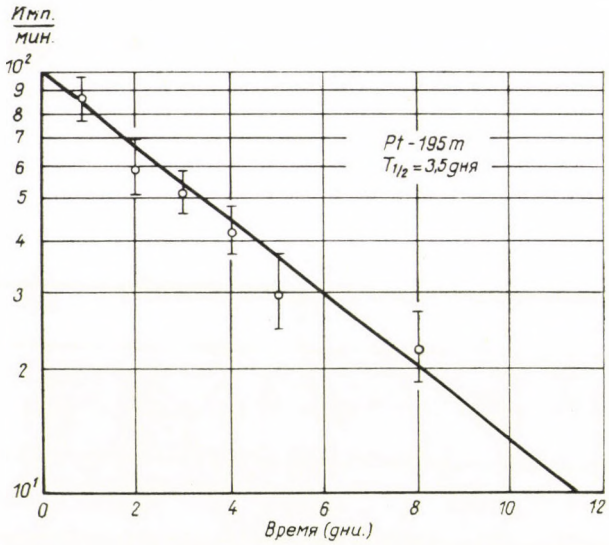

Рис. 10. Кривая распада Pt-195m

способность детектора у датчика типа Siemens 14%, у датчика типа GOM 9,2% было для линии с энергией 662 кэв Cs-137 в течение измерений. Монтировочный слой кристалла изготовлен из алюминия с толщиной 0,5 мм.

Измерения изомеров, имеющих короткий полураспад, начались через 5—10 сек. после окончания облучения. В других случаях измерения начались через 5—60 мин. после окончания облучения. Фон, многократно проверенный между измерениями активностей, оказался равным около 170—180

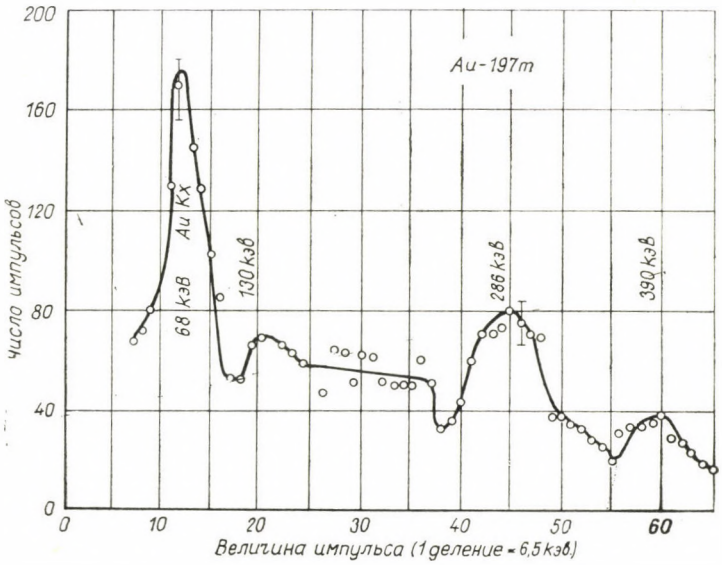

Рис. 11. Энергетический спектр Au-197m

и 230—240 имп. в мин. в зависимости от усиления. При снятии кривых полураспада параллельно, многократно определялся и спектр, форма которого не изменялась в течение распада (см. рис. 3—11). Данные измерений, сравниваемых с литературными данными, приведены в таблицу II.

Дискуссия

Из измерений и условий опыта можно оценить сечение активации для всех γ-квантов, выпущенных источником. Между активностью облученного образца (I) и сечением активации на метастабильный уровень (σ_m) существует следующее соотношение:

$$\sigma_m = \frac{IA\,(a+1)}{\Omega\varepsilon\, N\, \Phi\, a\, m(1-e^{-\lambda t})}\,, \tag{1}$$

где I — активность облученного образца (имп/сек.), экстраполированная к концу облучения,
A — массовое число возбуждаемого ядра,
a — коэффициент внутренней конверсии,
Ω — геометрический фактор,
ε — эффективность счетчика,
Φ — поток γ-квантов от источника (γ cm^2/sec),
a — содержание возбуждаемого ядра в образце,
m — вес образца (г),
и фактор $(1 - e^{-\lambda t})$ служит для определения кривой насыщения, зависящей от соотношения образовавшихся и распадающихся ядер.

По расчету в данном опыте поток γ-квантов от источника $\Phi \sim 1{,}4 \cdot 10^{12}\,\gamma/\text{см}^2$ sec. Значение $\Omega\varepsilon$ определили с помощью препаратов, имеющих форму облученной мишени и так по известным литературным данным экстраполировали на разные энергии.

Из условий опыта, при пороговой энергии ($\sim$ 1,1 Мэв) число рассеянных γ-квантов $n = 1{,}7 \cdot 10^{-7}$ эв$^{-1}$ для одного γ-кванта в интервале 1 эв.

Поэтому

$$\sigma_{\text{int}} = \frac{\sigma_m}{n} \text{ см}^2 \text{ эв}. \tag{2}$$

Дальше известно, что

$$\sigma(E) = \frac{\lambda^2}{8\pi}\, g\, \frac{\Gamma_{\gamma 0}\,\Gamma_{\gamma m}}{(E - E_r)^2 + \frac{1}{4}\Gamma_t^2} = \frac{\lambda^2}{2\pi}\, g\, \frac{\Gamma_{\gamma 0}}{\Gamma_t}\, \frac{\Gamma_{\gamma m}}{\Gamma_t}\, \frac{1}{\left(\frac{E - E_r}{\Gamma_t/2}\right)^2 + 1}, \tag{3}$$

где

$$g = \frac{2J_a + 1}{2J_m + 1};$$

J_a и J_m — спины соответствующие возбужденным состояниям E_a и E_m,
Γ_t — полная ширина уровня E_a,
Γ_{γ_0} и $\Gamma_{\gamma m}$ — ширины уровней относящихся к переходам из состояния E_a в основное состояние E_g и в метастабильное состояние E_m,
E — энергия излучения, E_r — резонансная энергия.
λ — длина волны для энергии E.

Интегрируя уравнение (3) по энергии, получим интегральное сечение в единицах см^2 эв если принять λ в см-ах и $\Gamma_{\gamma m}$ в эв-ах,

$$\sigma_{\text{int}} = \int_0^\infty \sigma(E)\, dE = \frac{\lambda^2}{4}\, g\, \frac{\Gamma_{\gamma 0}}{4}\, \Gamma_{\gamma m}\,. \tag{4}$$

Если значение g и $\frac{\Gamma_{\gamma 0}}{\Gamma_t}$ принимаем в первом приближении за единицу, по принципу не означающее большую погрешность, то для парциального уровня $\Gamma_{\gamma m}$ можно дать численные значения по уравнениям (2) и (4).

Если переход с уровня E_a на уровень E_m происходит путем каскадного процесса, то естественно, что $\Gamma_{\gamma m}$ является суммой всех уровней каскадного процесса, т. е.

$$\Gamma_{\gamma m} = \sum_i \Gamma_{\gamma i}. \tag{5}$$

Как видно из рисунков и данных таблицы, стало возможным обнаружение изомеров Se-77m, Sr-87m, Rh-103m, Ag-107m + 109m, Pt-195m, Au-197m и определение их энергии, времени жизни и других данных по полученной активности. У изомеров У-89m, Hf-179m, Ir-191m, и Hg-199m небольшие

Таблица II

Измеренные значения после облучения, сравниваемые с другими литературными данными

Элемент	Активность облучения после первого измерения (имп/мин.)	Активн. экстрп. в конце облуч. (имп/мин.)	Лутературные данные		Данные измерений		σm (10^{-28}см^2)	$\Gamma_{\gamma m}$ (10^{-4}эв)
			$T_{1/2}$	E (кэв)	$T_{1/2}$	E (кэв)		
Se-77m	3842±96	5400	17,5 сек.	160	18,1±1 сек.	160±10	9,5	1,75
Sr-87m	191±5	200	2,8 ч.	390	2,9±0,1 ч.	365±25	0,85	0,2
У-89m	96±20	170	16 сек.	910	16,7±5 сек.		0,08	0,02
Rh-103m	28±5	31	57 мин.	40	58±2 мин.	20,5±0,5	0,08	0,01
Ag-107m	220±14	250	44 сек.	93	43,8±0,6 сек	91±10	0,8	0,2
Ag-109m			39 сек.	88				
Hf-179m	80±18	155	19 сек.	160; 215	19±2 сек.		1	0,2
Ir-191m	90±20	250	4,9 сек.	42; 130	5±2 сек.		5,6	1
Pt-195m	90±9	100	3,5 д.	31; 100; 130;	3,5±0,2 д.	32±3 67,5±5 96±5 130±10	0,2	0,04
Au-197m	240±16	520	7,2 сек.	130; 277; 407	7,2±1 сек.	68:130: 280±20 390±20	0,07	0,01
Hg-199m	9,6±3,2		42 мин.	160; 370			0,005	0,001

кти вности дают возможность только для грубой оценки. Результаты последней группы изомеров улучшаются с увеличением количества вещества мишени за исключением Hg-199m, в случае которого только при большем источнике можно ожидать лучшие результаты.

Оценку погрешностей полученных результатов производил с помощью «формулы разброса» по теории вероятности [19].

Исследования на ядрах In-115 и Cd-111 [18] повторил с помощью нового источника и новой мишени. Полученное значение для σ_m равняется предыдущему в пределах погрешности 15%-ов.

Области применения метода

а) *Физические исследования*

Обнаружение этого эффекта с источником такой активности позволяет сделать выводы, что возбуждение γ-лучами с помощью источников, активность которых на 1—2 порядка больше указанной активности, может служить для расширения данных о состояниях ядер.

б) *Исследования вопросов, связанных с применением больших источников*

Ныне очень распространено применение больших γ-источников порядка активности килокюри. С помощью настоящего метода можно определить степень образования разных ядерных изомеров, и с помощью этих, можно делать выводы насчет образованных активностей в некоторых облученных продуктах и потребности мероприятия безопасности. Полученные до сих пор данные позволяют сделать вывод, что образованные активности при облучении даже в случаях источников с активностью на 1—2 порядка больше, не вызывают никакого затруднения в дальнейшем применении облученных материалов.

в) *Активационный анализ*

В многочисленных отраслях промышленности имеет большое значение определение следов. Такими вопросами занимается анализ активации с нейтронами. Произведенные мною опыты доказали, что для некоторых элементов, в случае источника на 2—3 порядка большей активности, применение этого метода оказывается пригодным. Недостаток этого метода состоит в том, что эффективность на 2—4 порядка меньше эффективности активации с нейтронами. Преимущество метода заключается в том, что легко и быстро можно оценивать результаты опытов, поскольку этому не помешает присутствие других активизированных компонентов.

г) *Дозиметрия*

По произведенным измерениям In оказывается наиболее пригодным для точного определения активности большого источника Co-60. Преимущество метода заключается в том, что увеличение дозы многократно рассеянных и обратно рассеянных мягкий γ-излучений не помешает измерению вопреки другим методам, где правильная оценка степень рассеяний и его измерения оказывают много трудностей. Этот метод можно сделать пригодным для определения активности от 10 кюри до 10^4 кюри. Таким образом можно определить дозу порядка М-рад при известных условиях облучения изомеров, имеющих короткий полураспад.

ЛИТЕРАТУРА

1. O. Hahn, Chem. Berichte, **54,** 1131, 1921.
2. *Б. В. Курчатов* и др. Compt. Rend., **20,** 1201, 1935.
3. C. H. Johnson and F. T. Hamblin, Nature, **138,** 504, 1936.
4. C. F. von Weizsäcker, Naturwiss., **24,** 813, 1936.
5. *Б. С. Джелепов, Л. К. Пекер,* Схемы распада радиоактивных ядер, Москва (1958).
6. Nuclear data sheets, NRC (1960).
7. B. Waldman, G. B. Collins, E. M. Stubblefield and H. Goldhaber, Phys. Rev., **55,** 1129, 1939.
8. M. L. Wiedenbeck, Phys. Rev., **67,** 92, 1945.
9. M. L. Wiedenbeck, Phys. Rev., **68,** 1, 1945.
10. M. L. Wiedenbeck, Phys. Rev., **68,** 237, 1945.
11. W. C. Miller and B. Waldman, Phys. Rev., **75,** 425, 1949.
12. H. R. Lukens, Jr. J. W. Otvos and C. D. Wagner, Appl. Rad. and Isotopes, **11,** 30, 1961.
13. E. Guth, Phys. Rev., **59,** 325, *d*94*d*.
14. M. Goldhaber, R. D. Hill and L. Szilard, Phys. Rev., **55,** 47, 1939.
15. K. Siegbahn, Beta and Gamma Ray Spectroscopy, North-Holland Publishing Company, Amsterdam, 1955.
16. C. E. Crouthamel, Applied Gamma-Ray Spectrometry, Pergamon Press, Oxford, 1960.
17. Fay Ajzenberg-Selove, Nuclear Spectroscopy, Academic Press, New-York and London, 1960.
18. Á. Veres, Appl. Rad. a. Isotopes, **14,** 123, 1963.
19. L. Jánossy, Theory and Practice of the Evaluation of Measurement, Oxford (под редакцией).

PHOTOACTIVATION OF NUCLEAR ISOMERS BY Co^{60} IRRADIATION

Á. VERES

Abstract

Investigations have been carried out on the isomers of 10 stable nuclides by the A (γ, γ') A* photoactivation reaction using a 1310 C γ-source. This phenomenon has not been investigated until now by nuclear γ-radiation.

The activation cross-section and the activation level band belonging to the transition from activated to metastable level was estimated from the extent of photoactivation measured.

Some possible practical uses are suggested, based on the experimental results.

ON THE PRESSURE-DEPENDENCE OF SOME PARAMETERS OF A. C. DISCHARGES

By

J. BITÓ

INDUSTRIAL RESEARCH INSTITUTE FOR TELECOMMUNICATION TECHNIQUE, BUDAPEST

(Presented by G. Szigeti — Received 28. V. 1963)

The author describes the probe measurement method based on the pulse technique introduced by WAYMOUTH and its application to the examination of discharges operated by a supply voltage of 50 cps. In this connection the author examines the pressure-dependence of some characteristic parameters; he shows the dependence of the cathode-fall, the axial field strength and the plasma potentials and the pressure of the applied argon ground gas, for a mercury vapour discharge. The results obtained are discussed and compared with the data appearing in recent literature.

Introduction

The examination of gas discharges is at present chiefly experimental. The properties and the behaviour of more or less ionized gas or vapour have been examined for about 200 years, but until now coherent results leading to an unambiguous theoretical picture have not been attainable from which the fundamental processes and the relations between them could unambiguously be explained, either in a closed form (by functions), or in any other one.

But, at the same time, the physical knowledge shows in more and more places the presence of the plasma state. The application of the advantageous properties (lighting, processing, rocket driving, etc.) of the discharges, of the discharge plasma, or of otherwise produced ionized gases and vapours becomes ever more and more extensive. This wide possibility of application necessitates the development of suitable examination methods, in order to obtain more detailed knowledge. One of the fundamental examining methods of experimental plasma physics is the probe measuring process introduced by LANGMUIR [1—3], by means of which relatively correct data can be obtained concerning the processes occurring in the discharges. By a great number of measurements of an improved accuracy further relations can be expected, which may contribute to a clarification of the properties so far known and to a further and wider application of the discharges and their plasma.

In this paper the author makes known the pressure-dependence of the fundamental discharge parameters determined by the process [4] extended to the case of a. c. discharges and based on LANGMUIR's probe measuring method, applied to a. c. discharges. Until now similar examinations of only

d. c. discharges have been discussed in the literature [5] and with the exception of the cathode-fall, the pressure-dependence of their parameters has been given only under specific circumstances [5].

For a. c. discharges a much more complicated measuring method must be used and so the examinations become much more difficult. As the character of the a. c. discharges differs essentially from that of d. c. discharges, this difference is expected to influence other important parameters also and therefore it is impossible to extend the d. c. experimental results simply and directly to the phenomena appearing under a. c. discharges.

The determination of the latter necessitates further measuring series.

Measuring method

Further extensions of the LANGMUIR's probe measuring system to the examination of a. c. discharges are known [6]. While developing this system, it was always in the mind of the researchers that during the measurement they should produce, if possible, only a negligible disturbance in the discharge field to be examined and in this way they should ensure the reality of the results obtained as far as possible.

Among the above-mentioned a. c. methods the author applied the measuring technique based on WAYMOUTH's pulse method [4].

By the transformation of this method in some degree [7] a measuring process of satisfactory accuracy and reproducibility could be obtained, by means of which the phenomena of the plasma of the cathodic side and of its field of low-pressure mercury-argon discharges around the cathode could be more quickly examined than by some other a. c. measuring methods.

The block diagram of the electric scheme applied can be seen in Fig. 1.

From the stabilizer S one pulse comes through a separating transformer in each period to the measuring probe M of the 50 cps voltage-supplied discharge tube T, by means of the impulse generator I. The measuring probe can be connected by a battery of about 150 V with various potentials corresponding to the place of the examined discharge field, relating to the chosen electrode.

In the present case the measurements took place on the cathode side of the discharge and so the probe was at the same or higher potential than the cathode. The bias comes from the square generator G, through the differentiator D, into the impulse generator I. The magnitude of the steep, nibbed, wedge-shaped pulse is generally of 80—90 V, its period 500 μsec. As soon as this pulse, in relation to one of the electrodes, reaches the probe and changes its voltage in time, the probe current passing through the resistance R_s of the probe circuit changes too and follows the time-variation of the probe current, according to the regularity observed by LANGMUIR [1—3].

Putting the voltage-variation arising on the ends of the resistance R_s through the difference-amplifier A to the vertical input of the oscilloscope O, the probe voltage characteristics can be observed, when the voltage of the applied pulse gets onto the horizontally deflecting pair of the sweep plates. In this way, during the period of the pulse, LANGMUIR's probe characteristics

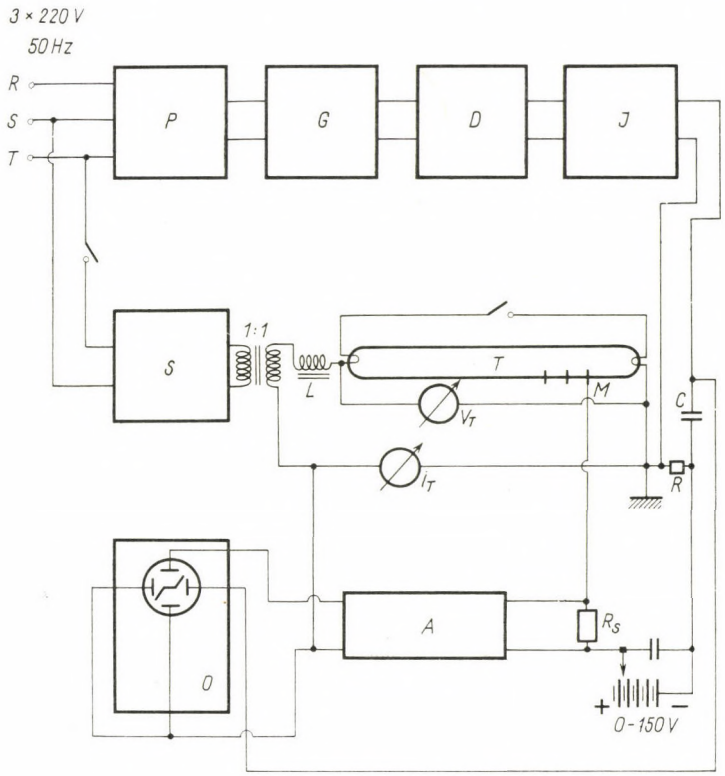

Fig. 1

can be plotted in a given discharge time, apart from its ion current part, which is, however, of no importance from the point of view of the further evaluations and discussions.

If the determination of the plasma characteristics and discharge parameters is desired in various phases of the a. c. discharge, the above-mentioned voltage pulse must be examined in the phase in question. In the course of the present experimental arrangement this was possible by means of the phase slider P, by the use of which the phase of the pulse given by the generator G could be adjusted arbitrarily.

The measurements took place in a half-period, with a probe circuit formed according to the cathode, by phase angles of 10°. In this case, if the electrode

chosen to the probe circuit was in the half-period, no pulse reacted the probe and so no measurement was performed.

The probe characteristics plotted fifty times/sec at a given phase angle could well be evaluated on an oscilloscope screen of suitable size.

The fundamental factors decisively influencing the accuracy of the probe measurement have always been taken into account during the measurements [8], e.g. the measuring conditions relating to the dimensions and purity of the probes, the measuring time, the removal of the impurities, etc.

Conditions of the examination

The examinations took place by means of glass discharge tubes of 1200 mm length and 38 mm diameter. Within the ends of these tubes there were electrodes of the same structure, tungsten coiled coils provided with an electron emitting coating, heated only by the discharge and protected by nickel auxiliary electrodes. Three probes reached into the discharge tube, and were placed near the electrode. The spacing between the probes was 100 mm. The probe nearest to the electrode was 1500 mm from it, sealed into the discharge tube. In the construction of the tube a usual vacuum technical procedure was used. The probes were made with glass insulation and their parts protruding into the discharge field and active from the point of view of the discharge current were made of nickel wire of 2 mm length and 0,2 mm diameter.

In the course of the earlier experiments it turned out [8] that the probe of such a diameter can be used with the same accuracy in 50 cps discharge conditions as that of 0,02 mm diameter. Therefore the use of thicker probes of greater solidity was more practical. The probes reached radially into the axis of the discharge tube. After a vacuum technical treatment, about 60 mg mercury and argon gas of the desired pressure were put into the tubes. The gas pressure was adjusted by measurements with a Mac Leod manometer. For the sake of ensuring the same experimental conditions in the measurements, as far as possible, at various gas pressures the same tube was used. The refilling of the gas from the discharge tubes into higher or lower pressure-values took place by transfer extension pieces [9, 10].

In this way the inaccuracies of the measurements resulting from the differences of the electrodes, tube- and probe-dimensions arising from the use of different tubes could be eliminated from the measurement series. During the examination the tube was operated in an ambient temperature of $25 \pm 1°$ C.

The discharge was maintained by a stabilized supply voltage and at various pressures the current of the discharge was adjusted to the same value of 410 mA and was limited by an inductive resistance. The base point of the discharge was always adjusted to the same end of the electrodes for the various measurements.

Measuring results

The experiments were carried out in argon gas of 1, 2, 3, 4 and 5 mmHg pressures and at a saturated mercury vapour pressure arising at a wall temperature of about 37° C, corresponding to an ambient temperature of 25 $\pm$ 1° C, at about 0.005 mmHg.

At every gas pressure the measurement took place at a discharge current of 410 mA. In this way the identical surface current loading of the cathode was ensured which is an indispensable condition for the comparison of cathodefalls.

Having used the measuring method mentioned in the second part of this paper, the course in time of the plasma potential on the place of each probe could be determined for every pressure. This follows, generally, the temporal progress of the supply voltage falling to the tube. From the plasma potential plotted on the various known points of the discharge field, the cathodefall belonging to each time, could be given by means of NÖLLE's method [11, 12], with a full knowledge of the extent of the cathodic dark space.,

The determination of the time-dependence of the cathodic dark space and the marking out of its limits for each pressure was made by the well-known stroboscopic system.

It was known that the end of the dark space, i.e. the meniscus of the cathodic side of the plasma of the positive column, idenpendently of time, is at a distance of 30 $\pm$ 1 mm from the electrode (cathode).

According to the measuring results, this distance does not change, even with the pressure of argon in the pressure range of 1—5 mmHg, or at least this change is within the inaccuracy range of the measuring method. This eventual small fluctuation was negligible from the point of view of further examinations. In full knowledge of the independence of the length of the pressure which proves to be a very valuable datum, the time-dependence of the cathode-falls could be given by means of NÖLLE's method [11, 12]. With an argon pressure of 2 mmHg, during the chosen half-period, the temporal process characteristic of the cathode-fall can be seen in Fig. 2.

The phase angle 0 means the moment of the beginning of the discharge, from the choice of the system of reference. At this moment the maximal voltage to the discharge field arrives. At a phase-angle of 180° the commutation point takes place at the end of the half period. From that point the chosen electrode — up to now the cathode — according to the sense of the alternating current — performs the duty of the anode.

From Fig. 2 it can be seen that the temporal progress of the cathodefall also follows to a certain degree the time-dependence of the voltage falling to the discharge. The cathode-fall is maximal at the beginning of the discharge, i.e. at the break-down of the discharge field, and after this it diminishes rapidly

to a value below 10 V. The cathode-fall could be revealed by measurements only to a phase angle of 160°. During the period corresponding to the last 20 phase angles which is about 0,001 sec, no discharge occurs. This is the decay interval preceding the commutation point.

If the two electrodes of the discharge tube can be considered as identical, from the point of view of the discharge, the temporal progress of the cathode-fall can be expected to be identical for both electrodes. According to the

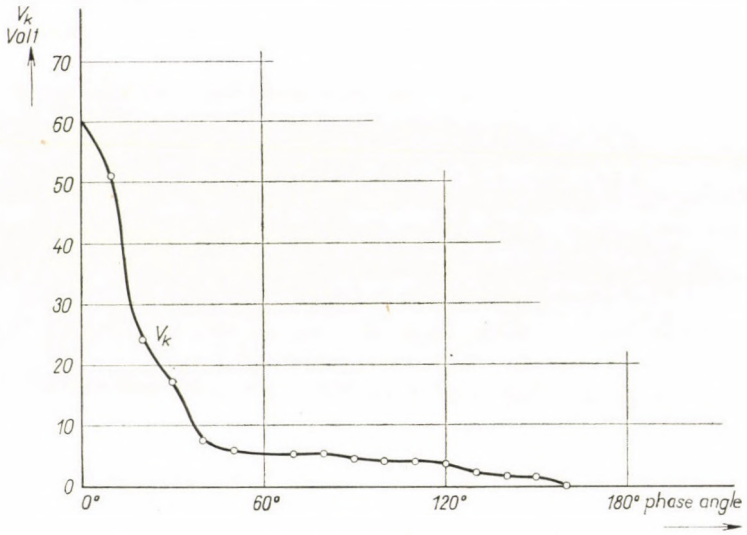

Fig. 2

author's opinion this method of comparison is suitable for the examination of the various electrode constructions relating one to the other and to their classification under discharge conditions.

Further on — for the sake of easier manageability and survey — instead of the curve describing the time-dependence of the cathode-fall V_{-k} given for a half period, it is more practical to take its integrated average:

$$V_k = \frac{2}{T} \int_0^{T/2} V_k(t)\, dt, \tag{1}$$

where T is the time of the period, and t the time.

This integrated average V_k will be characteristic of the cathode and of the discharge processes occurring in its neighbourhood.

Extended the measurements to the pressure range 1—5 mmHg, the time-dependence of the cathode-fall can be plotted to each pressure and the

curve describing the same can be formed, according to the integrated average (1), for the examined half period. The pressure dependence of these integrated averages V_k can be seen in Fig. 3.

As can be seen, the cathode-fall increases until 4 mmHg, with the increase of the argon pressure. Its value remains constant between 10 and 15 V. After the pressure of 4 mmHg it falls with a great diminution, at the pressure value of 5 mmHg to 11,8 V.

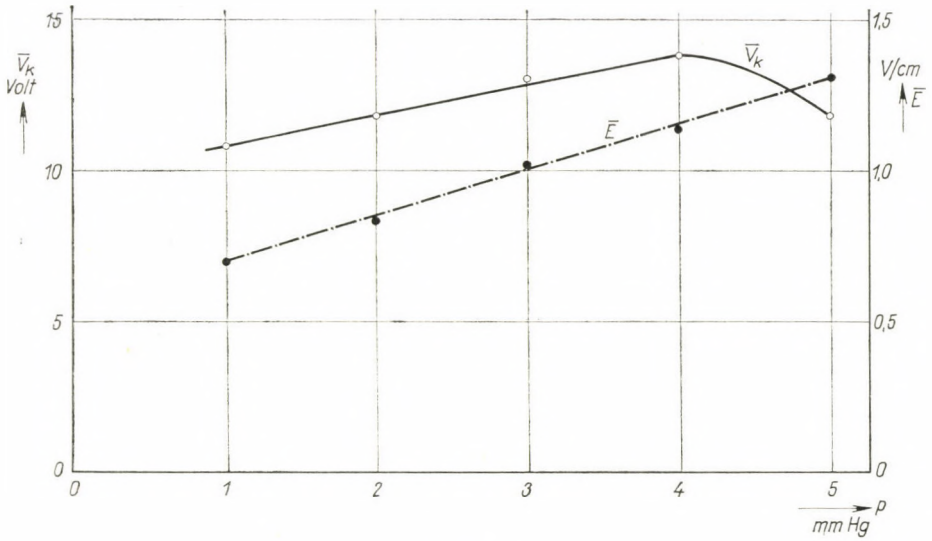

Fig. 3

The distance between the probes placed into the discharge tube being known, measuring the plasma potentials on the probes, it is possible to determine the time-dependence of the electric field strength.

The time-dependence of the plasma potentials and the gradient give a picture similar to that of the time-dependence of the cathode-fall. Plotting the time dependence of the potential gradient values belonging to the various pressures according to the above-mentioned method and forming the integrated average E of the obtained curves, according to the relation

$$\overline{E} = \frac{2}{T} \int_0^{T/2} E(t)\, dt, \tag{2}$$

where $E(t)$ is the function describing the time dependence of the gradient; t is the time and T the duration of the period.

To each pressure value a gradient value characteristic of it can be designated, i.e. the integrated average E. These potential gradients $\overline{E}$ are shown as a function of the pressures in Fig. 3. As can be seen, the measuring data fall with good approximation into the same straight line. According to this on the increase of the pressure the value of the gradient $\overline{E}$ also increases regularly within the pressure range of 1—5 mmHg.

Discussion

As the first results of the examinations it was found that the length of the dark field before the cathode — included all the cathodic fields to the meniscus of the cathodic side of the positive column — does not depend eithergon time, or on the variation of argon pressure.

It is known that the dimensions of the dark field, in case of d.c. discharges, are considerably influenced by the discharge current, or the heating current of the cathode, at otherwise identical cathodes [8]. But in the present examinations the effective value of the discharge current was from beginning to end always the same. The cathode, however, did not receive any external heating.

From the result that the dimensions of the fields before the cathode did not change, one can conclude that with the increase of the concentration of argon atoms no further considerable energy loss has arisen in the dark field before the cathode and so it was not necessary, for the purpose of compensation, to ensure the energy of the electrons needed to the increase of the cathodefall. In this way the hypothesis is evident that in the procedure of the cathodefall the decisive part in the argon pressure range of 1—5 mmHg is still played by the concentration of the mercury vapour and the fundamental processes occurring under the stationary discharge circumstances are connected with the latter. All this can be supported by the following line of reasoning.

The concentration of the argon atoms has increased by the increase of the pressure and so the mean free path of the electrons in argon is also changed. The mean free path of the electrons l_e in argon and the mean free path of argon atoms l_a for 1 and 5 mmHg pressures can be seen in Table I [13]:

Table I

p	l_e	l_a
1 mmHg	$4{,}38 \cdot 10^{-2}$ cm	$7{,}73 \cdot 10^{-3}$ cm
5 mmHg	$0{,}88 \cdot 10^{-2}$ cm	$1{,}55 \cdot 10^{-3}$ cm

On this basis calculating the number of the electron-argon-atom impacts, the energy given in the form of elastic impacts by the electrons and taken by argon atoms can be estimated.

Taking into consideration the 30 mm length of the field before the cathode and assuming in first approximation an undisturbed, linear running with impacts of minimal angles, it can be calculated that the electrons in this section impact about 70 times with argon atoms at a pressure of 1 mmHg and about 330 times at a pressure of 5 mmHg. Taking into consideration that at every elastic impact, as is known [13], the maximal energy given by the electrons by a central impact to the atoms is, by the law of conservation of energy, k-times the energy of the electrons, where

$$k = 4\frac{m_e}{m}, \tag{3}$$

m_e is the mass of the electron, m the mass of the atom impacting with the electron.

The mass of hydrogen is about 1840-times that of the electron, the mass of the argon atom, however, is about 40-times that of the hydrogen atom, so the relation m_e/m takes the value of $1{,}3 \cdot 10^{-5}$. Consequently the value of k of the equ. (3) becomes $5{,}2 \cdot 10^{-5}$.

According to what has been said, in the 30 mm length of the cathodic field at 5 mmHg argon pressure 330 impacts occur in the direction of the electric field between one electron and the argon atoms. In the course of so many impacts the electron loses the $330 \cdot k$-times of its energy, which corresponds to a value of $1{,}7 \cdot 10^{-2}$. This loss of energy is a negligible part of the whole energy of the electron. At an argon pressure of 1 mmHg that loss is still less. As is shown by this calculation, during the variation of the argon pressure between 1 and 5 mmHg, in the course of the elastic impact of the electrons the loss of energy is negligible and so does not influence all the losses of energy arising in the dark fields.

The inelastic impacts and the excitation and ionization connected with them have a role in the visible part of the field on the cathodic side of the cathodic dark field in question, but these inelastic impacts are not connected with argon atoms, but with those of mercury, since the ionization and excitation potentials of mercury are much lower than those of argon. The fact that in this field the number of inelastic electron impact with argon atoms did not increase, could also be proved by spectral examinations, because the intensity of argon lines leaving the field before the cathode did not change essentially in the pressure region examined.

As the probability of ionization generally coincides with the probability of excitation, presumably not even the number of ionized argon atoms increased.

In this way the experimentally found fact can be explained that in the pressure range of 1—5 mmHg the variation of argon pressure does not influence the whole extension of the dark fields before the cathode and the increase of the argon atom concentration in the pressure range probably does not alter the discharge processes in the neighbourhood of the cathode.

The pressure-dependence of the cathode-fall V_k represented in Fig. 3 in the pressure range of 1—4 mmHg can empirically be characterized by a straight section:

$$V_k = p + a, \tag{4}$$

where p is the pressure of argon gas, a a constant of a value of 9,8.

The section between 4 and 5 mmHg pressure of the curve representing the pressure-dependence of the cathode-fall V_k has a negative slope.

According to the author's opinion the decreasing character of the cathode-fall here can be explained by the potential gradients. Also the pressure-dependence of the integrated average E of the gradients can be seen in Fig. 3. It can be seen that the measuring points fall with a good approximation into the same straight line and the value of the gradient $\overline{E}$ increases with the increase of the pressure quite steeply, regularly in the pressure range of 1—5 mmHg.

This increase and the growth of the vapour pressure of Hg accompanying it can explain the behaviour of the last part of the cathode-fall curve V_k, i.e. the section of the pressure between 4—5 mmHg. Since during the experiments the current density of the discharge was the same, but with the increase of the pressure the gradient of the positive column increased, the energy received by the electrons and ions on the free paths increased too, but this fact did not mean a contribution to the current mentioned before.

Necessarily the electrons and ions had to give out some part of the energy-excess they had received in some or other form, e.g. by the impacts with mercury and argon atoms. In this way, however, supposing the linear shape of the cathode-fall, the ions having a greater energy and impacting on the cathode, can give out more energy on the surface of the latter and so they can facilitate the leaving of the electrons. In this way a smaller cathode-fall can be necessary for the production and acceleration in the field before the cathode than otherwise, at a positive column of a lower potential gradient, in case of a lower pressure. The pressure-dependence of the gradient $\overline{E}$ (integrated average) shown in Fig. 3 can be characterized by the following function relation:

$$\overline{E} = 0{,}15\, p + b\,, \tag{5}$$

where p is the pressure of argon gas, b a constant of the value of 0,55.

In case of a. c. discharges up to now the pressure-dependence of either the cathode-fall, or the potential gradient has not been mentioned in the litera-

ture. Their pressure-dependence could be described by the introduction of the integrated averages with the method given in that part of this paper.

In d. c. discharge conditions, in a thermostatic bath of 42° C at 400 mA discharge current, VERWEIJ performed such measurements [5], by which he gave, among other facts, the pressure-dependence of the gradient of the positive column for argon, within the pressure range of 0,01—100 mmHg, ensuring the constant mercury vapour pressure corresponding to 42° C. Representing the measuring result in a semi-logarithmic system, he obtained a curve rising exponentially with the increasing pressure. The gradient values obtained by VERWEIJ in d. c. measurements and the a. c. gradient values shown previously in Fig. 3 are compared in Table II.

Table II

The pressure-dependence of the gradient

Pressure (mmHg)	1	2	3	4	5
The gradient, the d.c. measuring result of VERWEIJ	0,7	0,75	0,8	0,85	0,9
The gradient, result of the present a.c. measurements V/cm	0,7	0,84	1,01	1,16	1,31

In the comparison of the data of Table II it must be taken into consideration that the d. c. measurements performed by VERWEIJ took place at 400 mA discharge current and with a discharge tube placed into a thermostatic water-jacket of 42° C [5], while in the present experiments for a. c. measurements the discharge current was 410 mA and the ambient temperature 25 $\pm$ 1° C, which corresponds to a wall temperature of about 32—39° C.

Representing the pressure dependence valid for d. c. discharges found by VERWEIJ [5] in a coordinate system of linear axes, in the pressure range of 1—5 a straight section is obtained. The slope of this section is 0,05 V/cm. mmHg, one third of that of the pressure-dependence found under a. c. discharge circumstances, i.e. of the value of 0,15 V/cm. mmHg. From this it can be seen that the plasma of the positive column of the a. c. discharge is more sensitive to variations of argon pressure within the given range, than the plasma of the d. c. discharge. It is perhaps practical to consider this fact for obtaining higher specific energies fed.

As there was some difference between the discharge current and the vapour pressure of mercury in the course of the two measurements, it would not be valid to draw further conclusions by comparing the absolute values of the results obtained. It is evident that the gradient values obtained by the a. c. measurements, because of the greater slope of the curve, apart from the

value obtained at the pressure of 1 mmHg, are all higher than the gradient data of the d. c. measurements. The pressure range examined is not wide enough to allow a reason to be given for the coincidence appearing at 1 mmHg. For the interpretation of the phenomenon observed further measurements are necessary at pressures lower than 1 mmHg. It may be surmised that there will not be a considerable difference in value between the two gradient curves in this region.

Up to now the pressure-dependence of the cathode-fall, the gradient and the plasma potentials in case of a. c. discharges has not been elaborated in the literature.

Previously the author took part in examinations connected with the time-dependence of some parameters of the a. c. discharges [12, 14], but apart from this, publications dealing with the relations between the parameters of a. c. discharges are not known in the special literature though the latter are already widely used in various domains. JURRIAANSE and previously MEISSNER too, have already made statements relating to the pressure-dependence of the normal cathode-fall under special circumstances [15], but in the course of their experiments they did not maintain the surface current density of the cathode at a constant value. Therefore they attributed the variations of the cathode-fall observed by them partly to this fact [15].

The measuring method used here is also suitable for the determination of further plasma- and discharge-parameters. So, by the same method the time-dependence of the electron temperature, electron concentration can be given too, which in the course of the survey of the previously mentioned a. c. current examinations has been dealt with in the literature [14]. But these measurements gave the time-dependence of the above-mentioned parameters only for some parts of the half period [14]. By the application of the present method, by characterization with integrated averages it is possible to obtain further knowledge also in the field of the processes connected with these parameters, for the whole duration of the half period. This was not the aim of the examinations now discussed, but from some of the performed measurements of an information character it turned out that the ionization degree calculated on the basis of the equation of EGGERT—SAHA is very low and does not change considerably with the argon pressure in the range examined. The degree of the plasma ionization arising in the course of the a. c. experiments ranges in the order of magnitude of 10^{-3}.

From the gradient of the positive column, from the density of the discharge current and from its distribution function [15], as well as from the geometric dimensions of the discharge tube the specific resistance of the positive column could be given approximately. Since during the experiments the value of the discharge current always remained the same, the distribution function of the current density for the cross-section of the tube did not change either.

Therefore the pressure-dependence of the specific resistance develops corresponding to the curve of the gradient (pressure-dependence shown in Fig. 3 of the integrated average). The directional tangent of the straight line obtained in this way is identical with that of the curve describing the pressure-dependence of the gradient.

The approximately calculated specific resistances range in the order of magnitude of 10^{-1} ohmcm^2/cm.

By the previously mentioned method still further characteristics of the plasma and discharge can be obtained. With full knowledge of them, among others, the characteristics of the oscillations causing the instability of the discharges can be calculated [17—20], by which the energy absorption of the detrimental oscillations and striations can possibly be restricted.

Acknowledgment

The author expresses his thanks to Mr. G. LAKATOS, for raising the subject and for his valuable discussions and remarks.

REFERENCES

1. I. LANGWUIR, J. Franklin Ist., **196,** 59, 1923.
2. I. LANGWUIR, Gen. El. Review, **26,** 731, 1923.
3. I. LANGMUIR, H. MOTH-SMITH, Gen. El. Review, **27,** 449, 538, 616, 762, 810, 1924.
4. J. F. WAYMOUTH, J. Appl. Phys., **30,** 9, 1404, 1959.
5. W. VERWEIJ, Probe Measurements and Determination of Electron Mobility in the Positive Column of Low-Pressure Mercury-Argon Discharges. Thesis, Utrecht, 1960.
6. J. BITÓ, Magy. Fiz. Folyóirat (Hung. Phys. Review), **X,** 411, 1962.
7. J. BITÓ, and I. SZEMZŐ, Acta Technica Hung., to be published.
8. J. BITÓ, Thesis, Szeged, 1960.
9. J. SZABÓ and G. LAKATOS, Hung. Patent No. 146. 209.
10. G. LAKATOS and J. BITÓ, Acta Phys. Hung. **13,** 193, 1961.
11. E. NÖLLE, Ann. der Phys., **18,** 328, 1956.
12. G. LAKATOS and J. BITÓ, Lecture, Electron and Vac. Phys. Sympos., Balatonföldvár, 1962; to be published.
13. W. UYTERHOEVEN, Elektrische Gasentladungen, Springer, Berlin, 1938.
14. G. LAKATOS and J. BITÓ, Acta Physik Hung., **13,** 271, 1961.
15. S. FLÜGGE, Handbuch der Physik, XXII, Gasentladungen, II., Springer, Berlin, 1956.
16. W. WEIZEL and R. ROMPE, Theorie Elektrischer Lichtbögen und Funken, J. A. Barth, Leipzig, 1949.
17. F. W. CRAWFORD and G. S. KINO, Proc. IRE, **49,** 12, 1767, 1961.
18. G. LAKATOS and J. BITÓ, Acta Phys. Hung., **13,** 245, 1961.
19. W. OTT, Z. für Naturforsch., **17***a*, 11, 962. 1962.
20. J. BITÓ, Magy. Fiz. Folyóirat, (Hung. Phys. Review.) **X,** 303, 1962.
21. G. SZIGETI and J. BITÓ, Acta Phys. Hung., **11,** 103, 196.
22. G. LAKATOS and J. BITÓ, Zs. T. F., **32,** 902, 1962.
23. G. LAKATOS and J. BITÓ, Lecture, 2nd Czechoslov. Electr. Conference, Prague, 1962; to be published.
24. G. LAKATOS and J. BITÓ, Lecture, Plasma-physical Discussions, Balatonszabadi, 1963.

О ЗАВИСИМОСТИ НЕКОТОРЫХ ПАРАМЕТРОВ ГАЗОВЫХ РАЗРЯДОВ ПЕРЕМЕННОГО ТОКА ОТ ДАВЛЕНИЯ

Я. БИТО

Р е з ю м е

Автором даётся анализ приёма измерений зондами, базирующегося на введенной Веймаусом импульсной технике, и расширение его на исследование разрядов, содержащихся в действии напряжением питания 50 Hz. Используя результаты этих исследований, автор приходит к выводу зависимости некоторых характерных для разряда параметров от давления. Так в работе даётся зависимость катодного падения потенциала, аксиальной напряжённости электрического поля и плазменного потенциала от давления применённого основного газа аргона в случае ртутного разряда. Полученные результаты дискутируются, сравниваются с новейшими литературными данными.

COMMUNICATIONES BREVES

A NEW METHOD FOR FINDING THE PHASE SHIFTS FOR THE SCHRÖDINGER EQUATION

By

T. TIETZ

DEPARTMENT OF THEORETICAL PHYSICS, UNIVERSITY OF ŁÓDŹ, ŁÓDŹ, POLAND

(Received 17. IV. 1963)

In this note we derive a new formula for finding the phase shift of the Schrödinger equation. We write the radial Schrödinger equation in the following form:[1]

$$\frac{d^2 y_l}{dr^2} + \left[k^2 - U(r) - \frac{l(l+1)}{r^2}\right] y_l = 0, \tag{1}$$

where $U(r)$ is related to the potential $V(r)$ as known, $U(r) = (2m/\hbar^2)\, V(r)$. We assume that $U(r)$ vanishes at infinity more rapidly than the Coulomb potential, for $r = \infty$ it is $U(\infty) = 0$. At $r = 0$ the potential $V(r)$ can be singular like the Coulomb potential or continuous. In order to obtain a relation for the phase shifts we write eq. (1) as two first order equations:

$$\frac{dy_l}{dr} - \frac{l+1}{r} y_l + k z_l = 0, \tag{2}$$

$$\frac{dz_l}{dr} + \frac{l+1}{r} z_l + \left[\frac{U(r)}{k} - k\right] y_l = 0. \tag{3}$$

The asymptotic forms of y_l and z_l as we see directly from eqs. (2) and (3) are

$$y(\infty) \to \sin\left(kr - \frac{l\pi}{2} + \eta_l\right), \tag{4}$$

$$z_l(\infty) \to \sin\left(kr - (l+1)\frac{\pi}{2} + \eta_l\right). \tag{5}$$

If we differentiate eq. (2) and eliminate $\frac{dz_l}{dr}$ using eq. (3) we obtain eq. (1).

[1] For reference see e.g. A. MESSIAH, Mecanique Quantique, Dunod, Paris, 1959 or any other book on quantum mechanics

In the same manner if we differentiate eq. (3) and eliminate dz_l/dr and dy_l/dr using eqs. (2) and (3) we obtain the equation

$$\frac{d^2 z_l}{dr} + \left[k^2 - U(r) - \frac{(l+1)(l+2)}{r^2}\right] z_l = -\frac{1}{k}\frac{dU}{dr} y_l. \tag{6}$$

Denoting by $\bar{y}_l$ and $\bar{z}_l$ the free solutions of eqs. (1) and (6) we have

$$\bar{y}_l(r) = \sqrt{\frac{\pi kr}{2}} I_{l+\frac{1}{2}}(kr), \tag{7}$$

$$\bar{z}_l(r) = \sqrt{\frac{\pi kr}{2}} I_{l+1+\frac{1}{2}}(kr), \tag{8}$$

where the symbol I denotes the Bessel function. The last two equations show that the solutions y_l and z_l of eqs. (1) and (6) in case of $U \neq 0$ have the same asymptotic form as given in eq. (4) and (5). To obtain a relation between the phase shifts we multiply eq. (2) for y_{l+1} by z_l and eq. (6) for z_l by y_{l+1}, subtract these equations and integrate making use of the asymptotic forms of y_{l+1} and z_l. We get the results

$$\sin(\eta_l - \eta_{l+1}) = \frac{1}{k^2}\int_0^\infty \frac{dU}{dr} y_l y_{l+1}\, dr. \tag{9}$$

Replacing l by $l-1$ in the last equation we have

$$\sin(\eta_{l-1} - \eta_l = \frac{1}{k^2}\int_0^\infty \frac{dU}{dr} y_{l-1} y_l\, dr. \tag{10}$$

Adding or subtracting the two last eqs. we have

$$\sin(\eta_l - \eta_{l+1}) + \sin(\eta_{l-1} - \eta_l) = \frac{1}{k^2}\int_0^\infty \frac{dU}{dr} y_l (y_{l+1} + y_{l-1})\, dr, \tag{11}$$

$$\sin(\eta_l - \eta_{l+1}) - \sin(\eta_{l-1} - \eta_l) = \frac{1}{k^2}\int_0^\infty \frac{dU}{dr} y_l (y_{l+1} - y_{l-1})\, dr. \tag{12}$$

If k is sufficiently large and the quantum number l is also sufficiently large, then the integral of the right side of eq. (12) goes to zero. In this case the left-hand side of eq. (12) vanishes if

$$\eta_l = \frac{\eta_{l+1} + \eta_{l-1}}{2} \,. \tag{13}$$

These relations between the phase shifts is the more accurate the larger k and l. In Table I we have compared the accuracy of the last formula for the THOMAS—FERMI potential.[2]

Table I

Table of phase shifts for the Thomas—Fermi potential with $k = Z$ and $Z = 80$ demonstrating our eq. (13), where the potential parametres were the same as in the reference [2]

l	Numerical exact values of η_l	$\eta_l = \frac{\eta_{l+1} + \eta_{l-1}}{2}$ of eq. (13)
0	203°	—
1	157°	166° 25′
2	129° 50′	134° 15′
3	111° 30′	113° 55′
4	98°	99° 40′
5	87° 50′	88° 50′
6	79° 40′	80° 25′
7	73°	—

Table I shows that formula (13) may be advantageous for calculating higher phase shifts for sufficiently large energies for the long-tailed potential like the Thomas—Fermi potential. To obtain approximate formulas for smaller l we substitute in eqs. (11) and (9) instead of y_l the free solutions given by eq. (7) and make the assumption that the difference $\eta_l - \eta_{l+1}$ is small. In this case eq. (9) gives

$$\eta_l - \eta_{l+1} = \frac{\pi}{2k} \int_0^\infty r \, \frac{dU}{dr} \, I_{l+\frac{1}{2}}(kr) \, I_{l+\frac{3}{2}}(kr) \, dr \,. \tag{14}$$

Eq. (11) using the well-known relation between the Bessel functions

$$I_{p+1}(z) + I_{p-1}(z) = \frac{2p}{z} \, I_p(z) \tag{15}$$

and the above-mentioned conditions concerning the difference $\eta_l - \eta_{l+1}$ gives

$$\eta_{l-1} - \eta_{l+1} = \frac{(l + {}^1/_2)\,\pi}{k^2} \int_0^\infty \frac{dU}{dr} I^2_{l+\frac{1}{2}}(kr)\, dr. \tag{16}$$

The two eqs. (14) and (15) allow us to calculate approximate phase shifts if η_0 is known.

[2] T. TIETZ, Ann. d. Phys. **3**, 105, 1959.

ZUR FRAGE DER WIRKUNGSSPHÄRE IN DEN AUF DIE KONZENTRATIONSDEPOLARISATION DES FLUORESZENZLICHTES BEZÜGLICHEN THEORIEN

Von

A. KAWSKI

PHYSIKALISCHES INSTITUT DER PÄDAGOGISCHEN HOCHSCHULE, GDAŃSK, POLEN

(Eingegangen: 18. IV. 1963)

In den Theorien über die Konzentrationsdepolarisation der Fluoreszenz von Lösungen wurden gewisse Konstanten eingeführt, die in verschiedener Weise definiert sind [1] [2] [3] [4]. SZALAY und SÁRKÁNY [5] haben neuerdings im Falle der Konzentrationsdepolarisation zwischen dem Radius R der JABŁOŃSKIschen Wirkungssphäre und dem FÖRSTERschen kritischen Abstand R_0 die Relation

$$R = 1{,}367\ R_0 \tag{1}$$

gefunden. Unabhängig, wurde von uns [6] die Relation

$$R = 3^{1/3}\ R_0 = 3^{1/3}\ R_W \approx 1{,}44\ R_0 \tag{2}$$

abgeleitet, wobei R_W den Radius der WAWILOWschen Konstante $\dfrac{\tau_0}{k_2} = \dfrac{4\pi}{3} \cdot R_W^3$ bedeutet.

SZALAY und SÁRKÁNY [5] wandten zur Ableitung der Beziehung zwischen R und R_0 die von JABŁOŃSKI hergeleitete Formel [4]

$$P = \frac{6\,P_0}{(3 - P_0)\,\dfrac{\nu^2}{\nu - 1 + e^{-\nu}} + 2\,P_0} \tag{3}$$

an. (Es bedeuten: P — der Polarisationsgrad, $\nu = v \cdot n$, $v = \dfrac{4\pi}{3} R^3$ eine für die Wahrscheinlichkeit der Energiewanderung charakteristische von n unabhängige Konstante, n — die Zahl der lumineszenzfähigen Moleküle in 1 cm^3, $P \to P_0$ für $\nu \to 0$.) Wir haben dagegen zur Ableitung der Beziehung (2) die JABŁOŃSKIsche Formel (3), die für kleine Werte von n ($\nu \ll 1$) die Form

$$\frac{1}{P} = \frac{1}{P_0} + \left(\frac{1}{P_0} - \frac{1}{3}\right)\frac{1}{3}\,\nu \tag{3}$$

annimmt, angewandt. Früher wurde schon von uns gezeigt, dass die experimentellen Ergebnisse für kleine Konzentrationen von Farbstoffen sehr gut die Gl. (4) erfüllen [7]. Die Messergebnisse von SZALAY und SÁRKÁNY [5] für die wässrig-glyzerinschen Na-Fluoreszeinlösungen zeigen auch, dass die

Depolarisationsmessungen für kleine Konzentrationen die JABŁOŃSKIsche Theorie [Gln. (3) und (4)] sehr gut bestätigen. Die Abweichung der letzten zwei gemessenen Punkte von der theoretischen Kurve kann durch die Vernachlässigung der Konzentrationslöschung in Gl. (3) oder auch dadurch, dass in der Wirkungssphäre sich eine endliche Zahl der Moleküle unterbringen lässt, verursacht sein (siehe auch unsere im Druck befindliche Arbeit [8]). Die beste Anpassung der von SZALAY und SÁRKÁNY [5] bestimmten experimentellen Polarisationswerte an die durch Gl. (3) dargestellte Kurve liefert einen Wert von $1{,}8 \cdot 10^{-18}$ cm^3 für das Volumen der aktiven Sphäre v. Dementsprechend ist der Radius der JABŁOŃSKIschen aktiven Sphäre $R = 75{,}46$ Å, aber nicht 70,8 Å, wie von SZALAY und SÁRKÁNY berechnet wurde.

Der FÖRSTERsche kritische Abstand R_0 kann aus der gegenseitigen Überlappung des Absorptionsspektrums mit dem zugehörigen Fluoreszenzspektrum nach der in [9], S. 176 gegebenen Formel (37,6) berechnet werden. Die Berechnung von SZALAY und SÁRKÁNY [5] auf Grund ihrer Messergebnisse liefert für den FÖRSTERschen kritischen Abstand den Wert $R_0 = 51{,}66$ Å. Somit erhält man auf Grund der Gln. (1) und (2) entsprechend $R_{\text{ber}} = 70{,}62$ Å (aus (1)) und $R_{\text{ber}} = 74{,}4$ Å (aus (2)). Man sieht, dass die Relation (2) eine bessere Übereinstimmung zwischen dem Radius R der JABŁOŃSKIschen aktiven Sphäre und dem FÖRSTERschen kritischen Abstand R_0 aufweist, als die Relation (1).

Auch in der Theorie der Fluoreszenzlöschung durch absorbierende Fremdstoffe wurde von JABŁOŃSKI [9] der Radius R' der aktiven Sphäre bei der Löschung, der in anderer Weise als der Radius R definiert ist, eingeführt. Nach JABŁOŃSKI [9] besteht für die durch die Energiewanderung bedingte Auslöschung die folgende Relation

$$R' = 1{,}327\ R_0. \tag{5}$$

Aus (2) und (5) folgt:

$$\frac{R}{R'} = 1{,}085$$

und man kann schliessen, dass die Radien der aktiven Sphären bei der Konzentrationsdepolarisation und bei der Fremdlöschung sich deutlich unterscheiden.

LITERATUR

1. S. I. WAWILOW, J. Phys. URSS, **7**, 141, 1943.
2. TH. FÖRSTER, Annalen der Physik, **2**, 55, 1948.
3. A. ORE, J. Chem. Physics, **31**, 442, 1959.
4. A. JABŁOŃSKI, Acta Phys. Polon., **14**, 295, 1955; **17**, 481, 1958.
5. L. SZALAY und B. SÁRKÁNY, Acta Phys. et Chem. Szeged, **8**, 25, 1962.
6. A. KAWSKI, Zesz. Nauk. WSP Gdańsk, Mat. Fiz., Chem., **1**, 17, 1961.
7. A. KAWSKI, Bull. Acad. Polon., **6**, 533, 1958; **6**, 671, 1958.
8. A. KAWSKI, Z. Naturforschg. 18a, 961, 1963.
9. A. JABŁOŃSKI, Bull. Acad. Polon., **6**, 663, 1958.

RECENSIONES

F. JONA and G. SHIRANE

Ferroelectric Crystals

International Series of Monographs on Solid State Physics Vol. I.

(Pergamon Press, London, 1962)

The main problems which arise in the theory of dielectric crystals are concerned with the polarization that can be induced in such non-conducting materials by means of an externally applied electric field. The polarization values which can be measured and the effects that the polarization is expected to have on a number of physical properties of the crystals (such as the elastic, optical or thermal behaviour) in normal dielectrics when applying experimentally attainable fields are usually small. Nevertheless, a rather large but limited number of crystals — such as potassium di-hydrogen phosphate (KH_2PO_4) and a number of isomorphous phosphates and arsenates, barium titanate ($BaTiO_3$) and other isomorphous oxides, Rochelle salts ($NaKC_4H_4O_6 \cdot 4\,H_2O$) and a few isomorphous crystals — exhibit polarization values and effects mentioned above which are many orders of magnitude larger than those observed in most dielectrics. Forty years have elapsed since the detailed study of some of these crystals — which it became customary to call ferroelectric crystals — revealed many peculiar effects which are interesting not only from the point of view of dielectric theory, but also from that of crystallography, crystal chemistry, thermodynamics, and, last but not least, with regard to practical applications in the field of electrical engineering. In contrast to some other branches of solid state physics, the understanding of the physical properties of ferroelectric crystals requires a wide range of experimental and theoretical approaches. The large reversible polarizations of these materials have both electric and ionic origins. The latter indicates the very close interdependence between ferroelectric activity and crystal structure. This nterdependence makes the most refined structural analysis a very essential tool for the investigations of the materials. On the other hand, the existence of linear electromechanical effects, which require the consideration of interactions between electrical and mechanical quantities, makes the treatment of the ferroelectric phenomena much more complex than, e.g. that of the ferromagnetic analogue. Several review articles and monographs have already been written by a number of authors on the subject of this field. Some of these treat the problem of ferroelectricity in terms of the properties which characterize the phenomenon. Others present the description of ferroelectricity in terms of compounds rather than properties, and are particularly concerned with the crystallographic aspects of the problem.

The authors' approach is to describe the properties of the various ferroelectric crystals individually, and to emphasize the dielectric character of the ferroelectric phenomenon as judged from the viewpoint of solid state physics, having in mind the graduated student and research scientist unfamiliar with the subject as well as researchers in the field. For the former a general introduction and for the latter a list of references as complete as possible up to May 1960 is given. To help the research worker the authors have adapted a presentation in terms of chapters and sections devoted to one compound at a time and they have tried to quote as many numerical results as seemed to be desirable. In a presentation of this kind repetitions are often unavoidable; therefore the authors introduce a number of cross references to help the readers interested in following up a given phenomenon rather than in the characteristics of a given compound.

J. I. HORVÁTH

J. P. SUCHET

Chimie physique des semiconducteurs

Monographies Dunod, Paris, 1962 (French), 222 p.

This new volume of the well-known series, Monographies Dunod, is a good survey of the physico-chemical problems of semiconductors. The treatment is based essentially on the work of a conference held at Bordeaux University, in 1957, entitled "Structure Defects and Semiconduction". In line with the main problems dealt with at that conference, the monograph deals with problems of impurity interactions and the extent to which it is possible to predict the semiconducting properties of a special compound. As recent suggestions indicate that the essential properties of special semiconductors are governed by the nature of interatomic bonds, the present treatment is focussed in that direction. As the author avoids mathematics, whereever possible and only refers to special literature, the book is of particular interest to chemists.

The first two of the eight chapters of the book contain an elementary description of bonding and of crystal defects. Chapter III is devoted to the question of impurity diffusion, *e.g.* the diffusion of oxygen in silicon. Chapter IV summarizes the rules for predicting semiconducting properties. Chapter V contains a survey of semiconducting-oxide ceramics, and Chapter VI the calculation of activation energies. The problems connected with the mobilities of charge carriers, such as the scattering on centre of different nature, the problem of the effective mass, *etc.*, can be found in Chapter VII. The last chapter contains the main problems and recent results in the field of organic semiconductors, including the problem of double bonds and, *e.g.* the semiconducting plastics.

The up-to-date treatment of the book and the survey of the corresponding literature included ensures that the book will be of wide interest, especially among scientists whose work is connected with the preparation of semiconductors.

J. GYULAI

R. W. B. PEARSE and A. G. GAYDON

The Identification of Molecular Spectra

Edited by Chapman Ltd., London 347 pp, third edition

In this book the authors have collected information about the appearance and occurrence of each known band spectrum which may assist in its identification. Several excellent books have been written dealing with the theory of molecular spectra and some have included collections of molecular constants derived from the analysis of these spectra but until now it has been necessary to search through original papers or to calculate the positions of bands from the tables of derived constants in order to identify a given system of bands. This task is usually tedious and sometimes impossible to one without considerable experience. The present work renders such efforts unnecessary.

In the first part of the book the band heads occurring most frequently are given in order of wave length; the second part includes all recorded systems of diatomic molecules arranged alphabetically; of triatomic and more complex molecules only those are included which show well-defined banded structure and are of frequent occurrence in spectroscopical investigation. The absorption spectra of complex organic molecules and of solutions have been omitted. The wavelength region considered is from 10,000 Å to 2,000 Å, that is roughly, from the photographic infra-red to the ultraviolet limit of quartz spectrographs. In addition to the wave lenghts of the band heads the tables include information about the appearance and occurrence of each band spectrum.

Where the available literature has proved to be incomplete, the authors have made new wave length measurements. In a large number of cases where no estimates of intensities are given but a photograph is included in the original papers estimations of intensities have been made from the photographs. In other cases where the analysis alone is given without mention of the position and intensities of the most prominent band

heads, the positions of these heads has been determined from the analysis where possible, and, if necessary the corresponding wave numbers have been converted to wave lengths.

The wide success and practical applicability of the book is shown by the fact that the first edition (1941) was followed by a second in 1950, and now, in 1963, the third has appeared. The publication of the present, third edition was prompted by the fact that during the twelwe years which have elapsed since the completion of the second edition many fields of research have found a new interest in spectroscopy. One result of this has been a greater output of papers recording observation of molecular spectra. For this reason an even greater amount of additional material has been added to this edition than to the second. This augmentation includes new data up to the end of 1961. The authors have attempted to present the resulting volume in as concise a form as possible. The tables are presented in a more compac- form than previously.

I. Kovács

* Department of Atomic Physics, Polytechnical University, Budapest, Hungary

Printed in Hungary

A kiadásért felel az Akadémiai Kiadó igazgatója — Műszaki szerkesztő: Farkas Sándor

A kézirat nyomdába érkezett: 1963. VIII. 9. — Terjedelem: 9,75 (A/5) ív, 32 ábra

3.57599 Akadémiai nyomda, Budapest — Felelős vezető: Bernát György

The *Acta Physica* publish papers on physics, in English, German, French and Russian.
The *Acta Physica* appear in parts of varying size, making up volumes.
Manuscripts should be addressed to:

Acta Physica, Budapest 502, Postafiók 24.

Correspondence with the editors and publishers should be sent to the same address.
The rate of subscription to the *Acta Physica* is 110 forints a volume. Orders may be placed with "Kultúra" Foreign Trade Company for Books and Newspapers (Budapest I., Fő u. 32. Account No. 43-790-057-181) or with representatives abroad.

Les *Acta Physica* paraissent en français, allemand, anglais et russe et publient des travaux du domaine de la physique.
Les *Acta Physica* sont publiés sous forme de fascicules qui seront réunis en volumes.
On est prié d'envoyer les manuscrits destinés à la rédaction à l'adresse suivante:

Acta Physica, Budapest 502, Postafiók 24.

Toute correspondance doit être envoyée à cette même adresse.
Le prix de l'abonnement est de 110 forints par volume.
On peut s'abonner à l'Entreprise du Commerce Extérieur de Livres et Journaux «Kultúra» (Budapest I., Fő u. 32. — Compte-courant No. 43-790-057-181) ou à l'étranger chez tous les représentants ou dépositaires.

«*Acta Physica*» публикуют трактаты из области физических наук на русском немецком, английском и французском языках.
«*Acta Physica*» выходят отдельными выпусками разного объема. Несколько выпусков составляют один том.
Предназначенные для публикации рукописи следует направлять по адресу:

Acta Physica, Budapest 502, Postafiók 24.

По этому же адресу направлять всякую корреспонденцию для редакции и администрации.
Подписная цена «*Acta Physica*» — 110 форинтов за том. Заказы принимает предприятие по внешней торговле книг и газет «*Kultúra*» (Budapest I., Fő u. 32. Текущий счет: № 43-790-057-181) или его заграничные представительства и уполномоченные.

28,— Ft

INDEX

COMMUNICATIONES BREVES

RECENSIONES

Acta Phys. Hung. Tom. XVI. Fasc. 3., Budapest, 16. XI. 1963.

Index: 26.022

ACTA PHYSICA

ACADEMIAE SCIENTIARUM HUNGARICAE

TOMUS XVI FASCICULUS 4

AKADÉMIAI KIADÓ, BUDAPEST
1964

ACTA PHYS. HUNG.

ACTA PHYSICA

A MAGYAR TUDOMÁNYOS AKADÉMIA FIZIKAI KÖZLEMÉNYEI

SZERKESZTŐSÉG ÉS KIADÓHIVATAL: BUDAPEST V., ALKOTMÁNY UTCA 21.

Az *Acta Physica* német, angol, francia és orosz nyelven közöl értekezéseket a fizika tárgyköréből.

Az *Acta Physica* változó terjedelmű füzetekben jelenik meg: több füzet alkot egy kötetet.

A közlésre szánt kéziratok a következő címre küldendők:

Acta Physica, Budapest 502, Postafiók 24.

Ugyanerre a címre küldendő minden szerkesztőségi és kiadóhivatali levelezés.

Az *Acta Physica* előfizetési ára kötetenként belföldre 80 forint, külföldre 110 forint. Megrendelhető a belföld számára az Akadémiai Kiadónál (Budapest V., Alkotmány utca 21. Bankszámla 05-915-111-46), a külföld számára pedig a „Kultúra" Könyv- és Hírlap Külkereskedelmi Vállalatnál (Budapest I., Fő u. 32. Bankszámla 43-790-057-181 sz.), vagy annak külföldi képviseleteinél és bizományosainál.

Die *Acta Physica* veröffentlichen Abhandlungen aus dem Bereiche der Physik in deutscher, englischer, französischer und russischer Sprache.

Die *Acta Physica* erscheinen in Heften wechselnden Umfanges. Mehrere Hefte bilden einen Band.

Die zur Veröffentlichung bestimmten Manuskripte sind an folgende Adresse zu richten:

Acta Physica, Budapest 502, Postafiók 24.

An die gleiche Anschrift ist auch jede für die Redaktion und den Verlag bestimmte Korrespondenz zu senden.

Abonnementspreis pro Band: 110 Forint. Bestellbar bei dem Buch- und Zeitungs-Aussenhandels-Unternehmen »Kultúra« (Budapest I., Fő u. 32. Bankkonto Nr. 43-790-057-181) oder bei seinen Auslandsvertretungen und Kommissionären.

EXPECTED α-DECAY DATA OF THE RARE EARTH NUCLIDES ON THE BASIS OF DIFFERENT SYSTEMATICS

By

T. FÉNYES

INSTITUTE OF NUCLEAR RESEARCH OF THE HUNGARIAN ACADEMY OF SCIENCES, DEBRECEN

and

Z. BŐDY

INSTITUTE FOR EXPERIMENTAL PHYSICS OF THE KOSSUTH UNIVERSITY, DEBRECEN

(Presented by A. Szalay. — Received 28. I. 1963)

This work summarizes the α-decay data of rare earth nuclides. The α- and β-decay energies measured up to present allow the computation of the decay energy of some 30 further nuclides. By plotting the α-decay energy vs. the atomic number, the expected α-decay energy of nuclides, the α-activity of which has not yet been detected experimentally, has been estimated. The estimation of the α-decay energies for the above nuclides on the basis of the available mass data and p and n separation energies has also been performed. The expected α-partial half-lives were also estimated from the gained α-decay energies using a semi-empirical relation (see [15], p. 6) expressing explicitly the dependence of the half-life on the atomic number. Finally, some questions regarding the possibility of experimental detection of those α-activities, which have not yet been measured, are discussed.

1. Introduction

It is known that for nuclides having mass number greater than about 140 α-decay is allowed energetically [1], but in most cases the half-lives are so high that the disintegrations have not yet been detected experimentally.

The probability of the α-decay in the region of great mass numbers is high, especially for nuclides containing protons or neutrons of magic number plus 2, 3, ... [2], because the binding energy of nucleons just above a closed shell is small and so the energy loss of the α-particles due to the binding energy is small. In the medium heavy region those are the nuclides of neutron number 84, 85, ... etc.

It is known too that among the nuclides of the same atomic number (far from magic numbers) the smaller is the number of neutrons in the nucleus, the greater is the disintegration energy [2], as the repulsive effect of protons in that case has relatively more influence.

Starting from these points the α-radiation of many neutron deficient rare earth nuclides has been experimentally detected — especially during the last 14 years. A detailed discussion of the literature up to 1959 can be found in paper [3].

The aim of this work is to summarize up to the middle of 1962 the data of α- and β-decays of the rare earth nuclides recently measured and computed

Table I

Nuclide	Mass number (A)	α-particle energy (MeV) In brackets: the total alpha-decay energy (MeV)	Method of detection	Total half-life	Other decay modes observed
$_{60}$Nd	144	1,90 ± 0,1	nuclear emulsion		natural β-stable
		1,83 ± 0,03 (1,902)	ionization chamber		
$_{61}$Pm	145	2,24 ± 0,04 (2,32)	,,	17,7 ± 0,4 years	e^--capture
$_{62}$Sm	146	2,55 ± 0,05 (2,64)	nuclear emulsion		β-stable
	147	2,18 ± 0,02	ionization chamber		natural β-stable
		2,23 ± 0,02	,,		
		2,20 ± 0,02	,,		
		2,19 ± 0,01	,,		
		2,21 ± 0,01 mean (2,293)			
	148	2,14 ± 0,03 (2,220)	ionization chamber		natural β-stable
	149	1,84 ± 0,05 (1,91)	ionization chamber		natural β-stable
$_{63}$Eu	147	2,88 ± 0,10 (2,98)	ionization chamber	24 ± 2 days	e^--capture
		2,91 ± 0,01 (3,01)	,,		

Data of α -active rare earth nuclides

α/total decay ratio	α-partial half-life T_α	Method of measuring T_α	Production (bombarding energy)	Reference
	$\approx 1{,}5 \cdot 10^{15}$ years	from decay rate of a given number of atoms	natural	[3]
	$(2{,}4 \pm 0{,}3) \cdot 10^{15}$ years	,,	23,83%	[5]
$(2{,}8 \pm 0{,}6) \cdot 10^{-9}$	$(6{,}3 \pm 1{,}4) \cdot 10^{9}$ years	$\frac{\alpha}{\text{x-ray}}$ ratio	$Sm^{144}(n, \gamma)Sm^{145}$ $Sm^{145} \xrightarrow{e^- \text{-capture}} Pm^{145}$ with thermal neutrons	[18]
	$\approx 5 \cdot 10^{7}$ years	estimated from reaction yield	$Nd^{143}(\alpha, n)$	[3]
	$< 3 \cdot 10^{8}$ years		Gd^{150} ($>10^5$ years) $\xrightarrow{\alpha}$	[5]
	$\approx 1{,}3 \cdot 10^{11}$ years	from decay rate of a given number of atoms	natural 15.09% Pm^{147} (2,6 years) $\xrightarrow{\beta^-}$	[3]
	$(1{,}15 \pm 0{,}05) \cdot 10^{11}$ years	,,	$U^{235}(n, \text{fission})$	[5]
	$(1{,}17 \pm 0{,}05) \cdot 10^{11}$ years	,,		[7]
				[6]
	$(1{,}18 \pm 0{,}05) \cdot 10^{11}$ years mean			[7] see also [26]
	$(1{,}2 \pm 0{,}3) \cdot 10^{13}$ years	,,	natural	[7]
	$> 2 \cdot 10^{14}$ years		$(11{,}35 \pm 0{,}09)$ %	[5]
	$(4 \pm 2) \cdot 10^{14}$ years	,,	natural	[7]
	$> 1 \cdot 10^{15}$ years		$(13{,}96 \pm 0{,}10)$ %	[5]
$\approx 10^{-5}$	$4{,}4 \cdot 10^{3}$ years $\approx 6 \cdot 10^{3}$ (within a multiplying factor 3.)	$\frac{\alpha}{\text{x-ray}}$ ratio	$Sm^{147}(p, n)$ 8,5 MeV $Sm^{147}(d, 2n)$ 19 MeV $Sm^{148}(d, 3n)$ 19 MeV	[3] [22]
$(2{,}2 \pm 0{,}6) \cdot 10^{-5}$		$\frac{\alpha}{\gamma\text{-ray}}$ ratio	$Sm^{147}(p, n)$ 9,5 MeV	[26]

Table I

Nuclide	Mass number (A)	α-particle energy (MeV) In brackets: the total alpha-decay energy (MeV)	Method of detection	Total half-life	Other decay modes observed
$_{64}$Gd	148	$3{,}16 \pm 0{,}10$ (3,27)	ionization chamber	$>$ 35 years ≈130 years	β-stable (?)
		$3{,}18 \pm 0{,}01$ (3,29)	,,		
	149	$3{,}00 \pm 0{,}15$ (3,11)	,,	$9{,}0 \pm 1$ days	e^--capture
	150	$2{,}70 \pm 0{,}15$ (2,80)	,,	$\approx 3 \cdot 10^5$ years	β-stable
		$2{,}53 \pm 0{,}05$ (2,62) $2{,}55 \pm 0{,}05$ mean of the first two data (2,64)	,,		
		$2{,}73 \pm 0{,}01$ (2,83)	,,		
	152	1,7	nuclear emulsion		
		$2{,}14 \pm 0{,}03$ (2,22)	ionization chamber		natural β-stable
$_{65}$Tb	149	4,0			
		$3{,}95 \pm 0{,}02$ (4,08)	α-spectroscope	$(4{,}10 \pm 0{,}05)$ hours	β^+
	149^m m = metastable	$3{,}99 \pm 0{,}03$	ionization chamber	$(4{,}3 \pm 0{,}2)$ minutes	e^--capture and β^+
	151	$3{,}44 \pm 0{,}1$ (3,55)	,,	19 ± 1 hours $17{,}5 \pm 0{,}7$ hours	e^--capture
	152			$17{,}4 + 0{,}3$ hours $(4 \pm 0{,}5)^m$ minutes	β^+-stable e^--capture $(\beta^+, e^-$-capture$)^m$

(continued)

α/total decay ratio	α-partial half-life T_α	Method of measuring T_α	Production (bombarding energy)	References
>25%	≈1,3 · 10^2 years (within a multiplying factor 3)	estimated from reaction yield	Sm^{147} (α, 3n) 36 MeV Eu^{151} (p, 4n) 32 MeV	[3] [22]
	84 ± 9 years	from decay rate of a given number of atoms	Eu (p, xn) 100 MeV	[26]
7 · 10^{-6}	≈4 · 10^3 years (within a multiplying factor 3)	$\frac{\alpha}{\text{x-ray}}$ ratio	Sm^{147} (α, 2n) 30 MeV Tb^{149} (4,1^h) e^--capture	[22] [3]
	≈3 · 10^5 years	from decay rate of a given number of atoms	Eu^{151} (d, 3n) 19 MeV Eu^{150} (13,7^h) β−	[3]
	3 · 10^6 years	,,	Eu^{151} (γ, n) Eu^{150} Eu^{150} (13,7^h) β−	[19] pre-liminary report
	(2,1 ± 0,3) · 10^6 years	,,	Sm^{150} (p, n) 9,5 MeV Eu^{150} (13,7^h) β−	[26]
	≈10^{15} years	,,	natural 0,2%	[23]
	(1,08 ± 0,08) · 10^{14} years	,,		[5]
0,1				[21]
0,16 ± 0,04	36 ± 7 hours	$\frac{\alpha}{\text{total decay}}$ ratio	Eu^{151} (α, 6n) 60 MeV Gd (p, xn) 32—200MeV Bi (p, fission)	[3]
			La^{139} (O^{16}, 6n) Tb^{149m} 80—140 MeV linear accelerator	[17]
3 · 10^{-6}	7,4 · 10^2 years	$\frac{\alpha}{\text{x-ray}}$ ratio	Gd (p, xn) 100 MeV Eu^{151} (α, 4n) 45 MeV	[3] [21]
$\frac{\alpha}{\text{x-ray (K)}}$ ratio ≈ (2 · 10^{-5}) for the meta-stable state)			Eu^{151} (α, 3n) 44 MeV Gd^{152}(p, 4n) 41 MeV	[8] [21]

Table I

Nuclide	Mass number (A)	α-particle energy (MeV) In brackets: the total alpha-decay energy (MeV)	Method of detection	Total half-life	Other decay modes observed
$_{66}$Dy	150	4,21 ± 0,06 (4,35)	ionization chamber	7 ± 2 minutes	e^--capture and β^+
	151	4,06 ± 0,04 (4,19)	,,	19 ± 4 minutes	e^--capture and β^+
	152	3,66 ± 0,05 (3,78)	,,	(2,3 ± 0,2) hours	e^--capture and β^+
	153	3,48 ± 0,05 (3,59)	,,	5 ± 0.5 hours	indirect proof for e^--capture
	154	3,35 ± 0,05 (?)	,,	13 ± 2 hours (?)	no observed
		2,85 ± 0,05 (2,95)	,,	>10 years if β^+ exists	no observed
$_{67}$Ho	151	4,48 (4,62)	,,	31 sec	
	152	4,40 (4,54)	,,	64 sec	
	153	4,34 (4,48)	,,	187 sec	
	154	4,12 (4,25)	,,	5,6 minutes	
	155	3,96 (4,09)	,,	16,5 minutes	
$_{68}$Er	152	4,80 ± 0,02 (4,95)	solid state ion. chamber	10,7 ± 0,5 sec	e^--capture β^+
	153	4,67 ± 0,02 (4,82)	,,	36 ± 2 sec	,,
	154	4,15 ± 0,02 (4,28)	,,	4,5 ± 1,0 min	,,
$_{69}$Tm	153	5,11 (5,27)		1,12 sec	
	154	5,04 (5,20)		3,10 sec	

The total decay energy was gained from the expression

$$Q = E + \frac{m}{M} E + (65{,}3\, E^{7/5} - 80\, E^{2/5})\, 10^{-6},$$

(continued)

α/total decay ratio	α-partial half-life T_α	Method of measuring T_α	Production (bombarding energy)	References
			$Tb^{159}(p, xn)$ 100 MeV	[3]
				[3]
	$\approx$ 1,45 years	estimated from reaction yield		[3]
	$\approx$13,4 years	,,		[3]
			Gd (α, ...)	[3]
	$\approx 10^6$ years (within a multiplying factor 3)	,,	Gd (α, ...) 48 MeV from a sample enriched in Gd^{154}	[9]
$\approx$0,1			Nd (N^{14} ions, ...) 65—130 MeV	[25]
$\approx$0,1			,,	[25]
$\approx$0,005			,,	[25]
0,017			,,	[25]
0,0078			,,	[25]
$0{,}90 \begin{matrix} +0{,}05 \\ -0{,}20 \end{matrix}$		detection of daughter	Nd^{142} (0^{16}, 6n) 75—151 MeV	[27]
$0{,}95 \begin{matrix} +0{,}05 \\ -0{,}20 \end{matrix}$		excitation function	N^{142} (0^{16}, 5n) 75—151 MeV	[27]
			Nd^{142} (0^{16}, 4n) 75—151 MeV	[27]
			Nd^{142} (F^{19}....) 190 MeV	[28]
			,,	[28]

where Q = total decay energy (MeV), E = kinetic energy of α-particle (MeV), m = mass of α-particle, M = mass of daughter nucleus, Z = atomic number of parent nucleus.
The first term of the expression gives the kinetic energy of the α-particle, the second the kinetic energy of the recoil daughter nucleus, the third the correction for electron screening.

from mass data, to complete them by adding the disintegration energies calculated from α—β decay cycles and to draw conclusions with respect to the α-decay energy of the rare earth nuclides the α-decay of which has not yet been observed. The disintegration energies mentioned above were computed also by means of energy cycles composed by using known α-decay and proton (neutron) separation energies. Conclusions have also been drawn regarding the expected partial half-lives from the disintegration energies, using the semi-empirical formula discussed in [15].

2. Summary of experimental α-decay data

The sources from which the data were taken are indicated in the last column of Table I. We have sometimes used the data of works [4] and [10],

Table II

α — β decay cycles in the rare earth region

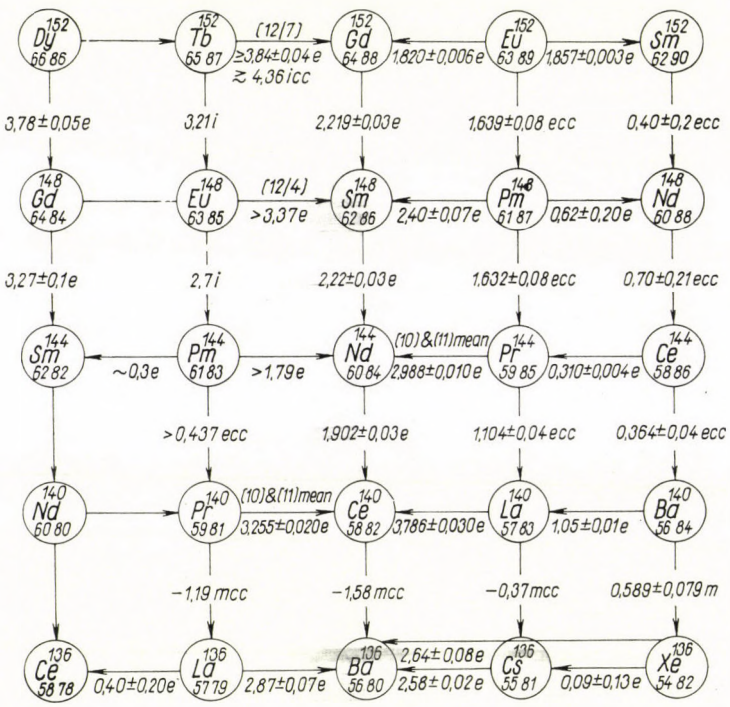

e	Explanation of the symbols written after decay energies: experimental value,
ecc	value computed from decay cycle containing only experimental data,
m	value gained from mass data having an error $\leq$200 keV,
mcc	value computed from decay cycle containing beside the experimental values also a decay energy calculated from mass data,
i	inter- or extrapolated value on the basis of Fig. 1
icc	value computed from decay cycle containing besides the experimental data also an inter-, or extrapolated value on the basis of Fig. 1 or [13].

but have not referred to them specifically. Paper [3] is a comprehensive work containing further references.

3. β-decay data

The disintegration energy values of the $\beta^{\pm}$-decays (including electron captures) are contained in Tables II, III, IV and V concerning the α — β decay cycles. The data are taken from [10] and [11], as well as from the recent papers (up to about the middle of 1962). In the latter case the source is indi-

Table III

α — β decay cycles in the rare earth region (for the explanation of symbols see the caption of Table II)

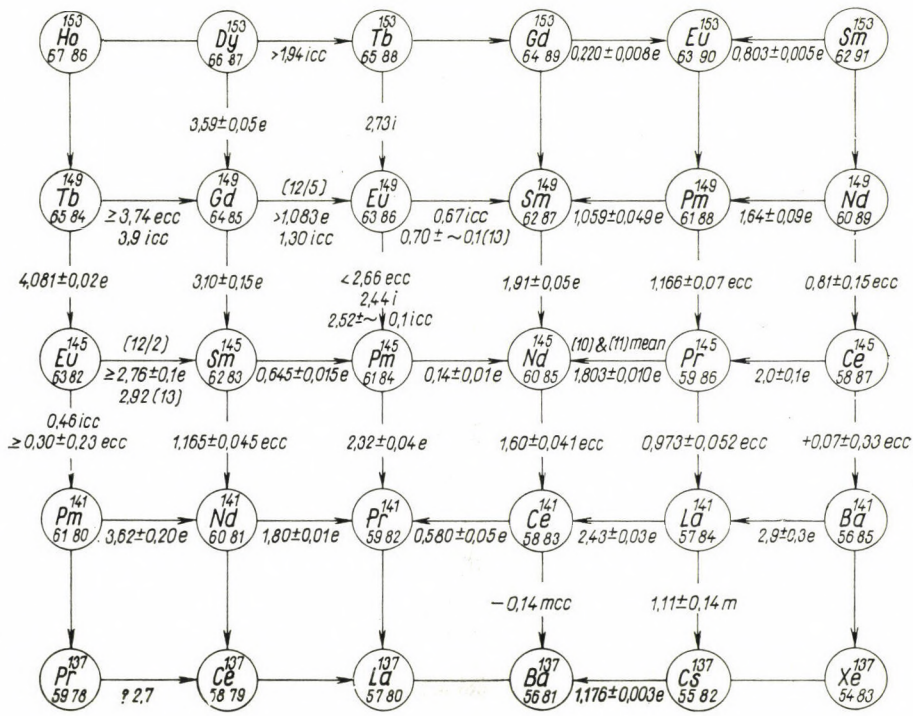

cated in the Tables. The EVERLING, GOVE, LIESHOUT systematics [13] recently published shows the $\beta^{\pm}$-decay and e^{-}-capture energies vs. mass number for even and odd nuclides, respectively. This systematics in some cases makes it possible to estimate the energy released in $\beta^{\pm}$-decay (electron capture) processes, where this has not yet been measured.

Table IV

$\alpha - \beta$ decay cycles in the rare earth region (for the explanation of symbols see the caption of Table II)

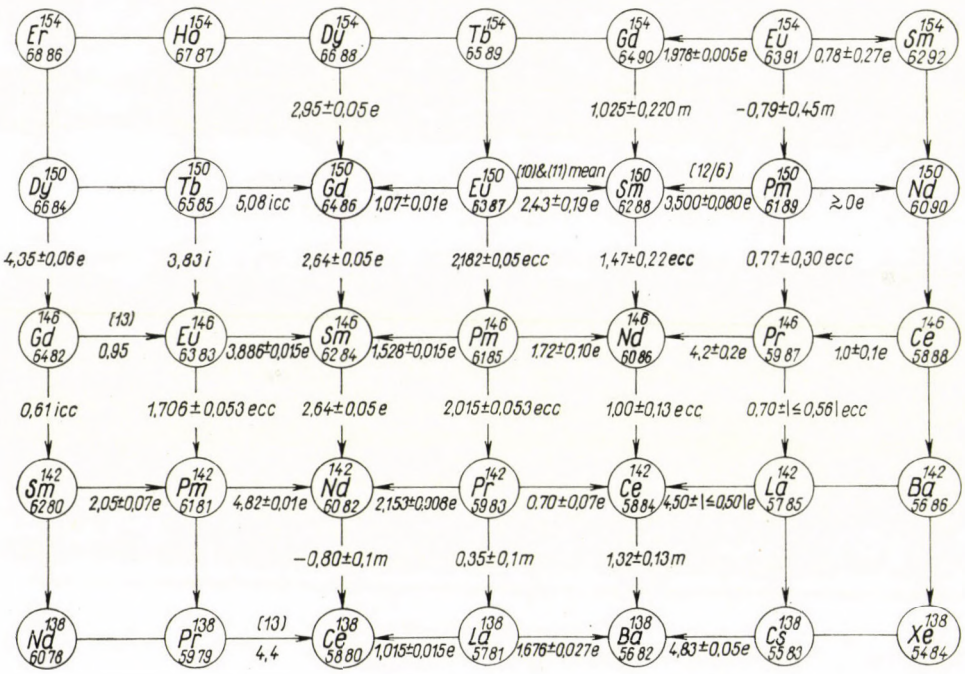

4. Computation of α- and β-decay energies by means of closed decay cycles

Tables II, III, IV and V allow to compute new energy values from known decay energies by means of closed decay cycles.

The alpha-disintegration energies computed from closed decay cycles, containing only experimentally measured disintegration energies, are presented in Table VI.

The β-decay energies computed from $\alpha - \beta$ decay cycles are shown in Table VII. Throughout the calculations cycles were used containing only experimental data and only occasionally single inter- or extrapolated α-decay energy values from Fig. 1.

5. Dependence of α-decay energy on mass number

Fig. 1 shows the decay energies (Q_α) vs. mass number (A).

In the systematics the curves $Z = \text{const.}$ and $N = \text{const.}$ are drawn for the most part through the measured points within the limits of error in order to get a better agreement with the general tendency of the curves.

Table V

$\alpha - \beta$ decay cycles in the rare earth region (for the explanation of symbols see the caption of Table II)

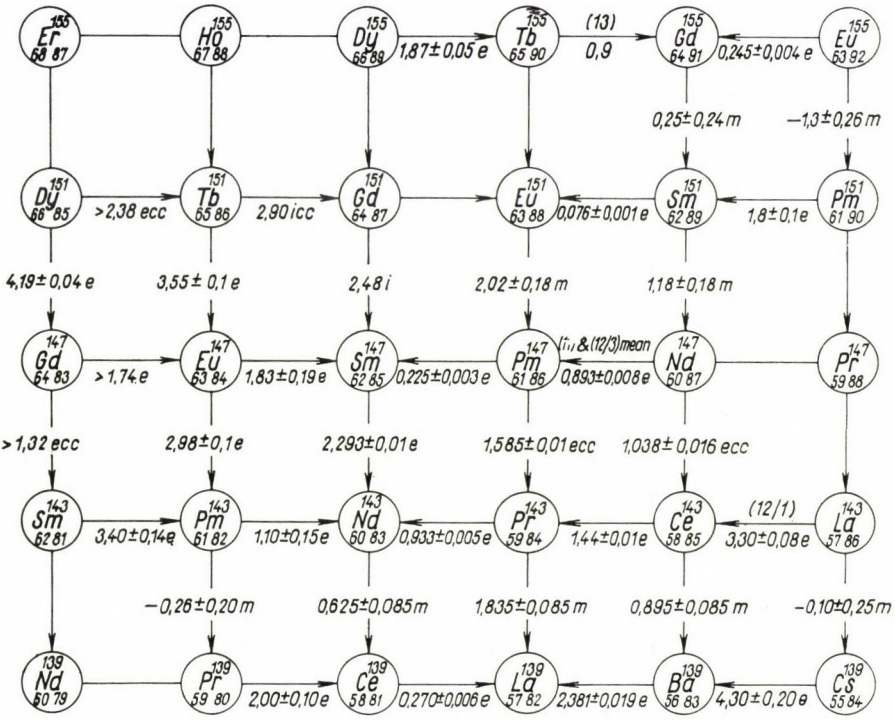

Linearity or at least quasi-linearity was supposed to be the general tendency; this was supported by an analogy with the behaviour of the corresponding curves in the region of heavy nuclides (far from magic numbers).

In one single case, that of Nd^{149}, the curves are drawn beyond the limits of error. This was suggested by some experimental evidences. The decay cycle, from which the β^--decay energy of Nd^{149} was computed, contains the β^--decay energy of Ce^{145}. We accepted the value $2{,}0 \pm 0{,}1$ MeV for this energy given in [10] and [11], while paper [20] gives $2{,}6 \pm | \leq 0{,}5 |$ MeV for it. Therefore it is probable that the α-decay energy of Nd^{149} is lower than 0,81 MeV.

The effect of the magic number $N = 82$ is evident from Fig. 1. For a given atomic number the α-decay energy increases gradually as the number of neutrons decreases down to $N = 84$ where there is a sharp cut off. See the cases of Pr_{83}^{142}, Nd_{83}^{143}, Sm_{83}^{145}, Eu_{83}^{146}, and Eu_{82}^{145}, Gd_{82}^{146}, respectively.

It is also clear that passing on from atomic number 64 to 65 the α-decay energy increases more rapidly than it generally does, this fact being related to a closed subshell at $Z = 64$ predicted by the independent-particle model. (See for example [14].)

Table VI

α-decay energies computed only from experimental data on the basis of $\alpha - \beta$ decay cycles as well as some data gained from other sources for the purpose of comparison

1	2	3	4
Nuclide	Expected α-decay energy		Deviation of the data of Column 2 from the lines in Fig. 1 (MeV)
	from $\alpha - \beta$ cycle Q_α (MeV)	from mass data Q_α (MeV) See [11]	
Ce^{144}	$0{,}364 \pm 0{,}04$	$0{,}345 \pm 0{,}09$	0,0
Ce^{145}	$0{,}07 \pm 0{,}33$	$-0{,}095 \pm 0{,}34$	—
Pr^{144}	$1{,}104 \pm 0{,}04$	$1{,}075 \pm 0{,}084$	$-0{,}04$
Pr^{145}	$0{,}973 \pm 0{,}052$	$0{,}815 \pm 0{,}16$	$+0{,}052$
Pr^{146}	$0{,}7 \pm \lvert\leq 0{,}54\rvert$	—	—
Nd^{145}	$1{,}60 \pm 0{,}041$	$1{,}435 \pm 0{,}16$	0,0
Nd^{146}	$1{,}00 \pm 0{,}13$	$0{,}975 \pm 0{,}17$	$-0{,}12$
Nd^{147}	$1{,}038 \pm 0{,}016$	$0{,}975 \pm 0{,}085$	0,0
Nd^{148}	$0{,}70 \pm 0{,}21$	$0{,}415 \pm 0{,}16$	—
Nd^{149}	$0{,}81 \pm 0{,}15$	$0{,}925 \pm 0{,}235$	$+0{,}2$
Pm^{144}	$(\sim 0{,}647)$ $> 0{,}437$	—	—
Pm^{146}	$2{,}015 \pm 0{,}053$	$1{,}995 \pm 0{,}1$	0,0
Pm^{147}	$1{,}585 \pm 0{,}01$	$1{,}515 \pm 0{,}084$	0,0
Pm^{148}	$1{,}632 \pm 0{,}08$	$1{,}335 \pm 0{,}15$	$+0{,}075$
Pm^{149}	$1{,}166 \pm 0{,}07$	$1{,}275 \pm 0{,}2$	0,0
Pm^{150}	$0{,}77 \pm 0{,}3$	$1{,}21 \pm 0{,}49$	—
Sm^{145}	$1{,}165 \pm 0{,}045$	—	0,0
Sm^{150}	$1{,}47 \pm 0{,}22$	$1{,}595 \pm 0{,}19$	—
Sm^{152}	$0{,}40 \pm 0{,}2$	$0{,}365 \pm 0{,}18$	—
Eu^{145}	$\geqq 0{,}30 \pm 0{,}23$	—	—
Eu^{146}	$1{,}706 \pm 0{,}053$	—	0,0
Eu^{149}	$< 2{,}66$	—	—
Eu^{150}	$2{,}182 \pm 0{,}05$	$2{,}305 \pm 0{,}17$	$-0{,}03$
Eu^{152}	$1{,}639 \pm 0{,}08$	$1{,}615 \pm 0{,}175$	$-0{,}03$
Gd^{147}	$> 1{,}32$	—	—

It is surprising that the decay energies of Sm^{152}, Gd^{153} and Gd^{154} are considerably lower than one might expect on the basis of the general tendency. It seems that the disintegration energy decreases markedly in many cases as the neutron number increases from 88 to 90. This effect has already been noted by TOTH and RASMUSSEN [3] and the new data support them definitely. It is to be noted that MACFARLANE [24] found 1.5 MeV for the α-decay energy of Dy^{156} having calculated it from the Cameron mass formula. This also confirms the effect mentioned above.

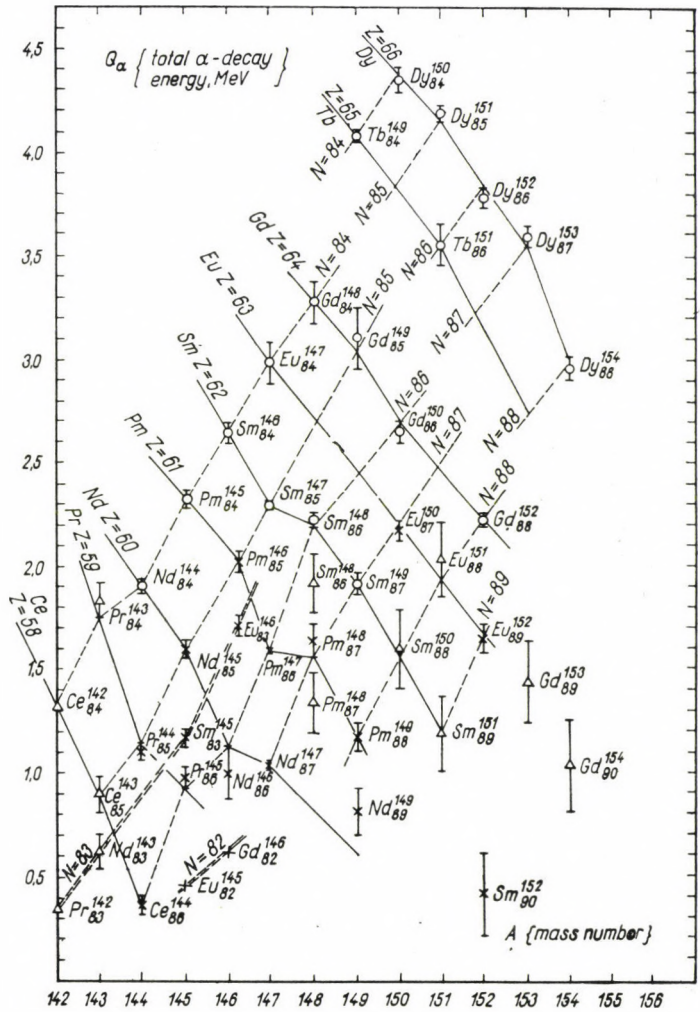

Fig. 1. The total α-decay energy (Q_α) as function of the mass number of the parent nuclide. Table of symbols:

o experimentally measured value,
× value computed from experimental data on the basis of $\alpha - \beta$ decay cycles (only those are presented which have an error $\leq$200 keV),
△ value gained from mass data (see [11]) (also only those which have an error $\leq$200 keV),
\+ Q_α computed from $\alpha - \beta$ decay cycle containing besides the experimental data also an inter-, or extrapolated value gained from β-systematics [13].
——— connects the values belonging to the same atomic number,
- - - - - - - - connects the values belonging to the same neutron number

From Fig. 1 some inter- and extrapolated energy data can be obtained for nuclides, the α-decay of which has not yet been observed or, if it has, the value of the α-decay energy has not been measured. The data gained by this method are presented in the second column of Table X. In the second place of the same column values of α-decay energies computed from mass data as given by [11] and in the third place α-decay energies calculated on the basis of closed decay cycles from proton (neutron) separation energies are also listed. The proton and neutron separation energies are given in [20].

Table VII

Electron capture and $\beta^{\pm}$ -decay energies computed from closed decay cycles

Nuclide	Type of decay	Q_β from decay cycles based on experimental data only (MeV)	Q_β from decay cycles containing beside the experimental data a single inter- or extrapolated Q_α (MeV)	Q_β from systematics [13] (MeV)
Eu^{149}	e^--capture or β^+		0,67	0,70
Gd^{149}	,,		1,30	—
Tb^{149}	,,	$\geqq 3{,}74$	3,9	—
Tb^{150}	,,		5,08	—
Tb^{151}	,,		2,90	—
Tb^{152}	,,		$>4{,}36$*	—
Dy^{151}	,,	$>2{,}38$		—
Dy^{153}	,,		1,94	—

"Decay cycles" constructed by taking separation energy data into account can be found in Tables VIII and IX. The last method of computation was used only in cases where we gained an energy value also by other methods.** Finally, there are data in Table X calculated from $\alpha - \beta$ decay cycles too.

6. Dependence of half-life on the disintegration energy

It is known that the connection between half-life T_α and decay energy Q_α for the ground state transition of even-even nuclides is given by the equation

$$\log T_\alpha = A + \frac{B}{\sqrt{Q_\alpha}} , \tag{1}$$

* The decay energy of Eu^{148} in systematics [13] is about 3,4 MeV, while the experimental value is $>3{,}37$ MeV. It seems therefore that the true value of the decay energy of Tb^{152} does not exceed the calculated one very much, probably they are equal.

** This way of computation was not followed for other nuclides because of the great errors in separation energies (although these errors seem to be overestimated in many cases).

Table VIII

Computation of α -decay energies using proton and neutron separation energies [20] on the basis of closed decay cycles

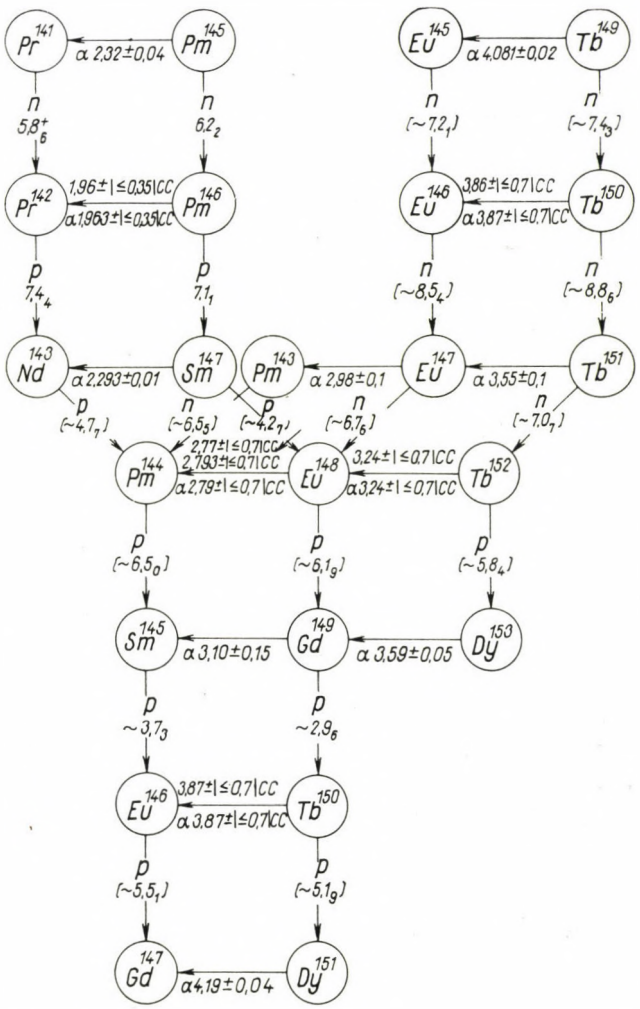

Table of symbols:

* experimental value,
\+ experimental value corrected within the limit of error,
( ) estimated value,
a value without mark: computed value,
cc value computed from cycle.
Errors: the last numeral written below: 0,04 < error (MeV) ≤0,25,
the last numeral written below and mark ~: 0,25 < error (MeV) ≤0,50

Table IX

Computation of α -decay energies using proton and neutron separation energies [20] on the basis of closed decay cycles (for the explanation of symbols see the caption of Table VIII).

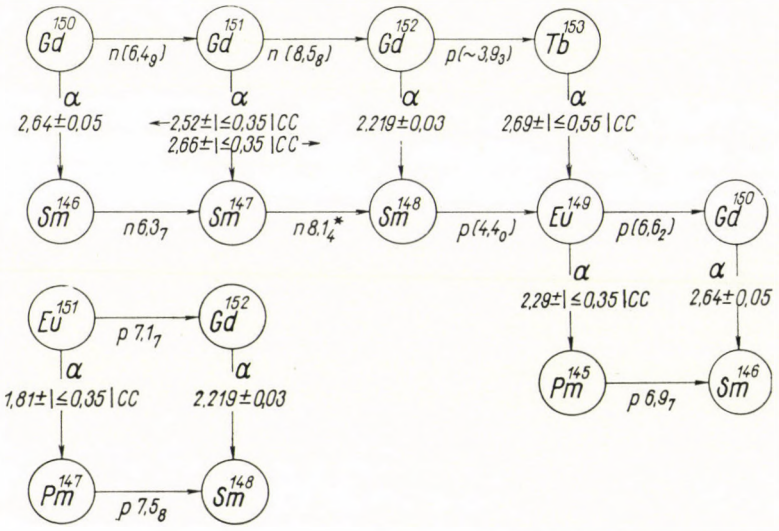

where the coefficients A and B are functions of the atomic number only. For this reason in the region of heavy nuclei one usually connects the points belonging to the same Z when plotting the function $T_\alpha = f(Q_\alpha)$. This method of plotting does not seem to be suitable in the medium heavy region because there are only a few isotopes belonging to the same atomic number the α-partial half-life of which is known. (Even the known half-life values are not too reliable.)

Recently TAAGEPERA and NURMIA [15] suggested an approximate formula, derived from the α-decay theory of quantum mechanics, which gives explicitly the Z dependence of the coefficients A and B. According to this formula for the transition between the ground states of even-even nuclei we have

$$\log T_\alpha = C + D\left[\frac{Z_d}{\sqrt{E}} - Z_d^{2/3}\right], \tag{2}$$

where C and D are constants independent of the atomic number,
T_α = partial half-life of α-decay, Z_d = atomic number of daughter nucleus,
E = kinetic energy of α-particle.

In Fig. 2 the known values of Q_α and T_α are presented for rare earth nuclides, the points representing the data of even-even nuclides being connected by a straight line.

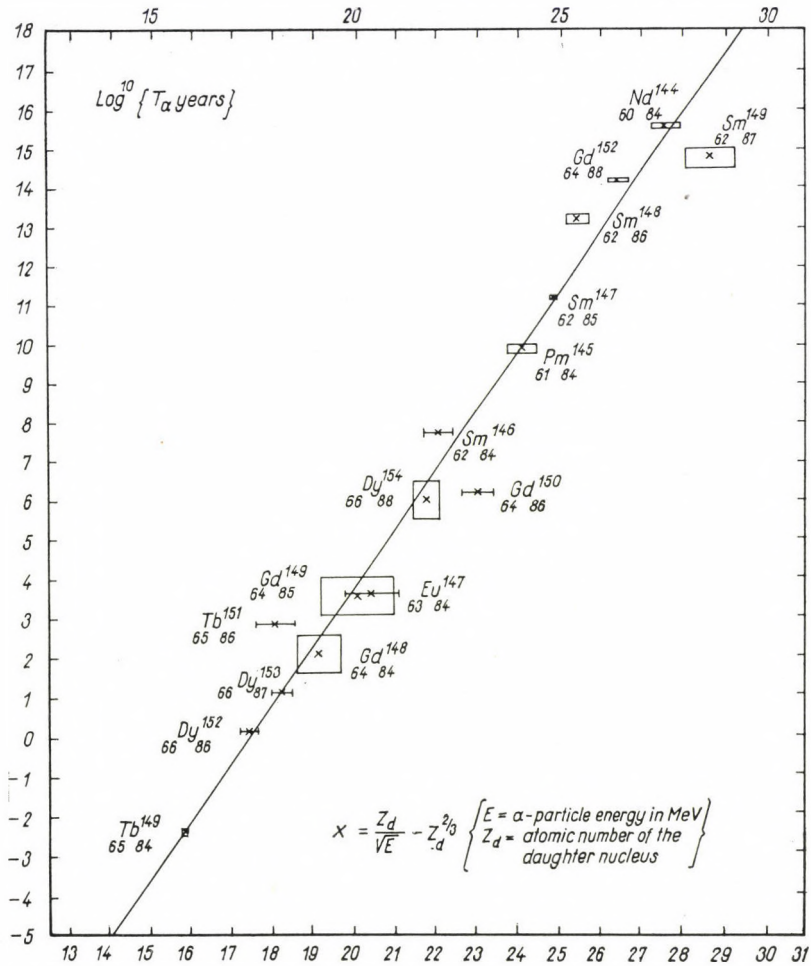

Fig. 2. Relation between the logarithm of α-partial half-life and α-particle kinetic energy of rare earth nuclides. Z_d is the atomic number of the daughter nucleus. The straight line connects the data of even-even nuclides [see formula (2)]. Only experimentally measured data are presented in the figure.

There are four nuclides for which the data deviate considerably from this straight line: Sm^{148}, Sm^{149}, Gd^{150}, and Tb^{151}.

As for the data of Sm^{148} we refer to paper [7]. The kinetic energy of the α-particle, given by that paper, seems to us too high for several reasons. First, it does not fit the decay-systematics of Fig. 1, second, it is much larger than the value gained from mass data, third, the Q_α of Pm^{148}, calculated from the closed decay cycle containing Q_α of Sm^{148}, is also higher than Q_α of Pm^{148} computed from mass data and it does not fit the systematics either. If we had decreased the Q_α value of Sm^{148} then X would have increased and so the fit would have been better, although — according to reference [5] —

the value of T_a is also larger here than that of [7], to be more exact $T_a > > 2 \cdot 10^{14}$ years.

We took $4 \cdot 10^{14}$ years for the partial half-life of Sm^{149}, i.e. the value given in [7]. If $T_a > 1 \cdot 10^{15}$ years had been accepted, given by [5], the fit would have been better.

The kinetic energy of Gd^{150} according to [3] is $2{,}7 \pm 0{,}15$ MeV, while according to [19] this is $2{,}53 \pm 0{,}05$ MeV. The value we accepted was the mean of these weighted by the reciprocal square of errors. [3] gives $T_a \approx 3 \cdot 10^5$ years and [19] gives $T_a = 3 \cdot 10^6$ years. There is no reference to the errors in either paper but in both cases the half-lives are probably approximate ones as indicated by symbol $\approx$ in [3], and by the remark in [19] stating that this is only a preliminary report and that the more exact results will be published later.

As for the case of Tb^{151} the α-decay is likely to be hindered which is the more probable because the number of protons in this nucleus is odd. The logarithmic hindrance factor H will then be in the case of Tb^{151}

$$H = \log^{10} \frac{T_{\text{experimental}}}{T_{\text{predicted}}} = 2{,}88 - 0{,}92 = 1{,}96,$$

where $T_{\text{predicted}}$ is the value given by the straight line in Fig. 2.

The data of the other nuclides either fit the straight line within the limits of error or their H value is lower than 0,8.

Heavy even-even nuclides containing protons or neutrons of magic number $+2$ or a little more, exhibit higher half-life than indicated by the general tendency. (See e.g. Po^{214}_{130}, Po^{212}_{128} in [16].) This fact is probably connected with the sharp change in nuclear radius taking place on account of the α-decay process. We disregarded this effect in the medium heavy region when plotting the straight line of Fig. 2 for two reasons. First, in the region of the rare earths there is but one single magic neutron number, 82, influencing the α-decay, the number of protons is not magic and a smaller deviation from the general tendency in the nuclear radius and the half-life can be expected than in the case of the Po-isotopes mentioned above. Second, the known energy and half-life data in the rare earth region are not exact enough to make any difference beyond the limits of error, when this effect is also considered.

It can be seen from Table I that the decay energies of Dy^{150} and Dy^{151} have been measured but their α-partial half-lives are unknown. We computed these half-lives on the basis of Fig. 2 and data [3]. The results are presented at the end of Table X.

From the straight line in Fig. 2 we estimated the α-partial half-lives to be expected for those rare earth nuclides, the α-decay of which has not yet been observed or, if it has been, the α-decay energies or the partial half-lives have not been measured. The results can be seen in Table X.

The assumption that no substantial hindrance arises by α-decay is justifiable only for transitions between the ground states of even-even nuclei. For nuclides of odd mass number nothing more can be expected than that H does not surpass the value of 1,5. This suggestion is based on the analogy between heavy nuclides where the proton number is $82 + 2, 3, 4, 5$ (and neu-

tron number >127) and nuclides where the neutron number is $82 + 2, 3, 4, 5$ (and proton number also far from the magic). Indeed, using data obtained spectrometrically the logarithmic hindrance factor does not surpass the value of 1,5 and in most cases it is even below 1. See [2], p. 122. This suggestion is also supported by the work [15] of TAAGEPERA and NURMIA who concluded, on the basis of generally accepted experimental data which may be assumed to be fairly accurate, that for nuclei far from magic numbers the value of H rarely surpasses 1,2.

Here "nucleus far from magic number" means such a nucleus the proton and neutron numbers of which are beyond the environment ± 1 of any magic number.

Paper [15] presents the mean logarithmic hindrance factors (H) of 71 nuclides for which Z and N are far from the magic numbers in the above sense. Taking $H = 0$ for even-even nuclides we get

		mean H	
Z odd,	N even	0,38	
Z even,	N odd	0,16	(3)
Z odd,	N odd	0,69	

Column 5 of Table X shows the α-partial half-lives for each type of nuclide gained by supposing hindrance (3).

It is to be noted that for the nuclides presented in Table X there are no known spin values except in a few cases.

In column 5 of Table X the errors of the predicted α-partial half-lives arise from three sources.

First, there is a contribution from the error of the decay energy. For example in the case of Eu^{148}, attributing an approximate error $\pm 0{,}1$ MeV to the value of Q_α taken from Fig. 1, we get $\Delta \log^{10} T_\alpha = \pm 1{,}1$, i.e. an error a little greater than one order of magnitude. This error would be reduced if we had taken into account the possibility of computing T_α from Q_α values obtained by different methods.

Second, the estimation of T_α is influenced by the uncertainty in drawing the straight line of Fig. 2 through the experimental points for even-even nuclides. The experimental data deviate from this straight line by not more than a value $\Delta \log^{10} T_\alpha = \pm 0{,}8$ apart from the four nuclides mentioned above (Sm^{148}, Sm^{149}, Gd^{150}, Tb^{151}) which cases can be more or less explained.

Finally, a hindrance fluctuation can take place in the case of the nuclides of Table X, although the mean hindrance was taken into account by (3). The mean hindrance is of course of an approximate character, nevertheless, it is probable that the error due to the hindrance is $\Delta \log^{10} T_\alpha < 1{,}2$.

If all these facts are taken into account we have an error $\approx (\pm 1{,}5)$ for the values $\log^{10} T_\alpha$ mean.

Table X

The expected parameters of α-activity from atomic number 60 to 66 and from neutron number 84 to 88.*** In this Table only those nuclides are presented which have an expected α-decay energy greater than 1,8 MeV**** and the α-partial half-life and α-decay energy of which have not yet been measured (except for the cases of Dy^{150} and Dy^{151} where the α-decay energies are known)

1	2	3	4	5
Nuclide	Basis for calculation of energy data	The expected: total energy of α-decay Q_α (MeV)	The expected: log T_α not taking into account hindrance (T_α in years)	The expected: T_α partial half-life (in years) taking into account average hindrance given by (3)
$_{65}Tb^{150}_{85}$	Fig. 1	3,83 $\pm$ / $\sim$ 0,1 /	−0,87	6,7 10^{-1}
	mass data			
	separation energy	3,87 $\pm$ | $\leq$ 0,7 |	−1,15	3,5 10^{-1}
	$\alpha - \beta$ cycle			
$_{65}Tb^{152}_{87}$	Fig. 1	3,22 $\pm$ / $\sim$0,1/	3,42	1,3 10^{4}
	mass data			
	separation energy	3,24 $\pm$ | $\leq$0,7|	3,28	0,93 10^{4}
	$\alpha - \beta$ cycle			
$_{65}Tb^{153}_{88}$	Fig. 1	2,73 $\pm$ / $\sim$0,1 /	7,95	2,1 10^{8}
	mass data			
	separation energy	2,69 $\pm$ | $\leq$ 0,55 |	8,35	5,4 10^{8}
	$\alpha - \beta$ cycle			
$_{64}Gd^{151}_{87}$	Fig. 1	2,48 $\pm$ / $\sim$0,1 /	10,1	170 10^{8}
	mass data			
	separation energy	2,59 $\pm$ | $\leq$ 0,35 |	8,8	9,1 10^{8}
	$\alpha - \beta$ cycle			
$_{63}Eu^{148}_{85}$	Fig. 1	2,69 $\pm$ / $\sim$ 0,1 /	7,1	56 10^{6}
	mass data			
	separation energy	2,78 $\pm$ | $\leq$ 0,7 |	6,14	6,8 10^{6}
	$\alpha - \beta$ cycle			
$_{63}Eu^{149}_{86}$	Fig. 1	2,44 $\pm$ / $\sim$ 0,1 /	9,9	17 10^{9}
	mass data			
	separation energy	2,29 $\pm$ | $\leq$ 0,35 |	11,8	1400 10^{9}
	$\alpha - \beta$ cycle			
	(See[13], $Q\beta$interpol)	2,52 $\pm$ / $\sim$ 0,1 /	8,91	2 10^{9}
$_{63}Eu^{150}_{87}$	Fig. 1	2,19 $\pm$ / $\sim$ 0,1 /	13,1	66 10^{12}
	mass data	2,305 $\pm$ 0,17	11,5	1,7 10^{12}
	separation energy	2,182 $\pm$ 0,05	13,5	78 10^{12}
	$\alpha - \beta$ cycle			
$_{63}Eu^{151}_{88}$	Fig. 1	1,93 $\pm$ / $\sim$ 0,1 /	17,2	360 10^{15}
	mass data	2,025 $\pm$ 0,180	15,6	9,1 10^{15}
	separation energy	1,81 $\pm$ | $\leq$ 0,35 |	19,3	46000 10^{15}
	$\alpha - \beta$ cycle			
$_{61}Pm^{146}_{85}$	Fig. 1	1,995 $\pm$ 0,1	14,5	14 10^{14}
	mass data	1,96 $\pm$ | $\leq$0,35|	15,0	49 10^{14}
	separation energy	2,015 $\pm$ 0,053	14,2	6,9 10^{14}
	$\alpha - \beta$ cycle			
$_{66}Dy^{150}_{84}$	experimental	4,35 $\pm$ 0,06	−3,36	4,37 10^{-4}
$_{66}Dy^{151}_{85}$	experimental	4,19 $\pm$ 0,04	−2,54	4,17 10^{-3}

*** Beyond this region the estimation is rather uncertain

**** At present this value seems to be the lowest limit of detectability.

7. Concluding remarks

Although some progress has been made in the α-spectroscopy of neutron-deficient rare earth nuclides (the α-spectrum of some 18 nuclides were measured) still many nuclides exist the disintegration energy and half-life of which are in the measurable region but where the α-decay has not been detected.

One of the main difficulties, if one uses an ionization pulse chamber, is the fact that the value of the branching ratio $\left(\frac{\alpha}{\text{total}} \text{ decay ratio}\right)$ is very small in many cases. The expected value of the branching ratio, as given in Table X, is $\lesssim 10^{-9}$ for the majority of nuclides which makes difficult and in some cases even impossible to carry out measurements by means of ionization chambers.

A significant development can be expected in this region by using an electromagnetic "giant" spectrometer where the electron capture or the $\beta^{\pm}$-decay have but a very small disturbing effect. If the source area is some cm^2, the effective solid angle is about 10^{-3} of 4π and the thickness of the source is somefold $10 \frac{\mu g}{cm^2}$, the α-partial-half-life is measurable up to $T_\alpha \approx 10^{10}$ years. It can be seen from Table X that many α-partial half-lives are below the above-mentioned limit.

The authors are much indebted to Professor A. SZALAY for his interest in this work.

Note. Reports on Ho [25], Er [27], Tm [28] and some Eu and Gd isotopes [26] were brought to our knowledge only after submitting the paper for publication. The data of [25], [26], [27] and [28] have been included in Table I but otherwise they have not been used.

REFERENCES

1. T. P. KOHMAN, Phys. Rev., **76,** 448, 1949.
2. Experimental Nuclear Physics, editor SEGRÉ, III. Vol., 1959. p. 65. New York, J. Wiley & Sons.
3. K. S. TOTH and J. O. RASMUSSEN, Nucl. Phys., **16,** 474, 1960.
4. W. KUNZ and J. SCHINTLMEISTER, Tabellen der Atomkerne, Berlin, Akad. Verlag, 1959.
5. R. D. MACFARLANE and T. P. KOHMAN, Phys. Rev., **121,** 1758, 1961.
6. *А. А. Воробьев, А. П. Комар, В. А. Королев, Г. Е. Солякин,* ЖЭТФ, **37**, 546, 1959.
7. M. KARRAS, Annales Acad, Sci. Fennicae, Ser. A., VI. Physica, No. 65, 1960.
8. J. OLKOWSKY, I. GRATOT, M. LE PAPE and L. COHEN, Nuclear Phys., **12,** 159, 1959.
9. R. D. MACFARLANE, J. Inorg. Nucl. Chem., **19,** 9, 1961.
10. LANDOLT-BÖRNSTEIN, New Series, Group I. Vol. 1, Springer, Berlin, 1961.
11. L. A. KÖNIG, J. H. E. MATTAUCH and A. H. WAPSTRA, Nuclear Phys., **31,** 18, 1962.
12/1. K. FRITZE, T. J. KENNETT and W. V. PRESTWICH, Can. J. Phys., **39,** 662, 1961.
12/2. *Ю. А. Александров, М. К. Никитин,* Изв. АН СССР, сер. физ. **25**, 1176, 1961.
12/3. R. P. SHARMA et al., Phys. Rev., **125,** 2071, 1962.
12/4. K. SUGIYAMA, J. Phys. Soc. Japan, **17,** 264, 1962.
12/5. H. J. PRASK, J. J. REIDY, E. G. FUNK and J. W. MIHELIC, Nucl. Phys., **36,** 441, 1962.
12/6. N. B. GOVE, Bull. Am. Phys. Soc., Ser. II., **7,** 352, XA8. 1962.
12/7. *К. Я. Громов, Ъ. С. Джелепов, Ж. Т. Желев, А. В. Кудрявцева,* Изв. АН СССР сер. физ., **25**, 1084, 1961,

13. F. Everling, N. B. Gove and R. van Lieshout, Beta-Disintegration Energy Charts, Nuclear Data Sheets, NAS—NRC 61—3—142, 1962.
14. G. J. Nijgh, A. H. Wapstra and R. von Lieshout, Nuclear Spectroscopy Tables, North Holland, Amsterdam, p. 111. 1959.
15. R. Taagepera and M. Nurmia, Ann. Acad. Sci. Fennicae, Ser. A., VI. Physica, No. **78**, 1, 1961.
16. *И. Перлман, Дж. Расмуссен,* Альфа-радиоактивность, p. 72, Изд. Иностранной Лит., Москва, 1959.
17. R. D. Macfarlane, Phys. Rev., **126**, 274, 1962.
18. M. Nurmia, P. Kauranen and A. Siivola, Phys. Rev., **127**, 943, 1962.
19. T. Doke, Canad, J. Phys., **40**, 607, 1962.
20. M. Yamada—Z. Matumoto, J. Phys. Soc. Japan, **16**, 1497, 1961.
21. K. S. Toth, B. Bjørnholm, M. H. Jørgensen, O. B. Nielsen, O. Skilbreid and A. Svanheden, J. Inorg. Nucl. Chem., **14**, 1, 1960.
22. J. O. Rasmussen, S. G. Thompson and A. Ghiorso, Phys. Rev., **89**, 33, 1953.
23. W. Riezler and G. Kauw, Z. Naturforsch., **14a**, 196, 1959.
24. R. D. Macfarlane, Natural Alpha Radioactivity in Medium-Heavy Elements (Thesis), NYO—7687, 1959. p. 148. Carnegie Institute of Technology, Pittsburg, Pennsylvania.
25. R. D. Macfarlane and R. D. Griffioen, Phys. Rev., **130**, 1491, 1963.
26. A. Siivola, Ann. Acad. Sci. Fennicae, Ser. A., VI. Physica, No **109**, 1, 1962.
27. R. D. Macfarlane, Private communication.
28. R. D. Macfarlane, Bull. Am. Phys. Soc., Ser. II., **8**, No. 4, 387, X5. 1963.

СИСТЕМАТИКА α-РАСПАДА ЯДЕР РЕДКОЗЕМЕЛЬНЫХ ЭЛЕМЕНТОВ

Т. ФЕНЕШ и З. БЁДИ

Р е з ю м е

В статье суммируются данные α-распада редкоземельных нуклидов и даются предсказанные энергии распада дальнейших 30-и нуклидов методом полных циклов распадов, исходя из известных в настоящее время энергий α- и β-распадов.

Путём экстраполирования и интерполирования кривых, показывающих зависимость энергии α-распада от массового номера, были получены энергии α-распада таких ядер, α-активность которых ещё не была найдена экспериментально. Энергии α-распада этих ядер оценивались также на основе известных масс ядер и энергий связи протона и нейтрона.

Из полученных энергий распадов оценились ожидаемые α-парциальные периоды полураспада при помощи полуэмпирической зависимости [15, стр. 6.], содержащей явную зависимость от атомного номера Z.

В конце статьи обсуждаются некоторые вопросы экспериментального обнаружения новых α-активностей.

FISSION PRODUCT PRECIPITATION FROM THE ATMOSPHERE IN DEBRECEN, HUNGARY, DURING 1961 AND 1962

By

A. SZALAY and Á. KOVÁCH

INSTITUTE OF NUCLEAR RESEARCH OF THE HUNGARIAN ACADEMY OF SCIENCES, (ATOMKI), DEBRECEN

(Received: 21. II. 1963)

The results of measurements carried out in the years 1961 and 1962 to determine the radioactivity due to fission products of precipitation from the atmosphere in Debrecen are given. The relation between the specific activity and the quantity of precipitation is treated and conclusions are drawn as to the variation of the radioactive contamination of the surface of the Earth. Based on the measurement of the decay of samples the activity measured in the individual periods is approximately assigned to the series of atomic weapon tests which began in the autumn of 1961.

To investigate the radioactive contamination of the atmosphere due to fission products two methods are available. The one is concerned with the radioactivity of atmospheric aerosol, while the other widely used method allows to draw conclusions as regards the variation of the radioactive contamination of the surface of the Earth by determining the radioactivity due to fission products of atmospheric precipitation.

At this Institute since 1952 we have continuously been investigating the radioactivity due to fission products in the precipitation fallen over Debrecen using throughout essentially the same methods [1, 2, 3, 4, 5, 6]. In our previous investigations (before 1953) the samples of precipitation were collected by means of a normal meteorological ombrometer of 1/50 m^2 surface. However, owing to the small collection surface the activity values we obtained were often very low. Experience also showed that part of the fission products in the precipitation were adsorbed by the metal surfaces of the meteorological ombrometer. To eliminate these disadvantages, from 1954 we have been using an ombrometer made of PVC and glass. Precipitation is collected from over a circular surface 40 cm in diameter, through a PVC funnel.

Precipitation is collected daily. During longer dry periods the dust deposited on the surface of the PVC funnel is washed from time to time into the collecting vessel and measured together with the next precipitation. Experience shows, however, that dustfall brings but a fraction of the total activity to the surface of the Earth, the majority of fission products being gathered by atmospheric precipitation.

After evaporation to dryness the activity of the samples is determined in a glass measuring vessel of normal size, in a GM-counter arrangement of constant geometry. As regards the details of the methodics the reader is referred to [4].

Results of measurements

Fig. 1 shows the results of our measurements in the years 1961 and 1962. To facilitate comparison with our measurements described in previous papers the results of actual activity measurements have been referred to a surface of 1/50 m^2, i.e. the surface of the normal meteorological ombrometer. As in our previous papers only the activity and the quantity of the precipitation are plotted against calendar time, experience showing that the specific activity of the precipitation, regarded by some authors as a characteristic value, is a function also of the quantity of the precipitation.

In a previous paper [4] SZALAY and BERÉNYI found a linear correlation between the quantity and the specific activity of the precipitation. By comparing the quantity and the activity of the precipitation containing only old fission products in the first nine months of 1961 it could be stated that the correlation existed in a logarithmic sense, which means that a correlation could be established between the logarithm of the specific activity and the quantity of the precipitation. Our measurements in the above period showed that with an increase of the quantity of the precipitation by 10 mm the specific activity decreased by approximately one order of magnitude. This experience confirms the assumption that precipitation from the atmosphere leaks through the air layers between the level of cloud formation and the surface of the Earth to a very large extent and further the logarithmic character of the correlation corresponds to the expectation that on the basis of geometrical probabilities the transport of the precipitation can be described by an exponential function.

The above experience supports our opinion, which is in agreement with that of other authors [7], that at least under the precipitation conditions in temperate zones it is by precipitation that the majority of fission products are carried down to the surface of the Earth and thus activity measurements on precipitations offer an approximately complete survey of the variation of the radioactive contamination of the surface of the Earth.

Studying Fig. 1 it can be stated that up to September 1961 the contamination of the atmosphere due to fission products continued to decrease. The rate of decontamination was somewhat lower than in the years 1959 to 1960. The increase of the rate of exchange between stratosphere and troposphere in the Spring 1961, reflected by the increase of the activity and the specific activity of the precipitation can be very well observed. The monthly quantity of fission products increased gradually from January and attained its maximum late in May and early in June (see the data in Table 1). The effect of increased exchange is also reflected by the increase of the monthly average specific activity (see Table 2).

Owing to atmospheric atomic weapon tests resumed in the autumn of 1961, from October 1961 we observed a considerable increase, approximately

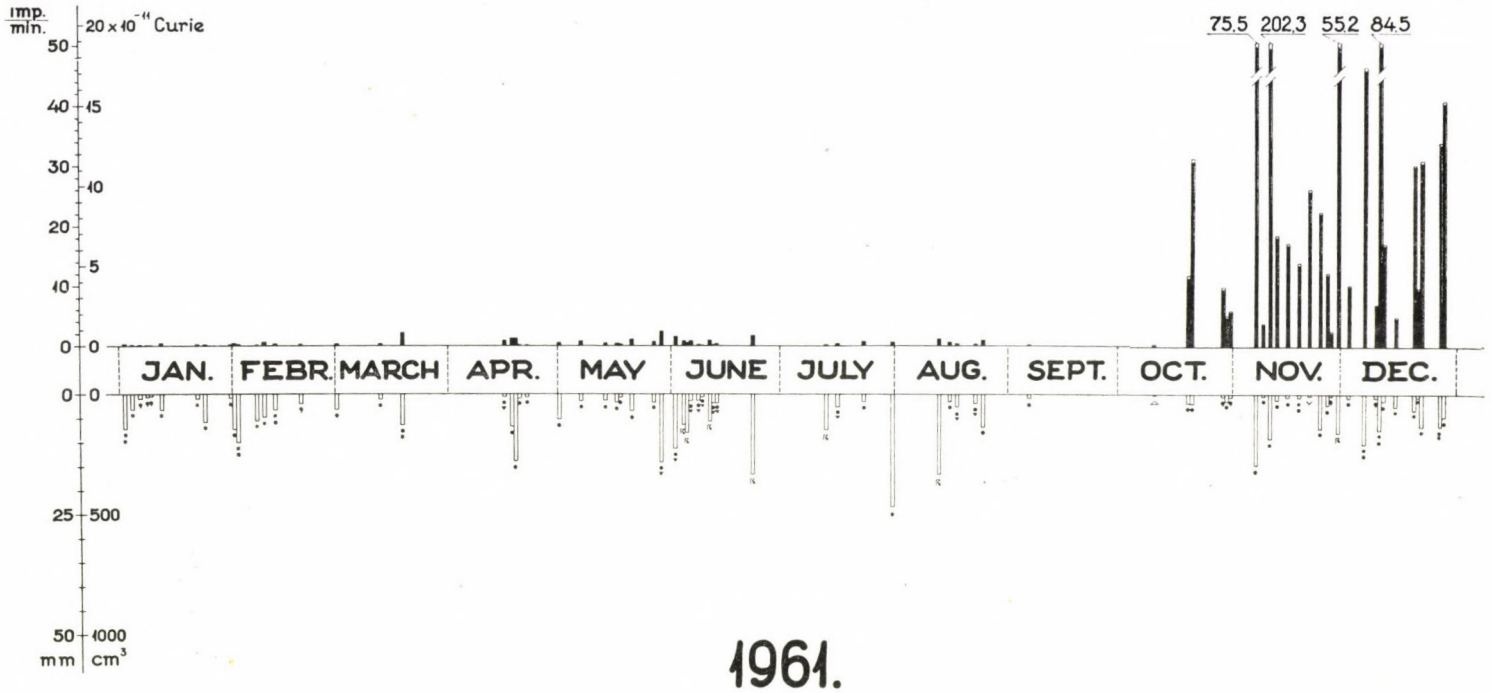

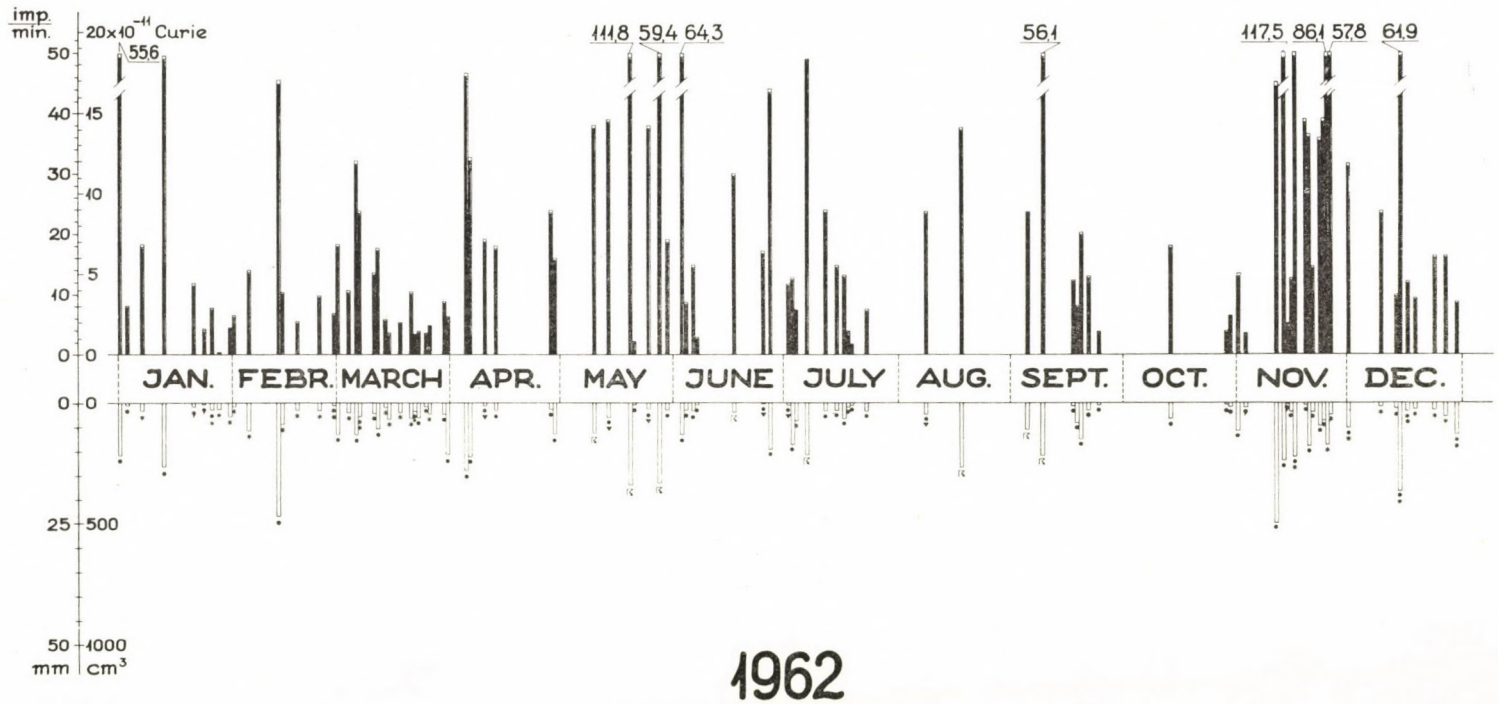

Fig. 1. Fission product precipitation from the atmosphere in Debrecen, Hungary, in 1961 and 1962. Ordinate upwards, right: activity in 10^{-11} Curie units, corrected for the geometry of the counting equipment. Ordinate upwards, left: activity observed in cpm reduced to 1/50 m² ombrometer surface. Very large activities are not shown linearly but by numbers indicating cpm values. Ordinate downwards, right: One day's rainfall expressed as volume collected from an exposed area of 1/50 m². Ordinate downwards, left: One day's rainfall in mm. Abscissa: calendar time

by two orders of magnitude, of the radioactive contamination due to fission products of the atmosphere. During the month of September and the beginning of October there was very little rainfall. Therefore we are unable to state exactly when atmospheric radioactivity began to increase. It is worth noting, however, that the activity of dust samples taken early in October 1961 was somewhat greater than the average. The precipitation fallen on the 20th and 21st October already showed a definitely increased specific activity.

Table I

Monthly total quantities of fission products measured in the precipitation fallen over Debrecen

Year	Month	mC/km²	Year	Month	mC/km²
1961	January	0,29	1962	January	29,9
	February	0,35		February	13,3
	March	0,53		March	32,1
	April	0,65		April	29,2
	May	1,25		May	58,1
	June	1,34		June	34,1
	July	0,43		July	27,1
	August	0,67		August	11,5
	September	0,06		September	26,1
	October	11,8		October	5,3
	November	85,0		November	105,0
	December	59,2		December	35,6

The monthly total quantities of fission products in the precipitation fallen over Debrecen are exhibited in Table 1 in mC/km² units. The monthly total values have been determined by direct summation of the activities measured in each sample of the precipitation, without taking the effect of radioactive decay into account.

The strikingly small values in September 1961 and October 1962 can be attributed to the relative dryness of these months.

As regards the number, date and yield of atmospheric atomic weapon tests in the period under consideration we had to rely on the announcements of news agencies and the official communications of the USAEC. In the years 1961 and 1962 three main series of atomic weapon tests were carried out: the USA carried out atmospheric and partly upper-atmospheric tests (4 tests) in the areas of the Christmas Islands and Johnston Island belonging to the Marshall Islands between 25th April and December 1962; the atmospheric atomic weapon tests of the Soviet Union were carried out during the periods

between September and November 1961 and between 5th August and 20th November 1962.

The assignment of the individual values of the activity due to the fission products found in the precipitations to particular explosions encountered some difficulties. Although, since the cessation of atomic weapon tests in the Autumn of 1958, the radioactive contamination of the atmosphere decreased to such an extent [6] that the background caused by the residual activity

Table II

Variation of the average specific activity of precipitation in Debrecen during 1961 and 1962

Year	Month	Specific activity pico C/ml	Year	Month	Specific activity pico C/ml
1961	January	0,013	1962	January	0,84
	February	0,011		February	0,47
	March	0,051		March	0,56
	April	0,029		April	0,81
	May	0,042		May	1,25
	June	0,024		June	0,53
	July	0,012		July	0,80
	August	0,023		August	0,71
	September	0,075		September	0,82
	October	1,96		October	1,15
	November	1,90		November	1,17
	December	1,33		December	0,90

would not have prevented assignment on the basis of the WAY—WIGNER formula [5], with regard to the fact that the tests carried out in 1961 and 1962 were numerous and followed each other in long uninterrupted series, apart from activities observed in October 1961, the individual activities could only be assigned to certain series of the explosion tests.

Similar to the practice of previous years in 1961 and 1962 we observed only the radioactive decay of samples of higher radioactivity. On the basis of the radioactive decay of the precipitation fallen on the 20th and 21st October 1961 conclusions could be drawn concerning the explosion tests which took place on the 23rd and 26th September, respectively. This result is in agreement with our previous experience that the appearance of activity due to Soviet explosion tests in the precipitation over Debrecen is delayed approximately four weeks (one month).

In the precipitations measured later mixed activity was present, it could be stated, however, that an overwhelming part of the fission products in the

precipitation fallen up to the Summer of 1962 was due to tests carried out in the Autumn of 1961.

It was first in the precipitation fallen in July 1962 that the presence of fission products of recent origin could be established with full certainty. A precise analysis of the decay curves was not possible owing to the lack of a sufficient number of measured results, it could, however, be established that an overwhelming part of the activity of the precipitation fallen in the Summer of 1962 was due to the atomic weapon tests carried out in the areas of the Christmas Islands and Johnston Island.

For the evaluation of the radioactive decay measured in the Autumn of 1962 a sufficient number of measured data are not yet available, it can, however, be established that the radioactive contamination of the atmosphere continued to increase owing to the series of tests carried out simultaneously in the Pacific and in the Polar area. In precipitations fallen in the Autumn of 1962 fission products from tests carried out after August 1962 prevail. The average specific activity of the precipitation in the Autumn of 1962 did not change substantially.

The variation of the average specific activity of the precipitation during the years 1961 and 1962 is shown in Table 2. The data listed in the Table have been calculated on the basis of the values of the uncorrected monthly total activity and of the monthly total quantity of precipitation.

Current official regulations [8] permit a maximum quantity of 0,1 pico-Curie/ml of unknown fission products to be contained in drinking water. Since October 1961 the average specific activity of precipitation fallen over Debrecen has exceeded this value. If, however, fission products in precipitation are regarded as the mixture of fission products due to an atomic bomb explosion which took place in the average 30 days previously, on the basis of the fission isotope spectrum it can be stated that taking the permitted concentration of each single fission product into account the observed average specific activity attains about 1/20 part of the level of contamination permitted in drinking water. This relatively high value results essentially on the basis of the calculated Sr^{90} concentration, the activity level calculated for other fission products remains well below the level of contamination permitted for drinking water. On the basis of and in order to check the above conclusion it seems desirable in any case to extend our measurements, in addition to the determination of the total activity, to that of the Sr^{90} content.

REFERENCES

1. A. Szalay and D. Berényi sen., Acta Phys. Hung., **5,** 1, 1955.
2. A. Szalay and D. Berényi sen., MTA III. Mat. Fiz. Oszt. Közl. (Reports of the Class for Math. and Phys. of the Hung. Acad. Sci.) **5,** 89, 1955.
3. A. Szalay and D. Berényi sen., MTA III. Mat. Fiz. Oszt. Közl. (Reports of the Class for Math. and Phys. of the Hung. Acad. Sci.,) **9,** 175, 1959.
4. A. Szalay and D. Berényi sen., Proc. 2nd Geneva Conf., P/1953, Vol. 18, p. 570.
5. A. Kovách and A. Szalay, ATOMKI Közlemények (Reports of the Inst. of Nucl. Res.,) **2,** 229, 1960.
6. A. Szalay and A. Kovách, Acta Phys. Hung., **13,** 281, 1961.
7. W. Anderson et al., Nature, **186,** 925, 1960.
8. Hungarian Standard Nr. 61—62, 1962. Protection against radiation of radio-isotopes.

ПРОДУКТЫ РАСПАДА В ОСАДКАХ, ВЫПАВШИХ В ДЕБРЕЦЕНЕ В 1961—62 ГГ.

А. САЛАИ и А. КОВАЧ

Р е з ю м е

Работа ознакомливает читателя с результатами измерения, которые проводились в 1961—62 гг. для определения радиоактивности, происходящей от продуктов деления в атмосферных осадках, выпавших в Дебрецене. Рассматривается зависимость между удельной активностью и количеством осадков, делается вывод по отношению формирования радиоактивного загрязнения земной поверхности. На основании измерения распада измеренных образцов, относящиеся к определенным периодам, активности сопоставляются сериям по испытанию атомного оружия, проведенным от осени 1961 г.

ON THE ROLE OF THE AUXILIARY ELECTRODE APPLIED BESIDE THE CATHODE IN A. C. DISCHARGES

By

G. LAKATOS and J. BITÓ

INDUSTRIAL RESEARCH INSTITUTE FOR TELECOMMUNICATION TECHNIQUE, BUDAPEST

(Presented by G. Szigeti. — Received 25. VI. 1963)

The authors examine the cathode fall by probe measurements in a.c. low pressure mercury vapour discharge tubes with oxide cathodes. By determining the potentials at three points of the plasma and the dimension of the cathode dark space they calculate the cathode fall. The plasma potential is determined by a pulse technique based on LANGMUIR'S method. The time-dependence of the cathode fall is determined and the influence of the applied auxiliary electrode is discussed.

1. Introduction

Various measuring methods are known [1] for determining the cathode fall. The most extensively applied method is based on the LANGMUIR probe measuring principle [2]. LANGMUIR worked out this method for the examination of d.c. gas discharges, but the method has been used by some workers also in case of a.c. discharges [3].

In a previous paper [4] the authors reported their study of the characteristics of 50 cps. a.c. discharges with the a.c. probe measurement method by FAJT and KONCZ [5] which is based on the LANGMUIR probe principle.

In the present paper the pulse technique for probe measurements in gas discharges developed by WAYMOUTH [6] is applied by the authors. With this method good time resolution, greater accuracy of measurement and a decrease of the measuring time were obtained in the case of an a.c. discharge of 50 cps.

According to this method in each half-cycle a pulser supplies positive saw-tooth shaped pulses (500 usec) to the probe which is normally biased negative to the discharge.

The WAYMOUTH pulse technique based on LANGMUIR probes consists in the following: the drop across the measuring resistance of the probe circuit is passed through a differential amplifier to the vertical deflecting plates of an oscilloscope. The pulse voltage is fed to the other pair of plates of this oscilloscope. The current-voltage characteristics of the probe is observed on an oscilloscope during the pulse.

In the measurements the duration of the pulses used (500 μsec) was much longer than the time needed to restore equilibrium in the space charge region around the probe.

2. Measuring method and arrangement

A block diagram of the setup is shown in Fig. 1. The pulse applied to the probe P_1 from the pulser G with the aid of a phase-sliding B and the drop across the measuring resistance R_p are fed to the vertical input of oscilloscope O through a differential amplifier A. To the horizontal input of this oscilloscope

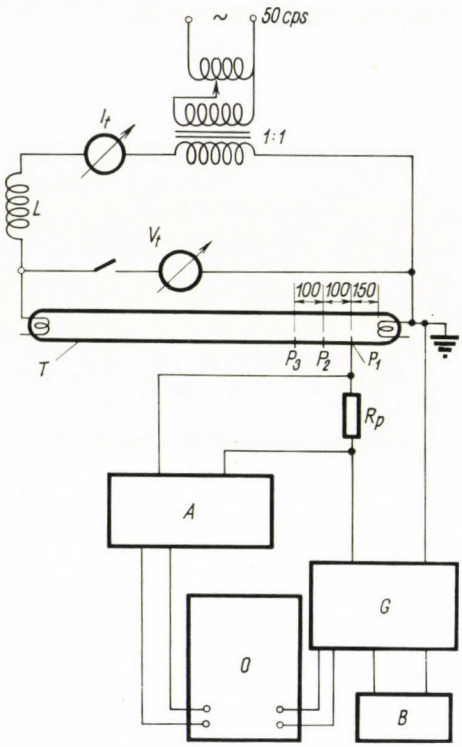

Fig. 1. Block diagram of setup

the pulse voltage from pulser G is fed. The current of discharge tube T was stabilized by an inductive ballast L. In all measurements an oxide-coated cathode was used which was heated by the discharge only, no external heating being applied. The measurements were carried out in ambient temperatures of 22,5—24° C. Data of the examined discharge tubes were: 1200 mm length, 38 mm outer diameter; they were filled with a mixture of mercury and argon of 3 mm Hg total pressure. The tubes had glass walls (of a thickness about 1 mm). The probes reached into the axis of the discharge tube. Their exposed free length was 2 mm and their diameter 0,2 mm each. In the gas discharge tube there were three probes: the distance from each other was 100 mm, and the distance of the first probe from the tube end was 150 mm.

3. Experimental results

Applying WAYMOUTH's pulse technique [6] mentioned above, the potential of the plasma is determined at three points near the cathode. At the measuring places, the probes reached into the homogeneous part of the positive column. From the plasma potentials obtained by WAYMOUTH's pulse technique the potentials of the cathodic end of the positive column were calculated by NÖLLE's method [7]. These potential values can be regarded in good approximation as the cathode fall.

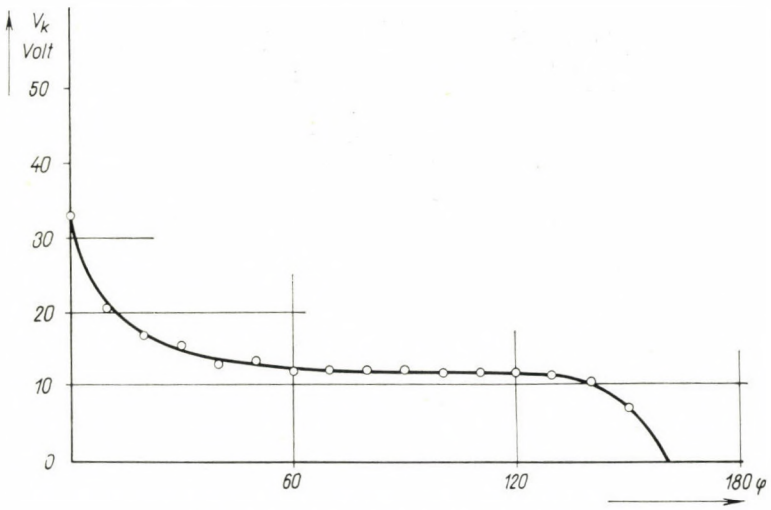

Fig. 2. Time-dependence of cathode fall V_k

The distance of the cathodic end of the positive column at the various phase angles was determined by stroboscopic measurements. The results of these measurements showed this distance to be approximately constant.

The plasma potentials were determined with WAYMOUTH's pulse technique and from these results applying NÖLLE's extrapolating method [7] for various phases the time-dependence of the cathode fall could be obtained in the observed half-cycle. The plasma potentials were determined for 18 phase angles in the observed half-cycle. The zero phase angle value was determined by the maxima of the tube voltage, so that the results were well reproducible.

By this method the cathode fall can be determined in both half-cycles.

The characteristic time-dependence of the cathode fall is shown in Fig. 2. It can be seen, that the cathode fall is approximately constant in the greater part of the observed half-cycle. Its value is about 12 V and this value is in good agreement with the results of GEHRTS [8] and KÜHL [9].

The relatively great value of the cathode fall at the beginning of the half-cycle signifies the moment of the breakdown. At this moment the tube voltage has a maximum.

The time-dependence of the cathode fall shown in Fig. 2 is similar to the time-dependence of the tube voltage.

As it can be seen from the above results this measuring method can be applied to the determination of the time-dependence of the cathode fall in a.c. discharges.

In the second part of our experiments the influence an auxiliary electrode placed near the electrode exerts on the time-dependence of the cathode fall

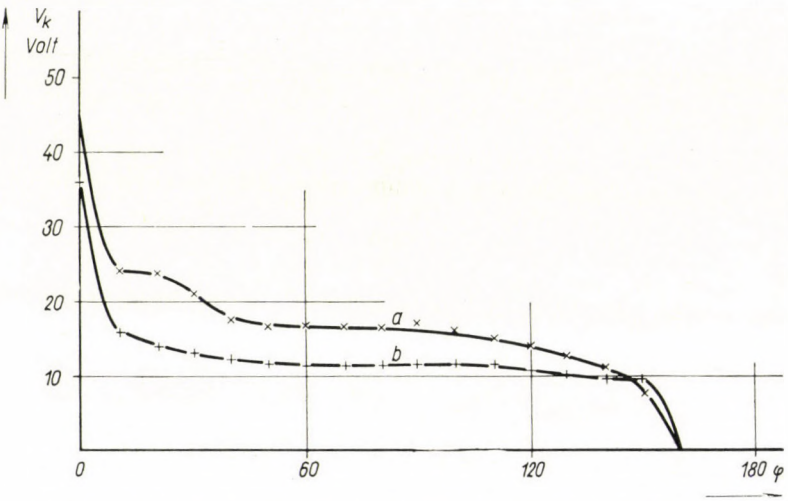

Fig. 3. Influence of the auxiliary electrode on the cathode fall V_k

was investigated. HINMAN and FOX [10] stated that such an auxiliary electrode decreases the energy loss of discharge tubes and that the decrease of the energy loss in an interval is proportional to the surface of the auxiliary electrode applied. The discussion [10] of their work showed that it was doubtful whether this decrease of losses originated from the decrease of the anode fall or from that of the cathode fall. Neither do they give experimental or theoretical results or considerations for its explanation. The purpose of our further experiments was the study of this problem. We note that in general, also in the paper by HINMAN and FOX [10], the auxiliary electrodes are called anodes [11].

The further investigations were carried out with tubes in which the auxiliary electrodes had a separate output. In this way it was possible to examine the same cathode with or without auxiliary electrodes. The material of the auxiliary electrodes was an iron-nickel alloy. They were placed parallel to the coiled cathode and coated by an alkaline-earth oxyde sheet. The distance

of the auxiliary electrodes from the cathode was 3 mm. They had the shape of a rod with a diameter of 0,5 mm.

The time-dependence of the cathode fall without (curve *a*) and with (curve *b*) auxiliary electrode is shown in Fig. 3. It can be seen that the auxiliary electrode decreases the value of the cathode fall. Determining the average value of the cathode fall on the basis of the following equation

$$\overline{V}_k = \frac{1}{T} \int_0^T V_k(t)\, dt \,,$$

it was found that $\overline{V}_{ka} - \overline{V}_{kb} = 3{,}8$ V, where V_{ka} and V_{kb} are the average values of the cathode fall without and with auxiliary electrode, respectively.

The change of the voltage across the tube was measured and it was found that its value was 4,3 V. Calculating from this value the decrease of the anode fall for the case when the auxiliary electrode is applied led to a value of 0,5 V. It can be seen, therefore, that the auxiliary electrode has a most important role in the decrease of the cathode fall.

This gives a definite experimental answer to the problem concerning the importance of the auxiliary electrode of a.c. discharges, which was doubtful in the work of HINMAN and FOX [10].

On the basis of our experimental results it can be concluded that the auxiliary electrode has a very important role in the cathodic half cycle.

The same result is found also in measurements in the case of d.c. discharges.

In the previous investigations the auxiliary electrode had the same potential as the cathode or anode. Further investigations were made with auxiliary electrodes not having the same potential as the cathode. It was found that in this case the cathode fall was greater than in the case when the auxiliary electrode was at cathode potential. For example 2 V difference in potential of any polarity increased the cathode fall by about 7—9 V.

4. Discussion

From the results of the investigation it can be seen that in the a.c. discharges the auxiliary electrode applied to the electrodes plays an important role in the cathodic half-cycle: it decreases the instantaneous and the average value of the cathode fall. This was observed in the case of a stationary discharge process.

One of the authors together with E. SZEMZŐ [12] found previously that the auxiliary electrode also plays an important role in the cathodic half-cycle at the moment of the breakdown. It can be thus concluded that in the case

of the negative polarity of the electrode the auxiliary electrode plays an important role both in the stationary and the non-stationary processes.

From the results of d.c. measurements with auxiliary electrodes not having the same potential as the cathode the following can be concluded: when the auxiliary electrode has a potential higher than the cathode potential it attracts part of the electrons liberated from the cathode and for this reason the increase of the cathode fall is needed to increase the number of liberated electrons required by the discharge conditions. In the other case, when the potential of the auxiliary electrode is lower than that of the cathode it attracts some positive ions from the space charge region. Consequently, the concentration of the ions is decreased and so the increase of the energy of these ions is needed for the production of the required number of electrons. On the other hand the increase of the cathode fall is required to increase the energy of the remaining ions. The reasons for the decrease of the cathode fall have not yet been examined.

The authors wish to thank E. Szemző and I. Zakár for their contributions to the construction of the electronic detecting apparatus.

REFERENCES

1. K. G. Emeleus, The Conduction of Electricity through Gases, Methuen Monogr. 1951, London.
2. I. Langmuir and H. Mott-Smith, General Electric Review, **27,** 449, 538, 616, 762, 1924.
3. J. Bitó, Thesis, 1960. Institute of Exp. Physics of the Univ. Szeged, Hungary.
4. G. Lakatos and J. Bitó, Acta Phys. Hung., **13,** 271, 1961.
5. J. Fajt and J. Koncz, Meeting on Gas Discharges, Balatonvilágos, 1958.
6. J. F. Waymouth, J. Appl. Phys., **30,** 1404, 1959.
7. E. Nölle, Techn.-Wiss. Abhandlungen der Osram Ges., **7,** 65, 1958.
8. A. Gehrts and H. Vatter, Z. Phys., 79, 241, 1932.
9. B. Kühl, Techn.-Wiss. Abhandlungen der Osram Ges., **7,** 73, 1958.
10. D. D. Hinman and R. S. Fox, Ill. Eng., **56,** 222, 1961.
11. E. F. Lowry, Ill. Eng., **45,** 289, 1951.
12. G. Lakatos and E. Szemző, Proc. of 5th Int. Conference on Ionization Phenomena in Gases, Vol. II.

О РОЛИ ВСПОМОГАТЕЛЬНОГО ЭЛЕКТРОДА, ПРИМЕНЯЕМОГО ПРИ КАТОДЕ РАЗРЯДОВ ПЕРЕМЕННОГО ТОКА

Г. ЛАКАТОЩ И Й. БИТО

Резюме

Авторами исследовано катодное падение потенциала при пробными измерениями в ртутных парах низкого давления в разрядной трубке с оксидными катодами при переменном токе. Катодное падение вычислялось определением потенциала в трех точках плазмы и размера темного пространства при катоде. Потенциал плазмы определялся пульсированной техникой, базирующейся на методе Лэнгмюира. Устанавливается зависимость катодного падения от времени, далее истолкуется влияние использованного вспомогательного электрода.

ÜBER EINIGE OPTISCHE EIGENSCHAFTEN VON AUS MIKROKRISTALLINEN KÖRNERN BESTEHENDEN LUMINESZIERENDEN SCHICHTEN

Von

G. T. BAUER

FORSCHUNGSINSTITUT FÜR DIE NACHRICHTENTECHNISCHE INDUSTRIE, BUDAPEST

(Vorgelegt von G. Szigeti. — Eingegangen: 27. VII. 1963)

Es wurde die Transmission von aus mikrokristallinen Körnern bestehenden Schichten bei der Wellenlänge $\lambda = 5461$ Å gemessen, bei der die verschiedenen Stoffe, aus denen die Schichten bestanden als durchsichtig angesehen werden können. Die Messungen und Berechnungen ergaben, dass die Streuung dieser Schichten grösser ist, als dies aus dem sogenannten »Modell der planparallelen Platte« folgen würde, welches zur Beschreibung der optischen Eigenschaften diffuser Schichten dient. Auf Grund der Messungen wurde das Modell modifiziert. Es wurde gezeigt, dass die Transmission der aus Körnern verschiedener Grösse bestehenden nicht absorbierenden Schichten ausschliesslich von der Anzahl der elementaren Schichten abhängt, die die einzelnen Schichten bilden. Durch Messung der Transmission kann ein spezieller Mittelwert der Grösse der Körner, die die Schicht bilden, bestimmt werden.

Bekanntlich lassen sich die meisten Kristallphosphore nur in Form mikrokristalliner Körner herstellen. Die Messung der für den untersuchten Stoff charakteristischen physikalischen Grössen (Absorptionskoeffizient, Brechungsindex, elektrische bzw. Wärmeleitfähigkeit, Photokonduktion, usw.) an den aus Körnern des lumineszierenden Materials bestehenden Schichten stösst auf Schwierigkeiten. Zahlreiche mit der mikroskristallinen Struktur der Schichten zusammenhängende Probleme treten auch bei deren industriellen Anwendungen auf.

In der älteren Theorie der diffusen Schichten [1, 2, 3, 4, 5] und bei ihrer Anwendung auf lumineszierende Schichten [6, 7, 8] wurde angenommen, dass die streuenden Zentren kontinuierlich in der Schicht verteilt sind. Die neueren Untersuchungen zeigten, dass die Strahlung am Rande der Körner gestreut wird; daher hängen die optischen Eigenschaften auch von der Grösse der Körner der Schicht ab [9, 10, 11]. Das Näherungsmodell von BODÓ, nach dem die aus Körnern gleicher Grösse bestehende Schicht als aus planparallelen Schichten zusammengesetzt angesehen werden kann, deren Dicken gleich der Korngrösse sind, gab die Möglichkeit zur approximativen Berechnung der Länge des von der Strahlung in der Schicht zurückgelegten Weges. Die Brauchbarkeit des Modells wurde durch BODÓ [9] und auch durch andere Autoren [12, 13, 14] durch Messung des Absorptionskoeffizienten einiger mikrokristalliner Stoffe auch experimentell bewiesen. Später hat ANTONOFF—ROMANOVSKI [15] darauf hingewiesen, dass die Länge des von dem Licht in den einzelnen Mikrokristallen zurückgelegten Weges auch von der Form

der Kristalle abhängt. Bei gewissen Kristallen kann auch totale Reflexion zustande kommen, so dass die Weglänge grösser sein kann, als dies bei dem obigen Modell zu erwarten wäre.

In der vorliegenden Arbeit soll über die Resultate von Untersuchungen an lumineszierenden mikrokristallinen Zinksilikat-Kalziumphosphat- und Zinksulfidschichten berichtet werden. Die Messungen der diffusen Transmission und Reflexion wurden, im Gegensatz zu den in der Literatur veröffentlichten Untersuchungen, bei einer Wellenlänge durchgeführt, bei der die Materiale praktisch durchsichtig sind ($\lambda = 5461$ Å). Daher brauchte der nicht genügend genau bekannte Absorptionskoeffizient der Materiale nicht berücksichtigt zu werden; die Messungen bezogen sich ausschliesslich auf die Streuungseigenschaften und indirekt auf die Struktur der Schichten.

I. Berechnung der optischen Eigenschaften von aus durchsichtigen Körnern bestehenden mikrokristallinen Schichten

a) *Die Schicht bestehe aus Körnchen gleicher Grösse*

Man betrachte im Inneren der aus homogenen mikrokristallinen Körnchen bestehenden Schicht der Dicke d, eine Elementarschicht der Dicke dx (Abb. 1). Die Schicht werde mit Licht der Wellenlänge λ_0 und der Intensität I_0, das vom Material der Schicht nicht absorbiert wird, beleuchtet. Die Elementarschicht der Dicke dx werde von vorne mit der Intensität I_1, von der entgegengesetzten Richtung mit der Intensität I_2 beleuchtet. Bezeichnet $\overline{R}$ die diffuse Reflexion, $\overline{T}$ die diffuse Transmission, $r = \left(\frac{d\overline{R}}{dx}\right)_{x=0}$ die diffusen Reflexionskoeffizienten der Schicht, so erhält man aus den SCHUSTERschen Differentialgleichungen [1]

$$\frac{dI_1}{dx} = \frac{dI_2}{dx} = -rI_1 + rI_2. \tag{1}$$

Berücksichtigt man auch die Randbedingungen, so lautet die Lösung von (1) folgendermassen:

$$\overline{T}(d) = \frac{1}{1 + r \cdot d}, \tag{2}$$

$$\overline{R}(d) = 1 - \overline{T}(d) = \frac{r \cdot d}{1 + r \cdot d}. \tag{3}$$

Bedeutet l den Durchmesser der Körnchen, d die Dicke der Schicht, so besteht die Schicht aus

$$c = \frac{d}{l} \tag{4}$$

Elementarschichten. Diese Anzahl ist im Abstand x von der Oberfläche gleich $c(x) = \dfrac{d}{l}$.

Aus der Definition von r folgt

$$r = \left(\frac{dR}{dc}\right)_{(0)} \cdot \left(\frac{dc(x)}{dx}\right)_{x=0} . \tag{5}$$

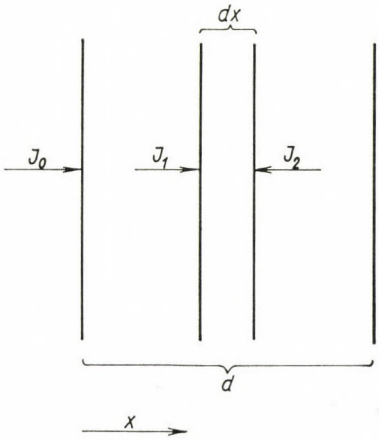

Fig. 1

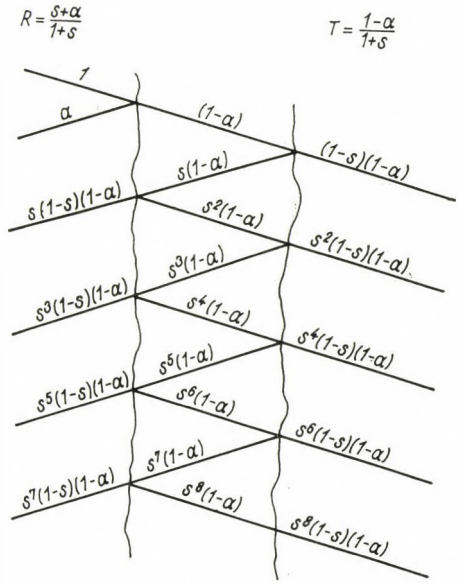

Fig. 2

Führt man die für eine bestimmte Form der Körnchen von der Korngrösse unabhängige Grösse $r^* = \left(\dfrac{dR}{dc}\right)_{c(0)}$ ein, so erhält man

$$r = \frac{r^*}{l} . \tag{6}$$

Die Transmission der Schicht kann wegen (2), (4) und (6) durch c und r^* folgendermassen ausgedrückt werden:

$$T(c) = 1 - R(c) = \frac{1}{1 + r^* c} . \tag{7}$$

Die Transmission und Reflexion der Schicht hängt von der Anzahl c der Elementarschichten und von r^* ab, r^* wird dagegen durch die optischen Eigenschaften der einfach bedeckten Schicht bestimmt. Die nächste Aufgabe ist also, den Zusammenhang zwischen r^* und den optischen Eigenschaften

der Schicht zu bestimmen. Es sei angenommen, dass die einfach bedeckte Schicht das $\left(\frac{n-1}{n+1}\right)^2 = \alpha$-fache des von aussen und das s-fache des von innen auffallenden Lichtes reflektiert und dass $s \geq \alpha$ ist (Abb. 2). Dann gilt für die Transmission bzw. Reflexion der einfach bedeckten Schicht

$$T(1) = 1 - R(1) = \frac{1-\alpha}{1+s}. \tag{8}$$

Aus (7) und (8) erhält man

$$\frac{1-T_1}{T_1} = r^* = \frac{\alpha+s}{1-\alpha}. \tag{9}$$

Die in (7) auftretende Schichtenanzahl c kann durch das spezifische Gewicht ϱ des Materials, durch das Gewicht eines cm^2 der Schicht und durch die Grösse der Körnchen ausgedrückt werden.

Mit Hilfe der experimentell bestimmten [16] auf die Schicht senkrechten Dimension l_3 der Körnchen, die im allgemeinen Ellipsoide sind, erhält man

$$c = \frac{3m}{2\varrho l_3}, \tag{10}$$

ferner aus (7), (8), (9) und (10)

$$T(m) = 1 - R(m) = \frac{2\varrho l_3(1-\alpha)}{2\varrho l_3(1-\alpha) + 3(\alpha+s)m}. \tag{11}$$

b) *Die Schicht bestehe aus Körnchen inhomogener Grösse*

Sind die folgenden Bedingungen erfüllt, so lassen sich die Formeln (7) und (11) auch auf aus Körnchen inhomogener Grösse bestehende Schichten verallgemeinern.

1. Die durchschnittliche Gestalt der Körnchen verschiedener Grösse ist die gleiche.[1]

2. Die diffuse Transmission und Reflexion der aus Körnchen inhomogener Grösse bestehenden Schicht hängt nicht von der Lage der verschieden grossen Körnchen in der Schicht ab.

Sind die Bedingungen 1 und 2 erfüllt, so hängt die diffuse Transmission und Reflexion der aus inhomogenen Körnchen bestehenden Schicht nur von der diffusen Konstante r^* und der Anzahl c der Elementarschichten ab.

Bei der aus inhomogenen Körnchen bestehenden Schicht kann c mit Hilfe der Wahrscheinlichkeitsverteilung $E(l)$ der Korngrösse ausgedrückt

[1] Hieraus folgt, dass für jede aus Körnchen derselben Grösse bestehende Schicht des untersuchten Materials die Grösse $r^* = \left(\frac{dR}{dc}\right)_{c(0)}$ eine von der Korngrösse unabhängige Konstante ist.

werden. Ist $\int_{k_1}^{k_2} E(l)\,dl$ das Gewicht des Materials, deren Korngrösse zwischen k_1 und k_2 liegt (das ganze Material soll das Gewicht 1 haben), so erhält man aus (10)

$$c = \frac{3\,m}{2\,\varrho} \int_a^b \frac{E\,(l)}{l}\,dl. \tag{12}$$

Hier bedeuten a bzw. b die kleinste bzw. grösste vorkommende Korngrösse. Der Unterschied zwischen (10) und (12) besteht darin, dass bei der letzten Formel

$$l^* = \frac{1}{\int_a^b \frac{E(l)}{l}\,dl} \tag{13}$$

an die Stelle von l_3 tritt. Setzt man in (7) für die Schichtenanzahl c den Ausdruck (12) ein bzw. ersetzt man in (11) l_3 durch l^* so erhält man die Transmission bzw. Reflexion der inhomogenen Schicht.

II. Messergebnisse

In der vorliegenden Untersuchungen wurden die diffuse Transmission von Schichten gemessen, die aus mit Mangan aktivierten Kalziumhalophosphat und Zinksilikat und aus mit Silber aktiviertem Zinksulfid bestanden. Bei den Messungen an homogenen Schichten war das Ziel die experimentelle Bestimmung von r^* und s. Bei den Messungen an inhomogenen Schichten sollte die Richtigkeit der Annahmen 1 und 2 geprüft werden.

Für die Messungen wurden durch Sedimentierung Fraktionen hergestellt, die aus Körnchen gleicher Grösse bestanden. Kalziumhalophosphat und Zinksilikat wurden in Wasser, Zinksulfid in Alkohol im Dunkeln sedimentiert. Von den homogenen Fraktionen wurden auf Glasplatten Schichten verschiedener Dicke sedimentiert. Die auf die Platte senkrecht durchschnittliche Dimension l_3 und die parallele Dimension l_1 wurde an Schichten von der Bedeckungszahl $c \approx 0{,}3$ gemessen [16].

Die Messung der Transmission wurde mit einer in [17] und [18] dargestellten Einrichtung durchgeführt. Diese bestand im wesentlichen aus einer Photometerkugel, einem Monochromator und einem Elektronenvervielfacher. Bei der Messung der diffusen Transmission und Reflexion wurden Kontrollmessungen durchgeführt, die zeigten, dass die Schichten bei der Wellenlänge 5461 Å nur einen vernachlässigbaren Teil des Lichtes absorbieren.

Auf den Abb. 3, 4 und 5 sind die Resultate der Transmissionsmessungen auf homogenen Kalziumhalophosphatschichten ($l_3 = 10{,}6\ \mu$), Zinksilikat-

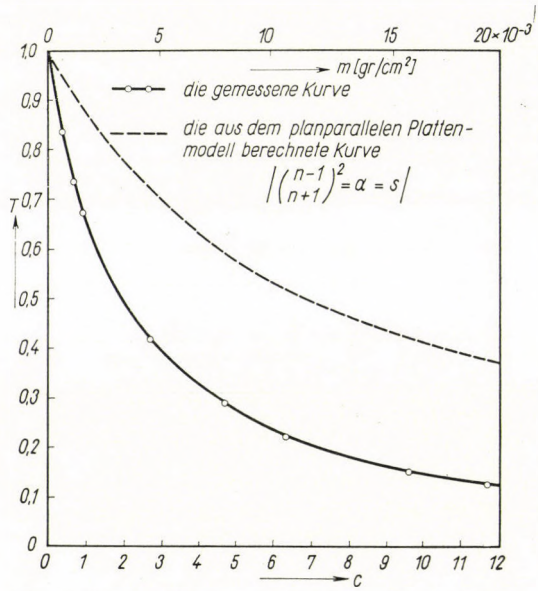

Fig. 3. Transmission von Halophosphatschichten

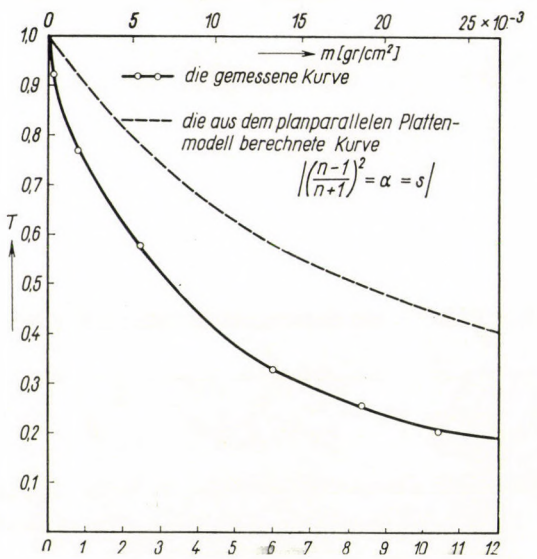

Fig. 4. Transmission von Willemitschichten

schichten ($l_3 = 6{,}6\ \mu$) und Zinksulfidschichten ($l_3 = 7{,}7\ \mu$) dargestellt. Zeichnet man den Ausdruck $(1 - T)/T$ als Funktion von c auf, so bekommt man im Einklang mit (7) eine Gerade mit der Richtungstangente r^* (Abb. 6). Aus r^* und α, welches aus (19), (20) und (21) bekannt ist, lässt sich s mittels (9) ausrechnen. Tabelle I enthält die Werte von r^* und s bei den untersuchten Stoffen.

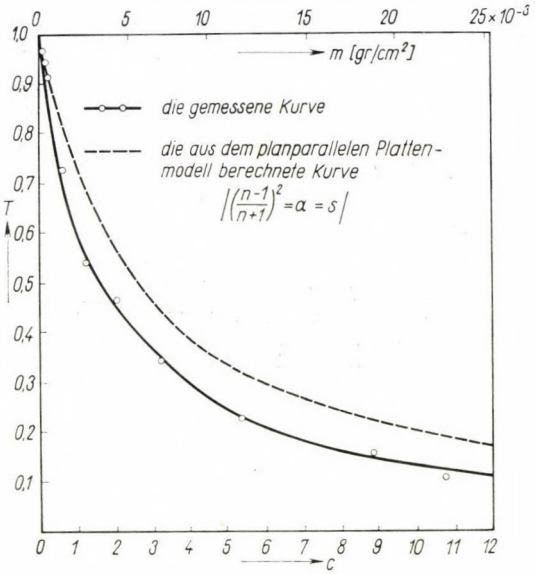

Fig. 5. Transmission von Zinksulfidschichten

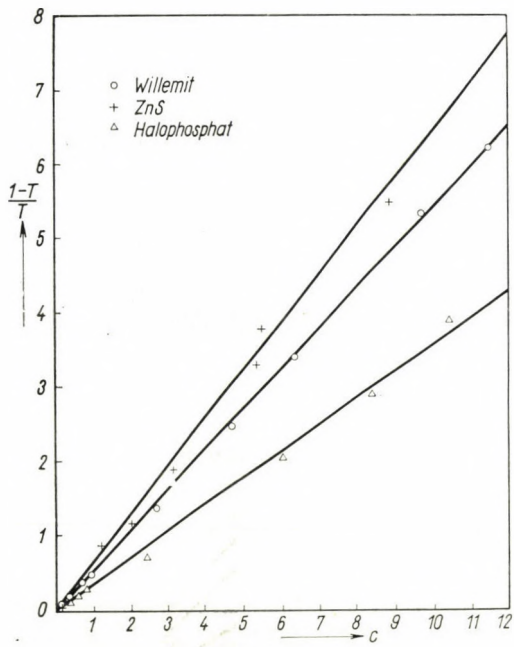

Fig. 6

Für die Untersuchung inhomogener Schichten wurden aus der Fraktion von Leuchtpulver, das aus Körnchen 5 verschiedener Grössen besteht, zwei Mischungen mit verschiedenen Mischproportionen hergestellt (Tab. II), und

die Transmission und das Gewicht der Schichten pro Flächeneinheit gemessen. Auf Abb. 7 ist das Resultat als Funktion der Schichtenanzahl dargestellt; c wurde dabei aus (12) berechnet. Bei der Berechnung wurde der experimentell gewonnene Wert von r^* verwendet, der in Tabelle I angegeben ist.

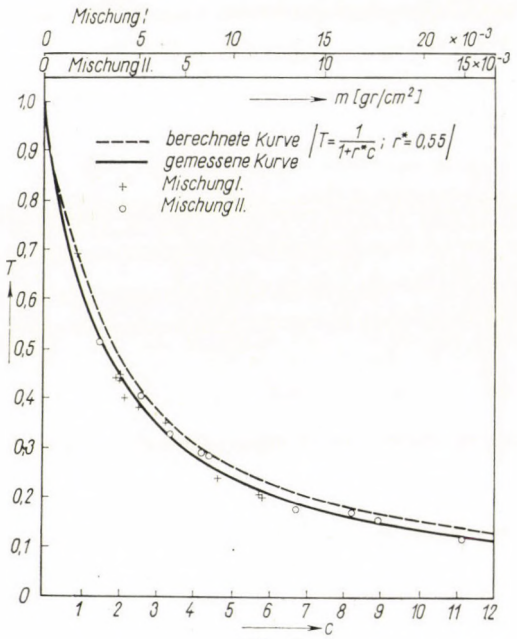

Fig. 7

Dies bedeutet, dass die Streuung der Schichten grösser ist, als dies zu erwarten wäre. Es ist möglich, dass eine Ursache der grösseren Streuung die totale Reflexion ist, die im Inneren der einzelnen Körnchen zustandekommt [15]. Ein anderer Umstand, den das planparallele Modell ausser acht lässt, ist der folgende. In den Elementarschichten läuft ein Teil des Lichtes nicht senkrecht zur Schicht, sondern in der Ebene der Schicht und wird an der Grenzflächen der einzelnen Körnchen gestreut, wodurch die Streuung der ganzen Schicht vergrössert wird [17, 18]. Es kann ferner angenommen werden, dass ein Teil der sedimentierten Körnchen zusammenklebt und solche Körnchen streuen das Licht stärker als die homogenen.

III. Diskussion

Aus der Tabelle I und den Abb. 3 und 5 wird ersichtlich, dass bei der homogenen Schicht das experimentell bestimmte r^* grösser (also die Transmission kleiner) ist als der mit dem planparallelen Modell berechnete Wert.

Die grössere Streuung hat zur Folge, dass die durchschnittliche Weglänge des Lichtes im Inneren der nicht absorbierenden Schicht grösser ist. Bei der experimentellen Bestimmung des Absorptionskoeffizienten mikrokristalliner Stoffe [9, 12, 15, 22] und bei der Berechnung des Lichtes, das an den beiden Seiten der angeregten lumineszierenden Schicht austritt [23, 24, 25], muss dieser Umstand berücksichtigt werden. Aus den beschriebenen Messun-

Tabelle I

	r^* (gemessen)	r^* aus dem planparallelen Modell gerechnet Fall $\left(\frac{n-1}{n-1}\right)^2 = \alpha = s$	$\alpha = \left(\frac{n-1}{n+1}\right)^2$	s
Kalziumhalophosphat	0,355	0,122	0,0578	0,277
Zinksilikat	0,55	0,146	0,068	0,445
Zinksulfid	0,65	0,396	0,165	0,378

Tabelle II

	Gewicht %	Korngrösse $l_3(\mu)$	
Mischung I	10	3,04	
	12	6,17	$l^* = 7{,}87\ \mu$
	15	6,6	$\bar{l} = 11{,}27\ \mu$
	35	8,93	
	28	21,85	
Mischung II	28	3,04	
	35	6,17	$l^* = 5{,}27\ \mu$
	15	6,6	$\bar{l} = 7{,}27\ \mu$
	12	8,93	
	10	21,85	

gen kann man schliessen, dass die Genauigkeit solcher Messungen und Berechnungen erhöht werden kann, wenn die auf Abb. 2 dargestellte modifizierte Form des Plattenmodells benutzt wird, und wenn der innere Reflexionskoeffizient s auf die obige Weise experimentell bestimmt wird.

Beim Zinksulfid, das unter den hier untersuchten Stoffen den grössten Brechungsindex hat, ist r^* am grössten (Tab. I). Der innere Reflexionskoeffizient s des Zinksulfids ist jedoch kleiner als der des Zinksilikats, das kleineren Brechungsindex hat. Die mikroskopischen Bilder des Zinksilikats und des Zinksulfids weichen stark voneinander ab. Die Zinksilikatkörnchen weisen keine so regelmässige Form auf, wie die Zinksulfidkörnchen, unter welchen

auch viele kugelförmige vorkommen [17, 26]. Durch die Messung wird die Annahme [15] bestätigt, nach der die Diffusion und Absorption nicht nur vom Brechungsindex, sondern auch von der Form der Körnchen abhängt.

Die Resultate der Versuche haben die Annahmen bestätigt, die wir in Ib über die inhomogene Schicht gemacht haben. Die auf Abb. 7 zu sehende kleine Abweichung zwischen dem gemessenen und berechneten Wert kann den bekannten Schwierigkeiten der Bestimmung der Korngrösse zugeschrieben werden.

Falls r^* bekannt ist, so lässt sich aus (7) mit einer Transmissionsmessung die Schichtenanzahl c einer homogenen oder inhomogenen, nichtabsorbierenden diffusen Schicht bestimmen [27]. Sind r^* und m bekannt, so lässt sich aus (7) und (10) mit einer Transmissionsmessung die Korngrösse l_3 bestimmen:

$$l_3 = \frac{3\, m r^*\, T}{2\,\varrho\,(1-T)} \,. \tag{14}$$

Ist die Schicht inhomogen, so ergibt (14) die durchschnittliche Korngrösse l^*. Es sei bemerkt, dass l^* von der in der Praxis gebräuchlichen Grösse $\bar{l} = \int_a^b l \cdot E(l)\, dl$ abweicht; die SCHWARZsche Ungleichung ergibt

$$l^* \equiv \frac{1}{\int_a^b \frac{E(l)}{l}\, dl} \leq \bar{l} \equiv \int_a^b l \cdot E(l)\, dl \tag{15}$$

z. B. bei den zwei in Tab. II angegebenen Mischungen ist l^* um 28%, bzw. 30% kleiner als l.

LITERATUR

1. A. SCHUSTER, Astrophys. Journ., **21,** 1, 1905.
2. M. GUREVIC, Phys. Zeitschr., **31,** 753, 1930.
3. P. KUBELKA und F. MUNK, Z. techn. Phys., **12,** 593, 1931.
4. P. KUBELKA, J. Opt. Soc. Am., **38,** 448, 1958.
5. P. KUBELKA, J. Opt. Soc. Am., **44,** 330, 1951.
6. H. C. HAMAKER, Philps Res. Rep., **2,** 55, 1947.
7. J. S. COLTMAN, E. G. EBBIGHAUSEN und W. ALTAR, J. Appl. Phys., **18,** 530, 1947.
8. J. BROSER, Ann. d. Phys., **5,** 401, 1950.
9. R. L. LONGINI, J. Opt. Soc. Am., **39,** 551, 1949.
10. P. P. JOHNSON und F. J. STUDER, J. Opt. Soc. Am., **40,** 121, 1950.
11. Z. BODÓ, Acta Phys. Hung., **1,** 135, 1951.
12. P. P. JOHNSON, J. Opt. Soc. Am., **42,** 978, 1952.
13. O. P. GIRIN und B. J. STEPANOFF, J. E. T. F., **27,** 281, 1954.
14. I. P. SHAPIRO, Optika i Spektroskopia, **7,** 798, 1959.
15. V. V. ANTONOV-ROMANOVSKY, J. E. T. F., **26,** 459, 1954.
16. Z. BODÓ und I. HANGOS, Acta Phys. Hung., **3,** 155, 1954.
17. G. T. BAUER, G. GERGELY und J. ÁDÁM, Festkörperphysik, Akademie Verlag, Berlin, 1961.
18. G. T. BAUER, Acta Phys. Hung., **14,** 311, 1962.

19. Ch. D. Hodgman, Handbook of Chemistry and Physics, Chemical Rubber Publishing Co., Cleveland.
20. W. P. Piper, Phys. Rev., **92,** 23, 1953.
21. C. K. Coogan, Proc. Phys. Soc., »B« **70,** 845, 1957.
22. B. Mühlschlegel, Ann. d. Phys., **6,** 29, 1951.
23. A. P. Ivanoff, J. E. T. F., **26,** 275, 1954.
24. A. P. Ivanoff, Optika i Spektroskopia, **4,** 225, 1958.
25. A. P. Ivanoff, Optika i Spektroskopia, **4,** 236, 1958.
26. G. Gergely, Acta Phys. Hung., **7,** 2, 1957.
27. R. L. Longini, J. Opt. Soc. Am., **39,** 377, 1949.

НЕКОТОРЫЕ ОПТИЧЕСКИЕ СВОЙСТВА ЛЮМИНЕСЦИРУЮЩИХ СЛОЁВ, СОСТОЯЩИХ ИЗ МИКРОКРИСТАЛЬНЫХ ЗЁРЕН

Г. Т. БАУЭР

Р е з ю м е

При длине волны $\lambda = 5461$ Å, где выбранные вещества практически прозрачны, измеряется трансмиссия изготовленных из разных веществ слоёв, состоящих из микрокристальных зёрен. По проведённым измерениям и вычислениям рассеяние света у этих слоёв больше той величины, которая следует из так называемой модели «плоскопараллельная пластинка», описывающей оптические свойства диффузных слоёв. На основании измерений модель подвергалась уточнению. Показывается, что трансмиссия рассмотренных неабсорбирующих слоёв, состоящих из зёрен неоднородных размеров, зависит исключительно от числа элементарных слоёв, образующих данные слои. Специальный средний размер образующих данный слой зёрен определяется измерением трансмиссии.

THE HYDRODYNAMICAL MODEL OF WAVE MECHANICS II

THE MOTION OF A SINGLE PARTICLE IN AN EXTERNAL ELECTROMAGNETIC FIELD

By

L. JÁNOSSY and MARIA ZIEGLER-NÁRAY

CENTRAL RESEARCH INSTITUTE OF PHYSICS, BUDAPEST

(Received 22. X. 1963)

In the present paper our investigations referring to the hydrodynamical model of wave mechanics [1] are continued and extended to the case of a single charged particle moving under the influence of an electromagnetic field. After establishing the appropriate basic equations describing the motion of a deformable medium, we investigate by means of the hydrodynamical model the effect of the external electromagnetic field upon the atom.

I. Basic considerations

§ 1. In our attempt to replace the wave mechanical description of a system by a mathematically equivalent hydrodynamical model, we have already dealt with the simplest case, i.e. with a particle of mass m and charge e moving under the influence of an external force represented by the scalar potential V. [1]. In the present paper we extend our investigations to the case of an external electromagnetic field, the field strengths ($\boldsymbol{E}$ and $\boldsymbol{H}$) of which may be given by the scalar and vector potentials, Φ and A, in the usual way:

$$\boldsymbol{E} = -\operatorname{grad}\Phi - \frac{1}{c}\frac{\partial \boldsymbol{A}}{\partial t}$$

and

$$\boldsymbol{H} = \operatorname{rot}\boldsymbol{A}. \tag{1}$$

A similar extension of the calculations relating to the simple Schrödinger equation can be found in the article of TAKABAYASI [2].

§ 2. The first task is the determination of the hydrodynamical variables by which the wave function can be replaced. The wave equation of a charged particle moving in an external electromagnetic field has the form:

$$\frac{1}{2m}\left(-i\hbar\nabla - \frac{e}{c}\boldsymbol{A}\right)^2\psi + (e\Phi - V)\psi = i\hbar\dot{\psi}. \tag{2}$$

(Here we have added a potential V to the scalar potential Φ, which may represent the external non-electromagnetic force.)

From equ. (2), just as in the case without an external electromagnetic field, we obtain the equation of continuity:

$$\operatorname{div}(\varrho \boldsymbol{v}) + \frac{\partial \varrho}{\partial t} = 0 \tag{3}$$

with

$$\varrho = \psi^* \psi \tag{4}$$

and

$$\varrho_m \boldsymbol{v} = -\frac{i\hbar}{2}(\psi^* \operatorname{grad} \psi - \operatorname{grad} \psi^* \cdot \psi) - \frac{1}{c}\varrho_e \boldsymbol{A}, \tag{5}$$

where $\varrho_m = m\varrho$ and $\varrho_e = e\varrho$ are the mass and charge density, respectively.

Similar to the case without external electromagnetic field also here the rotation of an arbitrary vector might be added to the right-hand expression of the velocity vector and the distribution of $\varrho \boldsymbol{v}$ thus obtained would still satisfy (3). We shall return to this question later, when discussing the equations of motion of the spinning particle.

§ 3. So as to obtain equations of motion, we may differentiate (5) with respect to time. Expressing the time derivatives of ψ in terms of spatial derivatives with help of the wave equation (2) we obtain as the result of some calculation for the acceleration of an element of the fluid using the well-known hydrodynamical expression

$$\frac{\mathrm{d}\boldsymbol{v}}{\mathrm{d}t} = \frac{\partial \boldsymbol{v}}{\partial t} + (\boldsymbol{v} \operatorname{grad}) \boldsymbol{v} :$$

$$\varrho_m \frac{\mathrm{d}\boldsymbol{v}}{\mathrm{d}t} = -\varrho \operatorname{grad}(V + Q) + \varrho_e \left(\boldsymbol{E} + \frac{1}{c}[\boldsymbol{v} \times \boldsymbol{H}] \right), \tag{6}$$

where

$$Q = -\frac{\hbar^2}{2m} \frac{\nabla^2 \varrho^{1/2}}{\varrho^{1/2}} .$$

This means that in this case, i.e. when there exists an external electromagnetic field, the elements of the fluid are moving under the influence of the external force (which includes the well-known Lorentz force) and the internal quantummechanical forces. We see thus that the electromagnetic field acts upon the fluid of charge and mass density ϱ_e and ϱ_m — representing the particle of charge e and mass m — as is to be expected from the classical theory. According to (6) the action of the charge upon itself has to be omitted.

As the internal quantummechanical force in this case has the same form as in the simplest case, where there is no external electromagnetic field, it follows from the calculations of Part I that the rate of change of momentum of the system is given in this case also by the integral over the external forces only, and similarly the change of the angular momentum is caused by the moment of the external forces.

II. Connection between hydrodynamical equations and wave equation

§ 4. Let us investigate now how far the hydrodynamical equations are equivalent to the wave equation. For this purpose we introduce real variables R and S, such that

$$\psi = Re^{iS}. \tag{7}$$

Introducing (7) into (4) and (5) we find for points with $R \neq 0$

$$\varrho = R^2, \qquad \boldsymbol{v} = \frac{\hbar}{m} \operatorname{grad} S - \frac{e}{mc} \boldsymbol{A}. \tag{8}$$

From (8) using (1) we find

$$\operatorname{rot} \boldsymbol{v} = -\frac{e}{mc} \boldsymbol{H} \quad \text{for points in which } \varrho \neq 0.$$

Thus the flow (apart from singularities with $\varrho = 0$) is free of vortices in the absence of a magnetic field. A magnetic field, however, gives rise to a continuous distribution of vortices, the angular velocity vector having the direction $-eH$, as $mc > 0$. As can be seen easily such vortices of a charged fluid can be treated as magnetic dipoles orientated in directions opposite to the direction of the external magnetic field.

We conclude thus that the term of (5) containing A corresponds to the diamagnetic susceptibility of the fluid.

Returning to the connection between wave equation and hydrodynamical equations we integrate the second equation of (8) along a line starting from an arbitrary point r_0 to some point r. If the path of integration avoids singular points with $\varrho = 0$, we find

$$S = \frac{m}{\hbar} \int_{r_0}^{r} \left(\boldsymbol{v} + \frac{e}{mc} \boldsymbol{A} \right) \mathrm{d}\boldsymbol{r} + S_0(t), \tag{9}$$

where the integration constant $S_0(t)$ is a function of t, but independent of the coordinates.

In case S is a multiple-valued function of $\boldsymbol{r}$ we obtain from (7) unique values for ψ if the values of S for given $\boldsymbol{r}$ differ from each other only by integer multiples of 2π. With this condition (9) may be written in the form

$$\oint \boldsymbol{v} \, \mathrm{d}\boldsymbol{r} = \frac{2\pi k\hbar}{m} - \frac{e}{mc} F, \tag{10}$$

with

$$F = \int \boldsymbol{H} \, \mathrm{d}\boldsymbol{f} \qquad \text{and} \qquad k = 0, \pm 1, \pm 2, \ldots$$

the value of k depending on the choice of the path of integration.

Introducing (8) resp. (9) into (7) we obtain an explicit expression for ψ in terms of ϱ and v. So as to show that the expression thus obtained does indeed satisfy the wave equation, we insert it into (2). The equation obtained in this way reduces to the hydrodynamical equation of motion (6) provided we put

$$S_0(t) = \frac{1}{\hbar} \int_0^t E(t)\, \mathrm{d}t\,,$$

with

$$E(t) = -\left(Q + V + e\Phi + \frac{1}{2} m \boldsymbol{v}^2\right)_{\cdot = t_0}.$$

We find thus that

$$\psi = \sqrt{\varrho} \exp\left\{\frac{im}{\hbar} \int_{r_0}^{r} \left(\boldsymbol{v} + \frac{e}{mc} \boldsymbol{A}\right) \mathrm{d}\boldsymbol{r} + i\, S_0(t)\right\} \tag{11}$$

satisfies the wave equation (2) provided ϱ and $\boldsymbol{v}$ satisfy the hydrodynamical equation of motion and the condition (10).

We note that the time derivative of (10) is zero provided ϱ and $\boldsymbol{v}$ obey the hydrodynamical equations and rot $\boldsymbol{E} = -\frac{1}{c} \boldsymbol{H}$. Thus equ. (10) is valid at any time provided it is satisfied at an initial moment $t = 0$, i.e. it can be regarded as an initial condition. As a further initial condition we may postulate the condition of normalization of ϱ, i.e.

$$\int \varrho \, \mathrm{d}\tau = 1\,. \tag{12}$$

Thus we may conclude: if a distribution $\varrho, \boldsymbol{v}$ satisfies the initial conditions (10) and (12) at $t = 0$, then the hydrodynamical variables describing the motion correspond exactly to the solution of wave equation (2), where ψ is given by (11).

§ 5. A further possibility for the ambiguity of ψ arises from the fact that wave equation (2) and also the equation defining ψ (11) contain the potentials Φ respectively $\boldsymbol{A}$ explicitly. As is well known, the potentials are not uniquely determined from the field strengths $\boldsymbol{E}$ and $\boldsymbol{H}$. The given fields $\boldsymbol{E}$ and $\boldsymbol{H}$ which can be represented by potentials $\boldsymbol{A}$ and Φ can also be represented by potentials

$$\boldsymbol{A}' = \boldsymbol{A} + \operatorname{grad} \chi \qquad \text{and} \qquad \Phi' = \Phi - \frac{1}{c} \frac{\partial \chi}{\partial t}\,,$$

where χ is an arbitrary function of the time and the coorditnates. Replacing $\boldsymbol{A}$ and Φ by $\boldsymbol{A}'$ and Φ' we obtain instead of (11) a wave function

$$\psi' = \psi \exp\left(-\frac{ie}{c\hbar} \chi\right), \tag{13}$$

which obeys the corresponding modified form of the wave equation, i.e. equ. (2), where $\boldsymbol{A}$ and Φ have been replaced by $\boldsymbol{A}'$ and Φ'. This means that the wave equation is not independent of the gauge of the potentials, i.e. in the case of a given initial condition for ψ, the variation of ψ with time depends upon the gauge of the potentials. However, the physical results obtained from the wave equation are independent of the gauge of the potentials. Indeed, by introducing (13) into (4) and (5) it can be shown that the hydrodynamical variables ϱ and $\boldsymbol{v}$ corresponding to the new values of the potentials ($\boldsymbol{A}'$ and Φ') are identical with their original values:

$$\varrho' = \varrho \qquad \text{and} \qquad \boldsymbol{v}' = \boldsymbol{v}.$$

Consequently, the gauge invariance of the hydrodynamical equation of motion is trivial.

III. Radiation damping

In the following — basing ourselves on the hydrodynamical model — we shall make some qualitative remarks on the behaviour of an electron in cases, where the effect of the spin can be neglected.

§ 6. As was shown in (1) for the stationary states of the electron the hydrodynamical variables describing its motion, say in the Coulomb field of the nucleus, are independent of time, i.e. $\varrho = 0$ and $\boldsymbol{v} = 0$, thus the system does not emit radiation. However, if the electron is disturbed the Coulomb attraction of the nucleus will not be any more compensated by the internal quantummechanical force and thus the elements of the fluid representing the electron start to oscillate around their equilibrium position, the frequencies of the oscillation being equal to the Bohr frequencies, $\omega_{kl} = \dfrac{E_k - E_l}{\hbar}$. This oscillating charge gives rise to electromagnetic radiation, which in first approximation may be regarded as a dipole radiation.

On the other hand the superposition of stationary states gives rise to undamped oscillation.

This difficulty can be overcome, as is well known from the classical theory of the electron, by taking into account also the electromagnetic field of the emitted radiation. The radiation reaction upon itself can be obtained by including in equ. (2) in the total vector potential the vector potential

$$\boldsymbol{A}_i = \int \frac{[\boldsymbol{i}]}{|\boldsymbol{r} - \boldsymbol{r}'|}\, \mathrm{d}\tau', \tag{14}$$

corresponding to the field of the radiation. In (14) the bracket denotes, in the usual way, that the retarded values of $\boldsymbol{i} = \varrho_e \boldsymbol{v}$ have to be taken, $\boldsymbol{v}$ being given by (8).

The electromagnetic field of the radiation is thus shown to act upon the moving charge and to damp down the oscillation, so that the energy irradiated by the system becomes equal to the energy loss of the emitting system.

In a similar way the radiation reaction gives rise to recoil and angular recoil of the atom and thus the conservation laws are satisfied if the reactions are properly taken into account.

§ 7. When considering the radiation reaction in the hydrodynamical model, we apply in effect the same procedure as is applied in the theory of radiation damping in the usual quantum mechanical treatment (see e.g. [3]).

It must be pointed out, however, that it is not the full reaction of the charge upon itself which has to be introduced. We have to omit the purely static action of the charge upon itself and also the action of the stationary currents upon themselves; we have thus to take into account only the field produced by the oscillating part of the currents. The above restriction is very essential. If we were to introduce e.g. the static Coulomb action of the charge upon itself, this action would give rise to forces comparable to the Coulomb attraction of the nucleus, and would lead to complete distortion of the cloud. The distorted cloud, however, would presumably have frequencies very different from the observed ones. The fact that we obtain the correct frequencies when omitting the action of the charge upon itself proves that the cloud does not act statically upon itself.

On the other hand, the fact that the radiation damping as calculated from the reaction of the charge upon itself leads to the correct description of e.g. the natural width of spectral lines, can be regarded as an empirical proof to the effect that the latter reaction does exist.

Thus we have to take it as an empirically established fact that the electron cloud acts upon itself through its radiation field but not through its stationary field. We note that this result is not brought about through the hydrodynamical model: it is already implied in the usual quantum mechanical treatment of stationary states and of radiation damping; the hydrodynamical model only forcefully draws the attention to this circumstance.

IV. Effects of an external electric field upon the atom

§ 8. We give a brief qualitative account in terms of the hydrodynamical model of the effect of an external electric field upon the atom.

According to equ. (6) each element of the fluid representing an electron starts to move under the influence of such a field.

As a result of the displacement of the cloud relative to the nucleus, the Coulomb attraction between nucleus and elements of the cloud changes, tending to compensate the external field. Finally the electron cloud settles

down into its new position in which in first approximation the Coulomb field, the external field and the internal force compensate each other. The detailed calculations (see [4]) show further that the displacement is in first approximation proportional to the strength of the external field.

Considering, however, the effect of the external field in greater detail one finds that the cloud is not simply displaced by it, but also suffers certain distortions. Further, the displacement, in particular for strong external fields, deviates noticeably from proportionality to the external field strength. Carrying out the calculations to this higher approximation finer details of the process of polarization of the atom can be obtained:

As the Coulomb attraction of the nucleus decreases with distance, there exist always regions in which the external force exceeds the Coulomb attraction and thus the charge from this region is carried away through the effect of the external field.

In the region bordering on these depleted parts the quantum mechanical force becomes weaker or even repulsive and thus charge starts to flow from the inner parts to the depleted parts. This process goes on until in the end the whole of the charge evaporates under the influence of the outer force [4].

From the above consideration it follows that no real stationary state exists if the atom is under the influence of a constant electric field. However, as the process of evaporation is a slow one the state of the atom, immediately after an external electric field has been switched on, may be considered as pseudo-stationary, such a state persisting for a comparatively long time. The effects of polarization have thus to be understood in terms of such pseudo-stationary states. The effect of evaporation described above is the process of photoelectric emission: a weak photoemission can indeed be induced by strong electric fields.

§ 9. The above consideration points to a difficulty of the theory. Atoms are always subjected to external electric fields. Taking e.g. the atoms of a gas, there are always ions present, some atoms are at least temporarily polarized, etc., thus every atom in the course of its history is continually subjected to the action of external fields and as the result, the electrons of atoms must be assumed to evaporate slowly all the time. We have to suppose that the atoms can also capture charges floating about, from which it follows that the charge of atoms at any time should show a distribution corresponding to thermodynamical equilibrium. This means that for a long time the effect of these processes ought to be that the charges of the bound parts of the electrons of individual atoms ought to differ from the elementary charge e, i.e. we should expect something like a thermodynamical distribution of the charges. As real atoms have always charges which are integer multiples of e, it is clear that some effect must exist which keeps the charges together. We wish to point

out here that describing the motion of the charges by the wave equation, we cannot account for the actually observed stability of the charges.

§ 10. It must be pointed out that the latter difficulty is not connected with the question of the interpretation of the wave function and thus the difficulty is not caused by the hydrodynamical treatment. One might argue that according to the usual probability interpretation the evaporation described by the wave equation should be interpreted as a slowly increasing probability for the electron as a whole to leave the atom. Thus one might expect the atom to retain the electron until a photoeffect occurs when suddenly the whole of the electron disappears.

While we think that the latter picture does indeed more or less correctly describe the behaviour of the real atom, we wish to point out that it does not follow from the description of the atom by means of its wave equation. On the contrary, the description through the wave equation leads to continuous evaporation — a picture which does not seem to be in accordance with the real behaviour of atoms.

Indeed, quite independent of the interpretation of the wave function, the field of the electron can be derived from a vector potential of the form (14) and from a scalar potential of similar form. If ψ is spread out over a large area these potentials exactly represent the field of a correspondingly spread out charge and current distribution, thus the electron acts upon its vicinity exactly like a classical charge distributed over the area over which ψ is spread out.

Furthermore, consider an atom in a partly ionized state, i.e. in a state where the ψ function consists of two parts, ψ_1 and ψ_2. The part ψ_1 should be concentrated around the nucleus corresponding to the part of the electron not yet evaporated and the other part ψ_2 should have values noticeably different from zero only in regions distant from the nucleus. The part ψ_2 of ψ corresponds to the already evaporated part of the electron. If an externa electric field is suddenly applied to the atom, we find from the hydrodynamical equation (6) that this field will act upon the atom in exactly the manner as is to be expected from the classical picture for the action of a field upon a partly ionized atom. Indeed, the action will be such, as if the charge of the electron were exactly

$$e_1 = e \int |\psi_1|^2 d\tau$$

which means $e_1/e < 1$.

It is true that the field if sufficiently extended will also act upon the evaporated part of the electron with charge $e_2 = e_1$, however, as the latter part is already torn off the atom, it does not react noticeably on the nucleus.

We see thus that according to the description through the wave equation the atom possessing a partly evaporated electron should produce a field corresponding to a fractional charge and it should react to an external field like

a fractionally ionized atom. As real atoms seem always to behave as if they possessed charges which are integral multiples of the elementary charge e it seems to us that this analysis shows that the wave equation does not give a complete description of the behaviour of the electron.

REFERENCES

1. L. JÁNOSSY and MARIA ZIEGLER, Acta Phys. Hung., **16,** 37, 1963.
2. T. TAKABAYASI, Prog. of theor. Phys., **8,** 143, 1952.
3. W. HEITLER, Quantum theory of radiation, Oxford, 1954.
4. M. HUSZÁR and MARIA ZIEGLER-NÁRAY, Reports of the Central Research Institute of Physics, in print.

ГИДРОДИНАМИЧЕСКАЯ МОДЕЛЬ ВОЛНОВОЙ МЕХАНИКИ II

Л. ЯНОШИ и МАРИЯ ЦИГЛЕР-НАРАИ

В настоящей работе мы продолжаем наши расчеты (1) в связи с гидродинамической моделью квантовой механики, распространяя их на случай заряженных частиц, движущихся в электромагнитном поле.

После составления подходящих основных уравнений деформируемой среды мы анализируем влияние внешнего магнито-электрического поля на атом с помощью гидродинамической модели.

ON THE QUASI-ELASTIC CHARACTER OF INELASTIC TWO-PRONG $\pi^- - p$ INTERACTIONS AT 7 AND 16 GeV/c

By

G. Bozóki, E. Fenyves, A. Frenkel and Éva Gombosi

CENTRAL RESEARCH INSTITUTE OF PHYSICS, BUDAPEST

(Presented by L. Jánossy. — Received 14. I. 1964)

The quasi-elastic diffraction character of inelastic two-prong $\pi^- - p$ interactions was confirmed by investigating the distribution of the four-momentum transfer t. From the similarity of the t distribution obtained for the secondary π^--mesons with the t distribut on in $\pi^- - p$ elastic scattering it was concluded that the incident pion undergoes quasi-elastic scattering and has a tendency to maintain its charge.

The quasi-elastic diffraction character of inelastic two-prong $\pi^- - p$ interactions was pointed out first by Morrison [1, 2] and supported later by several authors [3—5]. In the present paper we would like to present some additional evidence confirming this suggestion.

A certain sample of inelastic $\pi - p$ interactions can be considered to be quasi-elastic if it has properties similar to the basic characteristics of the $\pi - p$ elastic interaction at the same energy. We have chosen as one such basic property the distribution of the invariant four-momentum transfer $t = (q_1 - q_2)^2$ (where $q_1^2 = q_2^2 = m_\pi^2$) between the incident and the scattered π. (q_1 and q_2 are the four momenta of the incident and scattered π and m_π is the rest mass of the pion.) The rapid, approximately exponential decrease of the differential scattering cross-section (or of the distribution of t) with increasing $|t|$ is one of the most characteristic properties of the high-energy strong elastic interaction. The choice of the t distribution is also motivated by its independence of the coordinate system used.

In order to compare a sample of inelastic events with a sample of elastic ones from the point of view of the t distribution, we have to select in each inelastic event a secondary π and consider it as the quasi-elastically scattered primary. For this purpose several selection criteria can be conceived. In the present investigation we selected the quasi-elastically scattered π in two different ways using selection criteria which are independent of the frame of reference:

1. Selection of secondary pions produced in reactions of the type

$$\pi^- + p \to p + \pi^- + k\pi^\circ, \qquad (k = 1, 2, \ldots) \tag{1}$$

and

$$\pi^- + p \to n + \pi^- + \pi^+ + k'\pi^\circ, \quad (k' = 0, 1, \ldots) \tag{2}$$

according to their *charge*.

2. Selection of secondary pions according to their *four-momentum transfer.* Namely, let us assume that the quasi-elastically scattered primary emerges as the secondary having the smallest $|t|$ value among all the π^+, π^- and π° secondaries of the given event.* (This criterion can be applied also for many-prong events.) Due to the lack of data on π°-mesons, in the present paper this criterion could be applied only to the charged pions of interactions of type (2).

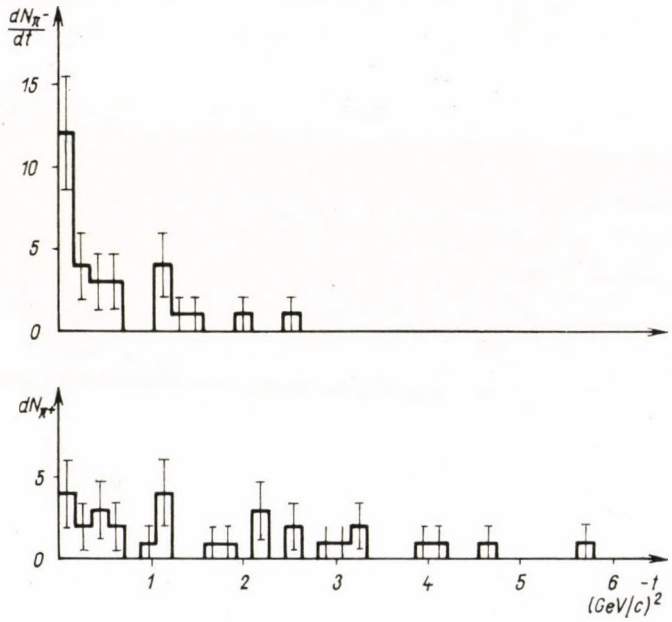

Fig. 1. Four-momentum transfer distribution for a) π^--mesons and b) π^+-mesons produced in

$$\pi^- + p \to n + \pi^- + \pi^+ + k'\,\pi^\circ \qquad (k' = 0, 1, \ldots)$$

interactions at 7 GeV/c

Applying the first selection criterion we have calculated the t distribution separately for π^- and π^+-mesons produced in interactions of type (2) at 7 GeV/c measured by the Berlin group [6] with the 24 l propan chamber of the Joint Institute of Nuclear Research, Dubna (Fig. 1).** It can be seen clearly that the t distribution of π^--mesons is rapidly falling off, a feature characteristic of elastic scattering, while the t distribution of π^+-mesons is rather flat with a long tail. The difference between the two distributions is significant.

* This secondary pion has generally the largest energy in the laboratory system and is emitted strongly forward in the $\pi - p$ C. M. S. a selection criterion often used by other authors.

** The histograms in Figs. 1—5 are actually cut off at values of $|t| \ll \mu^2$ for purely kinematical reasons.

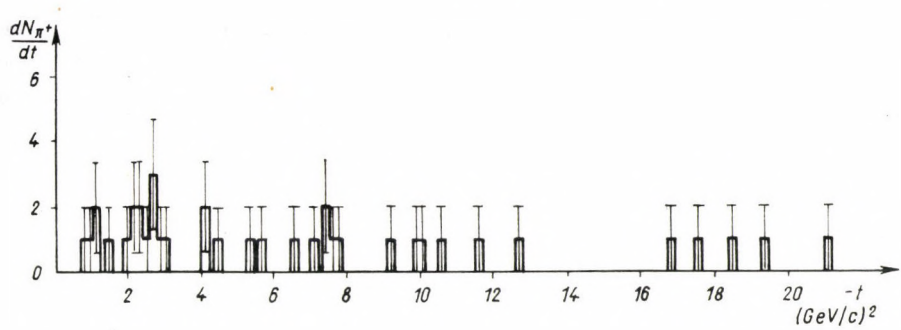

Fig. 2. Four-momentum transfer distribution for π^+-mesons produced in

$$\pi^- + p \to n + \pi^- + \pi^+ + k' \pi^0 \qquad (k' = 0, 1, \ldots)$$

interactions at 16 GeV/c

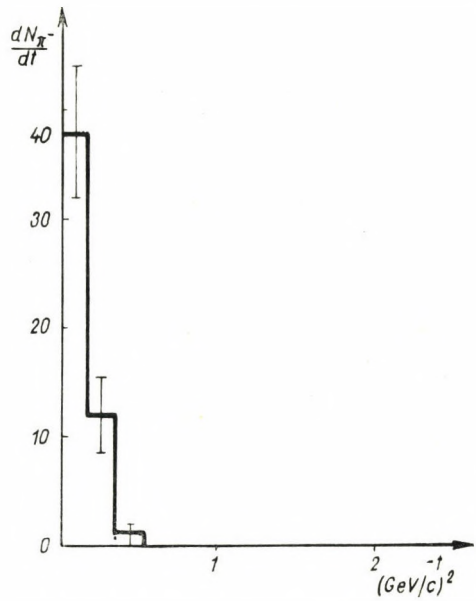

Fig. 3. Four-momentum transfer distribution for π^--mesons produced in

$$\pi^- + p \to p + \pi^- + k\pi^0 \qquad (k = 1, 2, \ldots)$$

interactions at 7 GeV/c

Similar results have been found for the t distribution of π^+-mesons produced in interactions of the same type at 16 GeV/c measured by MORRISON [2] with the CERN 32 cm hydrogen chamber (Fig. 2).

The rapid falling off of the t distribution of π^--mesons shown in Fig. 1 manifests itself also i) in the t distribution of π^--mesons produced in interactions of the type (1) at 7 GeV/c as obtained from the emulsion measurements

of the collaborating groups in Alma-Ata, Berlin, Budapest, Dubna and Prague (Fig. 3) and ii) in the t distribution of π^--mesons produced in both reactions (1) and (2) at 16 GeV/c as calculated from the experimental data by MORRISON [2] (Fig. 4).

Applying the second selection criterion we have calculated the t distribution of the quasi-elastically scattered pions produced in interactions of

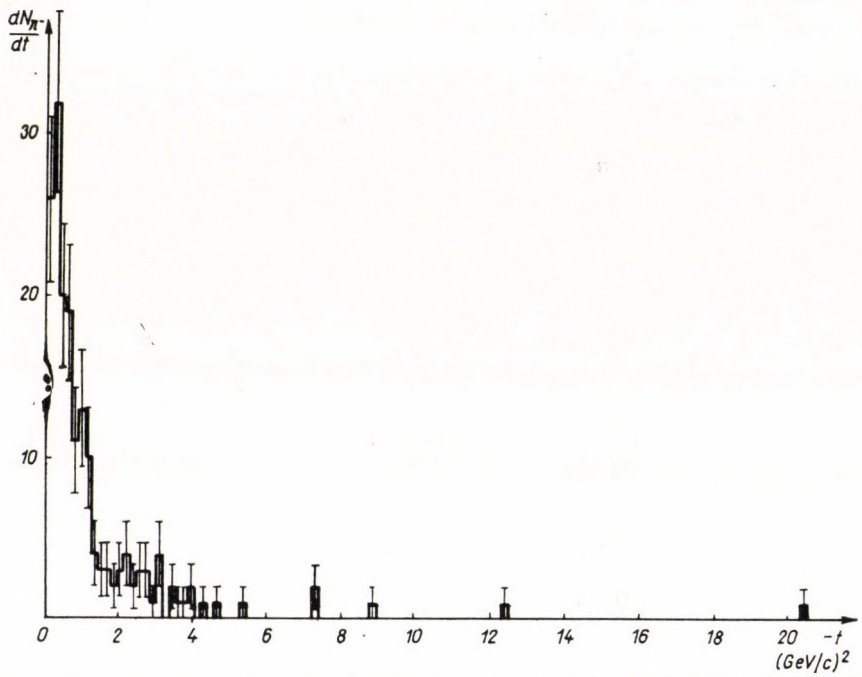

Fig. 4. Four-momentum transfer distribution of π^--mesons produced in the reactions

$$\pi^- + p \to p + \pi^- + k\pi^0 \qquad (k = 1, 2, \ldots)$$

and

$$\pi^- + p \to n + \pi^- + \pi^+ + k'\pi^0 \qquad (k' = 0, 1, \ldots)$$

at 16 GeV/c

type (2) at 7 GeV/c [6] (Fig. 5). The rapid falling off of this distribution is still more pronounced than in the former case obtained for π^--mesons. Furthermore it can be seen from Fig. 5 that the quasi-elastically scattered pion emerges as π^+ in about 1/4 of the cases, consequently "charge-exchange diffraction scattering" cannot be neglected [5].

From the above results we can conclude that in the inelastic two-prong $\pi^- - p$ interactions the incident pion undergoes a quasi-elastic scattering and has a certain tendency to maintain its charge.

We would like to point out that it is not possible to interpret the *quasi-elastic character* of the analysed sample as the result of a simple Regge-

pole exchange since the condition $z \gg 1$ in $P_{\alpha(t)}(-z)$ (where $P_{\alpha(t)}(-z)$ is the well-known Legendre function applied in the Regge formalism of scattering theory) necessary for the dominance of a Regge-pole is not fulfilled in the great majority of our events.

The authors are very much indebted to the laboratories in Alma-Ata, Berlin, Dubna, and Prague for letting us have their experimental data. It is also a pleasure to thank to Drs. G. Domokos, K. Lanius, D. R. O. Morrison and P. Surányi for valuable discussions.

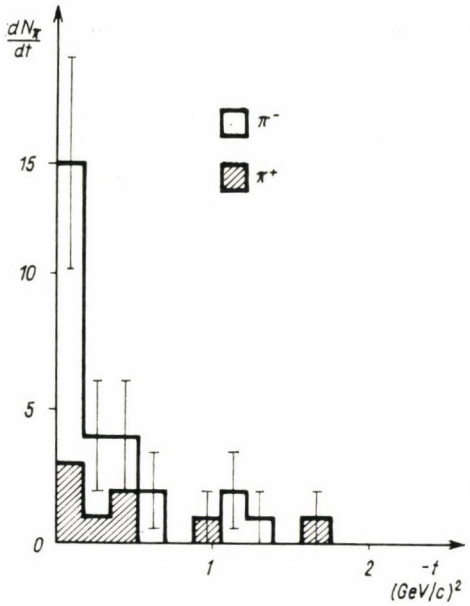

Fig. 5. Four-momentum transfer distribution of the quasi-elastically scattered pions produced in

$$\pi^- + p \to n + \pi^- + \pi^+ + k'\pi^\circ \qquad (k' = 0, 1, \ldots)$$

interactions at 7 GeV/c. The quasi-elastically scattered pions were selected by applying the second criterion. The shaded area corresponds to the contribution of π^+-mesons

REFERENCES

1. D. R. O. Morrison, Proc. Int. Conf. on Theor. Aspects of Very-High Energy Phenomena, CERN 61—22 (Geneva, 1961) p. 153; D. R. O. Morrison, Proc. Int. Conf. on Elementary Particles, Aix-en-Provence, Vol. 1 (Saclay: C. E. N., 1961) p. 407.
2. D. R. O. Morrison, Proc. Int. Conf. on High Energy Physics at CERN (Geneva 1962), p. 606.
3. G. Bellini, E. Fiorini, A. J. Herz, P. Negri and S. Ratti, Proc. Int. Conf. on High Energy Physics at CERN (Geneva 1962), p. 613.; G. Bellini, E. Fiorini, A. J. Herz, P. Negri, S. Ratti, C. Baglin, H. Bingham, M. Bloch, D. Drijard, A. Lagarrigue,

P. MITTNER, A. ORKIN-LECOURTOIS, P. RANCON, A. ROUSET, B. DE ROAD, R. SALMERON and R. VOSS, Nuovo Cimento, **27**, 816, 1963.
4. G. BOZÓKI, E. FENYVES, A. FRENKEL and E. GOMBOSI, Nuovo Cimento, **27**, 668, 1963.
5. M. I. FERRERO, C. M. GARELLI, A. MARZARI CHIESA and M. VIGONE, Nuovo Cimento, **27**, 1066, 1963.
6. Unpublished data. The authors are very much indebted to dr. LANIUS for letting them have these experimental data prior to publication.

О КВАЗИ-УПРУГОМ ХАРАКТЕРЕ НЕУПРУГИХ ДВУХЛУЧЕВЫХ $\pi^- - p$ ВЗАИМОДЕЙСТВИЙ ПРИ 7 И 16 Гэв/с.

Г. БОЗОКИ, Е. ФЕНЬВЕШ, А. ФРЕНКЕЛЬ и Е. ГОМБОШИ,

Р е з ю м е

Квази-упругий диффракционный характер неупругих двухлучевых $\pi^- + p$ взаимодействий подтверждается изучением распределения квадрата передачинного импульса t. Сходство t-распределения вторичных π^- мезонов с t-распределением упругого $0^- - p$ рассеяния указывает на то, что первичный п ион рассеивается квази-упруго и имеет тенденцию сохранить свой заряд.

DETERMINATION OF THE FREQUENCY OF VARIOUS TYPES OF EVENTS BY THE MAXIMUM LIKELIHOOD METHOD

By

ÉVA GOMBOSI and L. JÁNOSSY

CENTRAL RESEARCH INSTITUTE OF PHYSICS, LABORATORY FOR COSMIC RAYS, BUDAPEST

(Received 30. I. 1964)

The actual intensity of nuclear events and the statistical fluctuation of this value have been determined by means of the Maximum Likelihood Method from the number of events found in emulsion plates scanned l times. At the same time investigations were made on scanning efficiency to solve the problem whether, in order to reduce statistical errors, it is better to scan a small surface several times or a larger one less often.

1. Brief outline of the problem

When scanning emulsions* we often try to ascertain the rate of a certain type of event to be found in the emulsion. Denote the type of event, e.g. stars with some given specification, as the event "a". The number of such events produced in the emulsion in the course of exposre may be N.

Physically not N itself but its expected valuue

$$A = \langle N \rangle$$

is of interest. Indeed, exposing similar emulsions under similar conditions the total number N of events "a" produced by the irradiation will show random fluctuation around the expected number A of events.

When the emulsion is scanned for events of the type "a" each individual event is found in one scanning with a probability p, the quantity p being characteristic of the scanner and also of the type of event which is looked for. As a rule neither the "intensity" A nor the probability p are known.

In the following by using the Maximum Likelihood Method (MLM) we shall determine measured values $\bar{A}$ and $\bar{p}$ of A and p. The measured values thus obtained have minimum scatter. Further we consider the problem of how to spend the time available for scanning in a way that ensures greatest efficiency.

* The method described here is applicable not only to the case of nuclear emulsion plates but also to the evaluation of cloud- and bubble chamber and hodoscope experiments.

2. Determination of the frequency of events

Consider a material which has resulted from the l-fold scanning of an emulsion plate. In these scannings there will have been events "a" which were found exactly once, twice,..., l times. Let us denote the number of these events by $N_1, N_2, \ldots, N_l$ and by k the total number of events found in the process of scanning. Thus we have

$$k = \sum_{i=1}^{l} N_i .$$

The probability that precisely N_1 events will be found only once,..., and N_l events l times is given by a Poisson distribution:

$$W(N_1, \ldots, N_l, A_1, p) = \prod_{i=1}^{l} e^{-AP_i} (AP_i)^{N_i} \frac{1}{N_i!} = e^{-A(1-P_0)} A^k \prod_{i=1}^{l} \frac{P_i^{N_i}}{N_i!},$$

where P_i is the probability that by scanning the plate l times an event will be found precisely i times:

$$P_i = \binom{l}{i} p^i (1-p)^{l-i}.$$

By means of the MLM the values $\bar{A}$ and $\bar{p}$ as well as their scatters can be obtained from the following relations:

$$\left[\frac{\partial \ln W}{\partial A}\right]_{A=\bar{A}, p=\bar{p}} = 0 , \tag{1}$$

$$\left[\frac{\partial \ln W}{\partial p}\right]_{A=\bar{A}, p=\bar{p}} = 0 , \tag{2}$$

$$\langle (\delta \bar{A})^2 \rangle = \frac{W_{pp}}{W_{AA} W_{pp} - W_{Ap}^2} , \tag{3}$$

$$\langle (\delta p)^2 \rangle = \frac{W_{AA}}{W_{AA} W_{pp} - W_{Ap}^2} , \tag{4}$$

where

$$W_{pp} = -\frac{\partial^2 \ln W}{\partial p^2}, \quad W_{AA} = -\frac{\partial^2 \ln W}{\partial A^2}, \quad W_{Ap} = -\frac{\partial^2 \ln W}{\partial A \, \partial p} . \tag{5}$$

Substituting now $K = \sum_{i=1}^{l} iN_i$, we obtain from equations (5)—(9)

$$\bar{A} = \frac{k}{1-(1-\bar{p})^l} = \frac{K}{l\bar{p}},$$

$$\frac{\bar{p}}{1-(1-\bar{p})^l} = \frac{K}{lk}, \tag{6}$$

$$\langle(\delta\bar{A})^2\rangle = \bar{A}\,\frac{1 - l\bar{p}\,(1-\bar{p})^{l-1}}{1 - l\bar{p}\,(1-\bar{p})^{l-1} - (1-\bar{p})^{l}}\,,$$

$$\langle(\delta\bar{p})^2\rangle = \frac{1}{\bar{A}l}\,\frac{\bar{p}\,(1-\bar{p})[1-(1-\bar{p})^{l}]}{1 - l\bar{p}\,(1-\bar{p})^{l-1} - (1-\bar{p})^{l}}\,. \tag{7}$$

In order to simplify the computations required in an actual experiment graphs are given which permit to determine the quantities in question immediately from the measured values.

Thus in a given experiment K has to be calculated and then from the given graphs 1 and 2 the values of $\bar{A}$ and $\langle(\delta\bar{A})^2\rangle$ can be read off immediately.

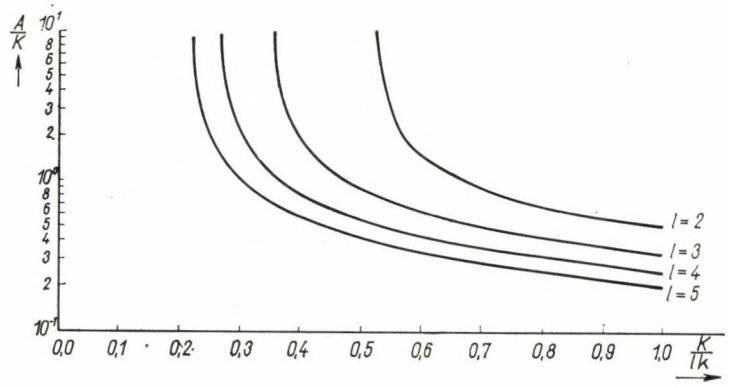

Fig. 1

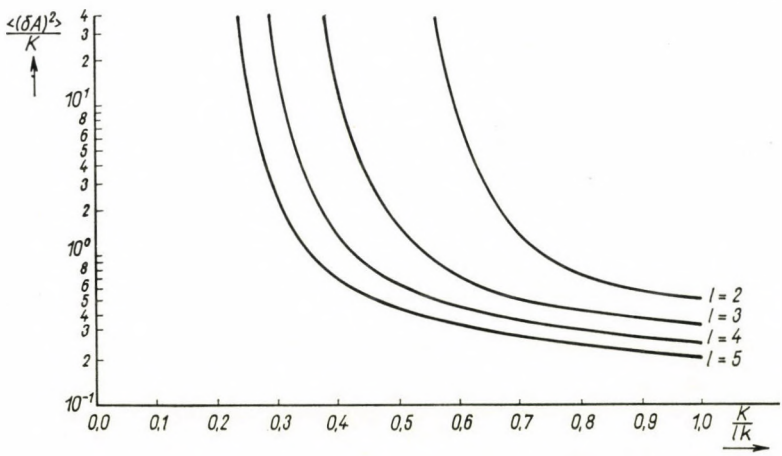

Fig. 2

3. The optimum number of scannings

Now the question arises what is the best choice of l ? It is clear that each scanning gives some new information, and therefore the accuracy of $\bar{A}$ and $\bar{p}$ increases monotonically with l.

However, if we intend to spend a specified length of time on scanning, we can put the question, whether it is more useful to scan a large area a few times, or a smaller area several times.

If a plate having surface F is scanned l times, the intensity $\bar{A}$ and the statistical error of this value are given by eqs. (6) and (7). Now, if the surface of the plate is $f = F/\gamma$, the scanning times being equal, this plate can be scanned $L = l\,\gamma$ times. The number of events to be expected in a plate having surface f is $\langle N_f \rangle = A'f = a$. This value, as obtained with the MLM is given by

$$\bar{a} = \frac{K}{L\bar{p}}$$

and for its statistical error we have

$$\langle (\delta \bar{a})^2 \rangle = \bar{a}\,\frac{1 - L\bar{p}\,(1-\bar{p})^{L-1}}{1 - L\bar{p}\,(1-\bar{p})^{L-1} - (1-\bar{p})^{L}} \,,$$

from which the intensity $\bar{A}'$ can be expressed as

$$\bar{A}' = \frac{\bar{a}}{f}$$

and the statistical error as

$$\langle (\delta \bar{A}')^2 \rangle = \frac{\bar{a}}{f^2}\,\frac{1 - L\bar{p}\,(1-\bar{p})^{L-1}}{1 - L\bar{p}\,(1-\bar{p})^{L-1} - (1-\bar{p})^{L}} \,. \tag{8}$$

If we note that $\bar{a} = \dfrac{f}{F}\,\bar{A} = \dfrac{\bar{A}}{\gamma}$, upon multiplying by l (8) becomes

$$l\,\langle (\delta \bar{A}')^2 \rangle = \frac{\bar{A}}{F^2}\,L\,\frac{1 - L\bar{p}\,(1-\bar{p})^{L-1}}{1 - L\bar{p}\,(1-\bar{p})^{L-1} - (1-\bar{p})^{L}} \,.$$

Thus γ has to be so chosen that the condition

$$\frac{\partial}{\partial \gamma}\,[l\,\langle (\delta \bar{A}')^2 \rangle] = 0$$

is satisfied.

Thus

$$\frac{\partial}{\partial\gamma}\left[l\langle(\delta\bar{A}')^2\rangle\right] = \frac{\partial}{\partial L}\left[l\langle(\delta\bar{A}')^2\rangle\right]\frac{\partial L}{\partial\gamma} = l\frac{\partial}{\partial L}\left[l\langle(\delta\bar{A}')^2\rangle\right] = 0\,,$$

$$\frac{\partial}{\partial L}\left[l\langle(\delta\bar{A}')^2\rangle\right] = 0\,.$$

The result of this extreme-value problem, taking into account that l may have only the values 2, 3, 4, ..., gives the number of scannings required if the probability of finding the event is p. The computed values are shown in Table I.

Table I

Interval of probability	Number of scannings
$1 < p < 0{,}53$	2
$0{,}53 < p < 0{,}38$	3
$0{,}38 < p < 0{,}30$	4
$0{,}30 < p < 0{,}25$	5

The problem has still to be considered what happens when p is not a constant. We hope to come back to this question in a later paper. We note, however, that to get information on whether a material is consistent with the assumption of constant p requires the results of several scannings.

ОБ ОПРЕДЕЛЕНИИ ЧАСТОТЫ СОБЫТИЙ РАЗЛИЧНЫХ ТИПОВ МЕТОДОМ НАИБОЛЬШЕГО ПРАВДОПОДОБИЯ

Е. ГОМБОШИ и Л. ЯНОШИ

Р е з ю м е

Определялась действительная интенсивность событий методом наибольшего правдоподобия и её статистическая флуктуация из числа событий, получаемых при l-кратном просмотре эмульсионных пленок ядра. Исследовался также тот вопрос, что с точки зрения доступной точности при одном и том же времени просмотра пленок, что является более преимущественным: многократный просмотр небольших поверхностей или небольшое число просмотров больших поверхностей плёнки.

COMMUNICATIO BREVIS

EFFECT OF THE SOLVENT ON THE FLUORESCENCE SPECTRUM OF TRYPAFLAVINE AND FLUORESCEIN

By

L. SZALAY and E. TOMBÁCZ

INSTITUTE OF EXPERIMENTAL PHYSICS, THE UNIVERSITY, SZEGED

(Received 21. IX. 1963)

In connection with recent investigations carried out at our Institute and concerning the polarization of fluorescence in various dyestuff solutions of different glycerol content several absorption and emission spectra had been determined in the visible range in order to control the purity acquired by the samples and to adapt these spectra to certain calculations related to the polarization of fluorescence. Meanwhile some features of the influence of the solvent on the position of these spectra have been found which may be considered interesting in themselves.

1. Both the absorption and emission spectra [$\varepsilon(\lambda)$ and $f_q(\lambda)$] were obtained with a photoelectric spectrophotometer (Optica Milano CF—4). $f_q(\lambda)$, the true normalized emission quantum spectrum (corrected for secondary fluorescence) was determined by a method given in [1] using exciting light of 460 mμ or 440 mμ wavelength (the half band width was about 6 mμ).[1] The solutions to be investigated were composed of trypaflavine (in a concentration of $5 \cdot 10^{-4}$ mol/l), acetic-acid (in a concentration of 2 per cent) and glycerol-ethanol mixtures (in different compositions shown in Fig. 1 and Table I).

The results are shown in Fig. 1. For a better comparison of the shift of the maxima with the glycerol content, both the absorption and emission spectra are represented in arbitrary units. As it is seen the absorption spectra of the different solutions coincide, the emission spectra, however, exhibit — small but well marked — shifts of the maxima towards the higher wavelengths with increasing glycerol amounts. The half band widths of the emission spectra, being about 48 mμ and 52 mμ in solutions possessing glycerol concentrations of 0 per cent and 88,2 per cent, respectively, are the broader, the higher is the glycerol concentration of the solution. The total emitted energy ($E = \int_0^\infty f_q(\lambda)\, d\,\lambda$) decreases with increasing glycerol amount. Taking

[1] The condition for the layer thickness $l \leqslant 0{,}1 \cdot \ln 10 \cdot \varepsilon(\lambda)_{max} = 5{,}2$ cm was fulfilled (actually $l = 0{,}10$ cm was chosen), consequently — according to [1] — the photometer values of the emission spectra need not be corrected for secondary luminescence by calculations.

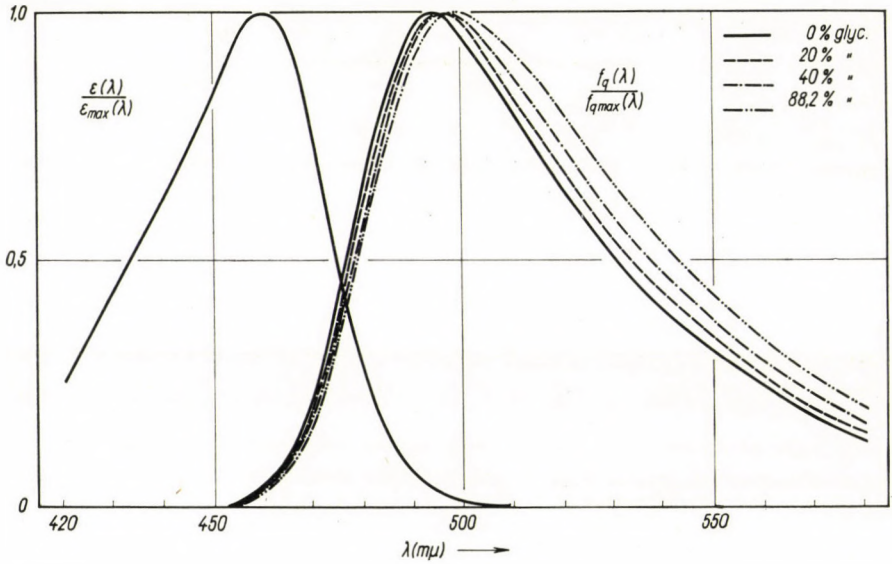

Fig. 1

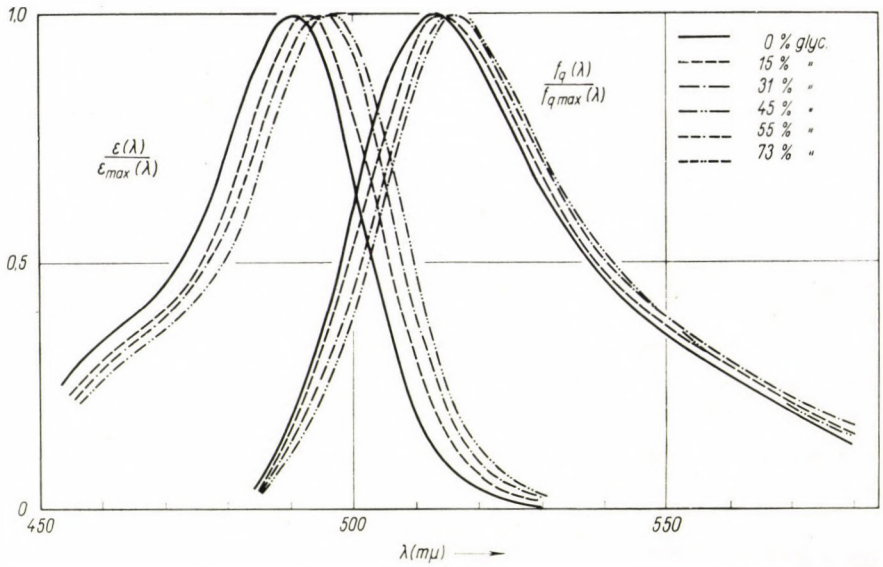

Fig. 2

the emitted total energy of a solution of 0 per cent glycerol content arbitrarily as $E_0 = 1$, there is $E_{19,6} = 0{,}95$; $E_{39,2} = 0{,}89$; $E_{58,8} = 0{,}86$; $E_{78,4} = 0{,}85$; $E_{88,2} = 0{,}89$.

In connection with the behaviour of trypaflavine, it seems worth while to remind the reader of the results of similar investigations referring to fluor-

escein[2] given in [2]—[3] and shown in Fig. 2. In this case both the absorption and emission spectra are shifted towards higher wavelengths with increasing glycerol concentration.

2. According to FÖRSTER [4] the critical distance between two molecules, characteristic of the migration of energy is given by the expression

$$R_0 = \sqrt[6]{\frac{9\,\varkappa^2\,(\ln 10)^2\,c\tau\,I_\nu}{16\,\pi^4\,n^2\,N'^2\,\nu_0^2}}\,, \tag{1}$$

where $c(= 3 \cdot 10^{10}\ \mathrm{cmsec}^{-1})$; τ, n, ν_0 and I_ν denote the velocity of light, the mean lifetime of the excited state, the refractive index of the solution, the

Table I

τ and R_0 for trypaflavine in glycerol-ethanol mixtures

Glycerol %	0,0	19,6	39,2	58,8	78,4	88,2
τ in ns	4,00	4,05	3,90	3,80	3,63	3,60
R_0 in Å	39,7	38,7	36,6	35,5	34,5	34,8

frequency of the mirror symmetry of the absorption and fluorescence spectrum and the product integral of the absorption and emission spectrum, respectively. $N' = 6{,}02 \cdot 10^{20}$ and $\varkappa^2 = 2/3$ in isotropic solutions ($\varkappa^2$ is a factor depending in general on the mutual orientation of the absorption and emission oscillators).[3] R_0 is the distance between two such solute molecules for which the migration of energy has the same probability as the emission of the primary excited molecules. In [4] an estimate of $R_0 = 50$Å is given for fluorescein in water and the lack of necessary data for eq. (1) is mentioned in cases of viscous solutions. The present measurements rendered possible the calculation of R_0 in viscous solutions as well. In the case of trypaflavine $\tau = 4{,}00$ ns was taken for ethanol solution [6] and for glycerol ethanol mixtures τ was calculated according to [7]. Table I contains the results obtained. Similar calculations using the results given in (2) and (3) lead to the values summarized in Table II for fluorescein solutions.

$\tau = 5{,}05$ ns was taken for the solution containing 60 per cent glycerol,[4] for the different glycerol mixtures τ was calculated according to [7]. In the

[2] The solutions were composed of $1 \cdot 10^{-4}$ mol/l fluorescein, 2 per cent NaOH and glycerol-water mixtures (in different compositions shown in Fig. 2 and Table II).

[3] In (5) a modified formula containing the absolute quantum yield is given, which results in somewhat smaller R_0 values (see also in [6]). At present, however, eq. (1) was used.

[4] τ was fluorometrically determined by J. HEVESI.

case of trypaflavine solutions (see Table I) R_0 is decreasing with the increase of the glycerol amount; in the case of fluorescein solutions, however, R_0 is practically independent of the glycerol amount of the solution (see Table II).

Table II

τ and R_0 for fluorescein in glycerol-water mixtures

Glycerol %	0,0	15,0	31,0	45,0	60,0	73,0	96,0
τ in ns	4,56	4,42	4,17	4,88	5,05	4,25	4,25
R_0 in Å	53,9[5]	54,2	54,1	53,7	53,4	53,7	53,2

$$R_{0,\text{mean}} = 53{,}7^{6}$$

Consequently, it may be concluded that the dependence of R_0 on viscosity is not always of the same character; trypaflavine in glycerol-ethanol mixtures and fluorescein in glycerol-water mixtures are representing two typical cases of different behaviour. Why is R_0 changed in trypaflavine solutions and why is it unchanged in fluorescein solutions when the glycerol amounts are altered in both cases? This is a question which is connected with the shift of the spectra.[7]

3. As for the shift of the spectra with increasing glycerol amounts the cases of trypaflavine and of fluorescein considerably differ. In the case of trypaflavine solutions the difference of the influence of the solvent on the absorption and emission spectra may be associated with a difference in the strength of the interaction of the solvent with the solute molecule in the ground and the excited state. In fluorescein solutions, where the influence of the solvent is practically of the same type on both the absorption and emission spectra, no significant difference can occur in the strength of the interactions in the ground and the excited state.

In [8] it is supposed that the microstructure of the solvent around the solute molecules will change when these go over into the excited state. This, however, can be established through the effect of the solvent on the fluorescence spectra only in cases where the lifetime of the excited state (τ) is greater

[5] This value is smaller than that given in [4] (50 Å).

[6] The modified formula given in [5] and [6] yields a mean value of 52,0 Å.

[7] According to [9] n_{AB}, the number of processes involving energy transition between the particles A and B in unit time decreases with the increase of viscosity of the solution. $n_{AB} = \frac{1}{\tau}\left(\frac{R_0}{R_{AB}}\right)^6$ (R_{AB} is the distance of the particles A and B); Tables I and II show that in trypaflavine solutions n_{AB} decreases when the viscosity is increased, in fluorescein solutions, however, it remains practically unchanged.

than the time required for the rearrangement which latter is characterized chiefly by the relaxation time of the solvent (τ'). Accepting these considerations the effect of the solvent described above may be explained.

Since $\tau \approx 4$ ns $> \tau' \approx 0.01$ ns — 1 ns in both cases, the different behaviour of the two systems may only be understood by assuming a different behaviour of the solute particles relative to their surroundings even in the ground state. In the case of fluorescein solutions investigated the particles capable to fluoresce are negative ions, thus hydrogen bonds between the solute and solvent may possibly be formed (similarly as it was supposed in [8] in the case of excited acetylanthracene in hydroxyl-containing solvents) even in the ground state. This phenomenon can not occur in trypaflavine solutions where the fluorescing particles are positive ions. The effect of the solvent in trypaflavine solutions is thought to represent a case of weaker close-order interaction between solvent and solute molecules predicted in [8], the effect of the solvent in fluorescein solutions, however, is supposed to be determined chiefly by the macroscopic properties of the solvent (as it was mentioned in [3]). These differences lead to a decreasing or unchanged overlap of the absorption and emission spectra resulting in a decrease and constancy of R_0 in trypaflavine and fluorescein solutions, respectively.

REFERENCES

1. I. KETSKEMÉTY, J. DOMBI, R. HORVAI, J. HEVESI and L. KOZMA, Acta Phys. Chem. Szeged, **7**, 17, 1961.
2. L. GÁTI, Diss., Szeged, 1958.
3. L. GÁTI and L. SZALAY, Acta Phys. Chem. Szeged, **5**, 87, 1959.
4. TH. FÖRSTER, Fluoreszenz Organischer Verbindungen, Vandenhoeck und Ruprecht, Göttingen, 1951.
5. I. KETSKEMÉTY, Cand. diss. Szeged, 1963.
6. L. SZALAY and B. SÁRKÁNY, Acta Chem. Phys., Szeged, **8**, 25, 1962.
7. S. I. STRICKLER and R. A. BERG, J. Chem. Phys., **37**, 814, 1962.
8. A. S. CHERKASOV and G. I. DRAGNEVA, Opt. Spectr. USSR, **10**, 466, 1961.
9. A. WEINREB and H. KALLMANN, Luminescence of Organic and Inorganic Materials. John Wiley and Sons Inc., 1962, p. 44.

RECENSIONES

ALLADI RAMAKRISHNAN

Elementary Particles and Cosmic Rays

Pergamon Press, Oxford—London—New York—Paris, 1962.

"Elementary Particles and Cosmic Rays", the work of ALLADI RAMAKRISHNAN, Professor of the University of Madras, Director of the Institute of Mathematical Sciences in Madras, is the result of an interesting experiment. It does not follow in the steps of monographs dealing minutely with the problems of one special narrow field, but offers a wide spectrum of subjects to its readers. It surveys all those fundamental principles, formalisms, methods and ideas which may today be considered to belong indispensably to the basic knowledge of those who deal with the physics of elementary particles and cosmic rays.

In the preface the author describes with engaging sincerity and modesty the circumstances under which the book came to be produced. At the suggestion of Prof. HEITLER he planned to write about the theory of the phenomena of cosmic radiation. While writing the introduction to the quantum theory — yielding to temptation — he became absorbed in the exciting problems of the fundamental theory of elementary particles. Therefore two-thirds of the book are taken up by chapters about quantum and field theory, and the physics of fundamental elementary particles.

"The writing of any text book is considered a drudgery, but to me it has been a most profitable and exciting experience" — writes the author in the preface. This circumstance, which certainly exerted a favourable influence on the didactic structure of the book, the author ascribes first to his personal contacts with prominent physicists, established during his journeys in Japan, in the United States of America and in Europe, secondly to the ardent cooperation of his pupils and to the constructive debates in connection with various chapters of the book.

Excitement and enthusiasm, felt for the theory and exciting mysteries of the physics of elementary particles, emanate from this book, together with the humility necessarily felt by a researcher facing the secrets of nature and striving to find the explanation of phenomena.

In his preface the author underlines service to scientific education in India as one of his chief aims. "This book is just the projection of the newly awakened hopes and aspirations of the young scientific community in my home town and university and its nascent interest in mathematical sciences." There can be no doubt, that by his aim the author endeavours to meet a demand manifested in the present period of the expansion of scientific research activity all over the world.

The book opens with the introduction of the fundamental postulates of quantum mechanics, the principles of complementarity and superposition. After a survey of the single particle wave equations (PAULI, KLEIN-GORDON and WEYL equations) the first chapter ends with a review of wave mechanics of the photon, based on the well-known monograph of AKHIEZER and BERESTETSKY. The second chapter, dealing with quantum electrodynamics describes the perturbation methods and their applications (COMPTON effect, annihilation, bremsstrahlung, pair production, electron-electron interaction), furthermore the problem of self-energy, the anomalous magnetic moment, the LAMB-shift, and finally the removal of divergences. The formalism of quantum field theory is the theme of the third chapter; within this the chapter deals with perturbation expansions, with the character of the interaction, WICK's theorem, with the use of HEISENBERG operators (based on KÄLLEN's Handbuch article), with propagators, and finally with the principles of invariance and the conservation laws. In the fourth chapter pion physics is discussed, beginning with the basic experimental facts and low-energy pion-nucleon interaction; a historical review follows describing the theoretical attempts (weak coupling, strong coupl-

ing and phenomenological theories), then a short report is given of HEITLER's theory of radiation damping and the TAMM—DANCOFF approximation, ending with a discussion of pion-nucleon scattering and photomeson production within the framework of CHEW—LOW formalism. The fifth chapter of only eighteen pages, gives an account of the non-perturbative approach (LEHMANN—SYMANZIK—ZIMMERMANN) to the problem of quantum fields in strong interaction, the method of dispersion relations, including the MANDELSTAM representation of the scattering amplitude. This is followed by the treatment of the problematics of strange particles in considerable detail. The sixth chapter first reviews the types of interaction which play a part in the processes of elementary particles, the selection rules operative in the course of the formation of strange particles, and further with the effective cross-section correlations following from the assumption of charge independence, and the chief questions of weak decay processes ($\tau - \vartheta$ puzzle, kinematics, decay of neutral caons, $|\Delta I| = 1/2$ rule). The seventh chapter deals with weak interactions and gives a detailed account of the violation of P and C invariances and some older and some more recent ideas concerning the universal FERMI interaction, finally it touches on the open questions of the theory. The eighth chapter summarizes the experimental results concerned with the scattering processes of caons, the hypernuclei and the relative parity between strange particles. The nineth chapter is devoted to the symmetry properties of strong interactions; the D'ESPAGNAT—PRENTKI' scheme, the hypothesis of global and cosmic symmetries; furthermore the mass formula of PAIS, SALAM-POLKINGHORNE and FEYNMAN, and the philosophical ideas which relate to this; about the model of FERMI—YANG, SAKATA and GOLDHABER, finally HEISENBERG's nonlinear theory. The "fundamental" part of the book which is complete in itself ends here.

The second part dealing with cosmic radiation is also a whole in itself and can be studied separately. It is divided into five chapters. The first, i.e. the tenth in the book, deals with primary cosmic radiation, its mass- and energy spectrum, its spatial distribution and time variations. The eleventh chapter on the geomagnetic effects describes, based on JÁNOSSY's well-known monograph, the motion of a charged particle in the field of a magnetic dipole, (the STÖRMER-cone theory) and touches on the problem of the latitude effect. Dealing with interactions of cosmic rays with matter, the twelfth chapter gives survey of the various theories of multiple production of particles (HEISENBERG, LEWIS—OPPENHEIMER—WOUTHUYSEN, FERMI, PEASLEE—TAGAKI, LANDAU—POMERANCHUK, SUDARSHAN—SRIVASTAVA, BHABHA). The length of the thirteenth chapter on cascade processes and the detailed mathematical treatment reveal that this is a favourite subject of the author. The last, relatively brief fourteenth chapter deals with the origin of cosmic radiation.

The Appendix of more than fifty pages contains good summaries of the general conceptions, useful mathematical aids and a collection of formulas. Thus a survey is given of the dimensions and units of physical quantities, the employed units, the most important formulas of the much-used CLEBSCH—GORDAN coefficients and the WIGNER $3j$, $6j$, $9j$ symbols. The following further sub-titles are included in the Appendix: The Density of States, Relativistic Transformation, Invariant Fun ction, Quantization of the Equivalence of the FEYNMAN and S-matrix Formalisms, On the Connection between Spin and Statistics, Phase Shift Analysis of Scattering, Resonance States of Strongly Interacting Particles, Gauge Theories of Elementary Particles, The Principle of Equivalence for all Strongly Interacting Particles.

The above description shows that the book — though not a monograph discussing in detail a special subject — cannot be considered a textbook either, which may be followed for instance in a university lecture-course. The senior university student, following up a subject on his own, a research-worker reading for a scientific degree or doing scientific research is given a useful hand-book, which offers basic information in the field of elementary particles and gives a good survey of the physical principles which form the basis of the sometimes complicated mathematical formalism and which deals with questions still under discussion. With its ready approach to problems and its abundant references to the literature, the book may well serve as a guide to further, more intensive studies. Written in an advanced didactic spirit and a polished style, the book is published and excellently produced by Pergamon Press.

G. GYÖRGYI

Halbleiterprobleme VI Tagung Erlangen 1960.

Herausgegeben von Prof. Dr. F. SAUTER, Köln. Verlag Fr. Vieweg und Sohn, Braunschweig. VIII + 345 Seiten, 234 Abbildungen. — Preis DM 48. —

"Halbleiterprobleme VI" comprises the general lectures of the 1960 national semiconductor conference in Erlangen, Federal Republic of Germany. Due to the national character of the conference, the topic covers a somewhat wider field than is customarily understood under this heading. It should be pointed out first that practical applications are also discussed, and second, that an everincreasing tendency makes itself felt nowadays to transfer the concepts, so successfully developed in the case of Ge and Si, to oxide semiconductors as well, motivated undoubtedly by the possibility of new technical applications. The intermetallic semiconductors are notable by their absence in this volume.

Nine papers are published in the volume, the first one being a short and somewhat belated paper by G. A. BUSCH on the experimental determination of the effective mass in semiconductors and metals. The second paper by G. LAUTZ deals with the electrical properties of semiconductors at low temperatures. The experimental and theoretical advances are discussed in the light of the impurity band conduction. This concept had to be introduced, its theoretical treatment, however, is one of the most formidable problems now confronting semiconductor physics. We find a large variety of new experimental facts, the reversible breakdown, its dependence on the magnetic field, the dependence of the noise spectrum on the frequency, the phonon drag effect, etc. One can, however, hope for a substantial theoretical advance in this field in the near future. The next paper by G. H. JONKER and S. VAN HOUTEN deals with semiconducting metal oxides. The theory presented is largely phenomenological, attention being gradually directed towards the experimental determination of impurity levels in various host crystals. We are clearly in the stage of data collection yet, but important practical applications are already indicated, because of the very wide variation of conductivity with impurity content, and the large coefficient of absolute thermoelectric power. The paper of A. HOFFMANN describes the methods used for the physical determination of the impurity content of very pure silicon. It is claimed that during vacuum zone melting, some of the boron evaporates from silicon, so that after about 50—70 zone passes specific resistivity in excess of 10^5 Ohmcm can be obtained, corresponding to a boron content below 10^{11} cm^{-3}. The next paper by F. KUHRT deals with practical applications of the Hall-effect. Magnetic field measurement, contact-free pulse signal generation and multiplication by the Hall generator is discussed. U. BIRKHOFF's paper summarizes the advances in the construction of semiconductor thermoelements. Here the main problem is to find materials with a high thermoelectric power, high electrical, but low thermal conductivity. Bars of Bi_2Te_3 — one of the most thoroughly investigated materials in this connection — have been produced by powder metallurgy methods. The paper of F. LÜTY deals with electron transitions in the colour centres of alkali halides. The theoretical problems are already solved for the simplest cases, but there is an immense variety of center complexes, the interaction of which, the chemical impurities and dislocations make a fruitful field of research for still a good many years to come. F. STÖCKMANN treats of the current-voltage characteristics of ohmic contacts in semiconductors and insulators. The problem centres around the development of space charge and its effect on the charge carriers. The last paper, written by F. W. DEHMELT, informs the reader of new advances in crystal diodes and transistors, with a brief account of the parametric and tunnel diode, the four-layer diode and the tunnel transistor.

The book published by Fr. Vieweg & Sohn, Braunschweig is of the usual high-quality printing, easily readable, and is of great value to the solid state scientist and the engineer engaged in semiconductor work.

E. NAGY

I. PRIGOGINE

Introduction to Thermodynamics of Irreversible Processes

Second, revised edition, Interscience Publishers,
John Wiley and Sons, New York, London, 1961. XII + 119 p.

The aim set by the author in his booklet, the first edition of which appeared in 1955, was to give an elementary introduction to the theory of irreversible thermodynamics, as developed on the foundations given by ONSAGER in 1931, and to present at the same time applications of the theory to some simple but practically relevant problems. The author being one of the masters of classical thermodynamics and one of the pioneers of the new theory as well, it is no wonder that this astoundingly clear and concise outline was a world success and that the first edition rapidly disappeared from the bookshops. In the following years, several excellent monographs and textbooks dealing with these topics have been published, but there is no other introductory work to be found that could parallel PRIGOGINE's in its simplicity, and which at the same time is as comprehensive and suggestive. The publication of the present new, revised edition is to be warmly welcomed, the more so, as it has been enlarged by a paragraph dealing with continuous systems and by a new chapter on non-linear problems, which may stimulate the development of a coherent non-linear theory, and which itself is a remarkable contribution to this end.

From the seven chapters of the book, the first three introduce the fundamental concepts and laws of the classical theory (reversible thermodynamics or thermostatics), but in a manner different from most of the usual treatments. The main emphasis is laid on the description of the fundamental and distinctive properties of systems closed, respectively open to mass transfer, and on the deduction of the relevant balance equations for mass, energy and entropy. In chapter iii the simple manner is impressive in which the concept of entropy production is introduced, and also its explicit determination in a variety of typical irreversible processes. This procedure conveys to the reader an essential knowledge of the concepts occurring in the general theory, these being illustrated by several concrete examples of practical interest. The reader is thus well prepared for the study of ONSAGER's theory of irreversible processes given in chapter iv.

The special structure of ONSAGER's theory raises a methodological problem: though this theory is, similarly to the classical theory essentially a phenomenological one, it is nevertheless based at present to a great extent directly on considerations of a statistical nature. There is thus a gap between the foundations of the classical and the new thermodynamics, which could be eliminated only by expanding the latter also in a purely phenomenological way, such a departure from ONSAGER's original treatment having been urged recently by more than one author. PRIGOGINE, who is obviously quite aware of this dilemma, tries to diminish the existing difficulty didactically at least, by defining with the aid of the phenomenological methods of the classical theory such quantities, as are introduced in ONSAGER's theory by statistical considerations, through the fluctuation theory. The fundamentals of ONSAGER's theory, the theory of fluctuations, the theorem of reciprocity and the presentation of the underlying mechanical principle, the hypothesis of microscopic reversibility are to be found of course in chapter iv.

Chapter v and vi deal with some simpler applications, and serve rather as illustrations of the theory than as detailed discussions of the studied phenomena, complete from the practical viewpoint. In chapter vi, special attention should be called, however, to the masterly analysis of the principle of minimum entropy production and the concept of the stationary state ensuing from it. This part of the book may be easily understood by any practical chemical engineer with stationary working process units, and is a very useful guide in the handling of industrial problems. The paragraph on biological applications of the theory is also of great interest.

The last chapter deals with problems of non-linearity, the treatment being based on the theorem of GLANSDORF and PRIGOGINE concerning the differential behaviour of entropy production. This chapter is mainly a program for the elaboration of a non-linear theory, by generalization of ONSAGER's linear one. The need for such a theory is felt most urgently by chemists dealing with chemical reactions, thus the incorporation of the ideas expounded in this last chapter into the new edition has to be warmly welcomed from this side.

The whole booklet is, besides being clear and concise, more than a simple introduction, for it does not shrink back from the discussion of the most actual and difficult problems, being thus a stimulating lecture for the beginner and equally for the advanced reader. The elegant get-up and clear typography of the book represent an agreeable feature.

G. SCHAY

A kiadásért felel az Akadémiai Kiadó igazgatója Műszaki szerkesztő: Farkas Sándor
A kézirat nyomdába érkezett: 1964. II. 29. — Terjedelem: 6,75 (A/5) ív, 28 ábra, 1 melléklet

64.58533 Akadémiai Nyomda, Budapest. Felelős vezető: Bernát György

The *Acta Physica* publish papers on physics, in English, German, French and Russian.
The *Acta Physica* appear in parts of varying size, making up volumes.
Manuscripts should be addressed to:

Acta Physica, Budapest 502, Postafiók 24.

Correspondence with the editors and publishers should be sent to the same address.
The rate of subscription to the *Acta Physica* is 110 forints a volume. Orders may be placed with "Kultúra" Foreign Trade Company for Books and Newspapers (Budapest I., Fő u. 32. Account No. 43-790-057-181) or with representatives abroad.

Les *Acta Physica* paraissent en français, allemand, anglais et russe et publient des travaux du domaine de la physique.
Les *Acta Physica* sont publiés sous forme de fascicules qui seront réunis en volumes.
On est prié d'envoyer les manuscrits destinés à la rédaction à l'adresse suivante:

Acta Physica, Budapest 502, Postafiók 24.

Toute correspondance doit être envoyée à cette même andresse.
Le prix de l'abonnement est de 110 forints par volume.
On peut s'abonner à l'Entreprise du Commerce Extérieur de Livres et Journaux «Kultúra» (Budapest I., Fő u. 32. — Compte-couraut No. 43-790-057-181) ou à l'étranger chez tout les représentants ou dépositaires.

«*Acta Physica*» публикют трактаты из области физических наук на русском, немецком, английском и французском языках.
«*Acta Physica*» выходят отдельными выпусками разного объема. Несколько выпусков составляют один том.
Предназначенные для публикации рукописи следует направлять по адресу:

Acta Physica, Budapest 502, Postafiók 24.

По этому же адресу направлять всякую корреспонденцию для редакции и администрации.
Подписная цена «*Acta Physica*» — 110 форинтов за том. Заказы принимает предприятие по внешней торговле книг и газет «*Kultúra*» (Budapest I.,) Fő u. 32. Текущий счет: № 43-790-057-181) или его заграничные представительства и уполномоченные.

20,— Ft

INDEX

COMMUNICATIO BREVIS

RECENSIONES

Acta Phys. Hung. Tom. XVI. Fasc. 4, Budapest, 20. VI. 1964

Index: 26.022